STRINGQFT

String-Theoretic Construction
of Quantum Field Theory

VOLUME XIV

F-Theory: Geometric Dictionary and Four-Dimensional Theories

Xingyang Yu

StringQFT v1.0 / Source build candidate

Drafted with AI assistance under the supervision of the author.
Manuscript free to read. All rights reserved.

Contents

XIV.1 The physical dictionary of F-theory **1**
XIV.1.1 What the elliptic fibre describes 1
XIV.1.2 The axiodilaton and a seven-brane 1
XIV.1.3 The elliptic curve and its marking 3
XIV.1.4 The M-theory torus and the emerging circle 5
XIV.1.5 A compact elliptic K3 and its discriminant 7
XIV.1.6 Dimensions, supercharges and background data 9
XIV.1.7 Exercises 11

XIV.2 A first four-dimensional gauge theory from a Calabi–Yau fourfold **13**
XIV.2.1 A seven-brane wrapped on a surface 13
XIV.2.2 The twist and four-dimensional multiplets 14
XIV.2.3 A split SU(5) Tate family 15
XIV.2.4 Resolved curves and their charges 17
XIV.2.5 Matter curves and enhanced fibers 20
XIV.2.6 Forced and adjustable gauge sectors 22
XIV.2.7 Local geometry and the scales still present 23
XIV.2.8 Exercises 26

XIV.3 Four-form flux and supersymmetric backgrounds **28**
XIV.3.1 Which background data the geometry leaves open 28
XIV.3.2 The shifted integral lattice 29
XIV.3.3 Four-dimensional transversality 30
XIV.3.4 Gauge-preserving flux and its alternatives 34
XIV.3.5 Hodge type and primitivity 37
XIV.3.6 D3 charge in a compact completion 41
XIV.3.7 Local flux and extension data 45
XIV.3.8 Exercises 47

XIV.4 Chiral spectra, zero modes and matter multiplicities **50**
XIV.4.1 From a matter surface to a chiral index 50
XIV.4.2 The bundle seen by a matter curve 54
XIV.4.3 Counting actual cohomology groups 59
XIV.4.4 Bulk modes on the seven-brane surface 62

XIV.4.5 Equal index with different pairs . . . 65
XIV.4.6 Spectral data and what it does not fix . . . 67
XIV.4.7 Exercises . . . 70

XIV.5 Yukawa couplings, Higgs backgrounds and T-branes 73
XIV.5.1 The holomorphic coupling problem . . . 73
XIV.5.2 A diagonal Higgs background and its zero modes . . . 77
XIV.5.3 A worked residue at an intersection . . . 80
XIV.5.4 Recombination and changed matter . . . 83
XIV.5.5 A nilpotent Higgs background . . . 87
XIV.5.6 Holomorphic and normalized couplings . . . 90

XIV.6 Abelian charges and the global gauge group 95
XIV.6.1 An extra section and a gauge field . . . 95
XIV.6.2 Removing vertical and Cartan components . . . 98
XIV.6.3 The charge-two and charge-one fibers . . . 101
XIV.6.4 The character and cocharacter lattices . . . 106
XIV.6.5 A torsion section and a quotient group . . . 110
XIV.6.6 The charge-two field to be Higgsed . . . 112
XIV.6.7 Exercises . . . 114

XIV.7 Genus-one fibrations and discrete gauge symmetry 117
XIV.7.1 Higgsing the continuous gauge group . . . 117
XIV.7.2 The deformed genus-one equation . . . 119
XIV.7.3 The bisection and its Jacobian . . . 122
XIV.7.4 Following charged states through the transition . . . 127
XIV.7.5 Selection rules and a changed charge . . . 131
XIV.7.6 What the global geometry establishes . . . 133
XIV.7.7 Exercises . . . 137

XIV.8 Effective action, vacuum conditions and decoupling 140
XIV.8.1 The circle lift and four-dimensional data . . . 140
XIV.8.2 What the flux superpotential tests . . . 143
XIV.8.3 Gauge kinetic terms and the D condition . . . 146
XIV.8.4 How a vector eats an axion . . . 149
XIV.8.5 Chirality, anomalies and the axion counterterm . . . 152
XIV.8.6 Growing the bulk at fixed gauge scale . . . 155
XIV.8.7 Which fields remain dynamical in a local limit? . . . 157
XIV.8.8 Exercises . . . 162

XIV.9 The Sen limit and the heterotic comparison 165
XIV.9.1 The weak-coupling question . . . 165
XIV.9.2 The Sen polynomial and its discriminant . . . 166
XIV.9.3 O7 and D7 data on the cover . . . 168
XIV.9.4 Where the approximation fails . . . 171
XIV.9.5 Elliptic K3 and the heterotic torus . . . 175

XIV.9.6 Stable degeneration and bundle data . . . 179
XIV.9.7 Comparing the already constructed sectors . . . 184
XIV.9.8 Exercises . . . 186

XIV.10 Nonperturbative superpotentials and geometric instantons 189
XIV.10.1 Which coupling can an instanton generate? . . . 189
XIV.10.2 One instanton, two descriptions . . . 191
XIV.10.3 Count neutral fermions on a vertical divisor . . . 194
XIV.10.4 What flux requires the instanton to absorb . . . 197
XIV.10.5 A contributing divisor and two failures . . . 201
XIV.10.6 The action when the bulk grows . . . 205

XIV.11 Completing the $SU(5)$ construction 210
XIV.11.1 The data already constructed . . . 210
XIV.11.2 Hypercharge as a background . . . 211
XIV.11.3 Masslessness and ambient pushforward . . . 214
XIV.11.4 Splitting the matter spectrum . . . 217
XIV.11.5 Quantization and combined flux . . . 225
XIV.11.6 Global extension and the resulting theory . . . 227
XIV.11.7 Exercises . . . 232

XIV.12 Strongly coupled sectors and conformal matter 235
XIV.12.1 When a matter curve stops being ordinary . . . 235
XIV.12.2 What the three blowups separate . . . 238
XIV.12.3 Which six-dimensional theory is on the curve? . . . 241
XIV.12.4 Why only one flavor is gauged . . . 242
XIV.12.5 A protected weak-gauging test . . . 246
XIV.12.6 Changing flux or changing the geometry . . . 249
XIV.12.7 Exercises . . . 252

XIV.13 Atlas of four-dimensional constructions 255
XIV.13.1 Choosing a construction from field-theory data . . . 255
XIV.13.2 Ordinary seven-brane sectors . . . 257
XIV.13.3 Continuous and discrete gauge data . . . 260
XIV.13.4 Instanton supports and strongly coupled sectors . . . 263
XIV.13.5 Changing one input and checking the output . . . 267
XIV.13.6 What remains unspecified . . . 270
XIV.13.7 Exercises . . . 272

Chapter XIV.1

The physical dictionary of F-theory

XIV.1.1 What the elliptic fibre describes

A D7-brane occupies eight spacetime directions. In the transverse plane, a loop around the brane changes the IIB axion by one period. The point in spacetime returns to itself, while the coupling returns in a different duality frame. This is the physical problem for which the elliptic fibre is useful. Its complex structure specifies the axion and dilaton, and its integral cycles give a way to compare charge frames along paths in the base.

A second question arises once we give that fibre a metric. In M-theory its area sets a length scale. When the area shrinks, a membrane wrapped on the whole fibre becomes light. The mass spacing of this tower lets us calculate the radius of the IIB circle. The same limit therefore has a small length scale in one description and a growing length scale in the other. Keeping the two mass metrics explicit will be essential.

We use the IIB duality and charge conventions of Volume II and the elliptic surface and Weierstrass tools of Volume III. A single compact example will connect the local logarithm to the global discriminant, including what happens when twelve simple zeros coalesce. We then use the dictionary to locate the four- and six-dimensional construction routes and identify the background data required to specify a theory.

XIV.1.2 The axiodilaton and a seven-brane

How does the field know that a loop encloses a seven-brane? The magnetic flux of the axion measures the charge. Its supersymmetric completion ties the angular axion profile to a radial dilaton profile. The variable that makes this relation simple is the axiodilaton,

$$\tau = C_0 + ie^{-\phi} = \tau_1 + i\tau_2, \qquad \tau_2 > 0, \qquad g_s = e^{\phi} = \frac{1}{\tau_2}. \tag{XIV.1.1}$$

Here C_0 has unit period and g_s denotes the local string coupling. For the local calculation set the three-form and five-form field strengths to zero. With a mostly-plus Einstein metric, the scalar and gravity terms are

$$S = \frac{1}{2\kappa_{10}^2} \int d^{10}x \, \sqrt{-g} \left(R - \frac{\partial_M \tau \, \partial^M \bar{\tau}}{2\tau_2^2} \right). \tag{XIV.1.2}$$

The factor τ_2^{-2} is the upper half-plane scalar metric. It gives the axion a kinetic coefficient $e^{2\phi}$ and lets a varying axion source the dilaton. We work with the holomorphic supersymmetric seven-brane branch in the coordinate $u = x^8 + ix^9$. The field equations then provide a local check of the coupled profile.

On a punctured patch, write the transverse metric as $e^{2D} du \, d\bar{u}$ and keep the worldvolume metric flat. Holomorphy makes both $\nabla^2 \tau = 4e^{-2D} \partial_u \partial_{\bar{u}} \tau$ and $(\nabla \tau)^2 = 4e^{-2D} \partial_u \tau \partial_{\bar{u}} \tau$ vanish. These are the two terms of the scalar equation. The trace-reversed Einstein equation from (XIV.1.2) then gives

$$-2\partial_u \partial_{\bar{u}} D = \frac{\partial_u \tau \, \partial_{\bar{u}} \bar{\tau}}{4\tau_2^2} = -\partial_u \partial_{\bar{u}} \log \tau_2. \tag{XIV.1.3}$$

For the second equality, differentiate $\tau_2 = (\tau - \bar{\tau})/(2i)$ and use $\partial_u \partial_{\bar{u}} \tau_2 = 0$. The difference $2D - \log \tau_2$ is harmonic. Locally it is the real part of a holomorphic function, so the metric is $ds_\perp^2 = \tau_2 |h(u)|^2 du \, d\bar{u}$ with h holomorphic and nonzero. This calculation determines the part of the conformal factor forced by the varying scalar. The choice of h on overlapping patches and the boundary conditions at the source belong to the global background.

Put n units of D7 charge at the origin in the local model and orient the loop counterclockwise. The single-valued part of the holomorphic scalar contributes zero to $\oint dC_0$. With a cut used to choose the logarithm, the required multivalued part is

$$\oint dC_0 = n, \qquad \tau(u) = \tau_* + \frac{n}{2\pi i} \log(u/u_*) + f_{\text{reg}}(u), \qquad \tau \longmapsto \tau + n. \tag{XIV.1.4}$$

The regular term f_{reg} is single-valued, and u_* fixes a reference point. The logarithm gains $2\pi i$ around the loop, giving the sign of the shear. On the cut patch, set $f_{\text{reg}} = 0$ to see its two effects at once. With $u/u_* = re^{i\theta}$,

$$C_0 = C_{0*} + \frac{n\theta}{2\pi}, \qquad \tau_2 = \tau_{2*} - \frac{n}{2\pi} \log r. \tag{XIV.1.5}$$

At $r = e^{-2\pi}$ and $\tau_{2*} = 4$, one D7 gives $\tau_2 = 5$. Increasing the enclosed charge to two gives $\tau_2 = 6$ and a shift by two periods, as illustrated in Figure XIV.1.1. The angular winding and the change in the radial slope are tied by holomorphy. The local formula applies on the portion with $\tau_2 > 0$. In particular, its decrease of g_s toward the puncture concerns the loop expansion. Control of the derivative expansion near the source requires separate information.

The shear acts on an upper half-plane coordinate. To use it around more than one degeneration, we need a way to record the coordinate together with the charge basis in which it is measured. A marked elliptic curve supplies that pair of data.

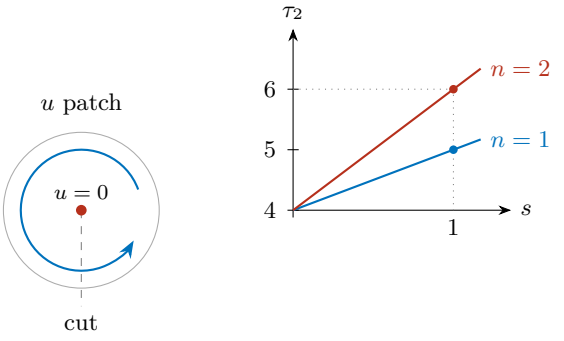


Figure XIV.1.1: The local D7 logarithm. The left panel fixes the counterclockwise orientation and downward cut. The right panel shows the pure logarithmic profile at $\tau_{2*} = 4$, using $s = -\log r/(2\pi)$. Changing the enclosed D7 charge from one to two changes both the radial slope and the monodromy.

XIV.1.3 The elliptic curve and its marking

What does a torus remember about the IIB coupling? A smooth elliptic fibre has a holomorphic differential ω. Choose an oriented basis of cycles A, B with $A \cdot B = 1$. Their periods and the modulus are

$$\Pi = \begin{pmatrix} \omega_A \\ \omega_B \end{pmatrix}, \qquad \omega_A = \int_A \omega, \qquad \omega_B = \int_B \omega, \qquad \tau = \frac{\omega_B}{\omega_A}. \tag{XIV.1.6}$$

A common nonzero rescaling of the periods leaves the modulus fixed. The marked curve is $\mathbb{C}/(\mathbb{Z} + \tau\mathbb{Z})$ in the coordinate divided by ω_A. The F-theory identification gives this shape the value of the IIB axiodilaton modulo its modular duality group. Its marking is local, just as the IIB charge convention is local.

Fix downward cuts for a brane of primitive string charge $z = (p, q)^T$, with the entries measured in F1 and D1 units. In a left-to-right crossing below the brane the string charge column v is transformed by

$$K_z = I + zz^T \begin{pmatrix} 0 & -1 \\ 1 & 0 \end{pmatrix} = \begin{pmatrix} 1 + pq & -p^2 \\ q^2 & 1 - pq \end{pmatrix}. \tag{XIV.1.7}$$

For a simultaneous change of chart, the same cycle period must satisfy $(v')^T\Pi' = v^T\Pi$ for every v. Substituting $v' = Kv$ gives $K^T\Pi' = \Pi$. Thus for $K = \left(\begin{smallmatrix} a & b \\ c & d \end{smallmatrix}\right)$,

$$\Pi' = K^{-T}\Pi, \qquad \tau' = \frac{a\tau - b}{d - c\tau}. \tag{XIV.1.8}$$

The inverse transpose acts on the column of periods. The fractional linear transformation in (XIV.1.8) then follows by dividing its second entry by its first. An active continuation of a string through a cut is a transport operation. The pairing argument concerns a relabeling of both columns at the same time.

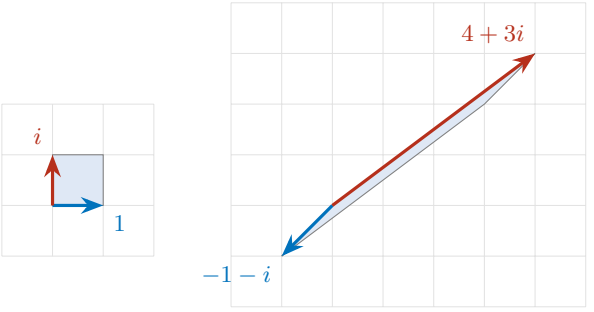


Figure XIV.1.2: Two oriented period bases for the same lattice in the complex plane. The square marking on the left has periods $1, i$. On the right the periods $-1-i, 4+3i$ span a parallelogram with the same oriented area. Their ratio gives the chart value in (XIV.1.9).

For a D7, $z = (1,0)^T$. Equation (XIV.1.7) is an upper triangular charge shear with entry -1, while (XIV.1.8) gives $\tau + 1$. To see the role of the period ordering when both charges are nonzero, set $z = (2,1)^T$, $v = (3,-2)^T$ and $\Pi = (1,i)^T$. The same calculation gives

$$K = \begin{pmatrix} 3 & -4 \\ 1 & -1 \end{pmatrix}, \qquad v' = \begin{pmatrix} 17 \\ 5 \end{pmatrix}, \qquad \Pi' = \begin{pmatrix} -1-i \\ 4+3i \end{pmatrix}, \qquad \tau' = \frac{-7+i}{2}. \tag{XIV.1.9}$$

Indeed $17(-1-i) + 5(4+3i) = 3 - 2i = v^T\Pi$. The imaginary part of the modulus changes under the modular chart change, even though the complex torus is the same. Applying the charge matrix directly to the period column would break this identity. Figure XIV.1.2 shows the two period bases used in this example.

When only the shape matters, the normalized j-invariant forgets the marking. Recall the short Weierstrass form from Volume III. With $P(x) = x^3 + fx + g$, its discriminant data are

$$\Delta_b = \operatorname{Res}(P, P') = 4f^3 + 27g^2, \qquad \Delta_{\mathrm{EC}} = -16\Delta_b, \qquad j = 1728\,\frac{4f^3}{\Delta_b}. \tag{XIV.1.10}$$

The resultant vanishes precisely when the cubic and its derivative share a root. A simple zero of Δ_b at which f stays nonzero produces a simple pole of j. In a cusp marking, $j = \mathfrak{q}^{-1} + 744 + O(\mathfrak{q})$ for $\mathfrak{q} = e^{2\pi i\tau}$. If u is a local complex coordinate vanishing at the zero, then

$$j = \frac{a}{u} + O(1), \quad a \neq 0 \qquad \Longrightarrow \qquad \mathfrak{q} = \frac{u}{a} + O(u^2), \qquad \tau = \frac{\log u}{2\pi i} + \text{regular}. \tag{XIV.1.11}$$

The primitive logarithm is recovered in the local vanishing-cycle marking. The pole locates the degeneration, while the marking is needed to identify that cycle in a common charge frame. In the compact example below, this distinction will separate an

exact discriminant count from the much stronger problem of computing the ordered monodromies.

XIV.1.4 The M-theory torus and the emerging circle

What happens to the physical length scales when the auxiliary fibre shrinks? First work with an ordinary flat M-theory torus. Its coordinates σ^1, σ^2 each have period one. Write its physical area in the eleven-dimensional metric as $\mathcal{A}$, including both circumferences. The shape determines the metric at fixed area,

$$ds^2_{T^2} = \frac{\mathcal{A}}{\tau_2}|d\sigma^1 + \tau d\sigma^2|^2, \qquad G = \frac{\mathcal{A}}{\tau_2}\begin{pmatrix} 1 & \tau_1 \\ \tau_1 & |\tau|^2 \end{pmatrix}. \tag{XIV.1.12}$$

Since $|\tau|^2 - \tau_1^2 = \tau_2^2$, the area integral over the unit square is $\sqrt{\det G} = \mathcal{A}$. The squared length of the cycle column $(p, q)^T$ is $\mathcal{A}|p + q\tau|^2/\tau_2$. Thus changing the area at fixed shape scales all cycle lengths together, while their length ratios and angles stay fixed.

The first mass comparison uses torus momentum. In the source ordering the momentum wave has phase $2\pi(\ell_2\sigma^1 + \ell_1\sigma^2)$, with ℓ_1, ℓ_2 integers. Its covector is $k = 2\pi(\ell_2, \ell_1)^T$, and the eigenvalue of the negative torus Laplacian is

$$M^2_{\text{torus KK},11} = k^T G^{-1} k = \frac{(2\pi)^2}{\mathcal{A}\tau_2}\left[(\ell_1 - \ell_2\tau_1)^2 + \ell_2^2\tau_2^2\right]. \tag{XIV.1.13}$$

The inverse metric makes the sign of the mixed term opposite to that in the cycle norm with the same ordered components. For example, take $\tau = 1/2 + i$ and $\ell_1 = \ell_2 = 1$. The shape factor in the brackets is $5/4$, whereas the squared direct-cycle factor for $(1, 1)^T$ is $13/4$. The two agree for this pair on a square torus, so a tilted torus is needed to expose the difference.

For a nonzero torus momentum pair $\ell = (\ell_1, \ell_2)$, set $d = \gcd(|\ell_1|, |\ell_2|)$ and write $\ell = d\mathbf{q}$. In the IIB description, this is d windings of the string with primitive source charges $\mathbf{q} = (q_1, q_2)$. Each winding contributes the circumference times the primitive tension. With reference tension T_0 and IIB Einstein radius R_B, the winding mass is

$$T_{\mathbf{q}} = T_0\frac{|q_1 - q_2\tau|}{\sqrt{\tau_2}}, \qquad M_{\text{wind},B} = 2\pi R_B T_\ell, \qquad T_\ell = dT_{\mathbf{q}}. \tag{XIV.1.14}$$

The source's second charge is the negative of the second component of our plus-sign cycle convention. The two mass formulas refer to different external metrics, both evaluated along the nine common noncompact directions. Define $M_{11} = \beta M_B$ for a fixed background. Comparing the squared masses in (XIV.1.13) and (XIV.1.14) cancels the charge-dependent shape factor and gives $\beta^2 R_B^2 T_0^2 = 1/\mathcal{A}$.

The second comparison involves an M2 wrapping the whole torus with degree m, independent of the string winding number d. With physical membrane tension T_M, the area action gives mass $|m|\mathcal{A}T_M$. Its IIB partner is the Fourier mode of integer momentum m on the IIB circle, with mass $|m|/R_B$. Consequently the two independent comparisons are

$$\beta^2 R_B^2 T_0^2 = \mathcal{A}^{-1}, \qquad \frac{\beta^2}{R_B^2} = \mathcal{A}^2 T_M^2. \tag{XIV.1.15}$$

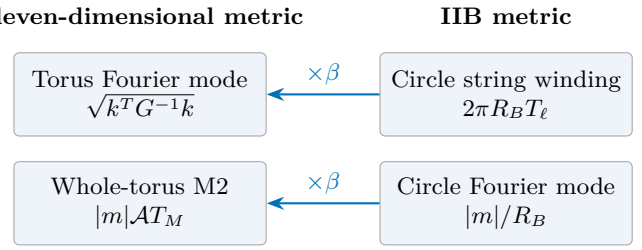


Figure XIV.1.3: The two mass comparisons for the flat torus. The upper pair compares one torus Fourier mode and the corresponding winding of a primitive IIB string. The lower pair compares a whole-torus membrane wrapping of degree m and IIB circle momentum m. The IIB masses are multiplied by β before comparison.

Both matching equations have dimensions of inverse length squared. Here T_0 has dimension L^{-2} and T_M has dimension L^{-3}, with $\hbar = c = 1$. The factor β is dimensionless. Multiplying the two equations gives $\beta^4 T_0^2 = \mathcal{A} T_M^2$. Taking the positive solution and then solving for R_B yields

$$\beta^2 = \sqrt{\mathcal{A}}\frac{T_M}{T_0}, \qquad R_B^{-2} = T_0 T_M \mathcal{A}^{3/2}. \tag{XIV.1.16}$$

The powers follow from matching two types of excitations. A comparison of only the wrapped membrane and circle momentum would determine the radius in one mass metric, leaving the relative Weyl factor undetermined.

To express the IIB circle scale in the eleven-dimensional length measure, use $M_{11} ds_{11} = M_B ds_B$ for the matched mass action. The equivalent circle radius is therefore

$$R_{B,11} = \frac{R_B}{\beta} = \frac{1}{\mathcal{A} T_M} = \frac{(2\pi)^2 \ell_p^3}{\mathcal{A}}, \qquad T_M = \frac{1}{(2\pi)^2 \ell_p^3}. \tag{XIV.1.17}$$

Here ℓ_p is the eleven-dimensional Planck length. $R_{B,11}$ expresses the scale of the emergent circle in common mass units. The finite M torus itself still has its two original cycles. The last equality keeps the full area rather than the product of two angular radii with the circumference factors removed.

At fixed τ, T_0, T_M, divide $\mathcal{A}$ by sixteen. Then

$$\frac{R_B'}{R_B} = 8, \qquad \frac{\beta'}{\beta} = \frac{1}{2}, \qquad \frac{R_{B,11}'}{R_{B,11}} = 16, \qquad \frac{M_{\text{wrap},11}'}{M_{\text{wrap},11}} = \frac{1}{16}. \tag{XIV.1.18}$$

The last ratio agrees with the inverse common-metric radius. Both radii grow as the area goes to zero. Their different powers describe the metric conversion in Figure XIV.1.3. Holding the shape fixed also holds τ_2 fixed, so the shrinking-area limit does not force weak IIB coupling.

The comparison uses the physical M/IIA lift and circle T-duality to identify the mass sectors. To pass from the flat torus to an elliptic fibration, we use the fibrewise

correspondence in its regime of validity and take its continuation as a physical premise. Near a degenerating fibre the smooth-torus approximation loses control. The F-theory description uses the IIB base and the elliptic shape data in that limit. Its emerging direction is the one associated with the light wrapped-M2 tower.

XIV.1.5 A compact elliptic K3 and its discriminant

Can we see every degeneration in one compact example? The discriminant of a Weierstrass equation is a section over the whole base. Its apparent behaviour in one affine coordinate must be translated before counting zeros on the sphere. We will also distinguish singularities of the individual cubic fibres from singularities of the surface in which they sit.

Take the base $\mathbb{P}^1$ with homogeneous coordinates $[T : U]$ and fundamental line bundle $L = \mathcal{O}(2)$. Choose the sections

$$f = -3U^8 \in H^0(L^4), \qquad g = T^{12} + cU^{12} \in H^0(L^6), \qquad y^2 z = x^3 + fxz^2 + gz^3. \tag{XIV.1.19}$$

The parameter c changes complex structure. In the base chart $U \neq 0$, let $t = T/U$. With $z = 1$, the equation is $y^2 = x^3 - 3x + t^{12} + c$. To examine $t = \infty$, set $w = U/T$ and use the powers of L on the fibre coordinates,

$$x_\infty = w^4 x, \qquad y_\infty = w^6 y, \qquad y_\infty^2 = x_\infty^3 - 3w^8 x_\infty + 1 + cw^{12}. \tag{XIV.1.20}$$

Every term of the affine equation scales by w^{12}. The discriminant scales by w^{24}, as a section of L^{12}. The transformed fibre at $w = 0$ is $y_\infty^2 = x_\infty^3 + 1$, with $\Delta_{b,\infty}(0) = 27$. Its nonzero discriminant rules out an additional zero at the point omitted by the first base chart.

The affine fibre coordinate $z = 1$ omits the zero section. At $z = 0$ the homogeneous equation forces $x = 0$, so the remaining point is in the chart $y = 1$. With $\xi = x/y$ and $\zeta = z/y$ the equation becomes

$$\zeta - \xi^3 - f\xi\zeta^2 - g\zeta^3 = 0, \qquad \frac{\partial}{\partial\zeta}(\zeta - \xi^3 - f\xi\zeta^2 - g\zeta^3)\Big|_{\xi=\zeta=0} = 1. \tag{XIV.1.21}$$

On the base overlap, $\xi_\infty = w^{-2}\xi$ and $\zeta_\infty = w^{-6}\zeta$, so this chart equation scales by w^{-6}. The derivative in (XIV.1.21) gives smoothness at the section in either trivialization. The two fibre charts cover the cubic over each base chart.

Start with $c = 0$. The resultant in the finite chart is

$$\Delta_b = 27(t^{24} - 4) = 27(t^{12} - 2)(t^{12} + 2), \qquad j = -\frac{6912}{t^{24} - 4}. \tag{XIV.1.22}$$

There are twenty-four simple roots because the two factors have disjoint roots, all of them nonzero. Each has a simple j pole and a nodal cubic, since $f = -3$ there. By contrast j vanishes at the smooth infinity fibre. A zero of j is a value of the complex structure, while a zero of Δ_b here indicates a degeneration.

To check the total space, use $F = y^2 - x^3 + 3x - t^{12}$. A finite affine singularity would solve $F = F_t = F_x = F_y = 0$. The three derivatives require

$$t = 0, \qquad x = \pm 1, \qquad y = 0, \qquad F(0, \pm 1, 0) = \pm 2. \tag{XIV.1.23}$$

Neither stationary point lies on the surface. At every nodal fibre the base derivative is nonzero, so the node does not make the total surface singular. Together with the infinity and section checks this proves smoothness. The relatively minimal elliptic surface classification identifies the simple nodes as fibres of type I_1.

The bundle choice also identifies the smooth compact surface. For a relatively minimal elliptic surface with section over $\mathbb{P}^1$, the canonical bundle is $K_X = \pi^*(K_{\mathbb{P}^1} \otimes L)$. The relative canonical bundle pushes forward to L. Relative duality gives $R^1\pi_*\mathcal{O}_X = L^{-1}$, so Leray yields

$$K_X = \pi^*\mathcal{O}(-2+2) = \mathcal{O}_X, \qquad h^1(X, \mathcal{O}_X) = h^1(\mathbb{P}^1, \mathcal{O}) + h^0(\mathbb{P}^1, \mathcal{O}(-2)) = 0. \tag{XIV.1.24}$$

These are the canonical and irregularity conditions for a K3 surface. The powers in (XIV.1.20) carry essential information. Choosing $L = \mathcal{O}(1)$ and $g = t^6$ would instead give twelve discriminant zeros and $K_X = \pi^*\mathcal{O}(-1)$ in the corresponding smooth elliptic surface.

Now tune c from zero to two, keeping the same bundles and chart transitions. Then

$$\Delta_b = 27t^{12}(t^{12} + 4), \qquad \operatorname{ord}_0(f, g, \Delta_b) = (0, 0, 12). \tag{XIV.1.25}$$

The discriminant has twelve units of multiplicity at $t = 0$ and twelve further simple zeros. Infinity is still smooth. This time the stationary point $(t, x, y) = (0, 1, 0)$ is on the surface. Writing $X = x - 1$ gives $y^2 - X^2(3 + X) = t^{12}$. The square root of $3 + X$ exists analytically near $X = 0$, so the coordinates

$$a = y - X\sqrt{3 + X}, \qquad b = y + X\sqrt{3 + X}, \qquad ab = t^{12} \tag{XIV.1.26}$$

have an invertible Jacobian at the point. This is an A_{11} surface singularity. The regular relatively minimal resolution has an I_{12} fibre at zero and twelve I_1 fibres elsewhere, using the indicated orders and the nodal reduction. The resolved surface again satisfies (XIV.1.24) with the same L and section. Figure XIV.1.4 depicts the change in the divisor on the base.

In the ordinary F-theory interpretation, the degree twenty-four counts seven-brane degenerations with multiplicity. Each isolated I_1 has the primitive shear of (XIV.1.11) in its own local marking. To multiply monodromies on the punctured sphere one must choose a common base point and transport the vanishing cycles along specified paths. If one assigns every root the same marked shear $\left(\begin{smallmatrix} 1 & 1 \\ 0 & 1 \end{smallmatrix}\right)$, the product is $\left(\begin{smallmatrix} 1 & 24 \\ 0 & 1 \end{smallmatrix}\right)$. This violates the sphere relation, which requires the ordered product of the corresponding based loops to be the identity. The computed divisor gives positions and multiplicities. The common marking and ordered paths supply additional information. Chapter 9 develops the K3 comparison with heterotic compactification and the weak-coupling limit.

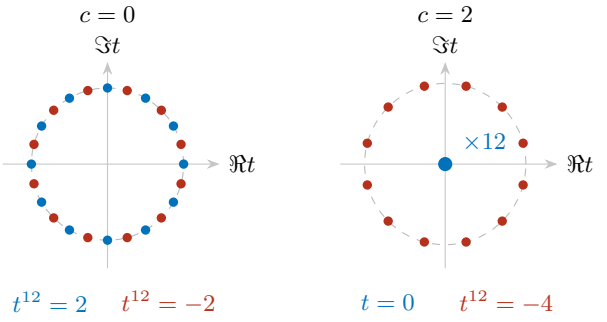


Figure XIV.1.4: The exact discriminant loci in the finite base chart. At $c = 0$ the two sets $t^{12} = \pm 2$ lie on the same circle and alternate in angle. At $c = 2$ one set has coalesced at $t = 0$ with multiplicity twelve. The remaining roots solve $t^{12} = -4$. The smooth infinity fibre is outside both finite plots.

XIV.1.6 Dimensions, supercharges and background data

Which part of the elliptic compactification occupies physical IIB space? For an elliptic complex n-fold $Y_n \to B_{n-1}$, the base has $2(n-1)$ real dimensions. In the IIB description only the base contributes to the internal spacetime count. In M-theory the entire $2n$-dimensional total space is internal. Hence

$$d_F = 10 - 2(n-1), \qquad d_M = 11 - 2n, \qquad d_F = d_M + 1. \tag{XIV.1.27}$$

The difference is the circle recovered in Section XIV.1.4. For the compact K3 example the base is a sphere, giving eight IIB spacetime dimensions. As a compact background it retains the eight-dimensional gravity sector. At finite fibre area the M description has seven spacetime dimensions, as expected for the circle reduction of that setting.

The spacetime count does not yet count supercharges. Consider the smooth reference M geometry with holonomy exactly $SU(n)$ and a compatible supersymmetric background. In the exterior-form model the complex internal spinor is $\Lambda^\bullet \mathbb{C}^n$, with chirality given by exterior degree modulo two. Under $SU(n)$ the scalar and the volume form are invariant. To see why there are no other singlets, act on the wedge e_I labelled by a subset I with a diagonal matrix g of eigenvalues $e^{i\theta_j}$. Its action is

$$g\, e_I = \exp\left(i \sum_{j \in I} \theta_j \right) e_I, \qquad \sum_{j=1}^{n} \theta_j = 0. \tag{XIV.1.28}$$

For a nonempty proper subset, pick one index inside I and one outside it. Give them angles θ and $-\theta$ and set the other angles to zero. The wedge acquires a nontrivial phase at generic θ. Only the empty and full wedges survive every diagonal action, and both are invariant under the full group. The external spinor in $11 - 2n$ dimensions has

Table XIV.1.1: Dimensions and reference supersymmetry for the ordinary elliptic F/M circle relation. The holonomy column refers to the M reference geometry. Compatible backgrounds and the untwisted circle are assumed.

Total space	Holonomy	M frame	F frame	Real Q
K3	$SU(2)$	7D minimal	8D minimal	16
CY threefold	$SU(3)$	5D $\mathcal{N}=1$	6D $(1,0)$	8
CY fourfold	$SU(4)$	3D $\mathcal{N}=2$	4D $\mathcal{N}=1$	4

complex dimension 2^{5-n}, so

$$\dim_{\mathbb{C}}(\Lambda^{\bullet}\mathbb{C}^n)^{SU(n)} = 2, \qquad Q_{\mathbb{R}} = 2\cdot 2^{5-n}. \tag{XIV.1.29}$$

The eleven-dimensional Majorana real structure commutes with holonomy. The real dimension of its invariant space equals the complex dimension of the complexified invariant space. In the fourfold case, the even forms have degrees zero, two and four. The odd forms have degrees one and three. They give the two chiral internal spinors

$$8_s = 1 \oplus 6 \oplus 1, \qquad 8_c = 4 \oplus \bar{4}. \tag{XIV.1.30}$$

The two singlets are both in 8_s. Each carries a two-component external spinor, giving four real supercharges.

With a compatible F uplift and an untwisted external circle, the same real supercharges organize into multiplets in the higher dimension. Table XIV.1.1 gives the corresponding assignments. The $(1,0)$ notation uses the six-dimensional chirality convention of Volume 0.

For a changed input at the same complex dimension, take K3 $\times$ K3 in the product metric. The holonomy now acts separately on the two complex two-planes. Each factor admits its own volume form, so the internal invariant basis is

$$1, \qquad \Omega_1, \qquad \Omega_2, \qquad \Omega_1 \wedge \Omega_2. \tag{XIV.1.31}$$

This gives eight real supercharges in the three-dimensional reference geometry when the sources and flux preserve them. The extra invariant forms explain precisely where the full-$SU(4)$ count changes. In a compact fourfold the flux and spacetime-filling sources must also satisfy the curvature-induced tadpole condition. Thus a reference spinor count describes the supersymmetry available to the geometry and leaves a separate consistency problem for the physical background.

The construction in Chapter 2 starts from seven-brane geometry on a base of complex dimension three. Its resolved fibres and intersections can specify a local gauge algebra and candidate representations. To determine the realized theory, we will need a Kähler chamber and scales, compatible flux and tadpole data, and a seven-brane gauge and Higgs background. Line bundles or sheaves enter the actual zero-mode calculation. For a local QFT, boundary conditions and scale limits must also isolate the fields under study. The six-dimensional route in XV instead starts from a base surface, where compact curves supply the tensor-branch data. Both routes use the same elliptic dictionary, with different physical background and isolation questions.

XIV.1.7 Exercises

1. For a primitive brane column $z = (1, 2)^T$, start with $v = (2, 1)^T$ and $\Pi = (1, i)^T$. Compute v', τ' and $(v')^T\Pi'$ under the simultaneous chart change. Explain why applying the charge matrix to the periods fails even when it preserves the integral lattice.

2. At fixed τ, T_0, T_M, set $\mathcal{A}'/\mathcal{A} = 1/81$. Find the ratios R'_B/R_B, β'/β, $R'_{B,11}/R_{B,11}$ and $M'_{\mathrm{wrap},11}/M_{\mathrm{wrap},11}$. Derive them from the two matching equations and explain how the circumference and metric conventions enter the result.

3. In the compact family (XIV.1.19), change c to -2. Compute the multiplicity of the discriminant at $t = 0$, the number of remaining simple roots, the value of $\Delta_{b,\infty}(0)$ and the affine singular point (t, x, y). Derive the local analytic normal form. Explain what the data determine about the resolved fibre and what would be needed to compare its vanishing cycle with the other roots.

4. A proposed compact four-dimensional construction specifies an elliptic CY fourfold and names the visible seven-brane divisors. Explain which parts of the dimension and supercharge assignment can be made conditionally from this information. Identify the further data needed to establish a consistent background, compute actual matter multiplicities and isolate a four-dimensional gauge sector. This exercise is assessed in writing.

Use `benchmark/tasks.json` to find the question IDs and `benchmark/PROTOCOL.md` for submission. Give exact numerical results for Exercises 1–3. Written derivations and interpretations, including all of Exercise 4, are assessed by a reader.

Status and sources

§XIV.1.2. The local Einstein scalar truncation, holomorphic branch and oriented magnetic logarithm are [SUGRA]. Schwarz (1995), v5, PDF p. 4, (6)–(7), fixes the scalar coefficient through $\frac{1}{4}\,\mathrm{tr}(d\mathcal{M}\,d\mathcal{M}^{-1}) = -d\tau\,d\bar{\tau}/(2\tau_2^2)$. Vafa (1996), v1, PDF p. 3, §2, supplies the seven-brane holomorphic branch and the logarithm. The calculation concerns the leading source-free patch and assumes the supersymmetric branch.

§XIV.1.3. The inverse-transpose period chart is [MATH] in the stated ordered charge and dual period convention. The oriented cut matrix appears in DeWolfe and Zwiebach (1999), v1, PDF pp. 8–9, (2.1)–(2.3) and Fig. 1. The physical identification of the elliptic shape with the IIB axiodilaton is [GEO-E], under the stated adiabatic and elliptic-IIB hypotheses, following Vafa (1996), v1, PDF pp. 3–4, 6 and 8. The resultant uses the Weierstrass convention $\Delta_{\mathrm{book}} = 4f^3 + 27g^2$. The displayed $27f^3 - 4g^2$ on Vafa v1 PDF p. 4 differs from the resultant of the cubic printed on that page. Equation (XIV.1.10) uses the defining cubic and its actual resultant.

§XIV.1.4. The torus norms and conditional mass algebra are [MATH]. The two-metric comparison follows Schwarz (1995), v5, PDF p. 6, (17)–(21), p. 7, (22)–(24), and pp. 8–9,

(25)–(30). Its source charge sign is translated by $q = -q_2$. The physical wrapped-membrane and circle momentum identification is [GEO-E] using the nonperturbative lift and ordinary circle T-duality. Fibrewise continuation adds the qualified adiabatic step of Vafa (1996), v1, PDF p. 6, §2, and p. 8, §3. The matched mass sectors leave general spectra and singular-fibre dynamics outside this calculation.

§XIV.1.5. The exact compact family, chart checks, canonical class, A_{11} analytic normal form and based-loop obstruction are [MATH]. The canonical bundle formula is Theorem 6.8 of Schütt and Shioda (2010), v3, PDF p. 26, with the source's bundle replaced by its dual to use positive L. The K3 criterion is Definition 12.1 on PDF p. 59. The Kodaira classification is used under the proper, sectioned, regular relatively minimal surface hypotheses stated above. The physical discriminant-count interpretation is [GEO-E] under the stated adiabatic and elliptic-IIB hypotheses, following Vafa (1996), v1, PDF pp. 3–4 and 6. A full marked global monodromy factorization is outside the calculation.

§XIV.1.6. The conditional dimension arithmetic is [MATH]. The invariant-spinor reference count and background constraints are [SUGRA], following Dasgupta et al. (1999), v3, PDF pp. 2–6, especially (2.11)–(2.12), with the eleven-dimensional Majorana real form. For the product example see Aspinwall and Kallosh (2005), v1, PDF pp. 3–4, §2 after (5). The compatible F uplift and resulting assignments are [GEO-E] under the stated adiabatic hypothesis. See Vafa (1996), v1, PDF pp. 11–12, §4, and Dasgupta et al. (1999), v3, PDF pp. 2–3, §1. The full-holonomy reference assignments require compatible supersymmetric backgrounds and the ordinary untwisted circle. The global constraints and actual matter data are developed in the following chapters.

The bounded exercise calculations admit exact rational submissions. Written derivations and physical interpretation are assessed separately.

References

Aspinwall, P. S. and R. Kallosh (2005). "Fixing all moduli for M-theory on K3 x K3". In: *JHEP* 10, p. 001. DOI: 10.1088/1126-6708/2005/10/001. arXiv: hep-th/0506014.

Dasgupta, K., G. Rajesh, and S. Sethi (1999). "M theory, orientifolds and G-flux". In: *JHEP* 08, p. 023. DOI: 10.1088/1126-6708/1999/08/023. arXiv: hep-th/9908088.

DeWolfe, O. and B. Zwiebach (1999). "String junctions for arbitrary Lie algebra representations". In: *Nucl. Phys. B* 541, pp. 509–565. DOI: 10.1016/S0550-3213(98)00643-3. arXiv: hep-th/9804210.

Schütt, M. and T. Shioda (2010). "Elliptic surfaces". In: arXiv: 0907.0298 [math.AG].

Schwarz, J. H. (1995). "An SL(2,Z) multiplet of type IIB superstrings". In: *Phys. Lett. B* 360, pp. 13–18. DOI: 10.1016/0370-2693(95)01138-G. arXiv: hep-th/9508143.

Vafa, C. (1996). "Evidence for F-Theory". In: *Nucl. Phys. B* 469, pp. 403–418. DOI: 10.1016/0550-3213(96)00172-1. arXiv: hep-th/9602022.

Chapter XIV.2

A first four-dimensional gauge theory from a Calabi–Yau fourfold

XIV.2.1 A seven-brane wrapped on a surface

A seven-brane can extend along four-dimensional spacetime and wrap a compact complex surface S in the base of an elliptic Calabi–Yau fourfold. The wrapped brane then supplies a gauge sector. To describe it in four dimensions we must determine which supersymmetries survive the curvature of S, which collapsing curves carry gauge charge, and where additional charged states can live. These questions use different pieces of the compactification. The twist acts on the fields on S. The root charges come from the fiber over a generic point of S. The charges of candidate matter come from the special fibers over curves in S.

We will work through one fourfold whose base is $\mathbb{P}^3$ and whose gauge surface is a smooth quadric. Its Tate equation admits a split I_5 fiber along S. We will construct the local resolution and compute what can be inferred about the four-dimensional gauge and matter sectors. The same surface and matter curves will serve as inputs when we introduce flux and count zero modes. A separate surface with a different normal bundle shows how a gauge sector can arise even in a generic Weierstrass equation.

We use the circle interpretation of the preceding chapter, the split-fiber criterion of Volume IV, and the quadratic brane action of Volume II. A fibral curve will mean a curve lying over a point of the base. A matter curve, by contrast, lies in the base itself. This distinction will let us follow a wrapped membrane as its position moves along the seven-brane.

XIV.2.2 The twist and four-dimensional multiplets

Which supercharges are still available after we wrap the brane? In an ordinary local seven-brane description, start with eight-dimensional supersymmetric Yang–Mills on $\mathbb{R}^{3,1} \times S$. The flat-space supersymmetry parameters are spinors. Parallel transport on S acts on their internal spinor index, so a flat-space parameter generally fails to give a global symmetry of the wrapped theory. The twist uses a background rotation in the two directions transverse to the brane to cancel this action on selected components. On a smooth Kähler surface the structure group reduces to $U(2)$, and the relevant compensating rotation is in its central $U(1)$.

Take J to be the central generator with charge $+1$ on $T^{1,0}S$ and R the generator of the transverse rotation. The eight-dimensional spinors $S_\pm$ arise from the real chiral spinor of the ten-dimensional theory. We denote a four-dimensional Weyl spinor by L_4 or R_4 according to chirality, and an internal Weyl spinor by L_S or R_S. In the orientation we use their decomposition is

$$\mathbf{16}_+ = (S_+, +\tfrac{1}{2}) \oplus (S_-, -\tfrac{1}{2}), \tag{XIV.2.1}$$

$$S_+ = (L_4 \otimes L_S) \oplus (R_4 \otimes R_S), \tag{XIV.2.2}$$

$$S_- = (R_4 \otimes L_S) \oplus (L_4 \otimes R_S). \tag{XIV.2.3}$$

The charges in the first line are R charges. Under the Kähler structure group, the internal spinors have the central weights

$$L_S \longrightarrow \mathbf{2}_0, \qquad R_S \longrightarrow \mathbf{1}_{+1} \oplus \mathbf{1}_{-1}. \tag{XIV.2.4}$$

The doublet has a nontrivial $SU(2)$ index. Even if its central charge vanished, it would still transform as a doublet. We therefore look for neutral singlets after combining J with R.

With $J_{\text{tw}} = J + 2R$, the $R = +1/2$ singlet of $J = -1$ and the $R = -1/2$ singlet of $J = +1$ become neutral. The other two singlets have charges $+2$ and -2, and the doublets have charges $+1$ and -1. The surviving singlets therefore give

$$J + 2R = 0 \quad \Longleftrightarrow \quad (J, R) = (-1, +\tfrac{1}{2}) \text{ or } (+1, -\tfrac{1}{2}), \tag{XIV.2.5}$$

$$(R_4 \otimes \mathbf{1}_0) \oplus (L_4 \otimes \mathbf{1}_0). \tag{XIV.2.6}$$

The last line consists of one Weyl supercharge and its conjugate because the parent spinor is real. It gives four real supercharges, the four-dimensional $\mathcal{N} = 1$ algebra. The two points at zero charge in Figure XIV.2.1 are therefore related by conjugation. A change to $J + R$ instead gives singlet charges $\pm 1/2$ and $\pm 3/2$. None is neutral. The factor of two follows from matching the spinor charges of the two rotations.

The same twist acts on the fields. The complex transverse scalar has $(J, R) = (0, -1)$. Its new charge is -2, the charge of the determinant of the holomorphic cotangent. If E is the gauge bundle, the local vector and chiral multiplet variables are thus

$$A_\mu, \qquad A^{0,1} \in \Omega^{0,1}(S, \operatorname{ad} E), \qquad \Phi \in \Omega^{2,0}(S, \operatorname{ad} E). \tag{XIV.2.7}$$

In particular the holomorphic Higgs field is valued in $K_S \otimes \operatorname{ad} E$. The geometric coordinate normal to S in the base transforms instead in $N_{S/B}$. Adjunction relates the

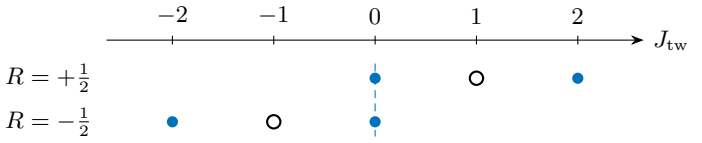


Figure XIV.2.1: Internal charges after twisting. Filled points represent singlets and open points represent $SU(2)$ doublets. The two neutral singlets accompany conjugate spacetime Weyl spinors.

bundles by $K_S = K_B|_S \otimes N_{S/B}$. For our quadric, $K_S = \mathcal{O}(-2,-2)$ and $N_{S/B} = \mathcal{O}(2,2)$. Confusing the two bundles would change the space of holomorphic sections from dimension zero to dimension nine.

For a reference calculation, take a trivial adjoint bundle and $\Phi = 0$ in the local bulk theory. The internal dependence of the massless vector, internal connection and Higgs comes respectively from $H^0(S,\mathcal{O})$, $H^1(S,\mathcal{O})$ and $H^0(S,K_S)$. On the product of projective lines, the Künneth formula gives

$$H^0(S,\mathcal{O}) = \mathbb{C}, \qquad H^1(S,\mathcal{O}) = 0, \tag{XIV.2.8}$$

$$H^0(S,K_S) = H^0(\mathbb{P}^1,\mathcal{O}(-2))^{\otimes 2} = 0. \tag{XIV.2.9}$$

The constant section supplies the four-dimensional gauge field. The internal connection and Higgs give no bulk adjoint chiral zero modes in this reference background. Modes supported on a matter curve solve a separate problem. Flux, bundle data and the corresponding zero-mode calculation enter in the next chapters. We first need the geometry on which those backgrounds are defined.

XIV.2.3 A split SU(5) Tate family

What global equation can support the desired gauge algebra on the quadric? Set $B = \mathbb{P}^3$ with hyperplane class H and coordinates $X_{00}, X_{01}, X_{10}, X_{11}$. The Segre map takes a pair $([u_0 : u_1],[v_0 : v_1])$ to $[u_0v_0 : u_0v_1 : u_1v_0 : u_1v_1]$. Its image is

$$S = \{w = 0\}, \qquad w = X_{00}X_{11} - X_{01}X_{10}. \tag{XIV.2.10}$$

The gradient of w can vanish only when all four coordinates vanish, so S is smooth. Let H_1, H_2 be the pullbacks of the two hyperplane classes on $\mathbb{P}^1$. Each X_{ij} restricts to a section of bidegree $(1,1)$. The divisor class, restricted hyperplane, and ruling intersections are

$$[S] = 2H, \qquad H|_S = H_1 + H_2, \qquad H_1^2 = H_2^2 = 0, \qquad H_1H_2 = 1, \tag{XIV.2.11}$$

$$N_{S/B} = \mathcal{O}_S(2,2), \qquad K_S = (K_B + 2H)|_S = \mathcal{O}_S(-2,-2). \tag{XIV.2.12}$$

In the elliptic construction take $L = K_B^{-1} = \mathcal{O}_B(4H)$. In the affine fiber chart x and y have bundles L^2 and L^3. The coefficient a_i has bundle L^i, so every term in the Tate

equation takes values in L^6. We impose the split tuning by choosing

$$y^2 + b_5xy + b_3w^2y = x^3 + b_4wx^2 + b_2w^3x + b_0w^5, \tag{XIV.2.13}$$

$$(a_1, a_2, a_3, a_4, a_6) = (b_5, wb_4, w^2b_3, w^3b_2, w^5b_0). \tag{XIV.2.14}$$

The residual degrees are found by subtracting $2v_i$ from $4i$, where v_i is the imposed order of w in a_i. In the order $(b_5, b_4, b_3, b_2, b_0)$ this gives

$$(4, 8-2, 12-4, 16-6, 24-10) = (4, 6, 8, 10, 14). \tag{XIV.2.15}$$

These are degrees of actual polynomials on $\mathbb{P}^3$. For example b_3 has degree eight and w^2b_3 has degree twelve as required for a_3. Treating the quadric as a degree-one divisor would already change this term's degree assignment.

To find the discriminant to first nonzero order, use $B_2 = a_1^2 + 4a_2$, $B_4 = a_1a_3 + 2a_4$ and $B_6 = a_3^2 + 4a_6$. Completing the square with $Y = y + (a_1x + a_3)/2$ and then shifting $x = X - B_2/12$ gives

$$Y^2 = X^3 + fX + g, \tag{XIV.2.16}$$

$$f = -B_2^2/48 + B_4/2, \qquad g = B_2^3/864 - B_2B_4/24 + B_6/4. \tag{XIV.2.17}$$

We use $\Delta = 4f^3 + 27g^2$. The conventional elliptic discriminant is -16Δ. In that convention one can collect the terms with $B_8 = (B_2B_6 - B_4^2)/4$. The order-four terms of B_2B_6 and B_4^2 both equal $b_5^2b_3^2w^4$ and cancel. The next two powers give

$$B_8 = w^5P + w^6(4b_4b_0 - b_2^2), \tag{XIV.2.18}$$

$$P = b_4b_3^2 - b_5b_3b_2 + b_5^2b_0, \tag{XIV.2.19}$$

$$-16\Delta = -B_2^2B_8 - 8B_4^3 - 27B_6^2 + 9B_2B_4B_6. \tag{XIV.2.20}$$

The last three terms begin at orders six, eight and six. Therefore at a generic point of S,

$$\Delta = \frac{w^5}{16}b_5^4P + O(w^6), \qquad (f, g)|_S = (-b_5^4/48, b_5^6/864). \tag{XIV.2.21}$$

Over the function field of S, b_5P is nonzero. Setting $w = 0$ gives the nodal cubic $y^2 + b_5xy = x^3$. Its node at the origin has tangent cone $y(y + b_5x) = 0$. The two tangent lines are distinct and defined over the function field. The orders $(0, 0, 5)$ and this split condition give a split I_5 in the regular minimal transverse model. The ordinary F-theory interpretation with the gauge background preserving the algebra gives $\mathfrak{su}(5)$. At $b_5 = 0$ the tangent lines coalesce. We will resolve that locus separately.

It is useful to record exactly which data remain available when the ambient geometry changes. Write $p : B_{\text{loc}} = \text{Tot}(N) \to S$ with $N = \mathcal{O}(2, 2)$ and use the tautological normal coordinate $w_N \in p^*N$. The relative tangent of the total space is p^*N. Taking determinants gives

$$-K_{B_{\text{loc}}} = p^*(K_S^{-1} \otimes N) = p^*\mathcal{O}(4, 4), \qquad B_{i,v_i} \in H^0(S, \mathcal{O}(4i - 2v_i, 4i - 2v_i)). \tag{XIV.2.22}$$

The restrictions of the original polynomials give these B_{i,v_i}. Every monomial of bidegree (d, d) on the quadric can be written as a product of d factors u_iv_j, by pairing the d

factors from each projective line. Thus the restriction from degree-d polynomials on $\mathbb{P}^3$ is surjective. In the split total space, $w_N^{v_i} p^* B_{i,v_i}$ realizes the prescribed leading terms. This construction fixes the leading jets and the local chart data they control. Higher normal coefficients in the original compact model require separate input.

We can also realize these jets in a compact ruled base. Take lines in $\mathcal{O} \oplus N$, write $T = \mathcal{O}(1)$ for the dual of the tautological line, and let U, V be the two projections of the tautological inclusion. They are sections of T and $T \otimes p^* N$. Figure XIV.2.2 shows the section $V = 0$ and the other section at $U = 0$. The tautological quotient has bundle $T \otimes p^* N$, and the relative tangent is the homomorphism bundle from the tautological line to this quotient. Hence

$$-K_{\mathbb{P}_S(\mathcal{O}\oplus N)} = T^2 \otimes p^*(K_S^{-1} \otimes N), \tag{XIV.2.23}$$

$$a_i = \sum_{k=v_i}^{2i} U^{2i-k} V^k p^* B_{ik}, \quad B_{ik} \in H^0(S, \mathcal{O}(4i-2k, 4i-2k)). \tag{XIV.2.24}$$

Each term has fiber degree $2i$ and acquires base degree $4i$ from V^k and B_{ik} together. At $U = 0$ the $k = 2i$ terms can be generic constants times V^{2i}. Keeping only the terms with $k = v_i$ would make all coefficients vanish there. If we instead change the normal bundle of the selected section to K_S, then $K_S^{-1} \otimes N$ becomes trivial and the leading B_{i,v_i} have bidegrees $(2v_i, 2v_i)$. This changes the model even though the gauge surface as an abstract surface is the same. The compact quadric, its split normal model and the ruled extensions furnish different global constraints on flux and bulk modes.

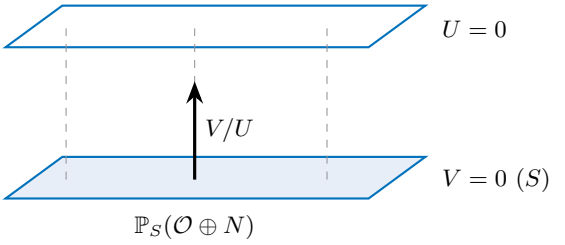


Figure XIV.2.2: Two sections of the projective bundle of lines. The chart $U \neq 0$ contains S and has fiber coordinate V/U in N. The independent highest powers of V control the Tate coefficients on the other section.

XIV.2.4 Resolved curves and their charges

Where does a simple root live in the geometry? We start with a transverse surface singularity $uv = z^2$, leaving the two surface coordinates of S as spectators. Its resolution has the two charts

$$(u, v, z) = (a, ab^2, ab), \qquad (u, v, z) = (c^2 d, d, cd). \tag{XIV.2.25}$$

Both maps satisfy $uv = z^2$. On the overlap $c = 1/b$ and $d = ab^2$. The curve $a = 0$ or $d = 0$ is a projective line, with coordinate b or c. The transverse coordinates transform

as the fiber coordinates of $\mathcal{O}_{\mathbb{P}^1}(-2)$, so the curve has self-intersection -2. The residue gives a separate check that the resolution preserves the canonical form.

$$\frac{du \wedge dz}{u} = da \wedge db = dc \wedge dd \quad \text{on the overlap.} \tag{XIV.2.26}$$

Each chart extends the form across the exceptional curve without a zero or pole. When these curves are fibered over the surface S, their union is a divisor in the fourfold. Its pairing with the exceptional curve is -2 because a transverse slice reduces that pairing to the self-intersection just computed.

A change of local equation shows how more curves can appear. Let t be one coordinate on S and replace the equation by $uv = z^2(z - t)$. Near $z = 0$ at fixed $t \neq 0$, $z - t$ is a unit, so rescaling v gives $uv = z^2$. At $t = 0$ the slice has $uv = z^3$, the A_2 surface singularity. The collision of roots of the polynomial changes the transverse root system. We will use this geometric idea in the elliptic fourfold, where the new charge vectors can be tracked by a particular resolution.

Return to the tuned quadric. We work in the affine fiber chart with projective coordinate $Z_f = 1$ and select toric resolution I with Cartan ordering e_1, e_2, e_3, e_4. The ambient blowups introduce e_1, e_4, e_2, e_3 in that order. A notation such as $(y, e_1) \mapsto (ye_4, e_1e_4)$ describes the substitution and the projective pair of directions. The four steps are

$$(x, y, w) \mapsto (xe_1, ye_1, e_0e_1), \qquad (y, e_1) \mapsto (ye_4, e_1e_4), \tag{XIV.2.27}$$

$$(x, e_4) \mapsto (xe_2, e_4e_2), \qquad (y, e_2) \mapsto (ye_3, e_2e_3). \tag{XIV.2.28}$$

The first blowup has center of ambient codimension three and the Tate polynomial has order two along (x, y, w). For example both y^2 and b_5xy have order two, whereas x^3 has order three. Dividing out e_1^2 gives the first proper transform

$$y^2 + b_5xy + b_3ye_0^2e_1 - x^3e_1 - b_4x^2e_0e_1 - b_2xe_0^3e_1^2 - b_0e_0^5e_1^3. \tag{XIV.2.29}$$

Its lowest order in (y, e_1) is one. To check the next two centers, retain only the linear terms in their defining ideals in the preceding proper transforms. They are

$$(x, e_4)\colon\ b_5xy + e_4(y^2 + b_3ye_0^2e_1), \tag{XIV.2.30}$$

$$(y, e_2)\colon\ y(b_5x + b_3e_0^2e_1e_4) - e_2(b_4x^2e_0e_1 + b_2xe_0^3e_1^2e_4 + b_0e_0^5e_1^3e_4^2). \tag{XIV.2.31}$$

Each linear part is nonzero. For a smooth ambient blowup center of codimension r and hypersurface multiplicity m, adjunction gives the discrepancy $r - 1 - m$. In the specified charts the pairs are $(3, 2), (2, 1), (2, 1), (2, 1)$, so the canonical form is preserved at every step. This calculation controls crepancy of the staged transforms. Global regularity would also require examining all strata and charts.

Composing the steps gives

$$x_{\text{old}} = xe_1e_4e_2^2e_3^2, \qquad y_{\text{old}} = ye_1e_4^2e_2^2e_3^3, \qquad w_{\text{old}} = e_0e_1e_2e_3e_4. \tag{XIV.2.32}$$

The term y_{old}^2 contains $e_1^2e_2^4e_3^6e_4^4$, whereas $x_{\text{old}}y_{\text{old}}$ contains $e_1^2e_2^4e_3^5e_4^3$. Removing the full common exceptional factor $e_1^2e_2^4e_3^5e_4^3$ from the equation leaves

$$\begin{aligned} F = {} & y^2e_3e_4 + b_5xy + b_3ye_0^2e_1e_4 - x^3e_1e_2^2e_3 - b_4x^2e_0e_1e_2 \\ & - b_2xe_0^3e_1^2e_2e_4 - b_0e_0^5e_1^3e_2e_4^2. \end{aligned} \tag{XIV.2.33}$$

The projective coordinate exclusions are part of this resolution. We will use the forbidden pairs $ye_1, ye_2, xe_4, e_0e_2, e_0e_3, e_1e_3$. For example ye_2 means y and e_2 cannot both vanish. At generic $b_5 \neq 0$, the pair $e_2 = e_4 = 0$ would reduce the proper transform to $F = b_5xy$. The coordinate exclusions make x, y nonzero there, so the two Cartan curves do not meet. This argument will change at the ten-matter locus.

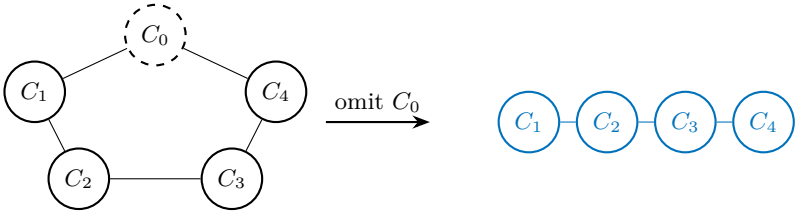


Figure XIV.2.3: Generic split I_5 fiber and its finite root chain. Vertices denote rational curves and edges denote single transverse intersections. The affine curve C_0 belongs to the fiber but is omitted from the finite Cartan basis.

In the regular split I_5 transverse model the resolved fiber is the five-curve cycle in Figure XIV.2.3. The curves C_i with $1 \leq i \leq 4$ are fibers of the Cartan divisors $D_i = \{F = e_i = 0\}$ over S. Adjunction on the crepant transverse surface gives self-intersection -2 for each rational component. Adjacent curves meet once. Omitting the affine component gives the finite chain and its intersection matrix

$$D_i \cdot C_j = -A_{ij}, \qquad A = \begin{pmatrix} 2 & -1 & 0 & 0 \\ -1 & 2 & -1 & 0 \\ 0 & -1 & 2 & -1 \\ 0 & 0 & -1 & 2 \end{pmatrix}. \tag{XIV.2.34}$$

The matrix gives a physical charge through the M-theory three-form. Write $C_3^{\text{M}} = \sum_i A_i \wedge \omega_i + \cdots$, with ω_i Poincaré dual to D_i. The membrane coupling on a worldline times an oriented curve C reduces to $\sum_i q_i \int A_i$, where

$$q_i = \int_C \omega_i = D_i \cdot C, \qquad M_C = T_{\text{M2}} \int_C J \quad \text{for a calibrated effective } C. \tag{XIV.2.35}$$

For the root curve C_j, q is the negative of the jth Cartan column. We use electric Dynkin labels $q^{\text{el}} = -q$ in the gauge basis below. This basis convention is independent of the orientation of the membrane. Reversing orientation conjugates the charge while leaving the positive rest mass unchanged. As the root curves collapse in the F-theory limit the additional charged gauge bosons become massless. A special fiber can carry other weights, which we now extract by applying the same pairing to its components.

XIV.2.5 Matter curves and enhanced fibers

What charged curves appear when the generic fiber changes? The leading discriminant on S locates two candidates, $C_{10} = \{b_5 = 0\} \subset S$ and $C_5 = \{P = 0\} \subset S$. Their subscripts anticipate the representation calculation. From the degrees in (XIV.2.15), the three terms of P have degrees $6 + 2 \cdot 8$, $4 + 8 + 10$, and $2 \cdot 4 + 14$. They all equal 22. Restricting to S gives

$$[C_{10}] = 4H_1 + 4H_2, \qquad [C_5] = 22H_1 + 22H_2. \tag{XIV.2.36}$$

Each locus is a curve in the threefold base. When a fibral component persists along such a curve, their union in the fourfold is called a matter surface. The fourth power of b_5 in (XIV.2.21) is an order of vanishing of the restricted residual discriminant. The number of massless fields comes from the mode problem on the curve.

We can verify the local inputs using actual degree-compatible coefficients. On $X_{00} = 1$, put $u = X_{10}$, $v = X_{01}$ and $w = X_{11} - uv$. Use $b_5 = X_{10}X_{00}^3$, $b_4 = X_{00}^6$, $b_3 = X_{00}^8$, $b_2 = X_{00}^{10}$ and $b_0 = X_{01}X_{00}^{13}$. Then

$$P = 1 - u + vu^2, \qquad P(0,0) = 1, \qquad P(1,0) = 0, \quad \partial_v P(1,0) = 1. \tag{XIV.2.37}$$

The first point lies on C_{10} with $P \neq 0$. At the second, P is a transverse coordinate and $b_5 = 1$. These polynomials provide jets in the displayed chart. Their special behavior on $X_{00} = 0$ is irrelevant to these two local calculations.

In the ideal (w, b_5), use total degree in its two generators. The leading terms of f, g, Δ at a generic point of C_{10} are

$$f = -b_4^2 w^2/3 + \cdots, \qquad g = 2b_4^3 w^3/27 + \cdots, \qquad \Delta = b_4^3 b_3^2 w^7 + \cdots. \tag{XIV.2.38}$$

For the discriminant, the degree-seven contribution comes from $-B_2^2 B_8$ in -16Δ. The degree-one part of B_2 is $4b_4 w$ and the degree-five part of B_8 is $b_4 b_3^2 w^5$. This explains why keeping only the generic $w^5 b_5^4 P$ term would miss the leading behavior near C_{10}. Near C_5 with $b_5 \neq 0$, f and g are units. The term $w^5 P$ has degree six in (w, P), and a possible w^6 term cannot cancel it. Thus the generic orders in the two ideals are $(2, 3, 7)$ and $(0, 0, 6)$. These orders locate changes in the geometry.

At a generic point of either matter curve, take a complex disk in the two-dimensional complex normal slice, with parameter t. Choose a generic first-order direction: the two ideal generators have nonzero linear coefficients in t, and the initial forms of f, g, Δ do not vanish on that direction. The disk then has the displayed orders in t. In the regular relatively minimal surface model of this slice, the Kodaira classification used in Volume IV gives I_1^* at C_{10} and I_6 at C_5, with transverse root systems D_5 and A_5, respectively. These slice types do not determine which curves split in the fourfold or establish regularity on special strata. The resolved components will tell us the charges.

On C_{10} the proper transform (XIV.2.33) gives

$$F|_{b_5 = e_2 = 0} = e_4 y(y e_3 + b_3 e_0^2 e_1), \tag{XIV.2.39}$$

$$F|_{b_5 = e_4 = 0} = -x^2 e_1 e_2 (x e_2 e_3 + b_4 e_0). \tag{XIV.2.40}$$

The excluded coordinate pairs make y a unit in the first restriction and x a unit in the second. The generic curves C_2 and C_4 split into two and three components as shown in Figure XIV.2.4. The two arrows pointing to $e_2 = e_4 = 0$ describe the same branch. At $x = y = e_0 = e_1 = e_3 = b_3 = b_4 = 1$ on this branch, both remaining cofactors are nonzero and the excluded pairs are respected. Thus it occurs with multiplicity one in each restriction. Its charge must agree in the two descriptions because the pairing uses the same curve and divisors.

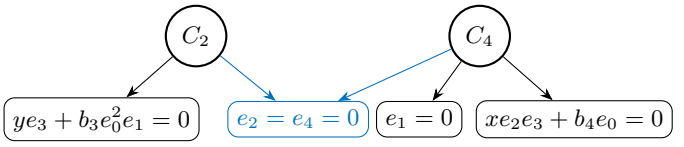


Figure XIV.2.4: Phase-I splittings at a generic point of C_{10}. Each arrow connects a parent curve to a branch of its restricted equation. The central branch occurs in both restrictions.

On C_5 we work in the $e_3 = 0$ chart with $e_0 = e_1 = 1$, allowed by the resolution's exclusions, and with b_5 a unit. To factor the restricted equation, group its terms linear in y and try to divide the remainder by their common coefficient. Set

$$L_p = b_5x + b_3e_4, \qquad Q = \frac{b_4x}{b_5} + \frac{b_5b_2 - b_4b_3}{b_5^2}e_4, \tag{XIV.2.41}$$

$$F|_{e_3=0,e_0=e_1=1} = L_p(y - e_2Q) - \frac{e_2e_4^2}{b_5^2}P. \tag{XIV.2.42}$$

To see the division, the first term of Q reproduces the x^2 coefficient, and the second adjusts the coefficient of xe_4. The residual term is proportional to e_4^2 and its coefficient is $-P/b_5^2$. As a polynomial in the fiber coordinates the displayed product equals the restriction precisely at $P = 0$. Particular values of e_2 or e_4 can kill the remainder off that locus. For a check take $(b_5, b_4, b_3, b_2, b_0) = (1, 1, 1, 2, 1)$ and $e_2 = e_4 = 1$. Then $P = 0$, $L_p = x + 1$ and $y - e_2Q = y - x - 1$. The points $(x, y) = (-1, 1)$ and $(1, 2)$ isolate the two factors. Changing b_0 to two leaves the product unchanged but adds a remainder -1. This is the split of C_3 over a generic point of C_5.

The Cartan intersections of the resolved curves in this phase give the geometric charge rows

$$\begin{aligned} C_2|_{C_{10}} &\longrightarrow (1, -1, 1, -1) + (0, -1, 0, 1), \\ C_4|_{C_{10}} &\longrightarrow (-2, 1, 0, 0) + (1, -1, 1, -1) + (1, 0, 0, -1), \\ C_3|_{C_5} &\longrightarrow (0, 1, -1, 0) + (0, 0, -1, 1). \end{aligned} \tag{XIV.2.43}$$

These are intersection data for the chosen resolution. Adding a row must reproduce the negative Cartan column of the parent curve. For C_2 the sum is $(1, -2, 1, 0)$. The repeated vector $(1, -1, 1, -1)$ satisfies the consistency condition from the common branch. This condition supplements charge conservation. For example the alternative C_2 pair $(0, -1, 0, 0), (1, -1, 1, 0)$ gives the same sum. Its two vectors belong to the

antisymmetric weight system or its conjugate, but neither appears in the displayed C_4 row. If both rows were allowed to change, the alternative C_4 triple

$$(-1,1,1,-1), \qquad (0,-1,0,0), \qquad (1,0,0,-1) \tag{XIV.2.44}$$

would restore the common vector and still sum to $(0,0,1,-2)$. Its first term is a root and the other two are allowed matter weights. These algebraic tests therefore leave ambiguity. The absolute entries of (XIV.2.43) are supplied by the resolved geometry.

We can identify the representations directly from the weights. Write ϵ_i for the five coordinate vectors and let $\lambda_i = \epsilon_i - \frac{1}{5}\sum_j \epsilon_j$. The coroots are $\epsilon_i - \epsilon_{i+1}$, so the Dynkin labels of a vector v are $v_i - v_{i+1}$. The Weyl group permutes the five coordinates. Starting from λ_1 gives the five fundamental weights, and starting from $\lambda_1 + \lambda_2$ gives the ten antisymmetric weights.

$$\mathbf{5} : \ \{\lambda_i\}_{i=1}^{5}, \qquad \mathbf{10} : \ \{\lambda_i + \lambda_j\}_{1\le i<j\le 5}. \tag{XIV.2.45}$$

For example the first geometric vector at C_5 is $-\lambda_3$ and the second is λ_4. The first C_2 vector is $-\lambda_2 - \lambda_4$ and the second is $\lambda_3 + \lambda_4$. The charge basis $q^{\mathrm{el}} = -q$ negates these labels. The resulting representation families are the fundamental and antisymmetric ones, with their conjugates under orientation reversal.

A second calculation shows why these families accompany the indicated root enhancements. In $\mathfrak{su}(6)$ the roots with both indices in the first five give the A_4 roots. Those with one index equal to six restrict to $\pm\lambda_i$. Of the five Cartan zero weights, four belong to $\mathfrak{su}(5)$. In $\mathfrak{so}(10)$ the roots are $\pm\epsilon_i \pm \epsilon_j$ for $i < j$. The opposite-sign pairs give the A_4 roots, and the same-sign pairs give $\pm(\lambda_i + \lambda_j)$. Again one Cartan zero weight remains after subtracting the A_4 adjoint. This accounts for every weight in the branchings

$$\mathbf{35} \longrightarrow \mathbf{24} \oplus \mathbf{5} \oplus \overline{\mathbf{5}} \oplus \mathbf{1}, \tag{XIV.2.46}$$

$$\mathbf{45} \longrightarrow \mathbf{24} \oplus \mathbf{10} \oplus \overline{\mathbf{10}} \oplus \mathbf{1}. \tag{XIV.2.47}$$

The restriction agrees with the resolved charge rows at the A_5 and D_5 enhancements. It identifies candidate matter charges. To decide which chiral fields actually occur, we must choose background data and solve the mode problem along the matter curves. At crossings the local geometry changes again. In particular $P|_{b_5=0} = b_4 b_3^2$ shows two possible crossing loci. Their interactions are a separate calculation after flux and zero modes have been introduced.

XIV.2.6 Forced and adjustable gauge sectors

Could we remove the gauge sector by changing the Weierstrass coefficients at fixed base? For the compact quadric, an untuned choice $f = X_{00}^{16}$, $g = X_{11}^{24}$ already answers the question. Evaluating at a point on the quadric gives

$$\Delta([1:0:0:0]) = 4(1^{16})^3 + 27(0^{24})^2 = 4. \tag{XIV.2.48}$$

Hence the discriminant need not contain S, and the I_5 sector comes from the Tate tuning.

Now put a different surface $S_f = \mathbb{P}^2$ in $B_f = \mathrm{Tot}(\mathcal{O}_{\mathbb{P}^2}(-n))$ as the zero section. Write w_f for its tautological normal coordinate. The canonical bundle calculation used above gives $-K_{B_f} = p^*\mathcal{O}(3-n)$. If f_k is the coefficient of w_f^k in f, and g_k is the corresponding coefficient in g, their degrees on S_f are

$$\deg f_k = 12 - (4-k)n, \qquad \deg g_k = 18 - (6-k)n. \tag{XIV.2.49}$$

For example a term $f_k w_f^k$ has degree $\deg f_k - kn$ and must have degree $4(3-n)$. This is an order-by-order section constraint. A negative degree on $\mathbb{P}^2$ forces the corresponding section to vanish. In the split total space a permitted coefficient pulls back to an actual section before multiplication by w_f^k.

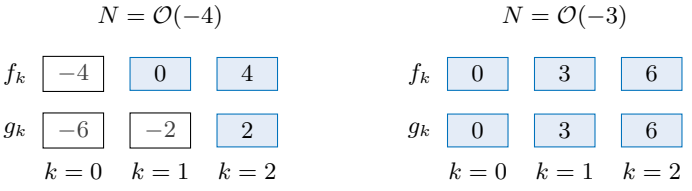


Figure XIV.2.5: Degrees of the first three normal coefficients for the two normal bundles. Shaded cells have section spaces of nonnegative degree. A negative entry forces the coefficient to vanish.

For $n = 4$, the first admissible f coefficient is $f_1 \in H^0(S_f, \mathcal{O})$ and the first admissible g coefficient is $g_2 \in H^0(S_f, \mathcal{O}(2))$. The actual sections $f = w_f$, $g = w_f^2 Q_f$, with $Q_f = X_0^2 + X_1^2 + X_2^2$, realize the minimal orders.

$$\Delta = 4w_f^3 + 27Q_f^2 w_f^4, \qquad \mathrm{ord}_{S_f}(f, g, \Delta) = (1, 2, 3). \tag{XIV.2.50}$$

At a zero of Q_f the leading discriminant still has order three. The coefficient f_1 is constant and nonzero. The generic transverse geometry is type III, supplying a geometric $\mathfrak{su}(2)$ sector. The coefficients extend to the corresponding compact projective bundle of lines. For instance $f_k w_f^k$ on $U \neq 0$ is homogenized by $U^{8-k}V^k$ times the pulled-back coefficient, with $U^{12-k}V^k$ for g. The leading powers $k = 1, 2$ are within these bounds.

Changing n to three removes the obstruction because f_0 and g_0 are now constants, as Figure XIV.2.5 shows. Taking both equal to one gives

$$\Delta|_{S_f} = 4 + 27 = 31, \qquad \mathrm{ord}_{S_f}(f, g, \Delta) = (0, 0, 0). \tag{XIV.2.51}$$

The example distinguishes a sector forced at generic complex structure by the normal bundle from one obtained by tuning coefficients on a fixed base. In each case the geometric algebra describes the unbroken sector in an appropriate background. The analysis of actual flux backgrounds and their effect on gauge symmetries comes next.

XIV.2.7 Local geometry and the scales still present

At which energies can we treat the wrapped gauge field as four dimensional? The zero mode is constant along S, and its kinetic coefficient therefore grows with the volume

over which it extends. For an unwarped reduction at constant coupling, write h_8 and h_4 for the two metrics. Integrate the kinetic action over S to obtain

$$-\frac{1}{4g_8^2}\int_{\mathbb{R}^{3,1}\times S}\sqrt{|h_8|}\,F^a_{\mu\nu}F^{a\mu\nu} = -\frac{1}{4g_4^2}\int_{\mathbb{R}^{3,1}}\sqrt{|h_4|}\,F^a_{\mu\nu}F^{a\mu\nu}, \tag{XIV.2.52}$$

$$\frac{1}{g_4^2} = \frac{\mathrm{Vol}(S)}{g_8^2}. \tag{XIV.2.53}$$

In the weak D7 reference take an unwarped string-frame metric and uniform g_s. With fundamental trace $\mathrm{Tr}_f(T_aT_b) = \delta_{ab}/2$, the quadratic DBI term has coefficient $\tau_7(2\pi\alpha')^2/4$ multiplying $\mathrm{Tr}_f F^2$. Thus

$$\tau_7 = \frac{1}{(2\pi)^7 g_s \alpha'^4}, \qquad \frac{1}{g_8^2} = \frac{\tau_7(2\pi\alpha')^2}{2}, \qquad g_8^2 = 2(2\pi)^5 g_s \alpha'^2. \tag{XIV.2.54}$$

Here g_8^2 has dimension length to the fourth power, so g_4 is dimensionless. A varying axio-dilaton or a warped reduction requires the corresponding kinetic integral. The absolute coefficient above belongs to the stated weak reference frame.

The truncation to the constant mode also requires energies below the relevant Kaluza–Klein masses. Even in a simple metric model this scale depends on shape. For a product of round two-spheres with radii R_1, R_2, scalar eigenvalues add. The first positive eigenvalue and the volume are

$$m^2_{\mathrm{KK,scalar}} = \min(2/R_1^2, 2/R_2^2), \qquad \mathrm{Vol}(S) = (4\pi)^2 R_1^2 R_2^2. \tag{XIV.2.55}$$

Compare $R_1^2, R_2^2 = (1,1)$ and $(2,1/2)$ in common length units. The volume stays fixed and the first eigenvalue halves. Its mass changes by $1/\sqrt{2}$. These are stipulated product metrics. The unequal areas do not lie in the Kähler class induced on the quadric by a hyperplane polarization of $\mathbb{P}^3$. The example isolates the dependence on the metric that enters a Kaluza–Klein calculation.

A matter curve introduces another scale, the width of a mode in the direction normal to the curve inside S. Consider a flat transverse patch with complex coordinate s and a linear diagonal Higgs mass proportional to κs, with $\kappa > 0$ of dimension inverse length squared. Neglecting derivatives along the curve, the local first-order system for two components ψ, χ takes the schematic form

$$\partial_s\psi + \kappa\bar{s}\chi = 0, \qquad \partial_{\bar{s}}\chi + \kappa s\psi = 0. \tag{XIV.2.56}$$

Taking both components equal to $e^{-\kappa|s|^2}$ solves the equations because the two derivatives bring down $-\kappa\bar{s}$ and $-\kappa s$. In polar coordinates the squared transverse L^2 norm of one component and its normalized mean-square radius are

$$\|\psi\|_\perp^2 = 2\pi\int_0^\infty re^{-2\kappa r^2}dr = \frac{\pi}{2\kappa}, \tag{XIV.2.57}$$

$$\langle|s|^2\rangle = \frac{\int_0^\infty r^3 e^{-2\kappa r^2}dr}{\int_0^\infty re^{-2\kappa r^2}dr} = \frac{1}{2\kappa}. \tag{XIV.2.58}$$

Figure XIV.2.6 shows the effect of quadrupling the slope. The root-mean-square width halves. The growing exponential fails the fixed-sign equations and the plane norm diverges. This model estimates the transverse profile when the flat patch is large compared with the width. A four-dimensional mode must also have the required dependence along the curve, where the bundle and its boundary or compactness conditions enter. A transverse Gaussian times a constant on an infinite tangent plane would fail the full norm test.

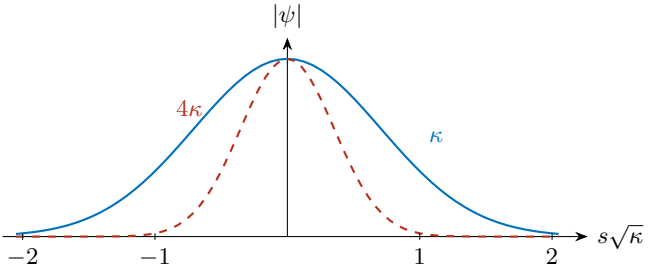


Figure XIV.2.6: One component of the transverse solution along the real axis, with the horizontal scale set by the reference slope κ. Both amplitudes are one at the curve. The dashed profile at 4κ has half the reference root-mean-square radius in the transverse plane.

Finally, consider gravity in the compact control. In $B = \mathbb{P}^3$ the classical Kähler cone has one parameter $J = tH$ with $t > 0$ of area dimension. Using $[S] = 2H$ and $\int_B H^3 = 1$ gives

$$\mathrm{Vol}(S) = \frac{1}{2}\int_B (2H)(tH)^2 = t^2, \tag{XIV.2.59}$$

$$\mathrm{Vol}(B) = \frac{1}{6}\int_B (tH)^3 = \frac{t^3}{6}. \tag{XIV.2.60}$$

In the leading unwarped gravitational reduction at fixed microscopic parameters, M_{Pl}^2 is proportional to $\mathrm{Vol}(B)$. At fixed finite gauge coupling, (XIV.2.53) holds t fixed. Sending t to infinity instead sends g_4 to zero. This specific volume path cannot separate gravity while keeping an interacting gauge sector of fixed coupling. The F-theory limit discussed in Chapter 1 concerns the elliptic fiber and the M-theory circle, whereas this constraint involves the base Kähler cone. A split normal model gives local geometric data for the gauge construction. To obtain an isolated four-dimensional theory from it one must also control couplings to bulk modes and the gaps of retained sectors. The later effective-action analysis returns to those conditions.

XIV.2.8 Exercises

1. **Change the normal bundle.** Take the zero section of $\mathrm{Tot}(\mathcal{O}_{\mathbb{P}^2}(-5))$. Give the degrees of f_k and g_k for $k = 0, 1, 2, 3$. Find their first allowed powers, give a choice of leading sections that realizes them, and compute the generic discriminant order. Explain why an allowed restricted coefficient gives an actual section in this total space.

2. **Transfer a Tate coefficient.** Use the same-normal ruled base with $N = \mathcal{O}(2, 2)$. For a_4 in (XIV.2.24), give the exponents of (U, V) and the degree on each ruling of B_{4k} at $k = 3$ and $k = 8$. Explain the role of the latter term at $U = 0$.

3. **Track a repeated branch.** Use the alternative C_2 pair discussed after (XIV.2.43). Give its total charge, the common vectors it shares with the displayed C_4 row, and the common vectors it shares with (XIV.2.44). Then explain what geometric information is needed to determine the absolute intersection entries.

4. **Change the transverse slope.** Change κ to 9κ with the peak amplitude kept fixed. Give the ratio of squared transverse norms and the ratio of root-mean-square radii. Explain why those ratios give no count of modes along the curve.

5. **Compare two limits.** In the compact $\mathbb{P}^3$ model double the volume of S with the microscopic coupling fixed. Find the change factors for $1/g_4^2$ and $\mathrm{Vol}(B)$. For JSON, give the square of the bulk-volume factor. For a noncompact replacement at finite gauge coupling, explain what isolation requires of the kinetic norm, the gap to additional compact modes, and the coupling to a bulk continuum.

Submit the bounded parts using `benchmark/PROTOCOL.md`.

Status and sources

§2. Surface twist and bulk reference. The ordinary twisted seven-brane description and the trivial-bundle bulk mode interpretation are [GEO-E]. The spinor and bundle calculation is [MATH]. See Beasley et al. (2009), arXiv:0802.3391v2, §3.2, eqs. (3.10)–(3.24), and §3.3.2, eqs. (3.44)–(3.50). The twist presupposes the ordinary local worldvolume description on a smooth Kähler surface. The bulk calculation specifies a trivial bundle and zero Higgs field locally. Admissible global flux is a separate condition.

§3. Tate family and extensions. The section classes, discriminant and two ambient extensions are [MATH]. The geometric gauge interpretation is [GEO-E], with the ordinary resolved transverse and wrapped-brane hypotheses. See Hayashi et al. (2013), arXiv:1304.1678v2, physical PDF p. 13, eqs. (3.1)–(3.3). Their $(b_1, b_2, b_3, b_4, b_6)$ are our $(b_5, b_4, b_3, b_2, b_0)$. Their base coordinate z and homogeneous fiber coordinate w are our w and Z_f. The calculation uses the Weierstrass convention $\Delta_{\mathrm{book}} = 4f^3 + 27g^2$. The extension constructs sections with prescribed leading classes and does not establish equivalence of full neighborhoods or all-strata regularity.

§4. Resolution and Cartan charges. The transverse charts, staged local crepancy and generic Cartan pairing are [MATH]. See Hayashi et al. (2013), pp. 11–15, eqs. (2.13)–(2.15),(3.4)–(3.12), and Appendix A, p. 36, eq. (A.1). The chosen geometry is Toric Resolution I, Cartans 1. The membrane coupling and calibrated mass interpretation are [GEO-E], using that source's §2.3, the M2 calibration and the M/F interpretation of Chapter 1. The electric basis sign is $q^{\mathrm{el}} = -q$. No junction cut sign or new duality convention is used.

§5. Matter curves and representations. The local orders, factorization, sourced intersections and weight calculations are [MATH]. See Hayashi et al. (2013), pp. 13–16, eqs. (3.3)–(3.14), in particular the full affine-first rows in eqs. (3.13)–(3.14). Equation (XIV.2.43) drops the affine entry of each row. The row sums, weight membership and common-branch condition constrain the source data. The joint-row alternative in the text illustrates the freedom left by those tests. The candidate matter dictionary is [GEO-E] in the stated ordinary fourfold regime, with Beasley et al. (2009), §4.2, for the defect interpretation. Matter multiplicity and the codimension-three calculation are deferred to later chapters.

§6. Forced sector. The normal degree and order calculations are [MATH]. The geometric type-III and tuned split-I_5 interpretations are [GEO-E]. See Morrison and Taylor (2015), arXiv:1412.6112, published JHEP05(2015)080, physical PDF pp. 7–9 and 16, §3.1 eqs. (3.7)–(3.8) and §5.1 eq. (5.3). The model with $N = \mathcal{O}(-4)$ is a separate fourfold setting from the tuned quadric. Forcedness concerns the generic Weierstrass coefficients for the chosen base.

§7. Volume reduction and localization. The conditional classical gauge and gravitational reductions are [SUGRA]. The quadratic D7 normalization is in the constant-dilaton weak-brane frame. The Gaussian and metric or volume calculations are [MATH]. The local equation uses Beasley et al. (2009), §4.2.3, eqs. (4.72)–(4.73). Its one-component squared norm is transverse. The compact gravity statement assumes a fixed microscopic coupling, a classical rank-one Kähler cone and the leading unwarped volume reduction. The decoupling question for other ambient geometries requires additional data.

References

Beasley, C., J. J. Heckman, and C. Vafa (2009). "GUTs and Exceptional Branes in F-theory - I". In: *JHEP* 01, p. 058. DOI: 10.1088/1126-6708/2009/01/058. arXiv: 0802.3391 [hep-th].

Hayashi, H., C. Lawrie, and S. Schäfer-Nameki (2013). "Phases, Flops and F-theory: SU(5) Gauge Theories". In: *JHEP* 10, p. 046. DOI: 10.1007/JHEP10(2013)046. arXiv: 1304.1678 [hep-th].

Morrison, D. R. and W. Taylor (2015). "Non-Higgsable clusters for 4D F-theory models". In: *JHEP* 05, p. 080. DOI: 10.1007/JHEP05(2015)080. arXiv: 1412.6112 [hep-th].

Chapter XIV.3

Four-form flux and supersymmetric backgrounds

XIV.3.1 Which background data the geometry leaves open

In the previous chapter a split elliptic fiber supplied the root curves of a seven-brane gauge algebra. Knowing the curves tells us what charges wrapped membranes can carry. It does not tell us whether there is an internal field strength that couples to those charges. In this chapter we hold the geometry fixed and ask which four-form field strengths it can support. We then change the geometry to see which parts of a flux calculation must be done again.

We use the M-theory description on a smooth Calabi–Yau fourfold Y, with the complex orientation. When Y is elliptically fibered, $\pi : Y \to B$, with a zero section Z, the ordinary M/F-theory dictionary relates the three-dimensional circle description to a four-dimensional one. Denote the internal curvature of the three-form by F_4. The dimensionless real cohomology class we will use is $G = [F_4/(2\pi\ell_p)^3] \in H^4(Y, \mathbb{R})$. This normalization keeps both the flux periods and the induced brane charge dimensionless.

The class G is less data than the three-form background. For instance, a flat change of the three-form leaves its curvature unchanged, while its holonomy on closed three-cycles can change. Refined descriptions of algebraic flux can likewise contain information that disappears upon taking the real cohomology class. Here we compute intersections and charge using G, and make a stronger algebraic pushforward calculation in one case. Neither operation reconstructs holonomy or a seven-brane sheaf.

A quantized flux can still violate transversality, couple to Cartan fields, or fail a supersymmetry test. The smooth elliptic model over $\mathbb{P}^3$ separates the transversality periods. The resolved quadric model supplies an integral witness for a flux candidate, and two products of K3 surfaces separate Hodge type from Kähler primitivity. We use the circle and resolution dictionaries from the preceding chapters and the elliptic geometry of Volume III. The charged zero-mode calculation comes after the background

data have been chosen.

XIV.3.2 The shifted integral lattice

Why need a flux period be half integral rather than integral? A membrane amplitude includes both the coupling to the three-form and a fermion determinant. Compare two ways of sweeping a membrane between the same configurations. The difference of sweeps gives a closed four-cycle M. With membrane tension $T_{\mathrm{M2}} = 1/((2\pi)^2 \ell_p^3)$, its curvature phase is $\exp(2\pi i \int_M G)$. The determinant can contribute a sign. In the spin M-theory setting, the sign is $(-1)^{\int_M \lambda}$, with $\lambda = p_1(TY)/2$ when the spacetime factors outside Y are trivial for the comparison. Cancellation requires

$$\exp\left(2\pi i \int_M G\right) (-1)^{\int_M \lambda} = 1, \qquad \int_M (G - \lambda/2) \in \mathbb{Z}. \tag{XIV.3.1}$$

The two possible signs in the representative half shift differ by the integral class λ. We use the convention $G - \lambda/2$. For a complex tangent bundle with Chern roots x_i, the Pontryagin class of the underlying real bundle satisfies

$$p_1 = \sum_i x_i^2 = \left(\sum_i x_i\right)^2 - 2\sum_{i<j} x_i x_j = c_1^2 - 2c_2. \tag{XIV.3.2}$$

Consequently $c_1(Y) = 0$ gives $\lambda = -c_2(Y)$ and the flux law reads

$$G + \tfrac{1}{2} c_2(Y) = \alpha_{\mathbb{R}}, \qquad \alpha \in H^4(Y, \mathbb{Z}). \tag{XIV.3.3}$$

Here $\alpha_{\mathbb{R}}$ denotes the image under the coefficient map, which forgets torsion. The lattice under discussion is the image of integral cohomology in real cohomology. Equation (XIV.3.3) makes no choice of flat three-form data. It defines a translate of a lattice, and the translate need not contain the origin.

Take a smooth sextic $Y_6 \subset \mathbb{P}^5$, with H the restriction of the hyperplane. This example needs no elliptic interpretation. The Euler sequence and the normal bundle $\mathcal{O}(6)$ give, through degree four,

$$c(TY_6) = \frac{(1+H)^6}{1+6H}, \tag{XIV.3.4}$$

$$c_1 = (6-6)H = 0, \tag{XIV.3.5}$$

$$c_2 = (15 - 36 + 36)H^2 = 15H^2, \tag{XIV.3.6}$$

$$c_4 = (15 - 120 + 540 - 1296 + 1296)H^4 = 435H^4. \tag{XIV.3.7}$$

To see that the shift is nontrivial, it is not enough to point to the odd coefficient 15: the generator H^2 could itself have been even in the full lattice. Instead intersect Y_6 with four hyperplanes. Their intersection in $\mathbb{P}^5$ is a line and the sextic cuts it in six points counted with multiplicity. If $H^2 = 2\xi$ modulo torsion, we would have

$$6 = \int_{Y_6} H^4 = 4 \int_{Y_6} \xi^2 \in 4\mathbb{Z}. \tag{XIV.3.8}$$

This contradiction also rules out divisibility of $15H^2$ by two, since $15H^2$ and H^2 agree modulo twice the lattice. Thus $G = 0$ fails the shift. In contrast,

$$G = \tfrac{1}{2}H^2 \quad \Longrightarrow \quad G + \tfrac{1}{2}c_2 = 8H^2. \tag{XIV.3.9}$$

The product of two hyperplane divisors is integral, so the right side is an actual integral witness. Testing only the H^2 period would miss the failure of $G = 0$: the period of $c_2/2$ on that test is already 45. The square test diagnoses what the sampled period misses.

The witness is a statement about the lattice, not about a supersymmetric configuration. At the hyperplane polarization $J = H$ it gives

$$\int_{Y_6} H\,(J \wedge G) = \tfrac{1}{2}\int_{Y_6} H^4 = 3. \tag{XIV.3.10}$$

In particular $J \wedge G$ is nonzero. In the elliptic examples we must first ask how much of a quantized class can be seen by the four-dimensional transversality periods, then impose the separate supersymmetry conditions.

XIV.3.3 Four-dimensional transversality

Which curvature components can lift from the circle description without violating four-dimensional Poincaré invariance? With a section, the ordinary M/F-theory identification requires two kinds of vanishing period:

$$\int_Y G\,\pi^*D_a\,\pi^*D_b = 0, \qquad \int_Y G\,Z\,\pi^*D_a = 0 \quad \text{for all base divisors } D_a, D_b. \tag{XIV.3.11}$$

The base/base test probes the flux integrated over the whole fiber. The section/base test can detect a four-form pulled back entirely from the base, which the first test misses. The two tests impose different restrictions in the ordinary circle dictionary; neither tests the couplings with a Cartan divisor.

Start with the smooth Weierstrass fourfold over $\mathbb{P}^3$ and use H also for its pullback. In the ordinary projective-bundle cubic the three coordinate divisors are $r, r+8H, r+12H$; r is the divisor of the cubic coordinate W. Near the section $[W : x : y] = [0 : 0 : 1]$ we can set $y = 1$. The local equation solves for W as x^3 times a unit. Thus $r|_Y = 3Z$, including the multiplicity. Adjunction on the section in the Calabi–Yau gives $N_{Z/Y} = K_Z = \mathcal{O}(-4H)|_Z$. It follows that

$$H^4 = 0, \qquad \int_Y ZH^3 = 1, \qquad Z^2 = -4HZ. \tag{XIV.3.12}$$

The first equality is pulled back from the base; the second integrates over the actual section. The last accounts for its nontrivial normal bundle. The period map on the span of H^2 and ZH is therefore

$$\begin{pmatrix} \int GH^2 \\ \int GZH \end{pmatrix} = \begin{pmatrix} 0 & 1 \\ 1 & -4 \end{pmatrix} \begin{pmatrix} a \\ b \end{pmatrix} = \begin{pmatrix} b \\ a - 4b \end{pmatrix}, \qquad G = aH^2 + bZH. \tag{XIV.3.13}$$

The class $4H^2 + ZH$ has moments $(1, 0)$ and the class H^2 has moments $(0, 1)$. Each fails only one constraint. Imposing both forces $(a, b) = (0, 0)$ in this span, with no conclusion about the complement in H^4.

We also need the topology of the smooth example for the charge comparison. Let $K_0 = 3r + 24H$ be the cubic class. The relative Euler sequence and hypersurface adjunction give

$$c(TY) = \left.\frac{(1+H)^4(1+r)(1+r+8H)(1+r+12H)}{1+K_0}\right|_Y . \tag{XIV.3.14}$$

The numerator has first Chern class K_0, so division cancels the first-order term and leaves its second-order term unchanged. This gives

$$c_2 = 182H^2 + 52Hr + 3r^2 = 182H^2 + 48HZ. \tag{XIV.3.15}$$

Here we used both identities for r and Z; in particular the shift is even by an explicit divisor expression. To find the Euler number, let s_j denote the degree-j numerator term in (XIV.3.14). In degree four the terms $-K_0^3 s_1$ and K_0^4 cancel because $s_1 = K_0$. The combination to expand is

$$c_4 = s_4 - K_0 s_3 + K_0^2 s_2. \tag{XIV.3.16}$$

For example the highest power of r comes from $-3r \cdot r^3 + (3r)^2 \cdot 3r^2 = 24r^4$. The degree-four term, retaining only terms with H degree at most three, is

$$c_4 = 48696H^3 r + 9362H^2 r^2 + 784Hr^3 + 24r^4 = 23328H^3 Z. \tag{XIV.3.17}$$

For example, $r^3 = 27Z^3 = 432H^2 Z$ on Y. Integration of the reduced expression gives $\chi = 23328$. This is the smooth model; the singularity resolved in the gauge model changes the answer.

Now consider the degree-two gauge divisor $S \subset \mathbb{P}^3$ from the preceding chapter. For the compact calculation assume a smooth projective crepant member of the ordinary split Tate family in the specified phase-I resolution. The following calculation is conditional on that hypothesis; it does not prove smoothness, flatness or regularity at every stratum for a specified tuple of coefficient polynomials. To see which data enter the intersection numbers, temporarily write the gauge divisor class as dH. Put $X = r + 8H$ and $Y_0 = r + 12H$ for the coordinate divisor classes of x and y; Y_0 here is not a fourfold. Over $W = 1$, use the split Tate form

$$y^2 + b_5 xy + b_3 w^2 y = x^3 + b_4 w x^2 + b_2 w^3 x + b_0 w^5, \tag{XIV.3.18}$$

where $w = 0$ defines S. The blowups are ordinary coordinate blowups. Their new coordinate names, total exceptional classes, center classes and multiplicities in the current hypersurface are as follows:

Step	Coordinate	Total class	Center classes	Multiplicity
1	e_1	A	X, Y_0, dH	2
2	e_4	B	$Y_0 - A, A$	1
3	e_2	C	$X - A, B$	1
4	e_3	D	$Y_0 - A - B, C$	1

The four substitutions can be read off from which coordinates vanish at each center. In the first one put $x = e_1 x_1$, $y = e_1 y_1$ and $w = e_1 w_1$. Divide by the common factor e_1^2 to find

$$y_1^2 + b_5 x_1 y_1 + b_3 e_1 w_1^2 y_1 = e_1(x_1^3 + b_4 w_1 x_1^2) + b_2 e_1^2 w_1^3 x_1 + b_0 e_1^3 w_1^5. \tag{XIV.3.19}$$

The first two terms on the left are the order-two part of the original equation along the first center. At the second center (y_1, e_1) the terms $b_5 x_1 y_1$ and $e_1 x_1^3$ are already linear. Under $y_1 = e_4 y_2$ and $e_1 = e_4 a_2$, division by one factor e_4 gives

$$e_4 y_2^2 + b_5 x_1 y_2 + b_3 e_4 a_2 w_1^2 y_2 = a_2(x_1^3 + b_4 w_1 x_1^2) + b_2 e_4 a_2^2 w_1^3 x_1 + b_0 e_4^2 a_2^3 w_1^5. \tag{XIV.3.20}$$

Here a_2 temporarily denotes the strict first exceptional coordinate, not a coefficient of the Tate equation. The third center (x_1, e_4) again has order one. Put $x_1 = e_2 x_3$ and $e_4 = e_2 a_4$. After division the leading terms relevant to the last center are $a_4 y_2^2 + b_5 x_3 y_2$ and $a_2 b_4 e_2 w_1 x_3^2$. Their order along (y_2, e_2) is one. Put $y_2 = e_3 y$ and $e_2 = e_3 a_3$. Up to renaming (a_2, a_3, a_4, w_1) as the final strict (e_1, e_2, e_4, e_0), the composite map on the original affine coordinates is

$$(x_{\mathrm{old}}, y_{\mathrm{old}}, w_{\mathrm{old}}) = (x e_1 e_4 e_2^2 e_3^2,\ y e_1 e_4^2 e_2^2 e_3^3,\ e_0 e_1 e_2 e_3 e_4). \tag{XIV.3.21}$$

In the last step it is the strict y coordinate, not the strict x coordinate, that occurs in the center. Keeping track of this choice fixes which normal classes enter the intersection calculation.

The proper hypersurface class and its strict Cartan divisors are

$$K = K_0 - 2A - B - C - D = -K_{\mathrm{amb}}, \tag{XIV.3.22}$$

$$(D_1, D_2, D_3, D_4) = (A - B, C - D, D, B - C). \tag{XIV.3.23}$$

The equality with the ambient anticanonical class follows because each multiplicity equals the codimension of the center minus one. The strict divisors subtract later exceptional divisors precisely when the corresponding coordinate occurs in the later center. The first center is disjoint from the section, and all later centers lie over the first. Thus Z remains disjoint from the four Cartans and its normal-bundle relation survives. Figure XIV.3.1 shows why the order of the pushforwards is the reverse of the coordinate substitutions.

For a quartic P in the divisor classes, insert K to integrate P in the ambient fivefold. A blowup f in a smooth complete intersection of k divisors $z_1, \dots, z_k$ has exceptional divisor E. Its normal bundle is the tautological line of degree -1 on the projective normal fibers. Restricting all but one copy of E to that divisor and integrating over the normal fibers gives

$$f_* E^n = (-1)^{k-1} z_1 \cdots z_k \, h_{n-k}(z_1, \dots, z_k) \quad (n > 0), \qquad f_* 1 = 1. \tag{XIV.3.24}$$

Here h_m is the complete homogeneous polynomial of degree m, with $h_0 = 1$ and $h_m = 0$ for $m < 0$. The vanishing for $n < k$ expresses the shortage of fiber degree. In particular

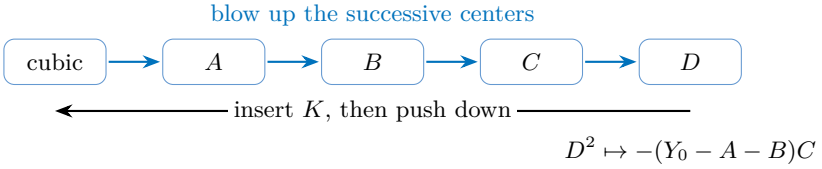


Figure XIV.3.1: Ambient blowups above the affine Weierstrass chart. The upper row constructs the proper transform. To integrate a quartic on the final hypersurface, insert K and push down in the opposite order. At the last step the normal divisors are $Y_0 - A - B$ and C.

for the last step $f_*D = 0$, $f_*D^2 = -(Y_0 - A - B)C$. In the unblown projective bundle the coordinate divisors have no common zero, so $r(r + 8H)(r + 12H) = 0$; the fiber integral of r^2 is one.

As a test sensitive to the small resolution, compute the period of $D_2D_4H^2$. Set $T = X - A$, $L_4 = Y_0 - A - B$, and $M = K_0 - 2A - B$. Before the fourth push, the integrand is $H^2(B - C)(C - D)(M - C - D)$. The coefficient of D is killed; the remaining terms give the first line of

$$f_{D*}(KD_2D_4H^2) = H^2(B - C)C(M - C - L_4), \tag{XIV.3.25}$$

$$f_{C*}f_{D*}(KD_2D_4H^2) = H^2TB(M - L_4 - T). \tag{XIV.3.26}$$

In the second line one uses $f_{C*}C^2 = -TB$ and $f_{C*}C^3 = -TB(T + B)$; terms linear in C have disappeared. The remaining parenthesis is $K_0 - X - Y_0 = r + 4H$, independent of B. The next push kills the entire expression because it is linear in B. Hence the quartic period is zero.

One can diagnose the center error without recomputing the whole table. Formally change just L_4 to $T - C$, keeping the same Cartan polynomials and the same K. Equation (XIV.3.25) becomes $H^2(B - C)C(M - T)$. The C and B pushes now give, successively,

$$H^2TB(M - T) \longmapsto H^2T(Y_0 - A)A \longmapsto H^2XY_0(dH). \tag{XIV.3.27}$$

The first arrow uses the term $-B$ in M and $f_{B*}B^2 = -(Y_0 - A)A$; the second uses the coefficient $+1$ of A^3 and kills lower powers of A. The projective-bundle integral is d, since the coefficient of r^2H^3 is d. A changed center therefore changes a specific period even though the divisor polynomials have been kept fixed. The calculation is a diagnostic of the tower, not an identification with a different physical phase.

The characteristic classes can be obtained in the same tower. The factor in the ambient Chern class at one blowup is $(1 + E)\prod_j(1 + z_j - E)/(1 + z_j)$. Its first two positive-degree pieces are $(1 - k)E$ and $E\sum_j z_j + k(k - 3)E^2/2$. Consequently the change to the degree-two term is

$$\Delta c_2 = (1 - k)Ec_1^{\text{old}} + E\sum_j z_j + \tfrac{1}{2}k(k - 3)E^2. \tag{XIV.3.28}$$

The second Chern class on the hypersurface is the final ambient one restricted to it, since the final ambient c_1 is K. In this notation the whole polynomial can be organized as

$$\begin{aligned} c_2 = {} & 182H^2 + 52Hr + 3r^2 + A(X + Y_0 + dH - 2K_0) \\ & + B(Y_0 - K_0 + 2A) - B^2 \\ & + C(X - K_0 + A + 2B) - C^2 + D(Y_0 - K_0 + A + 2C) - D^2. \end{aligned} \tag{XIV.3.29}$$

This formula retains the total exceptional transforms. Substituting strict Cartans before doing the push would change the blowup formula. In the quadric case, pushforward of Kc_2^2 gives 2736. Adjunction to degree four and pushforward give $\int_Y c_4 = 6768$. A characteristic-number check independent of the phase-specific quartic table uses the resolved $SU(5)$ Euler polynomial

$$\chi(d) = 23328 - 12000d + 2100d^2 - 120d^3. \tag{XIV.3.30}$$

It gives $\chi(2) = 6768$. The quartic calculation in (XIV.3.27) is why agreement on χ alone cannot justify reusing a period from another tower. We now use the computed periods to impose the Cartan conditions.

XIV.3.4 Gauge-preserving flux and its alternatives

How can an algebraic surface carry flux without inducing a Cartan background? An intersection with a fibral Cartan divisor measures the coupling to the corresponding Cartan gauge field. A first set of tests comes from pairing with classes on B:

$$\int_Y G D_i \pi^* D_a = 0, \qquad i = 1, \dots, 4. \tag{XIV.3.31}$$

These are necessary in the ordinary F-limit dictionary for the absence of a Cartan gauge background. The full geometric test uses the pushforward of the restriction from D_i to S, which can have components not detected by restrictions of base divisors.

Keep the smooth phase-I quadric hypothesis. Start with the surface product $V = D_2 D_4$ and use the six classes

$$U = (H^2, ZH, HD_1, HD_2, HD_3, HD_4), \qquad P_{ij} = \int_Y U_i U_j, \quad v_i = \int_Y U_i V. \tag{XIV.3.32}$$

The first block of P is the smooth section matrix. The mixed blocks vanish: Z is disjoint from the Cartans, and the degree of the Cartan image is too low for three generic base hyperplanes to meet it. To obtain the last block, intersect S with the two hyperplanes. Each point of the intersection sees the generic transverse A_4 resolution, with self-intersections -2 and adjacent intersections $+1$. There are d such points. Thus

$$P = P_0 \oplus (-d\mathcal{C}), \qquad P_0 = \begin{pmatrix} 0 & 1 \\ 1 & -4 \end{pmatrix}, \qquad \mathcal{C} = \begin{pmatrix} 2 & -1 & 0 & 0 \\ -1 & 2 & -1 & 0 \\ 0 & -1 & 2 & -1 \\ 0 & 0 & -1 & 2 \end{pmatrix}. \tag{XIV.3.33}$$

This also follows by reducing the quartics in the ambient tower. The determinant of P_0 is -1. The determinants of the consecutive Cartan blocks obey $\Delta_n = 2\Delta_{n-1} - \Delta_{n-2}$ with $\Delta_0 = 1$, $\Delta_1 = 2$, so $\det \mathcal{C} = 5$. Both blocks are invertible over $\mathbb{Q}$.

Define $b_i = \frac{1}{2}\int_Y U_i c_2$. On the quadric the inputs to the linear system are

$$v = (0, 0, 8, -8, 8, -8)^t, \qquad b = (24, -5, -4, 4, 40, 12)^t. \tag{XIV.3.34}$$

For an example of how to obtain them, replace the H^2 factor of (XIV.3.25) by $H(A-B)$. The first two pushes again leave $TB(r+4H)$ multiplied by this factor. Now the $-B$ in $D_1 = A - B$ supplies a quadratic power of B. The result no longer vanishes:

$$H(A-B)TB(r+4H) \longmapsto HT(Y_0 - A)A(r+4H) \longmapsto dH^2XY_0(r+4H). \tag{XIV.3.35}$$

Here $\pi_* r^3 = -20H$, so the last expression integrates to $d(24-20) = 4d$. The second component of b can instead be computed directly on the section. Restrict the smooth expression to Z, where $Z|_Z = -4H$, obtaining $c_2|_Z = (182-192)H^2 = -10H^2$. It follows that $\int_Y ZHc_2/2 = -5$. For the first component of b, pushing Kc_2H^2 down the four blowups and dropping terms with H degree above three gives

$$228H^3r^2 + 9H^2r^3. \tag{XIV.3.36}$$

The remaining bundle push is $228 - 9 \cdot 20 = 48$. Half of this is the first component of b. In contrast to the normal-bundle argument for ZH, this computation does not rely on restricting to a section. The other entries follow from (XIV.3.29) and the same pushforward.

There are two different linear problems. To project V to the null space of the six periods, subtract $(P^{-1}v)\cdot U$. For the quadric this means subtracting a class with Cartan coefficients $(-8, 4, -4, 8)/5$. The fractions are expected because P is invertible over $\mathbb{Q}$. This construction produces a vanishing set of periods but is not a proof of shifted integrality.

Instead start with an integral ansatz $\alpha = x \cdot U - 2V$ and set $G_* = \alpha - c_2/2$. The six vanishing periods require

$$Px = b + 2v = (24, -5, 12, -12, 56, -4)^t. \tag{XIV.3.37}$$

The first row sets $x_Z = 24$ and the second sets $x_H = -5 + 4x_Z = 91$, with x_H, x_Z the coefficients of H^2, ZH. For the Cartans, write t_i for the four remaining coefficients. Dividing the Cartan block by -2, one has

$$2t_1 - t_2 = -6, \qquad -t_1 + 2t_2 - t_3 = 6, \tag{XIV.3.38}$$

$$-t_2 + 2t_3 - t_4 = -28, \qquad -t_3 + 2t_4 = 2. \tag{XIV.3.39}$$

The first two equations give $t_2 = 2t_1 + 6$ and $t_3 = 3t_1 + 6$; the third gives $t_4 = 4t_1 + 34$. The final equation reduces to $5t_1 + 62 = 2$. Thus the shifted witness is

$$x = (91, 24, -12, -18, -30, -14)^t, \tag{XIV.3.40}$$

$$\begin{aligned}\alpha = {} & 91H^2 + 24ZH - 12HD_1 - 18HD_2 \\ & - 30HD_3 - 14HD_4 - 2D_2D_4.\end{aligned} \tag{XIV.3.41}$$

Every product on the right uses integral divisors on the smooth fourfold. The occurrence of ZH uses the actual section; it does not assert that $r/3$ is integral in the ambient space. This is why (XIV.3.41) is a witness rather than a list of sample periods. The Gram matrix of the 21 unordered divisor products from $H, Z, D_1, \dots, D_4$ has numerical rank seven under the quartic pairing. Even c_2 periods on these 21 products do not establish evenness on the full lattice.

The Cartan correction changes something measurable even after transversality. Starting from G_*, add V or add HD_1. Both additions are integral, leave the shift satisfied, and preserve the first two moments. Their changes to the four Cartan moments are

$$\delta_V(\text{Cartan moments}) = (8, -8, 8, -8), \tag{XIV.3.42}$$

$$\delta_{HD_1}(\text{Cartan moments}) = (-4, 2, 0, 0). \tag{XIV.3.43}$$

The first uses the column v and the second the first Cartan column of P. Thus the two requirements are independent even within this small collection of divisor products.

The stronger pushforward test has a direct calculation in this example. Write the quadric as a Segre surface, with ruling divisor classes u, v_S; the subscript distinguishes v_S from the vector in (XIV.3.32). They satisfy $u^2 = v_S^2 = 0$, $\int_S uv_S = 1$, and $H|_S = u + v_S$. For a strict ambient exceptional divisor T_i with map $p_i : T_i \to S$, the restriction of the flux to its fourfold Cartan and the pushforward can be computed together:

$$\rho_i = (p_i)_*\big((G_*^{\mathrm{amb}}|_{T_i})(K|_{T_i}) \cap [T_i]\big) \ \in \mathrm{CH}^1(S)_{\mathbb{Q}}. \tag{XIV.3.44}$$

The ambient polynomial G_*^{amb} uses $r/3$ as a rational lift of Z. Insertion of K cuts T_i by the hypersurface and represents the same restricted cycle for this purpose. The projection formula identifies $\int_S \rho_i(H|_S)$ with $\int_Y G_* D_i H$.

Represent the Segre equation as the determinant of a two-by-two matrix of projective coordinates. Transposition interchanges the rulings and preserves the equation. It lifts to the projective bundle and the blowup centers in the table, and leaves the classes $T_i, K, G_*^{\mathrm{amb}}$ invariant. The individual Tate coefficients need not be fixed: the ambient intersection depends on the invariant class K. Therefore ρ_i is invariant under exchange of the two rulings. A symmetric divisor class has the form $c_i(u + v_S)$, and the projection formula now gives

$$2c_i = \int_S c_i(u + v_S)^2 = \int_Y G_* D_i H = 0. \tag{XIV.3.45}$$

So the pushforward vanishes in rational Chow for this class. The inference uses the symmetry of the actual ambient representative. An arbitrary class can have an antisymmetric restriction that this moment does not see, and the calculation does not settle flat or refined gauge data.

We can see the missing direction using only the inclusion $\iota : S \hookrightarrow \mathbb{P}^3$. The coefficient of H^2 in $\iota_*(au + bv_S)$ is its degree paired with H, so

$$\iota_*(au + bv_S) = (a + b)H^2, \qquad \left(\int_S (au + bv_S)u, \int_S (au + bv_S)v_S\right) = (b, a). \tag{XIV.3.46}$$

In particular $u - v_S$ vanishes under the inclusion pushforward and still has ruling periods $(-1, 1)$. Figure XIV.3.2 shows both intersections: a probe of one ruling meets

the component of the opposite ruling. The kernel of the pushforward is not a kernel for the local field.

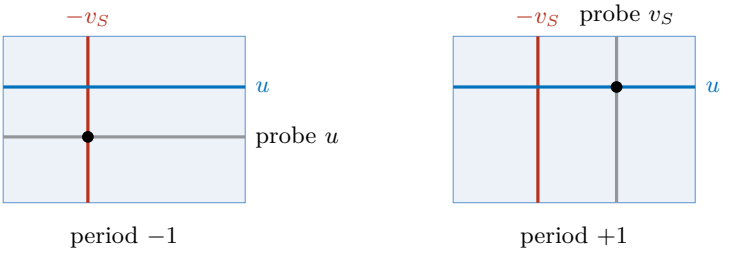


Figure XIV.3.2: The two rulings on the quadric. The class $u - v_S$ has periods -1 and $+1$ on the two ruling probes; their sum is its intersection with the inherited hyperplane. This is the antisymmetric direction omitted by that single test.

For a concrete gauge interpretation, put the local ruling class along $T_{\mathrm{diag}} = \mathrm{diag}(-2, -2, -2, 3, 3)$. On an off-diagonal generator E_{ij} the commutator with T_{diag} gives $(t_i - t_j)E_{ij}$. Within the two blocks there are $3 \cdot 2 + 2 \cdot 1 = 8$ neutral roots. Each direction between blocks has $3 \cdot 2 = 6$ roots of charge $+5$ or -5. A background along this generator has centralizer algebra

$$\mathfrak{su}(3) \oplus \mathfrak{su}(2) \oplus \mathfrak{u}(1). \tag{XIV.3.47}$$

This is a local gauge-algebra calculation. It gives neither a compact lift of the ruling flux nor a massless abelian gauge field. Even when the compact Cartan pushforwards vanish, we have still to test the Hodge and Kähler conditions on the flux.

XIV.3.5 Hodge type and primitivity

What can change when the flux class is fixed but the geometry is varied? Quantization sees the integral lattice. Supersymmetry sees how that class decomposes at the chosen complex structure and how it pairs with the chosen Kähler class. For the leading smooth M-theory supersymmetry conditions used here, an internal flux must obey

$$G \in H^{2,2}(Y), \qquad J \wedge G = 0. \tag{XIV.3.48}$$

The second condition is called primitivity. It is an equality of degree-six cohomology classes, not a condition that the integral vector have relatively prime coefficients. We first construct a class whose primitivity can be turned off without changing its Hodge type or charge. Then we compare two equal-charge classes of different Hodge type.

For the first control take a product $Y = X_1 \times X_2$. The first factor is the resolved sectioned elliptic K3 with affine equation

$$y^2 = x^3 - \Phi(t)^2 x, \qquad \Phi(t) = t^4 - 1, \qquad 4f^3 + 27g^2 = -4\Phi^6. \tag{XIV.3.49}$$

Here Φ is a homogeneous quartic written on a base chart. On the double cover $s^2 = \Phi(t)$, the substitution $x = s^2 X$, $y = s^3 Y'$ makes the fiber equation $Y'^2 = X^3 - X$ away from the branch points. At the simple zeros of Φ, the minimal resolved fibers have type I_0^*. The change $t \mapsto -t$ exchanges the fibers at 1 and -1. Let E_1, E_2 be corresponding nonidentity outer curves in these fibers and $\xi = E_1 - E_2$ their divisor-class difference on the surface. The curves are disjoint, each has square -2 by adjunction on K3, and neither meets the zero section. The fiber class F pairs to zero with either. Therefore

$$\int_{X_1} \xi^2 = -4, \qquad F \cdot \xi = Z_1 \cdot \xi = 0, \qquad E_1 \cdot \xi = -2. \tag{XIV.3.50}$$

To arrange $J_1 \cdot \xi = 0$, average a Kähler class with its pullback by the fiber-exchanging involution. Positivity is preserved by averaging. The volumes of both outer curves are now equal and positive.

Take X_2 to be a smooth $(2,2,2)$ hypersurface in $(\mathbb{P}^1)^3$ and h_1, h_2, h_3 the restricted factor hyperplanes. Each square vanishes. For $i \neq j$, the only surviving term after multiplication by the hypersurface class $2(h_1 + h_2 + h_3)$ uses the third hyperplane, so $\int_{X_2} h_i h_j = 2$. The class $J_2 = h_1 + h_2 + h_3$ is ample, and $J_2 \cdot h_i = 4$ for each i. Set

$$\beta = m(h_1 - h_2) + n(h_1 - h_3), \qquad G_{m,n} = \xi \boxtimes \beta, \tag{XIV.3.51}$$

with integers m, n and $\boxtimes$ denoting the product of the two pullbacks. Both factors of the tensor are integral $(1,1)$ classes. On the product $c_2/2 = 12([\mathrm{pt}]_1 + [\mathrm{pt}]_2)$, since each K3 has $c_2 = 24[\mathrm{pt}]$ and $c_1 = 0$. Hence the flux obeys the shifted law. For the product Kähler class $J = J_1 + J_2$,

$$J \wedge G_{m,n} = (J_1 \xi) \boxtimes \beta + \xi \boxtimes (J_2 \beta). \tag{XIV.3.52}$$

These terms belong to different Künneth summands. The first vanishes by symmetry of J_1. The second vanishes because the coefficients of β sum to zero and the three $J_2 \cdot h_i$ are equal. This gives a primitive class at the specified polarization.

The elliptic projection of the product has base $\mathbb{P}^1 \times X_2$. In a base/base or section/base moment the first-factor insertion either has the wrong degree or pairs ξ with F or Z_1. Both relevant pairings vanish. But a Cartan probe $E_1 \pi^* h_1$ for $(m,n) = (1,0)$ gives

$$\int_Y G_{1,0} \, (E_1 \pi^* h_1) = (-2) \Big(\int_{X_2} (h_1 - h_2) h_1 \Big) = 4. \tag{XIV.3.53}$$

Thus even a primitive algebraic flux passing transversality can be Cartan sensitive. This product has reduced holonomy; we are comparing cohomological tests here.

Now keep $G_{1,0}$ fixed and use the ample $J_2' = h_1 + 2h_2 + h_3$. The intersections with (h_1, h_2, h_3) become $(6,4,6)$. Thus $J_2' \beta = 2[\mathrm{pt}]_2$, and the second term in (XIV.3.52) becomes $2\xi \boxtimes [\mathrm{pt}]_2$. Its nonvanishing cannot be removed by the other Künneth summand. There has been no change to the algebraic tensor, its Hodge type, or its square. That

square is controlled by a different calculation:

$$\int_{X_2} \beta^2 = 4\big((m+n)(-m) + (m+n)(-n) + mn\big)$$
$$= -4(m^2 + mn + n^2), \tag{XIV.3.54}$$
$$\tfrac{1}{2}\int_Y G_{m,n}^2 = 8(m^2 + mn + n^2). \tag{XIV.3.55}$$

In particular one must retain the mixed term mn when changing flux along both directions.

To test Hodge type independently, take two copies of the square Kummer K3. The quartic double cover in (XIV.3.49) has branch cross ratio -1, so its elliptic curve is square, like the fiber. The product of the two square elliptic curves gives the abelian surface of the Kummer construction. In unit real coordinates $z_i = x_i + iy_i$ on the two covering tori, the real and imaginary parts of the holomorphic two-form are

$$a = dx_1 \wedge dx_2 - dy_1 \wedge dy_2, \tag{XIV.3.56}$$
$$b = dx_1 \wedge dy_2 + dy_1 \wedge dx_2. \tag{XIV.3.57}$$

With orientation $dx_1\, dy_1\, dx_2\, dy_2$, the square of either form contains twice the volume form. For a, the minus sign in the cross term cancels the sign from moving dy_1 past dx_2. Every term in ab repeats a one-form, so $ab = 0$. These two real forms generate the integral transcendental lattice of the square abelian surface: they span the real holomorphic period plane and their coefficients in the integral exterior basis generate a saturated rank-two sublattice there. The Kummer lattice relation multiplies their intersection form by two. On each Kummer factor we can therefore take integral classes p, q with

$$p^2 = q^2 = 4, \qquad p \cdot q = 0, \qquad \Omega = p + iq. \tag{XIV.3.58}$$

Here the squared classes denote their integrated pairings; Ω is a choice of normalization for the holomorphic two-form.

On the product consider

$$G_+ = p_1p_2 + q_1q_2 = \Re(\Omega_1\overline{\Omega}_2), \tag{XIV.3.59}$$
$$G_- = p_1p_2 - q_1q_2 = \Re(\Omega_1\Omega_2). \tag{XIV.3.60}$$

The first tensor is of type $(2,2)$ and the second is of type $(4,0)+(0,4)$. The positive and negative relative signs are what select these types. Both squares integrate to $4 \cdot 4 + 4 \cdot 4 = 32$ because the cross-pairing vanishes. They are both shifted integral, since the product again has the integral $c_2/2$. An unnormalized holomorphic period distinguishes them. For $\Omega_4 = \Omega_1\Omega_2$, the two elementary periods are

$$\int \Omega_4 p_1p_2 = 4 \cdot 4 = 16, \qquad \int \Omega_4 q_1q_2 = (4i)(4i) = -16. \tag{XIV.3.61}$$

It follows that $\int \Omega_4 G_+ = 0$ and $\int \Omega_4 G_- = 32$. The second flux has the same charge as the first and still fails the Hodge test. For a product Kähler class the wedge on each K3

with its holomorphic or antiholomorphic two-form vanishes by type. The distinction exhibited here is therefore Hodge type, even though both fluxes satisfy the wedge test at such a product polarization.

Return to the compact quadric in phase I. The class G_* is algebraic by construction and has type $(2,2)$ under the smooth projective hypothesis. To test primitivity in the displayed divisor span, let

$$J = aH + bZ + \sum_{i=1}^{4} j_i D_i. \tag{XIV.3.62}$$

Pair JG_* with each D_i. The H contribution vanishes by (XIV.3.37) and the Z contribution by disjointness. The remaining intersections, using the quartic pairing on the same tower, are

$$\mathcal{W}_{ik} = \int_Y G_* D_i D_k = 56 \begin{pmatrix} 0 & 0 & 0 & 0 \\ 0 & 1 & 0 & -1 \\ 0 & 0 & -1 & 1 \\ 0 & -1 & 1 & 0 \end{pmatrix}. \tag{XIV.3.63}$$

For example the second and third rows require $j_2 - j_4 = 0$ and $-j_3 + j_4 = 0$. These are necessary equations, whether or not the divisor span exhausts all of $H^{1,1}(Y)$. It is useful to see where one nonzero entry comes from. With brackets denoting integration over Y, insert K and push down the tower for $D_2^2 = (C - D)^2$:

$$(\langle D_2^2 U_i \rangle)_i = (-4, 0, 12, 8, -20, -8), \tag{XIV.3.64}$$

$$\langle D_2^2 V \rangle = -32, \qquad \langle D_2^2 c_2 \rangle = 136. \tag{XIV.3.65}$$

The first entry -4 also follows from the transverse A_4 surface, and the second vanishes by section disjointness. Inserting x into the first row gives 60. Then subtract $2(-32)$ and $136/2$ to find 56. The Cartan/Cartan block is sensitive to different periods from the HD_i block: the vanishing of (XIV.3.31) does not set (XIV.3.63) to zero.

There is an effective curve on which the required equalities are incompatible with strict positivity. At a generic point of the matter curve $b_5 = 0$, use the component of the split second Cartan with intersections

$$(D_0, D_1, D_2, D_3, D_4) \cdot C_{\mathrm{fib}} = (0, 0, -1, 0, 1). \tag{XIV.3.66}$$

Here D_0 is the affine component divisor. The row is affine first, with the strict e_1, e_2, e_3, e_4 order of (XIV.3.23). It is the second component in the split of D_2, distinct from the component shared with the split of D_4. The curve is fibral and is away from the section, so both H and Z integrate to zero on it. It follows that

$$\int_{C_{\mathrm{fib}}} J = -j_2 + j_4 = 0 \tag{XIV.3.67}$$

for any primitive J in the stated span. An interior Kähler class integrates strictly positively over every nonzero effective holomorphic curve. Figure XIV.3.3 shows the resulting obstruction. It requires only one curve and necessary primitivity equations; it does not require a presentation of the full Kähler cone.

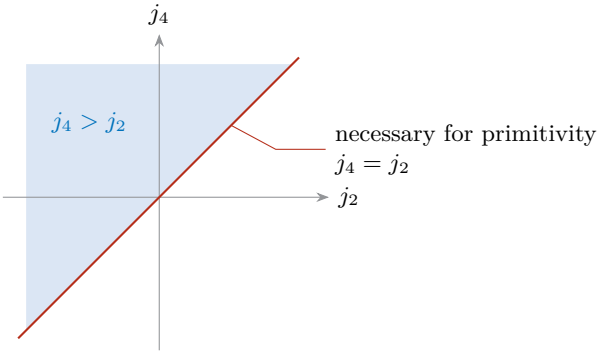


Figure XIV.3.3: Necessary conditions in the (j_2, j_4) projection of the displayed divisor span. The effective component with area $j_4 - j_2$ selects a strict half-plane. The Cartan equations for primitivity place J on its excluded boundary. The shaded half-plane is only one necessary Kähler inequality.

In the F-theory limit the base pullback is on a limiting face, where fibral curve areas can vanish. The four-dimensional D-term condition with vanishing charged-field expectation values uses the pairing with the pulled-back base Kähler class. The displayed class already passes $\int_Y G_* D_i \pi^* J_B = 0$, since J_B is proportional to the base hyperplane. This is different from setting the whole class JG_* to zero at a finite interior point. The obstruction (XIV.3.67) neither proves nor disproves F-limit supersymmetry. We can still evaluate the compact charge of the class without making either inference.

XIV.3.6 D3 charge in a compact completion

How much of the compact brane charge can a flux carry? The M-theory equation for the three-form has an electric membrane source, a quadratic term in the four-form and a curvature term. Integrate its internal eight-form part on a smooth compact fourfold without boundary. The integral of the total derivative is zero, so with the complex orientation the leading equation is

$$N_{\mathrm{M2}} + Q(G) = \int_Y I_8, \qquad Q(G) = \tfrac{1}{2} \int_Y G^2, \qquad I_8 = \frac{p_2 - p_1^2/4}{48}. \tag{XIV.3.68}$$

The count N_{M2} uses positive charge for a membrane filling the external spacetime. On the complex tangent bundle with $c_1 = 0$, $p_1 = -2c_2$ and $p_2 = c_2^2 + 2c_4$. Substitution cancels the c_2^2 term and gives

$$\int_Y I_8 = \frac{1}{24} \int_Y c_4 = \frac{\chi(Y)}{24}. \tag{XIV.3.69}$$

Under the ordinary elliptic M/F-theory identification N_{M2} becomes N_{D3}. In the stated supersymmetric charge budget we need $N_{\mathrm{D3}} \geq 0$, with branes rather than antibranes.

When the flux is primitive $(2,2)$, the Kähler Hodge-star identity for real primitive middle-degree forms gives $*G = G$ for the harmonic representative. Consequently

$$Q(G) = \tfrac{1}{2}\int_Y G \wedge *G = \tfrac{1}{2}\|G\|^2 \geq 0. \tag{XIV.3.70}$$

This positivity argument uses the supersymmetry conditions. One can compute the signed intersection $\int G^2$ without them.

Why is the formal remainder integral even when neither term is integral separately? In the strict compact Calabi–Yau case, $h^{0,0} = h^{0,4} = 1$ and $h^{0,i} = 0$ for $0 < i < 4$, so the degree-four Todd genus gives

$$\frac{3\int_Y c_2^2 - \chi}{720} = \chi(Y, \mathcal{O}_Y) = 2. \tag{XIV.3.71}$$

Insert $G = \alpha - c_2/2$ into the charge equation. The $c_2^2/8$ term cancels against the same term from $\chi/24$, leaving

$$N_{\mathrm{D3}} = -60 - \frac{1}{2}\int_Y (\alpha^2 - \alpha c_2). \tag{XIV.3.72}$$

The spin Wu formula says that $\lambda = -c_2$ is characteristic for the free middle pairing: $\int_Y \alpha^2 \equiv \int_Y \alpha\lambda \pmod 2$. The sign disappears modulo two, so the bracket in (XIV.3.72) is even. Integrality of the remainder is a consequence of the shift and the Todd identity; its sign remains to be tested. The constant 60 uses the strict Calabi–Yau Todd genus and will not be used on the K3 product.

For the smooth elliptic model of §XIV.3.3 the available curvature charge is $23328/24 = 972$. The only flux in the displayed transverse span is zero, and zero is allowed by its shift. The sextic is a separate M-theory comparison: $\chi = 435 \cdot 6 = 2610$ and $Q(H^2/2) = \frac{1}{2}\cdot\frac{1}{4}\cdot 6 = 3/4$, giving a formal $N_{\mathrm{M2}} = 108$. This integral value is compatible with the earlier failure of primitivity; the budget tests something else.

For the compact phase-I quadric, use $Px = b + 2v$ to simplify the square before doing the remaining quartics:

$$\begin{aligned}\langle G_*^2\rangle &= x^tPx - 4x^tv - 2x^tb + 4\langle V^2\rangle + 2\langle Vc_2\rangle + \tfrac{1}{4}\langle c_2^2\rangle \\ &= -x^tPx + 4\langle V^2\rangle + 2\langle Vc_2\rangle + \tfrac{1}{4}\langle c_2^2\rangle.\end{aligned} \tag{XIV.3.73}$$

The remaining pairings are computed by inserting K and using (XIV.3.24). The projective-bundle relation first gives $\pi_* r^3 = -20H$ and then $\pi_* r^4 = 304H^2$, $\pi_* r^5 = -4160H^3$. These follow by successively multiplying $r^3 = -20Hr^2 - 96H^2 r$ by r and pushing. For the quadric the polynomials after the four blowup pushes, retaining only terms with H degree at most three, are

$$KV^2 \longmapsto -96H^3r^2 - 4H^2r^3, \tag{XIV.3.74}$$

$$KVc_2 \longmapsto 96H^3r^2 + 4H^2r^3, \tag{XIV.3.75}$$

$$\begin{aligned}Kc_2^2 \longmapsto\ & 88704H^3r^2 + 13700H^2r^3 \\ & + 988Hr^4 + 27r^5.\end{aligned} \tag{XIV.3.76}$$

For the first line one can start with $K(B-C)^2(C-D)^2$. Write L_4 and M as in (XIV.3.25). Only the powers D^0, D^2, D^3 survive the last blowup push. Their combined result is

$$(B-C)^2C\big[C(M-C)-L_4(M+C)+L_4(L_4+C)\big]. \tag{XIV.3.77}$$

The formula shows how higher powers of a normal class enter a quadratic flux calculation even when the mixed transversality period was zero. The projective-bundle integrals give $\langle V^2\rangle=-16$, $\langle Vc_2\rangle=16$ and $\langle c_2^2\rangle=2736$. The dot product of (XIV.3.37) with (XIV.3.41)'s vector is 512, so the flux square is $-512-64+32+684=140$. A cross-check uses the projected surface of §XIV.3.4:

$$V_\perp = V-(P^{-1}v)\cdot U, \tag{XIV.3.78}$$

$$\langle V_\perp^2\rangle = -16-v^tP^{-1}v=\frac{112}{5}, \tag{XIV.3.79}$$

$$\begin{aligned}\langle G_*V_\perp\rangle &= -2\langle V^2\rangle + x^tv-\tfrac12\langle Vc_2\rangle\\ &= -56.\end{aligned} \tag{XIV.3.80}$$

The equality of the direct square and $(25/4)\langle V_\perp^2\rangle$ is a numerical check in the computed pairings. It does not identify a full basis of H^4 or transport a class between phases. In the compact quadric the charge and formal remainder are

$$Q(G_*)=70, \qquad N_{\mathrm{D3}}^{\mathrm{form}}=\frac{6768}{24}-70=212. \tag{XIV.3.81}$$

Odd rescalings preserve the affine shift: for an integer k,

$$kG_*+c_2/2=k\alpha+\frac{1-k}{2}c_2. \tag{XIV.3.82}$$

At $k=3$ the witness is $3\alpha-c_2$. The Cartan and transversality periods are still zero, but the charge is multiplied by nine and the formal remainder is $282-630=-348$. Thus a rescaling can preserve every tested linear equation while failing the budget.

Now replace the quadric with a smooth degree-one gauge plane. Work with the same phase-I tower and smooth projective crepant premise for this different compact model. The first center has $d=1$, so the normal divisor dH and the Chern polynomial both change. The independent Euler polynomial gives $\chi(1)=13308$, and the quartic reduction yields $\langle c_2^2\rangle=4916$. This time c_2 cannot be twice an integral class on the free lattice. Indeed if $c_2=2z$, then $\lambda=-2z$ and the characteristic property for z forces $\langle z^2\rangle$ to be even. This would give $8\mid\langle c_2^2\rangle$, whereas $4916\equiv 4 \pmod 8$. In particular zero flux and even multiples of any shifted-integral candidate are excluded by the shift on this plane model.

The section block has not changed, but the Cartan block is now $-\mathcal{C}$. In the Cartan rows the new b is $(-3,1,24,5)^t$ and the new v is $(4,-4,4,-4)^t$. Applying the old coefficients to the new block gives the error

$$(-\mathcal{C})\begin{pmatrix}-12\\-18\\-30\\-14\end{pmatrix}-\begin{pmatrix}5\\-7\\32\\-3\end{pmatrix}=\begin{pmatrix}1\\1\\-4\\1\end{pmatrix}. \tag{XIV.3.83}$$

Both section-block equations still hold. The old compensator therefore fails a test that the two transverse moments cannot detect. To repair it, solve the new Cartan equations with right side $(5,-7,32,-3)^t$. Substitution of $t_2 = 2t_1 + 5$ from the first row gives $t_3 = 3t_1 + 3$ and $t_4 = 4t_1 + 33$, and the fourth row gives $5t_1 = -60$. The new coefficient vector is $(91, 24, -12, -19, -33, -15)^t$. With $x^t P x = 1126$, $\langle V^2 \rangle = -4$ and $\langle V c_2 \rangle = 4$, (XIV.3.73) gives

$$\langle G^2_{\text{plane}} \rangle = -1126 - 16 + 8 + 1229 = 95, \qquad N^{\text{form}}_{\text{D3}}(k) = \frac{1109 - 95k^2}{2}. \quad \text{(XIV.3.84)}$$

Both the half-integral charge and half-integral curvature term matter. The new unit flux leaves 507, and tripling leaves 127, unlike tripling in the quadric. At $k = 5$ the plane budget is also exceeded. Figure XIV.3.4 compares the two budgets only at odd multiples, where the shift is satisfied by (XIV.3.82). The change of topology modifies both the shift and the budget. Neither positive remainder is a certificate of supersymmetry.

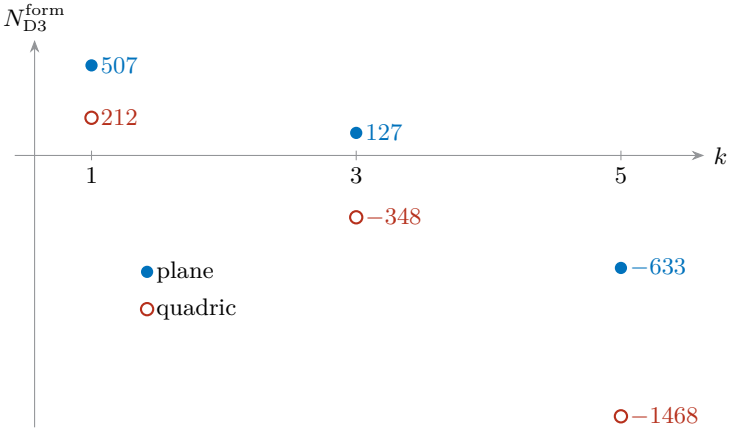


Figure XIV.3.4: Formal D3 remainder for odd rescalings of the separately solved quadric and plane candidates. The horizontal axis is the zero-budget line. The points at $k = 3$ fall on opposite sides; both models exceed the budget at $k = 5$.

For the K3 product, Euler characteristics multiply to $24 \cdot 24 = 576$ and the curvature charge is 24. At the product polarization of §XIV.3.5, the algebraic choices $(m, n) = (1, 0), (1, 1), (2, 0)$ in (XIV.3.55) give

$$(Q, N^{\text{form}}_{\text{D3}}) = (8, 16), \ (24, 0), \ (32, -8). \quad \text{(XIV.3.85)}$$

The third flux is still primitive at that polarization. The two Kummer tensors, by contrast, both give $(16, 8)$ even though only one is of type $(2, 2)$. When we pass to a local description the curvature term and the flux contribution no longer supply a compact charge budget by themselves.

XIV.3.7 Local flux and extension data

Can a traceless local spectral class specify the compact flux? To see which information it actually fixes, consider the local spectral description of a K_S-valued Higgs field on the quadric. Its spectral coordinate lives in K_S, not in the geometric normal bundle $N_{S/B}$ of the wrapped brane. Compactify the K_S fibers to projective lines with projection π_{loc} and zero section σ. The zero section has normal bundle K_S, so its self-intersection in the local projective bundle satisfies

$$\sigma^2 = -\sigma\pi_{\mathrm{loc}}^* c_1(S). \tag{XIV.3.86}$$

Assume a smooth finite cover $p : C \to S$ cut out by the local degree-five spectral equation. In the compactified bundle, its divisor class is $C = 5\sigma + \pi_{\mathrm{loc}}^*\eta$; the coefficient of σ measures the degree over a generic point of S. At the infinity section the cover equation reduces to the local coefficient $b_0|_S$. Its divisor class is η. In the Tate model $b_0 w^5$ has class $6c_1(B)$, so $[b_0] = 6c_1(B) - 5S$. Adjunction gives $c_1(B)|_S = c_1(S) + c_1(N_{S/B})$. Hence

$$\eta = (6c_1(B) - 5S)|_S = 6c_1(S) + c_1(N_{S/B}). \tag{XIV.3.87}$$

For the quadric $c_1(S) = 2u + 2v_S$ and $N_{S/B} = \mathcal{O}(2,2)$, so

$$\eta = 14(u + v_S), \qquad \delta = \eta - 5c_1(S) = 4(u + v_S). \tag{XIV.3.88}$$

The class δ records where the cover meets the zero section, as seen by multiplying C by σ and using (XIV.3.86).

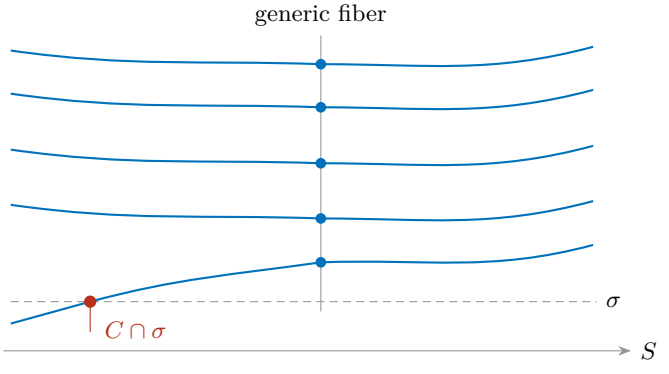


Figure XIV.3.5: The degree-five spectral projection, drawn over a small patch of S away from branch points. A generic projective-line fiber meets five sheets. The sheet meeting the zero section contributes to the intersection divisor of class δ. Pushing a pullback from the base counts all five sheets.

A spectral line bundle $\mathcal{L}$ on this smooth finite cover gives the local rank-five bundle $p_*\mathcal{L}$. The first Chern class must vanish for the local $SU(5)_\perp$ description. With r_{ram} the ramification class, Grothendieck–Riemann–Roch gives

$$c_1(p_*\mathcal{L}) = p_*\big(c_1(\mathcal{L}) - r_{\mathrm{ram}}/2\big) = 0, \tag{XIV.3.89}$$

This condition on $\gamma = c_1(\mathcal{L}) - r_{\rm ram}/2$ is separate from finding a line bundle with that Chern class. To construct a traceless γ, first use the intersection ring before pushing down:

$$\sigma C = 5\sigma^2 + \sigma\pi_{\rm loc}^*\eta = \sigma\pi_{\rm loc}^*\delta, \tag{XIV.3.90}$$

$$\sigma^2 C = -\sigma\pi_{\rm loc}^*(c_1(S)\delta). \tag{XIV.3.91}$$

A fiber meeting five cover sheets does not imply five copies of the zero-section intersection. The latter counts only the points of the cover with zero spectral coordinate. Since $\pi_{{\rm loc}*}\sigma = 1$, the zero-section intersection and a pulled-back divisor have respective traces

$$p_*(\sigma|_C) = \pi_{{\rm loc}*}(\sigma C) = \delta, \qquad p_*(p^*\delta) = 5\delta. \tag{XIV.3.92}$$

The second operation counts the generic degree, as in Figure XIV.3.5. Thus $\gamma_0 = 5\sigma|_C - p^*\delta$ is traceless. To see why the same factor of five matters in the square, expand into the zero-section square, the cross term and the pulled-back square. The first pairing uses (XIV.3.91); the other two use the projection formula:

$$\int_C (\sigma|_C)\, p^*\delta = \int_S \delta^2, \tag{XIV.3.93}$$

$$\int_C (p^*\delta)^2 = 5\int_S \delta^2. \tag{XIV.3.94}$$

There is one factor of the map degree in the last line. Each intersection on S is counted across the cover once, not independently for the two inserted divisors. With these pairings,

$$\begin{aligned}\int_C \gamma_0^2 &= \int_S \bigl(-25c_1(S)\delta - 10\delta^2 + 5\delta^2\bigr) \\ &= -5\int_S \eta\delta = -560.\end{aligned} \tag{XIV.3.95}$$

In the final step $(u + v_S)^2$ integrates to 2. If we add $p^*(u + v_S)$ to γ_0, the correction is seen on all five sheets:

$$p_*(\gamma_0 + p^*(u + v_S)) = 5(u + v_S). \tag{XIV.3.96}$$

Being pulled back from the base does not make the correction traceless. Conversely, the negative local self-intersection in (XIV.3.95) is not a negative compact D3 charge. It is a divisor intersection on the cover, whereas the charge uses the square of a degree-four class on Y. Comparing the two needs a map that carries the actual flux and controls its pairing.

The calculation of γ_0 gives a traceless class. Constructing a line bundle would also require the integrality of $r_{\rm ram}/2 + \gamma_0$; here the half shift involves ramification. These are conditions on local spectral data. Likewise $\iota_*(u - v_S) = 0$ in (XIV.3.46) concerns a different map, from the gauge surface into the base. It does not compute $p_*\gamma$ on the cover or extend a cover class to the fourfold.

A local patch can exchange charge through its boundary; the step of dropping the integral of a total derivative in (XIV.3.68) required compactness. To compare a local background with a compact one, one needs a restriction or gluing map and a background that obeys the global constraints with that restriction. Neither the local square in (XIV.3.95) nor the compact square in (XIV.3.73) supplies this matching. In particular the reference trivial bulk bundle of the previous chapter is not an assertion that $G = 0$ is allowed for a compact gauge model. To compute zero modes one must choose and verify a compatible bundle, sheaf or Higgs background, including the data seen by the matter curves. The class G_* in this chapter is not identified with such an object.

XIV.3.8 Exercises

1. In the smooth model use $G = 7H^2 + 2ZH$. Give the base/base and section/base moments in that order. Then give a nonzero change $(\Delta a, \Delta b)$ whose own base/base moment is zero but whose own section/base moment is nonzero, and report those two change moments.

2. In the phase-I calculation change the gauge divisor from the quadric to a plane. Keep the integral-witness coefficient of V equal to -2. Solve for the four Cartan coefficients, then compute the four residual Cartan moments obtained by using the old quadric coefficients on the plane instead. For $k = 7$ report the formal charge remainder. Would $k = 5$ also preserve shifted integrality?

3. Use $(m, n) = (1, -1)$ in the algebraic K3 product. Give the charge and the coefficient of $\xi \boxtimes [\mathrm{pt}]_2$ in JG first with $J_2 = h_1 + h_2 + h_3$, then with $J_2' = h_1 + 2h_2 + h_3$. State whether the change of polarization changes the Hodge type.

4. For the integral Kummer tensor $2p_1p_2 + q_1q_2$, calculate the integrated square, the period with Ω_4 and the formal remainder. Does the tensor have type $(2, 2)$?

5. For the quadric ruling class $u - 2v_S$, give its two ruling periods (first u, then v_S) and its ambient pushforward in units of H^2. Now project rationally to the inherited-trivial direction: subtract the component along $u + v_S$ so that the new coefficients sum to zero. Repeat the two period measurements and the pushforward. This subtraction is a specified rational operation, with no assertion of a canonical integral projection.

6. Explain why an integral witness, vanishing mixed moments, a finite Kähler obstruction and a formal compact remainder do not decide the F-theory limit or determine the data for a matter sheaf.

Use `benchmark/tasks.json` for the JSON fields and `benchmark/PROTOCOL.md` for submission. Written explanations, including Exercise 6, are assessed by a reader.

Take-home message of this chapter

A flux calculation has several independent steps. The integral witness tests the shifted lattice. Intersection periods test transversality and Cartan couplings. Hodge type and Kähler primitivity test the class at a particular geometry, and the square measures its charge in a compact budget. The quadric class constructed here passes the lattice and Cartan tests and has a nonnegative formal remainder. In the displayed divisor span, its finite resolved Kähler obstruction comes from one effective curve. The F-theory limit and the choice of a compatible local sheaf require further data.

Status and sources

§XIV.3.1. Background data. [**GEO-E**] The dimensionless curvature convention and distinction from refined background data use Weigand 2018, (9.1)–(9.5), (9.35)–(9.45). No flat or torsion classification is used.

§XIV.3.2. Shifted lattice. [**GEO-E**] The membrane sign uses Witten 1997, (1.2), (2.3)–(2.5), with $p_1/2 = -c_2$ on the Calabi–Yau. [**MATH**] Sextic adjunction, the indivisibility test and the witness are in (XIV.3.7)–(XIV.3.9).

§XIV.3.3. Transversality and resolution. [**GEO-E**] The ordinary sectioned M/F-theory conditions use Weigand 2018, (9.8) and Marsano and Schäfer-Nameki 2011, (4.3). [**MATH**] The smooth Weierstrass construction uses Sethi et al. 1996, §2.2. [**MATH**] The phase-I blowups and strict divisors use Hayashi et al. 2013, (3.1)–(3.10), Appendix A; Esole and Yau 2013, §§4–5 gives related small-resolution context. The pushforwards and Chern factors use Esole, Jefferson, et al. 2017, Theorem 3.3 and Lemma 3.4. Its Table 10, printed p. 29 (PDF p. 30), checks χ but not the phase-specific quartics.

§XIV.3.4. Cartan tests. [**GEO-E**] The inherited moments and stronger restriction use Weigand 2018, (9.13), (9.38)–(9.45). [**MATH**] Equations (XIV.3.37)–(XIV.3.46) give the witness, the rational-Chow symmetry argument and the independent local ruling calculation.

§XIV.3.5. Hodge and Kähler tests. [**GEO-E**] The leading supersymmetry conditions and the base-limit pairing use Gukov et al. 2000, §2 and Appendix I and Weigand 2018, (9.8)–(9.13). [**MATH**] The elliptic K3 uses Sen 1996, (2.9)–(2.13), the $(2, 2, 2)$ surface Dasgupta et al. 1999, §3.1, and the Kummer lattice relation Aspinwall and Kallosh 2005, (36). The affine-first effective row is the second row-component in the splitting of the second Cartan in Hayashi et al. 2013, (3.13), p. 16.

§XIV.3.6. Compact charge. [**GEO-E**] The charge equation and self-duality argument use Gukov et al. 2000, §2 and Appendix I. [**MATH**] The strict Calabi–Yau Todd identity is Marsano and Schäfer-Nameki 2011, (2.20), p. 14; the spin Wu congruence is Witten 1997, (3.5), p. 8. The remainder (XIV.3.72) follows by substituting the shifted class into the charge equation. The compact characteristic numbers and charge calculations are displayed above. The other resolved phase example in Marsano and Schäfer-Nameki 2011, (4.18) provides a normalization comparison, not a phase identification.

§XIV.3.7. Local data. [**MATH**] The Tate coefficient class uses Marsano and Schäfer-Nameki 2011, (2.25). The local cover ring and trace use Marsano and Schäfer-Nameki 2011, Appendix D, (D.1)–(D.11), (D.13)–(D.14), (D.18)–(D.25), (D.27)–(D.29), pp. 59–62 (PDF pp. 60–63). The value -560 is the worked quadric intersection in (XIV.3.95). [**GEO-E**] The role of boundary charge and missing global data uses Gukov et al. 2000, (2.16) and Weigand 2018, (9.35)–(9.45). No compact spectral correspondence is asserted.

References

Aspinwall, P. S. and R. Kallosh (2005). “Fixing all moduli for M-theory on K3 x K3”. In: *JHEP* 10, p. 001. DOI: 10.1088/1126-6708/2005/10/001. arXiv: hep-th/0506014.

Dasgupta, K., G. Rajesh, and S. Sethi (1999). “M theory, orientifolds and G-flux”. In: *JHEP* 08, p. 023. DOI: 10.1088/1126-6708/1999/08/023. arXiv: hep-th/9908088.

Esole, M., P. Jefferson, and M. J. Kang (2017). “Euler characteristics of crepant resolutions of Weierstrass models”. In: arXiv: 1703.00905.

Esole, M. and S.-T. Yau (2013). “Small resolutions of SU(5)-models in F-theory”. In: *Adv. Theor. Math. Phys.* 17, pp. 1195–1253. arXiv: 1107.0733.

Gukov, S., C. Vafa, and E. Witten (2000). “CFT’s from Calabi–Yau four-folds”. In: *Nucl. Phys. B* 584, pp. 69–108. arXiv: hep-th/9906070.

Hayashi, H., C. Lawrie, and S. Schäfer-Nameki (2013). “Phases, Flops and F-theory: SU(5) Gauge Theories”. In: *JHEP* 10, p. 046. DOI: 10.1007/JHEP10(2013)046. arXiv: 1304.1678 [hep-th].

Marsano, J. and S. Schäfer-Nameki (2011). “Yukawas, G-flux, and spectral covers from resolved Calabi–Yau’s”. In: *JHEP* 11, p. 098. arXiv: 1108.1794.

Sen, A. (1996). “F-theory and orientifolds”. In: *Nucl. Phys. B* 475, pp. 562–578. arXiv: hep-th/9605150.

Sethi, S., C. Vafa, and E. Witten (1996). “Constraints on low-dimensional string compactifications”. In: *Nucl. Phys. B* 480, pp. 213–224. arXiv: hep-th/9606122.

Weigand, T. (2018). “TASI Lectures on F-theory”. In: *PoS* TASI2017, p. 016. arXiv: 1806.01854.

Witten, E. (1997). “On flux quantization in M-theory and the effective action”. In: *J. Geom. Phys.* 22, pp. 1–13. arXiv: hep-th/9609122.

Chapter XIV.4

Chiral spectra, zero modes and matter multiplicities

XIV.4.1 From a matter surface to a chiral index

What does a four-form period tell us about the particles on a seven-brane? In Chapter 2 we found the curves that carry electric weights, and in Chapter 3 we constructed a shifted class and tested its Cartan periods. We will now select one matter surface, integrate the class on it, and compare this operation with the one that counts zero modes. The comparison requires two kinds of geometry. A wrapped membrane sees a curve in an elliptic fiber. A four-dimensional charged wavefunction may vary along an entire matter curve in the base. The surface swept out by the first curve over the second gives an index, while the wavefunctions are counted by cohomology.

Write $\pi : Y \to B_3$ for the resolved fibration and $C_R \subset S$ for a matter curve on the gauge divisor. Over a generic point $p \in C_R$, a fibral component $\gamma_w(p)$ carries a weight w. Its closure over C_R is a matter surface T_w. Both C_R and $\gamma_w(p)$ have complex dimension one, but they lie in different spaces. The complex dimension of T_w is two. The left panel of Figure XIV.4.1 shows which of these objects can be paired with a four-form. In the ordinary matter-surface dictionary, for an admissible background preserving the gauge algebra, one uses

$$\chi_R = n_R - n_{\overline{R}} = \int_{T_w} G. \tag{XIV.4.1}$$

Here w is one weight of the complex representation R, and its orientation is fixed in the common charge convention used to define χ_R. The algebra acts on the components of a multiplet, so each weight in one copy of R has the same multiplicity. Summing the periods of ten weights of a ten, for example, counts weight components with sign. It does not count ten independent generations.

There is a useful intersection check of this statement when a difference of two candidate surfaces is known. Let $j_i : D_i \hookrightarrow Y$ and $p_i : D_i \to S$ denote a Cartan inclusion and projection. If the difference is $\sum_i m_i (j_i)_* p_i^* [C_R]$, then the projection

formula gives

$$\int_{T_w - T_{w'}} G = \sum_i m_i \int_S (p_i)_* (j_i^* G)\, [C_R]. \tag{XIV.4.2}$$

The right hand side vanishes when the indicated Cartan pushforwards vanish. This is an implication for a specified difference of cycles. It does not establish that all pairs of weight lifts differ in this way; the physical weight independence in (XIV.4.1) uses the unbroken algebra.

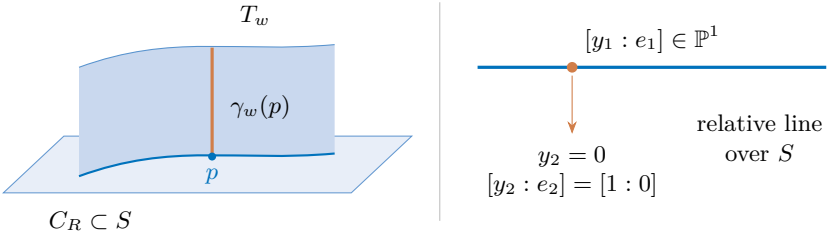


Figure XIV.4.1: Left: $\gamma_w(p)$ is vertical over a point, while C_R lies in the base. Their relative family closes to T_w, on which the period is taken. Right: over each point of S the third center retains the second exceptional direction $[y_1 : e_1]$. The fourth blowup replaces the point $y_2 = 0$ in this line by the indicated direction on its strict transform. Imposing $b_5 = 0$ then restricts the base from S to C_{10}.

For the calculation, assume the smooth projective crepant member of the phase-I Tate model over $B_3 = \mathbb{P}^3$, with the quadric $S = (w = 0)$ and the Cartan labels of Chapter 2. We will use the smooth curve $C_{10} = (w = b_5 = 0)$ described in the next section. Let A, B, C, D denote the total exceptional classes, in order. The strict Cartans are

$$(D_1, D_2, D_3, D_4) = (A - B, C - D, D, B - C). \tag{XIV.4.3}$$

In the affine fiber chart $W \neq 0$ the centers are successively (x, y, w), (y_1, e_1), (x_1, e_4), and (y_2, e_2), using the current strict coordinates at each stage. To determine what the intersection $D_2 D_4$ means on Y, we must first follow the corresponding intersection in the ambient space. Reading the fiber at a single generic point would leave open whether the same stratum contains an extra component over a special point of C_{10}.

Over a trivializing patch of S, the first exceptional plane has coordinates $[x_1 : y_1 : w_1]$. The second center inside it is the line $y_1 = 0$. Its exceptional divisor adds the normal direction $[y_1 : e_1]$ over each point of that line. The third center is cut out on this second exceptional divisor by $x_1 = 0$. This singles out the point $[0 : 0 : 1]$ on the first line and imposes no equation on $[y_1 : e_1]$. In the third blowup, the third exceptional divisor meets the strict second exceptional divisor at direction $[x_1 : e_4] = [1 : 0]$. The intersection is thus the full projective line of second exceptional directions over each point of S.

The fourth center meets that line at the section where $y_2 = 0$. On the strict transform of the line over this section, the relevant fourth blowup chart has direction $[y_2 : e_2] = [1 : 0]$. There $e_{2,\text{old}} = y_{2,\text{old}} e_2$, and the strict e_4 is unchanged. Thus the

common locus of the two strict divisors still maps isomorphically to the old line; away from the center the map is already an isomorphism. The first center does not meet $W = 0$, so there is no additional piece of the common locus there. This explains the relative line in Figure XIV.4.1 and also why its intersection with Y should be computed by restricting the defining equation.

In the final strict coordinates the composite substitution has the form

$$(x_{\text{old}}, y_{\text{old}}, w_{\text{old}}) = (xe_1e_4e_2^2e_3^2,\ ye_1e_4^2e_2^2e_3^3,\ e_0e_1e_2e_3e_4). \tag{XIV.4.4}$$

On substitution into the affine Tate equation, the common factor is $e_1^2e_4^3e_2^4e_3^5$. After division, the $b_5x_{\text{old}}y_{\text{old}}$ term becomes b_5xy. The y_{old}^2 term has a remaining factor e_4; the x_{old}^3 and $b_4w_{\text{old}}x_{\text{old}}^2$ terms have a remaining factor e_2. The terms with b_3, b_2, b_0 retain factors of e_4 or e_2 as well. Consequently

$$F_{\text{proper}}\big|_{e_2=e_4=0} = b_5xy. \tag{XIV.4.5}$$

The two blowup directions just described force the final x, y to be units along this stratum. Hence the cut by the hypersurface is the pullback of $b_5 = 0$. At the smooth C_{10}, b_5 is a parameter transverse to the curve in S and vanishes to order one. We obtain the complex-oriented class $V = [T_{\text{sh}}] = D_2D_4$ with multiplicity one. The argument concerns this common stratum and gives no flatness assertion about the other fibers of Y.

To identify the weight, let H be the pullback of a base hyperplane. For the four Cartans, $\int_Y VHD_i$ integrates their fiber degrees over the H-section of C_{10}. The Segre quadric has $H|_S = (1, 1)$ and C_{10} has bidegree $(4, 4)$, so this section has degree eight. Here is the intersection computation in the same ambient presentation as Chapter 3. Set $X = r + 8H$ and $Y_0 = r + 12H$, where r is the ambient class of $W = 0$. Use

$$K = 3r + 24H - 2A - B - C - D \tag{XIV.4.6}$$

for the proper hypersurface class. To integrate any quartic on Y, first multiply by K, then push down the four exceptional classes in reverse order. For a center of codimension k cut by normal divisors $z_1, \dots, z_k$, the term E^n with $n > 0$ is replaced by $(-1)^{k-1}(\prod z_i)h_{n-k}(z_1, \dots, z_k)$, where h_m is the complete homogeneous polynomial of degree m and $h_m = 0$ for $m < 0$. Constant terms survive. The ordered lists of normal divisors here are

$$(X, Y_0, 2H), \quad (Y_0 - A, A), \quad (X - A, B), \quad (Y_0 - A - B, C). \tag{XIV.4.7}$$

These are lists in the successive spaces. Using a later strict transform in an earlier list changes the normal bundle.

For example, put $L = Y_0 - A - B$, $T = X - A$, and $M = 3r + 24H - 2A - B$. In $KV = (B - C)(C - D)(M - C - D)$ the linear power of D drops out, while D^2 pushes to $-LC$. Pushing next in C leaves

$$KV \longmapsto (B - C)C(M - C - L) \tag{XIV.4.8}$$

$$\longmapsto TB(M - L - T) = TB(r + 4H). \tag{XIV.4.9}$$

The HD_1 insertion does not contain C or D and so multiplies this last expression by $H(A-B)$. Only the $-B^2$ term contributes in the B push, giving $HT(Y_0-A)A(r+4H)$. The A^3 coefficient then gives $2H^2XY_0(r+4H)$. On the original projective bundle the powers satisfy $\pi_* r^2 = 1$, $\pi_* r^3 = -20H$. Thus the last expression integrates to $2(24-20) = 8$.

For the remaining three insertions, one can keep C and D in the product until their own pushes. The intermediate polynomials after both pushes are displayed here with the common factor H removed:

D_i	push of KVD_i through D, C
D_1	$(A-B)TB(r+4H)$
D_2	$TB(T-L)(M-L-T)$
D_3	$LTB(M-L-T)$
D_4	$TB(B-T)(M-L-T)$

(XIV.4.10)

Only the coefficients of B in the factors multiplying $TB(M-L-T)$ survive after the B push, since $M-L-T = r+4H$. Their signs are $(-1,+1,-1,+1)$; relative to the D_1 computation the integrated moments are therefore $(8,-8,8,-8)$. With $D_0 = (e_0 = 0)$, the five strict divisors sum to $\pi^* S$, by the product for w_{old} in (XIV.4.4). A pullback from S has degree zero on a fiber. The four degrees sum to zero, so the affine degree is zero as well:

$$(D_0, D_1, D_2, D_3, D_4) \cdot \gamma_{\text{sh}} = (0, 1, -1, 1, -1). \tag{XIV.4.11}$$

This is the shared row in the phase-I splitting. The second split component of the second Cartan has row $(0,0,-1,0,1)$; it is a different fibral curve.

Our named electric charge reverses the four geometric signs. To identify it, use the standard basis $\mathbf{e}_i$ of $\mathbb{R}^5$ and write $\lambda_i = \mathbf{e}_i - \frac{1}{5}\sum_j \mathbf{e}_j$ for the five weights of the defining representation. They are not the four fundamental highest weights $\omega_k = \sum_{i=1}^{k} \lambda_i$. Pairing a weight with the four simple coroots takes consecutive differences of its five coordinates. For $\lambda_2 + \lambda_4$ this takes differences of $(0,1,0,1,0)$, giving

$$q_{\text{el}} = (-1,1,-1,1) = \text{Dynkin tuple of } \lambda_2 + \lambda_4 \in \wedge^2 \mathbf{5}. \tag{XIV.4.12}$$

The ten also contains $\lambda_1 + \lambda_2$, with electric row $(0,1,0,0)$, but reversing its signs fails the actual Cartan-moment test for V. Changing the charge convention does not change the integral on the complex-oriented V. Replacing V by $-V$ does change it; $-V$ denotes an orientation reversal rather than another effective component.

Now pair the class constructed in Chapter 3 with V. Let Z denote the genuine section, represented rationally by $r/3$ for the ambient integration, and write

$$U = (H^2, ZH, HD_1, HD_2, HD_3, HD_4), \tag{XIV.4.13}$$

$$G_* = (91, 24, -12, -18, -30, -14) \cdot U - 2V - \tfrac{1}{2} c_2(Y). \tag{XIV.4.14}$$

For the Chern term, the initial ambient Chern factors have roots H four times, r, X, Y_0. At a blowup with center divisors z_j the factor is $(1+E)\prod_j (1+z_j-E)/(1+z_j)$. Append $1/(1+K)$ for the hypersurface. If p_l is the sum of the l-th powers in the numerator minus that in the denominator, the degree-two Newton identity gives

$$c_2(Y) = \tfrac{1}{2}(p_1^2 - p_2) = -\tfrac{1}{2} p_2. \tag{XIV.4.15}$$

The equality uses $p_1 = 0$, since K is the final ambient anticanonical class. The degree-two coefficients and the square term are sensitive to different powers of the last exceptional divisor. For example, in KV^2, the D^0, D^2, D^3 terms give

$$(B-C)^2C\big[C(M-C) - L(M+C) + L(L+C)\big] \tag{XIV.4.16}$$

after the first push. The other pushes, discarding H^4 and higher powers, reduce the two products as follows:

$$KV^2 \longmapsto -96H^3r^2 - 4H^2r^3, \tag{XIV.4.17}$$

$$KVc_2(Y) \longmapsto 96H^3r^2 + 4H^2r^3. \tag{XIV.4.18}$$

The bundle push then gives $\int_Y V^2 = -16$ and $\int_Y Vc_2/2 = 8$. The first two entries of $\int_Y VU$ are zero: two generic hyperplanes miss the base curve and the section is disjoint from the exceptional locus. The other four entries are exactly those used in (XIV.4.11). It follows that

$$\int_V G_* = 8(-12+18-30+14) - 2(-16) - 8 = -56, \tag{XIV.4.19}$$

$$\int_{-V} G_* = +56, \tag{XIV.4.20}$$

$$\int_Y G_*\, D_2(4H) = 0. \tag{XIV.4.21}$$

For the last line, $D_2(4H) = 4U_4$ is the full second Cartan over the base curve, and the six U periods vanish. Replacing V by that whole Cartan loses the period. Inserting an additional H into G_*V is also invalid: this integrand is already of top degree.

What is missing if we want to interpret -56 as a particle count? First, (XIV.4.19) concerns a formal shifted class, without a compatible supersymmetric F-theory limit or an induced defect sheaf. Second, even in a background for which (XIV.4.1) applies, it is a signed difference. If $[R]$ denotes the character of R, the contribution of a conjugate pair is

$$\mathcal{X} = n_R[R] + n_{\overline{R}}[\overline{R}], \tag{XIV.4.22}$$

$$\mathcal{X} - \overline{\mathcal{X}} = \chi_R\big([R] - [\overline{R}]\big). \tag{XIV.4.23}$$

The identity trace of $\mathcal{X}$ is $(n_R + n_{\overline{R}})\dim R$; that of the difference is zero. The pairs $(6,2)$ and $(4,0)$ both give index four for the ten, but the former describes eighty weight components and the latter forty. We will obtain these two pairs from actual curve bundles. They will illustrate the distinction without assigning either pair to G_*.

XIV.4.2 The bundle seen by a matter curve

Which curve and which line bundle would a defect wavefunction see? The Tate model locates the ten-matter support at $b_5 = 0$ on S. In the quadric model let

$$S = \mathbb{P}^1_u \times \mathbb{P}^1_v, \qquad X_{ij} = u_i v_j, \qquad w = X_{00}X_{11} - X_{01}X_{10}. \tag{XIV.4.24}$$

The hyperplane pulls back to $\mathcal{O}_S(1,1)$. Thus a quartic b_5 on $\mathbb{P}^3$ has bidegree $(4,4)$ on S. We choose the actual homogeneous quartic

$$b_5 = X_{00}^4 + X_{10}^4 + X_{01}^4 + tX_{11}^4 + \epsilon X_{00}^2 X_{11}^2. \tag{XIV.4.25}$$

Here t, ϵ are complex parameters of the equation, unrelated to a fiber area or a three-form potential. The finite chart with $x = u_1/u_0$, $y = v_1/v_0$ has polynomial $1 + x^4 + y^4 + tx^4y^4 + \epsilon x^2y^2$. In this section x, y are base coordinates, rather than the fiber coordinates used in (XIV.4.4).

We need a smooth curve to use the ordinary smooth defect dictionary. Multiplying by the correct fourth powers on passing to inverse coordinates gives the four chart polynomials:

$$\begin{array}{c|l} (x,y) & 1 + x^4 + y^4 + tx^4y^4 + \epsilon x^2y^2 \\ (s,y),\ s = x^{-1} & 1 + s^4 + ty^4 + s^4y^4 + \epsilon s^2y^2 \\ (x,q),\ q = y^{-1} & 1 + q^4 + tx^4 + x^4q^4 + \epsilon x^2q^2 \\ (s,q) & t + s^4 + q^4 + s^4q^4 + \epsilon s^2q^2 \end{array} \tag{XIV.4.26}$$

In each chart singular points are the zeros of the polynomial and its two derivatives. On the boundary of the dense torus, the finite-chart edges give $1 + x^4$ or $1 + y^4$; at infinity the restrictions give $1 + tx^4$ or $1 + ty^4$ on the adjoining edge charts. For $t \neq 0$, all these edge roots are simple and none of the four corners lies on the curve. This accounts for every point in (XIV.4.26) outside the torus.

On the torus set $a = x^2$, $b = y^2$. This coordinate change is étale there. If the two derivatives of $1 + a^2 + b^2 + ta^2b^2 + \epsilon ab$ vanish, subtract $b\partial_b$ from $a\partial_a$. The result is $2(a^2 - b^2) = 0$, so $a = \sigma b$ with $\sigma = \pm 1$. In this sector the equation and remaining derivative condition become

$$1 + (2 + \sigma\epsilon)b^2 + tb^4 = 0, \qquad 2 + \sigma\epsilon + 2tb^2 = 0. \tag{XIV.4.27}$$

They require $(2 + \sigma\epsilon)^2 = 4t$. At $(2,0)$ the squares are $(4,4)$ rather than $(8,8)$; at $(2,1)$ and $(3,1)$ they are $(9,1)$, with $4t = 8$ and 12, respectively. Therefore the Jacobian ideals in all four charts are unit for these three fixtures. This exact test also locates the failure at $(1,0)$, when the finite polynomial is $(1 + x^4)(1 + y^4)$. At $(0,0)$ the finite polynomial has no singular point, but the (s,q) chart has a singular point at $(0,0)$. Checking one affine equation would give the wrong answer there.

Let H_1, H_2 be the two ruling classes, so $H_1^2 = H_2^2 = 0$ and $\int_S H_1H_2 = 1$. The normal bundle of a smooth Cartier curve of bidegree $(4,4)$ is $\mathcal{O}_C(4,4)$. Adjunction and the ruling intersections give

$$K_S = \mathcal{O}_S(-2,-2), \qquad K_C = \mathcal{O}_C(2,2), \tag{XIV.4.28}$$

$$\deg \mathcal{O}_C(a,b) = 4(a+b), \qquad \deg K_C = 16. \tag{XIV.4.29}$$

The smooth curve is connected: the Cartier sequence for $\mathcal{O}_C$ has left term $\mathcal{O}_S(-4,-4)$ with $H^0 = H^1 = 0$ by Künneth. Thus $H^0(\mathcal{O}_C) = \mathbb{C}$. A smooth connected curve is integral, and $2g - 2 = 16$ gives $g = 9$.

The choice of theta characteristic, a square root of K_C, is part of the twist. Here we declare

$$\Theta_C = \mathcal{O}_C(1,1) = \mathcal{O}_{\mathbb{P}^3}(1)|_C, \qquad \Theta_C^2 = K_C. \tag{XIV.4.30}$$

It also has an embedded description. The two divisors meeting in C are the smooth quadric and the quartic of (XIV.4.25). For the selected parameters, a singular point on the quartic would require $X_{10} = X_{01} = 0$. When $t \neq 0$, neither X_{00} nor X_{11} can then be zero, and the two remaining derivatives require $\epsilon^2 = 4t$, which fails. The two divisors are spin: their canonical bundles have degrees -2 and 0 in hyperplane units. The complete-intersection adjunction in $\mathbb{P}^3$ gives $K_C = \mathcal{O}_C(-4+2+4)$. Taking the reference roots in this prescription gives (XIV.4.30); the geometry does not imply uniqueness among all square roots.

In the linearized ordinary smooth defect problem, let L_R be the coefficient line bundle before the twist and put $M_R = \Theta_C \otimes L_R$. The Dolbeault operator $\bar\partial_{M_R}$ maps sections to $(0,1)$-forms. The Laplacian built from this operator and its adjoint gives harmonic representatives: sections obey $\bar\partial_{M_R} s = 0$ and $(0,1)$-forms obey $\bar\partial^\dagger_{M_R} a = 0$. With the same orientation as in (XIV.4.1), the two chiral sectors of charges R and $\overline{R}$ have spaces

$$H^0(C, M_R), \qquad H^0(C, K_C \otimes M_R^{-1}) \simeq H^1(C, M_R)^\vee. \tag{XIV.4.31}$$

The second group is written as the dual of H^1, rather than identifying opposite-charge modes with the same charged wavefunction. Riemann–Roch uses $\deg \Theta_C = g - 1$, so

$$\chi(C, M_R) = \deg M_R + 1 - g = \deg L_R. \tag{XIV.4.32}$$

For a coefficient vector bundle E_R of rank r_E, the spin degree is $r_E(g-1)$ and the Euler term is $r_E(1-g)$; the result is $\deg(\det E_R)$. Equation (XIV.4.32) assumes that the bundle placed in the cohomology is already twisted. Applying the root again would shift the predicted index by eight in our rank-one example.

For comparison, an honest genus-nine line bundle with $\chi = -56$ would have degree -48. A nonzero section would define an effective divisor of negative degree, which is impossible on this smooth integral curve. Hence such a line bundle has $(h^0, h^1) = (0, 56)$. This is a consequence of the degree assumption, not a determination of the matter bundle induced by G_*. We now check why even the type of curve on which to formulate that question can vary between sectors of a single Tate model.

The fundamental matter locus C_5 in S is cut by

$$P = b_4 b_3^2 - b_2 b_3 b_5 + b_0 b_5^2. \tag{XIV.4.33}$$

The five Tate coefficients have ambient degrees $4, 6, 8, 10, 14$ for b_5, b_4, b_3, b_2, b_0, respectively. Thus every term of P has bidegree $(22, 22)$. The shape of (XIV.4.33), not merely that divisor class, determines its singular points. We will hold b_5 at $(2, 0)$ and take the degree-eight ambient polynomial

$$b_3 = \prod_{j=2}^{9} \big(X_{11} - jX_{01} - (j+8)X_{10} + j(j+8)X_{00}\big). \tag{XIV.4.34}$$

On the finite chart a factor is $(x - j)(y - j - 8)$. On the whole quadric its two factors are the homogeneous linear ruling equations in the two projective coordinates. At $x = j$, the C_{10} equation is $(1 + j^4) + (1 + 2j^4)y^4 = 0$. The two coefficients are nonzero and

the four solutions are finite, nonzero and simple. At $y = j + 8$ the same reasoning applies with the variables exchanged. Every grid crossing of the rulings has positive real x, y, hence the curve polynomial is positive there. These facts give $8 \cdot 4 + 8 \cdot 4 = 64$ distinct transverse points of $C_{10} \cap (b_3 = 0)$, all lying on exactly one ruling of $b_3 = 0$. In particular b_5, b_3 are independent local parameters after a choice of local frames.

For the rest of the coefficients we vary the full spaces of homogeneous polynomials on $\mathbb{P}^3$. Their restrictions to S fill the respective spaces of bidegree $(6,6), (10,10), (14,14)$. To see this, take a monomial $u_0^{n-i} u_1^i v_0^{n-j} v_1^j$. Match its n factors in u with its n factors in v and multiply the corresponding X_{ab}; the resulting homogeneous monomial restricts to the desired section. The resulting linear system in $H^0(S, \mathcal{O}(22,22))$ is

$$\mathcal{V} = b_3^2 H^0(\mathcal{O}_S(6,6)) + b_3 b_5 H^0(\mathcal{O}_S(10,10)) + b_5^2 H^0(\mathcal{O}_S(14,14)). \tag{XIV.4.35}$$

The middle sign in (XIV.4.33) does not restrict the image. At any point with $b_5 \neq 0$, a b_0-only section can be chosen nonzero; at any point with $b_3 \neq 0$, a b_4-only section can be chosen nonzero. The base support consists of exactly the 64 intersections just found. At one of them, in coordinates $U = b_5$, $V' = b_3$ (using local trivializations), each coefficient system supplies a section that is a unit. The base ideal is therefore $(U^2, UV', (V')^2)$.

For irreducibility we use the Bertini criterion for a linear system with base support of codimension at least two on a geometrically integral variety. In the form needed here, two sections must have a common codimension-two component outside the zero set of a third section. This hypothesis matters: the dimension of the base locus alone does not exclude a system composed with a pencil. Here the variety is the smooth integral product S over $\mathbb{C}$. Choose three b_0-only sections with local representatives $1, x, y$ in the finite chart, homogenized in bidegree $(14,14)$. At the origin $b_5 = 1$. The two sections $b_5^2 x, b_5^2 y$ have an isolated common zero there, and b_5^2 does not vanish there. This supplies the codimension-two witness and gives a geometrically irreducible general member of (XIV.4.35).

To apply the smoothness criterion, separate the two opens in the base complement. On $b_5 \neq 0$ the b_0 subsystem generates the required line bundle, and cancelling its common unit b_5^2 identifies its map with the restriction of the very ample $(14,14)$ embedding. On $b_3 \neq 0$ the b_4 subsystem does the same with the very ample $(6,6)$ embedding. In either open the full map is an immersion: in a projective chart with a nonzero subsystem coordinate, its subsystem ratios give the immersion and the extra ratios give its graph. In terms of jets, at a point the values and two tangent derivatives of sections are then independent linear tests. The incidence of sections singular at a point has three conditions, while the point moves in dimension two. The Bertini smoothness lemma applies on both opens and gives smoothness off the base points for a general member. As a Cartier divisor on a smooth surface it has no embedded points. Smoothness away from a finite set gives generic reducedness, so together with irreducibility the curve is integral on a nonempty open.

At a base point p, write $A_p = b_4(p)$, $B_p = b_2(p)$, $C_p = b_0(p)$ in compatible frames. The tangent cone and its discriminant are

$$A_p (V')^2 - B_p U V' + C_p U^2, \qquad \Delta_p = B_p^2 - 4 A_p C_p. \tag{XIV.4.36}$$

The evaluation of each independent coefficient space at p is surjective. Thus $A_p \neq 0$ and $\Delta_p \neq 0$ can be required on a nonempty open for each p. Intersecting the finitely many such opens with the preceding opens still gives a nonempty open in the irreducible parameter space. Nonzero discriminant over $\mathbb{C}$ gives two distinct tangent lines and therefore an ordinary node. A repeated tangent does not determine the analytic singularity; higher terms are then needed. Figure XIV.4.2 shows the generic local picture with neither node tangent equal to the line $U = 0$.

In a neighborhood with $A_p \neq 0$ we can see the two branches directly. Set $V' = U\xi$ in the chart of the blowup of the base point that records slopes relative to U. After division by U^2 the strict transform has equation

$$A_p\xi^2 - B_p\xi + C_p + UR(U, \xi) = 0 \tag{XIV.4.37}$$

for a holomorphic R. The two roots at $U = 0$ are simple if $\Delta_p \neq 0$. The implicit function theorem gives two graphs $\xi = \xi_\pm(U)$, hence $V' = U\xi_\pm(U)$ downstairs. Their different first derivatives give a transverse crossing. No tangent is omitted from this chart because the quadratic coefficient of $(V')^2$ is nonzero. For example, $(A_p, B_p, C_p) = (1, 1, 1)$ gives $\xi_\pm = (1 \pm \mathrm{i}\sqrt{3})/2$. With $(1, 2, 1)$ the two roots coincide at $\xi = 1$ and the derivative needed for the graph argument vanishes. The intersection with $U = 0$ still has length two in both cases: the order of the restricted equation does not decide whether the branches of C_5 are distinct.

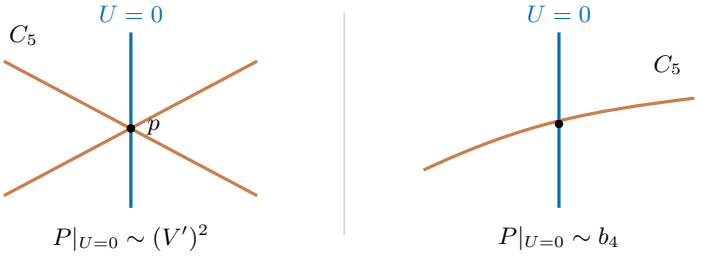


Figure XIV.4.2: Two kinds of intersection with C_{10}, which is $U = 0$ in both panels. At a base point p, $V' = b_3$ vanishes and the two branches of C_5 give order two in the restriction to C_{10}. At a simple zero of b_4 away from $b_3 = 0$, the restriction has order one. The drawings indicate tangent directions in local complex coordinates.

To count the other intersections with C_{10}, the restriction $P|_{C_{10}} = b_4 b_3^2$ is decisive. The restriction of the very ample $(6, 6)$ system to the smooth curve has general simple zeros and can avoid the 64 fixed points. More explicitly, a double zero at a specified point imposes two independent conditions, whereas the point moves in dimension one; avoiding each of the fixed points is one open condition. The degree of $b_4|_{C_{10}}$ is $4 \cdot 6 + 4 \cdot 6 = 48$. Thus the length of the intersection on the original curves is

$$(4, 4) \cdot (22, 22) = 176 = 48 + 2 \cdot 64. \tag{XIV.4.38}$$

At a node, restricting to $U = 0$ leaves $(V')^2$ times a unit. This explains why the length is two although the point belongs to the list of 64 only once.

For the Cartier curve C_5, adjunction gives $\omega_{C_5} = \mathcal{O}_{C_5}(20, 20)$. The dualizing bundle exists even though the tangent space has larger dimension at a node. Its degree is $22(20 + 20) = 880$, giving arithmetic genus 441. To see what changes on normalization, let $\nu : \widetilde{C}_5 \to C_5$ be the normalization. At a node functions on the two branches descend if and only if their values at the node agree. The normalization exact sequence therefore reads

$$0 \longrightarrow \mathcal{O}_{C_5} \longrightarrow \nu_*\mathcal{O}_{\widetilde{C}_5} \longrightarrow \bigoplus_{p\,\text{node}} \mathbb{C}_p \longrightarrow 0. \tag{XIV.4.39}$$

The quotient has length one at each node. Since the normalized curve is connected, its genus is $441 - 64 = 377$. A line bundle on the original curve has Euler characteristic $\deg +1 - 441$; using 377 would erase the matching constraints in (XIV.4.39). In the next section we compute two cohomology pairs directly on the original curve. They do not assign a physical five-matter sheaf or its ramification data.

XIV.4.3 Counting actual cohomology groups

How can we recover both multiplicities from the equation of an embedded curve? On the surface S, consider a nonzero bihomogeneous equation F of degree (d, e) and its Cartier divisor C. The ideal sheaf is generated locally by F. Twisting the corresponding exact sequence by $\mathcal{O}_S(a, b)$ gives

$$0 \longrightarrow \mathcal{O}_S(a - d, b - e) \xrightarrow{\cdot F} \mathcal{O}_S(a, b) \longrightarrow \mathcal{O}_C(a, b) \longrightarrow 0. \tag{XIV.4.40}$$

This is a resolution on the surface, so the method applies to the singular C_5 as well as to smooth C_{10}. It computes the cohomology of the stated restriction sheaf. Changing to a sheaf on the normalization would change the question.

First compute the ambient groups on one projective line. On its two standard affine charts a section of $\mathcal{O}(k)$ is represented in the finite frame by a polynomial in x on the first chart and by x^k times a polynomial in x^{-1} on the other. On the overlap the common representatives and the unremoved Laurent classes are, respectively,

$$H^0(\mathcal{O}(k)) = \mathbb{C}[x] \cap x^k\mathbb{C}[x^{-1}], \tag{XIV.4.41}$$

$$H^1(\mathcal{O}(k)) = \mathbb{C}[x, x^{-1}]/\big(\mathbb{C}[x] + x^k\mathbb{C}[x^{-1}]\big). \tag{XIV.4.42}$$

Thus in degree zero the exponents are $0, \dots, k$ when $k \geq 0$, and in degree one they are $k + 1, \dots, -1$ when $k \leq -2$. At $k = -1$ both groups vanish. For example on $\mathcal{O}(-4)$ the three classes have exponents $-3, -2, -1$. The negative signs on the exponents are important: multiplication can move a representative out of the surviving window without making the Laurent polynomial identically zero.

On S, the product cover gives tensor products of these bases. In total degree i, use $x^p y^q$ with exponents in the windows for degrees i_x, i_y such that $i_x + i_y = i$. For $F(x, y) = \sum f_{jk} x^j y^k$, the matrix entry of $m_i = H^i(\cdot F)$ from (p, q, i_x, i_y) to (p', q', i'_x, i'_y) is

$$(m_i)_{(p',q',i'_x,i'_y),(p,q,i_x,i_y)} = \delta_{i'_x i_x}\delta_{i'_y i_y} f_{p'-p,q'-q}. \tag{XIV.4.43}$$

Only exponents in the target window are listed as rows; terms outside it in a degree-one factor are coboundaries. This is the actual induced map on cohomology, rather than a multiplication on unrestricted Laurent polynomials. The long exact sequence from (XIV.4.40) places each $H^i(C, \mathcal{O}_C(a,b))$ between $\operatorname{coker} m_i$ and $\ker m_{i+1}$. In dimensions,

$$h^i_C = h^i_{mtarget} - \operatorname{rk} m_i + h^{i+1}_{msource} - \operatorname{rk} m_{i+1}. \tag{XIV.4.44}$$

The source here means the leftmost ambient line bundle in (XIV.4.40) and the target means the middle one.

Work first on $C = C_{2,0}$. For $\Theta_C = \mathcal{O}_C(1,1)$ the only source group is $H^2(\mathcal{O}_S(-3,-3))$ of dimension $2 \cdot 2 = 4$, and the only target group is $H^0(\mathcal{O}_S(1,1))$ of dimension $2 \cdot 2 = 4$. The two survive in different degrees on the curve, giving $(4,4)$. For $\mathcal{O}_C(2,0)$ the source $\mathcal{O}_S(-2,-4)$ instead has a $1 \cdot 3$ dimensional H^2, while the target $\mathcal{O}_S(2,0)$ has three polynomials. Thus

$$\mathcal{O}_C(1,1):\ (h^0,h^1) = (4,4), \qquad \mathcal{O}_C(2,0):\ (h^0,h^1) = (3,3). \tag{XIV.4.45}$$

Both bundles have degree eight. The ratio $\mathcal{O}_C(1,-1)$ is a nontrivial degree-zero twist: if it were trivial these two line bundles would be isomorphic and their cohomology dimensions could not differ.

At degree twelve, $\mathcal{O}_C(2,1)$ has six ambient polynomials and h^2 of its source $\mathcal{O}_S(-2,-3)$ is two. For $\mathcal{O}_C(3,0)$ the source has a factor of degree -1 and is acyclic, while the target has four polynomials. Hence

$$\mathcal{O}_C(2,1):\ (6,2), \qquad \mathcal{O}_C(3,0):\ (4,0). \tag{XIV.4.46}$$

The Serre-dual line bundles are $\mathcal{O}_C(0,1)$ and $\mathcal{O}_C(-1,2)$, respectively. The first has the two ruling sections, while the second has none by the same Cartier sequence: its target has a degree--1 factor and its source has only H^2. This is an independent way to keep track of which multiplicity is conjugate. Both pairs in (XIV.4.46) have index four; the extra two copies in each conjugate sector of the first bundle cancel in that difference.

Ambient polynomials are not always enough to count $H^0(C)$. At degree sixteen, $\mathcal{O}_C(2,2) = K_C$ has $(9,1)$, since the source $\mathcal{O}_S(-2,-2)$ contributes one H^2 and the target contributes nine H^0. On the other hand, for $\mathcal{O}_C(4,0)$ the source $\mathcal{O}_S(0,-4)$ has three H^1 and no other groups. The target has five H^0 and no H^1. The relevant part of the long exact sequence is

$$0 \longrightarrow \mathbb{C}^5 \longrightarrow H^0(C, \mathcal{O}_C(4,0)) \longrightarrow \mathbb{C}^3 \longrightarrow 0. \tag{XIV.4.47}$$

Thus the answer is $(8,0)$ rather than $(5,0)$. The last three sections are represented by local lifts that differ by multiples of F on overlaps. They descend to the curve even though they do not lift to global polynomials on S.

We can exhibit those last three sections in local frames. For each $q = -1, -2, -3$ the source Laurent class is y^q. On the overlap in the v factor at $(t,\epsilon) = (2,0)$ its image is

$$F_{2,0} y^q = (1 + x^4) y^q + (1 + 2x^4) y^{q+4}. \tag{XIV.4.48}$$

In the target the v degree is zero. The first term extends to the inverse v chart, and the second to the finite v chart; both coefficients in x are sections of $\mathcal{O}(4)$ on the

other projective line. Take the finite-chart lift $(1+2x^4)y^{q+4}$ and the inverse-chart lift $-(1+x^4)y^q$ in the common frame. Their difference is $F_{2,0}y^q$, so they agree after restriction to C. The connecting homomorphism sends these sections to the three distinct source classes y^q, up to the common Čech sign convention. This exhibits how a nonzero ambient degree-one class can produce a global curve section without extending to a global ambient section.

Now vary the smooth curve while keeping the ambient bundle $\mathcal{O}_S(5,-3)$ fixed. Both ambient groups in (XIV.4.40) are concentrated in degree one:

$$H^1(\mathcal{O}_S(1,-7)) \xrightarrow{m_1} H^1(\mathcal{O}_S(5,-3)), \qquad 2\cdot 6 = 6\cdot 2 = 12. \tag{XIV.4.49}$$

There are two output y-exponents, $j=-2,-1$. Since the equation has even y-exponents, the two output sectors receive disjoint input columns. For a fixed j the input exponents are $j, j-2, j-4$ and each comes with the x-basis $1, x$. The three multipliers in that sector are $1+x^4, \epsilon x^2, 1+tx^4$, respectively. Order the output for even x powers as $(1, x^4, x^2)$ and the input as the even columns of $(j, j-4, j-2)$. The odd columns have the same map with every exponent increased by one. Both j-sectors therefore give two copies of the block

$$N = \begin{pmatrix} 1 & 1 & 0 \\ 1 & t & 0 \\ 0 & 0 & \epsilon \end{pmatrix}, \qquad \det N = (t-1)\epsilon. \tag{XIV.4.50}$$

In particular the full determinant, up to basis ordering, is $(t-1)^4\epsilon^4$. Figure XIV.4.3 shows the coefficient paths. At $t=2$ the first two columns (from shifts 0 and 4) span the first two rows. If $\epsilon = 0$ the third row and column are zero in every block. The rank is 8 rather than 12. Since H^0 is the kernel and H^1 the cokernel of m_1, the two smooth curves give

$$(t,\epsilon) = (2,0) : \ (4,4), \qquad (t,\epsilon) = (2,1) : \ (0,0). \tag{XIV.4.51}$$

The degree is eight in both cases. The determinant vanishes when the section and coboundary conditions fail to be independent; no singularity of the curve is needed. At $(3,1)$ the block determinant is two, giving another smooth instance with no sections. These are changes of the embedded curve at a fixed ambient twist, not deformations of an established compact supersymmetric solution.

For an explicit kernel element at $\epsilon = 0$, choose the even column with exponent y^{j-2}. Its image in the degree-one quotient is zero because $F_{2,0}$ shifts that exponent by 0 or 4, and neither result is in the target window $\{-2,-1\}$. The two discarded terms extend to the two charts, just as in (XIV.4.48). For each j, the even and odd versions exhaust the lost columns. When ϵ is turned on their images acquire the new classes $\epsilon x^2 y^j$ and $\epsilon x^3 y^j$. These span the two missing target rows for that j. One change of coefficient thus removes a kernel and a cokernel of equal dimension. This accounts for the paired nature of the jump, independently of simply subtracting the two Euler characteristics.

On the original singular C_5 we can use (XIV.4.40) with $(d,e) = (22,22)$ without specifying the generic coefficients further. For $\mathcal{O}_{C_5}(10,10)$ the source $\mathcal{O}_S(-12,-12)$ has only H^2, of dimension $11\cdot 11$, and the target has only H^0, also of dimension $11\cdot 11$.

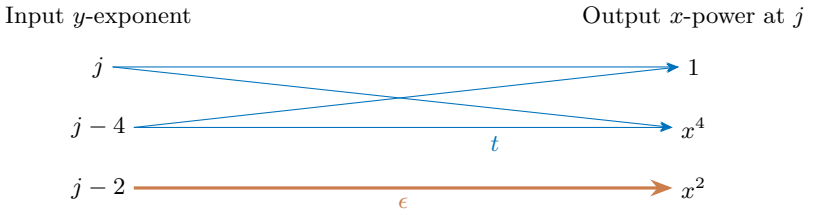


Figure XIV.4.3: One of the four blocks in the multiplication on H^1 for $\mathcal{O}_C(5,-3)$. Inputs are listed at fixed target y-exponent j and for the even x-parity block. The y-powers in the equation shift the three input exponents to j. Unlabeled arrows have coefficient one. In the odd block every target x-power acquires an additional factor of x.

For $\mathcal{O}_{C_5}(20,0)$ the source is $\mathcal{O}_S(-2,-22)$ and the target is $\mathcal{O}_S(20,0)$. Their nonzero dimensions are $1\cdot 21$ and $21\cdot 1$ in those same degrees. All three ranks in (XIV.4.44) vanish for both bundles, since source and target groups do not occur in the same degree. We obtain

bundle on C_5	deg	(h^0,h^1)
$\mathcal{O}_{C_5}(10,10)$	440	$(121,121)$
$\mathcal{O}_{C_5}(20,0)$	440	$(21,21)$

(XIV.4.52)

The first bundle squares to the dualizing bundle and the second need not be such a root. The arithmetic-genus index gives zero in both cases, as these computations require. Replacing the arithmetic genus by 377 would predict a difference of 64, contrary to the exact sequence on C_5. Having computed the groups on a declared line bundle, we still need to ask which sheaf, if any, the physical background supplies.

XIV.4.4 Bulk modes on the seven-brane surface

Which modes live on the whole gauge surface, rather than on a defect curve? Consider the twisted local seven-brane theory on S with zero background Higgs field and a holomorphic Hermitian Yang–Mills bundle. We use the zero-mode approximation of the twisted field equations. For a charged coefficient line T, the connection fluctuation is a $(0,1)$-form in T and the Higgs fluctuation is a $(2,0)$-form in T. The background Higgs field would couple their equations through a commutator. Here it is zero, so the connection fluctuation a is $\bar\partial_T$-closed modulo $\bar\partial_T$ of a gauge parameter, and a harmonic gauge fixes $\bar\partial_T^\dagger a=0$. The Higgs fluctuation φ is holomorphic. Thus the spaces are

$$a: \quad H^{0,1}_{\bar\partial}(S,T)=H^1(S,T), \tag{XIV.4.53}$$

$$\varphi: \quad H^0(S,K_S\otimes T)\simeq H^2(S,T^\vee)^\vee. \tag{XIV.4.54}$$

The same linearization has vector zero modes in $H^0(S,T)$. A scalar-valued vector wavefunction along S is different from either chiral fluctuation above. With the trivial coefficient on the quadric, $H^0(\mathcal{O}_S)=\mathbb{C}$, $H^1(\mathcal{O}_S)=0$ and $H^0(K_S)=0$. This yields the constant vector and no bulk chiral modes in that coefficient sector.

In this local reduction the internal norm is the L^2 norm on S from the product of the Hermitian metric on T and the surface metric. For a connection form the quadratic expression controlling the zero mode is

$$\big(a, \Delta_{\bar\partial_T} a\big)_{L^2(S)} = \|\bar\partial_T a\|^2_{L^2(S)} + \|\bar\partial_T^\dagger a\|^2_{L^2(S)}. \tag{XIV.4.55}$$

This identity follows by integration by parts on the closed surface. A zero eigenvector must obey both first-order equations, and a cohomology class has a unique harmonic representative for the chosen smooth metrics. The analogous norm for the holomorphic Higgs section uses the metric on $K_S \otimes T$. Compactness of S makes the norms finite for smooth representatives in this surface theory. It does not decide normalization in a larger noncompact space transverse to the brane, or a dynamical decoupling limit of the compact fourfold.

For a charged sector with no vector contribution in either T or $T^\vee$, the signed number in the orientation of T is

$$n_T - n_{T^\vee} = h^1(T) + h^2(T^\vee) - h^1(T^\vee) - h^2(T) \tag{XIV.4.56}$$

$$= \chi(T^\vee) - \chi(T). \tag{XIV.4.57}$$

Hirzebruch–Riemann–Roch gives the difference by multiplying Chern character and Todd class. In complex dimension two the rank term, which multiplies $\mathrm{td}_2(S)$, cancels, as does the quadratic Chern term. The two linear terms have opposite sign, each multiplying $c_1(S)/2$. Therefore

$$\chi(T^\vee) - \chi(T) = -\int_S c_1(T) c_1(S). \tag{XIV.4.58}$$

This is a signed count after separating the vector modes. If a vector contribution is present, discarding H^0 from an Euler characteristic without accounting for it changes the index argument.

Take the following separate local gauge background on the same S:

$$L_k = \mathcal{O}_S(k, -k), \qquad E = L_k \oplus L_k^{-1}, \qquad \Phi = 0. \tag{XIV.4.59}$$

The determinant is trivial. Under an off-diagonal fluctuation a field in L_k^{-1} is mapped to a field in L_k. The entry transforms as $\mathrm{Hom}(L_k^{-1}, L_k)$, and the reverse arrow takes values in its dual line $\mathrm{Hom}(L_k, L_k^{-1})$. The two coefficient lines are

$$T_+ = L_k^2 = \mathcal{O}_S(2k, -2k), \qquad T_- = L_k^{-2} = \mathcal{O}_S(-2k, 2k). \tag{XIV.4.60}$$

This explains the doubling in Figure XIV.4.4. A line carrying the defining charge of the rank-two bundle and a line carrying the root charge are different coefficients in the fluctuation problem.

For $k \geq 1$, the first factor of T_+ contributes $2k+1$ degree-zero modes and no degree-one modes. The second contributes $2k-1$ degree-one modes and no degree-zero modes. The product hence has no H^0 or H^2, and

$$h^1(S, T_+) = (2k+1)(2k-1) = h^1(S, T_-). \tag{XIV.4.61}$$

The result for T_- uses the exchanged ruling factors. The Higgs bundle $K_S T_+ = \mathcal{O}_S(2k-2, -2k-2)$ has no sections because its second exponent is negative; the first exponent of $K_S T_-$ gives the same conclusion. Consequently $k = 1$ yields the pair $(3, 3)$ and $k = 2$ yields $(15, 15)$, all from connection modes in the two charges. Using L_1 itself would instead give zero since $\mathcal{O}(-1)$ is acyclic. By (XIV.4.58) the index vanishes because $c_1(S) = 2(H_1 + H_2)$ pairs to zero with $2k(H_1 - H_2)$.

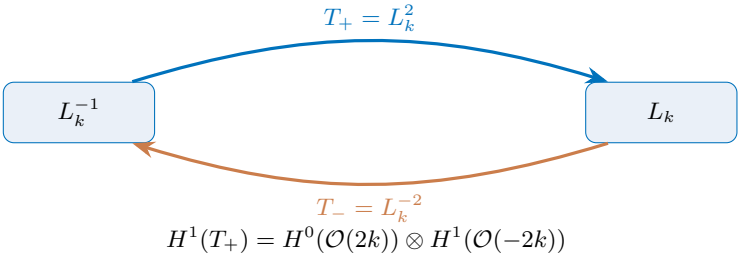


Figure XIV.4.4: The two off-diagonal entries of the local split connection act between opposite summands. A map $L_k^{-1} \to L_k$ carries coefficient L_k^2, whose positive ruling degree supplies polynomials and negative ruling degree supplies Laurent classes. The diagonal commutant has a different, neutral coefficient.

For example, at $k = 1$ a representative Čech basis for the positive root is $(1, x, x^2) \otimes y^{-1}$. The negative root exchanges the roles of the finite coordinate and the overlap coordinate. At $k = 2$ the positive root has five polynomial factors and the three Laurent factors y^{-3}, y^{-2}, y^{-1}. The number fifteen counts the tensor products of those two bases; it is not a multiple of the Cartan charge inserted in a trace. The diagonal sector of $\operatorname{End} E$ has no such shifted ruling exponents. This shows how the internal zero modes of a given adjoint multiplet can split according to the coefficient bundle seen by each entry.

There remains a supersymmetry check. Write $J = aH_1 + bH_2$ with $a, b > 0$. The degree with respect to this polarization is

$$\mu_J(L_k) = \int_S J c_1(L_k) = k(b - a). \tag{XIV.4.62}$$

The sign is fixed by the cross terms in $H_1 H_2$. For a product metric with normalized area forms ω_1, ω_2, choose the product Chern connection whose real normalized curvature represents $k(\omega_1 - \omega_2)$. It has type $(1, 1)$, and wedging it with $a\omega_1 + b\omega_2$ gives $k(b-a)\omega_1 \wedge \omega_2$ pointwise. At $a = b$ the two summands have primitive curvatures and the split determinant-one connection solves the zero-Higgs equation. Equivalently the two line summands are slope-zero stable bundles and their direct sum is polystable.

For unequal areas and $k \neq 0$ one summand has positive slope while E has zero slope; the same zero-Higgs split bundle cannot solve the HYM condition. The holomorphic dimensions in (XIV.4.61) are unchanged by this change of metric. A vector in the neutral commutant can still be distinguished from the charged fields counted above; the nontrivial split does not preserve a bulk $SU(2)$ vector multiplet. The local equal-area

example does not provide a compact $SU(5)$ gauge background. It shows which physical hypothesis must be tested in addition to the cohomology computation. Next we hold the component bundles fixed and change instead the way their wavefunctions are matched.

XIV.4.5 Equal index with different pairs

What changes when a matter curve degenerates into components? An equation on each component determines the local wavefunctions, but it leaves a second problem: which of these wavefunctions agree at the common points? We can see both problems in the $(t, \epsilon) = (1, 0)$ member of (XIV.4.25). Its homogeneous equation on S is

$$(u_0^4 + u_1^4)(v_0^4 + v_1^4) = 0. \tag{XIV.4.63}$$

There are four vertical rulings and four horizontal rulings. Each intersects all four of the opposite kind, once and transversely. The normalization is the disjoint union of eight rational curves and the incidence graph is the complete bipartite graph $K_{4,4}$. The curve is connected, so the normalization sequence for $\mathcal{O}_C$ gives

$$p_a = 1 - \chi(\mathcal{O}_C) = 1 - (8 - 16) = 9. \tag{XIV.4.64}$$

In this example the arithmetic genus is the number of independent cycles of the incidence graph. No individual normalized component has positive genus.

Fix $\mathcal{O}(1)$ on each component. To make an invertible sheaf M on the nodal curve, identify the two branch fibers at each node by a nonzero factor z_{ij}. In a local ring $\mathbb{C}[[s,t]]/(st)$, if the branch representatives are $f(s), g(t)$, the matching condition is $f(0) = z_{ij} g(0)$. Rescaling one of the frames at the node reduces it to the defining condition for a regular function on the nodal curve. Hence this construction gives a line bundle for every nonzero factor; setting a factor to zero is not an invertible identification. Globally we have the sequence

$$0 \longrightarrow M \longrightarrow \nu_* \nu^* M \xrightarrow{\mathrm{ev}_\Delta} \bigoplus_{i,j} \mathbb{C}_{p_{ij}} \longrightarrow 0, \tag{XIV.4.65}$$

where ev_Δ subtracts the evaluations in the matching equation. It is surjective as a sheaf map: at one node either branch has a local section with arbitrary value there. Its map on global sections need not be surjective.

Rescale each finite ruling coordinate by a fourth root of -1; the marked coordinates u_i and v_j on the two sets are then $1, \mathrm{i}, -1, -\mathrm{i}$, with indices $0, 1, 2, 3$. Here u_i, v_j denote scalar marked positions rather than the earlier pairs of homogeneous coordinates. Sections on the vertical lines have values $A_i + B_i v$, and those on the horizontal lines $C_j + D_j u$, in the affine frames of $\mathcal{O}(1)$. Each of the sixteen matching rows is

$$A_i + B_i v_j - z_{ij}(C_j + D_j u_i) = 0. \tag{XIV.4.66}$$

There are sixteen coefficients. Since $H^1(\mathcal{O}(1)) = 0$ on each normalized component, the cohomology on C is determined by this single matrix $Q(z)$:

$$0 \longrightarrow H^0(C, M) \longrightarrow \mathbb{C}^{16} \xrightarrow{Q(z)} \mathbb{C}^{16} \longrightarrow H^1(C, M) \longrightarrow 0. \tag{XIV.4.67}$$

The two dimensions are equal to $16 - \operatorname{rk} Q(z)$. If we simply counted the two sections on every rational component, we would miss both the matching constraints on H^0 and the cokernel giving H^1.

	$v_0 = 1$	$v_1 = \mathrm{i}$	$v_2 = -1$	$v_3 = -\mathrm{i}$
$u_0 = 1$	p_{00}	p_{01}	p_{02}	p_{03}
$u_1 = \mathrm{i}$	p_{10}	p_{11}	p_{12}	p_{13}
$u_2 = -1$	p_{20}	p_{21}	p_{22}	p_{23}
$u_3 = -\mathrm{i}$	p_{30}	p_{31}	p_{32}	p_{33}

orange: changed edge

blue: interpolation square

sixteen node conditions

Figure XIV.4.5: The sixteen evaluations for $K_{4,4}$. Each grid entry is an intersection of a vertical component (row) with a horizontal component (column). The blue square is enough to interpolate a bilinear polynomial, and the orange entry is the one whose gluing is changed.

Take $z_{ij} = 1$ except possibly at $(0,0)$. When all entries are one, the bundle is $\mathcal{O}_S(1,1)|_C$ in the compatible affine frames. We can compute the rank without assuming an ambient extension for other choices of z_{00}. Temporarily omit the $(0,0)$ row. The 2×2 square with $i, j \in \{1,2\}$ determines a unique bilinear polynomial

$$f(u,v) = c_0 + c_1 u + c_2 v + c_3 uv \tag{XIV.4.68}$$

from its four values, since the two marked coordinates in each direction are distinct. For each of the two chosen horizontal lines, matching at the two chosen vertical lines forces its affine section to be the restriction of f. Each vertical line then matches f at the two chosen horizontal lines and must itself be a restriction. Finally each remaining horizontal line agrees at the two chosen vertical lines. This proves that all solutions of the fifteen equations are parametrized by (XIV.4.68). It also proves that all four parameters are independent, since any such polynomial meets the fifteen constraints. Figure XIV.4.5 indicates the square used in the interpolation.

The last equation is now $(1 - z_{00}) f(u_0, v_0) = 0$. At $z_{00} = 1$ it adds no condition. If $z_{00} = 2$ or 3, it adds one independent condition because evaluation at a point is nonzero on the constant polynomial. Thus

z_{00}	$\operatorname{rk} Q$	(h^0, h^1)
1	12	$(4,4)$
2 or 3	13	$(3,3)$

(XIV.4.69)

while the multidegree remains $(1,1,1,1,1,1,1,1)$. The total degree is eight, so $8+1-p_a = 0$ independently of the rank. Neither a square-root property nor extension of the modified bundle to S entered the calculation.

One can read the removed mode directly in the interpolating basis. In the chosen marking, $u_0 = v_0 = 1$. For $z_{00} \neq 1$ the last row sets $c_0 + c_1 + c_2 + c_3 = 0$. The three polynomials $u - 1$, $v - 1$ and $uv - 1$ then span the kernel. The constant polynomial,

which matched at every node when $z_{00} = 1$, has a residual at precisely the changed edge. The index remains zero because the cokernel also loses one dimension. This interpretation identifies which local sections fail to assemble, rather than just giving a numerical rank.

Changing every factor in one row by the same nonzero number is a different operation. If $z'_{ij} = s_i z_{ij}$ with $s_i \neq 0$, replace (A_i, B_i) by $s_i(A_i, B_i)$. The new residual at each node in that row is then s_i times the old residual. This gives invertible changes of coordinates on both sides of (XIV.4.67). Hence a full row change cannot alter the rank. For example, starting with all factors one, every product

$$\frac{z_{ij} z_{k\ell}}{z_{i\ell} z_{kj}} \tag{XIV.4.70}$$

on a four-edge cycle stays one under such row changes and under analogous column changes. A single changed edge gives a nonunit product on any such cycle containing it. It cannot be absorbed by rescaling frames on the components.

The cycles can also be counted without assigning a new parameter to each of the sixteen edges. Pick seven edges forming a spanning tree of the eight-vertex graph. Given any nonzero factors on those edges, choose the frame at a root vertex, then determine the neighboring frames one at a time to turn each tree factor into one. The remaining nine factors are measured by products around cycles; a simultaneous rescaling of every component has no effect on any edge factor. Thus the line bundles with this fixed component data admit genuine matching choices modulo changes of frames. The computed rank jump is an example within that local space of choices, not a statement about the space of compact gauge potentials.

We have now seen three ways to change cohomology at fixed index. On the same smooth curve one can change the degree-zero part of the bundle, as in (XIV.4.45). With the same ambient bundle one can change the map induced by the smooth curve equation, as in (XIV.4.50). On the nodal curve one can keep every component bundle and change the matching itself. These are different operations. The nodal calculation illustrates what a gluing map can do to the dimensions; it does not identify z_{00} with a compact spectral-cover parameter or a three-form holonomy.

XIV.4.6 Spectral data and what it does not fix

What data must a physical construction supply before one of these cohomology pairs can be used as a spectrum? The answer starts with the distinction between a curvature class and a gauge potential that realizes it. For a smooth projective fourfold, the ordinary unshifted Deligne cohomology group fits into

$$0 \longrightarrow J^2(Y) \longrightarrow H^4_{\mathcal{D}}(Y, \mathbb{Z}(2)) \longrightarrow H^4(Y, \mathbb{Z}(2)) \cap F^2 H^4(Y, \mathbb{C}) \longrightarrow 0. \tag{XIV.4.71}$$

The notation on the right means integral classes whose complexification lies in the Hodge filtration F^2, with the indicated Tate normalization. In the free image they are of type $(2, 2)$. The intermediate Jacobian $J^2(Y)$ is the quotient

$$J^2(Y) = \frac{H^3(Y, \mathbb{C})}{F^2 H^3(Y, \mathbb{C}) + \operatorname{im}\big(H^3(Y, \mathbb{Z}(2))\big)}. \tag{XIV.4.72}$$

This follows from the description of Deligne cohomology by the comparison of integral cohomology and the filtered complex: the contribution from degree four is the kernel of the comparison and that from degree three is the cokernel. The flat ambiguity in (XIV.4.71) is a fiber over an allowed class, not a supply of independent arbitrary flat bundles on every defect. The characteristic shift of Chapter 3 must be taken into account separately in specifying the physical curvature and its lift; (XIV.4.71) is not itself the shift law.

In the ordinary algebraic construction a chosen gauge cycle $\mathcal{A}$ defines refined data by the cycle map. Suppose the curvature, refinement and spin convention are compatible, and take a smooth matter curve with its oriented matter surface T_w. Let $i : T_w \hookrightarrow Y$ be the inclusion and $p : T_w \to C_R$ the projection. The divisor class seen on C_R is obtained from the refined intersection on the surface and pushforward:

$$D_R = p_*\big(i^!\mathcal{A}\big) \in \mathrm{CH}_0(C_R), \tag{XIV.4.73}$$

$$L_R = \mathcal{O}_{C_R}(D_R), \tag{XIV.4.74}$$

$$M_R = \Theta_{C_R} \otimes L_R. \tag{XIV.4.75}$$

Here $i^!\mathcal{A}$ is the intersection class on T_w: apply the refined Gysin map of the diagonal of the smooth fourfold Y to $[T_w] \times \mathcal{A}$. This gives a zero-cycle class on T_w and agrees with Gysin pullback when i is a regular embedding. For an ordinary line bundle we require the pushed class to be integral. On the smooth curve, rational equivalence of these divisors is linear equivalence. The upper route in Figure XIV.4.6 retains this class before taking its degree.

Under the stated compatibility conditions, passing to degrees yields

$$\deg D_R = \deg(i^!\mathcal{A}) = \int_{T_w} G. \tag{XIV.4.76}$$

The first equality uses proper pushforward of zero-cycles and the second uses compatibility of the cycle class and orientation with the curvature pairing. This explains how the index in (XIV.4.32) can agree with the period in (XIV.4.1). It also describes precisely what that agreement forgets. For example the degree-eight twists of (XIV.4.45) have coefficients $L = \mathcal{O}_C$ and $L' = \mathcal{O}_C(1, -1)$ with respect to the same Θ_C. The ruling degrees cancel in $\deg L'$ but its class is nontrivial. It changes the cohomology even though the degree map in (XIV.4.76) could not detect it. This comparison does not place either bundle in the image of compact gauge data.

The same distinction applies when a construction imposes a root condition on L_R. A local root solves an equation in the Picard group of the curve. To conclude that it comes from a compact gauge potential requires an image calculation for the actual restriction or pushforward map. The exact sequence (XIV.4.71) cannot perform that calculation: it describes an ambiguity on Y and does not identify its effect on C_R. Compact examples with an additional section and particular Tate restrictions can realize specific curve sheaves. They do not give the curve sheaves for this quadric model. Even the degree agreement suggested by -56 would not identify the lift, establish supersymmetry, or justify a four-dimensional F-theory limit.

There is also a limit to the line-bundle calculation as a local description. When a nonzero Higgs field couples the connection and Higgs fluctuations, the local defor-

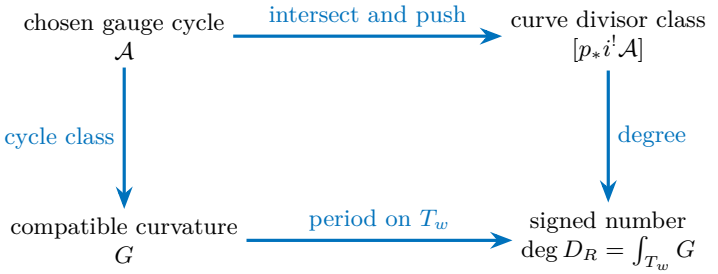


Figure XIV.4.6: Two routes out of refined algebraic data in the ordinary compatible setting. The divisor class is formed by intersecting on T_w and pushing to C_R. Taking its degree recovers the numerical period but forgets the class in the curve Picard group. Neither arrow from the upper-left object is specified by just supplying the number at lower right.

mation operator has two parts: the Dolbeault differential and the map induced by the background Higgs field. For an endomorphism-valued fluctuation, the latter is the commutator in the sheaf complex

$$\operatorname{End} E \xrightarrow{[\Phi,\cdot]} \operatorname{End} E \otimes K_S. \tag{XIV.4.77}$$

The hypercohomology keeps both maps. In a spectral description this problem can be expressed using Ext groups of the corresponding sheaves in the local spectral category. The spectral polynomial fixes support, but support is only where the sheaf can live. A sheaf on several components can also carry extension data.

To see why an extension can enter a count, take a short exact sequence of local spectral sheaves $0 \to F_1 \to F \to F_2 \to 0$, with extension class $\eta \in \operatorname{Ext}^1(F_2, F_1)$. Applying $\operatorname{Hom}(P_0, -)$ for a test sheaf P_0 gives a connecting map

$$\operatorname{Hom}(P_0, F_2) \xrightarrow{\delta_\eta} \operatorname{Ext}^1(P_0, F_1), \qquad \delta_\eta(f) = \eta \circ f. \tag{XIV.4.78}$$

Indeed a map f lifts to F precisely when the pullback of the extension by f splits. Exactness makes the image of $\operatorname{Hom}(P_0, F)$ the kernel of δ_η, and passes its cokernel to the next group. Thus the rank of this map can matter even though additivity in the Grothendieck group gives

$$\operatorname{ch}(F) = \operatorname{ch}(F_1) + \operatorname{ch}(F_2). \tag{XIV.4.79}$$

The characteristic class on the left is independent of the extension map. This is the same counting principle as in (XIV.4.67), with a different map in a different category. The rank calculated there is a rank of point evaluations, not of a spectral Ext connecting map.

For clarity, write $d = \operatorname{rk} \delta_\eta$. The long exact sequence gives, whenever the groups are

finite dimensional,

$$\dim \operatorname{Hom}(P_0, F) = \dim \operatorname{Hom}(P_0, F_1) + \dim \operatorname{Hom}(P_0, F_2) - d, \tag{XIV.4.80}$$

$$\dim \operatorname{Ext}^1(P_0, F) = \dim \operatorname{Ext}^1(P_0, F_1) - d + \dim \ker\bigl(\operatorname{Ext}^1(P_0, F_2) \longrightarrow \operatorname{Ext}^2(P_0, F_1)\bigr)\,. \tag{XIV.4.81}$$

The next connecting map can also depend on the extension. This is why knowledge of d alone would not in general compute a spectral spectrum. In the curve normalization calculation the normalized H^1 vanishes and the sequence stops at the one cokernel. This made it possible to compute both dimensions by a single matrix there.

One must also impose the appropriate stability or D-term condition on a local Higgs background. The example (XIV.4.62) shows why a holomorphic object and a compatible metric are separate inputs. Finally these constructions count linearized modes. Interactions can pair or lift some of them, depending on the background and couplings. The next chapter studies a local operation that produces couplings; its input includes the relevant wavefunctions and their charge data. The geometry and formal periods of the present example give neither the complete compact spectrum nor a physical identification of its local gluing choices.

XIV.4.7 Exercises

1. In the phase-I quadric presentation use the cycle $P = (C-D)(B-C)+8H(C-D)$ and then reverse its orientation. Give the codimension, orientation sign and resulting formal period. Enter the unoriented polynomial P in total exceptional classes with symbols `H,r,A,B,C,D` (and optional aliases `D1,D2,D3,D4`), using `*` for multiplication and `**` for powers. Report the geometric and electric four-entry tuples of the shared component in that order. Explain why adding a Cartan term with zero period does not identify the new cycle with a single effective matter component.

2. On $C_{4,0}$ use $M = \mathcal{O}_C(-3, 5)$. Check the four charts, then give the degree of M, the ranks of m_0, m_1, m_2 in order, and (h^0, h^1). Repeat the cohomology calculation for the same curve with $\mathcal{O}_C(0, 4)$ and explain where nonlifting sections enter. The bounded submission uses the first bundle; the second calculation is written practice.

3. On the eight-component curve set $z_{12} = 4$ and all other factors to one, using zero-based indices. Compare with the choice in which every factor in row 1 is 4 and all other factors are one. For each case give the matching rank and (h^0, h^1) at the stated fixed multidegree. Explain how a component frame change acts on the second matrix.

4. Use $k = 3$ in the local split bundle. Give the exponents of T_+ and T_- in that order, the connection and Higgs dimensions in both charges, and $\mu_J(L_k)$ and whether the zero-Higgs split is HYM at each of $(a, b) = (2, 2), (2, 5)$.

5. At one base point of the actual coefficient system use $(A_p, B_p, C_p) = (2, 1, 3)$; at another use $(1, 4, 4)$. Give the tangent discriminant, ordinary-node classification, and local intersection length with C_{10}. Compare with a point where b_3 is a unit and $b_4|_{C_{10}}$ has a simple zero. Compute the arithmetic genus and the normalization genus under the original generic 64-node assumption. Explain why the repeated tangent case by itself cannot fix a new normalization genus.

6. Explain why the formal G_* period and a smooth genus-nine line bundle of degree -48 do not yet give a compact four-dimensional spectrum. State the needed conditions on a refined lift, the induced defect data, and the supersymmetric limit. Distinguish this issue from computing the kernel and cokernel once the coefficient sheaf is given.

Use `benchmark/tasks.json` for the JSON fields and `benchmark/PROTOCOL.md` for submission. Written explanations, including Exercise 6, are assessed by a reader.

Take-home message of this chapter

A period on one oriented weight surface gives a representation index under the ordinary compatible background assumptions. Cohomology computes separate multiplicities only after the curve and its coefficient sheaf are specified. The difference can stay fixed while the dimensions change through a degree-zero twist, multiplication by a different curve equation, or a different node matching. A formal shifted period does not choose these data.

Status and sources

§XIV.4.1. Matter surface and index. [**GEO-E**] One oriented weight surface for the index under the ordinary algebra-preserving dictionary: Bies, Mayrhofer, and Weigand 2017, (2.9)–(2.10) and Grimm and Hayashi 2011, (2.1). [**MATH**] The projection formula, relative intersection and character are displayed above. Phase-I Cartans 1 and affine-first rows: Hayashi et al. 2013, (3.9)–(3.14), PDF pp. 15–16. Their b_1, b_2, b_3, b_4, b_6 are our b_5, b_4, b_3, b_2, b_0. The formal class and divisor presentation reuse Chapter 3; the actual weight and period are evaluated on the common stratum in (XIV.4.10)–(XIV.4.21). No physical index is asserted for G_*.

§XIV.4.2. Geometry and twist. [**MATH**] The chart, adjunction and Cartier calculations apply to the displayed quartic and the stated open in the actual residual coefficient system. The geometric irreducibility and open smoothness steps use The Stacks Project Authors n.d., Lemma 37.32.3, tag 0G4F, Lemma 33.47.3, section tag 0FD4; their hypotheses are verified separately. [**GEO-E**] The local defect groups and the embedded spin prescription use Beasley et al. 2008, (4.98)–(4.103) and Bies, Mayrhofer, and Weigand 2017, (2.15)–(2.21). The chosen twists are mathematical examples.

§XIV.4.3. Cohomology. [**MATH**] The product Čech multiplication, fixed-degree comparison and fixed ambient twist comparison are derived in (XIV.4.42)–(XIV.4.51). The original C_5 line-bundle calculations are in (XIV.4.52).

§XIV.4.4. Bulk fields. [**GEO-E**] The local zero-Higgs assignments and signed index use Beasley et al. 2008, (3.38)–(3.51). [**MATH**] The root counts and local HYM wall follow in (XIV.4.60)–(XIV.4.62).

§XIV.4.5. Nodal matching. [**MATH**] Equations (XIV.4.65)–(XIV.4.70) compute the invertible gluing comparison on the original nodal curve.

§XIV.4.6. Refined and spectral data. [**GEO-E**] For the curvature refinement, induced Chow divisor and its degree, see Bies, Mayrhofer, and Weigand 2017, (2.3)–(2.10), (2.15)–(2.21), App. A.2 and Bies, Mayrhofer, Pehle, et al. 2014, §3.1. Local roots need an additional global-image test, as in Bies, Cvetič, et al. 2021, Introduction and (5.2). The local spectral category, Ext and stability discussion use Donagi and Wijnholt 2011, (2.81), (2.86)–(2.89), §3. No compact lift, complete spectrum, or image of local flat data is determined here.

References

Beasley, C., J. J. Heckman, and C. Vafa (2008). "GUTs and Exceptional Branes in F-theory, I". In: arXiv: `0802.3391 [hep-th]`.

Bies, M., M. Cvetič, et al. (2021). "Root Bundles and Towards Exact Matter Spectra of F-theory MSSMs". In: arXiv: `2102.10115 [hep-th]`.

Bies, M., C. Mayrhofer, C. Pehle, et al. (2014). "Chow Groups, Deligne Cohomology and Massless Matter in F-theory". In: arXiv: `1402.5144 [hep-th]`.

Bies, M., C. Mayrhofer, and T. Weigand (2017). "Gauge Backgrounds and Zero-Mode Counting in F-theory". In: arXiv: `1706.04616 [hep-th]`.

Donagi, R. and M. Wijnholt (2011). "Gluing Branes, I". In: arXiv: `1104.2610 [hep-th]`.

Grimm, T. W. and H. Hayashi (2011). "F-theory Fluxes, Chirality and Chern–Simons Theories". In: arXiv: `1111.1232 [hep-th]`.

Hayashi, H., C. Lawrie, and S. Schäfer-Nameki (2013). "Phases, Flops and F-theory: SU(5) Gauge Theories". In: arXiv: `1304.1678 [hep-th]`.

The Stacks Project Authors (n.d.). *Bertini theorems*. Section 33.47 and Lemma 37.32.3 (tag 0G4F). URL: `https://stacks.math.columbia.edu/tag/0FD4`.

Chapter XIV.5

Yukawa couplings, Higgs backgrounds and T-branes

XIV.5.1 The holomorphic coupling problem

Which information about a seven-brane determines the cubic of its charged matter fields? In Chapter 2 the singular fiber located the 10 and 5 matter curves of the quadric model. Chapter 4 distinguished those supports from the sheaves that can carry zero modes. A cubic requires still more: we must know how the three modes meet and which components of their holomorphic profiles enter the invariant. We will compute this interaction in a small patch, first at a transverse intersection and then when two intersections merge. The calculation will distinguish the polynomial that describes the Higgs eigenvalues, the module on which the Higgs field acts, and the choice of modes inside that module.

Return to the split $SU(5)$ Tate family over $\mathbb{P}^3$. Let S be the quadric with homogeneous equation $W = X_0X_3 - X_1X_2 = 0$. Set $X_0 = 1$, put $x = X_1$, $y = X_2$, and use $w = X_3 - xy$ for the normal coordinate. The symbol $z = x + y$ below is a function on S, not this normal coordinate. In the chosen affine frames the Tate coefficients are

$$(a_1, a_2, a_3, a_4, a_6) = (b_5, wb_4, w^2b_3, w^3b_2, w^5b_0). \tag{XIV.5.1}$$

The homogeneous versions of the a_i have degree $4i$, so after removing a power W^v the residual degree is $4i - 2v$. In the order b_0, b_2, b_3, b_4, b_5 these degrees are $14, 10, 8, 6, 4$. The matter ideals on S are generated by

$$b_5 \quad (C_{10}), \qquad P = b_4b_3^2 - b_2b_3b_5 + b_0b_5^2 \quad (C_5). \tag{XIV.5.2}$$

The subscript in C_5 describes the support; it does not specify the chirality or even which conjugate representation has a mode in the compact model.

We want a specialization that lets us vary an intersection and an off-diagonal Higgs entry separately. In a local frame for the canonical bundle K_S, take the two light eigenvalues to be the roots of $Q(s)$, and choose three spectator eigenvalues r_i. We use

the following matrix and determinant:

$$M = \begin{pmatrix} x & \tau \\ mx+\delta & y \end{pmatrix}, \qquad d = xy - \tau(mx+\delta), \qquad Q(s) = \det(sI - M) = s^2 - zs + d. \tag{XIV.5.3}$$

Here m, δ, τ are constants; τ will be either zero or one. Set $(r_1, r_2, r_3) = (1, 2, -3-z)$ so that the trace of the complete five-dimensional matrix is zero. Multiplication gives

$$\begin{aligned} R_3(s) &= (s-1)(s-2)(s+3+z) \\ &= s^3 + zs^2 - (7+3z)s + (6+2z), \qquad \text{(XIV.5.4)} \\ Q(s)R_3(s) &= b_0 s^5 + b_2 s^3 + b_3 s^2 + b_4 s + b_5. \qquad \text{(XIV.5.5)} \end{aligned}$$

The s^4 term cancels between the two factors. The other coefficients are

$$b_0 = 1, \qquad b_2 = d - 7 - 3z - z^2, \tag{XIV.5.6}$$

$$b_3 = 6 + 9z + 3z^2 + dz, \qquad b_5 = (6+2z)d, \tag{XIV.5.7}$$

$$b_4 = -z(6+2z) - (7+3z)d. \tag{XIV.5.8}$$

This use of a local spectral polynomial assumes the ordinary meromorphic spectral description on the open $b_0 \neq 0$. Its eigenvalue s is a canonical-bundle coordinate. On the quadric, adjunction gives $K_S = \mathcal{O}_S(-2)$ while $N_{S/\mathbb{P}^3} = \mathcal{O}_S(2)$. The local numerical values of s and w belong to different constructions. A chosen affine frame and the monic ratios do not give a global endomorphism with five scalar eigenvalues.

The coefficients above really can be restrictions of the prescribed homogeneous sections. For residual degree n lift each term $cx^i y^j$ to $cX_0^{n-i-j}X_1^i X_2^j$; all degrees of the local polynomials are at most three. For example at $(m, \delta, \tau) = (1, 0, 1)$, $d = xy - x$ and the complete b_5 lift is

$$b_5^{\mathrm{hom}} = 2X_0X_1\big(-3X_0^2 - X_0X_1 + 2X_0X_2 + X_1X_2 + X_2^2\big). \tag{XIV.5.9}$$

Inserting the homogeneous residual coefficients and the corresponding powers of W in (XIV.5.1) gives homogeneous a_i of the required degrees. In particular $b_0^{\mathrm{hom}} = X_0^{14}$. These lifts are special members of the coefficient space, and the chart says nothing about minimality or regularity at $X_0 = 0$. Changing δ in (XIV.5.3) changes actual homogeneous coefficients by the same lift, rather than just drawing a new pair of matter curves.

There is also a compact formula for all five lifts. Write $X = X_0$, $Z = X_1 + X_2$, and $D_2 = X_1X_2 - \tau(mX_1X + \delta X^2)$. Then $z = Z/X$ and $d = D_2/X^2$. Pulling out the minimal power of X that clears the denominators in each term gives

$$b_0^{\mathrm{hom}} = X^{14}, \qquad b_2^{\mathrm{hom}} = X^8(D_2 - 7X^2 - 3XZ - Z^2), \tag{XIV.5.10}$$

$$b_3^{\mathrm{hom}} = X^5(6X^3 + 9X^2Z + 3XZ^2 + D_2Z), \tag{XIV.5.11}$$

$$b_4^{\mathrm{hom}} = -X^3\big(XZ(6X+2Z) + (7X+3Z)D_2\big), \tag{XIV.5.12}$$

$$b_5^{\mathrm{hom}} = X(6X+2Z)D_2. \tag{XIV.5.13}$$

For example, the term dz in b_3 becomes X^5D_2Z of degree eight, and the term 6 becomes $6X^8$. The coefficients of the global Tate equation can now be recovered in any projective chart from the homogeneous forms. The spectral interpretation below is narrower: the factors such as $6+2z$ and U are treated as units only where they do not vanish. In particular one should not use a degree-one equation $z=0$ as a global replacement for the degree-twenty-two polynomial P.

To see which factors of (XIV.5.2) matter locally, take the additive action on the exterior square of the five-dimensional matrix. Its ten eigenvalues are sums of distinct entries from the list of five eigenvalues. The constant term of its characteristic polynomial is the product of these ten sums, since the degree is even. The pair of light roots sums to z. The product of the two sums involving a given spectator r_i is $Q(-r_i)=r_i^2+zr_i+d$. The last three sums contain only spectators. Thus the additive exterior-square determinant is

$$-P=zU, \qquad U=\prod_{i=1}^{3}(r_i^2+zr_i+d)\prod_{i<j}(r_i+r_j). \tag{XIV.5.14}$$

The first equality uses the constant coefficient $-b_4b_3^2+b_2b_3b_5-b_5^2$ of the additive polynomial in the monic, traceless frame. In this family the factorization can also be checked without solving for either light root. Write $B=6+2z$, $C=7+3z$ and $D=B+zC+dz=b_3$. Substitution into P gives

$$\begin{aligned} P &= (-zB-Cd)D^2-(d-C-z^2)DdB+d^2B^2 \\ &= -z(1+z+d)(4+2z+d)(9+3z+d)\,3(2+z)(1+z). \end{aligned} \tag{XIV.5.15}$$

The spectator sums in (XIV.5.14) multiply to $3(2+z)(1+z)$, whereas $Q(-r_3)=9+3z+d$.

The determinant can also be computed directly on the modules, including points where M cannot be diagonalized. Decompose the auxiliary five-dimensional space as $V\oplus W_3$, with W_3 the spectator space. Then

$$\Lambda^2(V\oplus W_3)=\Lambda^2V\oplus(V\otimes W_3)\oplus\Lambda^2W_3. \tag{XIV.5.16}$$

The action on the first summand is scalar z. The middle summand consists of three copies of $M+r_iI$, whose determinants are $Q(-r_i)$. The last summand is diagonal with entries r_i+r_j. Taking the determinant of this block decomposition gives zU even at a non-diagonalizable value of M. The argument uses a direct sum of light and spectator blocks; it does not assume a decomposition into the two individual light eigenlines. That distinction matters when we keep the same determinant but change the light module.

At $z=d=0$ the factors of U are all nonzero and $U=216$. Also $b_5/d=6$ there. A holomorphic function nonzero at the point is a unit of its local ring, so in the germ the actual matter ideals are (d) and (z). In the simple example $d=x(y-1)$, the component $y=1$ is outside the germ. The two lines in Figure XIV.5.1 are the restrictions near the origin. We will use (z,d) as ordered equations for the residue. Replacing them by (P,b_5) preserves the supports but multiplies the numerator required in the residue by the determinant of the equation change.

At the simple origin the ordered tuple (b_0,b_2,b_3,b_4,b_5) equals $(1,-7,6,0,0)$. Its

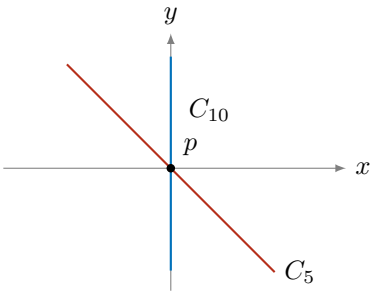


Figure XIV.5.1: Real slice of the two complex matter-curve germs in the chart $w = 0$ at $(m, \delta, \tau) = (1, 0, 1)$. The line $x = 0$ represents the nearby component of $d = 0$; the line $y = -x$ is $z = 0$. The component $y = 1$ lies outside the displayed germ. The picture shows neither the normal direction w nor an elliptic fiber.

linear jets have $b_5 = -6x + O(2)$ and $b_4 = x - 6y + O(2)$ on S, so

$$\det \frac{\partial(b_5, b_4)}{\partial(x, y)}(0) = \det \begin{pmatrix} -6 & 0 \\ 1 & -6 \end{pmatrix} = 36. \tag{XIV.5.17}$$

Here the $O(2)$ terms are in the ideal $(x, y)^2$. To test the Weierstrass orders we must include w as well. Define $B_2 = a_1^2 + 4a_2$, $B_4 = a_1a_3 + 2a_4$, and $B_6 = a_3^2 + 4a_6$. Completion of the square and cube gives

$$f = \frac{B_4}{2} - \frac{B_2^2}{48}, \qquad g = \frac{B_6}{4} - \frac{B_2B_4}{24} + \frac{B_2^3}{864}, \qquad \Delta_{\text{book}} = 4f^3 + 27g^2. \tag{XIV.5.18}$$

In (x, y, w), B_2 starts in degree two, B_4 in degree three and B_6 in degree four. In particular the degree-three part of B_4 is $(-36x - 14w)w^2$, from the linear jet of b_5, the value of b_3, and the value of b_2. The degree-four part of B_6 is $36w^4$. Therefore the leading nonzero terms are

$$f_3 = -18xw^2 - 7w^3, \qquad g_4 = 9w^4, \qquad (\Delta_{\text{book}})_8 = 27(9w^4)^2 = 2187w^8. \tag{XIV.5.19}$$

The cubic of f begins one degree higher than the square of g, so it cannot cancel the degree-eight term. Along with (XIV.5.17), this identifies the ordinary E_6-type Tate top-coupling locus in the example. Testing only $b_5 = P = 0$ elsewhere would also admit $b_3 = 0$ because $P = b_4b_3^2$ on $b_5 = 0$. Our use of the top channel needs b_3 a unit and the specified local exceptional description. The orders $(3, 4, 8)$ at a point on a threefold base do not give a Kodaira fiber diagram there. We next use the geometric equations to identify where the charged operators fail to be invertible in a prescribed Higgs background.

XIV.5.2 A diagonal Higgs background and its zero modes

What does a Higgs field add to the equations of the matter curves? A curve equation locates a possible charged mode. The matrix acting in its representation tells us which linear combinations can be removed by gauge transformations. On a smooth Kähler patch of S use the ordinary classical twisted seven-brane model with no explicit defect sources. Write $A^{0,1}$ for the holomorphic structure on the gauge bundle and Φ for the adjoint-valued $(2,0)$ field. We keep the commutative superpotential and work at leading order in the local worldvolume description. The holomorphic functional, up to its overall coefficient, is

$$W_8 = \int_S \mathrm{Tr}(\Phi \wedge F^{0,2}), \qquad F^{0,2} = \bar\partial A^{0,1} + A^{0,1} \wedge A^{0,1}. \tag{XIV.5.20}$$

Varying Φ tests $F^{0,2}$ directly. Varying $A^{0,1}$ brings down $\bar\partial_A \delta A^{0,1}$. With variations supported in the patch, integration by parts gives the two holomorphic equations

$$F^{0,2} = 0, \qquad \bar\partial_A \Phi = 0. \tag{XIV.5.21}$$

A Hermitian bundle metric H and a Kähler form ω also enter the unitary moment map. With wedge products understood in the commutator of forms, use

$$i\omega \wedge F + \tfrac{1}{2}[\Phi, \Phi^{\dagger_H}] = 0. \tag{XIV.5.22}$$

The first two equations can be solved using complex gauge transformations. Equation (XIV.5.22) asks for a compatible Hermitian representative. This distinction lets us compute holomorphic classes before specifying kinetic norms.

On a sufficiently small patch, $F^{0,2} = 0$ permits a holomorphic frame with $A^{0,1} = 0$. In a fixed frame of K_S, write a, φ for the fluctuations of $A^{0,1}, \Phi$. The linearized equations and infinitesimal complex gauge action, with the Higgs bracket written on its coefficients, are

$$\bar\partial a = 0, \qquad \bar\partial \varphi = [\Phi, a], \tag{XIV.5.23}$$

$$(a, \varphi) \longmapsto (a + \bar\partial \chi,\ \varphi + [\Phi, \chi]). \tag{XIV.5.24}$$

Locally set $a = \bar\partial \xi$. The two terms in $\bar\partial(\varphi - [\Phi, \xi])$ cancel since Φ is holomorphic. Gauging a to zero leaves the representative and equivalence

$$h = \varphi - [\Phi, \xi], \qquad \bar\partial h = 0, \qquad h \sim h + [\Phi, \chi_0] \quad (\bar\partial \chi_0 = 0). \tag{XIV.5.25}$$

Let $R = \mathbb{C}\{x, y\}$ be the ring of holomorphic germs at the origin, or the analogous ring at another chosen point. In a charged sector where the bracket acts as a matrix T, this construction gives $\mathrm{coker}\, T$. A class is torsion if some nonzero $f \in R$ kills it, or equivalently if $fh = T\eta$ for a holomorphic η. Away from $f = 0$ the class can be gauged to zero by dividing that equation by f. In the local matter description it is this torsion that represents localization. The quotient by itself does not compute normalizable four-dimensional fields.

For a scalar action $T = x$ this statement reduces to a familiar restriction: $R/(x)$ retains precisely $h(0, y)$. To see it directly, write

$$h(x, y) = h(0, y) + x\,\ell(x, y). \tag{XIV.5.26}$$

The second term is a complex gauge shift, and the first cannot be removed by dividing by x holomorphically unless it vanishes. If T is a unit, the entire quotient is zero. If $T = 0$, the quotient is R with no torsion, and the same argument gives no localization. These two extremes explain why an eigenvalue that stays nonzero can be eliminated while a bulk field with identically zero Higgs action is a different kind of mode.

We need the charged actions before taking the quotients. The gauge 10 is the antisymmetric rank-two tensor of the unbroken $SU(5)$. In the ordinary local exceptional description it carries a defining index of an auxiliary $\mathfrak{sl}(5)$, distinct from the gauge indices. The gauge 5 that can pair with two 10's carries a dual exterior-square index of the auxiliary algebra. At the points with $z = d = 0$, all the spectator factors in (XIV.5.14) and all the spectator eigenvalues are nonzero. They can be inverted in the local holomorphic quotient. Only the light two-dimensional space V and its dual determinant line enter this channel. For a basis e_1, e_2 of V, the additive action on $e_1 \wedge e_2$ is

$$(Me_1) \wedge e_2 + e_1 \wedge (Me_2) = z(e_1 \wedge e_2), \tag{XIV.5.27}$$

$$(M\lambda)(e_1 \wedge e_2) = -\lambda\big(z(e_1 \wedge e_2)\big). \tag{XIV.5.28}$$

For $\lambda \in \Lambda^2 V^*$ the notation $M\lambda$ denotes the induced dual action. Its sign ensures invariance of the evaluation between a line and its dual. This is why the 5 sees $-z$ even though its matter ideal can be written (z).

The same actions appear in the E_6 branching with respect to $\mathfrak{sl}(5) \oplus \mathfrak{sl}(2) \oplus \mathfrak{u}(1)$, where the two fields are $(10, 2)_{-3}$ and $(5, 1)_{+6}$. Decompose the doublet matrix as

$$M = M_0 + \frac{z}{2} I, \qquad M_0 = M - \frac{z}{2} I, \qquad c = -\frac{z}{6}, \qquad -3c = \frac{z}{2}, \qquad 6c = -z. \tag{XIV.5.29}$$

The central coefficient c reproduces both actions. These branching charges organize the local invariant; they do not introduce a dynamical four-dimensional $U(1)$. If $\epsilon_{12345} = 1$ on gauge indices and $\epsilon(e_1, e_2) = 1$ on the doublet, the invariant contracts the two gauge 10's and the gauge 5 by ϵ_{ijklm} and the two doublets by

$$\epsilon(u, v) = u^T J v, \qquad J = \begin{pmatrix} 0 & 1 \\ -1 & 0 \end{pmatrix}, \qquad \epsilon(Mu, v) + \epsilon(u, Mv) = z\epsilon(u, v). \tag{XIV.5.30}$$

In the cubic the singlet action cancels this variation, or equivalently $-3-3+6 = 0$. Using the opposite singlet action would double the trace term. The dual-action derivation fixes the sign without inferring it from the matter equation, which is insensitive to a unit such as -1.

Consider first the diagonal light matrix $\mathrm{diag}(x, y)$, obtained at $m = \delta = \tau = 0$. Its flat connection and identity metric solve the local equations: the field is holomorphic and commutes with its Hermitian adjoint. The two columns kill the two basis vectors separately. The split doublet module and the singlet module are

$$\mathcal{M}_{10}^{\mathrm{split}} = R/(x)e_1 \oplus R/(y)e_2, \qquad \mathcal{M}_5 = R/(z). \tag{XIV.5.31}$$

For example, the class of ye_1 is a varying profile on $x = 0$, whereas xe_1 is zero. The values of the two profiles at the node are independent.

For $\tau = 1$ the second column is $e_1 + ye_2$. Subtracting a multiple of it sets the first component of any representative to zero. In the remaining column subtract $x(e_1 + ye_2)$ from $xe_1 + (mx + \delta)e_2$ to obtain $-de_2$. This proves the exact quotient and identifies the map on a general column:

$$\mathcal{M}_{10}^{\mathrm{cyc}} = R/(d)e_2, \qquad \rho(u_1e_1 + u_2e_2) = u_2 - yu_1 \pmod{d}. \tag{XIV.5.32}$$

Indeed $(-y, 1)M = (-d, 0)$, and if $u_2 - yu_1$ is divisible by d, the two column operations express the representative in the image. The adjugate gives a lift for every torsion class. In particular

$$A = \operatorname{adj} M = zI - M, \qquad MA = AM = dI, \tag{XIV.5.33}$$

$$\eta_{10} = A\,(ue_2) = \begin{pmatrix} -1 \\ x \end{pmatrix} u, \qquad \eta_H = -h \quad \text{for } zh = (-z)\eta_H. \tag{XIV.5.34}$$

Here h denotes the scalar 5 profile and u a scalar 10 profile in the cyclic frame. Figure XIV.5.2 compares the elimination in the two presentations when both have determinant xy. A shared annihilator does not give the number of independent values at a node.

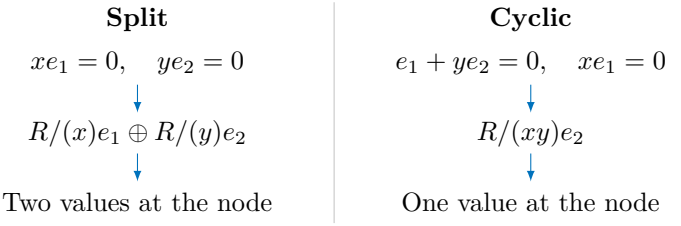


Figure XIV.5.2: Taking the 10 cokernel at fixed determinant xy. In the split case each column kills a multiple of one generator. In the cyclic case the unit in the second column eliminates e_1 and the remaining relation is $xye_2 = 0$. The dimensions below are those of the module fibers at the origin, not numbers of compact zero modes.

The determinant annihilates either doublet module in Figure XIV.5.2, but it is not the only useful test. At the node with $m = \delta = 0$, set $x = y = 0$ after taking the cokernel. Taking this fiber commutes with taking a cokernel, since it just evaluates the relation matrix at the point. Hence

$$\mathcal{M}_{10}^{\mathrm{split}} \otimes_R R/(x, y) \simeq \mathbb{C}^2, \qquad \mathcal{M}_{10}^{\mathrm{cyc}} \otimes_R R/(x, y) \simeq \mathbb{C}. \tag{XIV.5.35}$$

This is a test of generator values. At a smooth point of either branch away from the node both modules have one value. For instance on $x = 0$, $y \neq 0$, the split survivor is e_1, while the cyclic quotient sends e_1 to $-ye_2$, a nonzero generator there. At the node that coefficient vanishes. Thus a field that is a good generator on the punctured branch need not trivialize the whole module near the node.

The lift also records why a change of holomorphic representative need not alter the primitive pole. If u is a doublet column and $u' = u + M\chi$, then

$$Au' = Au + d\chi, \qquad \frac{Au'}{d} = \frac{Au}{d} + \chi. \tag{XIV.5.36}$$

The difference is holomorphic across $d = 0$, so only the meromorphic part is tied to the localized class. For the scalar action $-z$, a change $h \mapsto h + z\ell$ likewise adds a holomorphic term to $-h/z$. This is the mechanism that makes the subsequent residue insensitive to the extension of a mode off its own matter curve.

For comparison with the ordinary local E_6 block, the traceless part satisfies $M_0^2 = kI$, where $k = z^2/4 - d$. For $\tau = 1$ let $T = (M_0 e_2, e_2)$. Then $\det T = 1$, $M_0(Te_1) = kTe_2$ and $M_0(Te_2) = Te_1$. Consequently

$$T^{-1} M_0 T = \begin{pmatrix} 0 & 1 \\ k & 0 \end{pmatrix}, \qquad (x_{\mathrm{src}}, y_{\mathrm{src}}) = (k, -z/2). \tag{XIV.5.37}$$

At the simple point $\partial_x k = 1$, $\partial_y k = 0$, so the Jacobian of $(k, -z/2)$ is $-1/2$. At $d = xy$ one instead has $k = (x - y)^2/4$ and this Jacobian vanishes at the origin. The frame change still works, but the displayed functions are no longer surface coordinates at the collision. We will use the torsion lifts in the original coordinates. This avoids treating a multiple intersection as transverse by changing to a singular chart.

XIV.5.3 A worked residue at an intersection

Why does the holomorphic cubic depend on the germs near the meeting point rather than on an integral of their metric norms? At cubic order the superpotential in (XIV.5.20) contains $\mathrm{Tr}(\varphi \wedge a \wedge a)$. On a patch without explicit sources, represent two torsion classes by meromorphic gauge primitives η_i/f_i, and keep the third class holomorphic. To see the localization, choose smooth cutoffs ρ_i vanishing near $f_i = 0$ and equal to one outside slightly larger tubes. For each primitive a smooth representative is

$$\xi_i = -\rho_i \eta_i / f_i, \qquad a_i = \bar\partial \xi_i, \qquad \varphi_i = (1 - \rho_i) h_i, \qquad f_i h_i = [\Phi, \eta_i]. \tag{XIV.5.38}$$

Since ρ_i vanishes at the pole, the smooth representative still has the original holomorphic class. Its a_i is confined to the transition tube; the field is gauge trivial outside. When the divisors intersect only at isolated points, one can use the tubes to isolate the contribution of each point.

For our cubic the two denominators can be taken as $f_1 = z$, $f_2 = d$. Use the 5 as one torsion primitive and one 10 as the other. Keeping both denominators equal to d would leave a curve of common zeros and would not define the two-circle contour. In the two-tube calculation, trace invariance and integration by parts combine the cubic terms into the boundary class represented on the overlap by

$$\frac{\mathrm{Tr}([\eta_1, \eta_2]\varphi_3)}{f_1 f_2}. \tag{XIV.5.39}$$

Here the numerator is a holomorphic two-form. The integration by parts replaces the cutoff derivatives by the jumps from zero to one. Equivalently, integrate on the two

tube boundaries and take their oriented common contour. This is the local residue prescription for the classical undeformed cubic. It assumes holomorphic torsion modes, an isolated complete intersection, and the common invariant from the local exceptional model. In particular it does not require a flat metric for the variable background. It also does not calculate the normalizability of the modes used in the cubic.

The cutoff step can be seen explicitly at a transverse point. In local coordinates f_1, f_2, take each cutoff to depend only on $|f_i|$. Writing $f_i = r_i e^{i\theta_i}$, the relevant one-variable factor on its transition annulus is

$$\frac{1}{2\pi i}\bar\partial\rho_i \wedge \frac{df_i}{f_i} = \frac{\rho_i'(r_i)}{2\pi}\, dr_i \wedge d\theta_i. \tag{XIV.5.40}$$

The angular integral projects a holomorphic function to its constant term and the radial integral is the jump of ρ_i, namely one. In two variables the ordered product of these annulus integrals gives the two ordered Cauchy integrals. For a nontransverse isolated complete intersection the equations may fail to be coordinates. The boundary residue prescription still uses their two phase circles, and we will reduce it to one-variable Cauchy theory after a valid change of denominator. One must not divide by a Jacobian that vanishes at the common zero.

For scalar numerator N define the ordered residue with coordinate two-form $dx \wedge dy$ by

$$\mathrm{Res}_{(z,d),p}\, \frac{N\, dx \wedge dy}{zd} = \frac{1}{(2\pi i)^2}\int_{\Gamma_p} \frac{N\, dx \wedge dy}{zd}, \qquad \Gamma_p = \{|z| = \varepsilon_1,\ |d| = \varepsilon_2\}_p. \tag{XIV.5.41}$$

The orientation is increasing $\arg z$ followed by increasing $\arg d$. Figure XIV.5.3 shows the radial picture at a transverse point. The marked corner represents two independent phase circles. Interchanging the equations reverses the orientation even though their product is unchanged. A change $g = Bf$ between ordered pairs defining the same local complete intersection uses the residue transformation law:

$$\mathrm{Res}_f\, \frac{N\, dx \wedge dy}{f_1 f_2} = \mathrm{Res}_g\, \frac{N \det B\, dx \wedge dy}{g_1 g_2}. \tag{XIV.5.42}$$

In particular (P, b_5) differs from (z, d) by a diagonal matrix with entries $-U, 6 + 2z$, not by the identity.

Insert the lifts from (XIV.5.34) into (XIV.5.39). With u, v the doublet representatives, the pairing in the 10 sector for fixed singlet h is

$$B_h(u, v) = \mathrm{Res}_{(z,d),p}\, \frac{h\, \epsilon(Au, v)\, dx \wedge dy}{zd}. \tag{XIV.5.43}$$

We have factored out a single nonzero common coefficient κ, including the sign from $\eta_H = -h$. We use this same convention throughout. There is no separate normalization or sign choice at the second point in a two-point sum. The order of the denominators and the doublet convention $\epsilon(e_1, e_2) = 1$ fix the relative signs displayed below.

Three calculations show that (XIV.5.43) is a bilinear on the indicated holomorphic classes. For any two by two matrix A, $\epsilon(Au, v) + \epsilon(u, Av) = (\mathrm{tr}\, A)\epsilon(u, v)$. Here $\mathrm{tr}\, A = z$. Hence

$$\epsilon(Au, v) - \epsilon(Av, u) = z\epsilon(u, v). \tag{XIV.5.44}$$

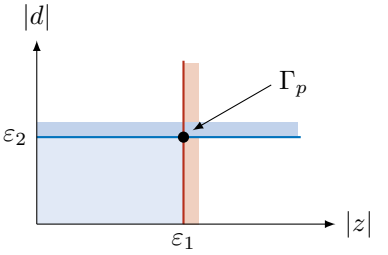


Figure XIV.5.3: Radial projection of the two tube boundaries for the transverse pair (z, d). The small rectangle marks their interiors. At the corner $|z| = \varepsilon_1, |d| = \varepsilon_2$, the full contour has two phase circles with the stated order. Cutoff derivatives are supported in the narrow transition bands.

The right side vanishes under the residue because its numerator is in the denominator ideal. This gives the required symmetry in the two 10 profiles. The tensor on their $SU(5)$ indices is symmetric under exchanging the two antisymmetric pairs. Next use $AM = dI$, the adjoint identity $\epsilon(a, Mb) = \epsilon(Aa, b)$ for the alternating form, and $A^2 - zA + dI = 0$. The variations under the two doublet shifts are

$$\epsilon(A(u + M\chi), v) - \epsilon(Au, v) = d\epsilon(\chi, v), \tag{XIV.5.45}$$

$$\begin{aligned} \epsilon(Au, v + M\chi) - \epsilon(Au, v) &= \epsilon(A^2 u, \chi) \\ &= z\epsilon(Au, \chi) - d\epsilon(u, \chi). \end{aligned} \tag{XIV.5.46}$$

Both vanish in the residue. Finally, changing h by $z\ell$ adds a multiple of z to the numerator. These tests are useful even for a double intersection, where a function vanishing at the point need not lie in the denominator ideal.

We can also change frames without changing the interaction. Let $G(x, y)$ be holomorphic and invertible, with $M' = GMG^{-1}$ and $u' = Gu$, $v' = Gv$. Then $A' = GAG^{-1}$ and

$$\epsilon(A'u', v') = (\det G)\epsilon(Au, v), \qquad h' = (\det G)^{-1} h. \tag{XIV.5.47}$$

Thus the doublet and dual singlet changes cancel pointwise. The trace and determinant stay fixed. In an $SL(2)$ frame the singlet component itself stays fixed; for example $G = \left(\begin{smallmatrix} 1 & x \\ 0 & 1 \end{smallmatrix}\right)$ changes the quotient row to $(-y, 1 + xy)$. It sends e_2 to $(x, 1)^T$, on which the new row is one. Omitting the representative transformation would compare different fields. No derivative of the holomorphic frame enters the pairing. For a coordinate or canonical-bundle frame change the numerator two-form must likewise be transported: the Jacobian acts on $dx \wedge dy$, and any units in the ordered equations are accounted for by (XIV.5.42). The contour formula uses the form and the equations together.

As a coordinate example, take $x' = (1 + y)x$, $y' = y$ near the simple point. This has Jacobian $1 + y$, a unit. Holding the represented two-form fixed gives

$$dx \wedge dy = \frac{dx' \wedge dy'}{1 + y'}, \qquad d = \frac{y' - 1}{1 + y'} x', \qquad z = \frac{x'}{1 + y'} + y'. \tag{XIV.5.48}$$

Thus the light determinant differs from the new coordinate equation $x' = 0$ by another unit. If we replace the second denominator by x' after changing coordinates, we divide the numerator by the determinant factor $(y' - 1)/(1 + y')$. Together with the volume factor this leaves $1/(y' - 1)$, the same unit that relates d to x in the original chart. A residue may be evaluated in any such coordinates; keeping the bare coefficient of the two-form fixed while changing the coordinates would instead change the form.

At the simple point $p = (0, 0)$, $d = x(y - 1)$ and

$$J_{(z,d)}(x, y) = \det \begin{pmatrix} 1 & 1 \\ y - 1 & x \end{pmatrix} = x - y + 1, \qquad J_{(z,d)}(p) = 1. \tag{XIV.5.49}$$

We can use (z, d) as local coordinates. The two Cauchy integrals select the constant term of the transformed numerator $N/J_{(z,d)}$, giving $N(p)/J_{(z,d)}(p)$. In the cyclic presentation the two 10 representatives are ue_2, ve_2 and $\epsilon(Ae_2, e_2) = -1$. Consequently

$$B_h(ue_2, ve_2) = -h(p)u(p)v(p), \qquad Y_{h=1}^{(1,x)} = \begin{pmatrix} -1 & 0 \\ 0 & 0 \end{pmatrix}. \tag{XIV.5.50}$$

The x profile vanishes as a class in this simple 10 germ: $d = x(y - 1)$ with $y - 1$ a unit. More generally the bilinear factors through a single evaluation functional on any selected 10 space of germs, and is zero if that functional vanishes or if $h(p) = 0$. There is a geometric intersection even if the chosen modes give zero coupling. For example $h = x$ is nonzero on the 5 curve but gives zero at this point.

A second transverse matrix separates vanishing at the point from vanishing in the matter module. Choose the profiles $(1, y)$ instead of $(1, x)$, still on the cyclic generator. The germ y is nonzero in $R/(x)$ and vanishes only at p on the matter curve. For any constants a, b the restriction of $a + by$ to the length-one intersection algebra is a, giving

$$B_1(a + by, c + ey) = -ac. \tag{XIV.5.51}$$

The same matrix now acts on two independent germs, with a one-dimensional null space. Either vanishing of a matter class or vanishing of its evaluation can give a zero entry; the underlying tests take place in different quotients.

As a numerical orientation check use the original geometric generators (P, b_5). Their ordered Jacobian at p is $(-216)(6) \cdot 1 = -1296$. Their numerator for $h = u = v = 1$ is $(-216)(6)(-1) = 1296$ and the residue stays -1. With unchanged numerator -1 the computation would give $1/1296$, a different coefficient. We now keep the conventions fixed and change the actual polynomials, so that one patch contains two contributions.

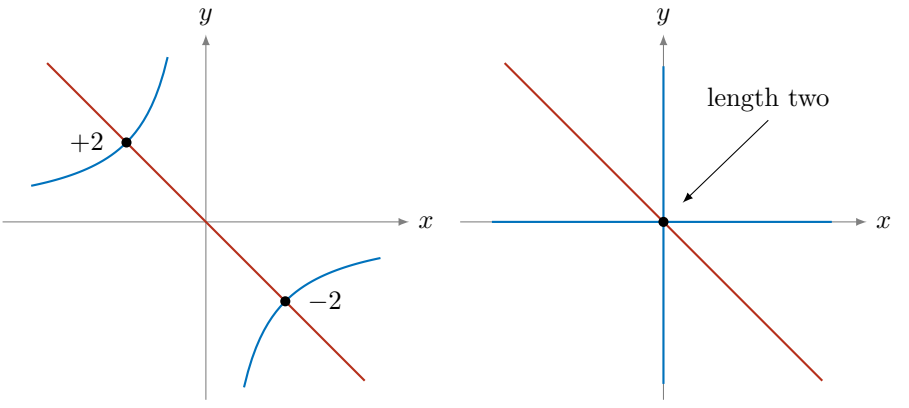
XIV.5.4 Recombination and changed matter

What becomes of the rank-one contribution when two points merge? Take $m = 0$ and $\tau = 1$. The light spectral equation and matter determinant are now

$$Q(s) = (s - x)(s - y) - \delta, \qquad d = xy - \delta. \tag{XIV.5.52}$$

In the spectral chart $s - x, s - y, s$ are coordinates; the first two satisfy a product equation. At $\delta = 0$ their zero loci cross. At $\delta \neq 0$ neither vanishes and the product

equation is smooth. The matter curve at $s = 0$ likewise changes from a pair of axes to a smooth $xy = \delta$. The 5 curve $z = 0$ stays fixed because the trace is fixed. We compare the two nearby points for $\delta = -r^2$, with r small and nonzero, and their collision at $r = 0$. The specialization with $r = 1/4$ is drawn in Figure XIV.5.4. At each intersection $z = d = 0$ and the spectator units used in Section XIV.5.1 have the same nonzero values as at the simple origin.



$\delta = -1/16$ $\qquad$ $\delta = 0$

Figure XIV.5.4: Real slices of the matter curves. Left: for $\delta = -1/16$, $xy = -1/16$ meets $z = 0$ at $x = -1/4$ and $x = 1/4$. The weights shown are for the cyclic profiles $h = u = v = 1$ at the separate points. Right: at $\delta = 0$ the 10 curve has two branches and the intersection with the 5 curve is a length-two scheme at the origin.

To check the character of the two points in the Tate system, differentiate (XIV.5.8) at $z = d = 0$. The map from (z, d) to (b_5, b_4) has first-order matrix

$$\frac{\partial(b_5, b_4)}{\partial(z, d)} = \begin{pmatrix} 0 & 6 \\ -6 & -7 \end{pmatrix}. \tag{XIV.5.53}$$

At $(x, y) = (t_0, -t_0)$ with $t_0 = \pm r$, the Jacobian of (z, d) with respect to (x, y) is $2t_0$. Thus the two b_5, b_4 collisions are both ordinary transverse ones, with Jacobians $72t_0$ and $b_3 = 6$. At the origin for $r = 0$, $d = xy$ has no linear term and the Jacobian degenerates. The intersection with $z = 0$ must then retain its scheme structure. The smoothing moves genuine Tate collision points; the matrix calculation below uses the original common frame to compare them.

Use $t = x$ along $z = 0$ and retain z as a coordinate normal to that curve in S. Since $y = z - t$, we have

$$dx \wedge dy = -dz \wedge dt, \qquad d = tz - t^2 - \delta, \qquad (z, d) \longmapsto (z, d - tz) = (z, -t^2 - \delta). \tag{XIV.5.54}$$

The equation change has determinant one. Integrating over the z phase first restricts

the numerator to $y = -t$ and leaves

$$\operatorname{Res}_{(z,d)} \frac{N\,dx \wedge dy}{zd} = \operatorname{res}_t \frac{-N(t,-t)}{-t^2-\delta}\,dt. \tag{XIV.5.55}$$

The notation on the right refers to the chosen point, or the sum of all enclosed points if a disk contains both. For cyclic representatives $N = -huv$. In the separated case the derivative of the remaining denominator at t_0 is $-2t_0$. Equivalently, the original ordered Jacobian $\partial(z,d)/\partial(x,y)$ at the point is $x - y = 2t_0$. The separate pairing is therefore

$$B_{h,t_0}(u,v) = -\frac{h(t_0)}{2t_0}\,u(t_0)v(t_0). \tag{XIV.5.56}$$

In the following formulas h, u, v denote profiles restricted to $y = -t$. They are held in one chart and frame while we add residues.

On the space of profiles $(1,t)$ and for $h = 1$, evaluate the vector $(1,t_0)^T$. At $r = 1/4$ this gives

$$Y_{-1/4} = \begin{pmatrix} 2 & -1/2 \\ -1/2 & 1/8 \end{pmatrix}, \quad Y_{+1/4} = \begin{pmatrix} -2 & -1/2 \\ -1/2 & -1/8 \end{pmatrix}, \quad Y_{-1/4}+Y_{+1/4} = \begin{pmatrix} 0 & -1 \\ -1 & 0 \end{pmatrix}. \tag{XIV.5.57}$$

Each determinant is zero, since each matrix is a single outer product. The two evaluation functionals are independent on $(1,t)$ for every $r \neq 0$. Their weighted sum here is nondegenerate; keeping only the point with $t > 0$ would leave rank one. The diagonal terms cancel and the off-diagonal terms add. This cancellation also explains why one should take the collision limit on the sum rather than separately on the two divergent constant-profile entries.

In general, write $F(t) = h(t)u(t)v(t)$ for fixed holomorphic profiles on a disk containing both points. The sum becomes a divided difference:

$$-\frac{F(r)}{2r} + \frac{F(-r)}{2r} = -F'(0) - \frac{r^2}{3!}F'''(0) + O(r^4). \tag{XIV.5.58}$$

The odd Taylor terms survive and even terms cancel. The sum on $(1,t)$ at $h = 1$ is independent of r, because products of those two profiles have degree at most two. This does not make the entire pairing independent of r: $F = t^3$ has sum $-r^2$. As a change of Higgs input at fixed r, take $h = t - r$. The point at r drops out, and the point at $-r$ has coefficient -1 times its evaluation outer product. Point count alone gives neither the weights nor the rank on the chosen mode space.

More generally, one can determine the rank of the two-point sum on $(1,t)$ without adding four entries. The evaluation matrix E takes the coefficients of a profile to its values at $-r$ and r. Thus

$$E = \begin{pmatrix} 1 & -r \\ 1 & r \end{pmatrix}, \qquad Y_h = E^T \operatorname{diag}\left(\frac{h(-r)}{2r}, -\frac{h(r)}{2r}\right) E, \qquad \det Y_h = -h(-r)h(r). \tag{XIV.5.59}$$

The determinant of E cancels the two inverse powers of r in the determinant of the diagonal factor. This shows why separate poles can diverge even as their sum has finite nonzero determinant. For $h = t$, both weights are $-1/2$ and the matrix is $\operatorname{diag}(-1, -r^2)$.

It has rank two at every nonzero separation but becomes rank one at collision. By contrast $h = 1$ leaves rank two at collision. These examples change the behavior of the same coalescing poles by changing which Taylor coefficients their weights probe.

The algebra of restrictions explains how two independent evaluations turn into a value and derivative. For $r \neq 0$, reducing a profile on the 5 curve modulo $t^2 - r^2$ keeps the same two evaluations. The inverse to the evaluation map sends their values a_-, a_+ to

$$a_- e_-(t) + a_+ e_+(t), \qquad e_-(t) = \frac{1 - t/r}{2}, \qquad e_+(t) = \frac{1 + t/r}{2}. \tag{XIV.5.60}$$

These are the two orthogonal idempotents: $e_+ e_- = 0$ and $e_\pm^2 = e_\pm$ modulo $t^2 - r^2$. Their pairing at $h = 1$ is diagonal with weights $1/(2r), -1/(2r)$. The idempotent basis becomes singular as r goes to zero. The regular basis $(1, t)$ can instead be carried across the collision, with

$$1 = e_- + e_+, \qquad t = r(e_+ - e_-), \qquad t^2 = r^2. \tag{XIV.5.61}$$

For any polynomial product $F(t)$ reduce it to $F_0(r) + F_1(r)t$ using this relation. The divided difference in (XIV.5.58) is $-F_1(r)$ exactly. For instance t^4 reduces to the constant r^4 and contributes zero, while t^5 reduces to $r^4 t$ and contributes $-r^4$. In the limit all terms of degree at least two are killed before extracting the linear term. Thus two point values determine two pieces of data while they are distinct. At the collision one can still extract two pieces if one transports the constant term and the divided difference, rather than transporting the evaluation basis. This gives an algebraic version of the fixed-contour limit.

At $r = 0$, the ordered reduction gives $\operatorname{res}(-F/t^2)\, dt$. The common zero is supported at one point, but its intersection algebra is

$$\mathcal{A} = R/(z, d) \simeq \mathbb{C}\{t\}/(t^2) = \mathbb{C} \cdot 1 \oplus \mathbb{C} \cdot t, \qquad t^2 = 0. \tag{XIV.5.62}$$

A nonzero class can have zero value at the point: t has that property. The residue takes the coefficient of t in $-huv$, not the value of huv at zero. It is the derivative limit in (XIV.5.58). The equality follows from Cauchy's formula on a fixed circle enclosing both poles, which also works when the two poles coalesce. Replacing the two point residues by twice the evaluation at zero would discard the t class.

Write $h = h_0 + h_1 t$ in $\mathcal{A}$. Multiplication by h followed by extraction of $-[t]$ gives

$$B_h(u, v) = -[t](huv), \qquad Y_h = -\begin{pmatrix} h_1 & h_0 \\ h_0 & 0 \end{pmatrix}, \qquad \det Y_h = -h_0^2. \tag{XIV.5.63}$$

For $h = 1, t, t^2$ this has rank two, one and zero, respectively. The last germ is nonzero on the 5 curve but restricts to zero in $\mathcal{A}$. To see the two rank-one and rank-zero mechanisms directly, note that multiplication by t sends the basis $(1, t)$ to $(t, 0)$, whereas multiplication by t^2 kills both. The functional $-[t]$ still detects the first image. Multiplication by a unit, characterized by $h_0 \neq 0$, is an automorphism of $\mathcal{A}$ and leaves the pairing nondegenerate there. These are choices of an external 5 mode in one cubic, rather than solutions for a Higgs expectation value.

In the transverse and colliding calculations the local rank bound comes from the dimension of the intersection algebra through which the two profile maps factor. Actual equality requires a sufficiently large image and the corresponding nonzero 5 input. Thus a change in rank can arise from smoothing the geometry, from changing the 5 profile, or from changing the allowed 10 profiles. The next comparison holds the spectral polynomial fixed and changes the holomorphic presentation itself.

XIV.5.5 A nilpotent Higgs background

Can the same spectral equation give different couplings of specified matter modes? Set $m = \delta = 0$ and compare two choices of τ:

$$M_{\mathrm{s}} = \begin{pmatrix} x & 0 \\ 0 & y \end{pmatrix}, \qquad M_{\mathrm{g}} = \begin{pmatrix} x & 1 \\ 0 & y \end{pmatrix}, \\ \det(sI - M_{\mathrm{s}}) = \det(sI - M_{\mathrm{g}}) = (s-x)(s-y). \tag{XIV.5.64}$$

The subscripts refer to the split and glued presentations. The two matrices give identical b_i, including their homogeneous lifts. At the origin M_{s} vanishes, whereas M_{g} has rank one and square zero. A nonsingular gauge change would conjugate their values at the origin, preserving rank, so no such change relates the germs. Away from $x = y$ a change of eigenbasis is possible: the eigenvectors of M_{g} can be taken as e_1 and $(1, y-x)^T$. Their determinant $y - x$ vanishes on the seam. Rescaling the second vector to determinant one replaces this degeneration by a pole. The matrix can therefore be diagonal on the punctured chart while its nilpotent behavior at the seam remains part of the background. We use T-brane for this type of Higgs data, which eigenvalues alone do not determine.

A spectral module keeps precisely the information lost by recording only the eigenvalues: it is R^2 with the additional variable s acting as the Higgs matrix. For M_{g} the vectors $(M_{\mathrm{g}}e_2, e_2)$ form a basis. Acting on the generator e_2 by $a + bs$ gives $ae_2 + bM_{\mathrm{g}}e_2$. The only polynomial relation needed is the characteristic equation, by division by the monic quadratic and independence of these two vectors. The two spectral modules are

$$\mathcal{S}_{\mathrm{g}} = R[s]/((s-x)(s-y)), \qquad \mathcal{S}_{\mathrm{s}} = R[s]/(s-x) \oplus R[s]/(s-y). \tag{XIV.5.65}$$

Evaluation on the two sheets takes $a + bs$ to $(a + bx, a + by)$. The difference is $b(x - y)$. Conversely, if $F - G$ is divisible by $x - y$, take $b = (F - G)/(x - y)$ and $a = F - bx$ to recover the section. This proves the matching condition

$$\mathcal{S}_{\mathrm{g}} \simeq \{(F, G) \in R \oplus R : F - G \in (x - y)\}. \tag{XIV.5.66}$$

The same map is injective because R is a domain and a linear representative vanishing on both sheets has $b(x - y) = 0$. The split module imposes no condition on F, G.

Passing to the 10 matter quotient means imposing $s = 0$. For $\mathcal{S}_{\mathrm{g}}$ this gives $R/(xy)$, and restricting to the two axes gives a different matching condition:

$$R/(xy) \simeq \{(F(y), G(x)) : F(0) = G(0)\}, \qquad (F, G) \longmapsto F(y) + G(x) - F(0). \tag{XIV.5.67}$$

The second map gives an inverse in the quotient, since all terms divisible by xy disappear. Here the agreement is at the base node, rather than all along $x = y$ in the spectral description. The split matter quotient in (XIV.5.31) still has independent constants. Figure XIV.5.5 distinguishes the two restrictions. In particular the intersection of the support with the zero section does not remove all memory of how the spectral module was assembled.

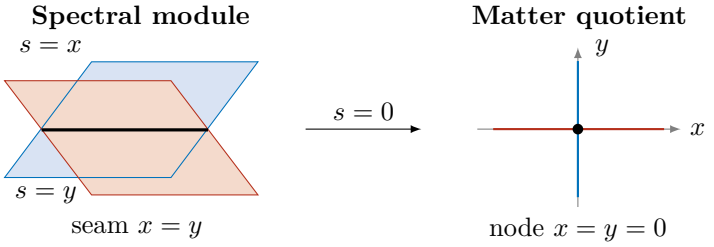


Figure XIV.5.5: The matching locus before and after taking the matter quotient. Left: on the spectral sheets $s = x$ and $s = y$, pairs in the cyclic module agree on the seam $x = y$. Right: after taking $s = 0$, the two matter branches meet at the base node; pairs in the cyclic matter quotient agree there. The split module has no matching condition in either description.

We can compare pairings on these presentations at $h = 1$. For the split matrix $A_{\mathrm{s}} = \mathrm{diag}(y, x)$. If both modes are on the same branch, both vectors in the alternating form are parallel and the numerator vanishes. For opposite branches the two orderings give

$$\epsilon(A_{\mathrm{s}} e_1, e_2) = y, \qquad \epsilon(A_{\mathrm{s}} e_2, e_1) = -x. \tag{XIV.5.68}$$

On $z = 0$ each numerator becomes $-t$. The one-variable residue in (XIV.5.55) extracts $[t]$ of that numerator at $\delta = 0$, giving -1 in both orders. Additional powers of x or y multiply this numerator by at least one power of t, so do not contribute. On the full split test space (e_1, ye_1, e_2, xe_2) the matrix is

$$Y_{\mathrm{s}} = \begin{pmatrix} 0 & 0 & -1 & 0 \\ 0 & 0 & 0 & 0 \\ -1 & 0 & 0 & 0 \\ 0 & 0 & 0 & 0 \end{pmatrix}. \tag{XIV.5.69}$$

It has rank two. On the same-branch list (e_2, xe_2) it restricts to zero. In the glued presentation that list is a cyclic value and first derivative and gives the rank-two matrix in (XIV.5.63) at $h = 1$. This comparison uses the listed representatives in each module. It does not identify the two abstract spaces of allowed modes, and there is no general inequality between their total ranks. In fact the two presentations here both exhibit rank two when the relevant directions are retained. What changed is the rule for which representatives couple.

The split calculation also exhibits a useful vanishing test for a changing 5 profile.

With general h on the 5 curve, the residue of the split cross term at the node is

$$[t]\big(-t\,h(t)F(-t)G(t)\big) = -h(0)F(0)G(0) \tag{XIV.5.70}$$

for a first-branch profile $F(y)$ and a second-branch profile $G(x)$. This follows because the adjugate has already supplied one power of t. Thus $h = t$ kills the whole split pairing, whereas the glued cyclic form at $h = t$ retains rank one. Both backgrounds have the same ideal (z, d); they do not place the same numerator into that ideal's residue. A derivative in the residue functional need not differentiate each input profile. It acts on the full product, including any zeros required by the representation and the matrix.

We now separate the role of the metric in an independent example. On a flat bidisc $|x| < 1$, $|y| < 1$ take $\Phi = N\,dx \wedge dy$ with constant

$$N = \begin{pmatrix} 0 & 1 \\ 0 & 0 \end{pmatrix}, \qquad N^2 = 0, \qquad \det(sI - N) = s^2. \tag{XIV.5.71}$$

The zero field has the same spectral equation. Its module is $(R[s]/s)^2$, while N has module $R[s]/s^2$ by the cyclic basis (Ne_2, e_2). The holomorphic equations hold for both in holomorphic gauge. For the zero field we can take $H = I$ and the flat connection. For N the same choice gives $[N, \bar{N}^T] = D_0$ with $D_0 = \mathrm{diag}(1, -1)$, so the moment map fails. This mismatch asks for a Chern curvature rather than a new spectral polynomial.

Choose a real function $f(x, \bar{x})$ and use

$$H = \mathrm{diag}(e^f, e^{-f}), \qquad \omega = \tfrac{i}{2}(dx \wedge d\bar{x} + dy \wedge d\bar{y}), \qquad A^{1,0} = H^{-1}\partial H = (\partial f)D_0. \tag{XIV.5.72}$$

The holomorphic Chern frame still has $A^{0,1} = 0$. With $F = \bar{\partial}A^{1,0}$, the ordered coefficient of $dx \wedge d\bar{x}$ in F is $-f_{x\bar{x}}D_0$. The adjoint with respect to H is

$$N^{\dagger_H} = H^{-1}\bar{N}^T H = \begin{pmatrix} 0 & 0 \\ e^{2f} & 0 \end{pmatrix}, \qquad [N, N^{\dagger_H}] = e^{2f}D_0. \tag{XIV.5.73}$$

The form $dx \wedge dy \wedge d\bar{x} \wedge d\bar{y}$ has a minus sign relative to $dx \wedge d\bar{x} \wedge dy \wedge d\bar{y}$. Thus the latter ordered volume coefficient of (XIV.5.22) is $(f_{x\bar{x}} - e^{2f})D_0/2$. The scalar equation has the positive metric solution

$$f = -\log(1 - |x|^2), \qquad \partial f = \frac{\bar{x}}{1 - |x|^2}\,dx, \qquad f_{x\bar{x}} = \frac{1}{(1 - |x|^2)^2} = e^{2f}. \tag{XIV.5.74}$$

All eigenvalues of H are positive on the stated open bidisc. If one used $\bar{N}^T$ for the adjoint in this frame, the curvature above would leave a residual coefficient $(e^{2f} - 1)D_0/2$ away from $x = 0$. The solution is local, and its behavior at the boundary is not a compact boundary condition.

The solution can be checked in an orthonormal frame as well. Write $G = H^{1/2}$, so a column in the orthonormal frame is G times its column in the holomorphic frame. With $A = A^{1,0}$ as in (XIV.5.72),

$$A_{\mathrm{u}} = GAG^{-1} - dG\,G^{-1} = \tfrac{1}{2}(\partial f - \bar{\partial} f)D_0, \qquad N_{\mathrm{u}} = GNG^{-1} = e^f N. \tag{XIV.5.75}$$

Here A_{u} is anti-Hermitian because f is real. The x derivative of N_{u} in the antiholomorphic direction is no longer zero, but $[D_0, N] = 2N$. Consequently

$$\bar{\partial}(e^f N) + [A_{\mathrm{u}}^{0,1}, e^f N] = (\bar{\partial} f) e^f N - (\bar{\partial} f) e^f N = 0. \tag{XIV.5.76}$$

In this frame the ordinary Hermitian adjoint is appropriate, and the commutator of N_{u} with its adjoint is still $e^{2f} D_0$. The two frames describe the same local solution. Using an ordinary adjoint on the old constant matrix with the new curvature would mix the two frames.

A positive Hermitian metric cannot make a nonzero nilpotent normal: such an operator would be unitarily diagonalizable and all its eigenvalues would vanish. Thus at the nilpotent point of the variable $SU(5)$ light block, any solution in this description needs nonzero curvature to cancel the commutator there. Equation (XIV.5.74) solves the separate constant problem. It gives neither a metric for (XIV.5.64) nor compact boundary data. The residue calculation uses the prescribed holomorphic Higgs classes, while a physical background and kinetic norms require additional compatible data.

XIV.5.6 Holomorphic and normalized couplings

When can the rank of a local pairing be used in a four-dimensional theory? The global modes must first restrict to the germs on which the residue acts. In a compatible compact Higgs background the mode space V_{10} is obtained from the appropriate twisted sheaf cohomology or Higgs complex. Write $j_p : V_{10} \to \mathcal{A}_p$ for the restriction to the cyclic intersection algebra at p, and assume a fixed global 5 mode with restriction h_p. On a common basis the point contributions give a holomorphic matrix of the form

$$Y = \sum_p j_p^T B_{h_p, p} j_p. \tag{XIV.5.77}$$

This equation uses the classical local residue prescription and consistently transported frames at all the points in the sum. An overall invariant coefficient has again been suppressed. The rank bound from an intersection algebra applies to its point contribution; the sum requires the actual maps from the same generation space. The formal flux period of Chapter 4 is not a prescription for any of these maps.

For a worked restriction take the glued collision with $h = 1$, so B_1 has rank two on $(1, t)$. The line spanned by 1 is isotropic for this symmetric bilinear: the residue of the product of two constants vanishes. In contrast, the line spanned by $1 + t$ gives $B_1(1+t, 1+t) = -2$. More generally, for the line with generator $1 + at$ the restriction is

$$B_1(1 + at, 1 + at) = -[t](1 + 2at + a^2 t^2) = -2a. \tag{XIV.5.78}$$

Both choices have one input direction, but one yields rank zero and the other rank one. There is a derivative in the residue, so having a nonzero value at the intersection does not by itself ensure a nonzero pairing. These examples specify the image of a toy restriction. They do not say which sections a compact quadric model realizes.

A restriction may preserve rank two even if the chosen global list is much larger than two. At a single point write the image of a field q_i as $a_i + b_i t$. For $h = 1$ the

matrix has entries

$$(j^T B_1 j)_{ij} = -a_i b_j - b_i a_j. \tag{XIV.5.79}$$

If the row vectors (a_i) and (b_i) are independent, j is surjective and j^T is injective. Since B_1 is invertible on the jet space, the rank is then exactly two. For example the two images $1+t$ and $1-t$ yield diagonal entries $-2, 2$ and a zero cross term. If the two rows are dependent, the rank is at most one; an isotropic image can still make the result zero. This reasoning uses only the fixed point contribution. A sum over points can mix different value and derivative rows or cancel parts of earlier contributions, so its rank cannot be read off by counting local algebras.

Suppose a finite set of normalizable modes and their positive kinetic forms are given. For one 5 field H_5 and a column q of 10 fields, omit gauge indices and use the rigid conventions

$$W = \tfrac{1}{2} q^T Y q\, H_5, \qquad K = q^\dagger Z_{10} q + Z_5 |H_5|^2. \tag{XIV.5.80}$$

The matrix Z_{10} is positive Hermitian and $Z_5 > 0$. In a dimensional reduction these are overlap norms of the full modes with the background metric and measure; their values do not follow from (XIV.5.77). Set $L = Z_{10}^{1/2}$, the positive Hermitian square root. Then $q_c = Lq$ and $H_{5,c} = \sqrt{Z_5}\, H_5$ have unit quadratic kinetic terms. Substituting the inverse redefinition in the holomorphic expression gives

$$Y_c = \frac{L^{-T} Y L^{-1}}{\sqrt{Z_5}}. \tag{XIV.5.81}$$

The first inverse is transposed because both occurrences of q in W are holomorphic. Hermitian conjugation occurred in the kinetic form; it does not occur in this substitution. Invertible left and right factors preserve matrix rank, although the entries and physical singular values generally change.

For an explicit complex example, stipulate

$$L = \begin{pmatrix} 2 & i \\ -i & 2 \end{pmatrix}, \qquad Z_{10} = L^2 = \begin{pmatrix} 5 & 4i \\ -4i & 5 \end{pmatrix}, \qquad Z_5 = 4, \qquad Y = \mathrm{diag}(-1, 0). \tag{XIV.5.82}$$

The eigenvalues of L are one and three, so it is the positive square root of Z_{10}. The example takes the same matrix form as the transverse pairing, now with a stipulated two-dimensional field space and kinetic data. The inverse $L^{-1} = \frac{1}{3}\left(\begin{smallmatrix} 2 & -i \\ i & 2 \end{smallmatrix}\right)$ has first row $(2, -i)/3$. The normalized matrix is minus the symmetric outer product of this row, divided by two:

$$Y_c = \frac{1}{18} \begin{pmatrix} -4 & 2i \\ 2i & 1 \end{pmatrix}. \tag{XIV.5.83}$$

Without the transpose one would obtain $(1/18)\left(\begin{smallmatrix} -4 & 2i \\ -2i & -1 \end{smallmatrix}\right)$, which is not symmetric. This diagnostic needs complex kinetic data; a real symmetric L would hide the mistake. In a holomorphic polynomial the antisymmetric part would drop out, and discarding it would not recover the stated congruence.

There is a basis freedom even after fixing unit kinetic terms. If L' is another invertible factor with $L'^\dagger L' = Z_{10}$, then $U = L' L^{-1}$ is unitary, since

$$U^\dagger U = L^{-1} L'^\dagger L' L^{-1} = I, \qquad Y_c' = U^{-T} Y_c U^{-1}. \tag{XIV.5.84}$$

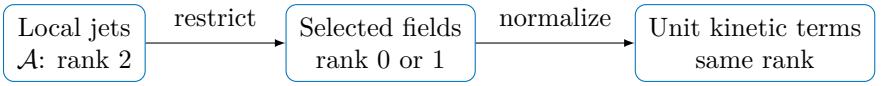


Figure XIV.5.6: Three steps in forming a four-dimensional coupling. The same rank-two local jet pairing can give rank zero or one under the two sample restrictions of (XIV.5.78). A subsequent invertible kinetic congruence preserves the rank on the selected field space. The arrows require a restriction map and a positive kinetic form, respectively.

A numerical entry of Y_c thus depends on the chosen unitary basis. Its singular values do not: both factors multiplying Y_c are unitary. In this example the normalized matrix is an outer product and its one nonzero singular value is the squared norm of $(2,-i)/3$ divided by two, namely $5/18$ in the stated units and with κ factored out. This number illustrates the dependence on the given positive norms. It is not a prediction for a compact model in which those norms and the overall coefficient have not been calculated.

Figure XIV.5.6 summarizes the order of these operations. The geometric equations determine the local intersection algebra. The holomorphic Higgs action, including its gluing, and the selected fields determine the residue on the image of their germs. Kinetic normalization then acts on the resulting field space. Replacing a projection by an invertible field redefinition would miss the possible rank loss in (XIV.5.78). In the compact supergravity theory additional normalization factors may enter. The local examples here establish neither the compatible global Higgs background nor the wavefunction metrics needed for that theory. Later effective-action and compact-model chapters use those inputs when they are available.

Exercises

1. **Change the equations and the doublet frame.** At the simple point use the ordered generators (ad, bz) for nonzero constants a, b, and $G = \left(\begin{smallmatrix} 1 & \lambda y \\ 0 & 1 \end{smallmatrix}\right)$ for the doublet frame. With $h = u = v = 1$ in the original cyclic frame, give the equation-change determinant, the new Jacobian and numerator at the point, and the transported residue. In the new frame give the coefficient of y^2 in the second entry of the transported quotient row and its value on Ge_2. Use $(a, b, \lambda) = (2, -3, 3)$ for the sample. Explain why leaving the doublet column fixed while transforming the row is not the same change of frame.

2. **Change the two poles and then collide them.** Use $\delta = -1/9$ and $h = t + 2$ with profiles $(1, t)$. Compute the negative and positive point matrices separately, their sum and its rank. At $\delta = 0$ instead take $h = 2t + t^2$, and give the new matrix and rank. Explain why this last pairing is not the limit of the separated pairing with $h = t + 2$ held fixed.

3. **Change the constant nilpotent amplitude.** On the same bidisc replace N by cN with $c = 2$ real and positive. Seek $f = -\log(1 - |x|^2) + k$ and give e^k and the coefficient of D_0 in the moment map with the correct and the ordinary transpose adjoints at $|x|^2 = 1/3$. Explain why this does not solve the variable background.

4. **Restrict and normalize.** Compute the restricted jet pairing and rank on $1 + 2t$. Separately take $L = \left(\begin{smallmatrix} 3 & 2i \\ -2i & 3 \end{smallmatrix}\right)$, $Z_5 = 9$ and $Y = \mathrm{diag}(-1, 0)$. Find the eigenvalues of L, the normalized matrix and its rank. Explain what extra input identifies the restriction of actual compact modes.

5. **Compare the full split space and one branch.** With $h = 1$, compare the full split test space with the list (e_2, xe_2) before and after gluing. Use the alternating form to account for each nonzero pairing. Explain how both full pairings can have rank two while the same-branch calculation changes. This is a written exercise.

Use `benchmark/tasks.json` for the JSON fields and `benchmark/PROTOCOL.md` for submission. Written explanations are assessed by a reader.

Status and sources

§1. Tate specialization and the spectral chart. The coefficient lift, factorization and point jets are [MATH]. The meromorphic spectral/Tate identification and ordinary top-channel interpretation are [GEO-E]. See Hayashi et al. (2013), arXiv:1304.1678v2, p. 13, eqs. (3.2)–(3.5); Marsano and Schäfer-Nameki (2011), arXiv:1108.1794v1, printed pp. 27–28 and 35–38, eqs. (3.24),(4.20)–(4.23),(4.46)–(4.48); and Donagi and Wijnholt (2014), arXiv:0904.1218v1, printed pp. 16–17 and 20–21, eqs. (2.45)–(2.53),(2.69)–(2.72). The Tate residuals use the names of Chapter 2. A local spectral frame gives no compact Higgs field or resolved codimension-three fiber incidence.

§2. Twisted fields and charged modules. The classical local equations and the exceptional representation input are [GEO-E]. The holomorphic quotient and frame calculations are [MATH] under the stated equations; the localization interpretation uses the seven-brane description. See Cecotti, Córdova, et al. (2011), arXiv:1010.5780v1, printed pp. 41–45, eqs. (4.1)–(4.2),(4.10)–(4.18), and printed pp. 76–79, eqs. (7.1)–(7.13). The singlet action follows from the dual wedge action and agrees with the E_6 branching and action in eqs. (7.2),(7.5)–(7.7).

§3. Residue and transverse rank. The classical local residue prescription is [GEO-E]; the class invariance, frame transport and simple matrix are [MATH]. See Cecotti, Córdova, et al. (2011), printed p. 49, eqs. (4.34)–(4.36), printed pp. 78–79, eqs. (7.12)–(7.14), and Appendix C, printed pp. 100–103, eqs. (C.3)–(C.24). The denominator order is (z, d) and κ is unassigned.

§4. Smoothing and first jets. The smoothing, point sum, double pole and fixed-background rank changes are [MATH] in the residue model. For the spectral recombination and nonreduced residue method see Cecotti, Córdova, et al. (2011), printed pp. 25–26, eqs. (2.84)–(2.86), and pp. 50–51, eq. (5.3).

§5. Gluing and the Hermitian representative. The equal-polynomial module comparison, specified pairings and constant bidisc solution are [MATH]. See Cecotti, Córdova, et al. (2011), printed pp. 28–29, eqs. (3.4)–(3.13), for the local nilpotent equation, and p. 79, eqs. (7.15)–(7.16), for the source's distinct split example. The constant metric is a separate solution, not a metric for the variable block.

§6. Restriction and kinetic normalization. The restriction and kinetic congruence are [MATH] once the global-mode map and positive norms are specified. See Cecotti, Cheng, et al. (2009), arXiv:0910.0477v2, printed pp. 31–33, eqs. (3.43)–(3.46), and Appendix A, printed pp. 67–68, for the commutative residue and rank bound. No compact restriction map, normalizable basis or physical Yukawa normalization is supplied here.

References

Cecotti, S., M. C. N. Cheng, et al. (2009). "Yukawa Couplings in F-theory and Non-Commutative Geometry". In: arXiv: 0910.0477 [hep-th].

Cecotti, S., C. Córdova, et al. (2011). "T-branes and Monodromy". In: *JHEP* 07, p. 030. arXiv: 1010.5780 [hep-th].

Donagi, R. and M. Wijnholt (2014). "Higgs Bundles and UV Completion in F-theory". In: *Commun. Math. Phys.* 326, pp. 287–327. arXiv: 0904.1218 [hep-th].

Hayashi, H., C. Lawrie, and S. Schäfer-Nameki (2013). "Phases, Flops and F-theory: SU(5) Gauge Theories". In: *JHEP* 10, p. 046. arXiv: 1304.1678 [hep-th].

Marsano, J. and S. Schäfer-Nameki (2011). "Yukawas, G-flux, and Spectral Covers from Resolved Calabi–Yau's". In: *JHEP* 11, p. 098. arXiv: 1108.1794 [hep-th].

Chapter XIV.6

Abelian charges and the global gauge group

XIV.6.1 An extra section and a gauge field

Which piece of an elliptic fourfold can supply a photon? In Chapter 2 the resolved root curves carried charge under the Cartan vectors. An extra section offers another route to a vector: it gives a divisor with which a wrapped membrane can have a nonzero intersection. The section itself still meets the generic elliptic fiber, just as the zero section does. To isolate an abelian direction we must first subtract that common intersection, then remove overlap with the zero section and with any roots. We will build both sections, perform these subtractions, and test the resulting charge on actual curves. The global gauge group will then require a further test: which integral weights and periods occur together?

Take $\pi : Y \to B$ with $B = \mathbb{P}^3$ and let H be its hyperplane class, normalized by $\int_B H^3 = 1$. We use the toric quotient description of elliptic fibers from Volume III. Here the ambient fiber is a blowup of $\mathbb{P}_{1,1,2}$, with coordinates (u, v, w, s) and two independent scalings. The excluded sets and the class of each coordinate divisor are

$$\begin{aligned} &(u, v, w, s) \sim (\lambda u, \lambda\mu v, \lambda^2\mu w, \mu s), \\ &\qquad (u, w) \neq (0, 0), \qquad (v, s) \neq (0, 0), \end{aligned} \tag{XIV.6.1}$$

$$([u], [v], [w], [s]) = (U, U + S + \alpha, 2U + S + \beta, S), \quad \alpha = \beta - \bar{K}, \quad \bar{K} = -K_B = 4H. \tag{XIV.6.2}$$

Here U, S denote ambient coordinate classes and later their restrictions to Y. We suppress base pullbacks in total-space divisor formulas. The twists are $\beta = 5H$ and $\alpha = H$. Twisting changes how the coordinates glue over B; it does not change either scaling on an individual fiber.

The ambient relative anticanonical class is the sum of the four toric coordinate divisors. Adding $\bar{K}$ from the base gives the required hypersurface class

$$-K_{\text{amb}} = 4U + 3S + \alpha + \beta + \bar{K} = 4U + 3S + 2\beta. \tag{XIV.6.3}$$

We call the following standalone family MP-Q2. Its equation is

$$\begin{aligned} P_1 = {} & sw^2 + b_0 s^2 u^2 w + b_1 suvw + b_2 v^2 w \\ & + c_0 s^3 u^4 + c_1 s^2 u^3 v + c_2 s u^2 v^2 + c_3 u v^3 = 0. \end{aligned} \tag{XIV.6.4}$$

For example, $v^2 w$ has class $4U + 3S + 2\alpha + \beta$, so its coefficient has class $2\bar{K} - \beta$. The monomial $s^2 u^3 v$ instead has class $4U + 3S + \alpha$, leaving $2\beta - \alpha = \bar{K} + \beta$ for its coefficient. Applying the same subtraction to all the terms gives

$$([b_0], [b_1], [b_2]) = (\beta, \bar{K}, 2\bar{K} - \beta) = (5, 4, 3)H, \tag{XIV.6.5}$$

$$([c_0], [c_1], [c_2], [c_3]) = (2\beta, \bar{K} + \beta, 2\bar{K}, 3\bar{K} - \beta) = (10, 9, 8, 7)H. \tag{XIV.6.6}$$

The term sw^2 has the required class without any coefficient bundle. We take its coefficient to be one. A bare v^4 cannot be added to (XIV.6.4): its S degree is four and the other terms have degree three. A coefficient pulled back from the base cannot repair a mismatch in a fiber scaling. The degree-four deformation will belong to the blown-down model.

The two nonvanishing conditions in (XIV.6.1) give four charts, according to which pair uv, us, vw, ws is nonzero. In the first three, the matrix of weights of the nonzero coordinates has determinant $+1$ or -1, so those coordinates can be set to one without a residual action. The last pair has determinant two. Setting $w = s = 1$ there leaves the action

$$(u, v) \longmapsto (-u, -v), \qquad P_1\big|_{u=v=0,\ w=s=1} = 1. \tag{XIV.6.7}$$

Thus the hypersurface misses the singular vertex of the ambient quotient in every fiber.

One can also recover the local meaning of this toric surface directly. In $v = 1$ the residual action sends (u, w, s) to $(\lambda u, \lambda w, \lambda^{-1} s)$. The invariant coordinates $u' = su$ and $w' = sw$ are constrained by

$$(u', w') \in \mathbb{C}(u, w), \qquad wu' - uw' = 0, \qquad [u : w] \in \mathbb{P}^1. \tag{XIV.6.8}$$

For $(u', w') \neq (0, 0)$ this fixes a unique direction. Over the origin the direction is free. In $u = 1$ the chart has coordinates $(w/u, su)$, and in $w = 1$ they are $(u/w, sw)$. This is the ordinary blowup of the affine chart $v' = 1$ at $(u', w') = (0, 0)$. Outside that center the projective map is an isomorphism; the quotient singularity in the other chart was not part of the blowup center. Over B the weighted projective bundle and its blowup along the section of centers are projective, giving the projective ambient morphism. In particular a new line exists in the ambient fiber over every point of B, but whether the hypersurface contains it must be tested with its equation.

To see why smoothness holds for a general choice of coefficients, temporarily allow the constant coefficient of sw^2 to vary as well. The four charts are covered by nonvanishing monomials:

$$uv \longrightarrow uv^3, \qquad us \longrightarrow s^3 u^4, \qquad vw \longrightarrow v^2 w, \qquad ws \longrightarrow sw^2. \tag{XIV.6.9}$$

The coefficient bundles of the first three monomials are generated by their global sections. For example, at any chosen base point one can choose a homogeneous polynomial of

degree seven that is nonzero there and multiply uv^3 by it. Thus at every ambient point some member of the linear system does not vanish. On the smooth ambient locus Bertini gives a smooth general member. Restrict to the open set where the coefficient of sw^2 is nonzero and normalize it to one. The remaining ambient singular locus is disjoint by (XIV.6.7). This argument uses the full coefficient spaces; it gives no smoothness conclusion for a particular sparse tuple of polynomials.

The toric ambient bundle is projective over the projective base and locally is a product with the toric surface. Its relative hypersurface equation is nonzero on every surface fiber, since the coefficient of sw^2 is fixed. The fibers of the ambient bundle are integral, so the nonzero equation is a nonzerodivisor on each of them. The relative Cartier divisor criterion gives flatness over B, and adjunction on the smooth locus gives

$$K_Y = (K_{\mathrm{amb}} + [P_1])|_Y = 0. \tag{XIV.6.10}$$

In this argument projectivity, smoothness of the general total space, and flatness have separate causes. Flatness still allows the shape and number of components of a fiber to change.

Now restrict the equation to the two coordinate divisors. At $u = 0$, the exclusion forces $w \neq 0$, and the remaining equation forces $v \neq 0$. In the $v = 1$ chart the residual scaling has weights $(+1, +1, -1)$ on (u, w, s). Set $w = 1$ there. On $s = 0$, again $v \neq 0$, and (u, w) are homogeneous coordinates of weight one. The restrictions give

$$Z = U: \qquad u = 0, \quad s = -b_2 \quad (v = w = 1), \tag{XIV.6.11}$$

$$S: \qquad s = 0, \quad b_2 w + c_3 u = 0 \quad (v = 1). \tag{XIV.6.12}$$

The first equation defines a holomorphic zero section, including over $b_2 = 0$. For the second, the projective point is $[u : w] = [b_2 : -c_3]$ off the locus $C_1 = \{b_2 = c_3 = 0\}$. There the two coefficients no longer select a point: the full projective line satisfies the equation. With b_2, c_3 independent transverse coordinates, this incidence equation is locally the blowup of their common zero locus on B. The generic point defines a rational section; its closure is the divisor S.

The blowdown coordinates have weights $(1, 1, 2)$, with the following map and polynomial identity:

$$[u' : v' : w'] = [su : v : sw], \tag{XIV.6.13}$$

$$\begin{aligned} P_0(u', v', w') = {} & w'^2 + (b_0 u'^2 + b_1 u' v' + b_2 v'^2) w' \\ & + c_0 u'^4 + c_1 u'^3 v' + c_2 u'^2 v'^2 + c_3 u' v'^3, \end{aligned} \tag{XIV.6.14}$$

$$P_0(su, v, sw) = s P_1(u, v, w, s). \tag{XIV.6.15}$$

On the chart $v' = 1$, write $W = w'/v'^2$. The restriction $u' = 0$ gives $W(W + b_2) = 0$. The two roots by themselves do not label the sections. The map of (XIV.6.15), applied to (XIV.6.11) and (XIV.6.12), assigns

$$Z \longmapsto [0 : 1 : -b_2], \qquad S \longmapsto [0 : 1 : 0] \qquad (b_2 \neq 0). \tag{XIV.6.16}$$

For $b_2 = 3$ in a local trivialization the roots are -3 and 0, in that order. At $b_2 = c_3 = 0$ the two images coincide, but only S contains the exceptional line. Figure XIV.6.1 separates the two situations.

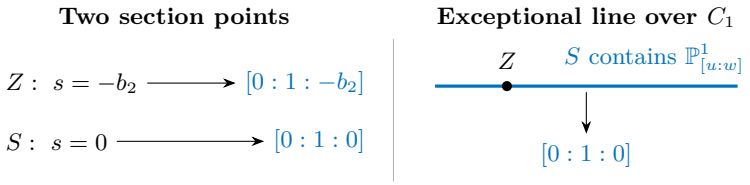


Figure XIV.6.1: The resolved section charts in the patch $v = 1$. Away from $b_2 = 0$, the blowdown keeps the two images distinct. Over C_1 it contracts the exceptional line inside S; the zero section meets that line at $[u : w] = [0 : 1]$.

There is a useful intermediate case. Suppose $b_2 = 0$ but $c_3 \neq 0$. Then (XIV.6.12) sets $u = 0$ and the two sections meet at the same resolved point. Nevertheless the exceptional line is not in the fiber. At the corresponding point of P_0 in $v' = 1$ one has

$$P_0(0, 1, 0) = 0, \qquad \left(\frac{\partial P_0}{\partial u'}, \frac{\partial P_0}{\partial w'}\right) = (c_3, b_2). \tag{XIV.6.17}$$

With either derivative nonzero the center lies on a smooth part of the fiber curve and the blowup only records its tangent direction. This explains why the coincidence class $[b_2]$ used in the height is a divisor, while containing a new component requires both derivatives to vanish and happens over a curve.

The generic fiber can also be checked in the primed coordinates. Put $B_2 = b_0 u'^2 + b_1 u' v' + b_2 v'^2$ and let C_4 denote the binary quartic in the last line of P_0. Completing the square gives

$$(2w' + B_2)^2 = B_2^2 - 4C_4. \tag{XIV.6.18}$$

For a generic evaluation of the coefficients there are four distinct branch points in $[u' : v']$. To check that squarefreeness is a nonempty open condition, take $b_i = c_1 = c_2 = 0$ and $c_0 = c_3 = 1$ at one point of the base. The right side is $-4u'(u'^3 + v'^3)$, which has four simple roots. Riemann–Hurwitz gives $2g - 2 = 2(-2) + 4 = 0$. Over a smooth fiber the blowup at a smooth fiber point preserves the curve. We therefore start with a genuine genus-one generic fiber and two points on it, with Z fixing the origin of the group law. The next question is what divisor combination of those points produces the gauge direction.

XIV.6.2 Removing vertical and Cartan components

Which intersections must vanish before the difference of two sections can be used as an abelian gauge divisor? The generic elliptic fiber F has degree one against either section. A divisor giving a new four-dimensional vector must be distinguished from the zero-section direction and any Cartan vectors in the circle description. In the ordinary M/F dictionary, we impose the following projection conditions:

$$\sigma \cdot F = 0, \qquad \pi_*(\sigma Z) = 0, \qquad \sigma \cdot C_j = 0 \quad \text{for each simple-root curve } C_j. \tag{XIV.6.19}$$

The last condition keeps the roots neutral under the additional abelian factor. The first is already satisfied by $S - Z$. The second uses the pushforward of an intersection surface to a divisor on the threefold base. If the surface maps into a curve, it has zero pushforward as a divisor. This is why the wrapping of S over a curve will affect the individual membrane charges, yet does not invalidate the divisor pushforward used here.

Compute the vertical subtraction directly. On Z the local equation of S is $s = -b_2$, so SZ pushes to the divisor $b_2 = 0$. For a general cubic this is a simple zero. Write $L = [b_2]$. Adjunction on Z gives $Z|_Z = K_B$ because $K_Y = 0$ and $Z \simeq B$. On the open subset where S is a section, the same argument gives $S|_S = K_B$ there. The omitted locus is over C_1 of codimension two in B, so it cannot change the pushforward divisor class. Thus

$$\pi_*(SZ) = L, \qquad \pi_*(Z^2) = -\bar{K}, \qquad \pi_*(S^2) = -\bar{K}, \tag{XIV.6.20}$$

$$D := \pi_*((S - Z)Z) = L + \bar{K}. \tag{XIV.6.21}$$

For a divisor D_B on the base the projection formula gives $\pi_*(Z\pi^* D_B) = D_B$. The same formula for S uses its generic degree one. Subtracting $\pi^* D$ from $S - Z$ therefore removes the entire zero-section pushforward without changing its intersection with any curve in a single fiber.

There is an equivalent way to see that the subtraction is fixed, without choosing a basis of the base divisors. For any candidate $S - Z - \pi^* D'$ and any base curve class γ, the intersection that measures overlap with Z is

$$\int_Y (S - Z - \pi^* D')Z\,\pi^*\gamma = \int_B (L + \bar{K} - D')\,\gamma. \tag{XIV.6.22}$$

For $\gamma = H^2$ this determines the single coefficient of D' in the present base. In the uncorrected class that number is 7, and subtracting any value other than 7 leaves a detectable pairing. At the same time, the pullback $\pi^* D'$ restricts to a trivial bundle on each fiber. This is why using a height calculation to change the charges of individual fibral curves would be inconsistent.

In the MP-Q2 family there are no generic root curves over a base divisor. The proof uses the two independent square conditions for the quadratic (XIV.6.18), derived in Section XIV.6.3. The Shioda divisor, the projection of the rational section into the gauge direction, is then

$$\sigma = S - Z - D = S - Z - 7H. \tag{XIV.6.23}$$

One can now compute the height directly from the divisor intersections. In the basis (S, Z, H) let P be the symmetric matrix whose entries are pushforwards of products. The pullback H^2 has zero divisor pushforward: its support maps into a base curve. Using (XIV.6.21) and the projection formula yields

$$\begin{aligned} P &= H \begin{pmatrix} -4 & 3 & 1 \\ 3 & -4 & 1 \\ 1 & 1 & 0 \end{pmatrix}, & v_\sigma &= \begin{pmatrix} 1 \\ -1 \\ -7 \end{pmatrix}, \\ P v_\sigma &= H \begin{pmatrix} -14 \\ 0 \\ 0 \end{pmatrix}, & h &:= -\pi_*(\sigma^2) = -v_\sigma^{\mathsf{T}} P v_\sigma = 14H. \end{aligned} \tag{XIV.6.24}$$

The calculation can be performed without coordinates on the space of divisors. Put $\mathcal{A} = S - Z$, so that $\pi_*(\mathcal{A}) = 1 - 1 = 0$ as a degree on the base. Expanding σ^2 gives

$$\pi_*\big((\mathcal{A} - \pi^* D)^2\big) = \pi_*(\mathcal{A}^2) - 2D\pi_*(\mathcal{A}) + \pi_*\big((\pi^* D)^2\big), \tag{XIV.6.25}$$

$$\pi_*(\mathcal{A}^2) = \pi_*(S^2) - 2\pi_*(SZ) + \pi_*(Z^2) = -2(\bar{K} + L). \tag{XIV.6.26}$$

The last two terms of the first line vanish. In particular, the self-pairing would have the same pushforward if we had used an incorrect D. This does not make the subtraction optional. The height is insensitive to a vertical shift of a degree-zero class, while the mixed pushforward with Z detects that shift. One should check both quantities. For a Cartan shift the situation is different, because the root divisors have nonzero mutual pushforwards.

The middle zero in Pv_σ checks the zero-section condition. Reversing the sign of the subtraction would give $14H$ in that entry. The last zero checks that the fiber degree vanished before the vertical subtraction. Figure XIV.6.2 follows the three projections and identifies the pairings each one preserves.

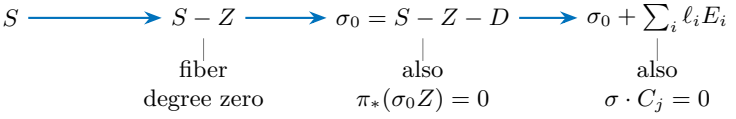


Figure XIV.6.2: Projection of an extra section into a gauge divisor. A vertical pullback changes the zero-section pushforward while leaving fibral intersections unchanged. If there are roots, the Cartan term changes their intersections and leaves the zero-section condition intact.

On the base ray $J_B = tH$ with $t > 0$, the geometric pairing of the height is $\int_B J_B^2 h = 14t^2$. The sign comes from the minus in the definition of h. This pairing does not fix the physical units of a gauge kinetic term. Its nonzero value shows that σ does not vanish in rational cohomology. Because the Shioda map is a homomorphism from sections to rational divisor classes, a torsion section would map to zero. In the ordinary F-theory limit and in the absence of a background that breaks this gauge direction, the non-torsional class gives an abelian vector. Counting all such vectors would require information about the other sections. Also, replacing σ by $m\sigma$ gives

$$q_{m\sigma}(C) = m q_\sigma(C), \qquad h_{m\sigma} = m^2 h_\sigma. \tag{XIV.6.27}$$

Positive height cannot decide whether the normalization is primitive. To do that we will find a unit intersection.

The twist parameter gives a useful test of the vertical part. Change β to $6H$ with the base fixed. The fiber scalings and the form of (XIV.6.4) stay fixed, but α becomes $2H$. The key coefficients now have

$$[b_2] = 2H, \qquad [c_3] = 6H, \qquad [c_4] = 4H. \tag{XIV.6.28}$$

Here c_4 is the coefficient of v'^4 after blowdown: v' has class $U + S + \alpha$, so this coefficient has class $2\beta - 4\alpha = 4\bar{K} - 2\beta$. For general coefficients the complete intersection (b_2, c_3)

has degree $2 \cdot 6 = 12$. The new coincidence class is $2H$, so the vertical subtraction is $6H$. In the matrix in (XIV.6.24), the off-diagonal 3 becomes 2, while the two self-intersection entries remain -4. Acting on $(1, -1, -6)^{\mathsf{T}}$ gives $(-12, 0, 0)^{\mathsf{T}} H$ and hence

$$\sigma_{\beta=6H} = S - Z - 6H, \qquad h_{\beta=6H} = 12H. \tag{XIV.6.29}$$

Keeping the old $7H$ subtraction would give a nonzero zero-section pushforward in the new geometry.

For comparison, suppose a distinct model has an ordinary split gauge divisor $W_B \subset B$. Let E_i be its Cartan divisors and fix the sign $E_i \cdot C_j = -\mathsf{C}_{ij}$ for the Cartan matrix C. The intersections of the unprojected section difference form the column a, with $a_j = (S - Z) \cdot C_j$. The vertical subtraction still has zero intersection with each C_j. Write $\sigma_0 = S - Z - D$ and add $\sum_i \ell_i E_i$. The root equations become

$$(\sigma_0 + \textstyle\sum_i \ell_i E_i) \cdot C_j = a_j - \sum_i \mathsf{C}_{ij} \ell_i = 0, \qquad \mathsf{C}^{\mathsf{T}} \ell = a. \tag{XIV.6.30}$$

The holomorphic zero section meets the identity component, so $\pi_*(E_i Z) = 0$ in this ordinary geometry. The Cartan term preserves the zero-section subtraction.

The inverse Cartan matrix, rather than one independent subtraction for each curve, is essential once roots intersect. For a split A_2 root pair with $a = (1, 0)^{\mathsf{T}}$ the two neutrality equations are

$$2\ell_1 - \ell_2 = 1, \qquad -\ell_1 + 2\ell_2 = 0, \qquad (\ell_1, \ell_2) = (2/3, 1/3). \tag{XIV.6.31}$$

A subtraction confined to the first root with $(\ell_1, \ell_2) = (1/2, 0)$ would neutralize the first pairing but give charge $1/2$ on the second curve. The second coefficient corrects that charge and thereby changes the first coefficient as well. The general height correction below uses the solution of the coupled system.

For a simply laced factor, the ordinary divisor pushforwards are

$$\pi_*(\sigma_0 E_i) = a_i W_B, \qquad \pi_*(E_i E_j) = -\mathsf{C}_{ij} W_B. \tag{XIV.6.32}$$

Indeed the generic fiber intersections over W_B give the multiplicities of that divisor; contributions over smaller loci do not push to divisors. Expanding the square shows the sign of the height shift:

$$h = h_0 - \big(2\ell^{\mathsf{T}} a - \ell^{\mathsf{T}} \mathsf{C} \ell\big) W_B = h_0 - a^{\mathsf{T}} \mathsf{C}^{-1} a \, W_B, \tag{XIV.6.33}$$

$$\mathsf{C} = (2), \quad a = 1 \quad \Longrightarrow \quad \ell = \tfrac{1}{2}, \qquad h = 2(\bar{K} + L) - \tfrac{1}{2} W_B \tag{XIV.6.34}$$

when the same section pushforwards as in (XIV.6.21) hold. For this A_1 example the cross term contributes $-W_B$ to h and the Cartan self-intersection contributes $+W_B/2$. An addition of $-E_1/2$ would instead leave root charge 2. The fraction in the correct projection is therefore forced by a root intersection. In Section XIV.6.4 it will also determine a relation between the global periods of the two gauge directions.

XIV.6.3 The charge-two and charge-one fibers

How can a section that contains a curve give a negative intersection with it? For a curve C lying in a divisor, the intersection with that divisor is the degree of its associated line

bundle restricted to C. It need not count points. In the charge-two fiber one section contains an entire component, so we will compute a normal line rather than count section crossings. In the charge-one fiber both intersections reduce to ordinary point counts.

At C_1 use $v' = 1$ in the blowdown and take b_2, c_3 as transverse coordinates near a smooth point of their intersection in B. On the total-space chart set

$$X = w', \qquad T_0 = u', \tag{XIV.6.35}$$

$$W_0 = w' + b_0 u'^2 + b_1 u' + b_2, \qquad Y_0 = c_3 + c_2 u' + c_1 u'^2 + c_0 u'^3. \tag{XIV.6.36}$$

Here T_0, W_0, Y_0 are coordinates and not divisor classes. The blowdown equation becomes

$$P_0 = XW_0 + T_0 Y_0. \tag{XIV.6.37}$$

To see that this is a genuine change of coordinates, hold X, T_0 fixed. At the node $X = T_0 = 0$ the derivative of (W_0, Y_0) with respect to (b_2, c_3) is the identity. Thus the transverse space is the conifold, with the coordinate along the base curve unaffected. Under $(T_0, X) = (su, sw)$ the factor s cancels and the proper transform is $wW_0 + uY_0 = 0$. The exceptional locus has one projective line $[u : w]$ over each point of C_1. It has dimension two in the fourfold, so this is a small resolution.

The same conifold coordinates make it possible to follow the resolution chart by chart. Retain $[u : w]$ as the direction of (T_0, X). The resolved conifold is locally described by the two equations

$$uX - wT_0 = 0, \qquad wW_0 + uY_0 = 0. \tag{XIV.6.38}$$

On $u = 1$, use (T_0, W_0, w) and eliminate $X = wT_0$ and $Y_0 = -wW_0$. On $w = 1$, use (X, Y_0, u) and eliminate $T_0 = uX$ and $W_0 = -uY_0$. In both charts two coordinates must vanish to reach the exceptional line. On their overlap the transition is

$$(X, Y_0) = (wT_0, -wW_0), \qquad u = 1/w. \tag{XIV.6.39}$$

Up to the sign on one coordinate, both transitions are the tautological ones. The charts exhibit smoothness along the exceptional line for a transverse C_1 independently of the generic total-space argument. They also distinguish a normal coordinate to S inside the total space, T_0 or X on the corresponding chart, from the direction $[u : w]$ along the curve.

Over a point of C_1 the actual fiber equation is

$$P_1 = sR, \qquad R = w^2 + b_1 uvw + b_0 su^2 w + c_2 u^2 v^2 + c_1 su^3 v + c_0 s^2 u^4. \tag{XIV.6.40}$$

The component C_s has $s = 0$, and we call the residual component C_r. On $R = 0$, $u = 0$ would force $w = 0$, which is excluded. After setting $u = 1$, the remaining scaling acts on (w, v, s) with equal weights, and the other exclusion removes $[1 : 0 : 0]$ from that projective chart. The conic does not contain that point, since its w^2 coefficient is one. In the resulting $\mathbb{P}^2$ the conic and its intersection with $s = 0$ are controlled by

$$R|_{u=1} = (w, v, s) \begin{pmatrix} 1 & b_1/2 & b_0/2 \\ b_1/2 & c_2 & c_1/2 \\ b_0/2 & c_1/2 & c_0 \end{pmatrix} \begin{pmatrix} w \\ v \\ s \end{pmatrix}, \tag{XIV.6.41}$$

$$R|_{u=1,\ s=0} = w^2 + b_1 vw + c_2 v^2.$$

Write M_r for the symmetric matrix. The conic is smooth if $\det M_r \neq 0$. Its two crossings with C_s are distinct and transverse if $b_1^2 - 4c_2 \neq 0$. The two tests answer different questions. For instance $R = w^2 + sv$ is a smooth conic, but at $s = 0$ its equation has a repeated root. In an ordinary I_2 fiber both tests must pass.

At a node of the fiber one may take $u = v = 1$. Near that point write the fiber coordinates as (w, s), and let w_* be a root of $R(w, 0)$. The gradients of the two equations $s = 0$ and $R = 0$ have determinant, up to ordering,

$$\left.\frac{\partial R}{\partial w}\right|_{w_*,\, s=0} = 2w_* + b_1. \tag{XIV.6.42}$$

Thus the discriminant test measures the actual intersection in the quotient chart. When it is nonzero the pair (s, R) gives local coordinates on the ambient fiber, and $sR = 0$ is a crossing of two branches. When it vanishes, the conic can remain smooth but these two local equations fail to be independent.

The Z intersection on C_s comes from $u = 0$ at one reduced point. To compute $S \cdot C_s$, use $v = 1$ and cover the line by $u \neq 0$ and $w \neq 0$. The two invariant normal coordinates to $s = 0$ are su and sw. Their relation on the overlap is

$$t_u = su, \qquad t_w = sw = \frac{w}{u}\, t_u. \tag{XIV.6.43}$$

This is the tautological line: the same vector on the line $[u : w]$ has first coordinate t_u in the first patch and second coordinate t_w in the second. Hence $\mathcal{O}_Y(S)|_{C_s} \simeq \mathcal{O}_{\mathbb{P}^1}(-1)$. By contrast C_r misses Z and meets S twice by (XIV.6.41). Base pullbacks have degree zero on either component, so the charge degrees in the effective orientations are

	$Z \cdot C$	$S \cdot C$	$\sigma \cdot C$
C_s	1	-1	-2
C_r	0	2	2
$C_s + C_r$	1	1	0

(XIV.6.44)

In particular the zero section meets the exceptional component, even though it is the other section that wraps it. The sum row gives the intersections with the full fiber. Assigning $+1$ to $S \cdot C_s$ would violate that sum.

The curve along which this happens can itself be checked by base intersection theory. For a transverse complete intersection of the cubic b_2 and septic c_3, adjunction on the base gives

$$[C_1] = (3H)(7H) = 21H^2, \qquad \deg_C H = 21, \tag{XIV.6.45}$$

$$K_{C_1} = (K_B + 3H + 7H)|_{C_1} = 6H|_{C_1}, \qquad 2g(C_1) - 2 = 6 \cdot 21 = 126. \tag{XIV.6.46}$$

This gives genus 64 for the general complete intersection. The genus describes the locus along which the fiber changes. A four-dimensional zero-mode calculation would also require the bundle of modes along that locus.

To find a unit charge, go instead to $b = b_2 \neq 0$. In (XIV.6.15) the fiber is a quadratic in w'. Reducibility is equivalent to factoring it into two monic linear polynomials in w' with quadratic homogeneous constant terms. This follows also from (XIV.6.18): the

binary discriminant must be a square, in which case half the sum and difference of its square root and B_2 give the constant terms. At $u' = 0$ they are 0 and bv'^2, which fixes the order of the factors. Write

$$P_0 = (w' + Au'^2 + B_1u'v')(w' + D_1u'^2 + Eu'v' + bv'^2). \tag{XIV.6.47}$$

The w' coefficient fixes $A + D_1 = b_0$ and $B_1 + E = b_1$. The $u'v'^3$ and $u'^2v'^2$ terms in the product of the constant terms fix $bB_1 = c_3$ and $bA + B_1E = c_2$. In order, one obtains

$$B_1 = c_3/b, \quad E = b_1 - B_1, \quad A = (c_2 - B_1E)/b, \quad D_1 = b_0 - A, \tag{XIV.6.48}$$

$$c_0 = AD_1, \quad c_1 = AE + B_1D_1. \tag{XIV.6.49}$$

The last line consists of the two remaining equations. At fixed b, b_0, b_1, c_2, c_3 they independently prescribe c_0, c_1. This gives a description of the square locus C_2 on the specified open chart. It does not describe all of its strata on $b = 0$.

These conditions also justify using no Cartan term for general MP-Q2. Over $b \neq 0$ the center of the blowup is a smooth point on the fiber, and the square condition is codimension two in the values of the coefficients. On $b = 0$, $c_3 \neq 0$, the binary discriminant has a simple root at $u' = 0$: its linear term there in the $v' = 1$ chart is $-4c_3u'$. Hence it cannot be square, and the center is again a smooth fiber point. Over $b = c_3 = 0$, the exceptional component appears, also subject to two independent conditions. At any fixed base point the evaluations of all the coefficient bundles are independently surjective. The incidence of reducible fibers in the product of coefficient space and B therefore has codimension at least two. Its components that dominate coefficient space have general fibers of dimension at most one. The nondominant components can be avoided by general coefficients. No base divisor carries a reducible fiber in this general family.

We must check ordinary crossings before assigning the charge-one fiber type. At an intersection the factors in (XIV.6.47) agree as graphs of w' over $[u' : v']$. They cannot meet at $u' = 0$, since $b \neq 0$. For $\tau = v'/u'$ their difference gives

$$b\tau^2 + (E - B_1)\tau + D_1 - A = 0, \tag{XIV.6.50}$$

$$\delta_{\text{node}} = (E - B_1)^2 - 4b(D_1 - A). \tag{XIV.6.51}$$

In the same patch put $\omega = w'/u'^2$. At a common point the equations of the two components are $\omega + A + B_1\tau = 0$ and $\omega + D_1 + E\tau + b\tau^2 = 0$. Their Jacobian in (ω, τ) is

$$\det \begin{pmatrix} 1 & B_1 \\ 1 & E + 2b\tau \end{pmatrix} = E - B_1 + 2b\tau. \tag{XIV.6.52}$$

At a root τ_* its square equals δ_{node}. For a repeated root the difference of the two graph equations starts at order $(\tau - \tau_*)^2$. Thus both components are individually smooth in that case, while their intersection multiplicity is two at one point. This difference is drawn in Figure XIV.6.4.

Nonzero δ_{node} means the difference of the graphs has two simple zeros. Each graph is itself a smooth projective line. Since $b \neq 0$, their intersections do not lie at the blowup center. Pulling the factors back gives $P_1 = FG$ with

$$F = w + Asu^2 + B_1uv, \qquad G = sw + D_1s^2u^2 + Esuv + bv^2. \tag{XIV.6.53}$$

On $s = 0$ one has $G = bv^2 \neq 0$, so the section cuts only the $F = 0$ component, at a reduced point by the linear equation in $[u : w]$. On $u = 0$, $F = w \neq 0$, so Z cuts only the $G = 0$ component, with multiplicity one as in (XIV.6.11). Let C_F, C_G be the corresponding curves. In the same normalization as (XIV.6.44),

	$Z \cdot C$	$S \cdot C$	$\sigma \cdot C$
C_F	0	1	1
C_G	1	0	-1

(XIV.6.54)

The projections are different from those at C_1 because neither section contains a component here. Figure XIV.6.3 shows both distributions of the section intersections.

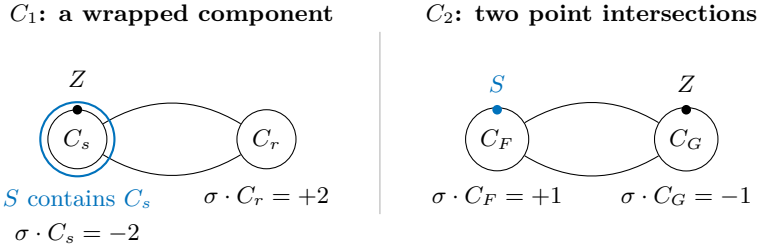


Figure XIV.6.3: Incidence graphs of the ordinary split fibers. Two edges represent the two transverse crossings. The labels give the Shioda degrees of the effective curves. On the left the blue outline marks the entire curve contained in S, whereas on the right each section meets a component at a point.

An explicit compact coefficient tuple lets us test whether both ordinary loci persist under coefficient variation. Use homogeneous base coordinates $[X_0 : X_1 : X_2 : X_3]$ and take

$$\begin{aligned} b_0 &= 5X_1^5, & b_1 &= 3X_1^4, & b_2 &= X_0^2X_2 + X_1^3, \\ c_0 &= -X_0^{10} + 4X_1^{10} + X_1^9X_2, & c_1 &= 9X_1^9 + X_1^8X_3, & & \\ c_2 &= -X_0^8 + 3X_1^8, & c_3 &= X_0^6X_3 + 2X_1^7. & & \end{aligned} \tag{XIV.6.55}$$

At $p = [1 : 0 : 0 : 0]$ the cubic and septic vanish, with derivatives $(1, 0)$ and $(0, 1)$ in the X_2, X_3 directions in the chart $X_0 = 1$. The conic is $w^2 - v^2 - s^2 = 0$, with determinant 1 and node discriminant 4. Its crossings in $u = v = 1$ are at $w = \pm 1$. At $p' = [0 : 1 : 0 : 0]$, in the chart $X_1 = 1$, the values are $(b_0, b_1, b) = (5, 3, 1)$ and $(c_0, c_1, c_2, c_3) = (4, 9, 3, 2)$. Substituting gives

$$(A, B_1, D_1, E; b) = (1, 2, 4, 1; 1), \qquad \tau^2 - \tau + 3 = 0, \qquad \delta_{\text{node}} = -11. \tag{XIV.6.56}$$

Here b, b_0, b_1, c_2, c_3 have zero X_2, X_3 derivatives, while c_0, c_1 have respective derivatives $(1, 0), (0, 1)$. The derivative matrix of the two remaining square equations is therefore the identity in those directions. In each case the equations can be solved locally in the base variables as the coefficients vary. More explicitly, if G_1, G_2 are the two defining

equations at either witness and λ_{coeff} denotes the coefficient tuple, a small change $\delta\lambda_{\mathrm{coeff}}$ is accompanied by a change of the two transverse coordinates satisfying

$$\begin{pmatrix}\delta X_2\\ \delta X_3\end{pmatrix} = -\left(\frac{\partial(G_1,G_2)}{\partial(X_2,X_3)}\right)^{-1}\frac{\partial(G_1,G_2)}{\partial\lambda_{\mathrm{coeff}}}\,\delta\lambda_{\mathrm{coeff}} \tag{XIV.6.57}$$

to first order in the chosen affine chart. The nonvanishing determinants and node discriminants persist near these points. The projection of each incidence locus to coefficient space is consequently dense, and its constructible image contains a nonempty Zariski open set. Intersect those open sets with the open set of general smooth members. The tuple proves occurrence of both local geometries for general coefficients; its own total space has not been certified smooth everywhere.

Changing D_1 and E to 1 and 2 in (XIV.6.56), with the other factor coefficients fixed, still gives a square discriminant in (XIV.6.18). But the node equation becomes $\tau^2 = 0$: the two graphs now touch at one point. Conversely, keeping $D_1 = 4$ and changing only E to 2 gives $\tau^2 + 3 = 0$ and two crossings. In both changed cases $2c_3 - b_1 b = 0$. Dividing by that expression would discard the ordinary second case. The factor equations need only division by b, while the crossing test is separate from the square test.

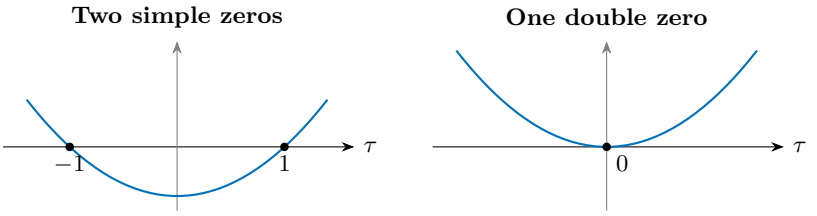


Figure XIV.6.4: The graph equation difference on the real τ axis for two real choices of the node polynomial. After subtracting the first graph, its height is zero. For $\tau^2 - 1$ there are two simple intersections; for τ^2 the two branches share a tangent. The complex intersection test is the same derivative test.

Finally, σ in (XIV.6.23) is an integral divisor class. If it were an integer multiple of another integral divisor modulo vertical divisors, say $\sigma = mD' + \pi^*V$, then $1 = \sigma \cdot C_F = m(D' \cdot C_F)$, forcing $|m| = 1$. This unit intersection fixes the primitive charge normalization for this direction. In the ordinary resolved M/F limit the membrane coupling gives $q(C) = \sigma \cdot C$ for the effective orientation and $-q(C)$ for the reverse. Equations (XIV.6.44) and (XIV.6.54) thus give geometric sectors of magnitudes two and one with the same height normalization. They do not count four-dimensional zero modes or decide whether one can condense. The joint charge lattice in the next example will require more than this single-direction divisibility test.

XIV.6.4 The character and cocharacter lattices

Can two geometries have the same Lie algebra but allow different large gauge transformations? An ordinary split I_2 fiber supplies the root of $\mathfrak{su}(2)$. If there is also an

abelian vector, the root alone cannot tell us whether a half period of the Cartan circle is equivalent to a half period of the abelian circle. The section placements on the two components provide that information. To see the effect we compare two resolved toric tops, separate from the standalone MP-Q2 fourfold.

The tops have a gauge divisor whose defining function pulls back to e_0e_1. Write $E_i = \{e_i = 0\}$ on the resolved space. At a generic point of the divisor the fiber consists of the identity component in E_0 and the simple-root component c in E_1. The two polynomials are

$$\begin{aligned} P_{\text{same}} &= c_0e_0^2s^3u^4 + c_1e_0s^2u^3v + c_2su^2v^2 + c_3e_1uv^3 \\ &\quad + b_0e_0s^2u^2w + b_1suvw + b_2e_1v^2w + sw^2, \\ P_{\text{mixed}} &= e_0(c_0s^3u^4 + c_1s^2u^3v + c_2su^2v^2 + c_3uv^3) \\ &\quad + w(b_0s^2u^2 + b_1suv + b_2v^2 + e_1sw). \end{aligned} \tag{XIV.6.58}$$

Here the letters b_i, c_i belong to these tops, with their own bundles. The displayed terms are useful for seeing what changes when a section equation is restricted:

	$u = 0$	$s = 0$
P_{same}	$w(b_2e_1v^2 + sw)$	$e_1v^2(b_2w + c_3uv)$
P_{mixed}	$w(b_2v^2 + e_1sw)$	$v^2(b_2w + c_3e_0uv)$

(XIV.6.59)

A factor in a restriction is not by itself a fiber component met by the section: the toric exclusions still decide which coordinate strata exist. We use as input the resolved topology of the two tops, including their triangulation data. It gives the following absolute placements, with one reduced intersection on the indicated component in each case:

	Z	S	$(S - Z) \cdot c$
same	E_0	E_0	0
mixed	E_0	E_1	1

(XIV.6.60)

Figure XIV.6.5 shows the placement data and the resulting charge lattice. The restrictions in (XIV.6.59) distinguish the two equations; the locations in (XIV.6.60) are inputs from their actual resolutions.

Using $E_1 \cdot c = -2$ in (XIV.6.30), the mixed model requires the addition of $E_1/2$, whereas the same-component model needs no Cartan addition. For any fibral curve C put $n = E_1 \cdot C$ and $q = \sigma \cdot C$. Here n is the integral Cartan weight in the sign convention of the intersection. With the mixed correction one has

$$q = (S - Z) \cdot C + \tfrac{1}{2}n, \tag{XIV.6.61}$$

$$Q := 2q, \qquad Q - n = 2(S - Z) \cdot C \in 2\mathbb{Z}. \tag{XIV.6.62}$$

We use the integer labels (n, Q) for the mixed model. Odd weights then have odd abelian labels; even weights have even labels. The root itself has $(n, Q) = (-2, 0)$ and obeys the condition. In the same-component model we keep q as the integer abelian label.

A character of a torus gives a phase. For coordinates (n, Q) and periods measured in turns, the phase on the pair (r, t) of Cartan and abelian angles is $\exp(2\pi i(nr + Qt))$.

The character lattice tells us which linear functionals must be integral on a period. Equation (XIV.6.62) gives a containing lattice, but to know that it is the actual lattice we need characters that span it. The mixed top supplies a doublet with $q = 1/2$ and a singlet with $q = 1$ in the geometric normalization. Choose the weight $+1$ of the doublet. Then

$$(1,1), \quad (0,2) \quad \text{occur}, \tag{XIV.6.63}$$

$$(n,Q) = n(1,1) + \tfrac{Q-n}{2}(0,2). \tag{XIV.6.64}$$

Every integral pair of the required parity is therefore generated. The $q = 3/2$ doublet gives the weight $(1,3) = (1,1) + (0,2)$, consistent with the same lattice. The character basis has index two in $\mathbb{Z}^2$. A subset of allowed characters need not determine that index: keeping $(1,3)$ and $(0,4)$ instead would generate an index-four sublattice and miss the actual primitive singlet.

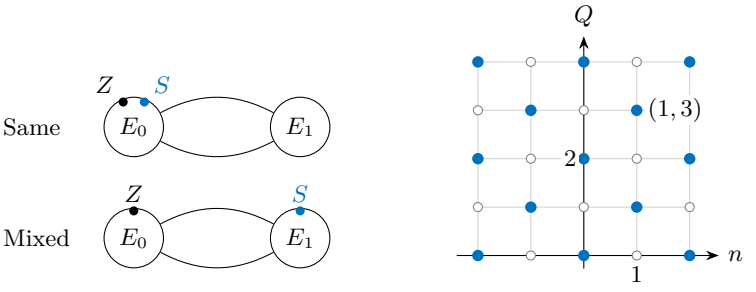


Figure XIV.6.5: Left: section placements on the generic resolved I_2 fibers of the two tops. Right: mixed character pairs (n,Q); filled dots satisfy the parity rule, and open dots fail it. Both signs of a doublet weight have the same parity.

A cocharacter is a homomorphism from a circle into the torus. In the same angle coordinates it is a period vector: traversing one circle gives a phase of one on every character. With the character generators as columns of M, the condition is $M^{\mathsf{T}}(r,t)^{\mathsf{T}} \in \mathbb{Z}^2$. Thus the cocharacter generators are columns of $M^{-\mathsf{T}}$:

$$M = \begin{pmatrix} 1 & 0 \\ 1 & 2 \end{pmatrix}, \qquad M^{-\mathsf{T}} = \begin{pmatrix} 1 & -1/2 \\ 0 & 1/2 \end{pmatrix}, \tag{XIV.6.65}$$
$$\Lambda^\vee = \mathbb{Z}^2 + \mathbb{Z}(\tfrac{1}{2}, \tfrac{1}{2}).$$

The second column differs from the half-diagonal by an integral vector. Pairing $(1,1), (0,2), (1,3)$ with the half-diagonal gives $1, 1, 2$ respectively. Pairing them with $(1/2, 0)$ gives $1/2, 0, 1/2$. In geometric terms the relation $q - n/2 = (S - Z) \cdot C$ means that the shifted half-diagonal is realized by the integral section difference, since vertical classes have no degree on C. One cannot retain a pure half-Cartan period with the odd doublet present. Likewise a singlet of label $(0,1)$ would detect the half-diagonal and is incompatible with this mixed lattice.

The same dual lattice can be derived without a matrix. The singlet fixes $2t \in \mathbb{Z}$, and the doublet weight fixes $r + t \in \mathbb{Z}$. If t is an integer, then so is r. If t is a half-integer

modulo integers, so is r. This gives exactly the two cosets in (XIV.6.65). One can see the identification in the two eigenangles of the defining $U(2)$ representation:

$$(r,t) \longmapsto (t+r, t-r), \qquad t+r \in \mathbb{Z}, \quad t-r \in \mathbb{Z} \quad \text{for a period.} \tag{XIV.6.66}$$

The determinant angle is $2t$, detected by $(0,2)$. The second eigenangle, corresponding to the other doublet weight, is integral whenever the first one and the determinant angle are. In particular the half-diagonal changes one eigenangle by a full turn and leaves the other unchanged. A pure half-Cartan shift changes the two eigenangles by half a turn in opposite senses and gives the matrix $-I$, not the identity.

In an $SU(2)$ representation of highest weight n the central element $-I$ acts by $(-1)^n$. The other weights differ by even integers. Hence the element $(-I,-1)$ in the product group acts by $(-1)^{n+Q}$, which is one on the mixed lattice. The $(0,2)$ singlet requires any central kernel element to have $z^2=1$ in the $U(1)$, and the $(1,1)$ doublet requires the two signs to coincide. Under the ordinary connected gauge-group dictionary the kernel is exactly the indicated $\mathbb{Z}_2$. There is a concrete realization of the quotient:

$$SU(2)\times U(1) \longrightarrow U(2), \qquad (g,z) \longmapsto zg, \qquad \ker = \{(I,1),(-I,-1)\}. \tag{XIV.6.67}$$

Surjectivity follows by choosing a square root z of the determinant of a unitary matrix and dividing the matrix by z. The ambiguity of that square root is precisely the kernel.

Changing the character basis also changes the generators of the dual basis. For example, replace the columns $(1,1),(0,2)$ by $(1,3),(0,2)$. With

$$N = \begin{pmatrix} 1 & 0 \\ 1 & 1 \end{pmatrix}, \qquad M' = MN, \qquad (M')^{-\mathsf{T}} = M^{-\mathsf{T}} N^{-\mathsf{T}}, \tag{XIV.6.68}$$

the second change of basis is also integral and unimodular. The periods in physical angle coordinates are therefore unchanged. Explicitly, $(1,3)$ paired with the old half-diagonal gives 2, and $(0,2)$ paired with it gives 1. The different-looking first column of M' is a change of generators, not a change of global form. By contrast, replacing $(0,2)$ by $(0,4)$ as well makes N nonunimodular. Its dual would admit, for instance, $(1/4,1/4)$: the two retained characters pair to integers, but the discarded $(0,2)$ pairs to $1/2$. A few surviving weights can thus suggest a spurious period unless they generate the full lattice.

In the same-component example the actual $q=0$ doublet and $q=1$ singlet give $(1,0)$ and $(0,1)$ in its own integral coordinates. They detect the two centers independently, giving the direct product $SU(2)\times U(1)$ in that example. Multiplying the mixed Shioda class by two makes the charges integral but also multiplies its height by four. It does not remove the parity constraint or produce the same-component product. The quotient identifies elements of a connected group; there is no extra discrete gauge factor in this identification. These lattices determine the indicated connected global form under the ordinary geometry dictionary, without specifying a dynamical line spectrum or a discrete theta angle. A pure half-Cartan period will become possible in a different model where the geometry excludes odd weights.

XIV.6.5 A torsion section and a quotient group

How can a second point on the elliptic fiber change the group without giving another photon? The Shioda map takes values in a rational vector space, so a finite-order point maps to zero. But the divisors appearing in that zero relation can encode a period that was absent from the coroot lattice. The distinction can be seen in a different Tate model, with a section T at a fixed point of elliptic inversion.

Take the Tate equation with $a_3 = a_6 = 0$ and coefficient classes $[a_i] = i\bar{K}$:

$$P_T = -y^2 - a_1xyz + x^3 + a_2x^2z^2 + a_4xz^4 = 0. \tag{XIV.6.69}$$

In the chart $z = 1$ elliptic inversion fixes x and sends y to $-y - a_1x$. It exchanges the two solutions of the quadratic in y for each x. The point $(x, y) = (0, 0)$ satisfies the equation and is invariant under this map. It is not the origin at infinity. Hence on the smooth generic elliptic curve it has exact order two.

To locate the ordinary singular fiber, first set $Y_T = y + a_1x/2$ and $A_T = a_2 + a_1^2/4$, then shift $x = X_T - A_T/3$ to remove the quadratic term. This gives

$$Y_T^2 = x^3 + A_Tx^2 + a_4x = X_T^3 + fX_T + g, \tag{XIV.6.70}$$

$$f = a_4 - \tfrac{1}{3}A_T^2, \qquad g = \tfrac{2}{27}A_T^3 - \tfrac{1}{3}A_Ta_4, \tag{XIV.6.71}$$

$$\Delta_{\text{book}} = 4f^3 + 27g^2 = a_4^2(4a_4 - A_T^2). \tag{XIV.6.72}$$

At a generic point of $a_4 = 0$ with $A_T \neq 0$, the discriminant order is two while f, g are nonzero. This is consistent with the ordinary resolved I_2 fiber of this model. The divisor relation of interest requires the resolution and cannot be read off from those orders.

Use the two toric substitutions $(x, y) \mapsto (sx, sy)$ and then $(x, s) \mapsto (tx, ts)$. The variables s, t here are the exceptional coordinates of this Tate resolution. In each substitution divide out the indicated exceptional factor once to obtain the proper transform. The two equations are

$$P_T^{(1)} = -sy^2 - a_1sxyz + s^2x^3 + a_2sx^2z^2 + a_4xz^4, \tag{XIV.6.73}$$

$$P_T^{(2)} = -sy^2 - a_1stxyz + s^2t^4x^3 + a_2st^2x^2z^2 + a_4xz^4. \tag{XIV.6.74}$$

At $x = 0$, the second polynomial reduces to $-sy^2$. The resolved ambient exclusions prohibit $s = x = 0$ and also $y = x = 0$. Therefore no point with $x = 0$ is on the proper transform. Omitting the second exclusion would introduce false solutions with $y = 0$ and $s \neq 0$. Figure XIV.6.6 marks where the exclusions enter the calculation.

One can now locate T in the resolved geometry. The composite blowdown to the original Tate coordinates is

$$(x_{\text{old}}, y_{\text{old}}, z_{\text{old}}) = (st^2x, sty, z). \tag{XIV.6.75}$$

The resolved exclusions include yt and tz, so along $t = 0$ one has $y, z \neq 0$. In the chart $x = 1$ the remaining two weights on y, z are respectively $(2, 1)$ and $(1, 1)$, allowing $y = z = 1$ there. The restriction of the proper transform at $t = 0$ is $-sy^2 + a_4z^4 = 0$,

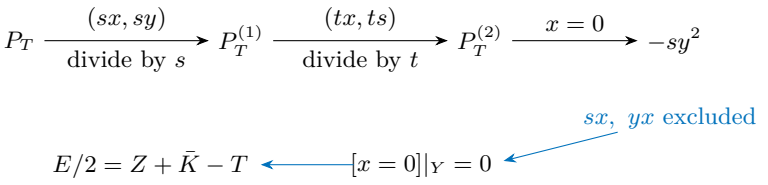


Figure XIV.6.6: The two proper transforms of the order-two Tate model. At $x = 0$ the resulting equation requires one of two simultaneous vanishings excluded by the ambient toric geometry. The absent divisor gives the half-coroot relation.

so it fixes $s = a_4$ in this patch. Its image under (XIV.6.75) is the finite point $(0, 0)$, as required for T. On the gauge divisor it lands on $s = 0$. The zero section lies at $z = 0$ and hence cannot meet $s = 0$ by the exclusion of sz. These placements are consistent with the integral representative of the half-coroot that we will obtain from the class of the absent x divisor.

Since x does not vanish, work in the chart $x = 1$ to examine the fiber above $a_4 = 0$:

$$P_T^{(2)}|_{x=1,\ a_4=0} = s(-y^2 - a_1yzt + st^4 + a_2z^2t^2). \tag{XIV.6.76}$$

Near a crossing of the two components one can take $z = t = 1$. Indeed $s = 0$ excludes $z = 0$, and if also $t = 0$ the second factor in (XIV.6.76) would force $y = 0$, which is excluded with $t = 0$. In this patch the component intersections satisfy

$$s = 0, \qquad y^2 + a_1y - a_2 = 0, \qquad \delta_y = a_1^2 + 4a_2 = 4A_T. \tag{XIV.6.77}$$

For $A_T \neq 0$ the crossings are distinct. The second component is given by $s = y^2+a_1y-a_2$ in this patch. Its derivative with respect to y is nonzero at each crossing, which recovers the ordinary transversality directly. The order of the Weierstrass discriminant and the resolved crossing calculation are therefore consistent.

The sourced resolved topology identifies the Cartan divisor E with the $s = 0$ component over this gauge divisor. Let X_{div} denote the ambient class of $x = 0$ restricted to the hypersurface. The coordinate classes of the resolution give $X_{\text{div}} = 2Z - E - 2T + 2\bar{K}$. The nowhere-vanishing coordinate on the hypersurface sets this class to zero. Rearranging gives

$$T - Z - \bar{K} + \tfrac{1}{2}E = 0 \qquad \text{in } H^2(Y, \mathbb{Q}). \tag{XIV.6.78}$$

The first three terms are integral divisors. Thus the class of $E/2$ in rational cohomology has an integral representative, namely $Z + \bar{K} - T$. This is the vanishing torsion Shioda combination and it supplies no extra vector. It does not assert that there is a nonzero order-two element of $H^2(Y, \mathbb{Z})$: the order-two period arises relative to the coroot lattice.

In the Cartan normalization where a root has weight -2, a weight n has pairing $n/2$ against the pure half-coroot. Intersecting (XIV.6.78) with any integral fibral curve forces $n/2$ to be integral. The root is allowed and the doublet weight 1 is not. The coroot-lattice extension is dual to this even weight lattice:

$$\Lambda_{\text{char}} = 2\mathbb{Z}, \qquad \Lambda_{\text{cochar}} = \tfrac{1}{2}\mathbb{Z}. \tag{XIV.6.79}$$

As a local control, take $a_1 = 0$, $a_2 = 1$ and let $a_4 = \rho$ vary near $\rho = 0$. Then

$$f = \rho - \tfrac{1}{3}, \quad g = \tfrac{2}{27} - \tfrac{\rho}{3}, \quad \Delta_{\text{book}} = -\rho^2 + 4\rho^3. \tag{XIV.6.80}$$

For $\rho \neq 0, 1/4$ the cubic is smooth and the finite point still has order two. At $\rho = 0$, the crossings of the two resolved components are $y = +1$ and $y = -1$ in the chart $z = t = 1$. The derivatives of the second component there are $+2$ and -2, so both crossings are transverse. The torsion section at $t = 0$ lies on the Cartan component and away from these crossings. The double discriminant zero is thus associated here with a two-component root fiber, rather than with the torsion point disappearing from the family.

The distinction between the two lattices can be measured directly with phases. The pure Cartan angle shifted by one half turn acts by -1 on weight one and by $+1$ on weight two. The former would distinguish the two lifts of a group element to $SU(2)$, while the latter descends. In the covering Cartan, a full turn is already a coroot period, so the additional half turn has order two only modulo that original period. This reproduces the meaning of the integral representative in (XIV.6.78) without treating the divisor itself as a torsion element.

The ordinary resolved gauge dictionary therefore gives $SU(2)/\mathbb{Z}_2 \simeq SO(3)$ for this connected sector. In the mixed top the doublet prevented a pure half-coroot and allowed a correlated half period involving the photon. Here the half-coroot occurs without a photon. Both effects change the global form of a connected gauge group. We now return to MP-Q2, where the primitive abelian charge makes a different operation possible.

XIV.6.6 The charge-two field to be Higgsed

Which electric charges can a charge-two condensate still distinguish? The distinction only makes sense once the unit of charge is fixed. Section XIV.6.3 found a curve of unit intersection, so the charge-two curve carries twice the primitive charge. There is also a corresponding geometric question: what happens to the two section points on the quartic if we deform the blowdown that contracted the charge-two curve?

Keep $B = \mathbb{P}^3$ and $\beta = 5H$. The map in (XIV.6.15) gives

$$[u'] = U + S, \quad [v'] = U + S + H, \quad [w'] = 2(U + S) + 5H. \tag{XIV.6.81}$$

Thus P_0 has class $4(U + S) + 10H$, and we can add the missing term in the quartic as

$$P_2 = P_0 + c_4 v'^4, \qquad [c_4] = 6H. \tag{XIV.6.82}$$

At the selected point p of C_1, this perturbation adds a constant in the chart $v' = 1$ when $c_4(p) \neq 0$. Equivalently, in a family with parameter ϵ multiplying c_4, the derivative of the equation with respect to ϵ is $c_4(p)$ at the node. This is the transverse deformation parameter of the local conifold equation (XIV.6.37).

Restrict to the displayed divisor $u' = 0$; the vertex $u' = v' = 0$ is off the hypersurface because w'^2 does not vanish there. In $v' = 1$ the two points are determined by

$$W^2 + b_2 W + c_4 = 0, \qquad W = w'/v'^2, \tag{XIV.6.83}$$

$$W_\pm = \tfrac{1}{2}(-b_2 \pm \sqrt{\Delta_{\text{br}}}), \qquad \Delta_{\text{br}} = b_2^2 - 4c_4. \tag{XIV.6.84}$$

Here Δ_{br} is the branch discriminant of this quadratic, not the Weierstrass discriminant of the whole elliptic fiber. Both summands in Δ_{br} have class $6H$, so the square test can be carried out after choosing a trivialization at the generic point. A different trivialization rescales by a square and gives the same test.

For the tuple in (XIV.6.55), consider two choices:

$$c_4^{\mathrm{ns}} = \frac{b_2^2 - X_0^5(X_0 + X_1)}{4}, \qquad c_4^{\mathrm{sp}} = \frac{b_2^2 - (X_0^3 + X_1^3)^2}{4}. \tag{XIV.6.85}$$

Both are nonzero homogeneous degree-six sections. At p the first choice gives $c_4^{\mathrm{ns}}(p) = -1/4$ in the $X_0 = 1$ chart. On $X_1 = 1$, its branch discriminant is $X_0^5(X_0 + 1)$, with valuation five at the prime $X_0 = 0$. A rational square has even valuation at every prime, so this quadratic is irreducible over $\mathbb{C}(B)$. The displayed divisor has degree two and its points are exchanged over the quadratic extension generated by $\sqrt{\Delta_{\mathrm{br}}}$. The second choice has $\Delta_{\mathrm{br}} = (X_0^3 + X_1^3)^2$, so both points remain rational despite the nonzero deformation. Figure XIV.6.7 distinguishes these outcomes. Neither test examines other points of the generic fiber. In particular, the nonsplit quadratic by itself does not prove absence of a rational section, a period or index assertion, or a discrete gauge interpretation.

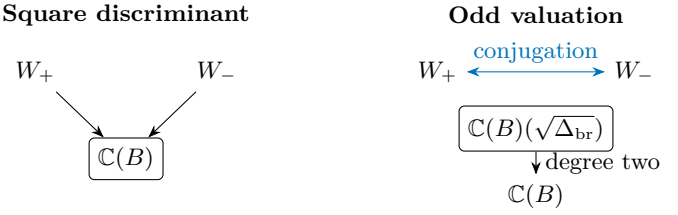


Figure XIV.6.7: The two roots on the displayed divisor $u' = 0$. A square discriminant gives separate rational points over $\mathbb{C}(B)$. An odd valuation gives a conjugate pair on a quadratic extension; the diagram concerns this divisor only.

The difference between these two cases is visible in the way the points can be labeled. For the split choice the labels W_+ and W_- are separately defined by rational functions on the base chart. For the nonsplit choice they become rational only after adjoining one square root. Over that extension they satisfy

$$W_+ + W_- = -b_2, \qquad W_+ W_- = c_4, \qquad (W_+ - W_-)^2 = \Delta_{\mathrm{br}}. \tag{XIV.6.86}$$

The first two quantities descend even when $W_+ - W_-$ does not. In the undeformed limit $c_4 = 0$, the product vanishes and the two labels can be assigned again by (XIV.6.16). Neither the primitive charge nor the sign of a field-theory phase can be read off from a choice of which root to call W_+.

The conditional field-theory calculation is independent of this square test. In the primitive $U(1)$ normalization the angle α is periodic modulo 2π and a charge q transforms by $e^{iq\alpha}$. If a charge-two field actually acquires a nonzero expectation value, its stabilizer is

$$e^{2i\alpha} = 1 \quad \Longleftrightarrow \quad \alpha = 0, \pi \pmod{2\pi}, \qquad e^{i\pi} = -1. \tag{XIV.6.87}$$

The last phase is the action on a unit-charge field. The surviving elements form a subgroup of the original $U(1)$ in this hypothetical Higgs background. This is different from the identifications by a center in the two connected group examples. Here the fiber calculation supplies charge two, and the quartic calculation supplies a test for the displayed pair of points. Neither shows that a suitable vacuum or flux exists. The next chapter takes up the additional geometry and physical input needed to connect a genus-one fibration to a discrete gauge sector. Axion gauging is a separate mechanism.

XIV.6.7 Exercises

Use `benchmark/tasks.json` for the JSON fields and `benchmark/PROTOCOL.md` for submission. The written explanations are human assessed.

1. **Change the twist.** With $\beta = 4H$ on $\mathbb{P}^3$, give the degree row in the order $(b_0, b_1, b_2, c_0, c_1, c_2, c_3, c_4)$ and the powers of (s, v) in $c_4 v'^4$ after pullback. Explain why $c_4 v^4$ fails as an extra term of P_1 even if its base degree is right.

2. **Move the section to another root.** In an ordinary split A_2 example take $\mathsf{C} = \left(\begin{smallmatrix} 2 & -1 \\ -1 & 2 \end{smallmatrix}\right)$ and $a = (0,1)^{\mathsf{T}}$. Give both entries of ℓ and the signed coefficient of W_B in $h - h_0$. Explain how you would detect a wrong sign before computing the height.

3. **Test a square fiber for tangency.** Take $(A, B_1, D_1, E; b) = (2, -1, 3, 3; 2)$ in (XIV.6.47). Compute the seven original coefficients, the discriminant of the node equation, and the signed degrees in order (C_F, C_G). Repeat for $D_1 = 4$. Explain why both quartics pass the square test but the two graphs have different intersection multiplicities.

4. **Change lattice generators.** Use mixed characters $(-1, 1)$ and $(0, -2)$ as columns. Give their matrix, its inverse transpose and the phase exponents in turns for the shifts $(1/2, -1/2)$ and $(1/2, 0)$ on both generators. Identify which shifts are periods. Explain why $(-1, 3)$ and $(0, -4)$ fail to generate the full lattice.

5. **Retest the Tate resolution.** Set $(a_1, a_2, a_4) = (2, 2, 1)$ in a local trivialization of the Tate model. Compute the inverse of $(0, 0)$, its order, and Δ_{book}. After the two substitutions give $P_T^{(2)}|_{x=0}$ and the coefficient of E in (XIV.6.78) when the coefficient of T is one. Explain why keeping only the exclusion of sx is insufficient.

6. **Separate the two kernels.** Take $b_2 = X_1^3$ and $4c_4 = b_2^2 - X_0^3(X_0 + X_1)^3$. Give the valuation at $X_0 = 0$ on $X_1 = 1$ and whether the displayed pair splits. In a separate $U(1)$ with primitive charge one, give the stabilizer angles in turns for a charge-three expectation value. Explain why the first answer does not prove the second is realized in a compactification.

Status and sources

§1. The family and its sections. The anticanonical class, general-member regularity, generic fiber, actual section charts and absence of a divisorial reducible fiber for general coefficients are [MATH]. See Mayrhofer, Palti, et al. (2014), arXiv:1408.6831v4, §2.1, eqs. (2.1)–(2.6), Tables 2.1–2.2. The compact base and twist are specialized here. The displayed Sec1 of source eq. (2.3) is the image of Z by direct substitution, although the prose after that equation associates Sec1 with the exceptional section. The regularity proof is for general coefficients. The gauge-direction interpretation is [GEO-E], under the ordinary M/F description of Chapter 1 and with no gauge-breaking background. No full Mordell–Weil rank assertion is used.

§2. Projection and height. The vertical, height and root calculations are [MATH]. See Morrison and Park (2012), arXiv:1208.2695v2, §3.1, eqs. (3.2)–(3.11), for the Shioda construction and pushforward, and Cvetič and Lin (2018), arXiv:1706.08521v3, §2.2, eqs. (2.4)–(2.8), for the root correction and charges. The older Calabi–Yau threefold rank proof is not used for this fourfold. The Cartan height calculation assumes the stated ordinary pushforwards over the gauge divisor.

§3. Charged fibers. The conifold chart, section degrees, complete intersection, square locus and open occurrence of the two ordinary fibers are [MATH]. See Mayrhofer, Palti, et al. (2014), §2.1, eqs. (2.5)–(2.11) and Figs. 2–3. The calculation here of C_2 assumes $b_2 \neq 0$ and does not use the saturated ideal on the remaining strata. The charge interpretation is [GEO-E]; see Morrison and Park (2012), eq. (3.11), and Cvetič and Lin (2018), eq. (2.8). It uses the ordinary wrapped-membrane and F-theory identification, and does not give zero-mode multiplicities.

§4. The two tops. The restrictions, section placement input and lattice deductions are [MATH]. The connected group identification is [GEO-E]. See Cvetič and Lin (2018), §4.2, eqs. (4.2),(4.5) and Fig. 1 for the two resolved top geometries and their matter representations, and §3.1, eqs. (3.1)–(3.4), for the group dictionary. The displayed restrictions do not replace the resolved topology. The conclusions concern the compact connected sector.

§5. The torsion Tate model. The exact torsion point, discriminant and half-coroot calculation are [MATH]. The connected gauge interpretation is [GEO-E]. See Mayrhofer, Morrison, et al. (2014), arXiv:1405.3656v2, §4.1, eqs. (4.1)–(4.20), especially the exclusions (4.8), absent divisor (4.18), and quotient (4.19)–(4.20). Their eq. (4.2) uses $\Delta_{\text{book}}/16$; here $\Delta_{\text{book}} = 4f^3 + 27g^2$. Our Cartan divisor is E. The relation is rational with an integral representative of the half-coroot, without a claim about torsion in integral cohomology.

§6. Deformation and conditional stabilizer. The quartic blowdown, square tests and conditional field-theory stabilizer are [MATH]. See Mayrhofer, Palti, et al. (2014), §2.2, eqs. (2.12)–(2.13) for the quartic and restriction. The stabilizer uses a primitive four-dimensional charge and an assumed expectation value. The circle-reduced combination in their §2.4 and the existence of a physical Higgs vacuum are outside this argument.

References

Cvetič, M. and L. Lin (2018). "The Global Gauge Group Structure of F-theory Compactification with $U(1)$s". In: *JHEP* 01, p. 157. DOI: 10.1007/JHEP01(2018)157. arXiv: 1706.08521 [hep-th].

Mayrhofer, C., D. R. Morrison, et al. (2014). "Mordell–Weil Torsion and the Global Structure of Gauge Groups in F-theory". In: *JHEP* 10, p. 016. DOI: 10.1007/JHEP10(2014)016. arXiv: 1405.3656 [hep-th].

Mayrhofer, C., E. Palti, et al. (2014). "Discrete Gauge Symmetries by Higgsing in Four-Dimensional F-Theory Compactifications". In: *JHEP* 12, p. 068. DOI: 10.1007/JHEP12(2014)068. arXiv: 1408.6831 [hep-th].

Morrison, D. R. and D. S. Park (2012). "F-Theory and the Mordell–Weil Group of Elliptically-Fibered Calabi–Yau Threefolds". In: *JHEP* 10, p. 128. DOI: 10.1007/JHEP10(2012)128. arXiv: 1208.2695 [hep-th].

Chapter XIV.7

Genus-one fibrations and discrete gauge symmetry

XIV.7.1 Higgsing the continuous gauge group

What survives when a field of charge two acquires an expectation value? A continuous gauge field can become massive while its gauge transformations still act nontrivially on some particles. In the preceding chapter, the two sections of a compact fourfold over $\mathbb{P}^3$ supplied an abelian gauge direction, and wrapped membranes supplied its charge lattice. We will follow the deformation that replaces those two sections by a divisor of degree two over the base. This will give us a geometry on which to ask separately whether there is still a rational section, what happens to the charged fibral curves, and under what assumptions there is a four-dimensional Higgs vacuum.

Recall that a fibral curve lies over a point of the base. Its abelian charge in the ordinary wrapped-M2 description is the intersection with the Shioda divisor. The unit-charge component in our parent fixes a primitive character of the $U(1)$; we may not divide all charges by two just because the proposed Higgs field has charge two. Write θ for the gauge angle, q_i for a charge, and v_i for the vacuum value of a scalar ϕ_i. The condition for a gauge transformation to fix the vacuum is

$$\theta \in \mathbb{R}/2\pi\mathbb{Z}, \qquad \phi_i \longmapsto e^{iq_i\theta}\phi_i, \qquad q_i\theta \in 2\pi\mathbb{Z} \quad \text{for every } v_i \neq 0. \tag{XIV.7.1}$$

A neutral expectation value imposes no condition. If at least one charged expectation value is nonzero, let d be the greatest common divisor of the absolute values of the participating charges. Since there are integers r_i with $\sum_i r_i q_i = d$, every angle fixing the vacuum obeys $d\theta \in 2\pi\mathbb{Z}$. Conversely, each q_i is a multiple of d. Thus the full stabilizer inside this gauge factor is

$$\mathrm{Stab}(v) = \left\{ \theta = \frac{2\pi j}{d} \pmod{2\pi} : 0 \leq j < d \right\} \simeq \mathbb{Z}_d. \tag{XIV.7.2}$$

For charge two, the allowed angles are 0 and π. A field of odd charge changes sign at π. Even though the Lie algebra of the stabilizer is zero, this sign distinguishes states and

constrains amplitudes. Figure XIV.7.1 shows why knowing the angle period is part of the calculation.

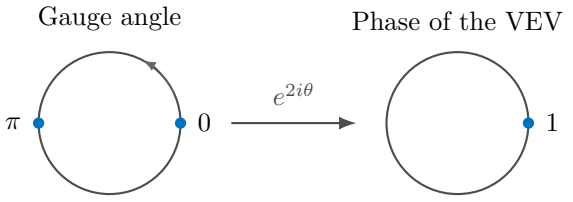


Figure XIV.7.1: The charge-two character sends both $\theta = 0$ and $\theta = \pi$ to the unit phase. With an additional charge-three expectation value, the same π rotation gives phase -1 and fails to fix the vacuum.

For example, with both a charge-two and a charge-three expectation value, subtracting 2θ from 3θ shows that θ itself must be a multiple of 2π. For charges four and six, the difference is instead 2θ and the sign group survives. A lone charge-one value leaves only the identity. A lone charge-three value would give $\mathbb{Z}_3$ in ordinary field theory; this does not change the number of sheets in the quartic we are about to construct.

The stabilizer calculation presupposes a vacuum. To see what it takes even in a toy theory, use two chiral multiplets with charges $+2, -2$, canonical kinetic terms, zero Fayet–Iliopoulos parameter and zero superpotential. Denote their scalar components by ϕ_+, ϕ_-. The moment map μ and its contribution to the potential are

$$\mu = 2|\phi_+|^2 - 2|\phi_-|^2, \qquad V_D = \frac{g_{\mathrm{YM}}^2}{2}\mu^2, \qquad V_F = \sum_i |\partial_i W|^2 = 0. \tag{XIV.7.3}$$

Here g_{YM} is the gauge coupling. Choosing $\phi_+ = \phi_- = v$ with $|v| > 0$ solves both sets of flatness equations. A single positively charged field could not do this at zero FI parameter. With $D_\nu \phi_i = (\partial_\nu - i g_{\mathrm{YM}} q_i A_\nu)\phi_i$ and the canonical vector mass term normalized with a factor of $1/2$, the kinetic terms give

$$m_A^2 = 2 g_{\mathrm{YM}}^2 \sum_i q_i^2 |v_i|^2 = 16 g_{\mathrm{YM}}^2 |v|^2. \tag{XIV.7.4}$$

The opposite charges cancel in μ and add in the vector mass. This realizes the sign stabilizer without a massless photon from the original factor. In polar coordinates $\phi_\pm = r_\pm e^{i\gamma_\pm}$ the equal radii solve the moment map, while the angle shifts are $(\gamma_+, \gamma_-) \mapsto (\gamma_+ + 2\theta, \gamma_- - 2\theta)$. The sum of the phases is gauge invariant, as is the product

$$\phi_+ \phi_- = |v|^2 e^{i(\gamma_+ + \gamma_-)}. \tag{XIV.7.5}$$

The phase difference moves along the gauge orbit. Its continuous motion is absorbed by the vector; the rotation by π leaves both phases fixed modulo 2π. A spectator of charge one still feels that rotation. This is why identifying the gauge invariant coordinate along the flat branch does not account for the full action on excitations.

For a monomial built from fields and conjugates, its charge is the sum of the charges of the factors, with a sign reversal for every conjugate. In the sign subgroup a monomial of total charge Q transforms by $(-1)^Q$. In a variant of the toy theory with a charge-one chiral field X_1, an allowed coupling and its effect at $X_1 = 0$, $\phi_- = v$, are

$$W = \lambda \phi_- X_1^2, \qquad (-2) + 1 + 1 = 0, \qquad W_{\text{quad}} = \lambda v X_1^2. \tag{XIV.7.6}$$

At the stated vacuum the derivatives with respect to X_1 and ϕ_- still vanish. The bilinear is permitted because it is even and follows here from an explicit invariant cubic. An allowed bilinear in a compactification need not have a nonzero coefficient. Odd total charge, in contrast, cannot be canceled by inserting fields whose charges all belong to $2\mathbb{Z}$.

This is the field theory pattern we will compare with the geometry. The two available signs in a fiber equation do not by themselves establish a vacuum or even exclude a rational point. To see what the compact construction does establish, we first need the equation in which the two old sections can join.

XIV.7.2 The deformed genus-one equation

How do the old section images become two sheets of one divisor? Let $B = \mathbb{P}^3_{\mathbb{C}}$ with hyperplane class H and homogeneous coordinates $X_0, \dots, X_3$. Use (u, v, w, s) for the parent fiber coordinates and U, S for the divisor classes of u, s. The two toric actions and the base twists are encoded by the classes

$$([u], [v], [w], [s]) = (U, U + S + H, 2U + S + 5H, S). \tag{XIV.7.7}$$

For example the coefficients of U, S in these four entries are the two weight rows $(1, 1, 2, 0)$ and $(0, 1, 1, 1)$. The forbidden simultaneous vanishings are $u = w = 0$ and $v = s = 0$. Write $\mathcal{O}_B(k)$ for the bundle of class kH. The coefficients (b_0, b_1, b_2) have degrees $(5, 4, 3)$ and (c_0, c_1, c_2, c_3) have degrees $(10, 9, 8, 7)$. With these twists the parent polynomial is

$$\begin{aligned} P_1 = {} & sw^2 + (b_0 s^2 u^2 + b_1 suv + b_2 v^2) w \\ & + c_0 s^3 u^4 + c_1 s^2 u^3 v + c_2 s u^2 v^2 + c_3 u v^3. \end{aligned} \tag{XIV.7.8}$$

For instance $b_1 suvw$ has class $4U + 3S + 10H$, the same as sw^2 and $c_3 uv^3$. Homogeneity fixes the bundle information needed for the deformation.

Consider the map $(u', v', w') = (su, v, sw)$. Its target has fiber weights $(1, 1, 2)$ for the single remaining fiber scaling; the coordinate classes are $U', U' + H, 2U' + 5H$, where on the parent the pullback ambient class is $U' = U + S$. This equality does not identify the divisor $u' = 0$ on the deformed space with either individual parent section. On $s \neq 0$ substitute $u = u'/s$, $v = v'$, $w = w'/s$ into sP_1. The inverse powers of s cancel, yielding

$$\begin{aligned} P_{\text{b}} = {} & w'^2 + (b_0 u'^2 + b_1 u' v' + b_2 v'^2) w' \\ & + c_0 u'^4 + c_1 u'^3 v' + c_2 u'^2 v'^2 + c_3 u' v'^3, \qquad P_{\text{b}}(su, v, sw) = sP_1(u, v, w, s). \end{aligned} \tag{XIV.7.9}$$

The last identity is polynomial and holds also at $s = 0$. Over a base point at which $b_2 \neq 0$, the section U has $u = 0$ and $w \neq 0$. Its equation then requires $sw = -b_2 v^2$, and $v = 0$ would force $s = 0$, which is forbidden there. The section S has $s = 0$, so $v \neq 0$ and $su = sw = 0$. Normalizing by v gives the ordered images

$$U \longmapsto [0 : 1 : -b_2], \qquad S \longmapsto [0 : 1 : 0]. \tag{XIV.7.10}$$

These are the two roots of $w'(w' + b_2 v'^2) = 0$ along $u' = 0$. Their order will matter when we read signed charges on the two components of another fiber.

The class of P_{b} is $4U' + 10H$. The absent monomial v'^4 has class $4U' + 4H$, so its coefficient c_4 has degree six. Define the quadratic B_2 and quartic C_4 by

$$B_2 = b_0 u'^2 + b_1 u' v' + b_2 v'^2, \tag{XIV.7.11}$$

$$C_4 = c_0 u'^4 + c_1 u'^3 v' + c_2 u'^2 v'^2 + c_3 u' v'^3 + c_4 v'^4. \tag{XIV.7.12}$$

Adding $c_4 v'^4$ gives $P_2 = w'^2 + B_2 w' + C_4 = 0$. The change of coordinate $z = 2w' + B_2$ gives

$$4P_2 = z^2 - F, \qquad F = B_2^2 - 4C_4, \qquad F = \sum_{i=0}^{4} a_i u'^{4-i} v'^i. \tag{XIV.7.13}$$

Both z and w' have class $2U' + 5H$. Counting powers of H in each monomial gives $\deg a_i = 10 - i$. In that order the coefficients are

$$(a_i)_{i=0}^{4} = (b_0^2,\ 2b_0 b_1,\ b_1^2 + 2b_0 b_2,\ 2b_1 b_2,\ b_2^2) - 4(c_0, c_1, c_2, c_3, c_4). \tag{XIV.7.14}$$

At fixed b_i, prescribing the five a_i independently prescribes five allowed c_i. This is the full family of quartics with these twists. Varying only c_4 at a fixed parent instead moves just a_4.

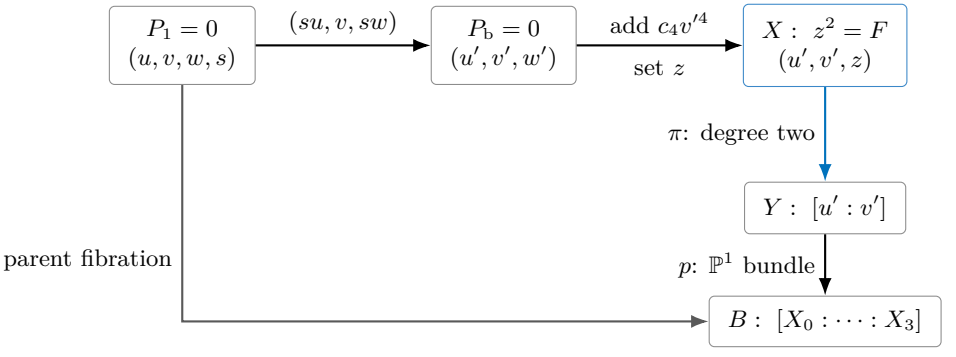


Figure XIV.7.2: The weighted blowdown followed by the quartic deformation. The upper row gives the coordinate map and the equation change; the arrow from X to Y forgets z. The degree-two map is to the ruled space Y, not to the threefold base B.

To make the geometry of Figure XIV.7.2 global, let $p : Y = \mathbb{P}_B(\mathcal{O}_B \oplus \mathcal{O}_B(H)) \to B$ parametrize one-dimensional quotients, and write $\zeta = c_1(\mathcal{O}_Y(1))$. Evaluating the two

summands in the quotient gives v' of class ζ and u' of class $\zeta - H$. Thus $U' = \zeta - H$. The two coordinate divisors do not intersect, and the tautological quotient has degree one on each projective line. In particular,

$$U'(U' + H) = 0, \qquad L = 2U' + 5H = 2\zeta + 3H, \qquad F \in H^0(Y, \mathcal{O}_Y(2L)). \quad \text{(XIV.7.15)}$$

Here and below classes from B are pulled back where used. The rank-two bundle defining Y is generated by its sections: one for the trivial summand and four for $\mathcal{O}_B(H)$. Evaluating them embeds Y into $B \times \mathbb{P}^4$ over B, with $\mathcal{O}_Y(\zeta)$ the second hyperplane class. Hence L is ample, as the restriction of $\mathcal{O}(3, 2)$. The class U' itself is not ample: on the section of Y associated to the trivial quotient, $\zeta = 0$ and $U' = -H$.

The weighted vertex $u' = v' = 0$ does not lie on $P_2 = 0$ because there w'^2 is nonzero. Off that vertex the weighted ambient is the total space of $\mathcal{O}_Y(L)$: on each of the charts $u' \neq 0$ or $v' \neq 0$, divide the weight-two coordinate by the square of the chart coordinate and use its base twist. For example in a common base trivialization,

$$z_v = z/v'^2, \qquad z_u = z/u'^2, \qquad z_u = (v'/u')^2 z_v. \quad \text{(XIV.7.16)}$$

The additional base twists of z_v and z_u are $3H$ and $5H$ respectively, consistent with the twist of the ratio on the overlap. The completion of the square in (XIV.7.13) respects this same transition since B_2 has the class of z. Thus the compact hypersurface X can be described by the double-cover algebra over Y:

$$\pi : X = \mathrm{Spec}_Y(\mathcal{O}_Y \oplus \mathcal{O}_Y(-L)) \longrightarrow Y, \qquad z^2 = F. \quad \text{(XIV.7.17)}$$

Locally this is a free rank-two algebra with basis $1, z$; multiplication of two elements from the second summand uses F. The map is finite flat, hence projective, and $p\pi$ is flat. Write $D = (F = 0) \subset Y$ for the branch divisor. At $F \neq 0$, the derivative in the z direction is $2z \neq 0$. At $z = 0$, the derivative of $z^2 - F$ is $-dF$. Therefore smooth D gives smooth X. A smooth divisor in the nontrivial ample class $2L$ is nonempty and reduced. Along one of its components the section F has odd order, in any rational trivialization up to a square. It follows that the generic double cover is a field extension and X is integral.

The quotient bundle formula gives $K_Y = -2\zeta + p^*(K_B + H) = -L$. The canonical bundle of the total space of $\mathcal{O}_Y(L)$ is the pullback of $K_Y - L$. The hypersurface has class $2L$ in this total space, so adjunction gives

$$K_X = \pi^*(K_Y - L + 2L) = 0, \qquad \pi_* \mathcal{O}_X = \mathcal{O}_Y \oplus K_Y. \quad \text{(XIV.7.18)}$$

The projective line fibers of p give $p_* \mathcal{O}_Y = \mathcal{O}_B$ and no higher direct images. Thus $H^i(Y, \mathcal{O}_Y) = 0$ for $i > 0$, and Serre duality in dimension four gives $H^i(X, \mathcal{O}_X) = 0$ for $0 < i < 4$. In characteristic zero the dominant map from smooth X to B has smooth generic fiber. On that fiber a smooth degree-two cover of $\mathbb{P}^1$ has four simple branch points, so $2g - 2 = 2(-2) + 4 = 0$. Smoothness of the total space concerns all its directions; a special fiber can still be singular.

It remains to produce a smooth branch member of this actual compact linear system.

Consider the diagonal quartic

$$F = Au'^4 + Ev'^4, \qquad (p_0, p_1, p_2, p_3) = (1, 4, 16, 64),$$
$$A = \sum_{i=0}^{3} X_i^{10}, \qquad E = \sum_{i=0}^{3} p_i X_i^6. \tag{XIV.7.19}$$

For example set $b_i = 0$, $c_0 = -A/4$, $c_4 = -E/4$ and the other $c_i = 0$. The gradients of A and E are nonzero at their respective projective zeros. Suppose they were proportional at a common zero. Computing the gradients in the affine cone, at each active coordinate $X_i \neq 0$ proportionality requires $X_i^4 = \kappa p_i$ with one common $\kappa \neq 0$. Fixing a square root of κ gives

$$X_i^2 = \pm\sqrt{\kappa}\sqrt{p_i}, \qquad E = \kappa^{3/2} \sum_{i \text{ active}} \pm p_i^{5/2}. \tag{XIV.7.20}$$

The magnitudes are $1, 32, 1024, 32768$. The largest active one exceeds the sum of all the smaller ones, so $E = 0$ is impossible. This proves transversality at every common zero, including points where some coordinates vanish.

At $v' = 0$, the branch equation is $A = 0$ and a base derivative of A makes the divisor smooth; the same argument uses E at $u' = 0$. In the interior, take the fiber chart $v' = 1$ and write $\tau = u'/v'$ in a local base frame. Vanishing of the fiber derivative requires $4A\tau^3 = 0$, so on D with $\tau \neq 0$ it forces $A = E = 0$. There the base derivative is $\tau^4 dA + dE$, which cannot vanish by transversality. This establishes smoothness everywhere, rather than testing a finite list of fibers.

The choice of weights matters. If all $p_i = 1$, then at $[1 : i : 0 : 0]$ both polynomials vanish. In the chart $X_0 = 1$, the only nonzero derivatives are in the X_1 direction, where $dA = 10i\, dX_1$ and $dE = 6i\, dX_1$. A ratio τ with $\tau^4 = -3/5$ makes the branch derivative vanish. Thus an allowed change of coefficients gives an actual singular branch divisor. The singular incidence is closed in the product of the projective variety Y with the parameter space of sections, and its projection to parameters is closed by properness. The first diagonal member proves the complementary open is nonempty. Its fiber at $[1 : 0 : 0 : 0]$ is already smooth, since $u'^4 + v'^4$ has distinct roots. The diagonal example tests the child geometry; it is not the resolved charged parent. In the irreducible full coefficient space this child open meets the nonempty open of smooth resolved parents, which imposes conditions on the coefficients other than c_4. This does not give a genericity assertion about the c_4-only line through an arbitrary special parent.

The double cover gives a specific degree-two divisor by pulling back $u' = 0$. We next ask whether the two points of this divisor, or any other points of the generic fiber, can be chosen over the base field.

XIV.7.3 The bisection and its Jacobian

Which calculation can rule out every rational section? The point of the base relevant to this question is its generic point, with field $K = \mathbb{C}(B)$. A rational section of $p\pi$ gives a K-rational point of the generic curve X_K, and a K-point gives a section over some

open set of B. First examine the displayed divisor $\mathcal{B} = \pi^{-1}(u' = 0)$. On this chart $v' \neq 0$, write $W = w'/v'^2$ in a base trivialization. The restriction of P_2 is

$$W^2 + b_2 W + c_4 = 0, \qquad \delta_2 = b_2^2 - 4c_4 = a_4 \in H^0(B, \mathcal{O}_B(6)). \tag{XIV.7.21}$$

For $\delta_2 \neq 0$ over K, its two roots are $(-b_2 \pm \sqrt{\delta_2})/2$. The change of base frame multiplies the representative of δ_2 by a square, so its square class in $K^\times$ is well defined. A nonsquare exchanges the two roots under the nonidentity automorphism of $K(\sqrt{\delta_2})/K$. This detects the two points of $\mathcal{B}$ only.

Even as a local test on a fiber, $\delta_2 = 0$ tests one branch position rather than all branch collisions. For example,

$$F_1 = u'v'(u' - v')(u' + v'), \qquad F_2 = (u'^2 + v'^2)^2. \tag{XIV.7.22}$$

For F_1 the point $u' = 0$ is a simple branch point, so the two intersections with $\mathcal{B}$ coalesce but the fiber is smooth. Its other branch points are $v' = 0$ and $u'/v' = \pm 1$. For F_2 the two intersections with $\mathcal{B}$ are distinct, yet the cover factors into two graphs meeting at the zeros of $u'^2 + v'^2$. Both are tests on specialized fiber coefficients, not assertions of total-space smoothness. The distinction can be seen directly from the gradient on the curve. For a fiber coordinate τ and local equation $z_v^2 - F(\tau, 1) = 0$, the fiber gradient vanishes exactly when

$$z_v = 0, \qquad F(\tau, 1) = 0, \qquad \partial_\tau F(\tau, 1) = 0, \tag{XIV.7.23}$$

with the other chart giving the same test at infinity. At a simple root, τ varies quadratically with z_v after moving the root to zero. In contrast, at a double root with nonvanishing quadratic coefficient the two local slopes in (τ, z_v) are distinct. Figure XIV.7.3 shows the difference on a real slice of the two local normal forms. To detect a collision anywhere on the projective line we need the binary quartic discriminant. To construct the Jacobian we need two invariants of the quartic.

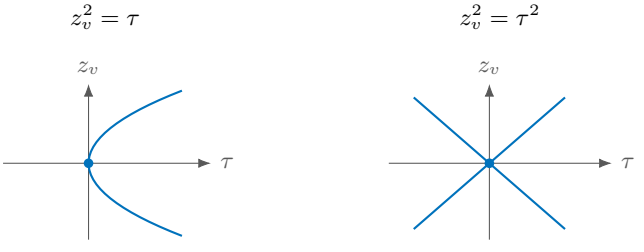


Figure XIV.7.3: Local fiber equations at zeros of the branch quartic, after absorbing a local unit. A simple root gives one smooth curve tangent to the line $\tau = 0$. A double root gives two crossing branches. The drawn real slices illustrate the complex tangent directions.

Write $(u', v') = (u_b, v_b)$ temporarily in a base frame, and write

$$F = au_b^4 + bu_b^3 v_b + cu_b^2 v_b^2 + du_b v_b^3 + ev_b^4. \tag{XIV.7.24}$$

The letters (a,b,c,d,e) denote $(a_0,\dots,a_4)$ in order. The alternating form on the two fiber coordinates identifies the coordinate vector with $(\partial_{v_b},-\partial_{u_b})$ in a determinant-one frame. For a quartic G with coefficients $(g_0,\dots,g_4)$ in the same order, applying the resulting differential operator gives the constant

$$\mathcal{T}_F(G)=F(\partial_{v_b},-\partial_{u_b})G=24(ag_4+eg_0)-6(bg_3+dg_1)+4cg_2. \tag{XIV.7.25}$$

Each term differentiates just one monomial to a nonzero constant. In particular $I=\mathcal{T}_F(F)/4=12ae-3bd+c^2$. For a cubic invariant, take G to be a quadratic expression in the coefficients of F which is again a binary quartic in the variables. The determinant of the 2×2 Hessian does this. With $G=\det\mathrm{Hess}(F)/3$ its five entries are

$$\begin{aligned} &g_0=8ac-3b^2, && g_1=24ad-4bc,\\ &g_2=48ae+6bd-4c^2, && g_3=24be-4cd, \qquad g_4=8ce-3d^2. \end{aligned} \tag{XIV.7.26}$$

For example, the u_b^4 term in the Hessian determinant is $(12a)(2c)-(3b)^2$. Substitution into (XIV.7.25) gives

$$J=\frac{\mathcal{T}_F(G)}{8}=72ace+9bcd-27ad^2-27b^2e-2c^3. \tag{XIV.7.27}$$

Under $v_b\mapsto v_b+\lambda u_b$ the coordinate vector and its alternating dual transform together, and the Hessian changes by conjugation with the shear and its transpose. The determinant of the shear is one, so I,J are unchanged. Under chart swap the contraction acquires four alternating signs and the Hessian determinant a square of a sign, so both are again unchanged. Equivalently, reversing the order of the five coefficients leaves the displayed formulas unchanged. These are coordinate checks in a base frame; the global line bundles will be read off from the coefficient degrees, without treating all five coefficients as sections of the same bundle.

The invariant theorem for a smooth genus-one double cover over a field of characteristic zero identifies its Jacobian over that field, using the differential of the cover. With the normalization of (XIV.7.24), its invariants are $c_4^{\mathrm{inv}}=16I$ and $c_6^{\mathrm{inv}}=32J$, where c_4^{inv} is unrelated to the coefficient c_4 of the deformation. In the theorem's cubic $y_F^2=x_F^3-27c_4^{\mathrm{inv}}x_F-54c_6^{\mathrm{inv}}$ set $x_F=6^2x$, $y_F=6^3y$ to get

$$J_K:\quad y^2=x^3+fx+g, \qquad f=-I/3, \qquad g=-J/27. \tag{XIV.7.28}$$

Here $J_K=\mathrm{Pic}^0(X_K)$ is the elliptic curve; J without a subscript in the formula for g is the cubic polynomial invariant. A check on the scale and sign is the split quartic $F=u_bv_b(u_b-v_b)(u_b-\lambda v_b)$, for $\lambda\neq 0,1$. In $v_b=1$ it is already the Legendre cubic $\tau^3-(1+\lambda)\tau^2+\lambda\tau$ in $\tau=u_b/v_b$. With its point at infinity as origin, setting $\tau=x+(1+\lambda)/3$ gives the short coefficients

$$f=\lambda-\frac{(1+\lambda)^2}{3}, \qquad g=\frac{\lambda(1+\lambda)}{3}-\frac{2(1+\lambda)^3}{27}. \tag{XIV.7.29}$$

The quartic coefficients $(0,1,-(1+\lambda),\lambda,0)$ give these same values in (XIV.7.28). A check of j alone would leave a possible twist over K. The invariant theorem fixes the actual K-Jacobian.

The binary discriminant can be calculated by elimination in a chart with $a \neq 0$. Divide $F(\tau, 1)$ by a, and translate $\tau = t - b/(4a)$. Write the depressed monic quartic as $Q(t) = t^4 + \alpha t^2 + \beta t + \gamma$. A repeated root is a common root of Q and Q'. The resultant is the determinant of multiplication by Q' in $K[t]/(Q)$: over a splitting field with simple roots its eigenvalues are Q' evaluated at those roots, and the equality extends as a polynomial identity. Reducing Q', tQ', t^2Q', t^3Q' with $t^4 = -\alpha t^2 - \beta t - \gamma$ gives

$$\det \begin{pmatrix} \beta & -4\gamma & 0 & 2\alpha\gamma \\ 2\alpha & -3\beta & -4\gamma & 2\alpha\beta \\ 0 & -2\alpha & -3\beta & 2\alpha^2 - 4\gamma \\ 4 & 0 & -2\alpha & -3\beta \end{pmatrix} = \frac{4(12\gamma + \alpha^2)^3 - (72\alpha\gamma - 27\beta^2 - 2\alpha^3)^2}{27}. \tag{XIV.7.30}$$

The right hand side follows by determinant expansion; for example its two terms independent of β combine to $16\gamma(\alpha^2 - 4\gamma)^2$. The two parenthesized factors are I/a^2 and J/a^3 for the monic translated quartic, by shear invariance and homogeneity. A degree-four discriminant is multiplied by a^6 when the polynomial is multiplied by a. The identity extends to $a = 0$ as an identity of binary forms and continues to test root collisions at infinity. With the Weierstrass convention used in this volume,

$$\begin{aligned} \operatorname{disc}_{\mathrm{bin}}(F) &= \frac{4I^3 - J^2}{27}, \\ \Delta_{\mathrm{book}} = 4f^3 + 27g^2 &= -\operatorname{disc}_{\mathrm{bin}}(F), \qquad \Delta_{\mathrm{ell}} = -16\Delta_{\mathrm{book}}. \end{aligned} \tag{XIV.7.31}$$

The last quantity is the usual discriminant of the Weierstrass equation. The distinction includes a sign and a factor even though the three quantities detect the same binary root collisions.

The degrees of (a, b, c, d, e) are $(10, 9, 8, 7, 6)$. In I each monomial has degree 16; in J the terms $ace, bcd, ad^2, b^2e, c^3$ each have degree 24. Thus $(f, g, \Delta_{\mathrm{book}})$ have degrees $(16, 24, 48)$, the fourth, sixth and twelfth powers of the anticanonical degree of the base. This recovers the expected Weierstrass bundles from the nontrivially twisted quartic. Compare the two smooth fiber quartics $u_b^4 + v_b^4$ and $u_b^4 + u_b^2v_b^2 + v_b^4$. Both have $\delta_2 = 1$, but the invariants are $(I, J) = (12, 0)$ and $(13, 70)$. Consequently $\operatorname{disc}_{\mathrm{bin}}$ is 256 and 144, respectively, and the corresponding $j = 1728 \cdot 4f^3/\Delta_{\mathrm{book}}$ values are different. The displayed pair of points is not enough information even to determine the complex elliptic modulus.

We can now ask if X_K itself has an origin. The Jacobian always has its own point at infinity; identifying X_K with J_K over K needs a point on X_K. To rule out every such point, we will show that every divisor on X_K has even degree. This requires a statement about line bundles on the compact fourfold, not just about the roots of one restriction.

Let $R = (z = 0) \subset X$ denote the ramification divisor and let $D = (F = 0) \subset Y$ be smooth as in Section XIV.7.2. The restriction $\pi_R : R \to D$ is an isomorphism: quotienting the local algebra by z also imposes $F = 0$. The divisor classes of D and R are $2L$ and π^*L. Both are ample, the latter by finite pullback. We apply the integral Grothendieck–Lefschetz restriction result separately to (Y, D) and (X, R). In the form we use, let T be a projective ambient variety and A an ample effective Cartier divisor.

The required depth and parafactoriality conditions are on the local rings of T, and the required cohomology vanishing is

$$H^1(A, \mathcal{O}_A(-nA)) = H^2(A, \mathcal{O}_A(-nA)) = 0 \qquad (n > 0). \tag{XIV.7.32}$$

Together these give the isomorphism $\mathrm{Pic}(T) \to \mathrm{Pic}(A)$. Here for both pairs the ambient closed-point local rings are regular of depth four. Off the divisor these regular local rings of dimension four are parafactorial, as required by the restriction result. Each divisor is a smooth projective threefold; for $i = 1, 2$,

$$H^i(A, \mathcal{O}_A(-nA))^\vee = H^{3-i}(A, K_A \otimes \mathcal{O}_A(nA)) = 0. \tag{XIV.7.33}$$

The twist on the right is ample, and the cohomological degree $3 - i$ is positive, so Kodaira vanishing applies. This checks both ambient and divisor hypotheses for both uses. At singular branch members this argument is not available.

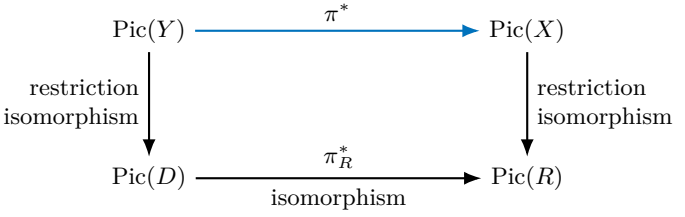


Figure XIV.7.4: The restriction square on integral Picard groups. The vertical isomorphisms require smooth ample divisors in the two smooth fourfolds; the lower isomorphism comes from the equation $z = 0$. Commutativity then gives the upper isomorphism.

Indeed pulling back a line bundle and restricting to R is the same as restricting it to D and pulling back by π_R. Following the arrows in Figure XIV.7.4 proves that $\pi^* : \mathrm{Pic}(Y) \to \mathrm{Pic}(X)$ is an integral isomorphism. Knowing only the ranks would leave open a subgroup of finite index. In particular it could not exclude a line bundle of degree one whose square was a pullback.

Let P be any closed point of X_K. Its closure in X dominates B and is generically finite over it. It therefore has dimension three and is a prime divisor in the smooth fourfold. Regularity makes it Cartier. Restricting its line bundle back to X_K gives $\mathcal{O}_{X_K}(P)$. Since this bundle comes from a pullback on X, for some $\mathcal{M} \in \mathrm{Pic}(Y)$ one has

$$[K(P) : K] = \deg \mathcal{O}_{X_K}(P) = \deg \pi_K^*(\mathcal{M}|_{Y_K}) = 2 \deg(\mathcal{M}|_{Y_K}), \qquad Y_K = \mathbb{P}^1_K. \tag{XIV.7.34}$$

So every closed-point degree is even. The displayed divisor $\mathcal{B}_K$ has degree two, since it is the pullback of a point by the finite flat degree-two map. The index, the gcd of all closed-point degrees, is exactly two, and there is no rational section.

A smooth genus-one curve is a torsor for its Jacobian: the elliptic curve acts simply transitively after choosing an origin over a splitting field. To see the degree dependence of this statement, choose $O \in X_K(\overline{K})$. In Pic^1 we may use $\mathcal{O}(O)$ as origin; the failure of this origin to descend is the cocycle with values $\mathcal{O}(gO - O)$ for a Galois element g.

With $\mathcal{O}(dO)$ as the origin of Pic^d the cocycle is multiplied by d. The degree-two divisor defined over K gives a K-point in Pic^2, so

$$[X_K] \neq 0, \qquad 2[X_K] = 0 \quad \text{in } H^1(K, J_K). \tag{XIV.7.35}$$

The first inequality follows from the absence of a K-point on the curve. The period, defined as the order of this Weil–Châtelet class, is therefore two. A geometric Tate–Shafarevich group would additionally require specifying a notion of local triviality and checking it on the base. The degree argument makes no such check.

Two allowed singular branch members show why global hypotheses matter. First, let $A = \sum_i X_i^{10}$ and $r = X_0^3 + X_1^3$. Then $F = Au'^4 + r^2 v'^4$ gives two K-points on $u' = 0$. Its generic fiber is smooth, but along $u' = r = 0$ the branch equation and all its first derivatives vanish. A smooth generic fiber alone could not have justified the use of the restriction theorem.

Next set $b_i = 0$ and take the quartic

$$F = X_0^9 u'^3 v' + X_0^5 (X_0 + X_1) v'^4. \tag{XIV.7.36}$$

On $X_1 = 1$ the order of δ_2 at $X_0 = 0$ is five. A square in K has even order there, so the displayed divisor does not split over K. In the generic fiber, $F = v'(A_1 u'^3 + E_1 v'^3)$ with $A_1 = X_0^9$ and $E_1 = X_0^5(X_0 + X_1)$ both nonzero. This has the simple root $v' = 0$ and three distinct roots in the chart $v' = 1$. Nevertheless $[u' : v' : w'] = [1 : 0 : 0]$ is a K-point. The index and period are one. At the base point $[0 : 1 : 0 : 0]$, in the fiber chart $u' = 1$ at $v' = 0$ the derivative in v' is $X_0^9 = 0$ and every base derivative vanishes. The total branch is singular. Thus even a nonsplit displayed divisor with smooth generic fiber is compatible with a trivial torsor on this boundary. To see how charges survive a transition, we need the degenerations of the actual parent and child, in addition to their generic fibers.

XIV.7.4 Following charged states through the transition

Which fibral curves disappear, and which keep track of the sign charge? The parent Shioda class for the two sections is $\sigma = S - U - 7H$, with height $14H$. The height is the negative pushforward of σ^2 to B. On any curve lying over a base point, H has degree zero, so its charge is simply the difference of its S and U intersections. These are intersection charges for wrapped membranes in the ordinary M-theory description; they do not yet count four-dimensional zero modes.

In the chart $v' = 1$ of the blowdown, use $\eta = u'$ and define

$$x_c = w', \qquad y_c = w' + b_0 u'^2 + b_1 u' + b_2, \qquad T = c_0 u'^3 + c_1 u'^2 + c_2 u' + c_3. \tag{XIV.7.37}$$

The polynomial is exactly

$$P_2 = x_c y_c + \eta T + c_4. \tag{XIV.7.38}$$

The base locus $C_1 = \{b_2 = c_3 = 0\}$ is a transverse complete intersection of degrees three and seven for general parent coefficients. At an ordinary point of C_1 we can use

b_2, c_3 as normal coordinates in the base, with a third coordinate along the curve. At $x_c = \eta = 0$ the determinant of the change from (w', b_2, u', c_3) to (x_c, y_c, η, T) is one: the linear terms of y_c are $w' + b_1 u' + b_2$ and those of T are $c_2 u' + c_3$. Thus for $c_4 = 0$ the transverse equation is a conifold, with the curve coordinate as a spectator. Its node is at the common image of the two branches of (XIV.7.10).

The parent resolves this node by retaining a rational curve. The charges can be obtained before taking the blowdown. At $b_2 = c_3 = 0$, the parent equation has a factor s. On $s = 0$ the fiber has $v \neq 0$ and $(u, w) \neq (0, 0)$. After setting $v = 1$, the remaining weight row is the first row minus the second, with weights $(1, 0, 1, -1)$ on (u, v, w, s). The exceptional component E_c is the projective line of (u, w); along it U has degree 1 and S has degree -1. The latter is the degree of the normal coordinate s, since the whole component lies in S. The map sends this entire curve to $[0 : 1 : 0]$.

The residual component M_c does not meet $u = 0$ at an ordinary point. Indeed $u = 0$ in the residual equation would force $w = 0$. In $u = 1$, after removing the factor s, the equation is the conic

$$w^2 + b_0 sw + b_1 vw + c_0 s^2 + c_1 sv + c_2 v^2 = 0. \tag{XIV.7.39}$$

At $s = 0$, v is nonzero and the equation in w/v is quadratic. For an ordinary transverse split fiber the two intersections are distinct. Therefore the degrees and charges are

	$U\cdot$	$S\cdot$	$\sigma\cdot$
E_c	1	-1	-2
M_c	0	2	2

(XIV.7.40)

Their sums are the degrees on the full fiber. The disappearing exceptional component is sign neutral because -2 is even. The signs refer to effective complex curve orientations; reversing the membrane reverses its charge.

Adjunction on the smooth complete intersection gives two different degrees that will enter the deformation:

$$\begin{aligned} [C_1] &= 21H^2, \qquad \deg_H C_1 = 21, \\ K_{C_1} &= \mathcal{O}_{C_1}(-4+3+7) = \mathcal{O}_{C_1}(6), \\ \deg K_{C_1} &= 6 \cdot 21 = 126, \qquad g(C_1) = 1 + 126/2 = 64. \end{aligned} \tag{XIV.7.41}$$

In particular a general degree-six section restricted to C_1 has 126 simple zeros. Write $c_4 = th$ for a small complex parameter t and a degree-six section h. At a point where $h|_{C_1} \neq 0$, the old node no longer belongs to the deformed hypersurface. At a simple zero of $h|_{C_1}$ the old point is still on the equation, but differentiating in the tangent direction r along C_1 gives $t\,\partial_r h \neq 0$ for $t \neq 0$. The old point is then smooth in the total space. This tangent derivative is absent when the base coordinates are fixed. At a zero on C_1 the fiber equation at that fixed base point is unchanged, so the fiber through the point can still be singular. Figure XIV.7.5 contrasts the contracted curve and the pair of graphs that will survive at a different locus.

An exact local test uses the same sparse parent coefficients at two base points. The

coefficients in this test are homogeneous:

$$\begin{aligned} b_0 &= 5X_1^5, & b_1 &= 3X_1^4, & b_2 &= X_0^2X_2 + X_1^3, \\ c_0 &= -X_0^{10} + 4X_1^{10} + X_1^9X_2, & c_1 &= 9X_1^9 + X_1^8X_3, & & \\ c_2 &= -X_0^8 + 3X_1^8, & c_3 &= X_0^6X_3 + 2X_1^7. & & \end{aligned} \tag{XIV.7.42}$$

We use these coefficients for transverse local calculations. Smoothness of a general compact member was established by the separate branch argument. At $P_\star = [1:0:0:0]$, the derivatives of (b_2, c_3) in (X_2, X_3) on $X_0 = 1$ form the identity matrix. There $b_i = c_1 = c_3 = 0$ and $c_0 = c_2 = -1$. For $h = X_0^6 + X_1^6$ we have $h(P_\star) = 1$, and the completed quartic and its invariants there are

$$F_t = 4(u'^4 + u'^2v'^2 - tv'^4), \tag{XIV.7.43}$$

$$I_t = 16(1 - 12t), \qquad J_t = -128(1 + 36t),$$

$$\Delta_{\text{book}}(F_t) = 65536\, t(4t + 1)^2. \tag{XIV.7.44}$$

The discriminant is nonzero for sufficiently small nonzero t, so this particular old fiber is smoothed. The other exceptional value in this one-parameter test, $t = -1/4$, has two repeated branch roots. Changing the deformation to $h = X_1^6$ gives $h(P_\star) = 0$ and the old singular fiber remains at $P_\star$ for every t. Checking the value of the deformation on a fixed fiber and checking its tangent derivative in the fourfold answer different questions.

Now look for fibers with two components that do not disappear. A square quartic $F = (ku'^2 + \ell u'v' + mv'^2)^2$ gives the two graphs $z = \pm(ku'^2 + \ell u'v' + mv'^2)$. A simple root of the quadratic is a transverse crossing of the two graphs. Indeed the derivative of their difference is twice the derivative of the quadratic, which is nonzero there. With two distinct roots, the components are projective lines meeting at two nodes. Write C_2 locally for the base locus of such squares, with $a_4 \neq 0$ so that we can solve for m, ℓ, k in that order. Equating the last three coefficients gives

$$m^2 = a_4, \qquad \ell = \frac{a_3}{2m}, \qquad k = \frac{a_2 - \ell^2}{2m} = \frac{N}{8a_4m}, \qquad N = 4a_4a_2 - a_3^2. \tag{XIV.7.45}$$

The remaining coefficient equations are

$$E_0 = a_0 - \frac{N^2}{64a_4^3} = 0, \qquad E_1 = a_1 - \frac{Na_3}{8a_4^2} = 0. \tag{XIV.7.46}$$

The sign of m changes the signs of all three quadratic coefficients and exchanges the graphs, leaving these equations invariant. In particular, a zero of the quartic discriminant does not by itself impose the two square equations.

At $Q_\star = [0:1:0:0]$, take the chart $X_1 = 1$ and hold $X_0 = 0$. The coefficients of (XIV.7.42) on this slice are $(b_0, b_1, b_2) = (5, 3, 1)$ and $(c_0, c_1, c_2, c_3) = (4+X_2, 9+X_3, 3, 2)$; the deformation is $c_4 = t$. Thus

$$(a_0, a_1, a_2, a_3, a_4) = (9 - 4X_2, -6 - 4X_3, 7, -2, 1 - 4t). \tag{XIV.7.47}$$

At $t = X_2 = X_3 = 0$ the quartic is $(3u'^2 - u'v' + v'^2)^2$. The quadratic discriminant is -11, so the two crossing points are distinct. To compute the motion, let $e = a_4$. Then

$N = 28e - 4$, and the e derivatives at $e = 1$ of the two subtracted terms in (XIV.7.46) are

$$\frac{d}{de}\frac{(28e-4)^2}{64e^3}\bigg|_1 = -6, \qquad \frac{d}{de}\frac{-2(28e-4)}{8e^2}\bigg|_1 = 5. \tag{XIV.7.48}$$

Multiplying by $de/dt = -4$ and including the minus signs in E_0, E_1 gives

$$\frac{\partial(E_0, E_1)}{\partial(X_2, X_3, t)} = \begin{pmatrix} -4 & 0 & -24 \\ 0 & -4 & 20 \end{pmatrix}, \qquad \left(\frac{dX_2}{dt}, \frac{dX_3}{dt}\right) = (-6, 5). \tag{XIV.7.49}$$

The invertible normal block permits the implicit function theorem. Along $X_0 = 0$ there is a local moving solution for $(X_2(t), X_3(t))$, and the same invertible block gives a local germ with X_0 free. The quadratic roots remain distinct near the point, since their discriminant starts nonzero. The old base point at fixed $(X_2, X_3) = (0, 0)$ is not this moving square locus. Writing $e = 1 - 4t$, the square condition on this slice gives the local solution itself:

$$X_2(t) = \frac{1}{4}\left(9 - \frac{(28e-4)^2}{64e^3}\right), \qquad X_3(t) = \frac{1}{4}\left(-6 + \frac{2(28e-4)}{8e^2}\right). \tag{XIV.7.50}$$

This solution vanishes at $t = 0$ and its linear terms are (XIV.7.49). A node of the fiber on this slice need not be a singular point of the total space: the two roots have $u' \neq 0$ near $Q_\star$, and in $z^2 - F$ the derivative in the X_2 direction is $4u'^4 \neq 0$ by (XIV.7.47). The fiber gradient alone cannot see this derivative. No claim about the global shape of C_2 is needed for this calculation.

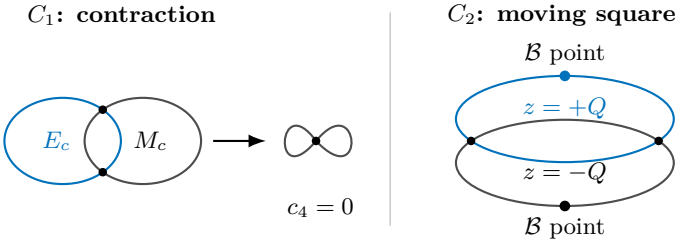


Figure XIV.7.5: Two different degenerations. Left: E_c at C_1 contracts; its Shioda charge is -2. Right: at the ordinary moving square, the two graphs $z = \pm Q$ meet at the two roots of the quadratic Q. The distinct marked points of the bisection lie off those nodes. At the parent point the upper graph meets S and the lower graph meets U.

Each graph meets $u' = 0$ in one reduced point, since in $v' = 1$ the graph is solved for z and u' is a coordinate on it. At $Q_\star$ we choose $m = 1$. The section images (XIV.7.10) have $w' = -1, 0$ in the order U, S. Since there $B_2(0, 1) = 1$, their z values are $-1, +1$ in that order. Therefore the plus and minus graphs have the following incidences on the parent and with the bisection on the nearby child:

	$U\cdot$	$S\cdot$	$\sigma\cdot$	$\mathcal{B}\cdot$
$z = +Q$	0	1	1	1
$z = -Q$	1	0	-1	1

$$Q = ku'^2 + \ell u'v' + mv'^2. \tag{XIV.7.51}$$

The charges $+1, -1$ also exhibit a primitive parent lattice. The modulo-two reduction agrees with the bisection intersection on each component. Over the moving germ with $a_4 \neq 0$, the two intersection points are still distinct and the two degrees are still one. With the ordinary wrapped-membrane interpretation this transports the odd assignment to the local surviving states. It does not give their zero-mode multiplicities.

At $a_4 = 0$ we cannot divide by m. For example $F = (u'^2 + u'v')^2$ has distinct nodes at $u' = 0$ and $u' = -v'$. Both graphs meet $u' = 0$ at the same node, so the two distinct marked points of Figure XIV.7.5 do not persist there. The calculation on the open chart distinguishes what is stable in the moving germ from what requires a separate boundary analysis. We now use the two different charge rows to compare the circle description to four dimensions.

XIV.7.5 Selection rules and a changed charge

Why can the three-dimensional description have a continuous gauge field if the four-dimensional Higgs mechanism leaves only a sign? In the ordinary circle reduction the three-dimensional charge lattice includes the Kaluza–Klein direction. Let R_{circ} be the circle radius, $n \in \mathbb{Z}$ the momentum label, q the original gauge charge, and ξ the Wilson-line variable in units of mass. In a frame with periodic fields the covariant momentum contributes the mass

$$m_n(q) = \left| \frac{n}{R_{\mathrm{circ}}} + q\,\xi \right| . \tag{XIV.7.52}$$

This is the mass from the circle and Wilson line for a tower with no other mass term. The integer labels are charges under $U(1)_{\mathrm{KK}} \times U(1)$. In the ordinary M/F identification used here the effective curve E_c has $(n, q) = (U \cdot E_c, \sigma \cdot E_c) = (1, -2)$. The residual conic has $(0, 2)$ in the same frame. Keeping n is essential because a shift of the Wilson line can cancel nonzero circle momentum.

At $\xi R_{\mathrm{circ}} = 1/2$ the $(1, -2)$ mode has zero mass in (XIV.7.52), whereas the residual conic row has nonzero circle mass. A unit-charge tower has half-integral covariant momenta there:

$$R_{\mathrm{circ}} m_1(-2) = 0, \qquad R_{\mathrm{circ}} m_0(2) = 1, \qquad \min_{n \in \mathbb{Z}} R_{\mathrm{circ}} m_n(\pm 1) = \min_{n \in \mathbb{Z}} |n \pm \tfrac{1}{2}| = \tfrac{1}{2}. \tag{XIV.7.53}$$

Figure XIV.7.6 shows the crossing and the neighboring unit-charge levels. A charge-three tower would also have half-integral covariant momenta at this Wilson line. These are statements about kinematics, independent of whether the necessary scalar actually has a vacuum value.

If the $(1, -2)$ mode acquires an expectation value in three dimensions, the two gauge angles, denoted (α, β) with periods 2π, must satisfy

$$\alpha - 2\beta = 0 \pmod{2\pi}, \qquad (\alpha, \beta) = (2\vartheta, \vartheta) \pmod{2\pi}. \tag{XIV.7.54}$$

Since the coefficient of α is one, each β determines exactly one α on the torus. The kernel is one connected circle with primitive generator $(2, 1)$, and a state (n, q) has

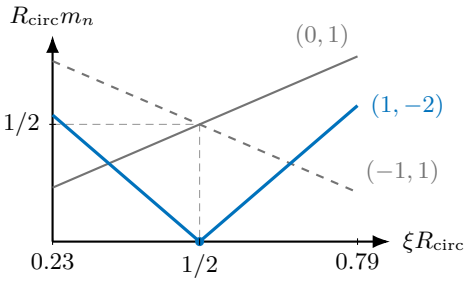


Figure XIV.7.6: Selected dimensionless masses $R_{\mathrm{circ}} m_n$ on the window $0.23 \le \xi R_{\mathrm{circ}} \le 0.79$. The $(1,-2)$ line reaches zero at $1/2$. The two shown unit-charge modes $(0,1)$ and $(-1,1)$ are the closest to zero there.

charge

$$Q_{\mathrm{circ}} = 2n + q, \qquad Q_{\mathrm{circ}} \equiv q \pmod 2. \tag{XIV.7.55}$$

For comparison, the hypothetical row $(2,-4)$ imposes

$$2(\alpha - 2\beta) = 0 \pmod{2\pi} \iff \alpha = 2\beta + \pi j \pmod{2\pi}, \qquad j = 0, 1. \tag{XIV.7.56}$$

The two values of j label distinct components. Its Lie algebra kernel is the same, but the actual $(1,-2)$ row is primitive. Discarding the Kaluza–Klein charge before finding the three-dimensional kernel would miss this difference. In Figure XIV.7.7, the connected kernel appears as two segments in a fundamental square, but their ends join when the square is identified. The second line in the comparison is a separate translate.

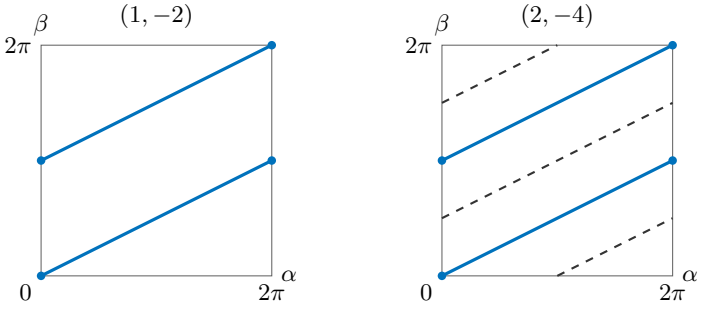


Figure XIV.7.7: Kernels in the square of gauge angles with opposite edges identified. Solid blue segments join to give the single circle of the $(1,-2)$ row. The nonprimitive row $(2,-4)$ retains that circle and the separate dashed translate.

The surviving continuous charge also has a direct geometric expression on a parent fibral curve C_f. Using $n = U \cdot C_f$ and $q = (S - U) \cdot C_f$ in this frame gives

$$2n + q = (U + S) \cdot C_f. \tag{XIV.7.57}$$

The class on the right is precisely the pullback ambient class of $u' = 0$. It has degree zero on the curve that contracts and degree one on each of the ordinary square components. This accounts for the bisection intersection in the same lattice that gives the three-dimensional circle.

Under the four-dimensional interpretation, a permitted D- and F-flat expectation value of charge magnitude two, with the remaining assumptions of Section XIV.7.1, leaves the subgroup $\mathbb{Z}_2$ of the original $U(1)$. On the three-dimensional circle of (XIV.7.54), take $\vartheta = \pi$. This gives $(\alpha, \beta) = (0, \pi)$ on the torus, so the character on a state is

$$e^{i\pi Q_{\mathrm{circ}}} = e^{i\pi(2n+q)} = (-1)^q. \tag{XIV.7.58}$$

This is how the same sign acts on states even though the three-dimensional stabilizer is connected. In particular the two local C_2 components have the same odd parity, while the C_1 row is neutral. This discrete stabilizer is also a different operation from taking a connected gauge group modulo a subgroup of its center, as in the preceding chapter. The local geometric transition and the stabilizer calculation identify a possible four-dimensional mechanism. We next examine which compact data still enter before it can be realized.

XIV.7.6 What the global geometry establishes

What additional information would be needed for an actual compact Higgs vacuum? Two conditions provide concrete tests. The compact D3 charge must balance, and the light fields must support the required expectation values. The two smooth compact geometries have different Euler characteristics, so changing the complex geometry can change the D3 charge budget even before considering the charged spectrum. We compute both Euler characteristics in their own ambient spaces.

For the child use the double cover of Y with smooth branch D. Write $P = U'$ temporarily in the intersection calculation. The projective bundle relation, base relation and integration normalization are

$$P^2 = -HP, \qquad H^4 = 0, \qquad \int_Y PH^3 = 1. \tag{XIV.7.59}$$

The last equality follows from degree one on the $\mathbb{P}^1$ fiber and $\int_B H^3 = 1$. The relative Euler sequence of the bundle and the Euler sequence of $\mathbb{P}^3$ give

$$c(TY) = (1+H)^4(1+P)(1+P+H). \tag{XIV.7.60}$$

By (XIV.7.59), the last two factors reduce to $1 + 2P + H$. In degrees one through four the expansion yields

$$\begin{aligned} c_1(Y) &= 2P + 5H, & c_2(Y) &= 8PH + 10H^2, \\ c_3(Y) &= 12PH^2 + 10H^3, & c_4(Y) &= 8PH^3. \end{aligned} \tag{XIV.7.61}$$

The class A_D of D is $2L = 4P + 10H$. Adjunction for the tangent bundle of D divides the total Chern class by $1 + A_D$. Since $c_1(Y) = A_D/2$,

$$c_3(TD) = \big(c_3(Y) - A_D c_2(Y) - \tfrac{1}{2}A_D^3\big)|_D = (-468PH^2 - 590H^3)|_D, \tag{XIV.7.62}$$

$$\chi(D) = \int_Y (4P + 10H)(-468PH^2 - 590H^3) = -5168. \tag{XIV.7.63}$$

For example $A_D c_2(Y) = 88PH^2 + 100H^3$ and $A_D^3/2 = 392PH^2 + 500H^3$; these two corrections come from the normal line to D. The Euler number of Y is 8 by (XIV.7.61). The cover has two sheets over $Y \setminus D$ and one over D, so additivity gives

$$\chi(X) = 2\chi(Y \setminus D) + \chi(D) = 2\chi(Y) - \chi(D) = 5184. \tag{XIV.7.64}$$

The branch correction is essential: counting two sheets everywhere would instead give 16.

For the resolved parent let $\mathcal{V}$ be the toric ambient bundle with the four fiber coordinates of (XIV.7.7), and write $A_P = 4U + 3S + 10H$ for the hypersurface class. The toric Chow calculation may be done over $\mathbb{Q}$. In addition to $H^4 = 0$, the forbidden pairs $u = w = 0$ and $v = s = 0$ give

$$U(2U + S + 5H) = 0, \qquad S(U + S + H) = 0, \qquad \int_{\mathcal{V}} USH^3 = 1. \tag{XIV.7.65}$$

Indeed $u = s = 0$ leaves nonzero v, w whose two weight columns have determinant -1. The quotient at this intersection has no finite stabilizer, so the fiber intersection multiplicity is one. The other possible nonunit determinant chart has w, s nonzero and $u = v = 0$; it misses the parent because $sw^2 \neq 0$ there. Thus tangent bundle adjunction on the smooth parent uses the ordinary smooth ambient chart along it. The calculation does not require an integral Chow presentation for the entire ambient quotient.

The toric Euler sequence, including the four base coordinates, yields

$$c(T\mathcal{V}) = (1 + H)^4(1 + U)(1 + U + S + H)(1 + 2U + S + 5H)(1 + S). \tag{XIV.7.66}$$

In particular $c_1(\mathcal{V}) = A_P$, so in $c(T\mathcal{V})/(1 + A_P)$ the last two degree-four terms $-A_P^3 c_1$ and A_P^4 cancel. For reproducibility, using $U^2 = -(US + 5UH)/2$ and $US = -S^2 - SH$ in the remaining terms gives

	H^3S	H^3U	H^2S^2
$c_4(\mathcal{V})$	45	19	-21
$A_P c_3(\mathcal{V})$	436	240	-122
$A_P^2 c_2(\mathcal{V})$	2278	1400	-536
$[c(T\mathcal{V})/(1 + A_P)]_4$	1887	1179	-435

(XIV.7.67)

Each row comes from the homogeneous component of (XIV.7.66), then multiplication and reduction with (XIV.7.65). For example the relations give $S^2H^3 = -USH^3$ and $U^2H^3 = -USH^3/2$. They reduce $A_P H^3 S$ and $A_P H^3 U$ to USH^3, and $A_P H^2 S^2$ to $-4USH^3$. To see the last reduction, multiply the first relation by S and the second by U to eliminate U^2S and obtain $US^2 = 3USH$; the second relation then

gives $S^3 = -3USH - S^2H$. These identities reduce the three terms of $A_P H^2 S^2$ to $(12-6-10)USH^3$. The resulting Euler number of the smooth resolved parent is

$$\chi(X_{\rm par}) = 1887 + 1179 + (-435)(-4) = 4806. \tag{XIV.7.68}$$

The difference $5184 - 4806 = 378 = 3 \cdot 126$ agrees with the Euler relation for this conifold transition, where 126 is the canonical degree of C_1 in (XIV.7.41). It is not obtained by just subtracting the Euler number of one rational component at each zero. We have used the smooth compact fourfolds, not assumed that the sparse local example is one of them.

With the dimensionless four-form convention of Chapter 3 let $Q = \frac{1}{2}\int G_4 \wedge G_4$. The D3 balance in the absence of further charge sources reads $N_{\rm D3} = \chi/24 - Q$. The curvature terms alone here are

$$\left(\frac{\chi(X_{\rm par})}{24}, \frac{\chi(X)}{24}\right) = \left(\frac{801}{4}, 216\right). \tag{XIV.7.69}$$

Their difference is $63/4$. An equality of complete D3 balances would require a compensating change of flux charge. We can compare two proposed flux expressions algebraically without assuming they give quantized supersymmetric backgrounds.

On the parent, take the formal product $G_{\rm par} = \sigma \wedge F_{\rm par}$ with base class $F_{\rm par} = mH$. The height $-\pi_{{\rm par}*}(\sigma^2) = 14H$ gives $Q_{\rm par} = -7m^2$. Here $\pi_{\rm par}$ is the fibration of the parent to B. On the child consider the specific factorized ansatz $c_4 = \rho\tau$ with $[\rho] = p_\rho H$ and $[\tau] = (6 - p_\rho)H$. Above $\rho = 0$, the restriction to the bisection splits. The sheet with $w' = -b_2 v'^2$ in $u' = 0$ defines a surface Σ_ρ over $\rho = 0$. The ansatz takes the combination $[\Sigma_\rho] - \frac{1}{2}\mathcal{B}\, p_\rho H$. Use its intersection formula on the base with $P_\rho = p_\rho H$:

$$Q_{\rm new} = \int_B P_\rho \left(-\frac{1}{4}P_\rho[c_3] + \frac{1}{2}[c_3][b_2]\right) = \frac{7}{4}p_\rho(6 - p_\rho), \qquad Q_{\rm par} = -7m^2. \tag{XIV.7.70}$$

The coefficient 7 comes from $[c_3] = 7H$, while $[b_2] = 3H$. This is the self-pairing formula for the stated surface ansatz. It makes no claim about an integral flux class on a smooth member at every choice of factorization.

Substituting (XIV.7.70) into the two balances and requiring equality gives

$$216 - \frac{7}{4}p_\rho(6 - p_\rho) = \frac{801}{4} + 7m^2 \quad \Longleftrightarrow \quad (p_\rho - 3)^2 = 4m^2. \tag{XIV.7.71}$$

The branches $p_\rho = 3 \pm 2m$ are interchanged by swapping ρ, τ. For the orientation $p_\rho = 3 + 2m$, effectiveness requires $0 \le p_\rho \le 6$, so the integral trial values of m are $-1, 0, 1$. At $m = 0$ the formal balance is $801/4$; at $m = \pm 1$ it is $829/4$. Neither is an integer. The equality compares two expressions in the bare trial lattice. It is not a D3-brane count and does not exclude other fluxes. A physical conclusion requires the shifted integral lattice, actual compatible classes, Hodge and primitivity conditions, the F-theory limit and any additional contributions to charge.

The fields needed for a vacuum give a separate calculation. Under the ordinary charged matter sheaf description, take the smooth curve $C = C_1$, the specified spin line

$\Theta = \mathcal{O}_C(3)$ with $\Theta^2 = K_C$, and a trial line bundle $\mathcal{L}_C = \mathcal{O}_C(m)$. The charge $+2$ contributes two powers of $\mathcal{L}_C$. The charges $(+2, -2)$ are counted by $(h^0(C, M), h^1(C, M))$, respectively, with

$$\begin{aligned} M &= \mathcal{L}_C^2 \otimes \Theta = \mathcal{O}_C(3 + 2m), \\ h^1(C, M) &= h^0(C, K_C \otimes M^{-1}) = h^0(C, \mathcal{O}_C(3 - 2m)). \end{aligned} \tag{XIV.7.72}$$

The equality is Serre duality. These are chosen line bundles on the curve, independently of whether the trial ambient flux induces them.

To compute $h^0(C, \mathcal{O}_C(d))$, twist the Koszul resolution for the $(3, 7)$ complete intersection by d. Its maps are multiplication by the equations of C and their relation:

$$0 \longrightarrow \mathcal{O}_B(d-10) \longrightarrow \mathcal{O}_B(d-3) \oplus \mathcal{O}_B(d-7) \longrightarrow \mathcal{O}_B(d) \longrightarrow \mathcal{O}_C(d) \longrightarrow 0. \tag{XIV.7.73}$$

In $\mathbb{P}^3$ the intermediate cohomologies of all line bundles vanish. Breaking the sequence at the twisted ideal sheaf therefore gives the exact count

$$h^0(C, \mathcal{O}_C(d)) = B(d) - B(d-3) - B(d-7) + B(d-10), \quad B(d) = \begin{cases} \binom{d+3}{3} & d \geq 0, \\ 0 & d < 0. \end{cases} \tag{XIV.7.74}$$

For example at $d = 5$ there are 56 polynomials, with 10 degree-two multiples of the cubic equation to subtract. No multiple of the degree-seven equation occurs. At $d = 7$ there is also the degree-seven equation itself to subtract. Applying the formula to the two powers in (XIV.7.72) gives Table XIV.7.1.

m	$(3 + 2m, 3 - 2m)$	$h^0(C, M)$	$h^1(C, M)$	$h^0 - h^1$
0	$(3, 3)$	$20 - 1 = 19$	$20 - 1 = 19$	0
1	$(5, 1)$	$56 - 10 = 46$	4	42
2	$(7, -1)$	$120 - 35 - 1 = 84$	0	84

Table XIV.7.1: Cohomologies for the fixed spin line $\Theta = \mathcal{O}_C(3)$. The two cohomology columns count charges $+2$ and -2, respectively. A positive index is compatible with the absence of the opposite charge.

Riemann–Roch gives the check

$$\chi(C, M) = \deg M + 1 - g = (3 + 2m)\, 21 + 1 - 64 = 42m. \tag{XIV.7.75}$$

At $m = 1$ both signs are present in the sheaf calculation even though the index is positive. At $m = 2$ the opposite sign is absent, so these fields alone could not supply the zero-FI D-flat pair of Section XIV.7.1. In particular $m = 2$ here is a cohomology test, not an allowed value in the preceding integral balance comparison. Even the cases with both signs require the actual compact moment map and superpotential. Computing the index alone cannot answer whether an expectation value exists.

The smooth branch geometry gives an index-two and period-two genus-one curve, and the local geometry gives intersection parities that agree with the charge-two Higgs

mechanism. Those results specify the geometric ingredients and the gauge action of the proposed transition. A compact background must also pass the flux and field conditions; the effective-action description in the next chapter separates these inputs from the charges of the geometric states.

XIV.7.7 Exercises

Use `benchmark/tasks.json` for the JSON fields and `benchmark/PROTOCOL.md` for submission. The written explanations are for discussion.

1. **Participating characters.** Take nonzero expectation values of charges 6 and 10. Find the stabilizer order and the two residues of the monomials $\phi_3^2\overline{\phi_5}$ and $\phi_5\overline{\phi_3}$, with subscripts giving charges. Repeat the stabilizer calculation after adding a charge-three expectation value. Explain why an allowed monomial need not have a nonzero coupling.

2. **Move the branch coefficients.** In (XIV.7.19) replace the four p_i by $(1, 9, 81, 729)$. Compute the four signed-sum magnitudes and the excess of each over the sum of its predecessors, in the given order. Use the excesses to prove transversality. For equal weights, give τ^4 at the singular point on $X_0 = 1$, $[X] = [1 : i : 0 : 0]$.

3. **A normalized cubic.** For $F = 2u_b^4 + u_b^3 v_b + 3u_b^2 v_b^2 - u_b v_b^3 + 2v_b^4$, find the displayed discriminant δ_2, the coefficients (f, g) and both Δ_{book} and Δ_{ell}. Explain which of these tests involves only the chart $u_b = 0$.

4. **A different normal motion.** Keep the sparse parent (XIV.7.42) and take $c_4 = 3tX_1^6$. On the slice through $Q_\star$, compute the two normal velocities in (X_2, X_3) and the discriminant of the reconstructed quadratic at $t = 0$, choosing $m = +1$ there. Give the parent charge and bisection degree of each labeled graph. Explain why the ordinary two-node condition is stronger than being a square.

5. **Circle lattice.** Suppose a three-dimensional mode of charge row $(3, -4)$ condenses. Give the number of connected components of the stabilizer, its primitive generator with positive second coordinate, and the Wilson-line value ξR_{circ} where its covariant momentum vanishes. Compute the minimum dimensionless mass in the unit-charge tower. Repeat the kernel calculation for $(6, -8)$.

6. **Line bundles and a formal balance.** On the same $(3, 7)$ curve and spin line use $m = -1$. Compute the two ordered cohomology dimensions and the index. In the separate trial flux formulas use $p_\rho = 3 + 2m$ at that m; give p_ρ, the formal parent and child flux charges, and the common formal balance. Explain why neither set of results gives a compact vacuum.

7. **What a nonsplit divisor does and does not tell us.** In (XIV.7.36) locate both the rational point and the place where the smooth-branch proof fails. Explain the difference between degree two of a particular divisor, index and period of a curve, local triviality over the base, and the unbroken gauge subgroup of an actual four-dimensional vacuum.

Status and sources

§1. Higgsing. The stabilizer and toy flatness calculations are [MATH]. The conditional compactification interpretation is [GEO-E]: see Mayrhofer et al. (2014), arXiv:1408.6831v4, §§2.2, 2.4 and App. A. The ordinary wrapped-M2 dictionary, the primitive parent charge lattice of Chapter 6, and a D- and F-flat expectation value are premises.

§2. Deformed equation. The blowdown, bundle calculation, double-cover description and smooth branch open are [MATH]. The parent is the compact specialization of Mayrhofer et al. (2014), §§2.1–2.2, eqs. (2.1)–(2.6), (2.12)–(2.13), Tables 2.1–2.2. Direct substitution gives the image of U as their displayed Sec1, and of S as their displayed Sec2; the prose following their eq. (2.3) associates the branch replaced by S with Sec1. The chapter uses the images from the equations. The compact transversality witness and its changed member are established here.

§3. Bisection and Jacobian. The three discriminants, Jacobian, integral Picard isomorphism, index, period and boundary calculations are [MATH]. See Fisher (2008), preprint pp. 4–5, Prop. 2.3 and Lemma 2.5, and p. 26, §7.1. Our f, g follow by the stated rescaling of Fisher's short equation. The discriminant follows the Weierstrass convention $\Delta_{\text{book}} = 4f^3 + 27g^2$. The two restriction isomorphisms use Grothendieck (2005), Exposé XII, Cor. 3.5–3.6, recomposed printed pp. 120–121; the degree and period interpretation uses Clark and Sharif (2010), §§1.1, 1.3. Compare Morrison and Taylor (2016), §§2.1, 2.3 for the genus-one and Jacobian distinction. The argument here does not determine geometric Tate–Shafarevich membership or a global resolution of the Jacobian.

§4. Fibral curves. The conifold chart, transverse locus, parent intersection rows and moving square jet are [MATH]. See Mayrhofer et al. (2014), §§2.1–2.2, eqs. (2.5)–(2.11), (2.19)–(2.25), and §2.4, Table 2.3. For incidence the root coordinate is the actual $z = 2w' + B_2$; no prefactor in their root formula (2.25) is needed. The interpretation of the geometric parity on the moving germ is [GEO-E], using their ordinary wrapped-M2 dictionary. The chosen germ has $a_4 \neq 0$ and two simple roots, and the calculation does not classify the remaining strata.

§5. Circle. The charge and operator arithmetic is [MATH]. The compactification interpretation is [GEO-E], with (n, q) ordered as in Mayrhofer et al. (2014), §2.4, eqs. (2.50)–(2.53), Table 2.3; see also Morrison and Taylor (2016), §6. The connected kernel is the kernel of the stated primitive charge row. It is not an independent determination of the vacuum dynamics.

§6. Compact geometry and backgrounds. The two Euler numbers and Koszul counts for the stated spin line are [MATH]. The topology difference agrees with Mayrhofer et al. (2014), eqs. (2.26)–(2.27). The background comparison is [GEO-E] conditional on the proposed flux expressions, eqs. (2.31)–(2.35), (2.45)–(2.48), with the D3 balance convention of Chapter 3. The charge assignment to the two cohomologies uses the matter line premise of their §2.3. No shifted quantization or compact flat vacuum has been inferred.

References

Clark, P. L. and S. Sharif (2010). "Period, Index and Potential, III". In: *Algebra & Number Theory* 4.2, pp. 151–174. DOI: 10.2140/ant.2010.4.151.

Fisher, T. (2008). "The Invariants of a Genus One Curve". In: *Proceedings of the London Mathematical Society* 97, pp. 753–782. DOI: 10.1112/plms/pdn021.

Grothendieck, A. (2005). *Cohomologie locale des faisceaux cohérents et théorèmes de Lefschetz locaux et globaux (SGA 2)*. Vol. 4. Documents Mathématiques. Société Mathématique de France. arXiv: math/0511279.

Mayrhofer, C. et al. (2014). "Discrete Gauge Symmetries by Higgsing in Four-Dimensional F-Theory Compactifications". In: *JHEP* 12, p. 068. DOI: 10.1007/JHEP12(2014)068. arXiv: 1408.6831 [hep-th].

Morrison, D. R. and W. Taylor (2016). "Sections, Multisections, and $U(1)$ Fields in F-Theory". In: *Journal of Singularities* 15, pp. 126–149. DOI: 10.5427/jsing.2016.15g. arXiv: 1404.1527 [hep-th].

Chapter XIV.8

Effective action, vacuum conditions and decoupling

XIV.8.1 The circle lift and four-dimensional data

A collapsing fiber can tell us which particles carry a gauge charge. How do we find the coefficient of their four-dimensional gauge kinetic term, or decide whether the vector remains massless after flux is turned on? We start in three dimensions, where the eleven-dimensional reduction gives a common description of vectors that will have quite different four-dimensional origins. We then compute the relevant Kähler, superpotential and gauge data and test them on separate examples. The last two sections ask what must be held fixed if the resulting action is to describe a local theory. We use the ordinary M/F dictionary of Chapter 1, the flux conditions of Chapter 3, and the section and charge dictionaries of Chapters 6 and 7. The calculation concerns the leading action, with large base volumes, a smooth resolved M-theory description before the lift, and only the indicated kinetic and matter blocks retained.

Write the Kähler form and the relevant part of the three-form on the resolved fourfold Y as

$$J_Y = v^0\omega_0 + v^\alpha\omega_\alpha + v^i\omega_i, \qquad \mathcal{V}_4 = \frac{1}{4!}\int_Y J_Y^4, \tag{XIV.8.1}$$

$$C_3 = A^0 \wedge \omega_0 + A^\alpha \wedge \omega_\alpha + A^i \wedge \omega_i + \cdots . \tag{XIV.8.2}$$

The vertical forms ω_α are pulled back from the base. The ω_i are Cartan forms associated to exceptional divisors of a split stack. The section direction ω_0 is understood in the circle matching basis; shifts by vertical classes are necessary when comparing different choices of section or KK divisor. Each coefficient of a two-form in C_3 is a three-dimensional vector. In three-dimensional Einstein variables their real scalar partners are

$$R = v^0/\mathcal{V}_4, \qquad L^\alpha = v^\alpha/\mathcal{V}_4, \qquad \xi^i = v^i/\mathcal{V}_4, \qquad R = r^{-2}, \qquad \xi^i = R\zeta^i. \tag{XIV.8.3}$$

Here r is the circle radius in the reduction convention and ζ^i is the corresponding Wilson scalar. Thus the coefficient R tends to zero when the circle decompactifies. One scaling in M-theory units has $v^0 \sim \epsilon$, $v^i \sim \epsilon^2$, and $v^\alpha \sim \epsilon^{-1/2}$. The leading fiber times base term of the quartic then has size $\epsilon(\epsilon^{-1/2})^3 = \epsilon^{-1/2}$. It follows that

$$R \sim \epsilon^{3/2}, \qquad \xi^i \sim \epsilon^{5/2}, \qquad \zeta^i \sim \epsilon, \qquad L^\alpha \sim \epsilon^0. \tag{XIV.8.4}$$

The scaling is a power count in the chosen M-theory variables. Finite four-dimensional base data are specified after the unit and Weyl rescalings; the growth of v^α in this example does not by itself give a four-dimensional limit of large physical base volume.

The circle vector A^0 is part of the four-dimensional metric: on reduction it occurs in the circle one-form $dy + A^0$. The Cartan pairs (ξ^i, A^i) reassemble into four-dimensional gauge fields; wrapped membranes on the root curves furnish the additional charged fields in the ordinary split nonabelian lift. An independent rational section gives a further gauge direction after the Shioda projection. In contrast, the vertical A^α are dual to periodic scalars ρ_α in three dimensions and give four-dimensional chiral coordinates. Figure XIV.8.1 distinguishes these operations. There can also be R–R gauge fields from C_4 with one external and three base indices. Their reduction uses harmonic three-forms of the base and is not the Shioda construction. The $\mathbb{P}^3$ examples have no such base three-forms.

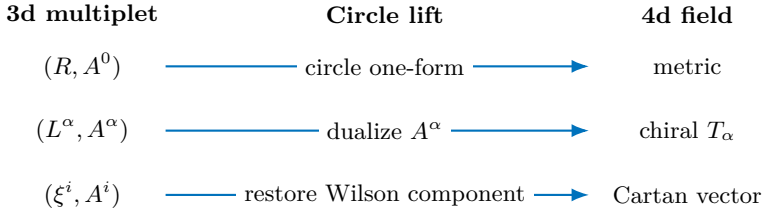


Figure XIV.8.1: The three displayed types of vector in the C_3 reduction. Only the vertical block is Legendre transformed when extracting the four-dimensional chiral coordinates. The gauge row concerns the Cartans at a split stack.

The radius factors can be checked directly in the circle reduction of a four-dimensional Maxwell term. Take the angle y to have fixed coordinate period and work locally at a constant radius in the three-dimensional Einstein frame:

$$ds_4^2 = r^{-2} ds_3^2 + r^2 (dy + A^0)^2, \qquad \sqrt{-g_4} = r^{-2}\sqrt{-g_3}, \tag{XIV.8.5}$$

$$A^i_{(4)} = A^i + \zeta^i (dy + A^0), \qquad F^i_{(4)} = F^i + \zeta^i F^0 + d\zeta^i \wedge (dy + A^0). \tag{XIV.8.6}$$

The conformal factor on ds_3^2 cancels the circle radius in the three-dimensional Einstein term: $\mathcal{R}_4$ includes $r^2 \mathcal{R}_3$, whereas the measure contributes r^{-2}. In the Maxwell term the two inverse horizontal metrics contribute r^4 to the horizontal field strength square. The mixed components use one horizontal and one vertical inverse metric and give $r^2 r^{-2} = 1$ before including the measure. With the constant coordinate circumference

absorbed into the reduction units, a gauge block $Z = \operatorname{Re} f$ therefore gives

$$\mathcal{L}_{3,\text{gauge}}/\sqrt{-g_3} = -\frac{1}{4} r^2 Z_{ij} (F^i + \zeta^i F^0)_{\mu\nu} (F^j + \zeta^j F^0)^{\mu\nu} \tag{XIV.8.7}$$

$$-\frac{1}{2} r^{-2} Z_{ij} \partial_\mu \zeta^i \partial^\mu \zeta^j. \tag{XIV.8.8}$$

Indices on the first line are raised with g_3. At fixed $R = r^{-2}$ the substitution $\zeta^i = \xi^i/R$ turns the scalar coefficient $r^{-2}Z$ into Z/R, the same scale as the vector coefficient. This is the factor to be extracted from the three-dimensional vector Hessian. At the nonabelian matching locus $\zeta = 0$ the horizontal field strengths reduce to F^i; a nonzero Wilson component would instead mix them with F^0. The powers of R arise from the dimensional reduction of the external action, rather than from interpreting a normalized fiber coefficient as an unrescaled area.

To see what dualization does to the kinetic terms, let u stand for the retained real vector coordinates, including R and ξ^i. Use $\widetilde{K}_M(L, u)$ for the real kinetic potential before dualization; complex coordinates such as the complex structure are suppressed in this notation. The dual real coordinates and new kinetic potential are defined by

$$\tau_\alpha = \partial_{L^\alpha} \widetilde{K}_M, \qquad T_\alpha = \tau_\alpha + i\rho_\alpha, \qquad K_M(\tau, u) = \widetilde{K}_M(L, u) - \tau_\alpha L^\alpha. \tag{XIV.8.9}$$

The subtraction cancels the variation in L when the real conjugate variable is held fixed. In particular, with other complex fields fixed,

$$dK_M = -L^\alpha d\tau_\alpha + (\partial_u \widetilde{K}_M)\, du, \qquad (K_M)_{T_\alpha} = -\frac{1}{2} L^\alpha. \tag{XIV.8.10}$$

The factor of $1/2$ follows from differentiating $\tau = (T + \bar{T})/2$. It will enter the moment map as well as the chiral metric. If $A = \widetilde{K}_{M,LL}$, $B = \widetilde{K}_{M,Lu}$ and $C = \widetilde{K}_{M,uu}$, keeping τ fixed gives $0 = A\, dL + B\, du$. In a regular block this yields

$$\partial_u L|_\tau = -A^{-1} B, \qquad (K_M)_{uu} = C - B^{\mathsf{T}} A^{-1} B, \qquad (K_M)_{T_\alpha \bar{T}_\beta} = -\frac{1}{4} (A^{-1})^{\alpha\beta}. \tag{XIV.8.11}$$

The Hessian of a retained vector is therefore evaluated with the dual scalars held fixed, not the original L. A mixed block can change it. In Section XIV.8.3 we will identify the locus where the mixed Cartan block vanishes.

In physical base units let $J_b = v^\alpha \omega_\alpha$, $\kappa_{\alpha\beta\gamma} = \int_B \omega_\alpha \omega_\beta \omega_\gamma$, and $\mathcal{V} = \int_B J_b^3/6$. At leading order the terms in $\widetilde{K}_M$ that survive for the base and complex structure are

$$\widetilde{K}_M = \log R + \log \mathcal{V}_L + K_{\text{cs}} + \cdots, \qquad \mathcal{V}_L = \frac{1}{6} \kappa_{\alpha\beta\gamma} L^\alpha L^\beta L^\gamma. \tag{XIV.8.12}$$

In this base block $L^\alpha = v^\alpha/\mathcal{V}$. Differentiating the cubic gives the divisor volumes; its homogeneity fixes the Legendre subtraction:

$$\tau_\alpha = \frac{\kappa_{\alpha\beta\gamma} L^\beta L^\gamma}{2\mathcal{V}_L} = \frac{1}{2} \int_B \omega_\alpha J_b^2, \qquad \mathcal{V}_L = \mathcal{V}^{-2}, \qquad \tau_\alpha L^\alpha = 3. \tag{XIV.8.13}$$

After separating the circle term and an additive constant, the four-dimensional potential for these kinetic terms is $K_4 = -2 \log \mathcal{V} + K_{\text{cs}}$. This use of homogeneity concerns the

leading block; brane and Wilson fields and corrected coordinates require their own terms in $\widetilde{K}_M$.

On $\mathbb{P}^3$ let $H^3 = 1$ denote the integrated triple intersection and set $J_b = tH$. The calculation is scalar:

$$\mathcal{V} = \frac{t^3}{6}, \qquad L = \frac{6}{t^2}, \qquad \tau = \frac{3}{L} = \frac{t^2}{2}, \tag{XIV.8.14}$$

$$K_4 - K_{\mathrm{cs}} = -3\log\tau + \text{constant}, \qquad K_T = -\frac{3}{t^2}, \qquad K_{T\bar{T}} = \frac{3}{t^4}, \tag{XIV.8.15}$$

$$K^{T\bar{T}} K_T K_{\bar{T}} = 3. \tag{XIV.8.16}$$

For example $t = 2$ gives $K_T = -3/4$ and $K_{T\bar{T}} = 3/16$; at $t = 8$ they become $-3/64$ and $3/4096$. The inverse metric compensates the changed slopes in the last line. This identity will remove one contribution to the potential, but a cancellation in a potential and a vanishing supersymmetry variation are different tests.

XIV.8.2 What the flux superpotential tests

Two fluxes can carry the same D3 charge and give different superpotentials. The charge depends quadratically on the flux class. The superpotential instead compares that class with a line that changes as the complex structure varies. Use the dimensionless oriented class $G = F_4/(2\pi\ell_p)^3$ of Chapter 3, and absorb the common normalization of W into the chosen period frame. If Ω is the holomorphic four-form, write

$$W = \int_Y \Omega \wedge G, \qquad N = \int_Y \Omega \wedge \bar{\Omega}, \qquad K_{\mathrm{cs}} = -\log N, \qquad D_i W = \partial_i W + K_i W. \tag{XIV.8.17}$$

Here the index i in the period discussion labels a complex-structure direction. The normalization of Ω can change by $\Omega \mapsto e^{h(z)}\Omega$ for holomorphic h. In this frame change $K_{\mathrm{cs}} \mapsto K_{\mathrm{cs}} - h - \bar{h}$. The derivative of the factor e^h cancels the new connection term:

$$D'_i W' = e^h(\partial_i W + K_i W), \qquad e^{K'}|W'|^2 = e^K |W|^2. \tag{XIV.8.18}$$

A zero of $\partial_i W$ alone depends on the choice of section of the period line.

The Hodge decomposition gives a physical reason for this subtraction. Write $\partial_i \Omega = c_i \Omega + \chi_i$, where χ_i has type $(3,1)$. Its pairing with $\bar{\Omega}$ is zero by type, hence $\partial_i N = c_i N$ and $K_i = -c_i$. Consequently

$$D_i W = \int_Y \chi_i \wedge G, \qquad W = \int_Y \Omega \wedge G^{0,4}, \qquad D_i W = \int_Y \chi_i \wedge G^{1,3}. \tag{XIV.8.19}$$

If the χ_i span the full $(3,1)$ tangent space, these vanishing conditions remove the indicated flux types and their conjugates for real G. They leave a $(2,2)$ class; they do not test $J_Y \wedge G = 0$. In a slice of the period domain, some of the pairings are untested. If a local seven-brane description is used for some deformations, its holomorphic equations must be included in a compatible set of variables. A deformation already counted by periods cannot simply be added again as an independent chiral field.

For comparison, on a smooth gauge surface the twisted connection has a $(0,1)$ part $\bar{A}$ and its adjoint Higgs field is a $(2,0)$ form Φ. The local functional $\int_S \operatorname{tr}(\Phi \wedge F^{0,2})$ illustrates how an F equation for a brane field is obtained. In a holomorphic gauge $\delta F^{0,2} = \bar{\partial}_A \delta \bar{A}$. Integrating by parts on the compact surface yields

$$\delta W_S = \int_S \operatorname{tr}\left(\delta\Phi \wedge F^{0,2} - \bar{\partial}_A \Phi \wedge \delta \bar{A}\right), \tag{XIV.8.20}$$

$$F^{0,2} = 0, \qquad \bar{\partial}_A \Phi = 0. \tag{XIV.8.21}$$

For the local functional these are the holomorphic equations. The real equation also involves $J_b|_S \wedge F$ and a commutator of Φ with its adjoint. The F equations make no reference to that surface volume. This is the twisted gauge system used in Chapters 4 and 5. In a simple adjoint truncation, expanding $F^{0,2}$ includes its background term and the square of the $(0,1)$ fluctuations. Pairing with a Higgs fluctuation produces respectively a linear flux term and a term with two Wilson fields and one Higgs field; the latter coefficient pairs two $(0,1)$ basis forms with a $(2,0)$ basis form over S. This construction of a local coupling supplies neither the full charged matter action nor additional copies of bulk moduli.

For an explicit period calculation, use the two marked Kummer lattices of Chapter 3. On each factor let $p_j^2 = q_j^2 = 4$, $p_j \cdot q_j = 0$, and $\Omega_j = p_j + i q_j$. Vary the first factor along a real vector n perpendicular to p_1, q_1, with $n^2 = -d < 0$. An isotropic ansatz requires a term in the conjugate period direction:

$$\Omega_1(z) = \Omega_1 + zn + cz^2 \bar{\Omega}_1, \qquad \Omega_1 \cdot \bar{\Omega}_1 = 8, \tag{XIV.8.22}$$

$$\Omega_1(z)^2 = (16c - d)z^2, \qquad c = \frac{d}{16}, \tag{XIV.8.23}$$

$$N_1(z) = 8 - d|z|^2 + \frac{d^2}{32}|z|^4 = 8\left(1 - \frac{d|z|^2}{16}\right)^2. \tag{XIV.8.24}$$

We use the connected positive chart about the origin, $d|z|^2 < 16$. The second factor is fixed and contributes a constant to K_{cs}. This abstract marked chart tests a variation of Hodge structure. It does not supply a complete elliptic family or a new integral flux construction along that chart.

Now pair $\Omega_1(z)\Omega_2$ with $G_\pm = p_1 p_2 \pm q_1 q_2$, where juxtaposition across factors denotes the exterior product. The cross term in $G_\pm^2$ vanishes, while the two squared terms are both $4 \cdot 4$. For the linear period pairing the signs matter:

$$\Omega_1(z) \cdot p_1 = 4(1 + cz^2), \qquad \Omega_1(z) \cdot q_1 = 4i(1 - cz^2), \tag{XIV.8.25}$$

$$W_\pm = 16(1 + cz^2) \mp 16(1 - cz^2), \qquad \int G_\pm^2 = 32, \tag{XIV.8.26}$$

$$W_+ = 2dz^2, \qquad W_- = 32. \tag{XIV.8.27}$$

The flux contributions to the charge budget are equal; the constants in the two period pairings cancel only for G_+. At the origin G_+ is the real part of $\Omega_1 \bar{\Omega}_2$ and has type $(2,2)$, whereas G_- is the real part of $\Omega_1 \Omega_2$. The difference is visible even before taking a derivative.

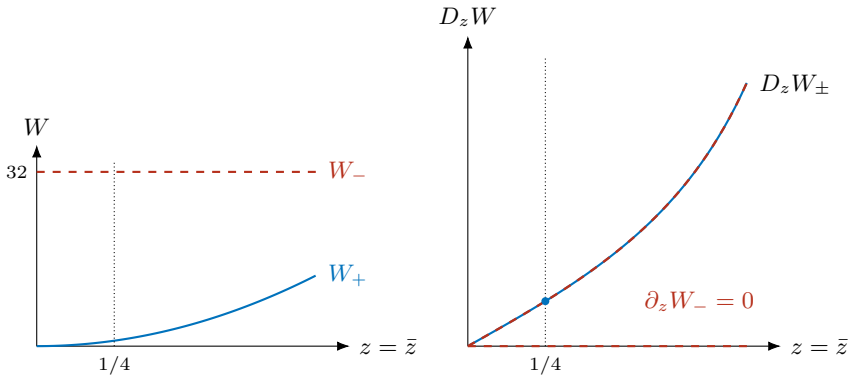


Figure XIV.8.2: The real slice at $d = 8$. The left panel shows $W_\pm$, and the right panel shows $D_zW_\pm$ and the vanishing $\partial_z W_-$. The dotted line at $z = 1/4$ locates the nonzero connection test. Both fluxes have squared pairing 32.

To test the connection itself, put $u = dz\bar{z}$. The potential in this chart is $-2\log(1 - u/16)$ plus a constant. Differentiating with respect to z and $\bar{z}$ independently gives

$$K_z = \frac{2d\bar{z}}{16 - u}, \qquad K_{z\bar{z}} = \frac{32d}{(16 - u)^2}, \tag{XIV.8.28}$$

$$D_zW_+ = 4dz + \frac{4d^2z^2\bar{z}}{16 - u} = \frac{64dz}{16 - u}, \qquad D_zW_- = \frac{64d\bar{z}}{16 - u}. \tag{XIV.8.29}$$

At $z = 0$ both covariant derivatives vanish, just as both ordinary derivatives do. Move to $d = 8$, $z = \bar{z} = 1/4$. Equation (XIV.8.29) now gives $D_zW_- = 256/31$, while $\partial_z W_- = 0$. The constant superpotential has not made its covariant derivative vanish. The same issue can be seen in the frame $e^z\Omega$: at the origin $\partial_z(32e^z) = 32$ and $K'_z = -1$, so the covariant derivative is zero. In the original frame at the origin the metric is $d/8$ and $W''_+ = 4d$. Raising d from 8 to 12 raises these quantities from 1 to 3/2 and from 32 to 48, respectively. A holomorphic second derivative in a chosen coordinate is not itself a canonically normalized mass.

To read these results as supersymmetry conditions, restore the base fields. In reduced Planck units the leading F potential is

$$V_F = e^K\big(K^{I\bar{J}}D_IW\,\overline{D_JW} - 3|W|^2\big), \qquad D_TW = K_TW \quad \text{if} \quad \partial_TW = 0. \tag{XIV.8.30}$$

Here I runs over all retained chirals. In the split Kähler and complex-structure truncation of Section XIV.8.1, the positive T contribution equals $3e^K|W|^2$ by (XIV.8.16). The same algebra follows for the isolated multi-modulus base block as long as it is regular: differentiate Euler's relation $\tau_\alpha L^\alpha = 3$ to obtain $AL = -\tau$, where A is the real L Hessian of Section XIV.8.1. Using (XIV.8.11),

$$K^{T\bar{T}}K_TK_{\bar{T}} = (-L/2)^{\mathsf{T}}(-4A)(-L/2) = -L^{\mathsf{T}}AL = \tau_\alpha L^\alpha = 3. \tag{XIV.8.31}$$

The scalar potential then measures the remaining F terms. On the G_- example at the origin the tested period derivative vanishes, but $W_- = 32$ gives a nonzero Kähler F term for any finite positive t in the one-modulus leading block. This use of the Kähler F equation is a comparison with the leading action, not an identification of the Kummer product with the $\mathbb{P}^3$ model. At a point where all $D_I W = 0$, $V_F = -3e^K|W|^2$; a supersymmetric Minkowski solution in the absence of a D contribution also requires $W = 0$. The cancellation uses the truncated kinetic metric and need not persist with corrected K or T-dependent W.

There is a separate way the charge test can miss supersymmetry. In the algebraic product of Chapter 3 at its flux choice $(m, n) = (1, 0)$, the flux square stays 16 when J_2 changes from $h_1 + h_2 + h_3$ to $h_1 + 2h_2 + h_3$, but the coefficient of $J_2\beta$ tested there changes from zero to two. The pairing with J_2 changes because J_2 enters the test itself. That example tests primitivity rather than Hodge type and uses a different flux from either marked Kummer control. We now apply both distinctions to the gauge and D blocks.

XIV.8.3 Gauge kinetic terms and the D condition

What can the volume of a gauge surface tell us about a proposed vacuum? Its first role is to set the coefficient of the gauge field strength. A different calculation, involving the flux and the Kähler form, sets the D term. We can obtain both in the same normalization and compare them without changing the model.

Let D_i be the Cartan divisors in the split resolution over S. The projection of their pairwise intersection to the base is

$$\pi_*(D_i D_j) = -C_{ij} S, \qquad C_{ij} = \mathrm{tr_f}(H_i H_j) = 2\delta_{ij} - \delta_{i,j+1} - \delta_{i+1,j}, \tag{XIV.8.32}$$

with $H_i = \mathrm{diag}(e_i - e_{i+1})$ in the defining representation of $SU(5)$. The negative sign comes from the resolved curve intersections; the kinetic matrix must instead be positive. To see how the sign changes, expand the normalized volume quartic inside $\widetilde{K}_M$. There are six placements of the two Cartan and two vertical factors in the quartic, so its coefficient is $6/4! = 1/4$. If $\kappa_{S\alpha\beta} = \int_B S\omega_\alpha\omega_\beta$, the relevant terms are

$$\widetilde{K}_M = \log\left(R\mathcal{V}_L - \frac{1}{4} C_{ij}\xi^i\xi^j\kappa_{S\alpha\beta}L^\alpha L^\beta + \cdots\right) + K_{\mathrm{cs}}. \tag{XIV.8.33}$$

There is no leading term linear in the Cartans at the matching locus, and therefore the leading L–ξ block vanishes there. The Schur subtraction in (XIV.8.11) leaves the Cartan Hessian unchanged at this order. Taking two derivatives of (XIV.8.33) gives

$$-R(K_M)_{\xi^i\xi^j} \longrightarrow \frac{C_{ij}\kappa_{S\alpha\beta}L^\alpha L^\beta}{2\mathcal{V}_L} = C_{ij}\tau_S, \qquad \tau_S = \frac{1}{2}\int_S J_b^2. \tag{XIV.8.34}$$

The circle matching identifies the left side with the real gauge kinetic matrix in the action $-\frac{1}{2}\int \mathrm{Re}\, f_{ij} F^i \wedge *F^j$. The leading holomorphic function in the corresponding trace frame is $f_{ij} = C_{ij}T_S$, using the $+C_4$ orientation for the axion in T_S. For the

smooth quadric of Chapter 2, $S = 2H$ and $J_b = tH$, giving $t^2 C_{ij}$. Replacing $2H$ by H in this intersection exercise gives $t^2 C_{ij}/2$ in the same generator basis. It does not make the coroot trace the identity, nor does the classical function determine all holomorphic thresholds.

The same expansion can use the Shioda self-intersection instead of the Cartan pairing. In the distinct rank-one example of Chapter 6, write U, S for the section divisors in their fixed order and let β denote the model's base divisor parameter. Put $c_1(B) = 4H$, with

$$\pi_* U^2 = \pi_* S^2 = -4H, \qquad \pi_*(US) = 8H - \beta, \qquad \sigma = S - U - (12H - \beta). \tag{XIV.8.35}$$

Indeed $\pi_*((S-U)U) = 12H - \beta$, which fixes the vertical subtraction. The mixed term from the subtraction has zero pushforward in σ^2, since $\pi_* S = \pi_* U$; the purely vertical term also pushes to zero. Thus

$$b_\sigma = -\pi_* \sigma^2 = 2(12H - \beta), \qquad Z_\sigma = \operatorname{Re} f_\sigma = \frac{1}{2} \int_B b_\sigma J_b^2. \tag{XIV.8.36}$$

For $\beta = 5H$ this gives $14H$ and $7t^2$; for $\beta = 6H$ it gives $12H$ and $6t^2$. The height is a divisor pairing; a particle's integer charge is instead the intersection of σ with its fibral curve. In particular, retaining the charge unit of Chapter 6 does not make the two heights equal.

Now include an ordinary non-R gauging. Let $\Theta_{\alpha a}$ be the coefficient in $DT_\alpha = dT_\alpha + i\Theta_{\alpha a} A^a$, and use $D\phi = d\phi + i q_a A^a \phi$ for a charged field. With constant leading matter metric Z_ϕ, the moment map and auxiliary-field energy in this convention are

$$D_a = K_{T_\alpha} \Theta_{\alpha a} + \sum_\phi q_a Z_\phi |\phi|^2, \qquad V_D = \frac{1}{2} D^{\mathsf{T}} (\operatorname{Re} f)^{-1} D. \tag{XIV.8.37}$$

For the shift and phase transformations above the holomorphic generators are $-i\Theta_{\alpha a}$ and $-iq_a\phi$. Multiplying each by i times the corresponding Kähler derivative produces the two terms in (XIV.8.37): $i(-i\Theta_{\alpha a}) K_{T_\alpha}$ and $i(-iq_a\phi) Z_\phi \dot{\phi}$. Thus an axionic contribution can have either sign even though Z_ϕ is positive. This choice of moment map uses an invariant Kähler potential and an ordinary gauge symmetry. The inverse gauge matrix appears because the real auxiliary variables have a quadratic term with coefficient $\operatorname{Re} f$ and a linear coupling to the moment map. Their equation of motion is $(\operatorname{Re} f)\, D_{\text{aux}} = -D$. In particular a positive kinetic coefficient cannot enforce $D = 0$.

For a formal flux trial in the Shioda model take $G = mH\sigma$. In the local reduction basis the coefficient entering the moment map is half the raw pairing, as derived in

Section XIV.8.4. For $\beta = 5H$ with no charged expectation values,

$$P_{H\sigma} = \int_Y G\, H\sigma = -14m, \qquad \Theta_{H\sigma} = -7m, \tag{XIV.8.38}$$

$$D_\sigma = \left(-\frac{3}{t^2}\right)(-7m) = \frac{21m}{t^2}, \qquad V_D = \frac{63m^2}{2t^6}, \tag{XIV.8.39}$$

$$\frac{1}{2}\int_Y G^2 = -7m^2, \qquad \frac{\chi(Y)}{24} - \frac{1}{2}\int_Y G^2 = \frac{801}{4} + 7m^2. \tag{XIV.8.40}$$

The sign of the flux changes the moment map but not its energy. At $t = 8$, the choices $m = 0, 1, -2$ have $D_\sigma = 0, 21/64, -42/64$ and V_D in the ratio $0 : 1 : 4$. If β changes to $6H$, then $\Theta = -6m$, $D = 18m/t^2$, and $V_D = 27m^2/t^6$. This changed-height comparison uses the altered intersection in both the gauging and the kinetic term.

A useful way to organize the two height calculations is to write $b_\sigma = \mathfrak{h}H$. With the same flux ansatz and classical base metric, the three input coefficients are

$$Z_\sigma = \frac{\mathfrak{h}t^2}{2}, \qquad \Theta = -\frac{\mathfrak{h}m}{2}, \qquad K_T = -\frac{3}{t^2}. \tag{XIV.8.41}$$

At fixed m, t, the kinetic coefficient and D term are linear in $\mathfrak{h}$. The energy is also linear, because one inverse power in the auxiliary-field elimination cancels a power in D^2. Figure XIV.8.3 illustrates the difference between changing the sign of m and changing the height. The sign flip changes the sign of D, while changing the height from $14H$ to $12H$ reduces the energy to $6/7$ of its original value (a reduction by $1/7$) at fixed nonzero m, t.

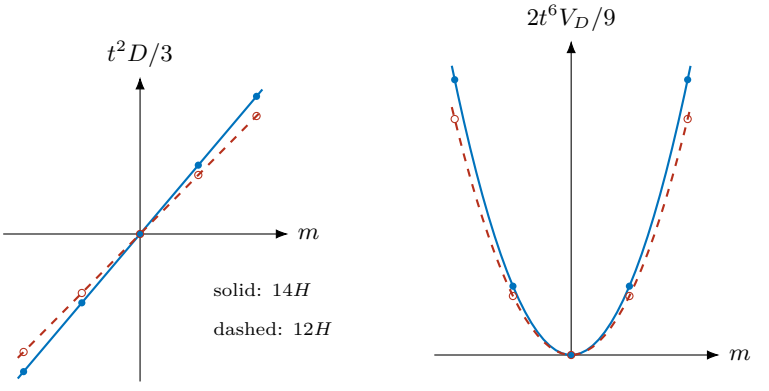


Figure XIV.8.3: Scaled moment map and auxiliary energy for the two height choices. Only the plotted integer points represent the specified integer flux trials; the curves show their algebraic dependence on m. The plots do not impose shifted quantization.

The charge expression in (XIV.8.40) counts a formal remainder before any claim of

shifted quantization. In fact

$$\int_Y (J_b \wedge G) \wedge \sigma = tP_{H\sigma} = -14tm \tag{XIV.8.42}$$

in the first model. Thus for $m \neq 0$ even the pullback Kähler form fails the primitive test. A negative $\int G^2$ is consistent with this failure: a real primitive $(2,2)$ class on a Kähler fourfold would be self-dual and would give $\int G^2 = \int G \wedge *G \geq 0$. The zero trial clears this particular D test but leaves the fractional formal remainder unchanged. This calculation supplies neither an allowed flux lattice point nor a charged expectation value. The genus-one transition of Chapter 7 is separate from choosing a flux vacuum in the resolved section model.

In the split $SU(5)$ example one can also fail a test after succeeding on the base pullback. Use the class G_* of Chapter 3, for which $\int_Y G_* H D_i = 0$ for the four strict Cartans. These periods make the corresponding base Kähler contribution to the D tests vanish at zero matter expectation values. But ask instead for primitivity at a resolved point. In the specified Kähler span the Cartan components of J_Y are j_i. Pairing $J_Y G_*$ with D_i gives the following necessary equations:

$$\begin{pmatrix} \int_Y J_Y G_* D_1 \\ \int_Y J_Y G_* D_2 \\ \int_Y J_Y G_* D_3 \\ \int_Y J_Y G_* D_4 \end{pmatrix} = 56 \begin{pmatrix} 0 & 0 & 0 & 0 \\ 0 & 1 & 0 & -1 \\ 0 & 0 & -1 & 1 \\ 0 & -1 & 1 & 0 \end{pmatrix} \begin{pmatrix} j_1 \\ j_2 \\ j_3 \\ j_4 \end{pmatrix} = 0. \tag{XIV.8.43}$$

The second and third rows force $j_2 = j_4$ and $j_3 = j_4$, so the last row adds no condition. An effective fibral curve in that resolution has strict Cartan intersections $(0, -1, 0, 1)$ and zero section and base contributions in this calculation. Its area is $-j_2 + j_4$, forced to zero by (XIV.8.43). A smooth Kähler class in the interior has positive area on the curve. Therefore this flux cannot be primitive at a point in that resolved interior of the declared span, even though it has a formal remaining charge of 212. A zero area can occur at a boundary, where the resolved interior argument no longer applies.

For an actual vacuum we must impose the supersymmetry equations, the shifted lattice and transversality conditions, and the charge budget on the same object. We must also identify the fields available to solve the equations and a scale range in which their action applies. The examples above separate those operations: a successful base moment or a nonnegative charge remainder cannot substitute for the resolved Kähler test.

XIV.8.4 How a vector eats an axion

A vector can exist geometrically before turning on flux and have a mass term afterward. The mechanism can be seen in the same three-dimensional dualization used to find T_α. In the eleven-dimensional Chern–Simons reduction the mixed entries involve the geometric pairing $P_{\alpha a} = \int_Y G\, \omega_\alpha \omega_a$. With the orientation of Section XIV.8.1, the two symmetric mixed entries combine by integration by parts into

$$-\int \Theta_{\alpha a} A^a \wedge F^\alpha, \qquad \Theta_{\alpha a} = \frac{1}{2} P_{\alpha a}. \tag{XIV.8.44}$$

Here F^α is the field strength of the vertical vector. The half in the reduction coefficient is essential; the sign is tied to the orientation of the dual axion.

More explicitly, with the common Chern–Simons action written in the source basis as $-\frac{1}{2}\int \Theta_{\Lambda\Sigma} A^\Lambda \wedge F^\Sigma$, each ordering occurs once in the sum. The mixed pieces are equal under the integral, up to a boundary term, because

$$A^\alpha \wedge dA^a = A^a \wedge dA^\alpha - d(A^\alpha \wedge A^a). \tag{XIV.8.45}$$

Combining the pieces removes the explicit factor in front of the symmetric action, leaving the factor in $\Theta = P/2$ intact. In the following local derivation we discard the boundary term; global periodic data do not follow from this step.

For dualization take F^α to be independent and use the term $-\int d\rho_\alpha \wedge F^\alpha$ to impose $dF^\alpha = 0$. Write M for the positive vertical kinetic matrix at a fixed point of the scalar fields. Then the first-order action for this sector is

$$S_{\text{first}} = -\frac{1}{2}\int M_{\alpha\beta} F^\alpha \wedge *F^\beta - \int (d\rho_\alpha + \Theta_{\alpha a} A^a) \wedge F^\alpha. \tag{XIV.8.46}$$

Varying F^α gives $M_{\alpha\beta} * F^\beta = -D\rho_\alpha$. In three-dimensional Lorentz signature $** = -1$ on one- and two-forms, so $F^\alpha = (M^{-1})^{\alpha\beta} * D\rho_\beta$. Substitution gives

$$S_\rho = -\frac{1}{2}\int (M^{-1})^{\alpha\beta} D\rho_\alpha \wedge *D\rho_\beta, \qquad D\rho_\alpha = d\rho_\alpha + \Theta_{\alpha a} A^a. \tag{XIV.8.47}$$

The shift $\rho_\alpha \mapsto \rho_\alpha - \Theta_{\alpha a}\lambda^a$ compensates $A^a \mapsto A^a + d\lambda^a$. If the sign of the C_4 axion is reversed to use the instanton phase convention of Chapter 10, both the shift and any axionic topological coefficient must be translated. Also, the coefficient Θ in this action does not by itself fix a primitive periodic charge. That requires a lattice of axion periods and compact gauge transformations.

At a regular point of the leading four-dimensional action set $Z = \operatorname{Re} f$ and $G_{\text{ax}} = 2K_{T\bar{T}}$, both positive, in reduced Planck units. The real axion term is $-\frac{1}{2}(D\rho)^{\mathsf{T}} G_{\text{ax}} (D\rho)$, so the vector quadratic form in the geometric basis is $\Theta^{\mathsf{T}} G_{\text{ax}} \Theta$. The canonically normalized vector is $A_{\text{can}} = Z^{1/2} A$. Its mass matrix and norm test are

$$M^2_{\text{can}} = Z^{-1/2} \Theta^{\mathsf{T}} G_{\text{ax}} \Theta Z^{-1/2}, \tag{XIV.8.48}$$

$$v^{\mathsf{T}} M^2_{\text{can}} v = \| G_{\text{ax}}^{1/2} \Theta Z^{-1/2} v \|^2, \qquad \ker M^2_{\text{can}} = Z^{1/2} \ker \Theta. \tag{XIV.8.49}$$

No positive finite change of kinetic matrices changes the rank. The coordinates of the massless direction do change. In the Shioda trial at $\beta = 5H$, use $G_{\text{ax}} = 6/t^4$, $Z = 7t^2$ and $\Theta = -7m$. The result is $42m^2/t^6$, and with $\beta = 6H$ it is $36m^2/t^6$. These are quadratic coefficients of an off-vacuum action in the stated frame. Since $D \neq 0$ at nonzero m in that test, the coefficient is not a mass pole in a constructed supersymmetric vacuum.

An independent two-vector example illustrates the difference between a kernel and its components. Take the charge map k, axion metric and gauge metric to be

$$k = \begin{pmatrix} 1 & 2 \\ 2 & 4 \end{pmatrix}, \quad G_{\text{ax}} = \operatorname{diag}(2, 3), \quad Z = \operatorname{diag}(1, 4). \tag{XIV.8.50}$$

The second row of k is twice the first, giving $k^{\mathsf{T}} G_{\mathrm{ax}} k = 14(1,2)^{\mathsf{T}}(1,2)$. With the two inverse gauge factors, the mass matrix becomes

$$M^2_{\mathrm{can}} = 14 \begin{pmatrix} 1 & 1 \\ 1 & 1 \end{pmatrix}, \qquad (m_0^2, m_1^2) = (0, 28). \tag{XIV.8.51}$$

The null vector is $(-1, 1)$ in the canonical coordinates but $(-2, 1)$ before rescaling. Figure XIV.8.4 shows the two coordinate planes. The field strength action fixes which axes measure equal physical amplitudes.

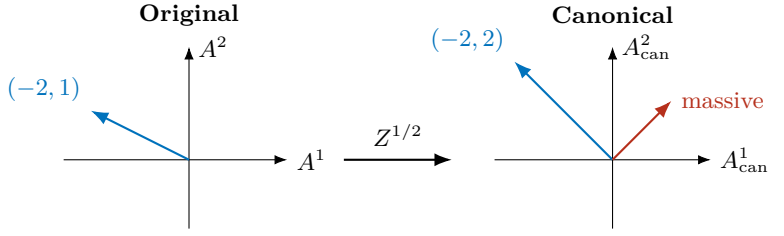


Figure XIV.8.4: The same null direction in the original and canonical vector coordinates of (XIV.8.50). The canonical coordinate change doubles the second component; in that basis the massive direction is orthogonal to the null direction in the Euclidean metric.

If a canonically normalized scalar of charge $q = (0, 1)$ has squared expectation value $|v_\phi|^2 = 2$, its kinetic term gives an additional matrix $2|v_\phi|^2 Z^{-1/2} q^{\mathsf{T}} q Z^{-1/2}$. It adds one to the bottom diagonal of (XIV.8.51). The new determinant is $14(15) - 14^2 = 14$. In general the new kernel is the intersection of the old one and the kernel of the transformed matter charge. Here the Higgs charge acts nontrivially on the old null vector and the intersection is zero.

To exhibit a solution of matter equations rather than prescribe a VEV, take a separate rigid model with charges ± 2, a neutral N, and $W = \lambda N(\phi_+\phi_- - \mu^2)$ with $\lambda \neq 0$ and $\mu^2 = 2$. Introduce a fixed effective FI parameter ξ only in this rigid model. The three F equations give $\phi_+\phi_- = 2$ and $N = 0$, since neither charged field can vanish. For $x = |\phi_+|^2$ and $y = |\phi_-|^2$ the remaining equations and positive solution are

$$xy = 4, \qquad 2(x - y) + \xi = 0, \tag{XIV.8.52}$$

$$x = \frac{\sqrt{\xi^2 + 64} - \xi}{4}, \qquad y = \frac{\sqrt{\xi^2 + 64} + \xi}{4}. \tag{XIV.8.53}$$

The phases can be chosen with product $+2$. This fixes their sum, while the relative phase transforms by the gauge action. With the gauge transformation of Section XIV.8.3, the individual shifts are -2λ and $+2\lambda$. At $\lambda = \pi$ both complex fields are unchanged. That transformation need not fix an axion in the same theory; to decide we have to specify the integer axion shift in a primitive period basis. At $\xi = 6$ the squared magnitudes are $(1, 4)$; at $\xi = -6$ they are $(4, 1)$; at $\xi = 0$ they are $(2, 2)$. The rigid FI parameter organizes this calculation without postulating a fundamental constant FI parameter for a compact non-R gauging.

A stabilizer question uses additional integral data. If the gauge transformation parameter and a periodic axion both have primitive period 2π, a nonzero Higgs of charge two and an independent axion charge k require

$$2\lambda = 0 \bmod 2\pi, \qquad k\lambda = 0 \bmod 2\pi \quad \Longrightarrow \quad \mathrm{Stab} = \mathbb{Z}_{\gcd(2,k)}. \tag{XIV.8.54}$$

For $k = 0, 2, 3$ the orders are $2, 2, 1$. In the last case $\lambda = \pi$ leaves the Higgs invariant but shifts the axion by an odd multiple of π. This is a four-dimensional stabilizer with specified periods; the connected kernel of the three-dimensional circle-and-charge row $(1, -2)$ in Chapter 7 answers a different question. Neither a nonzero Stückelberg mass nor the existence of an integral stabilizer removes the gauge redundancy. Its local anomaly must still cancel.

XIV.8.5 Chirality, anomalies and the axion counterterm

When a vector gets a Stückelberg mass, which anomaly test changes? Its field strength and the combination $D\rho$ are still gauge invariant. The shift of ρ, however, lets a topological coupling vary under the gauge symmetry. This variation can cancel a fermion anomaly. We first compute the relevant fermion traces, then compare the possible counterterm with explicit source data in a separate model.

Let F_{n} be the curvature of a simple gauge factor and F_A that of a $U(1)$. For a left Weyl fermion in R of charge q, the degree-six index density in characteristic-class normalization is

$$I_6(R, q) = \left[\mathrm{ch}_R(F_{\mathrm{n}})\, e^{qF_A/(2\pi)}\, \widehat{A}(T)\right]_6, \qquad \widehat{A}(T) = 1 - \frac{p_1(T)}{24} + \cdots . \tag{XIV.8.55}$$

Here gauge curvatures inside the characteristic classes are Hermitian with the indicated 2π normalization. In the cubic gauge term the two forms commute in the algebra because the abelian generator is scalar in R. Suppressing the common characteristic-class factors, the trace expansion is

$$\mathrm{tr}_R(F_{\mathrm{n}} + qF_A)^3 = \mathrm{tr}_R\, F_{\mathrm{n}}^3 + 3qF_A\, \mathrm{tr}_R\, F_{\mathrm{n}}^2 \tag{XIV.8.56}$$

$$+ 3q^2 F_A^2\, \mathrm{tr}_R\, F_{\mathrm{n}} + \dim(R) q^3 F_A^3. \tag{XIV.8.57}$$

The term linear in $\mathrm{tr}_R\, F_{\mathrm{n}}$ vanishes. The mixed gauge coefficient contains the factor $3/6 = 1/2$ from choosing one abelian field in the cubic. The dimension of R occurs in the purely abelian trace and in $\mathrm{tr}_R(F_{\mathrm{n}} + qF_A) = \dim(R) qF_A$ for the gravitational term. It is already accounted for by the trace when calculating the nonabelian indices.

Choose a scheme that preserves the simple gauge factor and local Lorentz symmetry for the mixed terms. For an axion with shift $-\Theta_\alpha \lambda$, the classical variation is

$$S_{\mathrm{top}} = \int \rho_\alpha X_4^\alpha, \qquad \delta_\lambda S_{\mathrm{top}} = -\int \lambda\, \Theta_\alpha X_4^\alpha. \tag{XIV.8.58}$$

Here X_4^α is built from invariant curvature polynomials. Descent from $F_A\, \Theta_\alpha X_4^\alpha$ produces the abelian variation with opposite sign when the coefficients match. A pure simple-group

cubic term has no F_A factor and must cancel in the chiral trace. Local counterterms can shift the assignment of the consistent anomaly among currents but do not change its polynomial. This analysis does not address global anomalies or large transformations.

To compute the $SU(5)$ indices, take a diagonal traceless generator with eigenvalues x_i and $\sum_i x_i = 0$. The weights of the $\mathbf{10} = \wedge^2\mathbf{5}$ are $x_i + x_j$ for $i < j$. Let $S_\ell = \sum_i x_i^\ell$. The cross terms of the trace reduce to the same power sums:

$$2\sum_{i<j} x_i x_j = -S_2, \qquad \sum_{i\neq j} x_i^2 x_j = -S_3, \tag{XIV.8.59}$$

$$\sum_{i<j}(x_i + x_j)^2 = 4S_2 - S_2 = 3S_2, \qquad \sum_{i<j}(x_i + x_j)^3 = 4S_3 - 3S_3 = S_3. \tag{XIV.8.60}$$

The $\bar{\mathbf{5}}$ has weights $-x_i$, hence quadratic index 1 and cubic index -1 relative to $\mathbf{5}$. In the separate $SU(5)$ source model over $\mathbb{P}^2 \times \mathbb{P}^1$, the signed left Weyl multiplicities are $\chi(\bar{\mathbf{5}}) = \chi(\mathbf{10}) = 162\lambda$, with λ the flux parameter in that example. Their pure coefficient in units of the defining cubic trace is $162\lambda(-1 + 1) = 0$. Replacing $\bar{\mathbf{5}}$ by $\mathbf{5}$ without changing χ gives 324λ instead. For instance at $\lambda = 1$ one can detect the difference on $(1, 1, 1, 1, -4)$, for which $S_3 = -60$. This test uses two representation copies with the stated multiplicities and their full traces, not a new chiral count for the quadric.

For a mixed comparison use the singlet-flux slice $(\lambda, \alpha) = (0, 0)$ of a separate $SU(5) \times U(1)$ source model, also over $\mathbb{P}^2 \times \mathbb{P}^1$. In its divisor order (H, S) the supplied numbers are

$$\begin{aligned} q = 5, \qquad \chi(\mathbf{1}_5) = -540\beta, \qquad \Theta = (-300\beta, 0), \\ b_U = (150, 70), \qquad b_{SU(5)} = (0, 1), \qquad a = (-3, -2). \end{aligned} \tag{XIV.8.61}$$

The last three vectors are the abelian, simple gauge and curvature coefficients of the axion couplings. Here β is the singlet-flux parameter of this source, not the Shioda model's divisor. This calculation takes χ and Θ as separate inputs. For comparing their coefficients use the source's F_A, defining gauge trace tr_f, and Lorentz vector trace $\mathrm{tr}\,\mathcal{R}^2$. In particular, the source gravity coefficient is $\sum \chi \dim(R) q/48$ in this trace. It is not the coefficient of $F_A p_1$ in (XIV.8.55).

In the order $F_A^3, F_A\,\mathrm{tr}_\mathrm{f}\,F_\mathrm{n}^2, F_A\,\mathrm{tr}\,\mathcal{R}^2$, the singlet contributes only to the first and third:

$$c_\mathrm{loop} = \left(\frac{\chi q^3}{6},\, 0,\, \frac{\chi q}{48}\right) = \left(-11250\beta,\, 0,\, -\frac{225}{4}\beta\right), \tag{XIV.8.62}$$

$$c_\mathrm{GS} = \left(\frac{b_U \cdot \Theta}{4},\, \frac{b_{SU(5)} \cdot \Theta}{4},\, -\frac{a \cdot \Theta}{16}\right) = \left(-11250\beta,\, 0,\, -\frac{225}{4}\beta\right). \tag{XIV.8.63}$$

The second line gives the coefficient to be matched by the loop, whose variation is canceled by the classical shift in (XIV.8.58). At $\beta = -2$ the signs reverse and the magnitudes double relative to $\beta = 1$. A nonzero Θ in the first divisor direction does not produce a nonabelian counterterm here: $b_{SU(5)}$ is supported in the second direction. Figure XIV.8.5 shows that projection and the two nonzero matches. No charged nonabelian spectrum was independently derived by this calculation.

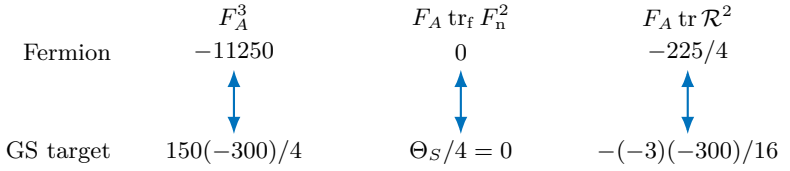


Figure XIV.8.5: Coefficients on the singlet slice, shown at $\beta = 1$. The first and third columns match the fermion coefficients after contracting the axion couplings with Θ. The simple gauge coefficient tests the orthogonal divisor component and vanishes.

There is a separate numerical comparison in three dimensions, and it does not give the same verdict. In the source's Coulomb chamber, the positively charged singlet has positive zero-mode mass. From the source loop formula its contribution is $\Theta_{55}^{\mathrm{loop}} = q^2\chi/2 = -6750\beta$; the printed geometric entry is $\Theta_{55}^{\mathrm{geom}} = 6750\beta$. The source comparison uses $-\Theta^{\mathrm{loop}} = \Theta^{\mathrm{geom}}/2$. Applying that conversion gives

$$-\Theta_{55}^{\mathrm{loop}} = 6750\beta, \qquad \frac{1}{2}\Theta_{55}^{\mathrm{geom}} = 3375\beta. \tag{XIV.8.64}$$

Both vanish at $\beta = 0$. For nonzero β their signs agree and the magnitudes differ by two. Dropping the factor of one half would manufacture an equality in a different normalization; reversing a sign would still leave a factor of two. The coefficient checks in (XIV.8.63) establish a limited equality between supplied four-dimensional rows, not a full spectrum and Chern–Simons match. The discrepancy does not determine a corrected chirality.

The mixed gravitational coefficient gives a different circle check, for which keeping only the zero mode would give the wrong result. In a small Wilson-line chamber $0 < |rq\zeta| < 1$ a tower has signed masses $m_n = n/r + q\zeta$ and KK charge n. For $n \neq 0$ the sign is the sign of n, and the zero mode contributes zero to the mixed level because its KK charge is zero. The source regulator assigns

$$\sum_{n\in\mathbb{Z}} n \operatorname{sign}(n + rq\zeta) = 2\zeta_{\mathrm{Riemann}}(-1) = -\frac{1}{6}, \tag{XIV.8.65}$$

$$\Theta_{0A}^{\mathrm{loop}} = \frac{\chi q}{2}\sum_n n \operatorname{sign}(n + rq\zeta) = -\frac{\chi q}{12} = 225\beta. \tag{XIV.8.66}$$

The origin of this sum is the charge product in the parity-odd three-dimensional term. A pair of nonzero modes with KK charges $n, -n$ and common charge q has opposite mass signs in this chamber. For the abelian self-level the two charge products are both q^2 and their signed sum vanishes. For the mixed level the charge products are nq and $-nq$, so the opposite mass signs make the contributions add:

$$q^2\big[\operatorname{sign} m_n + \operatorname{sign} m_{-n}\big] = 0, \qquad nq \operatorname{sign} m_n - nq \operatorname{sign} m_{-n} = 2nq \quad (n > 0). \tag{XIV.8.67}$$

This is why a zero-mode comparison such as (XIV.8.64) and the mixed KK sum use different parts of the circle spectrum. The sign of a charged zero mode matters for an

ordinary self-level; it cannot affect the mixed level because that mode has no KK charge. This relates the mixed loop level to the trace coefficient by $\Theta_{0A}^{\mathrm{loop}} = -4c_{\mathrm{loop,grav}}$. The sum is regulated, not an ordinary convergent series. A crossing of a KK mass through zero changes which signs occur, so the chamber matters. The geometric comparison also requires the shifted KK divisor. Here the computation uses the same stated χ as the four-dimensional trace and is a consistency check, not a second independent determination of the geometry. The KK modes in this calculation encode an anomaly on the circle. The next section considers a different tower, from enlarging a six-dimensional internal base at fixed four-dimensional spacetime.

XIV.8.6 Growing the bulk at fixed gauge scale

Can gravity become weak without making the gauge interaction weak as well? Work in fixed microscopic units, use the leading unwarped Einstein reduction, and keep the base and the relevant wrapped cycles large in string units when using this approximation. Denote physical Einstein volumes by V_E and dimensionless Kähler volumes by $\mathcal{V}$ and τ_D. In a product reduction the four-dimensional Einstein term results from integrating the internal constant graviton profile:

$$\frac{1}{2\kappa_{10}^2}\int_{B\times\mathcal{M}_4}\sqrt{-g_{10}}\,\mathcal{R}_4 = \frac{M_4^2}{2}\int_{\mathcal{M}_4}\sqrt{-g_4}\,\mathcal{R}_4, \qquad M_4^2 = \frac{V_E(B)}{\kappa_{10}^2}. \tag{XIV.8.68}$$

Warping would change the internal weight in the integral. For the weak D7 comparison with vanishing background gauge-invariant two-form, integrate the eight-dimensional quadratic gauge action on S. In the fundamental trace $\mathrm{tr_f}(T_aT_b) = \delta_{ab}/2$ it gives

$$-\frac{1}{2k_8}\int_{S\times\mathcal{M}_4}\sqrt{-g_8}\;\mathrm{tr_f}\,F_{\mu\nu}F^{\mu\nu} \;\longrightarrow\; -\frac{1}{2g_4^2}\int_{\mathcal{M}_4}\sqrt{-g_4}\;\mathrm{tr_f}\,F_{\mu\nu}F^{\mu\nu}, \qquad g_4^{-2} = \frac{V_E(S)}{k_8}, \tag{XIV.8.69}$$

where $k_8 = 2(2\pi)^5(\alpha')^2$. The gauge formula is dimensionless since k_8 and $V_E(S)$ have units of length to the fourth power. This weak-brane normalization is separate from the dimensionless geometric basis in Section XIV.8.3; both give the same dependence on the wrapped volume in their stated regimes. We will measure dimensionless J_b in units of ℓ_s^2 with $\ell_s = 2\pi\sqrt{\alpha'}$. In particular $V_E(B) = \ell_s^6\mathcal{V}$ and $V_E(S) = \ell_s^4\tau_S$ in these units.

For the rank-one base of the split quadric the relation between the volumes has no free shape parameter:

$$\mathcal{V} = \frac{t^3}{6}, \qquad \tau_S = t^2, \qquad \frac{\tau_S^{3/4}}{\mathcal{V}^{1/2}} = \sqrt{6}. \tag{XIV.8.70}$$

At $t = 2$ and $t = 8$ the volume grows by 64 and τ_S by 16. A divisor of degree one instead gives $\tau = t^2/2$, which has the same growth power. Thus the fixed-unit classical ray to infinite bulk volume cannot keep a positive finite gauge coupling for this sector. A uniformly rescaled reference metric $g(t) = t\,g(1)$ would have $\Delta(t) = t^{-1}\Delta(1)$, so

its KK masses scale as $t^{-1/2}$. The ratio of those masses to M_4 decreases along this illustrative metric family, but this is a path on which the gauge coefficient also diverges. It does not solve the fixed-coupling problem.

A separate geometry gives two independent volumes. Blow up a point in $\mathbb{P}^3$, writing H for the pulled-back hyperplane and $E \simeq \mathbb{P}^2$ for the exceptional divisor. On E, $H|_E = 0$ and $E|_E = -h$ for its hyperplane h. Consequently $\int E^3 = \int_E h^2 = 1$, all mixed cubic intersections vanish, and $\int H^3 = 1$. Write

$$J_b = aH - bE = (a-b)H + b(H-E), \qquad a > b > 0. \tag{XIV.8.71}$$

The pulled-back H and the class $H - E$ of projection hyperplanes generate the nef cone. The two elementary curve areas are b on an exceptional line and $a - b$ on the strict transform of a line through the point. The signs in (XIV.8.71) follow from those areas. Expanding the products gives

$$\mathcal{V} = \frac{a^3 - b^3}{6}, \qquad \tau_H = \frac{a^2}{2}, \qquad \tau_E = \frac{b^2}{2}, \qquad \tau_{H-E} = \frac{a^2 - b^2}{2}. \tag{XIV.8.72}$$

One can express the same path in terms of the curve areas directly. Put $c = a - b > 0$. Then

$$\mathcal{V} = \frac{c^3 + 3bc^2 + 3b^2c}{6}, \qquad \tau_{H-E} = \frac{c(c+2b)}{2}, \qquad \tau_E = \frac{b^2}{2}. \tag{XIV.8.73}$$

Increasing c grows both the bulk and the divisor $H - E$. It leaves the volume of the exceptional surface fixed because all its curve areas are controlled by b. In particular, choosing $H - E$ rather than E for a would-be local sector would not preserve the gauge scale along this ray. Now $a \to \infty$ at fixed b keeps the exceptional action finite. The ordinary smooth Weierstrass example of Chapter 10 supplies a geometry on this base. It does not place a gauge stack on E. If a separate construction supported such a sector, its leading volume scale would be controlled by τ_E; no flux or matter sector from the earlier compact examples has been moved here.

For an E3 on E the real classical action is $2\pi\tau_E$ in these Einstein units. Indeed its Einstein tension is $(2\pi)^{-3}(\alpha')^{-2} = 2\pi/\ell_s^4$; multiplying by $\ell_s^4\tau_E$ gives this result without a further dilaton factor. Whether this instanton contributes to a superpotential is a separate zero-mode and coupling question of Chapter 10. At $(a, b) = (7, 3)$ and $(14, 3)$ the bulk volumes are $158/3$ and $2717/6$, while the exceptional action is 9π at both points. On a uniform ray, compare $(7, 3)$ with $(14, 6)$: the action becomes 36π. Figure XIV.8.6 shows the two trajectories and their position relative to the cone wall.

The growth of M_4 tests the coupling of the four-dimensional graviton zero mode. It does not bound the masses or summed couplings of the other modes. If the bulk radii grow like $\sqrt{a}$ and the exceptional shape is controlled at fixed b, dimensional estimates give

$$m_{\mathrm{KK,bulk}} \sim \ell_s^{-1} a^{-1/2}, \qquad m_{\mathrm{KK},E} \sim \ell_s^{-1} b^{-1/2}. \tag{XIV.8.74}$$

These estimates require a metric hypothesis. A volume alone is not a spectral estimate. At finite a a global zero-mode action is restricted to energies below the lightest omitted tower. Such a bound cannot simply be continued to a fixed positive probe energy if the bound itself tends to zero.

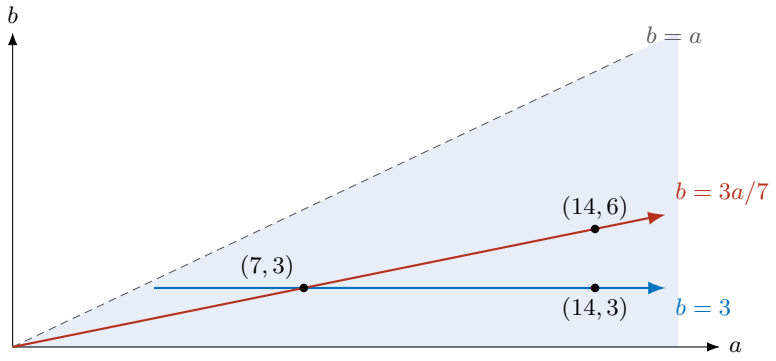


Figure XIV.8.6: Kähler coordinates of the point blowup. The shaded region is $0 < b < a$. The horizontal ray keeps the exceptional line area b fixed. The oblique ray holds $b/a = 3/7$ fixed and grows the exceptional action along with the bulk volume.

A flat torus comparison explains why even a small coupling to each mode does not settle the limit. For a six-torus with periods $2\pi R_{\mathrm{b}}$, normalized waves have $|\psi_{\mathbf{n}}(y)|^2 = (2\pi R_{\mathrm{b}})^{-6}$ at a fixed point. A momentum cutoff Λ keeps lattice points with $|\mathbf{n}| < \Lambda R_{\mathrm{b}}$. Thus at large R_{b},

$$N(\Lambda) \sim \frac{\pi^3}{6}(\Lambda R_{\mathrm{b}})^6, \qquad \sum_{|\mathbf{n}|<\Lambda R_{\mathrm{b}}} |\psi_{\mathbf{n}}(y)|^2 \sim \frac{\pi^3}{6(2\pi)^6}\Lambda^6. \tag{XIV.8.75}$$

For example the weight in a fixed shell $\Lambda_1 < |\mathbf{n}|/R_{\mathrm{b}} < \Lambda_2$ approaches $\pi^3(\Lambda_2^6 - \Lambda_1^6)/(6(2\pi)^6)$. A field confined to a small region can see this weight if it couples locally to the bulk wave; the calculation would change if the coupling imposed a selection rule or a momentum suppression. The remaining weight may be small at low energy in microscopic units, but its limit is not suppressed by R_{b} alone. The torus is an explicit comparison metric and not the point blowup's spectrum. A four-dimensional isolation claim requires control of couplings to any light continuum or a different limit that gives a suitable energy window. Before that step one also needs to know which local fields actually have finite kinetic norms.

XIV.8.7 Which fields remain dynamical in a local limit?

A period can remain nonzero when a region becomes noncompact. Does the corresponding field still have a finite kinetic term? A period fixes the normalization against cycles, while a kinetic term integrates a norm over the entire space. We first compute the compact norms in the point blowup. We then solve for period-normalized harmonic forms in an explicit auxiliary local metric. This second calculation is needed because the compact norm alone supplies no local representative.

Let ω_H, ω_E be harmonic $(1,1)$ forms representing H, E on the compact Kähler threefold. Define

$$A_{ij} = \int_B J_b \omega_i \omega_j, \qquad p_i = \int_B J_b^2 \omega_i, \qquad N_{2,ij} = \int_B \omega_i \wedge *\omega_j, \tag{XIV.8.76}$$

where $i, j = H, E$. Lefschetz contraction commutes with the Kähler Laplacian, so the trace part of a harmonic $(1,1)$ form is a constant multiple of J_b. Subtract it to get a primitive harmonic form:

$$\omega_i = \omega_i^{\mathrm{prim}} + \frac{p_i}{6\mathcal{V}} J_b, \qquad *\omega_i^{\mathrm{prim}} = -J_b \wedge \omega_i^{\mathrm{prim}}, \qquad *J_b = \frac{1}{2} J_b^2. \tag{XIV.8.77}$$

These star identities follow in a unitary coframe by taking the complement of each two-plane area form. The primitive trace condition is that the three coefficients sum to zero. For example, the star of a difference of two area forms equals minus the wedge of that difference with the sum of the three area forms. It follows that $*\omega_i = -J_b \omega_i + (p_i/4\mathcal{V}) J_b^2$ and

$$N_2 = -A + \frac{p p^{\mathsf{T}}}{4\mathcal{V}}, \qquad A = \mathrm{diag}(a, -b), \quad p = (a^2, b^2)^{\mathsf{T}}. \tag{XIV.8.78}$$

The entries of A and p are fixed by the same cubic intersection as in (XIV.8.72). As a check on the sign of the primitive term, the EE entry is $b + b^4/(4\mathcal{V}) > 0$. The determinant is $-ab + (a^3 - b^3)ab/(4\mathcal{V}) = ab/2$, so the matrix is positive throughout the cone.

A fixed-period C_4 axion is described by a four-form rather than the two-form for a divisor class. Let η^j be the harmonic basis specified by $\int_B \omega_i \wedge \eta^j = \delta_i^j$. Poincaré duality identifies these pairings with the integrals over the corresponding divisors. To obtain the basis from (XIV.8.78) we set $\eta^j = \sum_k *\omega_k (N_2^{-1})_{kj}$. The star is an isometry and its square on these forms is one, so the four-form Gram is $N_4 = N_2^{-1}$. Explicitly the rank-one update has denominator $4\mathcal{V} + p^{\mathsf{T}}(-A)^{-1} p = -2\mathcal{V}$. Hence

$$N_4 = \begin{pmatrix} -1/a & 0 \\ 0 & 1/b \end{pmatrix} + \frac{1}{2\mathcal{V}} \begin{pmatrix} a \\ -b \end{pmatrix} \begin{pmatrix} a & -b \end{pmatrix}. \tag{XIV.8.79}$$

The off-diagonal entry matters before taking the limit. A diagonal inverse taken entry by entry would miss that mixing.

The same four-form metric can be read from the leading $K = -2\log \mathcal{V}$ in chiral variables. With $\tau_H = a^2/2$, $\tau_E = b^2/2$,

$$\partial_\tau \mathcal{V} = \frac{1}{2}(a, -b), \qquad \partial_\tau^2 \mathcal{V} = \frac{1}{2}\,\mathrm{diag}(1/a, -1/b), \qquad 4\mathcal{V} K_{T\bar{T}} = \mathcal{V}\,\partial_\tau^2 K = N_4. \tag{XIV.8.80}$$

Restoring the factor of $\mathcal{V}$ is necessary because the dimensionless Kähler metric multiplies M_4^2 in the compact action. A four-form of unit period in fixed microscopic units should be tested with that physical coefficient. At fixed b the compact limits are

$$N_{2,HH} \sim a/2, \qquad N_{2,EE} \longrightarrow b, \tag{XIV.8.81}$$

$$N_{4,HH} \sim 2/a, \qquad N_{4,EE} \longrightarrow 1/b, \qquad N_{4,HE} \longrightarrow 0. \tag{XIV.8.82}$$

For example, at $(a,b)=(7,3)$ the compact exceptional two-form has squared norm $3+243/632$, whereas the four-form of unit exceptional period has squared norm $1/3+27/316$. The two-form answer would overestimate the axion coefficient even though both quantities are finite at that point. At $b=3$ the exceptional axion norm tends to $1/3$. The compact scalar variation of b has $d\tau_E = b\,db$ at fixed a, so its norm coefficient in this comparison is $b^2 N_{4,EE} \to b$. These statements refer to fixed-period kinetic coefficients and the compact leading moduli metric. They do not prove a normalizable solution of the linearized equations on a physical noncompact background. The H-axion norm tends to zero in this normalization; that is a degenerating compact coefficient, not a construction of a local field or a proof that it is a frozen source.

To find a local harmonic representative, restrict to the blowup of the affine patch about the point. This is the total space of $\mathcal{O}_{\mathbb{P}^2}(-1)$ with exceptional zero section E. The pullback H is cohomologically trivial there. With $s=\sum_{i=1}^{3}|z_i|^2$ on the complement of E, use the explicit auxiliary Kähler form

$$J_{\mathrm{loc}} = dd^c\phi(s), \qquad dd^c = \frac{i}{2\pi}\partial\bar\partial, \qquad \phi = s + b\log s. \tag{XIV.8.83}$$

In a blowup chart write $z=(w,wu,wv)$, so $s=|w|^2(1+|u|^2+|v|^2)$. Removing $\log|w|^2$ off the zero section leaves the smooth potential

$$|w|^2(1+|u|^2+|v|^2) + b\log(1+|u|^2+|v|^2). \tag{XIV.8.84}$$

At $w=0$ the first term supplies a positive normal direction and the second restricts to b times the Fubini–Study form with unit period on a line. On the complement the radial and two tangential coefficients are $\phi'+s\phi''$ and ϕ', both positive. They tend to one at infinity, so a path escaping to infinity has infinite length, and the extended metric is complete. It is a Kähler metric chosen for calculation. In particular, its determinant relative to the flat metric away from E is $(1+b/s)^2$, so it is not a Ricci-flat solution there. We have not imposed a seven-brane profile, flux, or warping.

Seek a two-form $\omega = dd^c u(s)$ with unit exceptional line period. For any radial potential, its tangential eigenvalue in the flat coordinates is u' and its radial eigenvalue is $(su')'$. Let $f=s\phi'=s+b$, $y=su'$. Dividing the eigenvalues by those of J_{loc} gives y/f twice and y'/f' once. A primitive form has zero sum of these eigenvalues. Thus the equation and boundary condition are

$$2\frac{y}{f}+\frac{y'}{f'}=0 \quad\Longleftrightarrow\quad (f^2y)'=0, \qquad y(0)=1. \tag{XIV.8.85}$$

The last condition fixes the coefficient of $\log s$ to one at E. The solution is

$$y=\frac{b^2}{(s+b)^2}, \qquad u(s)=\log\frac{s}{s+b}+\frac{b}{s+b} \quad \text{up to a constant.} \tag{XIV.8.86}$$

The $\log s$ term extends as in (XIV.8.84), and the other terms are smooth. Then $\int_{\mathbb{P}^1}\omega=1$. The form is closed; its star is $-J_{\mathrm{loc}}\wedge\omega$, also closed. It is therefore co-closed and harmonic. This construction imposes a differential equation in addition to the topological period.

To check its norm, the flat volume shell after angular integration in these units is $s^2 ds/2$, obtained from the ball volume $s^3/6$. The relative determinant multiplies it by $(f/s)^2 f'$, giving the shell $f^2 f' ds/2$ in the auxiliary metric. Put $q(s) = b^2/(s+b)^3$. The three eigenvalues of ω relative to J_{loc} are $(q, q, -2q)$, and their squares sum to $6q^2$. Consequently

$$\|\omega\|^2 = \int_0^\infty 6q(s)^2 \frac{f^2 f'}{2}\, ds = \int_0^\infty \frac{3b^4}{(s+b)^4}\, ds = b. \tag{XIV.8.87}$$

The period-dual harmonic form is $\eta = -*\omega/b$, since $*\omega|_E = -bh^2$. It has $\int_E \eta = 1$ and $\|\eta\|^2 = 1/b$. The positive line period of ω corresponds to the restriction of $-E$, since $E|_E = -h$. Its squared norm can be compared with that of the compact ω_E, but to compare periods one must reverse the latter's sign.

One can check the size of the region contributing to (XIV.8.87) without estimating a tail from a pointwise value. The norm inside a radius given by $s = S_0$ is

$$\|\omega\|^2_{s<S_0} = b\left[1 - \left(\frac{b}{S_0 + b}\right)^3\right]. \tag{XIV.8.88}$$

Already at $S_0 = b$ this contains $7/8$ of the squared norm. Here the finite normalization results from the radial equation and the volume density together. This estimate on a specified metric is different from a claim that fluctuations on a compact sequence have uniformly small tails.

The same line period also occurs for the smooth closed form obtained from $y = 1$. Its relative eigenvalues are $(1/f, 1/f, 0)$. The squared norm after multiplying by the shell is then $f' = 1$, so its integral diverges. Figure XIV.8.7 contrasts the two integrands. The harmonic form solves the primitive equation and decays in orthonormal components as r^{-6}, where $r = \sqrt{s}$. The other form's pointwise norm decays as r^{-2}, which is insufficient. Matching the compact limits b and $1/b$ is a comparison of norms in two specified calculations. It does not establish convergence of the compact metric, uniform isolation of a KK spectrum, or completeness of a space of normalizable modes.

A useful preliminary tail test is available on a six-dimensional conical end with bounded positive kinetic weight. A scalar of comparable magnitude $r^{-\delta}$ has tail norm proportional to $\int^\infty r^{5-2\delta} dr$. For a tangential p-form with coefficient size $r^{-\delta}$ in a fixed angular basis, each leg brings an additional inverse radius in the orthonormal norm. Thus

$$\int^\infty r^{5-2(p+\delta)} dr < \infty \quad \Longleftrightarrow \quad p + \delta > 3. \tag{XIV.8.89}$$

Equality gives a logarithm, and a constant scalar fails. Radial legs, a nontrivial weight, or a different asymptotic metric require the actual orthonormal norm. A convergent tail still has to be extended regularly through the core and satisfy the relevant fluctuation equation. In an actual F-theory limit the weights and the fluctuation operators can be different for different fields. A compact charge matrix determines a mass kernel only while its kinetic system is positive and regular. In a singular limit one must identify the surviving normalizable fields and their couplings before applying the kernel argument or claiming an isolated four-dimensional theory.

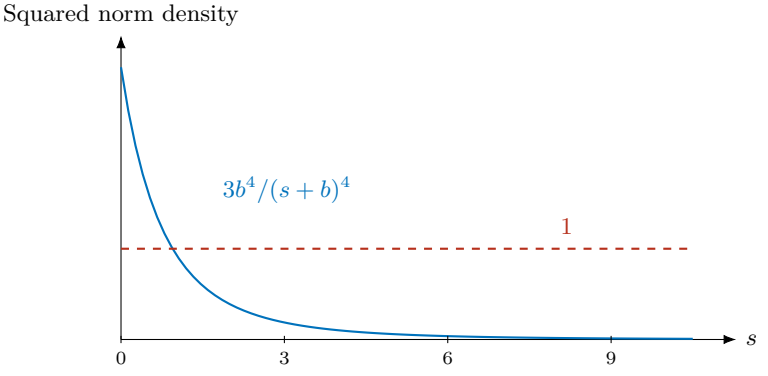


Figure XIV.8.7: Radial densities for squared two-form norms in the auxiliary metric at $b = 3$, after angular integration. Both profiles have line period one. The constant density for $y = 1$ gives infinite norm, while the integral of the primitive profile is 3.

XIV.8.8 Exercises

1. **Test the period connection.** In (XIV.8.24) take $d = 12$, use G_-, and set $z = \bar{z} = 1/3$. Find the compensator c, the coefficient of z^2 in $\Omega_1(z)^2$, $W(0)$, $D_z W(0)$, $K_{z\bar{z}}(0)$, $W''(0)$, and the ordinary and covariant derivatives at $z = 1/3$. Explain which supersymmetry test the common flux square misses.

2. **Change the Shioda height.** Use $\beta = 6H$, $t = 6$, $m = -3$ and zero charged expectation values in the factorized flux trial. Find the coefficient of H in b_σ, the raw pairing, D_σ and V_D. Explain why the trial is not a constructed quantized primitive vacuum.

3. **Change the kinetic and Higgs directions.** Keep k and G_{ax} of (XIV.8.50); take $Z = \mathrm{diag}(4, 9)$ and a Higgs field of charge $(1, -1)$ and $|v_\phi|^2 = 3$. Give the canonical matrix before and after the Higgs contribution and both nullities. In the separate charge-two stabilizer exercise take the integer axion charge to be $k = 5$ and give the order. Explain why the latter cannot be read off the canonical mass matrix.

4. **Change the anomaly data.** At $\beta = 3$ in the singlet slice, compute the three fermion and the three Green–Schwarz coefficients of (XIV.8.63), in the stated order and trace frame. In the *separate* pure $SU(5)$ example take $\lambda = 2$ and replace $\bar{\mathbf{5}}$ by $\mathbf{5}$. Give the cubic coefficient relative to the defining trace and say whether it vanishes. Explain why matching the mixed rows alone cannot address this failure.

5. **Choose a ray and a period.** For $(a, b) = (11, 4)$ give the cone verdict, $\mathcal{V}, \tau_H, \tau_E, \tau_{H-E}$ and the classical E3 action on E divided by π. Compute the compact EE two- and four-form squared norms separately. As $a \to \infty$ at this b, give both limiting norms and identify which divisor retains a positive finite fixed-period axion norm, H or E.

6. **Change the angular degree and decay.** On the six-dimensional cone take a tangential $p = 2$ form with angular coefficients comparable to r^{-1} at infinity. Give the exponent of r in the radial squared norm and classify convergence. Repeat with decay $r^{-3/2}$. Explain what else must be checked for a dynamical mode.

7. **Write a cutoff argument.** Suppose the fixed-b ray admits a sequence of bulk modes with masses tending to zero. Explain which conclusions the leading volume and period calculations still permit. Specify what would have to be shown about normalizable fields, their couplings to the tower, and a physical boundary condition to obtain an isolated four-dimensional theory.

Submit the bounded parts using `benchmark/PROTOCOL.md`. The written explanations are assessed by a reader.

Status and sources

§1. Fields and partial Legendre transform. The ordinary M/F field correspondence is [GEO-E]; the leading reduction is [SUGRA]; the rank-one Hessian and

no-scale identity are [MATH]. See Grimm (2011), arXiv:1008.4133v2, eqs. (2.17)–(2.35), (3.24)–(3.38), (4.16)–(4.17) and Appendix B. The circle interpretation is the Chapter 1 dictionary, with the ordinary adiabatic hypothesis. The field map is restricted to the displayed multiplets. The Legendre calculation does not give exact corrected chiral coordinates.

§2. Flux and Hodge type. The period reduction, leading F conditions and the restricted twisted-brane description are [SUGRA]. See Grimm (2011), eqs. (2.10)–(2.13), (2.39)–(2.47), (5.3)–(5.7) and (5.19)–(5.20), and the flux pairing of Gukov et al. (2000), hep-th/9906070v2, §2 and Appendix I. The Kummer chart and equal-charge comparison are [MATH]; the fixed-frame off-origin and transformed-frame tests discriminate the connection. The separate algebraic product example transfers the Chapter 3 result; its primitivity pairing is not computed in the Kummer chart. No elliptic-family completion or stabilization follows.

§3. Kinetic and moment-map blocks. The leading Cartan, Shioda and D coefficients are [SUGRA]: Grimm (2011), eqs. (3.18)–(3.20), (3.31)–(3.37), (5.12)–(5.16), and Cvetič et al. (2013), arXiv:1210.6034v2, §§3.1 and 3.3. The split quadric intersections use Chapter 2; the abelian section intersections use Chapter 6. The formal charge arithmetic and the resolved interior obstruction are [MATH]. The latter uses the same strict Cartan basis and G_* as Chapter 3; the former uses the separate Chapter 7 formal charge input. Warping and threshold corrections to leading gauge couplings are outside this calculation; see Grimm et al. (2013).

§4. Gauging and rank. The mixed term and its dualization are [SUGRA]; see Grimm (2011), eqs. (5.12)–(5.15), and Cvetič et al. (2013), eqs. (44)–(51). The canonical kernel, rigid solutions and integral stabilizer are [MATH]. The stabilizer assumes independently given primitive periods. Chapter 7 uses a different connected kernel; the comparison with Chapter 10 translates the axion orientation. The off-vacuum mass coefficient does not specify a pole mass.

§5. Anomaly and KK comparisons. The pure $SU(5)$ trace test and the singlet comparison are [ANOM], with one separate pure test and two matched nonzero local coefficients plus one mixed zero. See Cvetič et al. (2013), eqs. (13)–(16), (116)–(119), (127), (133)–(138), and Appendix A. The barred-five signs in the generic printed cubic row (136) are not used to set the cubic trace; the relevant multiplicities vanish on the singlet slice. The singlet Chern–Simons arithmetic uses eq. (64) and finds a factor of two, not an inferred spectrum. The regulated KK result is [SUGRA], using eqs. (64), (74)–(84), within the small-holonomy chamber. No independent derivation of all the chiralities, full Chern–Simons matching, or global anomaly test is claimed.

§6. Fixed units and the bulk. The Einstein and quadratic weak-brane reduction is [SUGRA]; see Córdova (2011), arXiv:0910.2955v2, eqs. (1)–(3), and the weak trace and tension normalization of Volume XV, Chapter 2. The two cone calculations are [MATH]; the smooth blowup geometry and E3 units use Chapter 10, separate from the split quadric or Shioda examples. Isolation at fixed probe energy is [DEC]; holding the exceptional action finite supplies a volume condition only.

§7. Norms and the auxiliary metric. The compact Gram computation, local radial solution and conical tail criterion are [MATH]. The Gram computation uses the stated Kähler star identities and the intersection ring of the point blowup. The radial computation proves existence of the two specified harmonic forms on the stated complete auxiliary metric. The compact comparison assumes the leading unwarped kinetic weight. A physical local mode spectrum or convergence of the compact background is outside these claims.

References

Córdova, C. (2011). "Decoupling Gravity in F-Theory". In: *Adv. Theor. Math. Phys.* 15, pp. 689–740. arXiv: 0910.2955 [hep-th].

Cvetič, M., T. W. Grimm, and D. Klevers (2013). "Anomaly Cancellation and Abelian Gauge Symmetries in F-theory". In: *JHEP* 02, p. 101. arXiv: 1210.6034 [hep-th].

Grimm, T. W. (2011). "The N=1 effective action of F-theory compactifications". In: *Nucl. Phys. B* 845, pp. 48–92. arXiv: 1008.4133 [hep-th].

Grimm, T. W., D. Klevers, and M. Poretschkin (2013). "Fluxes and Warping for Gauge Couplings in F-theory". In: *JHEP* 01, p. 023. arXiv: 1202.0285 [hep-th].

Gukov, S., C. Vafa, and E. Witten (2000). "CFT's from Calabi–Yau four-folds". In: *Nucl. Phys. B* 584, pp. 69–108. arXiv: hep-th/9906070.

Chapter XIV.9

The Sen limit and the heterotic comparison

XIV.9.1 The weak-coupling question

A seven-brane can be recognized by how charges change when they are transported around it. In an elliptic description the same transport acts on the cycles of the fiber. The twenty-four nodal fibers of the K3 in Chapter 1 furnish a first example. Each nodal fiber looks like a parabolic monodromy in a suitable local marking, but the marking need not be the same from one fiber to the next. Can we deform the geometry so that a single perturbative description accounts for the branes on a large part of the base? If so, what can that description tell us about the original elliptic model?

The first test is local. Let τ be the ratio of two oriented periods, chosen in the upper half plane. In the ordinary type IIB identification $\tau = C_0 + i/g_s$, with C_0 the axion and g_s the local string coupling. The modular invariant j is a function of the unmarked elliptic curve. We use $j(i) = 1728$. Near the cusp the local parameter is $q = e^{2\pi i\tau} = j^{-1} + O(j^{-2})$, and $\operatorname{Im}\tau = -\log|q|/(2\pi)$. Large $|j|$ therefore gives a local weakly coupled description in that chart. It does not give a global marking of the periods. In particular, taking $|j|$ large at each point of a region does not tell us how the period column closes around a hole in that region.

We will make two comparisons. In the first we use the Sen deformation to read a perturbative D7 and O7 configuration from a family of elliptic fibrations. The calculation has three parts: factor the leading discriminant, count divisors on the orientifold double cover, and follow actual periods around a region where the perturbative approximation breaks down. In the second comparison we split a different elliptic K3 into two surfaces meeting on a torus. The common curve and the two components give different pieces of the heterotic dictionary. We then work out what survives when the comparison is applied fiberwise. The O-plane and IIB charge conventions of Volume II and the K3 geometry of Volume IV are the prerequisites; the two limiting constructions are developed here. At the end we return to the split I_5 gauge divisor of Chapter 2 and test exactly what its weak-coupling comparison preserves.

XIV.9.2 The Sen polynomial and its discriminant

Which coefficients can make the generic fiber approach a cusp while keeping control of the singular fibers that remain at nonzero deformation parameter? For a Weierstrass model with anticanonical line $L = K_B^{-1}$ on the base B, write

$$y^2 = x^3 + fx + g, \qquad f \in H^0(B, L^4), \quad g \in H^0(B, L^6), \qquad \Delta = 4f^3 + 27g^2. \tag{XIV.9.1}$$

The discriminant of the elliptic curve with the conventional factor of 16 is -16Δ. Here $j = 1728(4f^3)/\Delta$. A double root $x = -h$ at a generic point gives a nodal cubic: with a third root at $2h$ we have

$$(x + h)^2(x - 2h) = x^3 - 3h^2x - 2h^3. \tag{XIV.9.2}$$

The coefficient h is a section of L^2. To vary this cubic, first add the term $\epsilon\eta(x + h)$, where ϵ is a complex parameter and η a section of L^4. This preserves the root at $-h$ and splits the double root. At the next order allow an independent constant-in-x perturbation using a section χ of L^6:

$$f = -3h^2 + \epsilon\eta, \qquad g = -2h^3 + \epsilon h\eta - \frac{\epsilon^2}{12}\chi. \tag{XIV.9.3}$$

The Sen parameter usually denoted C is our ϵ. In the original normalization the last term of g is $+C^2\chi_{\text{Sen}}$ and $j_{\text{Sen}}(i) = 24^3$, so $\chi_{\text{Sen}} = -\chi/12$ and $j_{\text{Sen}} = 8j$. The section degrees of the deformation terms and their relative signs both matter.

Expanding the two contributions separately exposes the cancellation:

$$4f^3 = -108h^6 + 108\epsilon h^4\eta - 36\epsilon^2h^2\eta^2 + 4\epsilon^3\eta^3, \tag{XIV.9.4}$$

$$27g^2 = 108h^6 - 108\epsilon h^4\eta + 27\epsilon^2h^2\eta^2 + 9\epsilon^2h^3\chi - \frac{9}{2}\epsilon^3h\eta\chi + \frac{3}{16}\epsilon^4\chi^2. \tag{XIV.9.5}$$

The first perturbation is tangent to the discriminant locus: the constant and linear terms cancel for every h and η. With $D = \eta^2 - h\chi$, the complete answer is

$$\Delta = -9\epsilon^2h^2D + \epsilon^3\left(4\eta^3 - \frac{9}{2}h\eta\chi\right) + \frac{3}{16}\epsilon^4\chi^2. \tag{XIV.9.6}$$

All three displayed coefficients have class $12L$. At $\epsilon = 0$, Δ vanishes everywhere. The relevant limiting divisor comes from the first nonzero coefficient after dividing by ϵ^2. It has the two parts h^2 and D. We will use the double cover to interpret those multiplicities; at this point they are just factors of a section.

To see the difference between a leading divisor and a finite-parameter divisor, work in a chart with $h = \chi = 1$ and $\eta = z$. The limiting residual polynomial is $D = z^2 - 1$, but the equation for the actual discriminant near $z = 1$ is

$$\frac{\Delta}{\epsilon^2} = -9(z^2 - 1) + \epsilon\left(4z^3 - \frac{9}{2}z\right) + \frac{3}{16}\epsilon^2. \tag{XIV.9.7}$$

At $z = 1$ this is $-\epsilon/2 + 3\epsilon^2/16$. The derivative of the zeroth-order polynomial there is -18, so the implicit function theorem gives a unique nearby root. Substituting $z = 1 + b\epsilon + O(\epsilon^2)$ fixes its displacement:

$$-18b - \frac{1}{2} = 0, \qquad z(\epsilon) = 1 - \frac{\epsilon}{36} + O(\epsilon^2). \tag{XIV.9.8}$$

The limiting root and the finite-parameter root agree to order zero, which is all the leading factorization promises. The change $\chi = 0$ is different. It gives the exact product

$$\Delta = \epsilon^2\eta^2(4\epsilon\eta - 9h^2). \tag{XIV.9.9}$$

At a simple zero of η with $h \neq 0$ the residual zero is now double. The exact factor η^2 does not describe two separated roots of this specialized discriminant.

The displacement calculation uses both the order in ϵ and the order of the limiting zero in the base. Write z_* for a simple zero of D with $h(z_*) \neq 0$. Expanding about z_* at fixed nonzero leading derivative gives

$$0 = -9h(z_*)^2 D'(z_*)\big(z - z_*\big) + \epsilon R_3(z_*) + O\big((z - z_*)^2, \epsilon(z - z_*), \epsilon^2\big), \tag{XIV.9.10}$$

where $R_3 = 4\eta^3 - 9h\eta\chi/2$ is the cubic-order coefficient. Terms from differentiating h^2 vanish here because $D(z_*) = 0$. In the same worked family the other root is initially at $z_* = -1$. There $D' = -2$ and $R_3 = +1/2$, so

$$z_+(\epsilon) = 1 - \epsilon/36 + O(\epsilon^2), \qquad z_-(\epsilon) = -1 - \epsilon/36 + O(\epsilon^2). \tag{XIV.9.11}$$

The two simple roots drift in the same direction at first order. At a double limiting zero the linear derivative in (XIV.9.10) instead vanishes. That is why the same first-order procedure cannot be used to split the residual η^2 in (XIV.9.9). It also cannot locate the roots near $h = 0$, where the factor $h(z_*)^2$ would vanish. The scaled calculation below treats that case.

We can use the same expansion to specify where weak coupling is uniform. Choose a compact set K in a trivializing chart disjoint from $hD = 0$. Then $|h|$ and $|D|$ have positive lower bounds on K and the coefficient functions have finite upper bounds. Write $R_3 = 4\eta^3 - 9h\eta\chi/2$ and $R_4 = 3\chi^2/16$. In this chart the two factors we divide are

$$4f^3 = -108h^6\left(1 - \frac{\epsilon\eta}{3h^2}\right)^3, \tag{XIV.9.12}$$

$$\Delta = -9\epsilon^2 h^2 D\left(1 - \frac{\epsilon R_3 + \epsilon^2 R_4}{9h^2 D}\right). \tag{XIV.9.13}$$

The terms subtracted from 1 are bounded in magnitude by a constant times $|\epsilon|$, uniformly on K for $|\epsilon| \leq 1$. For small enough $|\epsilon|$, each bracket has magnitude at least $1/2$. We can thus invert the denominator bracket uniformly, obtaining

$$j = \frac{20736h^4}{\epsilon^2 D}\big(1 + O_K(|\epsilon|)\big). \tag{XIV.9.14}$$

In particular, $|h^4/D|$ has both a positive lower bound and a finite upper bound there. The cusp estimate becomes

$$\operatorname{Im}\tau = -\frac{1}{\pi}\log|\epsilon| + O_K(1) \tag{XIV.9.15}$$

in local cusp representatives. A finite family of trivializations makes this argument on a compact exterior in the base. The constants depend on how far the set stays from the excluded loci. This can be seen directly in the chart $h = \chi = 1,\ \eta = z$ used for the moving root. On the disk $K = \{|z| \le 1/2\}$ the triangle inequality gives $|D| \ge 3/4$, $|R_3| \le 11/4$, and $|R_4| = 3/16$. For $|\epsilon| \le 1/4$ the sizes of the two subtracted terms in (XIV.9.13) are bounded by

$$\left|\frac{\epsilon z}{3}\right| \le \frac{|\epsilon|}{6}, \qquad \left|\frac{\epsilon R_3 + \epsilon^2 R_4}{9D}\right| \le \frac{(11/4)|\epsilon| + (3/16)|\epsilon|^2}{27/4}. \tag{XIV.9.16}$$

Both bounds are less than $1/2$, uniformly on that disk. In particular, fixing a compact set away from the residual divisor is a way of choosing an actual domain where the expansion can be truncated with a controlled error.

At $z = 1$, outside this disk, the issue is different. The finite root is displaced, so the fixed point is smooth for small nonzero ϵ, but $D = 0$ there and the preceding relative estimate is undefined. Equation (XIV.9.7) now gives

$$\Delta(1) = -\tfrac{1}{2}\epsilon^3 + \tfrac{3}{16}\epsilon^4, \qquad j(1) = 373248\,\epsilon^{-3}\big(1 + O(|\epsilon|)\big). \tag{XIV.9.17}$$

The cusp still occurs at the fixed point, but with a different rate. Closer to the moving zero the denominator depends on the displacement as well. By comparison, moving toward $h = 0$ can destroy the cusp altogether, because the numerator also tends to zero there. Thus the two parts of $h^2 D = 0$ are excluded for different reasons. First we interpret the limiting divisors; afterward we will follow a contour enclosing the $h = 0$ region.

XIV.9.3 O7 and D7 data on the cover

Where does the multiplicity h^2 enter D7 charge bookkeeping? The perturbative description uses a double cover of B. In the total space of L the tautological fiber coordinate ξ is a section of the pullback of L. Take

$$X: \quad \xi^2 = h, \qquad \pi : X \longrightarrow B, \qquad \iota(\xi) = -\xi. \tag{XIV.9.18}$$

The fixed locus $O = (\xi = 0)$ lies over the branch divisor $H = (h = 0)$. Near a smooth point of H, use h as one local coordinate. The normal map is $h = \xi^2$, so this local branch is smooth in X; away from H the cover is unramified. An arbitrary singular H would require a separate smoothness check.

Let $p : \mathrm{Tot}(L) \to B$ be the projection. The vertical tangent is p^*L, giving $K_{\mathrm{Tot}(L)} = p^*(K_B \otimes L^{-1})$. The cover equation is a section of p^*L^2. Adjunction on the smooth cover then gives

$$K_X = \pi^*(K_B \otimes L^{-1} \otimes L^2) = \pi^*(K_B \otimes L). \tag{XIV.9.19}$$

This line is trivial for $L = K_B^{-1}$. In additive divisor notation $H \sim 2L$; its scheme pullback is $2O$. Since O is itself cut out by ξ, its class is π^*L. The class of D is $8L$, so

$$\pi^*H = 2O, \qquad [D_{\mathrm{cov}}] = 8\pi^*L = 8[O], \qquad D_{\mathrm{cov}} = (\eta^2 - \xi^2\chi = 0). \tag{XIV.9.20}$$

The ordinary O7$^-$ interpretation pairs the geometric involution with the IIB orientifold operation. Its D7 charge is -8 in cover units and -4 in quotient units. Accordingly the D7 charge equation in cover units is

$$[D_{\mathrm{cov}}] - 8[O] = 0. \tag{XIV.9.21}$$

This equality concerns the D7 charge class. It does not compute curvature or flux contributions to other tadpoles. In particular, using the quotient charge -4 together with a count of both lifts of each generic D7 point would mix two conventions in one equation.

We can test the two counts on a compact base without assuming the zeros are generic. Take $B = \mathbb{P}^1$ with $z = U/V$ and $L = \mathcal{O}(2)$, and homogenize the following polynomials to degrees $4, 8, 12$:

$$h = z^4 - 1, \qquad \eta = z^8 + k, \qquad \chi = 2z^{12} + \ell. \tag{XIV.9.22}$$

The reference pair is $(k, \ell) = (2, 3)$; the changed pair is $(3, 5)$. Multiplying before specializing gives a residual polynomial that distinguishes the two:

$$D_{k,\ell} = -z^{16} + 2z^{12} + 2kz^8 - \ell z^4 + k^2 + \ell, \tag{XIV.9.23}$$

$$D_{2,3} = -z^{16} + 2z^{12} + 4z^8 - 3z^4 + 7, \tag{XIV.9.24}$$

$$D_{3,5} = -z^{16} + 2z^{12} + 6z^8 - 5z^4 + 14. \tag{XIV.9.25}$$

At $h = 0$, $z^4 = 1$ so $D = (1 + k)^2 \neq 0$ for both. Thus none of the residual points lies over a ramification point. To check simplicity, it is useful to compute the greatest common divisor of a polynomial with its derivative. The absence of such a common factor over $\mathbb{Q}$ excludes repeated complex roots.

Here the finite-parameter test can also use integer polynomials. With $\epsilon = 1/100$, let $A = 100f$, $G = 120000g$ and $N = 120000^2\Delta$. In the z-chart,

$$A = -300h^2 + \eta, \qquad G = -240000h^3 + 1200h\eta - \chi, \qquad N = 576A^3 + 27G^2. \tag{XIV.9.26}$$

The leading coefficients of A, G are $-299, -238802$. They are the same for both pairs since only lower coefficients changed. For example the z^{24} coefficient of N is $576(-299)^3 + 27(-238802)^2$, which is 2 mod 11. The Euclidean algorithm in $\mathbb{F}_{11}[z]$, with monic gcds, gives

(k, ℓ)	$\gcd(h, h')$	$\gcd(D, D')$	$\gcd(h, D)$	$\gcd(N, N')$	$\gcd(N, A)$
$(2, 3)$	1	1	1	1	1
$(3, 5)$	1	1	1	1	1

(XIV.9.27)

One way to reproduce the tests is to substitute $b = z^4$ first. Reduce A, G modulo 11 to $8(b-1)^2 + b^2 + k$ and $-2(b-1)^3 - b^3 - b^2 + kb - k - \ell$, respectively, then form N with coefficients $4, 5$ in front of A^3, G^2. For the derivative tests on D, N, the z-derivative adds a factor $4z^3$ to the derivative in b; the constant terms are nonzero modulo 11. For example, with the changed pair the reductions in b are

$$\overline{D} = -b^4 + 2b^3 - 5b^2 - 5b + 3, \tag{XIV.9.28}$$

$$\overline{N} = 2b^6 - 5b^5 + 3b^3 - 2b^2 + 4b + 4, \qquad \overline{A} = -2b^2 - 5b. \tag{XIV.9.29}$$

For $(\overline{D}, \partial_b \overline{D})$ the successive nonzero remainders, using these representatives, are

$$b^2 - 5b + 1, \quad b - 2, \quad -5. \tag{XIV.9.30}$$

For $(\overline{N}, \partial_b \overline{N})$ they are $3b^4 - 4b^3 - 3b^2,\ 4 - 4b,\ -4$; for $(\overline{N}, \overline{A})$ they are $4 - 4b,\ 4$. Each list ends at a nonzero scalar. Over the algebraic closure of $\mathbb{F}_{11}$, a common root of either derivative pair with $z \neq 0$ would make $b = z^4$ a common root of the reduced pair in b. The point $z = 0$ is excluded by $\overline{D}(0) = 3$ and $\overline{N}(0) = 4$. For the reference pair the corresponding remainder degrees are $(1, 0)$, $(4, 3, 2, 1, 0)$, and $(1, 0)$. This gives a short certificate even though the uncompressed finite polynomial has degree twenty-four.

The leading coefficients of the full polynomials retain their degrees, so a common factor in characteristic zero would give a common factor after reduction. Finally, the degrees $4, 16, 24$ equal the homogeneous degrees of h, D, Δ. Their leading coefficients are nonzero, so there are no omitted zeros at $V = 0$. The finite model has twenty-four simple zeros of Δ with $f \neq 0$; the corresponding fibers are I_1.

For the limiting cover, Riemann–Hurwitz uses four simple branch points, each with one preimage of local degree two:

$$2g(X) - 2 = 2(2g(\mathbb{P}^1) - 2) + 4 = 0. \tag{XIV.9.31}$$

Each of the sixteen D-points has two distinct lifts. In Figure XIV.9.1 the ramification identification and the two ordinary lifts are counted separately. Thus the degree of the left-hand side of (XIV.9.21) is $32 - 8 \cdot 4 = 0$, or $16 - 4 \cdot 4 = 0$ in quotient units. The finite count of twenty-four nodal fibers and the limiting charge calculation refer to different geometric objects.

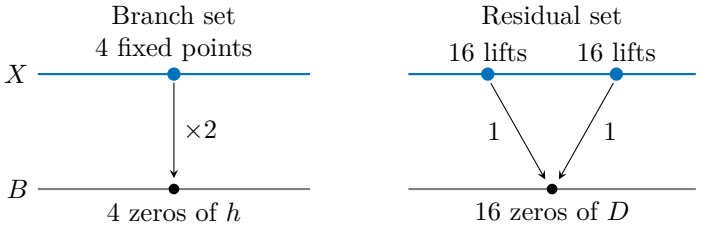


Figure XIV.9.1: Projection of the two sets of points in the compact Sen limit. Each of four branch points contributes one fixed point with projection multiplicity two. Each of sixteen residual points has two distinct lifts exchanged by ι. The lines indicate local maps of the two sheets, not globally disjoint sections of X.

A separate change of input tests the shape of the residual divisor. If $\chi = \psi^2$ with ψ a section of L^3, the equation on the cover becomes

$$\eta^2 - \xi^2 \chi = (\eta - \xi\psi)(\eta + \xi\psi). \tag{XIV.9.32}$$

The two factors, in $4\pi^* L$ each, are exchanged by the involution. There is no global square root of χ assumed in the general construction. To see the local distinction,

suppose η, ξ, χ are independent coordinates and write $F = \eta^2 - \xi^2\chi$. The derivative ideal and its radical are

$$(F, F_\eta, F_\xi, F_\chi) = (\eta, \xi\chi, \xi^2), \qquad \sqrt{(F, F_\eta, F_\xi, F_\chi)} = (\eta, \xi). \tag{XIV.9.33}$$

Away from $\chi = 0$ the two local branches can be separated by choosing a square root of χ. At $\chi = 0$ on the singular line that local separation fails, giving the Whitney pinch. The compact curve example has disjoint h- and D-points, so it does not realize this independent-coordinate singularity. Conversely, the global charge class does not require the local singularity type to be the same in every base dimension. To understand what is lost at the branch locus even when the cover is smooth, we now return to the unquotiented elliptic periods.

XIV.9.4 Where the approximation fails

How can a contour lie in a weakly coupled exterior and still enclose a region with order-one coupling? Consider a simple zero of h at which $\eta \neq 0$. At that fixed point (XIV.9.6) starts one order later in ϵ than it does at a generic exterior point. Substituting $h = 0$ gives

$$f = \epsilon\eta, \qquad \Delta = 4\epsilon^3\eta^3 + \frac{3}{16}\epsilon^4\chi^2, \qquad j = \frac{1728}{1 + 3\epsilon\chi^2/(64\eta^3)}. \tag{XIV.9.34}$$

Thus the fiber approaches the finite modular value $j(i)$, not the cusp. This does not contradict exterior uniformity: its proof divided by h^2.

The width of the region where the exterior estimate fails can be obtained by balancing the terms in Δ. Take a local family with constant $\eta \neq 0, \chi$, put $\epsilon = r^2$ and set $h = r\kappa$ with fixed scaled coordinate κ. Then $f = r^2(\eta - 3\kappa^2)$, and

$$r^{-6}\Delta = \eta^2(4\eta - 9\kappa^2) + r\chi\left(9\kappa^3 - \frac{9}{2}\kappa\eta\right) + r^2\frac{3}{16}\chi^2. \tag{XIV.9.35}$$

The leading j in this layer, away from the two scaled poles, is

$$j_{\text{layer}} = \frac{6912(\eta - 3\kappa^2)^3}{\eta^2(4\eta - 9\kappa^2)}. \tag{XIV.9.36}$$

It is finite for fixed generic κ, even as the region shrinks in the h-coordinate. In the reference layer $\eta = 1, \chi = 0$, the center $\kappa = 0$ gives 1728, while $\kappa = 1/\sqrt{3}$ gives 0 because f vanishes but the scaled discriminant does not. Both are finite modular values inside the layer. At large $|\kappa|$, away from the poles, the same rational function has the expansion

$$j_{\text{layer}} = \frac{20736}{\eta^2}\kappa^4\big(1 + O(\kappa^{-2})\big). \tag{XIV.9.37}$$

This reproduces the scaling $h^4/\epsilon^2 = \kappa^4$ of the exterior formula as its leading residual factor tends to $D = \eta^2$ near the branch. The large-κ check compares the two leading expressions; it does not make the compact-exterior estimate uniform in the layer.

The poles at $\kappa_0 = \pm 2\sqrt{\eta}/3$ are simple. The derivative of the first term in (XIV.9.35) at either pole is $-18\eta^2\kappa_0$, and the coefficient of r there is $-\chi\kappa_0\eta/2$. Therefore solving for the two nearby zeros gives

$$h_\pm = \pm\frac{2}{3}\sqrt{\epsilon\eta} - \frac{\chi}{36\eta}\epsilon + O(\epsilon^{3/2}). \tag{XIV.9.38}$$

The $\chi = 0$ locations are exact, by (XIV.9.9). The common shift in (XIV.9.38) uses constant η, χ; varying them along the base can affect the subleading expansion. If instead $\eta = \gamma h^2,\ \chi = 0$, for constant γ, substitution gives

$$f = (\epsilon\gamma - 3)h^2, \qquad \Delta = \epsilon^2\gamma^2(4\epsilon\gamma - 9)h^6, \qquad j = 1728\,\frac{4(\epsilon\gamma - 3)^3}{\epsilon^2\gamma^2(4\epsilon\gamma - 9)} \tag{XIV.9.39}$$

on the smooth fibers. For generic parameter values this has a sixth-order discriminant zero at a simple zero of h, with constant j elsewhere. There is no pair of distinct nearby roots in this changed family. The isolated-pair calculation requires the nonzero constant term of η at the branch.

We next follow the two periods for the exact pair at $\chi = 0,\ \eta = 1,\ \epsilon = 1/100$. We take h as the base coordinate and a counterclockwise exterior circle of radius $1/5$, based at the positive real point. The two discriminant points of the local model are at $\pm 1/15$ and lie inside the circle. We want a lift of monodromy that acts on actual periods, not only on their ratio. The marking starts with an integral over the real short cut of the cubic at the base point.

The factorization in x and the three roots are

$$x^3 + fx + g = (x + h)(x^2 - hx - 2h^2 + \epsilon\eta), \tag{XIV.9.40}$$

$$e_0 = -h, \qquad e_1 = \frac{h + d}{2}, \qquad e_2 = \frac{h - d}{2}, \qquad d^2 = 9h^2 - 4\epsilon\eta. \tag{XIV.9.41}$$

Use the branch $d/(3h)$ near $+1$ in the exterior. Set $\ell_{\mathrm{per}} = e_1 - e_0 = (3h + d)/2$ and $\lambda = (e_2 - e_0)/\ell_{\mathrm{per}}$. Since the two root differences multiply to $\epsilon\eta$, the change $x = -h + \ell_{\mathrm{per}} z$ gives

$$\lambda = \frac{3h - d}{3h + d} = \frac{\epsilon\eta}{\ell_{\mathrm{per}}^2}, \qquad y^2 = \ell_{\mathrm{per}}^3 z(z - 1)(z - \lambda),$$
$$\frac{dx}{2y} = \frac{dz}{2\sqrt{\ell_{\mathrm{per}}}\sqrt{z(z - 1)(z - \lambda)}}. \tag{XIV.9.42}$$

The affine coordinate change separates the moving cross ratio from the moving differential scale. A shift $z = Z + (1 + \lambda)/3$ removes the quadratic term from the Legendre cubic, giving $f_{\mathrm{Leg}} = -(1 - \lambda + \lambda^2)/3$. The product of squared root differences is $\lambda^2(1 - \lambda)^2 = -\Delta_{\mathrm{Leg}}$, so its modular invariant is

$$j(\lambda) = \frac{256(1 - \lambda + \lambda^2)^3}{\lambda^2(1 - \lambda)^2}. \tag{XIV.9.43}$$

The scale ℓ_{per} cancels out of j, but it remains in the periods in (XIV.9.42).

At the real base point $0 < \lambda < 1$. The cycle around the cut $[0, \lambda]$ traverses it on two opposite sheets, canceling the factor of two in the denominator of the differential. On that interval $z(z-1)(z-\lambda) = z(1-z)(\lambda - z)$. Substituting $z = \lambda \sin^2\theta$ into the resulting integral yields

$$A = \frac{1}{\sqrt{\ell_{\mathrm{per}}}} \int_0^{\lambda} \frac{dz}{\sqrt{z(1-z)(\lambda-z)}} = \frac{2K(\lambda)}{\sqrt{\ell_{\mathrm{per}}}},$$
$$K(m) = \int_0^{\pi/2} \frac{d\theta}{\sqrt{1 - m\sin^2\theta}}. \tag{XIV.9.44}$$

The next cut, $[\lambda, 1]$, gives an imaginary period. Substituting $z = 1 - (1-\lambda)\sin^2\theta$ cancels the factors from $1 - z$ and $z - \lambda$ against dz; with the orientation giving positive $\mathrm{Im}(B/A)$ the result is

$$B = \frac{2iK(1-\lambda)}{\sqrt{\ell_{\mathrm{per}}}}. \tag{XIV.9.45}$$

This fixes both the relative marking and the initial branch of the square root.

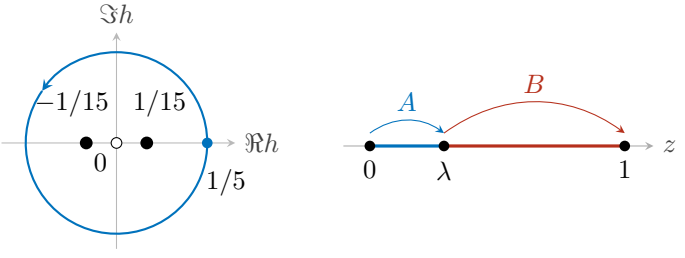


Figure XIV.9.2: The actual local pair for $\epsilon = 1/100, \eta = 1, \chi = 0$, and the marking at the positive real base point. Left: the branch center $h = 0$ and the two discriminant points lie inside the h-contour. Right: the adjacent cuts in the Legendre coordinate give the initial A and B periods. The second panel magnifies the short cut relative to the long one for legibility.

To continue these integrals, first track the scale and the cross ratio along the same path. On the radius-1/5 circle, $|4\epsilon\eta/(9h^2)| = 1/9$. The branch $\sqrt{1 - 4\epsilon\eta/(9h^2)}$ stays in the right half plane. Since

$$\frac{\ell_{\mathrm{per}}}{h} = \frac{3}{2}\left(1 + \sqrt{1 - \frac{4\epsilon\eta}{9h^2}}\right), \qquad \mathrm{wind}(\ell_{\mathrm{per}}) = 1, \qquad \mathrm{wind}(\lambda) = -2, \tag{XIV.9.46}$$

the scale winds once and the cross ratio winds twice in the negative direction. The lower bound $|\ell_{\mathrm{per}}/h| > 3/2$ gives $|\lambda| < 1/9$ on the whole circle. The only Legendre singularity enclosed by this λ-path in the unit disk is 0.

The two functions $K(\lambda)$, $K(1-\lambda)$ satisfy the same period equation,

$$\lambda(1-\lambda)P'' + (1-2\lambda)P' - \frac{1}{4}P = 0. \tag{XIV.9.47}$$

For example, expanding the first integral by the binomial series gives $P = K(\lambda) = (\pi/2)\sum_{n\ge 0} c_n\lambda^n$, where $c_0 = 1$ and $(n+1)^2 c_{n+1} = (n+\frac{1}{2})^2 c_n$. This is the recurrence from (XIV.9.47); the equation is invariant under $\lambda \mapsto 1-\lambda$. The indicial equation at 0 has a repeated root zero, so the logarithmic part of the second solution is a constant times $K(\lambda)\log\lambda$. In the complementary integral, the endpoint near $\theta = \pi/2$ gives the divergence $-\frac{1}{2}\log\lambda$: the singular part of the integral has the form $\int_0^\delta ds/\sqrt{s^2+\lambda}$ for fixed small δ. With $K(0) = \pi/2$, the logarithmic term is therefore

$$K(1-\lambda) = -\frac{K(\lambda)}{\pi}\log\lambda + \text{a function holomorphic near 0.} \tag{XIV.9.48}$$

A second route separates the logarithm from its normalization. Write $P = K(\lambda)W(\lambda)$ in (XIV.9.47). Dividing by $\lambda(1-\lambda)$ gives the coefficient of P' as $1/\lambda - 1/(1-\lambda)$. The first-order equation for W' then integrates to

$$W' = \frac{C}{\lambda(1-\lambda)K(\lambda)^2}. \tag{XIV.9.49}$$

Thus only the residue at zero changes W around the path. For $P = K(1-\lambda)$ the coefficient of $\log\lambda$ in W is $-1/\pi$ by the real-cut normalization, so $C = -\pi/4$. This calculation separates what the equation determines (the period multiplying the logarithm and the path dependence) from what the initial real integrals determine (the overall coefficient).

Each positive turn in λ adds $-2iK(\lambda)$ to $K(1-\lambda)$. Thus the two negative turns add $4iK(\lambda)$, sending B to $B - 4A$ if we temporarily hold the scale fixed. In the same continuation, $\sqrt{\ell_{\mathrm{per}}}$ changes sign. Combining both effects gives

$$\begin{pmatrix} A' \\ B' \end{pmatrix} = \begin{pmatrix} -1 & 0 \\ 4 & -1 \end{pmatrix}\begin{pmatrix} A \\ B \end{pmatrix}, \qquad \tau' = \tau - 4. \tag{XIV.9.50}$$

A continued ratio sees the shear. Equivalently, the inverse cusp coordinate $1/j(\lambda)$ winds -4 because its zero at $\lambda = 0$ has order two. The endpoint value of j is unchanged and by itself sees no shear. Neither the continued ratio nor the inverse-cusp winding sees the central sign: multiplying both periods by -1 leaves both quantities invariant.

The same marking can be checked by numerically continuing the two independent solutions of (XIV.9.47). For $h(\theta) = Re^{i\theta}$, the first-order continuation uses $dP/d\theta = P'\,d\lambda/d\theta$ and $dP'/d\theta = P''\,d\lambda/d\theta$ with P'' from the differential equation. To transport the scale separately, differentiation of ℓ_{per} gives $d\log\ell_{\mathrm{per}}/d\theta = 3ih/d$. Integrate on the moving λ-path with the real cut values and slopes as initial conditions, then multiply by the continued $1/\sqrt{\ell_{\mathrm{per}}}$. Representative periods rounded after the continuation are

path	A	B	A'	B'
$R = 1/5,\ \mathrm{CCW}$	4.14584	$8.29167i$	-4.14584	$16.58335 - 8.29167i$
$R = 1/4,\ \mathrm{CW}$	3.67794	$7.91008i$	-3.67794	$-14.71178 - 7.91008i$

(XIV.9.51)

For the first path, doubling the fourth-order integration steps from 256 to 512 to 1024 reduces the relative endpoint discrepancy with (XIV.9.50) from 6.4×10^{-7} to 4.0×10^{-8}

to 2.5×10^{-9}. Reversing direction and changing radius changes the starting periods and reverses the shear. The square root still changes sign because the new winding of the scale is -1. At either radius omitting the scale sign would give a different endpoint even though the continued B/A agreed.

Finally, compare the lift with the ordered charge calculation. In the charge column convention $K_v = I + vv^{\mathsf{T}}J$ with $J = \left(\begin{smallmatrix} 0 & -1 \\ 1 & 0 \end{smallmatrix}\right)$, the two charge names $B = [1, -1]$, $C = [1, 1]$ give

$$K_B = \begin{pmatrix} 0 & -1 \\ 1 & 2 \end{pmatrix}, \qquad K_C = \begin{pmatrix} 2 & -1 \\ 1 & 0 \end{pmatrix}, \qquad K_C K_B = \begin{pmatrix} -1 & -4 \\ 0 & -1 \end{pmatrix}. \tag{XIV.9.52}$$

These labels specify the chosen charge word, not a unique identification of each root of (XIV.9.38) with an individual brane in a global cut system. The inverse transpose acts on the period column because a charge and its period are paired. It is precisely the matrix in (XIV.9.50). In the chart of fractional transformations of τ, the lift is $-T^{-4}$ with $T : \tau \mapsto \tau + 1$. A single loop on the cover near $h = \xi^2$ projects to two base loops. Hence the lift for the cover loop is $(-T^{-4})^2 = T^{-8}$. The doubled exponent is consistent with the change from quotient to cover units in the divisor comparison. The exterior of the split pair can thus reproduce the orientifold monodromy while the resolved local elliptic periods retain information invisible in a perturbative coupling estimate.

XIV.9.5 Elliptic K3 and the heterotic torus

Can the geometry select one elliptic curve as the torus of a different string description? In the Sen calculation we kept the base and asked where the IIB coupling becomes weak. The heterotic comparison uses a different degeneration of an elliptic K3: the base itself splits into two rational curves. The elliptic fiber over the junction of those curves is the one we will compare with the heterotic torus. We start with the eight-dimensional setting, in which that torus is a single elliptic curve, before letting it vary in a fibration.

An elliptic K3 with section has a fiber class F_K and a section class S_K. The fiber can move off itself, the section meets a fiber once, and adjunction on the rational section gives $S_K^2 = -2$. Thus

$$F_K^2 = (S_K + F_K)^2 = 0, \qquad F_K \cdot (S_K + F_K) = 1. \tag{XIV.9.53}$$

These classes span a hyperbolic plane U. In the K3 lattice of signature $(3, 19)$, $U^\perp$ has signature $(2, 18)$. The holomorphic two-form defines an isotropic line in the projectivization of $U^\perp \otimes \mathbb{C}$; its positive norm with its conjugate selects the open period domain. The projective dimension 19 is reduced by one for the quadric:

$$\dim_{\mathbb{C}} \mathcal{D}_{U^\perp} = 19 - 1 = 18. \tag{XIV.9.54}$$

In the heterotic compactification on T^2 the complex structure τ_H, the complexified area ρ_H, and the sixteen complex Wilson-line parameters provide the same count. This checks a dimension required by the physical identification. It does not determine how the parameters map.

The generic eight-dimensional vector count is a different calculation. In the heterotic description sixteen vectors come from the Cartan of $E_8 \times E_8$; the metric and two-form give two each by reduction on the two torus cycles:

$$16 + 2 + 2 = 20 = 18 \text{ vector-multiplet vectors} + 2 \text{ graviphotons}. \tag{XIV.9.55}$$

This is the generic compact spectrum in the stated dictionary. The count of sections, or Mordell–Weil rank, is not the count of these fields. In particular, the vector count cannot be inferred by applying a rule for abelian vectors of a fourfold to an eight-dimensional K3 model. At zero Wilson lines the nonabelian $E_8 \times E_8$ geometry is visible in two type-II^* ends. The K3 with twenty-four I_1 fibers in Chapter 1 is a reference for the generic setting; here we will construct a different family with both ends already tuned.

To make the degeneration proper, take homogeneous coordinates $[U_0 : U_1]$ and $[V_0 : V_1]$ on two projective lines. The family of base curves is

$$\mathcal{B}_\mu : \quad U_1 V_1 = \mu U_0 V_0, \qquad \mathcal{L} = \mathcal{O}(1,1)|_{\mathcal{B}_\mu}. \tag{XIV.9.56}$$

For $\mu \neq 0$, projection to either line identifies $\mathcal{B}_\mu$ with a projective line: for example, $[V_0 : V_1] = [U_1 : \mu U_0]$. The two factors of $\mathcal{O}(1,1)$ each contribute degree one on this graph, so $\deg \mathcal{L} = 2$. At $\mu = 0$ the graph splits into $U_1 = 0$ and $V_1 = 0$, each with $\deg \mathcal{L} = 1$. They meet at $U_1 = V_1 = 0$. Defining $S_0 = U_0 V_0$, choose the coefficients

$$\mathcal{F} = a S_0^4, \tag{XIV.9.57}$$

$$\mathcal{G} = S_0^5 (U_1 V_0 + U_0 V_1 + c S_0). \tag{XIV.9.58}$$

The bidegrees $(4,4)$ and $(6,6)$ ensure that these are sections of $\mathcal{L}^4, \mathcal{L}^6$ throughout the family. The usual relative projective Weierstrass equation with these coefficients gives a proper model, including its section at infinity. There is no need to infer the ends of the family from a punctured affine chart.

On the chart $U_0 V_0 \neq 0$, use $u = U_1/U_0$ and $v = V_1/V_0$ and divide the coefficients by the appropriate powers of S_0:

$$uv = \mu, \qquad Y^2 = X^3 + aX + c + u + v. \tag{XIV.9.59}$$

The equation $uv = \mu$ smooths the intersection of the two base components. At $\mu = 0$ the elliptic surfaces on those components share the curve $E : Y^2 = X^3 + aX + c$. If E is smooth, the elliptic projection is smooth near it in these charts. In local analytic coordinates the two central surfaces meet along E with the two transverse directions u, v in the model $uv = \mu$. This explains what is being smoothed and what is common to both components.

We check the fibers at the ends before interpreting the middle. For $\mu \neq 0$ set $u = \mu t$, $v = t^{-1}$ and take $x = t^2 X$, $y = t^3 Y$. The change uses the degree-two line on the graph and gives the regular $t = 0$ equation with

$$f(t) = a t^4, \qquad g(t) = t^5 + c t^6 + \mu t^7, \tag{XIV.9.60}$$

$$\Delta(t) = t^{10} \left[4a^3 t^2 + 27(1 + ct + \mu t^2)^2 \right]. \tag{XIV.9.61}$$

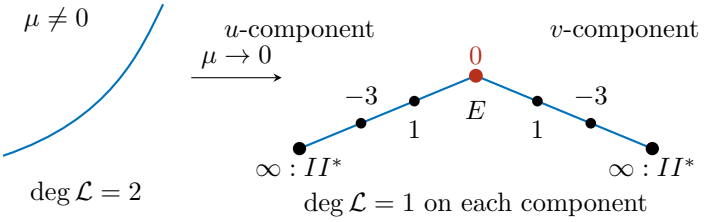


Figure XIV.9.3: The base of the proper plumbing family and its central fiber. On each central component the marked affine coordinates are u or v. For $(a, c) = (-3, 1)$ each end at infinity is II^*, and each arm has I_1 fibers at -3 and 1. Both central surfaces have the same smooth elliptic fiber at the base junction. The central diagram records incidence and labels; it is not a real coordinate axis.

The leading term in g is t^5 and that in Δ is $27t^{10}$. At the other end use $s = 1/t$, $\widehat{x} = s^4 x$, $\widehat{y} = s^6 y$, as required for a degree-two Weierstrass line. The regular coefficients there are

$$\widehat{f}(s) = as^4, \qquad \widehat{g}(s) = \mu s^5 + cs^6 + s^7, \tag{XIV.9.62}$$

$$\widehat{\Delta}(s) = s^{10}\left[4a^3 s^2 + 27(\mu + cs + s^2)^2\right]. \tag{XIV.9.63}$$

Thus for $a \neq 0, \mu \neq 0$, the orders $(4, 5, 10)$ hold at both ends. In characteristic zero they give II^* in the minimal elliptic-surface description. The reciprocal chart is essential: at $\mu = 0$, merely replacing μ by zero in the degree-two t-model does not give the two degree-one components.

For the finite member $a = -3,\ c = 1,\ \mu = 1$ we can test the four remaining fibers exactly. The polynomial in brackets in (XIV.9.61) reduces to

$$27(t^4 + 2t^3 - t^2 + 2t + 1) = 27t^2\big((t + t^{-1}) - 1\big)\big((t + t^{-1}) + 3\big). \tag{XIV.9.64}$$

Neither 1 nor -3 is a critical value ± 2 of $t + t^{-1}$. Hence each has two distinct preimages in $\mathbb{C}^\times$, and the two pairs are disjoint. At all four points $f \neq 0$, so the fibers are I_1. They account for the remaining four units in the discriminant degree $24 = 10 + 10 + 4$. The minimal resolution is the degree-two elliptic K3 in this example.

On the central component with coordinate u, the affine coefficients are a and $c + u$, and the second component has $c + v$ in place of $c + u$. For the first infinity chart put $\bar{u} = 1/u$ and $(\bar{X}, \bar{Y}) = (\bar{u}^2 X, \bar{u}^3 Y)$. For the second put $\bar{v} = 1/v$ and use $(\bar{v}^2 X, \bar{v}^3 Y)$. This time the degree is one, so the coefficient pairs are

$$(a\bar{u}^4,\ \bar{u}^5 + c\bar{u}^6), \qquad (a\bar{v}^4,\ \bar{v}^5 + c\bar{v}^6). \tag{XIV.9.65}$$

The leading discriminant term is $27\bar{u}^{10}$ or $27\bar{v}^{10}$, so the two ends retain the II^* fibers. For $a = -3, c = 1$, the remaining discriminants in the two affine charts are

$$4a^3 + 27(c+u)^2 = 27(u-1)(u+3), \qquad 4a^3 + 27(c+v)^2 = 27(v-1)(v+3). \tag{XIV.9.66}$$

They give the two I_1 fibers on each arm of Figure XIV.9.3. For the smooth common curve,

$$\Delta_E = 4a^3 + 27c^2 = -81, \qquad j(E) = 1728\frac{-108}{-81} = 2304. \tag{XIV.9.67}$$

The degree-one minimal resolutions are rational elliptic surfaces. Their individual elliptic Euler counts are $10 + 1 + 1 = 12$; subtracting $e(E) = 0$ when gluing gives $12 + 12 = 24$, consistent with the finite K3. The proper smoothing was obtained from (XIV.9.56) and (XIV.9.58); Euler arithmetic alone could not construct it. We have not supplied a global simultaneous resolution of the relative Weierstrass space.

The plumbing coordinates also allow us to track the four residual fibers as the base splits. In the neck the discriminant is $4a^3 + 27(c + u + v)^2$. In the smooth sample $a = -3, c = 1$, the two conditions on a residual point are $u + v = d_*$, with $d_* = 1$ or -3, and $uv = \mu$. For each value of d_* they give the unordered solutions of

$$u^2 - d_*u + \mu = 0, \qquad v = d_* - u. \tag{XIV.9.68}$$

Since $d_* \neq 0$, one point tends to $(d_*, 0)$ and the other to $(0, d_*)$. In particular, taking μ to zero while holding the finite-chart coordinate t fixed would miss some points: at fixed nonzero u the coordinate $t = u/\mu$ diverges. The two axes in the proper family retain the points that would otherwise run out of a single affine chart. For $d_* = 1$, the point tending to $(1, 0)$ has $u = 1 - \mu + O(\mu^2)$, $v = \mu + O(\mu^2)$; exchanging the two coordinates gives the other point. This is the finite-parameter origin of the two labels 1 in Figure XIV.9.3.

Changing c to 2 moves a discriminant root on each central component onto the common point. In the u-chart the residual polynomial is $27u(u + 4)$, and on the other component it is $27v(v + 4)$. The common cubic is $X^3 - 3X + 2 = (X - 1)^2(X + 2)$: the double curve is nodal, so the argument for gluing along a smooth elliptic curve no longer applies. A nodal fiber need not make the total Weierstrass space singular. For example on the u-component the derivative of $Y^2 - X^3 - aX - c - u$ with respect to u is -1 at the fiber node. In the family chart (XIV.9.59) one can eliminate μ and use the same derivative at the common node. The central union changes its local intersection geometry even though these total spaces can be smooth.

We now compare the elliptic modulus of the smooth junction to a heterotic modulus. The modular relation for the zero-Wilson-line $E_8 \times E_8$ locus uses a Weierstrass model with normalized end coefficients. For $\mu \neq 0$ set $t = s_*/\sqrt{\mu}$, $x = \mu^{-5/6}x_*$, $y = \mu^{-5/4}y_*$, with compatible branches on a simply connected parameter chart. Substitution in (XIV.9.61) yields

$$y_*^2 = x_*^3 + \alpha s_*^4 x_* + s_*^5 + \beta s_*^6 + s_*^7, \qquad \alpha = a\mu^{-1/3}, \quad \beta = c\mu^{-1/2}. \tag{XIV.9.69}$$

The two ends now have the same unit coefficient; α^3 and β^2 are independent of the branch choices. In the heterotic comparison put $J_\tau = j(\tau_H)/1728$, $J_\rho = j(\rho_H)/1728$,

with $\tau_H = iU,\ \rho_H = iT_{\mathrm{CLM}}$ in the convention of the modular relation. It gives

$$P = J_\tau J_\rho = -\frac{\alpha^3}{27} = -\frac{a^3}{27\mu}, \tag{XIV.9.70}$$

$$(J_\tau - 1)(J_\rho - 1) = \frac{\beta^2}{4} = \frac{c^2}{4\mu}, \tag{XIV.9.71}$$

$$S = J_\tau + J_\rho = 1 + P - \frac{c^2}{4\mu}. \tag{XIV.9.72}$$

The product and sum determine unordered roots of $J^2 - SJ + P = 0$. For the smooth sample with $a = -3, c = 1$, we have $P = 1/\mu$ and $S = 1 + 3/(4\mu)$. In general with $4a^3 + 27c^2 \neq 0$, the leading coefficient of S in μ^{-1} is nonzero, and $P/S^2 = O(\mu)$. Expanding the quadratic roots on the branch $\sqrt{1 - 4P/S^2} \to 1$ gives

$$J_{\mathrm{large}} = S + O(1), \qquad J_{\mathrm{finite}} = \frac{P}{S} + O(\mu) \ \longrightarrow\ \frac{4a^3}{4a^3 + 27c^2} = \frac{j(E)}{1728}. \tag{XIV.9.73}$$

In the sample the finite value is $4/3$. In the changed $c = 2$ sample, $S = 1$, so the expansion in P/S^2 no longer applies. The modular calculation therefore has the same smooth-common-curve condition as the geometric one.

The interpretation of the large root as the large-$\mathrm{Im}\,\rho_H$ cusp and the finite root as the complex structure of the heterotic torus uses the eight-dimensional duality and its choice of cusp. In particular, the heterotic complexified area and its cusp are different from the local IIB coupling measured in (XIV.9.14). Here μ is a complex-structure smoothing parameter of the K3 family. Its smallness does not say that the IIB coupling is uniformly weak. The finite modular root identifies which part of the degeneration can be used as the heterotic elliptic curve. The next calculation asks what information is carried by the two surfaces on its sides.

XIV.9.6 Stable degeneration and bundle data

What can be read from the two sides of the degeneration when the common elliptic curve varies over another base? The geometric starting point is the family of elliptic curves E at the junction of the two rational elliptic surfaces. Denote its base by B_H, so the common elliptic manifold is $\pi_H : Z \to B_H$. In the stable-degeneration dictionary the two rational elliptic surfaces encode the restrictions of the two heterotic E_8 bundles to that common elliptic curve. Applying this eight-dimensional comparison fiberwise is an additional adiabatic premise, appropriate to the large-base comparison. The section-class calculations below are geometric. They can be made without assuming that arbitrary coefficient choices solve the heterotic bundle or F-theory vacuum conditions.

On the F-theory side the K3 base varies over B_H. Choose the ruled base

$$B'_F = \mathbb{P}(\mathcal{O} \oplus \mathcal{T}) \longrightarrow B_H, \qquad t_H = c_1(\mathcal{T}), \qquad c_1 = c_1(B_H). \tag{XIV.9.74}$$

Write z, w for the homogeneous coordinates on its fibers, with divisors r and $r + t_H$ at $z = 0, w = 0$, respectively. We suppress pullbacks of base classes. The disjoint sections

give $r(r+t_H)=0$. The relative anticanonical class is the sum of the two coordinate divisors, so

$$c_1(B'_F) = c_1 + 2r + t_H. \tag{XIV.9.75}$$

This fixes the labels of the two ends; the minus end below is $z=0$. Interchanging z and w without changing the twist convention would interchange the two labels.

Expand g into homogeneous monomials $g_k z^k w^{12-k}$. The monomial alone has class $12r+(12-k)t_H$. Since g has class $6c_1(B'_F)$, subtracting the monomial class leaves $6c_1+(k-6)t_H$ for the coefficient. For f, the total class is $4c_1(B'_F)$ and the monomial $z^k w^{8-k}$ has class $8r+(8-k)t_H$. Thus

$$[f_k] = 4c_1 + (k-4)t_H, \tag{XIV.9.76}$$

$$[g_k] = 6c_1 + (k-6)t_H. \tag{XIV.9.77}$$

In particular the middle coefficients f_4, g_6 have the powers $4, 6$ of the anticanonical line $L_H = K_{B_H}^{-1}$; they supply the Weierstrass data of Z. The neighboring g coefficients have classes

$$[g_5] = \eta_- = 6c_1 - t_H, \qquad [g_7] = \eta_+ = 6c_1 + t_H. \tag{XIV.9.78}$$

To see the meaning of these neighbors, retain only f_4, g_5, g_6, g_7. In the chart $w=1$ the transverse powers are z^4 in f and z^5, z^6, z^7 in g. In the chart $z=1$ the same g-terms occur at powers w^7, w^6, w^5, so g_7 is the leading end coefficient there. At either generic end the orders are $(4,5,10)$ if the leading coefficients are nonzero. At a zero of the leading g coefficient, a fixed transverse slice instead has at least $(4,6,12)$. The zero-size instanton specialization uses those special points; it is not the general smooth-bundle description.

For $B_H = \mathbb{P}^1$ take t_H of degree n, so B'_F is F_n. A section of a line on $\mathbb{P}^1$ counts zeros with multiplicity by its degree. With $\deg c_1 = 2$, the two numbers associated with the ends are

$$(\deg g_5, \deg g_7) = (12-n, 12+n) = \begin{cases} (10,14), & n=2, \\ (8,16), & n=4. \end{cases} \tag{XIV.9.79}$$

Under the heterotic dictionary these are the instanton numbers k_-, k_+ in the no-separate-fivebrane balance for smooth heterotic K3. Indeed the sum 24 is required by $\int_{K3} c_2(TK3) = 24$. The degree derivation establishes the splitting of 24 between the labeled ends, while the heterotic identification supplies the physical meaning of these degrees. Changing n redistributes charge even though the sum does not change.

We can probe a different bundle restriction by allowing f_3, f_5 in addition to f_4. Call $a_{2,-} = f_3,\ a_{0,-} = g_5$ and $a_{2,+} = f_5,\ a_{0,+} = g_7$. Their respective classes at an end are $\eta_\pm - 2c_1$ and $\eta_\pm$. Near the minus end on $w=1$, writing $\zeta = z$ for the local transverse coordinate, the leading terms are

$$f = \zeta^3 a_{2,-} + \zeta^4 f_4 + O(\zeta^5), \tag{XIV.9.80}$$

$$g = \zeta^5 a_{0,-} + \zeta^6 g_6 + O(\zeta^7), \tag{XIV.9.81}$$

$$\Delta = 4\zeta^9 a_{2,-}^3 + \zeta^{10}(12 a_{2,-}^2 f_4 + 27 a_{0,-}^2) + O(\zeta^{11}). \tag{XIV.9.82}$$

In the other chart the corresponding calculation uses $\zeta = w$ and the plus coefficients. If $a_{2,\pm}a_{0,\pm} \neq 0$, the orders are $(3, 5, 9)$, the III^* geometry associated with an E_7 end in the ordinary dictionary. If $a_{2,-} = 0$ and $a_{0,-}f_4 \neq 0$, hold the coordinate of B_H fixed at that point and vary ζ. On this transverse slice the order-nine term disappears, f starts at order four, and the $27a_{0,-}^2$ term still survives. Thus the slice has $(4, 5, 10)$. The orders on that slice do not describe the full collision geometry in both base directions.

For a concrete F_2 example let s be the affine coordinate on B_H and take

$$(a_{2,-}, a_{0,-}) = (s^6 - 1, s^{10} - 3), \tag{XIV.9.83}$$

$$(a_{2,+}, a_{0,+}) = (s^{10} - 2, s^{14} - 5), \tag{XIV.9.84}$$

$$(f_4, g_6) = (s^8 + 1, s^{12} + 1). \tag{XIV.9.85}$$

All expressions have their full degrees after homogenizing, so none of these polynomials has a missing zero at infinity. For instance $s = 1$ is a simple zero of $a_{2,-}$; there $a_{0,-} = -2$ and $f_4 = 2$. At a fixed $s = 1$ the first terms are $2\zeta^4$ and $-2\zeta^5$, so the coefficient of ζ^{10} in Δ is 108. A nearby generic fixed value of s restores the order-nine term. There is no common zero of the two end coefficients at either end in (XIV.9.85): on the minus end their roots have moduli 1 and $3^{1/10}$, and on the plus end $2^{1/10}$ and $5^{1/14}$, which are distinct. Over F_4 the same form of construction requires degrees $4, 8$ for $a_{2,-}, a_{0,-}$ and $12, 16$ for $a_{2,+}, a_{0,+}$. The old minus-end exponents $6, 10$ exceed $4, 8$. At the plus end, homogenizing the old polynomials to degrees $12, 16$ multiplies both by the square of the coordinate that vanishes at infinity, giving a double zero there in each. To keep full affine degree at both ends, replace the four exponents by $4, 8, 12, 16$ and keep the constants $1, 3, 2, 5$.

Why is it natural to compare the a_2-degree to a bundle quantity? Suppose a stable holomorphic rank-two bundle V with trivial determinant is supplied on smooth heterotic K3, and use fundamental $SU(2)$ normalization for $k = \int_{K3} c_2(V)$. A nonzero global section would give a subsheaf of slope at least zero, incompatible with stability; the same applies to $V^\vee$. Serre duality with $K_{K3} \simeq \mathcal{O}$ therefore gives $h^0(V) = h^2(V) = 0$. In the degree-four integrand of Riemann–Roch, the trivial determinant removes the first Chern class and the rank multiplies the degree-four Todd term:

$$\chi(V) = 2\int_{K3} \mathrm{td}_2(K3) - \int_{K3} c_2(V) = 4 - k, \qquad h^1(V) = k - 4. \tag{XIV.9.86}$$

The degree of $\eta_\pm - 2c_1$ is also $k_\pm - 4$. This gives $6, 10$ on F_2, and the same rule gives $4, 12$ on F_4. The comparison uses the minimal (index-one) $SU(2) \subset E_8$ embedding with commutant E_7. It neither constructs V from the displayed polynomials nor counts localized states point by point.

For a four-dimensional specialization take $B_H = \mathbb{P}^1 \times \mathbb{P}^1$. In the ruling basis we write a divisor as (d, e). The two basis classes have square zero and intersect once, hence

$$(d, e) \cdot (d', e') = de' + ed', \qquad c_1 = (2, 2). \tag{XIV.9.87}$$

For $t_H = (2, 0)$, the classes in (XIV.9.78) are $\eta_+ = (14, 12)$, $\eta_- = (10, 12)$. Restrict to a ruling curve Γ of class $(0, 1)$. Pairing with Γ gives degrees $14, 10$, in that order. By

contrast $t_H = (0,2)$ gives classes $(12,14),(12,10)$. The same Γ now has degrees $12,12$, although the two classes still sum to $12c_1$:

t_H	η_+	η_-	$\eta_+ \cdot \Gamma$	$\eta_- \cdot \Gamma$
$(2,0)$	$(14,12)$	$(10,12)$	14	10
$(0,2)$	$(12,14)$	$(12,10)$	12	12

(XIV.9.88)

For the other ruling $\Gamma' \sim (1,0)$, the pairing in (XIV.9.87) reverses which twist is visible: the restrictions are $12,12$ for $t_H = (2,0)$ and $14,10$ for $t_H = (0,2)$. A useful way to extract this dependence without expanding each coefficient is

$$\eta_+ \cdot \Gamma - \eta_- \cdot \Gamma = 2t_H \cdot \Gamma, \qquad \eta_+ \cdot \Gamma + \eta_- \cdot \Gamma = 12c_1 \cdot \Gamma. \tag{XIV.9.89}$$

The sum is insensitive to the twisting line. The difference measures its degree on the chosen ruling. In either case $L_H|_\Gamma$ has degree two. The elliptic surface over Γ is a K3 under the usual smooth relatively minimal elliptic-surface hypotheses. Thus the common elliptic surface can have the same Weierstrass line degree while the two end restrictions change.

In the bundle dictionary, for the appropriate bundles the normalized degree-four E_8 characteristic class $\lambda(V_\pm)$ satisfies

$$\pi_{H*}\lambda(V_\pm) = \eta_\pm, \qquad \int_\Gamma \eta_\pm = \int_{\pi_H^{-1}(\Gamma)} \lambda(V_\pm). \tag{XIV.9.90}$$

For this index-one $SU(2) \subset E_8$ embedding, λ pulls back to the fundamental c_2. In this formula the pushforward integrates along elliptic fibers. A coefficient has the line-bundle class calculated in (XIV.9.77). Identifying that class with a pushforward uses the bundle correspondence and its hypotheses. Its restriction degree on Γ then uses a second operation, pairing with the curve. Neither operation recovers the full class on Z; for example, a degree-four class pulled back from B_H integrates to zero along an elliptic fiber. The ordered numbers in (XIV.9.88) are not an entire threefold bundle characteristic class.

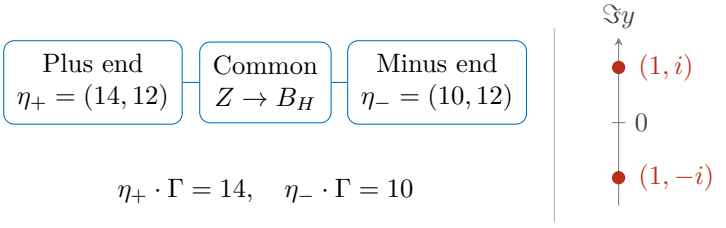


Figure XIV.9.4: The two labeled coefficient classes for $t_H = (2,0)$ and the common elliptic manifold Z. The degrees 14 and 10 refer to restriction to the ruling $\Gamma \sim (0,1)$. The inset records the two spectral points above $x = 1$ for $y^2 = x^3 - 3x + 1$, displayed along the imaginary y-axis. It records two points on one complex elliptic fiber.

The spectral equation explains why a coefficient of class $\eta - 2c_1$ enters the end geometry. On a smooth fiber of Z, a degree-zero line is represented by a point relative

to the origin. The opposite point gives the inverse line. For rank two with trivial determinant the unordered pair therefore consists of opposite points. In the short Weierstrass chart, opposite points have the same x and opposite y. They are selected by

$$a_0 + a_2 x = 0, \qquad a_0 \in H^0(B_H, \mathcal{M}), \quad a_2 \in H^0(B_H, \mathcal{M} \otimes L_H^{-2}), \qquad c_1(\mathcal{M}) = \eta. \tag{XIV.9.91}$$

The two terms have the same class because x has weight L_H^2. At a fiber with $a_2 \neq 0$ one substitutes $x = -a_0/a_2$ into the elliptic equation. On $y^2 = x^3 - 3x + 1$, the choice $(a_0, a_2) = (-1, 1)$ gives $(x, y) = (1, \pm i)$, shown in Figure XIV.9.4. Changing a_0 to zero at the same a_2 gives $(0, \pm 1)$. The two spectral points moved on the same elliptic curve. This computation concerns restrictions to that fiber and says nothing about how the two points assemble globally.

Near the origin section σ of Z, x has a pole of order two. A local parameter t_σ transverse to σ writes $x = U/t_\sigma^2$ with U a unit. Multiplying the spectral equation by t_σ^2 gives its regular equation

$$a_0 t_\sigma^2 + a_2 U = 0. \tag{XIV.9.92}$$

Intersecting with $t_\sigma = 0$ thus gives $a_2 = 0$ on the section. To interpret multiplicity at a smooth point of the divisor $a_2 = 0$ over a surface base, choose a curve through that point transverse to $a_2 = 0$, avoiding common zeros and with $a_0 \neq 0$ at the point. If s is a local coordinate on this curve, a_2 has a simple zero in s. In the elliptic surface restricted to the curve, the intersection ideal is (t_σ, s), of length one. It is an intersection multiplicity in that surface, even though the spectral equation on the one special elliptic fiber has a double root at the origin.

To compute this intersection it is necessary to use the completion of the affine x-chart. For example, near a smooth point of σ, write the projective cubic as $Y^2 Z_f = X^3 + f X Z_f^2 + g Z_f^3$. Trivialize the line on the base and choose the affine chart $Y = 1$. The section has $X = Z_f = 0$ and the equation gives $Z_f = X^3 + O(X^7)$. Consequently the affine $x = X/Z_f$ has a double pole. The corresponding regular equation of the divisor is obtained by multiplying by the square of the parameter X, as in (XIV.9.92), rather than by discarding the origin fiber point when the affine equation becomes constant.

The transverse intersection admits two different slices. At the special base point $s = 0$, the equation restricts to $a_0(0) t_\sigma^2 = 0$ on the elliptic fiber. Restricting to σ instead gives a unit times $a_2(s) = 0$. The first has multiplicity two and the second one. Locally $a_2(s) = sA(s)$ with $A(0) \neq 0$, so the derivative of the spectral equation in s is nonzero at the intersection. Over the chosen transverse base curve the spectral locus can be written $s = O(t_\sigma^2)$: two fiber points come together, while the spectral curve still intersects the origin section transversely. This description uses the nonzero a_0 hypothesis; at a common zero both coefficients vanish and the fiber equation has a different behavior.

The pole description also computes the intersection as a divisor class on the base. The spectral divisor C_{sp} has class $2\sigma + \pi_H^* \eta$. Since the normal to the zero section has class $-c_1$, the section satisfies $\sigma^2 = -\sigma \pi_H^* c_1$. Therefore

$$\pi_{H*}(C_{\mathrm{sp}} \cdot \sigma) = \eta - 2c_1. \tag{XIV.9.93}$$

This identity is geometric even when there are fibers on which the spectral equation vanishes identically. The latter are a serious obstruction if one wants to regard the divisor as a finite degree-two cover.

Indeed the two sections in (XIV.9.91) can vanish together. For the two choices of η at $t_H = (2, 0)$ the intersection numbers of their zero divisors are

$$(14, 12) \cdot (10, 8) = 14 \cdot 8 + 12 \cdot 10 = 232, \tag{XIV.9.94}$$

$$(10, 12) \cdot (6, 8) = 10 \cdot 8 + 12 \cdot 6 = 152. \tag{XIV.9.95}$$

For generic sections of these classes the intersections are proper and nonempty. Swapping the twist to $(0, 2)$ interchanges the two entries within each class and leaves the intersection numbers unchanged. At a common zero the equation imposes no condition on x, and (XIV.9.92) also vanishes along the fiber in the origin chart. The whole fiber belongs to the spectral divisor. Its generic degree two does not make its projection finite. Restricting to a smooth individual fiber with nonzero a_2, or choosing a base curve avoiding the common-zero points, gives a well-defined version of the local comparison. Even for an appropriate finite spectral cover, a spectral line bundle with a determinant constraint and a stable resulting bundle are additional data. The pushforward in (XIV.9.90) is used only where that bundle construction applies. The class calculation by itself furnishes neither a global stable bundle on Z nor a compact dual fourfold vacuum.

XIV.9.7 Comparing the already constructed sectors

Does the split I_5 gauge divisor of Chapter 2 survive a Sen deformation? The comparison can be made on the actual Tate equation rather than by looking for a D7 configuration with a similar gauge algebra. Use its local normal coordinate w to the quadric and its Tate coefficients

$$(a_1, a_2, a_3, a_4, a_6) = (b_5, wb_4, w^2 b_3, w^3 b_2, w^5 b_0). \tag{XIV.9.96}$$

Keep a_1, a_2 fixed, multiply a_3, a_4 by ϵ, and multiply a_6 by ϵ^2. With the capital B_i evaluated before scaling,

$$B_2 = a_1^2 + 4a_2 = b_5^2 + 4wb_4, \tag{XIV.9.97}$$

$$B_4 = a_1 a_3 + 2a_4 = w^2(b_5 b_3 + 2wb_2), \tag{XIV.9.98}$$

$$B_6 = a_3^2 + 4a_6 = w^4(b_3^2 + 4wb_0). \tag{XIV.9.99}$$

Completing the square in the Tate variable y puts the right-hand side in the form $x^3 + B_2 x^2/4 + \epsilon B_4 x/2 + \epsilon^2 B_6/4$. Shifting this x by $-B_2/12$ gives

$$f = -\frac{B_2^2}{48} + \frac{\epsilon B_4}{2}, \tag{XIV.9.100}$$

$$g = \frac{B_2^3}{864} - \frac{\epsilon B_2 B_4}{24} + \frac{\epsilon^2 B_6}{4}. \tag{XIV.9.101}$$

Matching terms with (XIV.9.3) fixes all three Sen sections:

$$h = -B_2/12, \qquad \eta = B_4/2, \qquad \chi = -3B_6. \tag{XIV.9.102}$$

The sign of h is required by the cubic and mixed terms of g, even though it would be invisible in the leading f.

We can now compare the residual divisor and the finite-parameter discriminant independently. The first is $D = (B_4^2 - B_2B_6)/4$. After pulling out $w^4/4$, the two terms inside the bracket have the same constant term $b_5^2b_3^2$. Their linear difference is $4w(b_5b_3b_2 - b_5^2b_0 - b_4b_3^2)$ and their quadratic difference is $4w^2(b_2^2 - 4b_4b_0)$. Thus

$$D = w^5\big[-P + w(b_2^2 - 4b_4b_0)\big], \qquad P = b_4b_3^2 - b_5b_3b_2 + b_5^2b_0. \tag{XIV.9.103}$$

The same P that enters the Tate construction has appeared in the Sen residual section. At a generic point of $w = 0$ with $b_5P \neq 0$, h is a unit, η has order at least two, and χ has order at least four. Consequently

$$\mathrm{ord}_w(4\eta^3 - \tfrac{9}{2}h\eta\chi) \geq 6, \qquad \mathrm{ord}_w(\chi^2) \geq 8. \tag{XIV.9.104}$$

The coefficient of w^5 in the full Δ is $9\epsilon^2 h|_{w=0}^2 P|_{w=0}$, nonzero for $\epsilon \neq 0$ there. Higher powers of ϵ cannot cancel it. Since $f|_{w=0} = -3h^2|_{w=0} \neq 0$, the generic fiber has multiplicative order five. Its nodal tangent slopes are $\pm b_5/2$: at $w = 0$, the cubic is $(x + h)^2(x - 2h)$ and the tangent coefficient at $x = -h$ is $-3h = b_5^2/4$. This realizes the split condition in the transverse I_5 model.

On the orientifold cover the same h restricts over the generic gauge divisor to a square,

$$\xi^2 = -b_5^2/12, \qquad \xi_\pm = \pm ib_5/\sqrt{12}. \tag{XIV.9.105}$$

The sheets are distinct there and exchanged by the involution. The multiplicity five from (XIV.9.103) lies on each sheet. This is a geometric comparison of the generic stack and its image. It does not require the full orientifold cover to be smooth. It also does not identify a D7 sheaf, a flux or the physical global form of the gauge group.

To see why the orders do not add on either sheet, trivialize L near a generic point of the gauge divisor and hold the tangent coordinates fixed. At either root in (XIV.9.105), the derivative of $\xi^2 - h(w)$ with respect to ξ is $2\xi_\pm \neq 0$. Thus the implicit function theorem expresses ξ as a holomorphic function of w in each chart. In particular w remains a normal coordinate upstairs. If $D = w^5U_D(w)$ with $U_D(0) = -P(0) \neq 0$, then its pullback to each chart is $w^5U_D(w)$ in that same coordinate. The two multiplicities five in Figure XIV.9.5 are separate. This is the unramified counterpart of (XIV.9.20), where the base branch equation instead vanishes quadratically in the covering coordinate.

The condition $b_5P \neq 0$ specifies what this calculation can see. For instance on a constant-coefficient transverse slice take $b_5 = b_3 = b_2 = b_0 = 1$ and $b_4 = 0$. Then $P = 0$, so $D = w^6$ while the two cover roots at $w = 0$ remain distinct. This result concerns D: the order-six term is of the same w-order as terms from ϵ^3 in the full discriminant, so the changed calculation of D alone cannot give a finite-parameter enhancement or a spectrum there. At $b_5 = 0$ even the distinct-sheet argument fails.

The two limits now answer different questions about four-dimensional constructions. The Sen calculation follows the same Tate coefficients, identifies a perturbative divisor

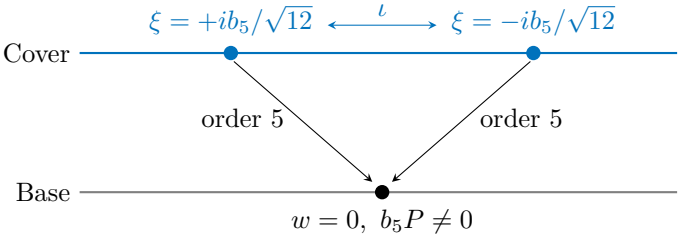


Figure XIV.9.5: The two roots over a generic point of the split Tate divisor. Each sheet is unramified there, and the pullback of the limiting residual divisor vanishes to order five on each. The horizontal arrow exchanges the two sheets under the involution.

with its multiplicity, and shows how the ordinary orientifold exterior arises around a locally nonperturbative region. The heterotic calculation identifies the modulus of a common curve and computes classes for restrictions of two bundles in a different geometric family. The common coefficient classes of the latter give neither a D7 charge computation nor a comparison of the split I_5 matter modes. To compare compact four-dimensional flux vacua one would have to identify a specific dual geometry and bundle with its extra data, and determine what becomes of the quantized G_4 class, the supersymmetry conditions, and the tadpole and zero-mode data. No such transport is implied by the equality of divisors or by the equality of restriction degrees. For an interacting theory one must also check the limit that isolates its degrees of freedom, as in the scale discussion of Chapter 2.

XIV.9.8 Exercises

1. **Change a Sen coefficient.** Replace the last term in g in (XIV.9.3) by $+\epsilon^2\chi/6$. Find the residual polynomial after normalizing the ϵ^2 term as $-9h^2D$. Give the coefficient of the mixed monomial $h\eta\chi$ at order three and of χ^2 at order four. Which cancellations are independent of this change?

2. **Count the points in a changed compact model.** Use $k = 3, \ell = 5, \epsilon = 1/100$ in (XIV.9.22). Submit the expanded or factored D, and the counts of branch points, residual base points, their lifts, and finite-parameter discriminant points. Explain the derivative gcd tests and why a degree check at infinity is necessary.

3. **Reverse the lifted path.** At $\eta = 1, \chi = 0, \epsilon = 1/100$, use the clockwise circle of radius $1/4$. Compute the winding of λ, the sign of the common differential factor, and the 2×2 matrix acting on the ordered period column $(A, B)^{\mathsf{T}}$. Which part could you recover from the inverse cusp winding alone?

4. **Change the common fiber.** Set $a = -3, c = 2$ in (XIV.9.59). Compute the common discriminant, the residual discriminant polynomial in each affine component chart, and whether the common fiber is smooth. Explain why your

answer about the fiber need not describe the smoothness of either component surface.

5. **Redistribute end data.** Replace F_2 by F_4. Compute the ordered g_5, g_7 degrees and the ordered minus, plus a_2 degrees. On $\mathbb{P}^1 \times \mathbb{P}^1$ instead use $t_H = (0, 2)$ and keep $\Gamma \sim (0, 1)$. Give the two restriction degrees in plus, minus order. Explain why the total degree alone does not determine the labeled data.

6. **Specialize the Tate residual polynomial.** Use $b_5 = b_3 = b_2 = b_0 = 1,\ b_4 = 0$ in (XIV.9.99). Compute the first nonzero term of D in w, and the unordered pair of cover roots at $w = 0$. This asks for the order of D only. Which higher-ϵ terms in Δ would need checking for a finite-parameter assertion?

7. **Compare the limits.** For each limit, specify one computed divisor or period quantity and explain where that calculation ceases to apply. What additional data would be required to compare a specified compact four-dimensional G_4 background?

Use `benchmark/tasks.json` for bounded answer fields and `benchmark/PROTOCOL.md` for submission. Written explanations require human assessment.

Status and sources

§1. The weak-coupling question. The ordinary identification of the period ratio with the local IIB axiodilaton is [GEO-E]. See Sen (1997), hep-th/9702165v1, physical pp. 2–3, eqs. (1)–(4), and Sen (1998), hep-th/9709159v1, physical pp. 6–7, eqs. (13)–(17). The identification uses the elliptic IIB dictionary of Chapter 1, in a local cusp chart.

§2. Exact Sen expansion and exterior. The expansion, exterior estimate and moving root are [MATH]. The family and normalization are translated from Sen (1997), v1 physical pp. 2–6, eqs. (1)–(24), into the Weierstrass convention $\Delta_{\text{book}} = 4f^3 + 27g^2$. The cited v1 page extracts have a corresponding discussion in v2.

§3. The orientifold cover. Cover geometry, compact counts, exchanged factors and the local derivative ideal are [MATH]. For ordinary I_1 recognition see Schütt and Shioda (2009), arXiv:0907.0298v3, §4.5, Table 1. Ordinary O7$^-$ charge and involution are [GEO-E]; see Sen (1997), v1 physical pp. 4–5, eqs. (17)–(20), especially the charge discussion on p. 5, and pp. 6–8, eqs. (24)–(32), for the later deformation and geometry. See also Sen (1998), v1 physical pp. 8–9, eqs. (24)–(29). The charge class is restricted to the ordinary D7 comparison.

§4. The core and the marked periods. The scaled limits, split pair, specialization, Legendre continuation and charge matrix are [MATH]. The source comparison is Sen (1997), v1 physical pp. 3–6, and Sen (1998), v1 physical pp. 7–9, eqs. (18)–(29). The central sign here is recovered from continued periods of the specified $\chi = 0$ cubic. The charge comparison uses the stated ordered cut frame and does not label both individual roots in a global cut frame.

§5. The K3 and its common curve. The lattice, relative model, selected fiber counts and modular-root algebra are [MATH]. See Morrison and Vafa (1996), hep-th/9603161v2, physical pp. 4–5, §2; Friedman et al. (1997), hep-th/9701162v2, physical pp. 36–38, §4.4, eqs. (4.22)–(4.23); and Schütt and Shioda (2009), v3 §§4.5, 4.10, 6.6–6.7. The common cubic in the Friedman–Morgan–Witten degeneration dictionary uses $a = -g_2/4, c = -g_3/4$ upon rescaling y_{FMW} by $1/2$. The generic vector breakdown is [GEO-E], using Douglas et al. (2014), arXiv:1403.1595v2, physical p. 8, printed p. 7, §2.1. The heterotic cusp and finite-modulus identification is [GEO-E], conditional on the zero-Wilson-line heterotic/F-theory comparison. See Cardoso et al. (1996), hep-th/9609111v1, physical p. 9, printed p. 8, eqs. (1.25)–(1.28), with the normalization shown in the text.

§6. Ruled bases and bundle restrictions. The two bundle restrictions and their fiberwise adiabatic interpretation, and the λ pushforward in the indicated bundle framework, are [GEO-E]. See Friedman et al. (1997), v2 physical pp. 36–38, 61–63, 73–77 and 83–85, §§4.4, 6, 7.2–7.3, 7.6. The ruled coefficient classes, transverse jets, conditional Riemann–Roch calculation, ruling restrictions, spectral pair and nonfinite divisor obstruction are [MATH]. See also Morrison and Vafa (1996), v2 physical pp. 7–8, eqs. (3.1)–(3.3), for the F_n specialization. The geometry does not establish the existence of a global stable bundle or a common compact flux vacuum.

§7. The split Tate comparison. The Tate-to-Sen substitution, residual and finite-parameter order checks, and generic cover sheets are [MATH]. The input is the exact split Tate family of Chapter 2; the Sen dictionary used to read its perturbative exterior has the scope stated above. The specialization at $P = 0$ computes the order of D only.

References

Cardoso, G. L. et al. (1996). "On the Duality between the Heterotic String and F-theory in Eight Dimensions". In: *Phys. Lett. B* 389, pp. 479–484. arXiv: `hep-th/9609111`.

Douglas, M. R., D. S. Park, and C. Schnell (2014). "The Cremmer–Scherk Mechanism in F-theory Compactifications on K3 Manifolds". In: *JHEP* 05, p. 135. arXiv: `1403.1595 [hep-th]`.

Friedman, R., J. Morgan, and E. Witten (1997). "Vector Bundles and F-theory". In: *Commun. Math. Phys.* 187, pp. 679–743. arXiv: `hep-th/9701162`.

Morrison, D. R. and C. Vafa (1996). "Compactifications of F-theory on Calabi–Yau Threefolds. I". In: *Nucl. Phys. B* 473, pp. 74–92. arXiv: `hep-th/9603161`.

Schütt, M. and T. Shioda (2009). *Elliptic Surfaces*. arXiv: `0907.0298 [math.AG]`.

Sen, A. (1997). "Orientifold Limit of F-theory Vacua". In: *Phys. Rev. D* 55, pp. 7345–7349. arXiv: `hep-th/9702165`.

Sen, A. (1998). "F-theory and Orientifolds". In: *Nucl. Phys. B Proc. Suppl.* 68, pp. 92–98. arXiv: `hep-th/9709159`.

Chapter XIV.10

Nonperturbative superpotentials and geometric instantons

XIV.10.1 Which coupling can an instanton generate?

Why can an isolated Euclidean brane generate a superpotential, while a brane in the same homology class can fail to do so? A finite action makes an exponential weight possible. The collective coordinates decide where that weight can appear. In four dimensions a superpotential is integrated over chiral superspace. A Euclidean brane can supply precisely this integral because it has a position in spacetime and breaks two of the supersymmetries of the vacuum. The broken generators yield two fermionic coordinates. An additional fermion changes the calculation: the integral is zero unless the integrand contains that coordinate.

We will follow this argument from an M5 wrapping an elliptic threefold to an E3, a Euclidean D3-brane wrapping a surface in the F-theory base. We use the circle dictionary, the resolved-fiber description of charged matter, and the bulk flux normalization developed earlier in the volume. The example will distinguish the modes of an isolated divisor from fermions localized where a spacetime D3 approaches it. A separate resolved model will show how bulk flux can make charged insertions obligatory.

Let X^{μ} be the instanton position in spacetime and θ^{1}, θ^{2} the two Goldstini in the orientation that gives a chiral term. Write S_{cl} for the classical Euclidean action and A for the remaining prefactor after the universal measure has been removed. If there are no other unsaturated modes and the integrand is gauge invariant, the candidate coupling is

$$\int d^{4}X\, d^{2}\theta\, W_{\mathrm{np}}, \qquad W_{\mathrm{np}} = A\, e^{-S_{\mathrm{cl}}}. \tag{XIV.10.1}$$

Here A can depend on the four-dimensional chiral fields. The conjugate instanton orientation yields the conjugate measure and term. If the saddle carries a gauge charge,

the same superspace integral can occur with charged fields multiplying the exponential.

To see the measure at work, introduce two extra independent Grassmann generators η_1, η_2. Choose the orientation $\int d\eta_2\, d\eta_1\, \eta_1\eta_2 = 1$ and let m be a complex mass in the convention that the exponent contains $+m\eta_1\eta_2$. In the exterior algebra,

$$(\eta_1\eta_2)^2 = 0, \qquad e^{m\eta_1\eta_2} = 1 + m\eta_1\eta_2, \tag{XIV.10.2}$$

$$\int d\eta_2\, d\eta_1\, e^{m\eta_1\eta_2} = m, \qquad \int d\eta_2\, d\eta_1\, 1 = 0. \tag{XIV.10.3}$$

The integral extracts the coefficient of the top monomial. This gives an elementary model for a prefactor that vanishes when a pair becomes massless. For two independent pairs (η_1, η_2) and (ξ_1, ξ_2), use the product orientation with top monomial $\eta_1\eta_2\xi_1\xi_2$. The two bilinears commute, and the full expansion is

$$e^{m\eta_1\eta_2 + n\xi_1\xi_2} = 1 + m\eta_1\eta_2 + n\xi_1\xi_2 + mn\eta_1\eta_2\xi_1\xi_2. \tag{XIV.10.4}$$

At $(m, n) = (2, 3)$ the coefficient is six. At $(2, 0)$ the first pair still saturates, but the four-coordinate integral vanishes. A polynomial in external fields can also saturate modes if it multiplies the correct Grassmann monomial. The result in that case is a coupling with those fields inserted. Counting modes tells us what must be saturated; it does not provide the couplings that saturate them.

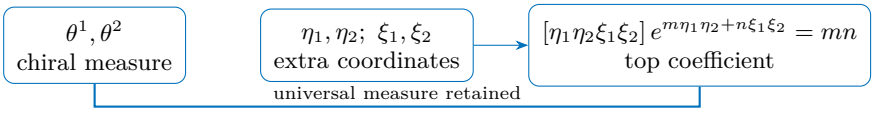


Figure XIV.10.1: The two universal coordinates remain the chiral measure. The two extra pairs are integrated out first. When $n = 0$ the integrand has no $\xi_1\xi_2$ coefficient, even when the η pair is massive.

There is a separate condition on the exponential. Let ρ be an axion of unit period, with the phase of the chosen instanton $e^{2\pi i\rho}$. An integer shift leaves that phase invariant. A continuous gauge transformation $\rho \mapsto \rho + q\lambda$, with dimensionless parameter λ, acts instead as

$$e^{-S_{\rm cl}} \longmapsto e^{2\pi i q\lambda} e^{-S_{\rm cl}}. \tag{XIV.10.5}$$

Let $\mathcal{O}$ be an operator of charge $q_{\mathcal{O}}$. Including it gives the phase and the period checks

$$\mathcal{O}\, e^{-S_{\rm cl}} \longmapsto e^{2\pi i(q+q_{\mathcal{O}})\lambda} \mathcal{O}\, e^{-S_{\rm cl}}, \tag{XIV.10.6}$$

$$\frac{e^{2\pi i(\rho+1)}}{e^{2\pi i\rho}} = 1, \qquad \frac{e^{2\pi i(\rho+1/2)}}{e^{2\pi i\rho}} = -1. \tag{XIV.10.7}$$

Thus a charge $q = -5$ requires a dressing of charge $+5$, while a half-period shift is not a symmetry of this first axion harmonic. The axion period makes the exponential single valued under a period shift; it does not neutralize its gauge charge.

The two tests already have different inputs. The Berezin integral needs the fermionic spectrum and its couplings. The gauge test needs the transformation of the action

and any operator it accompanies. We first construct a compact divisor so that we can calculate the neutral spectrum, and then ask what changes when flux can supply charge to the instanton.

XIV.10.2 One instanton, two descriptions

Which six-dimensional M5 worldvolumes give four-dimensional instantons? Let $\pi : Y \to B$ be an elliptically fibered Calabi–Yau fourfold, with complex threefold base B. If $S \subset B$ is a complex surface, its inverse image $D = \pi^{-1}(S)$ is a complex threefold. This is a *vertical* divisor: the brane wraps the whole elliptic fiber over a generic point of S. In a regular patch with a rectangular torus, write the two fiber circles as S^1_{11} and S^1_A. First reduce M-theory along S^1_{11}, then T-dualize along S^1_A. The worldvolumes and their real dimensions are

$$\text{M5}: \ S \times S^1_{11} \times S^1_A \ (6) \ \longrightarrow \ \text{D4}: \ S \times S^1_A \ (5) \ \longrightarrow \ \text{E3}: \ S \ (4). \tag{XIV.10.8}$$

The last duality is along a wrapped direction, so the E3 is localized on the dual circle. This describes the wrapping locally; the fiber need not split into two global circle bundles. At fixed IIB geometry the vertical saddle has a finite leading action, whose normalization we compute in the last section.

The zero section is a different threefold in Y. It covers the base and intersects a generic elliptic fiber at a point. An M5 on it lacks the wrapped circles in (XIV.10.8). In the same local description a horizontal M5 becomes an NS5 after reduction along a transverse M circle. T-duality along the remaining transverse circle gives a Kaluza–Klein monopole with that dual circle as its isometry direction. The fixed-IIB-scale comparison makes the suppression visible. With dual radius $R_B = \alpha'/R_A$ and coupling $g_B = g_A\sqrt{\alpha'}/R_A$, the local NS5 tension in IIA units becomes

$$\frac{1}{(2\pi)^5 g_A^2 \alpha'^3} = \frac{R_B^2}{(2\pi)^5 g_B^2 \alpha'^4}. \tag{XIV.10.9}$$

In this comparison the two string metrics agree along the directions transverse to the duality circle and tangent to the brane. As R_B grows at fixed IIB geometry the horizontal action grows. This is a local scaling explanation of the distinction; it does not assume a product metric for a compact fibration with seven-branes.

We now need a base with surfaces whose normals can be changed without changing the fourfold. Let $[Y_1 : Y_2 : Y_3 : Y_4]$ be homogeneous coordinates on $\mathbb{P}^3$ and put $p = [0 : 0 : 0 : 1]$. Projection from p has direction $[Y_1 : Y_2 : Y_3]$ away from p. To extend it at p, keep the direction $[X_1 : X_2 : X_3]$ as a second coordinate. The closure of the graph is

$$B = \{Y_i X_j = Y_j X_i, \quad 1 \le i < j \le 3\} \subset \mathbb{P}^3 \times \mathbb{P}^2. \tag{XIV.10.10}$$

On $Y_4 \neq 0$ these are the graph equations for the blowup of the origin in the three coordinates Y_i/Y_4. Over the marked point the full $\mathbb{P}^2$ of directions remains. Away from the point the direction is determined uniquely. Thus $B = \mathrm{Bl}_p \, \mathbb{P}^3$.

An equivalent presentation uses five homogeneous coordinates (x_1, x_2, x_3, u, v) and two rescalings. For both the direction and the point of $\mathbb{P}^3$ to be defined, use

$$(x_i, u, v) \sim (\lambda x_i, \mu u, \lambda\mu v), \qquad (x_1, x_2, x_3) \neq 0, \quad (u, v) \neq 0, \tag{XIV.10.11}$$

$$[X] = [x_1 : x_2 : x_3], \qquad [Y] = [ux_1 : ux_2 : ux_3 : v]. \tag{XIV.10.12}$$

The two displayed projective weights are constant within each list, and the incidence equations hold. To check the inverse, choose a direction chart $x_i \neq 0$. When $u \neq 0$, set $x_i = u = 1$ using the two rescalings. The three free coordinates are x_j/x_i for $j \neq i$ and $v/(ux_i)$; the latter equals Y_4/Y_i. When $v \neq 0$, use $x_i = v = 1$ instead, with third coordinate $ux_i/v = Y_i/Y_4$. These are the inverse coordinates on $X_iY_i \neq 0$ and $X_iY_4 \neq 0$ in the incidence variety. The six charts cover it and give affine three-spaces. An orbit with $x_1 = x_2 = x_3 = 0$ could still map to a point in $\mathbb{P}^3$ if $v \neq 0$, but it would have no direction and is excluded.

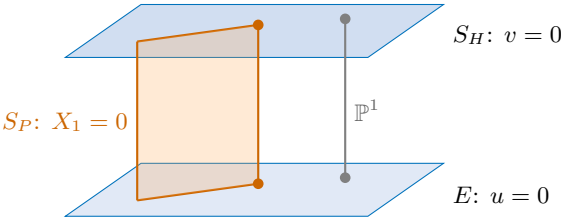


Figure XIV.10.2: The direction projection of the incidence blowup has a $\mathbb{P}^1$ fiber. Its two distinguished endpoints trace $E = \{u = 0\}$ and the disjoint plane $S_H = \{v = 0\}$. The inverse image of the direction line $X_1 = 0$ is the proper transform S_P of the plane through p. The drawing represents fibers over two directions.

Let H be the hyperplane class pulled back from $\mathbb{P}^3$ and $E = \{u = 0\}$ the exceptional divisor, also denoting its class by E. The weight $(1, 1)$ corresponds to H and $(0, 1)$ to E, so the direction hyperplane has class $H - E$. Figure XIV.10.2 identifies three actual surfaces:

$$S_E = E \simeq \mathbb{P}^2, \qquad S_H = \{v = 0\} \simeq \mathbb{P}^2, \qquad S_P = \{x_1 = 0\} \simeq \mathrm{Bl}_p\, \mathbb{P}^2. \tag{XIV.10.13}$$

The plane $v = 0$ is disjoint from p before the blowup. On $Y_1 = 0$ the proper transform retains the directions in that plane, exactly $X_1 = 0$. The two planes therefore have different normals. In particular $H|_E = 0$ because the blowdown contracts E. If h is the hyperplane on E, the direction class restricts as $(H - E)|_E = h$. Consequently

$$N_{E/B} = \mathcal{O}_E(-1), \qquad H^3 = E^3 = 1, \qquad HE = 0. \tag{XIV.10.14}$$

The negative normal gives $E^3 = \int_E (-h)^2 = +1$. The mixed products vanish by restriction to E. Three generic pullback hyperplanes intersect in one point away from p.

The Euler sequence for the smooth toric quotient expresses $c(TB)$ as a product over the five coordinate divisors. This fixes the Weierstrass coefficient bundles before any

choice of coefficients:

$$c(TB) = (1+H-E)^3(1+E)(1+H), \tag{XIV.10.15}$$

$$L = -K_B = 4H - 2E = 2H + 2(H-E), \qquad c_2(B) = 6H^2. \tag{XIV.10.16}$$

We write divisor classes and first Chern classes of their line bundles with the same symbols. The two terms in $2H + 2(H-E)$ come from the two projective factors. Thus L is the restriction of a very ample bundle under the incidence embedding.

Use an ordinary relative $\mathbb{P}^2$ bundle over B. Let α be the class of its coordinate z, so the coordinate divisors z, x, y have classes $\alpha, \alpha+2L, \alpha+3L$. The hypersurface Y is

$$y^2z = x^3 + fxz^2 + gz^3, \qquad [Y] = 3\alpha + 6L, \quad f \in H^0(B, L^4), \quad g \in H^0(B, L^6). \tag{XIV.10.17}$$

All terms are in the same bundle. The relative tangent Euler sequence gives relative canonical class $-3\alpha - 5L$. Adjunction then yields

$$K_Y = \pi^*(K_B + L) \simeq \mathcal{O}_Y. \tag{XIV.10.18}$$

Every fiber is a nonzero plane cubic with the same Hilbert polynomial, so the relative Cartier hypersurface is flat. In the affine chart $z = 1$, $y^2 = x^3 + fx + g$ is integral even at a nodal or cuspidal member: the polynomial in x is monic of odd degree and cannot be a square. At infinity there is a single reduced section Z_0 at $[z : x : y] = [0 : 0 : 1]$; as a divisor, $z = 0$ on Y is $3Z_0$. This multiplicity will matter in the Chern calculation.

Smoothness of the total space is a separate question from smoothness of each fiber. For a concrete simultaneous smoothness example put $f = 0$ and define

$$G_d = \sum_{i=1}^{3} x_i^d, \qquad g = v^{12}G_{12} + u^{12}G_{24}. \tag{XIV.10.19}$$

Both terms have weight $(24, 12)$, the weight of $6L$. In a direction chart $x_i = 1$ use $w = ux_i/v$ near E and $t = v/(ux_i)$ near S_H. In these trivializations g is $G_{12} + w^{12}G_{24}$ or $t^{12}G_{12} + G_{24}$. At either endpoint the corresponding projective Fermat equation is smooth. In the interior, $g = \partial_w g = 0$ would force $G_{12} = G_{24} = 0$. With $U_i = x_i^{12}$ this means

$$\sum_i U_i = 0, \qquad \sum_i U_i^2 = 0. \tag{XIV.10.20}$$

If one U_i were zero, the other two would have to be opposite and have zero sum of squares, forcing both to vanish. Hence all are nonzero. The gradients of the two equations in U_i are independent: proportionality would make all U_i equal. They both annihilate the radial direction at a common zero, so they remain independent on the projective chart. The power map is locally invertible there. It follows that $dG_{12} + w^{12}dG_{24}$ cannot vanish. On S_P the restricted polynomials have no common zero by the same two-coordinate calculation, and each endpoint has simple roots. On S_E and S_H the smooth endpoint equations already give the required result.

In the $z = 1$ chart of the fourfold, a singular point of $y^2 = x^3 + g$ would require $x = y = 0$ and $g = dg = 0$. These conditions fail both on the base and on the three

restricted bases. In the $y = 1$ chart the z derivative at Z_0 is one, also after restriction. This proves smoothness of Y and all three $D = \pi^{-1}(S)$ for (XIV.10.19); simultaneous smoothness then holds on a nonempty open set of the coefficient family.

A useful change is $G_{24} \mapsto G_{12}^2$. The two gradients at a common zero are now dependent. On $x_2 = 1$, at $x_1 = 0$, $x_3^{12} = -1$, $w = 1$, the derivative of $G_{12} + w^{12}G_{12}^2$ with respect to x_3 is $12x_3^{11} \neq 0$. This interior point is regular. At $t = 0$, however, $t^{12}G_{12} + G_{12}^2$ and all its first derivatives vanish wherever $G_{12} = 0$, and the corresponding cubic has a singular total-space point at $x = y = 0$. Smoothness must be checked across both endpoints and the interior. Our smooth member provides a geometric example on which to compute modes; its special $j = 0$ smooth fibers do not furnish a fluctuation determinant.

XIV.10.3 Count neutral fermions on a vertical divisor

How many neutral modes remain after removing the two universal fermions? Work first at zero bulk and worldvolume flux in the ordinary four-supercharge F-theory setting. Let $q : D \to S$ be the restriction of π, and let $r : P \to S$ denote the ambient relative $\mathbb{P}^2$ bundle for D. Cohomology of $\mathcal{O}_D$ will give the unfluxed neutral families. Instead of solving directly on the threefold, we resolve $\mathcal{O}_D$ using the cubic equation:

$$0 \longrightarrow \mathcal{O}_P(-D) \longrightarrow \mathcal{O}_P \longrightarrow \mathcal{O}_D \longrightarrow 0. \tag{XIV.10.21}$$

Here and below L in an expression over S means its restriction to S. Fiberwise, $\mathcal{O}_P$ has only H^0, while the cubic ideal restricts to $\mathcal{O}_{\mathbb{P}^2}(-3)$ with only H^2. To find the bundle of those top cohomology groups, use the relative canonical line bundle rather than treating $\mathbb{P}^2$ as a product:

$$K_{P/S} = \mathcal{O}_P(-3\alpha) \otimes r^*L^{-5}, \tag{XIV.10.22}$$

$$\mathcal{O}_P(-D) = K_{P/S} \otimes r^*L^{-1}, \qquad R^2r_*K_{P/S} = \mathcal{O}_S. \tag{XIV.10.23}$$

The last equality is relative Serre duality paired with $r_*\mathcal{O}_P = \mathcal{O}_S$. The long exact sequence of direct images now gives

$$q_*\mathcal{O}_D = \mathcal{O}_S, \qquad R^1q_*\mathcal{O}_D = L^{-1}, \qquad R^iq_*\mathcal{O}_D = 0 \quad (i > 1). \tag{XIV.10.24}$$

In particular it is the inverse *base* anticanonical bundle that occurs in the second row. As a check, adjunction gives $\omega_{D/S} = q^*L$, whose direct image is L.

Each of the surfaces above is rational. The Leray spectral sequence for q starts with $H^p(S, R^jq_*\mathcal{O}_D)$ in column p and row $j = 0, 1$. Its only possible differential goes from $(p, 1)$ to $(p + 2, 0)$. It is zero because $H^{>0}(S, \mathcal{O}_S) = 0$. The associated graded pieces on each diagonal give the dimensions

$$h^{0,k}(D) = h^k(S, \mathcal{O}_S) + h^{k-1}(S, L^{-1}), \qquad 0 \leq k \leq 3. \tag{XIV.10.25}$$

Cohomology outside $0 \leq p \leq 2$ on S is set to zero. The row shift by one reflects the additional elliptic cohomology degree. Applied over B, the same calculation has $H^{>0}(B, \mathcal{O}_B) = 0$ and $L^{-1} = K_B$. Serre duality then gives $h^k(Y, \mathcal{O}_Y) = (1, 0, 0, 0, 1)$.

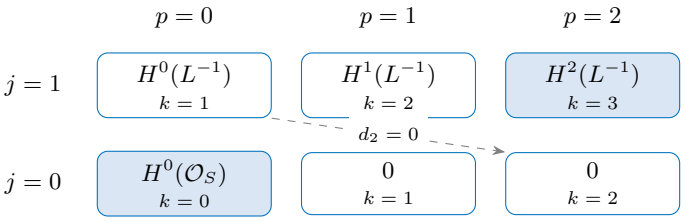


Figure XIV.10.3: Two Leray rows on a rational surface in the examples below. The labels inside the boxes are the base cohomology groups and k is the total degree. The lower left box supplies the universal doublet; the upper right box supplies the neutral deformation doublets. The possible arrow into the lower right box vanishes.

The relation of these groups to fermions uses the twist of the normal rotation of an M5. By adjunction in a Calabi–Yau, $N_{D/Y} = K_D$. Work in the orientation for which the M5 fermion uses the positive tangent chirality on D. On a Kähler threefold the Clifford generators act on $(0,k)$ forms by exterior multiplication and contraction. Positive chirality is the even part, with a canonical half-line from the spinor vacuum. The complex normal plane supplies a second spinor with opposite rotation charges on its two summands. In the normal-rotation convention we use, the two factors are

$$S_D^+ = K_D^{1/2} \otimes (\Omega^{0,0} \oplus \Omega^{0,2}), \qquad S_N = (K_D^{1/2})_{+1/2} \oplus (K_D^{-1/2})_{-1/2}. \tag{XIV.10.26}$$

The half powers cancel or combine in the tensor product; no separate square-root bundle is required. The branch of charge $-1/2$ uses ordinary $(0,0)$ and $(0,2)$ cohomology. The branch of charge $+1/2$ uses the same degrees with coefficients in K_D, because its two half powers multiply. The unfluxed Kähler Dirac operator acts as the Dolbeault operator plus its adjoint on each branch, so Serre duality gives the complementary degrees:

$$H^0(D, K_D) \simeq H^3(D, \mathcal{O}_D)^*, \qquad H^2(D, K_D) \simeq H^1(D, \mathcal{O}_D)^*. \tag{XIV.10.27}$$

In the M-theory derivation each family also carries an external spinor doublet from the three uncompactified directions. Thus the even degrees have charge $-1/2$ and the odd degrees $+1/2$. This charge is a rotation of the normal plane, not the $U(1)_X$ charge of the charged example. In particular the two coordinates for the constant form give the measure of charge $+1$, since a Berezin differential has the opposite charge to its coordinate. The signed total measure charge is

$$Q_{\mathrm{meas}} = \sum_{k=0}^{3} (-1)^k h^{0,k}(D) = \chi(\mathcal{O}_D), \qquad N_{\mathrm{ferm}} = 2 \sum_{k=0}^{3} h^{0,k}(D). \tag{XIV.10.28}$$

The normal-rotation anomaly assigns charge $-\chi(\mathcal{O}_D)$ to the exponential. In the unfluxed argument with no charged insertions, matching it to the chiral measure requires $\chi(\mathcal{O}_D) = 1$. An index of one can also arise by adding one even and one odd doublet to the universal pair. Their charges cancel in the index while their four

additional Grassmann coordinates still need saturation. To show that the universal pair is the entire neutral spectrum one needs the individual higher groups.

In IIB there is another useful assignment of the same cohomology dimensions. The duality line L describes the $SL(2,\mathbb{Z})$ rotation in the IIB description; the varying axio-dilaton makes this a genuine twist. In the unfluxed E3 convention, the left-handed families at degrees $p = 0, 1, 2$ use $H^p(S, \mathcal{O}_S)$, and the right-handed families use $H^p(S, L^{-1})$ up to complex conjugations in identifying the form fields. In particular the conjugate of the right-handed degree-two group is represented by holomorphic sections of $K_S \otimes L$. Adjunction gives

$$H^2(S, L^{-1}) \simeq H^0(S, K_S \otimes L)^*, \qquad K_S \otimes L = N_{S/B}. \tag{XIV.10.29}$$

The right-handed degree-two group therefore counts the deformation partners. The E3 left/right assignment by rows is not Witten's normal-rotation assignment by parity of k. For example the right-handed degree-two group has total M5 degree three. One can also count these deformations directly on D: $N_{D/Y} = q^* N_{S/B}$, $q_* \mathcal{O}_D = \mathcal{O}_S$, and Serre duality gives $h^{0,3}(D) = h^0(D, N_{D/Y})$.

The calculation on the exceptional surface starts from $L|_E = \mathcal{O}_E(2)$, using $H|_E = 0$ and $E|_E = -h$. On $\mathbb{P}^2$, $\mathcal{O}(k)$ has no middle cohomology and its top group is dual to $H^0(\mathcal{O}(-3-k))$. The negative bundle $\mathcal{O}(-2)$ therefore has no cohomology. Equation (XIV.10.25) gives

$$h^{0,\bullet}(D_E) = (1, 0, 0, 0), \qquad \chi(\mathcal{O}_{D_E}) = 1. \tag{XIV.10.30}$$

Rigidity also has a direct linear-system check. The exceptional section is the unique divisor of its linear system since

$$\begin{aligned} 0 \to \mathcal{O}_B \to \mathcal{O}_B(E) \to \mathcal{O}_E(-1) \to 0, \\ h^0(Y, \mathcal{O}_Y(D_E)) = h^0(B, \mathcal{O}_B(E)) = 1. \end{aligned} \tag{XIV.10.31}$$

The equality on Y uses $\pi_* \mathcal{O}_Y = \mathcal{O}_B$. This argument addresses deformations and representatives within the linear system. It does not evaluate a determinant.

On S_H the class E restricts to zero and $L|_{S_H} = \mathcal{O}(4)$. Now $H^2(\mathcal{O}(-4))$ is dual to $H^0(\mathcal{O}(1))$, with three independent linear monomials. Thus moving to the disjoint plane gives

$$h^{0,\bullet}(D_H) = (1, 0, 0, 3), \qquad \chi(\mathcal{O}_{D_H}) = -2. \tag{XIV.10.32}$$

The three deformations move the plane in the space of all planes. On S_P let h be the pullback of the line of the plane and e its exceptional curve. Here $K_{S_P} = -3h + e$ and $L|_{S_P} = 4h - 2e$. By Kodaira vanishing, $K_{S_P} + L$ has no higher cohomology, since L is ample. Serre duality gives

$$H^2(S_P, L^{-1}) = H^0(S_P, \mathcal{O}(h-e))^*, \qquad H^0(S_P, L^{-1}) = H^1(S_P, L^{-1}) = 0. \tag{XIV.10.33}$$

In plane coordinates $[s : t : r]$ with the marked point $[0 : 0 : 1]$, the line sections vanishing there are spanned by s, t. The monomial r would move the plane away from the marked point. For a conic through that point the corresponding list would be

s^2, st, t^2, sr, tr; this is a changed linear-system exercise, with no identification of its five coefficients with the deformations of the original plane. For the actual plane,

$$h^{0,\bullet}(D_P) = (1, 0, 0, 2), \qquad \chi(\mathcal{O}_{D_P}) = -1. \tag{XIV.10.34}$$

One can change the exceptional normal to a trivial normal by changing the base geometry. On $B' = \mathbb{P}^1 \times \mathbb{P}^2$, let $S' = \{\mathrm{pt}\} \times \mathbb{P}^2$. The coefficient bundle is $L' = \mathcal{O}(2, 3)$, and the restriction to S' is $\mathcal{O}(3)$. Smooth generic Weierstrass models exist both over B' and on the slice: L'^4 and L'^6 separate first jets, as do their restrictions. At a fixed affine fiber point, vanishing of the equation and its x derivative imposes independent conditions on g, f, and vanishing of the base derivatives imposes independent conditions on the first derivatives of g. The y derivative forces $y = 0$. Thus the singular incidence over the remaining (x, base point) has one more condition than its dimension, and the section is regular as before. On this product the second row is the top group of $\mathcal{O}(-3)$, of dimension one. Hence

$$h^{0,\bullet}(D') = (1, 0, 0, 1), \qquad \chi(\mathcal{O}_{D'}) = 0. \tag{XIV.10.35}$$

The one family moves the slice along $\mathbb{P}^1$. Using $K_E = \mathcal{O}(-3)$ in place of $L^{-1}|_E$ would produce the same number on paper but would falsely assign a displacement to the exceptional surface.

Finally the arithmetic genus can be computed without separating the groups. Write $\ell = c_1(L|_S)$ and $c = c_1(TS)$. Taking the alternating sum in (XIV.10.25) and applying surface Hirzebruch–Riemann–Roch yields

$$\chi(\mathcal{O}_D) = \chi(\mathcal{O}_S) - \chi(L^{-1}) = \int_S \left[(1 - e^{-\ell}) \operatorname{Td}(TS)\right]_2 \tag{XIV.10.36}$$

$$= \frac{1}{2} \int_S (\ell c - \ell^2) = -\frac{1}{2} \int_B L[S]^2. \tag{XIV.10.37}$$

In the first line the subscript means complex degree two. The last equality follows from $c = (L - [S])|_S$. For $E, H, H - E$, the three triple products are $-2, 4, 2$, respectively. They give precisely $1, -2, -1$. The index checks the alternating sum independently. It cannot diagnose any fermions localized at intersections with other branes, and an index evaluated on a class by itself does not construct a smooth divisor in that class.

XIV.10.4 What flux requires the instanton to absorb

When is a neutral mode count insufficient even to allow a bare exponential? Let $i : D \hookrightarrow Y$ be the inclusion of a compact M5 worldvolume. Use the dimensionless four-form $G_4 = F_4/(2\pi l_p)^3$, where l_p is the eleven-dimensional Planck length. Write T_3 for the invariant M5 three-form field strength. An incoming M2 wraps a fibral curve and follows an external worldline ending at the instanton position. Suppressing this common spacetime endpoint, denote the total membrane chain by P_{M2}, and its signed boundary by $C = \partial P_{\mathrm{M2}} \subset D$. With this choice of orientation the sourced Bianchi identity is

$$dT_3 = i^* G_4 - \delta_4(C). \tag{XIV.10.38}$$

Here $\delta_4(C)$ is the current Poincaré dual to C on D. A sign in the cycle describes an orientation or its CPT assignment. It does not mean an inverse matter field.

For any closed smooth two-form ω on D, integrating (XIV.10.38) against ω gives

$$0 = \int_D \omega \wedge dT_3 = \int_D \omega \wedge i^* G_4 - \int_C \omega. \tag{XIV.10.39}$$

The first equality follows from Stokes on the compact D and still holds in the sense of currents. Thus the restricted flux class must equal $\mathrm{PD}_D[C]$ in real cohomology. A nonzero period on D prevents a bare term in the sector $C = 0$: changing T_3 cannot change that period. Conversely, equality of real classes gives an unconstrained solution as a current, since the difference is exact in real current cohomology. It does not imply $T_3 = 0$, or solve the quantization, chirality or supersymmetry condition on T_3. For instance, with $C = 0$ a nonzero exact representative requires $dT_3 \neq 0$. Testing a pushforward only in the bulk can lose information about classes on D.

The boundary variation of the action explains the charge of the resulting insertion. Pullbacks of bulk potentials to D are implicit below. Write C_3, C_6 for the normalized bulk potentials and β_2 for the M5 two-form potential. With two-form gauge parameter Λ_2 the transformations used here are

$$\delta C_3 = d\Lambda_2, \qquad \delta C_6 = -\tfrac{1}{2}\Lambda_2 \wedge G_4 + d\Lambda_5, \qquad \delta\beta_2 = -\Lambda_2|_D, \qquad \delta T_3 = 0. \tag{XIV.10.40}$$

Only the following terms in the bosonic action vary:

$$S_{\mathrm{M5,top}} = -2\pi i \int_D \left(C_6 + \tfrac{1}{2} T_3 \wedge C_3\right) - \pi i \int_C \beta_2. \tag{XIV.10.41}$$

The signs make $T_3 = d\beta_2 + C_3|_D$ invariant away from sources. On the compact D, the exact term $d\Lambda_5$ drops out. Thus the three pieces give

$$\delta S_{\mathrm{M5}} = \pi i \int_D \Lambda_2 \wedge i^* G_4 - \pi i \int_D dT_3 \wedge \Lambda_2 + \pi i \int_C \Lambda_2 \tag{XIV.10.42}$$

$$= 2\pi i \int_C \Lambda_2. \tag{XIV.10.43}$$

In integrating by parts, $d(T_3 \wedge \Lambda_2) = dT_3 \wedge \Lambda_2 - T_3 \wedge d\Lambda_2$. The Bianchi identity supplies one copy of the boundary variation; the explicit β_2 term supplies the other. The membrane term is $-2\pi i \int_{P_{\mathrm{M2}}} C_3$, so

$$\delta S_{\mathrm{M2}} = -2\pi i \int_C \Lambda_2, \qquad \delta(S_{\mathrm{M5}} + S_{\mathrm{M2}}) = 0. \tag{XIV.10.44}$$

Dropping the explicit boundary coupling would leave an uncanceled variation after the membrane is added. Reversing only the membrane boundary would also spoil the cancellation. Figure XIV.10.4 shows which orientation enters both equations.

For an actual charged comparison, change the fourfold. Use the resolved, $U(1)$-restricted split $SU(5)$ Tate family in triangulation T_{11}. Write W for the seven-brane surface and a_1 for the Tate coefficient whose vanishing on W gives the **10** matter curve.

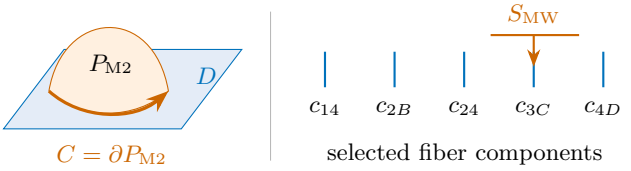


Figure XIV.10.4: An incoming membrane chain has oriented boundary C on D. For the split fiber considered below, only c_{3C} among the five indicated components meets the extra section S_{MW}. The pairing detects an obstruction that vanishes against the four Cartan divisors.

The restriction to an instanton base S meets that curve at transverse points p_ℓ of $S \cap W \cap \{a_1 = 0\}$. Assume these are ordinary points of the matter curve, away from higher enhancements. The resolved $U(1)$-restricted geometry has an extra rational section S_{MW}. Here and in the rest of this section the letter S alone still denotes the instanton base surface.

At each p_ℓ use the ordered component basis $(c_{14}, c_{2B}, c_{24}, c_{3C}, c_{4D})$ of the part of the split fiber that occurs in the calculation. Denote the four simple-root curves by r_i. The local resolution supplies

$$r_1 = c_{14}, \qquad r_2 = c_{2B} + c_{24}, \tag{XIV.10.45}$$

$$r_3 = c_{3C}, \qquad r_4 = c_{14} + c_{24} + c_{4D}. \tag{XIV.10.46}$$

To see why the splittings enter, choose the actual cycle representative of the flux. Let $\mathcal{S}_{24}$ be the matter surface $e_2 = e_4 = a_1 = 0$, with e_i the corresponding resolution coordinates. It is fibered by c_{24} over the **10** curve. Let $D_{a_1} = \{a_1 = 0\}$ in the base and let E_i be the Cartan divisors in the resolved fourfold $\widehat{Y}$. The specified codimension-two cycle is

$$\mathcal{D}_G = 5\mathcal{S}_{24} + \pi^{-1}(D_{a_1}) \cdot (2E_1 - E_2 + E_3 - 2E_4). \tag{XIV.10.47}$$

The second term restricts to root curves at the matter points because the base part puts those intersections on $a_1 = 0$. Transversality of S and the matter curve gives multiplicity one at each point. The first term of (XIV.10.47) therefore contributes $5c_{24}$ per point; the corrections contribute $2r_1 - r_2 + r_3 - 2r_4$. Expanding these corrections using (XIV.10.46) gives the signed curve and its column vector:

$$\begin{aligned} C_{G,\ell} &= 5c_{24} + 2r_1 - r_2 + r_3 - 2r_4 \\ &= -c_{2B} + 2c_{24} + c_{3C} - 2c_{4D} \;\longleftrightarrow\; (0, -1, 2, 1, -2)^t. \end{aligned} \tag{XIV.10.48}$$

The omitted fiber components have zero coefficients in this particular expression. The cycle represents the required restriction class on the M5, with the source specialization understood. A statement about a class alone would still leave the choice of representative and the chiral field on the M5 to be determined.

To find the Cartan charges, write the weight of any curve as the column of its four simple-coroot pairings. The simple roots α_i have the columns of the A_4 Cartan matrix

in these coordinates, and the effective root curve r_i has weight $-\alpha_i$. The resolved matter component c_{24} has weight $-\mu_{10}+\alpha_1+\alpha_2+\alpha_3$, where the highest weight μ_{10} has pairings $(0,1,0,0)^t$. Thus c_{24} has pairings $(1,-1,1,-1)^t$. The first and third splitting immediately give the columns of c_{14} and c_{3C}. Subtract the c_{24} column from the second splitting, and subtract both c_{14} and c_{24} from the fourth. The resulting Cartan matrix of pairings is

$$M = \begin{pmatrix} -2 & 0 & 1 & 0 & 1 \\ 1 & -1 & -1 & 1 & 0 \\ 0 & 0 & 1 & -2 & 0 \\ 0 & 1 & -1 & 1 & -1 \end{pmatrix}, \qquad MC_{G,\ell} = 0. \tag{XIV.10.49}$$

Here a curve in a matrix product means its column. The matter component alone would have nonzero Cartan charges; the Cartan corrections cancel them. They do not cancel the section degree. In the specified resolution, the section coordinate is s, with $s = 0$ for S_{MW}. The nonvanishing conditions on the split curves give

$$z \neq 0 \text{ on all five curves}, \qquad s \neq 0 \text{ on } c_{14}, c_{2B}, c_{24}, c_{4D}. \tag{XIV.10.50}$$

Thus the zero section cannot meet these curves, and only c_{3C} can meet S_{MW}. The intersection in the c_{3C} chart has degree one for the generic ordinary matter point. This local geometric input supplements the root splittings, which by themselves only determine the Cartan calculation. The section rows in this basis and the Shioda charge class are

$$S_{\mathrm{MW}} : (0,0,0,1,0), \qquad Z_0 : (0,0,0,0,0), \tag{XIV.10.51}$$

$$w_X = 5(S_{\mathrm{MW}} - Z_0 - \pi^* L) + 2E_1 + 4E_2 + 6E_3 + 3E_4. \tag{XIV.10.52}$$

These E_i are distinct from the exceptional surface of the preceding base. Pullbacks from the base have degree zero on fibral curves. Equations (XIV.10.48)–(XIV.10.52) give $\int_{C_{G,\ell}} S_{\mathrm{MW}} = 1$ and $\int_{C_{G,\ell}} w_X = 5$. The pullback of the section divisor to D is precisely a test class in (XIV.10.39). At a nonzero number of intersection points the bare M5 fails that test, although it passes every Cartan test.

Now supply the membrane ends. The five signed curves and their weights are as follows; the last column uses the same w_X as the flux curve.

End	Curve	Cartan pairings	X charge
1	$c_{24} + c_{3C}$	$(1,0,-1,0)$	1
2	$c_{14} + c_{24}$	$(-1,0,1,-1)$	1
3	$-c_{4D}$	$(-1,0,0,1)$	1
4	$-c_{2B}$	$(0,1,0,-1)$	1
5	$-c_{14} - c_{4D}$	$(1,-1,0,1)$	1

Table XIV.10.1: The five incoming M2 ends over one ordinary **10** point. Each Cartan row is obtained by multiplying the curve column by M.

For example the first curve has Cartan pairings $(1,0,-1,0)^t$ and section degree one. Its X charge is $5+2-6=1$. To identify the representation, let e_a, $a=1,\dots,5$, denote the defining weights with the trace direction removed; pairing with the ith coroot gives $\delta_{ai}-\delta_{a,i+1}$. The weights of $\overline{\mathbf{10}}$ are $-e_a-e_b$ for $a<b$. The five rows in the table are the pairs $(2,3),(1,4),(1,5),(3,4),(2,5)$, respectively. Summing the curve columns cancels c_{14} and leaves exactly $C_{G,\ell}$. If the first end is omitted, the residual curve is $c_{24}+c_{3C}$ and the residual section degree is one. Matching the full restriction is a stronger test than matching a chosen set of charges.

Zero total Cartan weight does not construct an $SU(5)$ singlet. For five independently labeled skew tensors $F_{j,ab}$ in $\overline{\mathbf{10}}$, a possible invariant projection uses two alternating tensors. For example define $v^a(F,G)=\epsilon^{abcde}F_{bc}G_{de}$, and form

$$v^a(F_1,F_2)v^b(F_3,F_4)F_{5,ab}. \tag{XIV.10.53}$$

This multilinear expression is nonzero, for instance with the five slots supported respectively in the $(23),(14),(15),(34),(25)$ entries listed above: the two vectors point in directions $5,2$. If all five slots are filled by the same commuting skew tensor, both vectors coincide and this contraction vanishes by skew symmetry. The available invariant projection in the tensor product therefore does not determine the actual flavors or contractions in the effective theory.

With $\Lambda_2=\lambda w_X$, (XIV.10.43) shows that the exponential has charge $-5n$, where n is the number of intersection points. Five incoming ends per point can supply a total $+5n$. As a concrete incidence specialization of this Tate bundle assignment, take $B=\mathbb{P}^3$, W a plane, a_1 a quartic, and S of degree d. Then

$$n=\int_{\mathbb{P}^3} dH\cdot H\cdot 4H=4d, \qquad (Q_{\exp},Q_{\text{ends}})=(-20d,+20d). \tag{XIV.10.54}$$

A line in W transverse to the quartic gives four points; a transverse smooth conic gives eight. Generic choices avoid the higher enhancements. Going from $d=1$ to $d=2$ changes the required dressing from charge $+20$ to $+40$. This calculation uses the specified local resolution and does not prove compact flux quantization, a tadpole solution or an instanton mode count for the specialization. In interpreting such membrane ends as four-dimensional matter insertions one takes the F-theory limit; at finite resolution volume a primitive M5 configuration with the attached curves need not exist. For example, replacing the first end by c_{24} alone leaves the residual c_{3C}. Its Cartan column is $(0,1,-2,1)^t$ and its section degree is one. Its Shioda charge vanishes because the contributions $5+4-12+3$ cancel. The replacement therefore passes the X charge sum but fails the Bianchi test and the Cartan test. The full set of specified ends has no such residual. It selects a possible dressed operator and excludes the bare one; it does not establish a nonzero charged amplitude.

XIV.10.5 A contributing divisor and two failures

Can the rigid exceptional divisor be used in a compact flux background, and what can make its prefactor vanish? Return to the smooth ordinary Weierstrass fourfold on

$B = \mathrm{Bl}_p\,\mathbb{P}^3$. In particular the Cartan divisors and extra section of the charged example are no longer present. First calculate the bulk constraints in the proposed zero-flux background. We will then vary the D3 position without varying the geometry of the instanton.

For the hypersurface (XIV.10.17), the relative Euler sequence gives three ambient tangent factors and adjunction divides by the normal factor. With base classes pulled back, the result is

$$c(TY) = c(TB)\,\frac{(1+\alpha)(1+\alpha+2L)(1+\alpha+3L)}{1+3\alpha+6L}\bigg|_Y . \tag{XIV.10.55}$$

To expand it, put $d_Y = 3\alpha + 6L$ and let e_j be the jth elementary symmetric polynomial of $(\alpha, \alpha+2L, \alpha+3L)$. Write R_k for the component of complex degree k in the fraction. Multiplying back by $1 + d_Y$ gives a convenient recurrence:

$$R_0 = 1, \qquad R_1 = e_1 - d_Y = -L, \tag{XIV.10.56}$$

$$R_2 = e_2 - d_Y R_1 = 3\alpha^2 + 13\alpha L + 12L^2, \tag{XIV.10.57}$$

$$R_3 = e_3 - d_Y R_2, \qquad R_4 = -d_Y R_3. \tag{XIV.10.58}$$

The linear term R_1 cancels $c_1(B)$. In degree two we obtain

$$c_2(Y) = c_2(B) + 11L^2 + 13\alpha L + 3\alpha^2 . \tag{XIV.10.59}$$

The divisor of z is $3Z_0$, so $\alpha|_Y = 3Z_0$. Adjunction on the reduced section gives $Z_0^2 = -LZ_0$: indeed $N_{Z_0/Y} = K_{Z_0} = K_B$. Using these relations before integrating gives

$$c_2(Y) = c_2(B) + 11L^2 + 12LZ_0 \tag{XIV.10.60}$$

$$= 182H^2 + 44E^2 + 48HZ_0 - 24EZ_0 . \tag{XIV.10.61}$$

In particular the displayed class is twice an integral class. Using $\alpha = Z_0$ would miss the multiplicity at the section and change the quantization test.

To compute the Euler number, retain degree four in (XIV.10.55). Terms of degree four pulled back entirely from B vanish. The remaining terms from $R_4 + LR_3 + c_2(B)R_2 + c_3(B)R_1$ are

$$c_4(Y) = 24\alpha^4 + 196\alpha^3 L + 584\alpha^2 L^2 + 756\alpha L^3 + c_2(B)(3\alpha^2 + 13\alpha L) \tag{XIV.10.62}$$

$$= Z_0\big(360L^3 + 12Lc_2(B)\big). \tag{XIV.10.63}$$

The second line follows by replacing α by $3Z_0$ and successive powers by $Z_0^k = (-L)^{k-1}Z_0$. Integration over the section is integration over B. In our base ring $HE = 0$, so

$$\int_B L^3 = 4^3 - 2^3 = 56, \qquad \int_B Lc_2(B) = 4 \cdot 6 = 24, \tag{XIV.10.64}$$

$$\chi_{\mathrm{top}}(Y) = \int_Y c_4(Y) = 360 \cdot 56 + 12 \cdot 24 = 20448. \tag{XIV.10.65}$$

The topological Euler number here controls the D3 budget. It is a different invariant from the arithmetic genus of D_E.

Use the shifted free-flux law and the leading D3 tadpole in the dimensionless normalization of (XIV.10.38):

$$\begin{gathered} G_4 + \tfrac{1}{2}c_2(Y) \text{ integral in the free class sector,} \\ N_{\mathrm{D3}} + \tfrac{1}{2}\int_Y G_4 \wedge G_4 = \frac{\chi_{\mathrm{top}}(Y)}{24}. \end{gathered} \tag{XIV.10.66}$$

Equation (XIV.10.61) permits $G_4 = 0$ in this law. Zero flux satisfies the leading transversality, type and primitivity conditions. Equation (XIV.10.66) then gives $N_{\mathrm{D3}} = 852$. Distinct points in the complement of E and the discriminant realize this charge count without putting any D3 on E. The budget does not fix their positions, determine the warped geometry or solve the vacuum equations. One can isolate how the blowup affects the budget by comparing with an ordinary smooth Weierstrass model over $\mathbb{P}^3$. There $L = 4H$ and $c_2(\mathbb{P}^3) = 6H^2$, so $\int Lc_2$ remains 24 but $\int L^3$ increases to 64. The change is

$$\frac{\chi_{\mathrm{top}}(Y_{\mathbb{P}^3}) - \chi_{\mathrm{top}}(Y)}{24} = \frac{360(64-56)}{24} = 120. \tag{XIV.10.67}$$

This compares two smooth models at zero bulk flux. It is a change of charge budgets, without an assumption about an interpolation or about the motion of individual D3 branes. In a trivial relevant C-field sector, $T_3 = 0$ and $C = 0$ solve the displayed instanton Bianchi identity; the real-class calculation does not settle additional differential or torsional data.

It is useful to see how a nonzero restriction would be detected before invoking any proposed physical flux. In this same smooth Y consider the two formal classes π^*H^2 and π^*E^2. For any one of our surfaces, test the restriction to $D = \pi^{-1}(S)$ against $Z_0|_D$. The section is isomorphic to S there. For either base divisor class $A = H$ or E,

$$\int_D Z_0|_D \wedge i^*\pi^*A^2 = \int_S (A|_S)^2. \tag{XIV.10.68}$$

The pairs of values for (H^2, E^2) are $(0,1)$ on E, $(1,0)$ on S_H and $(1,-1)$ on S_P. For the last value use $e^2 = -1$ on $\mathrm{Bl}_p\,\mathbb{P}^2$, rather than the cube $E^3 = 1$ on B. On E the H^2 restriction vanishes as a class because $H|_E = 0$; this conclusion does not follow from a single zero period in general. The nonzero E^2 period also equals the bulk test

$$\int_Y \pi^*E^2 \wedge Z_0 \wedge \pi^*E = 1. \tag{XIV.10.69}$$

A four-dimensional F-theory flux must have zero in this transversality test. Thus π^*E^2 diagnoses a local obstruction but cannot be used as the background of a physical fluxed comparison.

We can now separate the two ways a proposed bare term can fail in the actual zero-flux setting. First change the wrapped surface from E to S_H or S_P. The neutral calculation gives three or two additional deformation doublets, respectively. In the unfluxed bare integral with no lifting interactions or insertions to absorb these modes,

the Berezin coefficient vanishes. The rigidity and flux conclusions for E do not apply to the moved plane.

Next keep D_E fixed. In the sourced semiclassical exceptional-divisor construction, a generic isolated unfluxed saddle has a nonzero contribution away from additional zero loci, with the relevant C-field sector trivial and the spacetime D3 branes disjoint. This is the regime in which the neutral measure, vanishing source and absence of the localized D3 obstruction work together. Write the term as

$$W_E = A_E\, e^{-S_E}. \tag{XIV.10.70}$$

The existence statement uses the semiclassical analysis of the exceptional-divisor example. The cohomology does not compute A_E, and the special $j = 0$ smoothness example does not exhibit a particular nonzero value of A_E. Nor does the one-saddle analysis determine the total superpotential.

Now move one spacetime D3 toward E in a patch with regular elliptic fiber. Choose a holomorphic coordinate ζ normal to E, so the intersection is at $\zeta = 0$. At the intersection the localized fermion pair becomes massless. In a local trivialization its mass has a simple zero, $m(\zeta) = \zeta\, u(\zeta)$, with $u(0) \neq 0$. Applying the oriented integral from (XIV.10.3) gives

$$\int d\eta_2\, d\eta_1\, e^{m(\zeta)\eta_1\eta_2} = m(\zeta), \qquad A_E(\zeta) = \zeta\, U(\zeta), \quad U(0) \neq 0 \tag{XIV.10.71}$$

when the other prefactor factors are regular and nonzero there. The prefactor is expressed in a local frame, so U is not a universal normalization. An additional unsaturated pair would make the answer zero even off E, by (XIV.10.4).

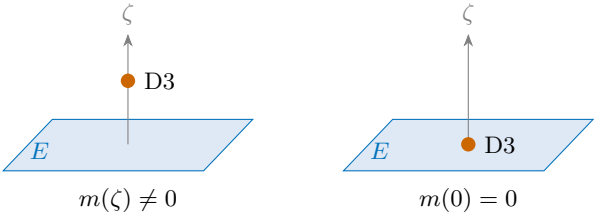


Figure XIV.10.5: The same exceptional surface is kept fixed in both panels. The spacetime D3 is displaced in its normal direction in the left panel and sits on the surface on the right. The localized factor in the prefactor vanishes in the second configuration. Neither the neutral groups of D_E nor the total D3 count changes.

This is a failure of the coefficient at a fixed instanton geometry, not a failure of the arithmetic genus test. It also makes no statement that derivatives of the full superpotential or the scalar potential vanish at the intersection. With the prefactor separated from the exponential, we can now ask what the classical weight does as the bulk grows.

XIV.10.6 The action when the bulk grows

Can the leading exceptional instanton weight remain finite while the compact regulator grows? There are two limits in this question. The F-theory limit shrinks the M fiber at fixed IIB geometry. After that identification, a Kähler limit within the base can enlarge the bulk relative to E. To compare them we first restore physical volumes and tensions.

Let $\ell_M = 2\pi l_p$ and $\ell_s = 2\pi\sqrt{\alpha'}$. Let $V_6(D)$ be the eleven-dimensional volume of the M5, and let $\rho_M = \int_D C_6$ in the unfluxed phase convention above. The leading Euclidean action is

$$S^{(0)}_{\mathrm{M5}} = 2\pi \left(\frac{V_6(D)}{\ell_M^6} - i\rho_M \right). \tag{XIV.10.72}$$

The tension is $2\pi/\ell_M^6 = 1/((2\pi)^5 l_p^6)$. The exponential has phase $e^{+2\pi i \rho_M}$ for the chosen orientation. Work in the regular isometric patch of (XIV.10.8), with IIA string coupling g_A and string radius R_A. The standard M/IIA calibration is $R_{11} = g_A\sqrt{\alpha'}$ and $l_p^3 = g_A \alpha'^{3/2}$. The first circle reduction gives

$$(2\pi R_{11})\, T_{\mathrm{M5}} = \frac{R_{11}}{(2\pi)^4 l_p^6} = \frac{1}{(2\pi)^4 g_A \alpha'^{5/2}} = T^{\mathrm{str}}_{\mathrm{D4}}. \tag{XIV.10.73}$$

The remaining wrapped circle has circumference $2\pi R_A$. Using $g_B = g_A\sqrt{\alpha'}/R_A$, its T-dual tension is

$$(2\pi R_A)\, T^{\mathrm{str}}_{\mathrm{D4}} = \frac{R_A}{(2\pi)^3 g_A \alpha'^{5/2}} = \frac{1}{(2\pi)^3 g_B \alpha'^2} = T^{\mathrm{str}}_{\mathrm{E3}}. \tag{XIV.10.74}$$

The two circle lengths thus convert the wrapped tension to the E3 tension as the local duality is applied. The computation uses the physical horizontal metrics in their respective frames; no global rectangular fiber metric is required. It explains why the vertical action remains finite at fixed IIB surface geometry in the F-theory limit.

For a constant dilaton patch $g_E = e^{-\phi/2} g_{\mathrm{str}}$, where here g_E, g_{str} are metrics and $g_B = e^{\phi}$ is the coupling. A real four-volume scales as $V_{\mathrm{str}} = g_B V_E$. The two factors of the metric in the volume cancel the explicit $1/g_B$ in (XIV.10.74). With dimensionful Einstein Kähler form J_E, define $V_E(S) = \frac{1}{2}\int_S J_E^2$. For a unit-period axion ρ_S the result is

$$S^{(0)}_E = 2\pi \left(\frac{V_E(S)}{\ell_s^4} - i\rho_S \right). \tag{XIV.10.75}$$

In the IIB convention in which the action contains $+i\int_S C_4$ with positive coefficient, $\rho_S = -\int_S C_4/\ell_s^4$. The two oriented phases are matched by the wrapped duality. This does not identify differently normalized bulk potentials. A second $1/g_B$ in (XIV.10.75) would count the frame conversion twice. The calibrated action controls the leading classical weight; it is not an exact quantum Kähler coordinate.

Now set $j = J_E/\ell_s^2 = aH - bE$. The two generators H and $H - E$ are nef, being pullbacks from the incidence factors. Since $j = (a-b)H + b(H-E)$, it is ample for $a > b > 0$ by the incidence embedding. To see necessity, a line l_E in E and the proper transform l_p of a line through p have areas

$$\int_{l_E} j = b, \qquad \int_{l_p} j = a - b. \tag{XIV.10.76}$$

The second line meets E once and has pullback hyperplane degree one. Both areas must be positive. In particular $(a, b) = (3, 7)$ is outside the cone even though the squared expressions for the first two surface volumes would be positive.

Let $\widehat{V}(S) = V_E(S)/\ell_s^4$. Integrating $j^2/2$ against the three surface classes and $j^3/6$ over the base gives

$$\widehat{V}(E) = \tfrac{1}{2}b^2, \qquad \widehat{V}(S_H) = \tfrac{1}{2}a^2, \qquad \widehat{V}(S_P) = \tfrac{1}{2}(a^2 - b^2), \tag{XIV.10.77}$$

$$V_E(B)/\ell_s^6 = \tfrac{1}{6}(a^3 - b^3). \tag{XIV.10.78}$$

The mixed terms vanish by $HE = 0$. At $(a, b) = (7, 3)$ the surface volumes are $9/2, 49/2, 20$, and $\operatorname{Re} S_E^{(0)} = 9\pi$. The distinct numbers reflect the distinct surface classes and would change if we exchanged the labels H and E.

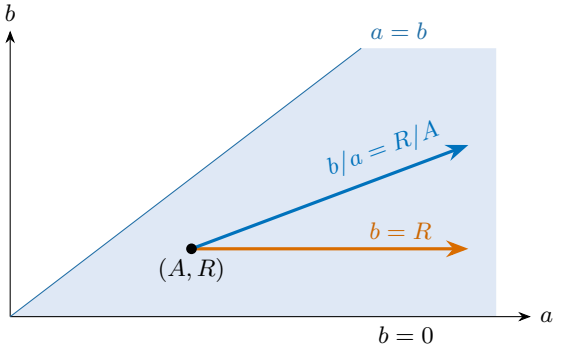


Figure XIV.10.6: The Kähler cone $0 < b < a$ in (a, b) coordinates. From the same starting point, the horizontal path fixes the exceptional area, whereas the ray along constant b/a increases it. The boundaries correspond to shrinking l_E or l_p.

There is a simple geometric interpretation of the fixed exceptional area. The patch $v \neq 0$ is the total space of $\mathcal{O}_{\mathbb{P}^2}(-1)$ with zero section E. Indeed fixing $v = 1$ leaves the rescaling $(x_i, u) \mapsto (\lambda x_i, \lambda^{-1}u)$, the line bundle of degree -1; the disjoint section S_H is outside this patch. Put $a = A + r$ with $A > R > 0$ and fix $b = R$ as $r \to \infty$. With ℓ_s and ρ_E fixed, (XIV.10.78) gives

$$\left|e^{-S_E^{(0)}}\right| = e^{-\pi R^2}, \qquad \frac{V_E(B)}{\ell_s^6} = \frac{r^3}{6} + O(r^2), \tag{XIV.10.79}$$

$$\left|e^{-S_H^{(0)}}\right| = e^{-\pi(A+r)^2}, \qquad \left|e^{-S_P^{(0)}}\right| = e^{-\pi((A+r)^2 - R^2)}. \tag{XIV.10.80}$$

Here $S_H^{(0)}$ and $S_P^{(0)}$ denote the leading actions on the surfaces S_H, S_P. A large fixed R keeps the exceptional cycle in a geometric semiclassical regime while its leading weight remains fixed. In contrast, on the uniform ray $b = \kappa a$ with $0 < \kappa < 1$, its weight tends to zero as $e^{-\pi\kappa^2 a^2}$.

The growing compact volume has a direct gravitational effect in the unwarped approximation. With ten-dimensional Einstein coupling κ_{10} fixed, integrate the coefficient

of the four-dimensional Ricci scalar over the base. In a product metric this term is

$$\frac{V_E(B)}{2\kappa_{10}^2}\int d^4X\,\sqrt{g_4}\,\mathcal{R}_4, \qquad M_{4,\mathrm{lead}}^2=\frac{V_E(B)}{\kappa_{10}^2}. \tag{XIV.10.81}$$

The ten-dimensional coupling squared has dimension length to the eighth power, so the ratio has dimension mass squared. The coefficient grows on both paths, even though the exceptional actions behave differently. The calculation assumes fixed microscopic length and omits the warp factor. The behavior of a classical action is a weaker statement than isolation of a four-dimensional theory. Neither ray evaluates the warped fluctuation determinant, bounds the bulk spectrum, nor shows that a finite dynamical superpotential coefficient survives in a decoupled local theory. The calculation identifies a surface whose classical weight is retained on one specified path in Kähler moduli space.

Exercises

The bounded answers use the conventions in the chapter. Use `benchmark/tasks.json` for the JSON fields and `benchmark/PROTOCOL.md` for submission. Written arguments and interpretations are assessed by a reader.

1. **Change the normal.** Compare E with the product slice S' of Section XIV.10.3. For each, use its geometric normal and K_S to obtain $L^{-1}|_S$, then submit the two surface rows, the vertical cohomology vector and its Euler characteristic. Why is using K_E for the second row a change in the calculation even if it happens to reproduce a correct number elsewhere?

2. **Change the planes.** At the same $p=[0:0:0:1]$, replace the coordinate planes by $Y_2+2Y_4=0$ and $Y_1-Y_2=0$. For each labeled plane, submit the proper-transform class, both Leray rows, the total cohomology, and the number of right-handed deformation doublets. Work with a smooth member of the same Weierstrass family whose pullbacks to these planes are smooth. Explain which monomial condition distinguishes the deformation spaces.

3. **Change a membrane end.** At each of the eight intersection points on the degree-two surface, replace the first row of Table XIV.10.1 by c_{3C} and leave the other four ends unchanged. Submit the residual curve $C_{G,\ell}-C_{\mathrm{ends},\ell}$, its Cartan and rational-section tests, the exponential and insertion charges, and their sum. Also give the residual section period if all ends are omitted. Explain why matching one set of charges does not remove the Bianchi obstruction.

4. **Change the localized spectrum.** At a fixed exceptional divisor, take two independent pairs of masses 3 and -2 with the product orientation of (XIV.10.4). Then take the second mass to zero. Submit the two top coefficients and the neutral arithmetic genus in both situations. Explain which factor was varied and why it is not the full determinant.

5. **Change the Kähler path.** Start at $(a, b) = (9, 4)$ and compare the surface volumes and real exceptional action at $a = 15$ on the fixed-b and fixed-b/a paths. Submit the three normalized volumes at the start and at both endpoints, the cone tests there and at $(4, 9)$, and the real actions in units of π at the three allowed points. What else would you need to infer isolation from either path?

6. **Separate two implications.** Explain in writing why cancellation of the cohomological Bianchi obstruction is neither a neutral mode calculation nor proof of a nonzero term. Use one compact example from the chapter, and state a limitation of the fixed exceptional ray.

Status and sources

§1. Chiral measure. The isolated semiclassical Goldstino interpretation is [GEO-E]; see Witten (1996), arXiv:hep-th/9604030v2, §2, eqs. (2.3)–(2.9). The Berezin coefficients are [MATH] in the specified exterior algebra. This algebra alone does not determine the microscopic fermion action.

§2. Wrapped descriptions and geometry. The M5/E3 interpretation and horizontal distinction are [GEO-E], using the M/F dictionary of Chapter 1 and Witten (1996), v2, §3, printed pp. 14–17. Incidence, base classes, and the flat smooth-member construction are [MATH]. In Witten's printed p. 16 the second Cox exclusion has an extra equation $u = 0$. The incidence charts give the defining open in (XIV.10.12); the extra equation would leave $(0, 0, 0, 1, 1)$ in the quotient. There the direction is undefined and the polynomial in (XIV.10.19) and all its first derivatives vanish on the free $u = v = 1$ chart. The Weierstrass frame uses the Weierstrass convention $\Delta_{\text{book}} = 4f^3 + 27g^2$. The ordinary $\mathbb{P}^2$ ambient bundle is that of Sethi et al. (1996), arXiv:hep-th/9606122v1, §2.2, eqs. (2.3)–(2.12).

§3. Neutral modes. The two relative direct images, four cohomology calculations and surface Riemann–Roch are [MATH]. The unfluxed M5 normal-rotation selection and E3 mode interpretation are [GEO-E], from Witten (1996), v2, §2, eqs. (2.3)–(2.9), and Bianchi et al. (2011), arXiv:1107.3732v2, §3.2–3.4, eqs. (3.17)–(3.20),(3.25)–(3.35). Their duality line L_Q is L here. The right-handed cohomology row refers to the unfluxed operator; flux can change the mode problem.

§4. Sourced Bianchi identity. The M5 action, sign and real-cohomology selection premise are [GEO-E]; the variation and finite curve/weight calculations are [MATH] with the indicated input. See Martucci and Weigand (2015), arXiv:1507.06999v2, §2.1–2.2, eqs. (2.3)–(2.23), and §5.1, eqs. (5.5)–(5.16), Fig. 1 and nn. 13–16. For the exact T_{11} charts and nonvanishing coordinates see Krause et al. (2012), arXiv:1109.3454v2, App. A.2, eqs. (A.11)–(A.19). The potential dressed term is [GEO-E], using the singlet projection in Martucci and Weigand, eq. (5.14), with independently labeled slots and no assumption of a realized flavor tensor or nonzero charged amplitude.

§5. Compact example. The Chern/Euler expansion and pullback periods are [MATH]; the leading zero-flux budget and semiclassical exceptional term are [GEO-E] within their stated backgrounds. See Sethi et al. (1996), v1, §2.2 and §3, and Witten (1996), v2, §3,

for the exceptional contribution. The flux shift follows Chapter 3 and Witten (1997), arXiv:hep-th/9609122v2, eq. (1.2), with the smooth-model comparison in Collinucci and Savelli (2012), arXiv:1011.6388v2, §2–3, eqs. (6)–(12). For the localized simple zero and the prefactor's local frame see Ganor (1997), arXiv:hep-th/9612077v1, §2–2.1, printed pp. 2–4. This is not an evaluation of the determinant at the smooth $j = 0$ example.

§6. Leading action and Kähler ray. The normalized wrapped action and its limit are [GEO-E]; the cone and intersection volumes are [MATH]. The E3 phase and frame use Bianchi et al. (2011), v2, §3, eqs. (3.2)–(3.3), with our ρ_S of opposite sign to their normalized C_4 integral. The M5 phase uses Martucci and Weigand (2015), v2, eq. (2.3); the M5 tension in Planck units agrees with Asano et al. (2025), §2.1, eqs. (2)–(4). The leading string tension uses the standard DBI normalization, and the two metric measures of the radius are those of Chapter 1. No exact quantum action or four-dimensional isolation is inferred.

References

Asano, Y., G. Ishiki, and Y. Yoshida (2025). "Classical BPS M5-Brane on the Plane-Wave Background". In: *PTEP* 2025, 123B09. DOI: 10.1093/ptep/ptaf145.

Bianchi, M., A. Collinucci, and L. Martucci (2011). "Magnetized E3-brane instantons in F-theory". In: *JHEP* 12, p. 045. arXiv: 1107.3732 [hep-th].

Collinucci, A. and R. Savelli (2012). "On Flux Quantization in F-Theory". In: *JHEP* 02, p. 015. arXiv: 1011.6388 [hep-th].

Ganor, O. J. (1997). "A Note On Zeroes Of Superpotentials In F-Theory". In: *Nucl. Phys. B* 499, pp. 55–66. arXiv: hep-th/9612077.

Krause, S., C. Mayrhofer, and T. Weigand (2012). "G4 flux, chiral matter and singularity resolution in F-theory". In: *Nucl. Phys. B* 858, pp. 1–47. arXiv: 1109.3454 [hep-th].

Martucci, L. and T. Weigand (2015). "Hidden Selection Rules, M5-instantons and Fluxes in F-theory". In: *JHEP* 10, p. 131. arXiv: 1507.06999 [hep-th].

Sethi, S., C. Vafa, and E. Witten (1996). "Constraints on low-dimensional string compactifications". In: *Nucl. Phys. B* 480, pp. 213–224. arXiv: hep-th/9606122.

Witten, E. (1996). "Non-Perturbative Superpotentials in String Theory". In: *Nucl. Phys. B* 474, pp. 343–360. arXiv: hep-th/9604030.

Witten, E. (1997). "On Flux Quantization in M-Theory and the Effective Action". In: *J. Geom. Phys.* 22, pp. 1–13. arXiv: hep-th/9609122.

Chapter XIV.11

Completing the $SU(5)$ construction

XIV.11.1 The data already constructed

A gauge field can survive the breaking of a nonabelian group and still acquire a mass. In the quadric model of Chapter 2 we would like to break $SU(5)$ by a field strength along the hypercharge generator. The commutant of that generator includes a $U(1)$, but a compactification also has axions. If any dynamical axion shifts under this $U(1)$, its kinetic term can give the vector a mass without a charged Higgs expectation value. This makes the embedding of the gauge surface relevant even when the field strength is specified entirely on the surface.

We will follow one ruling difference from a line bundle on the surface to a four-cycle in the resolved fourfold. There are two useful normalizations. One comes from an honest $SU(5)$ cocharacter and gives an integral Cartan cycle. The other gives the smallest nontrivial line seen by an off-diagonal root. It removes charged bulk modes in the local calculation. The main question is whether either choice can accompany the chirality background of Chapter 3. To answer it we will need a pairing with inherited divisors, a pairing with a particular matter surface, and an integral quantization test. The three have different domains.

Recall the input. The base is $\mathbb{P}^3$ and the gauge surface S is the smooth quadric $X_0X_3 - X_1X_2 = 0$. The residual Tate coefficients b_5, b_4, b_3, b_2, b_0 give a split I_5 along S. In the affine fiber chart the leading matter equations are $b_5 = 0$ and $P = b_4b_3^2 - b_2b_3b_5 + b_0b_5^2 = 0$. We use the phase-I resolution and its four strict Cartan divisors $D_1, \dots, D_4$. The compact intersection and quantization calculations assume a smooth projective crepant member. The construction of a special curve on S will not prove regularity of every fiber of the associated compact fourfold.

Two results will enter as inputs. Chapter 3 gave an algebraic shifted class G_*, an integral witness $\alpha = G_* + c_2/2$, and the inherited intersection matrix. Chapter 4 identified the complex-oriented common matter surface $V = D_2D_4$ over the smooth ten curve. Its geometric Cartan row is $(1, -1, 1, -1)$; the electric row is the negative of this

vector. Our new calculation will restrict G_* to that surface and push to the curve. We will then compare the resulting line with a line on a local spectral cover.

Keep three other computations separate from this restriction. The smooth-curve example will change a quartic at fixed degree to show why an index does not count pairs. The split-five example uses a different coefficient specialization and a separately chosen starting line, so it has its own matching conditions. The classical Yukawa computation of Chapter 5 uses another specified local coefficient and Higgs system. It gives neither a global space of sections of the lines used here nor their normalized couplings. These distinctions will matter when we ask which outputs can be put together into one background.

XIV.11.2 Hypercharge as a background

Which normalization of hypercharge removes the charged modes on the surface? Begin with the action of the generator itself. Put the three color entries first and the two weak entries last, and use integer charges q for $T = 6Y$:

$$T = \operatorname{diag}(-2,-2,-2,3,3), \qquad T = \sum_{i=1}^{4} t_i \alpha_i^\vee, \qquad t = (-2,-4,-6,-3). \tag{XIV.11.1}$$

Here $\alpha_i^\vee$ is the diagonal matrix with $1, -1$ in positions $i, i+1$. Its coefficient is the sum of the first i entries of T, since those partial sums cancel the intermediate diagonal terms in the expansion. In particular T exponentiates to a circle in the simply connected matrix group. Dividing it by five does not give another cocharacter of that group.

A vector in the fundamental transforms with the charge of its entry; the dual transforms with the opposite charge. A wedge of two fundamental vectors transforms with the sum of their charges. This gives

$$\mathbf{5} = (\mathbf{3},\mathbf{1})_{-2} \oplus (\mathbf{1},\mathbf{2})_{3}, \tag{XIV.11.2}$$

$$\overline{\mathbf{5}} = (\overline{\mathbf{3}},\mathbf{1})_{2} \oplus (\mathbf{1},\mathbf{2})_{-3}, \tag{XIV.11.3}$$

$$\mathbf{10} = (\overline{\mathbf{3}},\mathbf{1})_{-4} \oplus (\mathbf{3},\mathbf{2})_{1} \oplus (\mathbf{1},\mathbf{1})_{6}. \tag{XIV.11.4}$$

There are three ways to take two different color entries, six ways to take one of each kind, and one weak pair. In the adjoint, a matrix entry maps one basis vector to another, so its charge is a difference. Thus the neutral blocks contain dimensions $8+3+1$, and the two rectangular blocks have charges ± 5 and dimension six each:

$$\mathbf{24} = (\mathbf{8},\mathbf{1})_0 \oplus (\mathbf{1},\mathbf{3})_0 \oplus (\mathbf{1},\mathbf{1})_0 \oplus (\mathbf{3},\mathbf{2})_{-5} \oplus (\overline{\mathbf{3}},\mathbf{2})_{5}. \tag{XIV.11.5}$$

The centralizer in the simply connected $SU(5)$ is $S(U(3)\times U(2))$. The determinant constraint links the two block phases. To see the resulting quotient, send (A_3, A_2, z) in $SU(3)\times SU(2)\times U(1)$ to $\operatorname{diag}(z^{-2}A_3, z^3 A_2)$. The map is onto: choose a sixth root of the inverse determinant of the color block and then strip the block phases. Its kernel is

$$(A_3, A_2, z) = (z^2 I_3, z^{-3} I_2, z), \qquad z^6 = 1. \tag{XIV.11.6}$$

This quotient follows from the specified starting matrix group. It does not determine the global form of a compact physical gauge group with further sectors.

The weights also tell us what it means to preserve this subalgebra. In a connection with curvature proportional to T, the internal covariant derivative of an adjoint entry a_{ij} contains the difference of the diagonal connections. In a local line-bundle frame, if $\nabla_L = d + A_L$, then

$$\nabla a_{ij} = da_{ij} + (T_i - T_j)A_L a_{ij}, \qquad \nabla^2 a_{ij} = (T_i - T_j)F_L a_{ij}. \tag{XIV.11.7}$$

In particular a block generator can be covariantly constant while the off-diagonal entries see a magnetic field. A covariantly constant off-diagonal section would have to be annihilated by that curvature, which a nonzero parallel section cannot be if the corresponding curvature is nonzero. This is the local breaking mechanism. The axion charge of the remaining diagonal generator is a separate question because it depends on fields that propagate outside the seven-brane.

On $S = \mathbb{P}^1_u \times \mathbb{P}^1_v$, write u, v for the two pulled-back point classes. For a line $\mathcal{O}_S(a, b)$ these are its first Chern class coordinates. Write $h = u + v = H|_S$ and choose $L = \mathcal{O}_S(1, -1)$ with $f = c_1(L)$. The basic intersections and normal data are

$$\begin{aligned} &u^2 = v^2 = 0, \qquad \int_S uv = 1, \qquad f^2 = -2, \\ &K_S = \mathcal{O}_S(-2, -2), \qquad N_{S/\mathbb{P}^3} = \mathcal{O}_S(2, 2). \end{aligned} \tag{XIV.11.8}$$

The normal class is the degree-two equation restricted to S. Adjunction gives the canonical class by adding it to $-4h$. The two bundles enter different constructions below.

An honest flux along T gives each fundamental component the line associated to its charge. The bundle and its determinant are therefore

$$E = (L^{-2})^{\oplus 3} \oplus (L^3)^{\oplus 2}, \qquad \det E = L^{-6+6} = \mathcal{O}_S. \tag{XIV.11.9}$$

The charged roots see the Hom lines $L^{\pm 5}$. To relate this holomorphic bundle to the local gauge equations, let the polarization be $J_S = au + bv$, with $a, b > 0$. The slope of a line L^m, in a convention without dividing by volume, is

$$\mu_{J_S}(L^m) = \int_S J_S c_1(L^m) = m(b - a). \tag{XIV.11.10}$$

For $a = b$ the summands of E have the same zero slope. The split bundle is polystable for the ordinary zero-Higgs problem. For $(a, b) = (1, 2)$ the color and weak slopes are $-2, 3$; their weighted sum still vanishes. That cancellation in the determinant does not solve the individual slope conditions. The holomorphic cohomology calculated next is unchanged when the polarization changes.

There is a direct realization of the slope comparison at the level of differential forms on the product. Take the volume forms ω_u, ω_v on the two factors normalized to have integral one, pull them back to S, and use the product polarization. In the convention $c_1(L) = [iF_L/(2\pi)]$, the product of the unit monopole and its inverse has

$$\frac{iF_L}{2\pi} = \omega_u - \omega_v, \qquad J_S \wedge \frac{iF_L}{2\pi} = (b - a)\omega_u \wedge \omega_v. \tag{XIV.11.11}$$

This flux is of type $(1,1)$ and is primitive at equal areas. Tensor powers multiply both terms by the same integer. With unequal areas one cannot correct the nonzero integrated slope by changing the Hermitian metric on the same holomorphic summand. This local product construction explains why the induced polarization is useful, but it is a statement about the surface equation at zero Higgs field. It does not solve the fourfold primitivity equations.

The surface twist with zero Higgs field associates bulk chiral fields to $H^1(S,M)$ and $H^0(S,K_S\otimes M)$, and vector fields to $H^0(S,M)$, for a given adjoint line M. Take $M=L^k$ for $k\geq 1$. One projective line contributes sections of $\mathcal{O}(k)$ and the other contributes $H^1(\mathcal{O}(-k))$. Serre duality on $\mathbb{P}^1$ turns the latter into the dual of sections of $\mathcal{O}(k-2)$:

$$h^0(\mathbb{P}^1,\mathcal{O}(k))=k+1, \qquad h^1(\mathbb{P}^1,\mathcal{O}(-k))=k-1, \tag{XIV.11.12}$$

$$h^1(S,L^k)=(k+1)(k-1), \tag{XIV.11.13}$$

$$h^0(S,L^k)=h^2(S,L^k)=h^0(S,K_S\otimes L^k)=0. \tag{XIV.11.14}$$

In the last line the negative degree prevents H^0; for H^2, the nonnegative factor has no H^1. Interchanging the two projective lines gives the same dimensions for L^{-k}. The adjoint branching now has a useful test: $k=1$ gives no charged bulk fields of this type, $k=2$ gives three copies of each charged representation, and $k=5$ gives twenty-four copies of each. These are copies of the six-dimensional representations in (XIV.11.5), not counts obtained by interpreting every matrix entry as an independent copy. The two signs contribute in conjugate pairs in this ordinary zero-Higgs interpretation.

Can we use the first root size in a split rank-five $SU(5)$ bundle? If the common color and weak line classes are a_c,a_w, the determinant condition and the color-to-weak charge difference require

$$3a_c+2a_w=0, \qquad a_c-a_w=-f \quad\Longrightarrow\quad a_c=-2f/5, \qquad a_w=3f/5. \tag{XIV.11.15}$$

The primitive class f has no fifth root in $\mathrm{Pic}(S)\simeq\mathbb{Z}^2$. This prevents the proposed standalone bundle. It still makes sense to compare two integral component lines on a curve by a relative factor $L|_C$ when their T-charges differ by five. That comparison assigns no fractional bundle to an individual weight. Figure XIV.11.1 shows why the distinction matters: the charge gap determines the line seen by a root, whereas the determinant constrains both block lines.

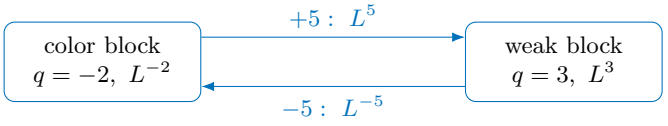


Figure XIV.11.1: The two charge blocks of the fundamental and the two oppositely directed Hom lines. The arrows show the charge of the target minus that of the source.

A compact flux could in principle use additional data to satisfy quantization without a standalone split bundle of root size one. The next step is to construct the integral cocharacter cycle and determine what the compact geometry can measure about it.

XIV.11.3 Masslessness and ambient pushforward

When does the ambient geometry detect the ruling difference? Use the Segre coordinates

$$(X_0, X_1, X_2, X_3) = (u_0 v_0, u_1 v_0, u_0 v_1, u_1 v_1). \tag{XIV.11.16}$$

The divisor u is a fixed point of the first projective line times the second line, and v is the opposite ruling. Their images in the base are both lines, so both represent the generator of $\mathrm{CH}_1(\mathbb{P}^3)$. Writing $i : S \hookrightarrow \mathbb{P}^3$, we obtain

$$i_* \,\mathrm{PD}_S(f) = [\text{line}] - [\text{line}] = 0, \qquad \left(\int_S f u, \int_S f v\right) = (-1, 1). \tag{XIV.11.17}$$

The first equality holds already for integral cycles modulo rational equivalence. The second shows how the surface itself detects f. Inherited divisor classes on S are multiples of h, for which the two periods cancel.

In the ordinary classical reduction, the coupling of a bulk two-form to the four-dimensional field strength is linear in $\int_S i^* \omega_\alpha f$ for the inherited two-form classes ω_α. The trace along the generator is nonzero:

$$\mathrm{tr}_{\mathbf{5}}\, T^2 = 3 \cdot 4 + 2 \cdot 9 = 30, \qquad Q_\alpha \;\propto\; 30 \int_S i^* \omega_\alpha f. \tag{XIV.11.18}$$

After dualizing the two-forms, the axion kinetic terms have the form $g_{\alpha\beta}(da^\alpha + Q^\alpha A)(da^\beta + Q^\beta A)$ in an axion basis. A positive metric on these dynamical axions gives zero vector mass from this mechanism precisely for the vanishing charge vector. Equation (XIV.11.17) makes that vector vanish in the inherited $\mathbb{P}^3$ sector. It does not replace the other conditions on a compact background.

The distinction can also be seen without dualizing explicitly. In a basis of normalized vector kinetic terms, the quadratic mass associated to one gauged direction is proportional to $Q^{\mathsf{T}} g Q$. After diagonalizing g with positive eigenvalues g_α,

$$Q^{\mathsf{T}} g Q = \sum_\alpha g_\alpha |Q'_\alpha|^2. \tag{XIV.11.19}$$

Opposite charges for two independent axions do not cancel in this expression. The cancellation in the quadric model takes place earlier, in the period of one inherited class, since $i^* H = u + v$. In the ruled comparison the independent periods do not first add to a single charge. The distinction is between the linear map that defines Q and the positive quadratic map that sets the mass.

The normal bundle alone cannot predict this kernel. For comparison put the same S in $B' = \mathbb{P}_{\text{lines}}(\mathcal{O} \oplus \mathcal{O}(2,2))$ as the section of lines in the first summand. Its normal line is the Hom from the first summand to the second, $\mathcal{O}(2,2)$. But $p : B' \to S$ is a retraction of the section i', so

$$p_* i'_* = \mathrm{id} \quad \text{on curve cycles}, \qquad \int_{i'_*\,\mathrm{PD}_S(f)} (p^* u, p^* v) = (-1, 1). \tag{XIV.11.20}$$

Now the ambient space measures both periods. This is a comparison of two embeddings with the same normal line. It neither transports the Tate coefficients to the ruled base nor assumes that the compact theories have the same spectra.

To lift f to the resolved fourfold, let $j_i : D_i \hookrightarrow \widetilde{Y}$ be the inclusion and $p_i : D_i \to S$ the projection. Above a generic point of S, the four divisors supply the four simple exceptional curves of the split fiber. Sweeping the i-th curve over each of the two rulings and taking the difference produces a surface class. The precise definition uses Cartier intersection:

$$\Gamma_i(a) = (j_i)_*\big(c_1(p_i^*\mathcal{O}_S(a)) \cap [D_i]\big), \qquad a \in \mathrm{Pic}(S). \tag{XIV.11.21}$$

For $a = f$ this is the difference of two integral algebraic cycles. Pullback here is the pullback of a line bundle followed by capping with the divisor cycle. The definition does not need a smooth D_i or a flat fibration over every point of S.

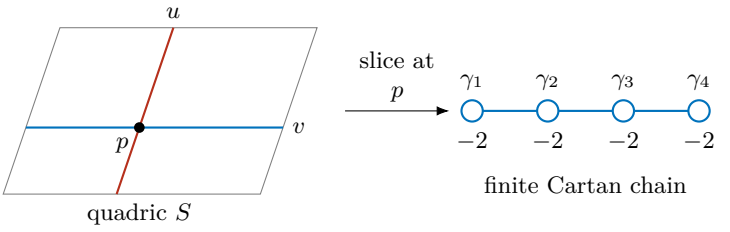


Figure XIV.11.2: Two transverse rulings on the quadric meet at a generic point of S. Over that point the Cartan fiber curves are paired in an elliptic surface slice. Two distinct representatives of a single ruling can be made disjoint, and the two opposite-ruling terms enter the square of the difference with minus signs.

To compute the pairing, first choose two ruling representatives with transverse intersections away from all enhanced points. Moving inside each ruling system permits this choice; two different representatives of the same ruling can be made disjoint. At a crossing of opposite rulings, intersect the two pulled-back base equations first. The remaining intersection is the pairing of the two exceptional curves on the ordinary elliptic surface normal slice. The self-intersection of a simple exceptional curve is -2; adjacent curves meet once and nonadjacent curves miss each other. Thus with A_4 the positive Cartan matrix,

$$\Gamma_i(a) \cdot \Gamma_j(b) = -(A_4)_{ij} \int_S ab, \qquad \big(\Gamma_i(f) \cdot \Gamma_j(f)\big) = 2A_4. \tag{XIV.11.22}$$

The sign in the second identity comes from two signs: the surface pairing is negative on the simple roots, and the two cross terms in f^2 give -2. Bilinearity proves the formula from the moved ruling calculation. A crossing in the base alone would supply only the multiplicity $\int_S ab$; it would miss the Cartan matrix.

We now use the electric convention to fix the sign of the four-cycle. If γ_w has

geometric Cartan row d_w, its T-charge is $-t \cdot d_w$. Define

$$K = \sum_{i=1}^{4} (-t_i)\Gamma_i(f), \qquad -t = (2, 4, 6, 3). \tag{XIV.11.23}$$

For the push to S, test the restriction of K to each D_i against the two rulings. Applying the slice argument again gives

$$\big((p_i)_*(j_i^* K)\big)_{i=1}^{4} = -A_4(-t)\, f = (0, 0, -5, 0)\, f. \tag{XIV.11.24}$$

The push is written in the geometric convention. It vanishes for the simple directions within the two blocks and measures the full root gap for the direction joining them. Pairing it with h would give zero in all four positions. That weaker compact test would lose the third component. The square tests the same nonzero direction:

$$K^2 = 2\, t^{\mathsf{T}} A_4 t = 2\,(2, 4, 6, 3) \cdot (0, 0, 5, 0) = 60. \tag{XIV.11.25}$$

For a concrete period test, consider the third Cartan over a curve of class u. The two terms from K are weighted by the third row of $-A_4$, and the curve period of f is -1. Over v the same local row is weighted by $+1$:

$$\int_{\Gamma_3(u)} K = +5, \qquad \int_{\Gamma_3(v)} K = -5, \qquad \int_{\Gamma_3(h)} K = 0. \tag{XIV.11.26}$$

The last cycle uses both rulings. The opposite signs are periods on two complex-oriented surfaces; no individual surface orientation has been reversed. These are enough to see how a nonzero root flux may be invisible to the compact inherited base test.

We need a stronger vanishing than the four HD_i tests: the mixed products with all inherited divisor pairs, including those of two Cartans. Work in the ambient projective bundle after its four coordinate blowups, and call the strict ambient exceptional divisors T_i. On the stipulated ordinary phase-I member the Cartans are their proper restrictions. In cycle notation in the ambient space,

$$[D_i] = [T_i] \cap [\widetilde{Y}]. \tag{XIV.11.27}$$

The restriction is the Cartier intersection with the proper cubic; in the ordinary strict Cartan geometry it is the indicated divisor, with multiplicity one. In particular the enhanced fibers are not extra components of this ambient divisor restriction.

Let P_2 be a degree-two polynomial in the inherited ambient divisor classes. These are H, the cubic class $r = [W = 0]$, and the total exceptional classes A, B, C, and D. Write $\widehat{p}_i : T_i \to S$ for the ambient map. Equations (XIV.11.21) and (XIV.11.27) let us push the product down before applying f:

$$\int_{\widetilde{Y}} \Gamma_i(f) P_2 = \int_S f\, \rho_i(P_2), \qquad \rho_i(P_2) = (\widehat{p}_i)_*\big(P_2[\widetilde{Y}] \cap [T_i]\big). \tag{XIV.11.28}$$

Here $\rho_i(P_2)$ is a divisor class on S. Transposition of the Segre matrix exchanges the two rulings. It is linear on $\mathbb{P}^3$ and preserves the determinant equation. It lifts to the

ambient bundle since its coordinate lines are powers of H, and to each blowup because the coordinate centers are preserved. It fixes all six ambient divisor classes and the proper cubic class. Equivariance of proper pushforward therefore fixes $\rho_i(P_2)$ under $u \leftrightarrow v$, even if transposition changes the chosen Tate coefficients. The formula uses the class of the hypersurface and does not require an automorphism of the hypersurface. We get

$$\rho_i(P_2) = m_i h, \qquad \int_{\widetilde{Y}} \Gamma_i(f) P_2 = m_i \int_S (u-v)(u+v) = 0. \tag{XIV.11.29}$$

There is a small additional step for the zero section Z. In the ordinary cubic, $W = 0$ implies $x = 0$ on the fiber, leaving the section in the chart with $y \neq 0$. In that chart the cubic has W times a unit equal to x^3, so W cuts the section with multiplicity three. The centers lie off this chart near the section. Thus

$$r|_{\widetilde{Y}} = 3[Z], \qquad Z = \tfrac{1}{3} r|_{\widetilde{Y}} \quad \text{in rational Chow.} \tag{XIV.11.30}$$

This gives an ambient rational representative for the actual integral section. It does not make $r/3$ an integral ambient class. The inherited products H^2, ZH, HD_i, D_iD_j now all have zero K-pairing by (XIV.11.29). The Chern polynomial of the fourfold also comes from this ambient ring by the coordinate blowup factors and adjunction. Since G_* is built from these products and $c_2/2$, the result includes

$$G_* \cdot K = 0. \tag{XIV.11.31}$$

In particular the inherited test for G_* and the one for K do not conceal the same local Cartan data. The class G_* has an ambient polynomial representative. Its local Cartan push is $\rho_i(G_*^{\mathrm{amb}})$, hence lies in $\mathbb{Q}h$ by the same transposition argument. The inherited HD_i moment is zero and $h^2 = 2$, so the coefficient of h is zero. In contrast K has the antisymmetric push in (XIV.11.24). For the sum $G_k = G_* + kK$ we can therefore write

$$(p_i)_*(j_i^* G_*) = 0, \qquad \big((p_i)_*(j_i^* G_k)\big)_{i=1}^4 = k(0,0,-5,0) f. \tag{XIV.11.32}$$

The vanishing inherited test for G_k measures neither the separate coefficients in the local Cartan push nor the class on a single split matter component.

This is an orthogonality statement for the named classes. Arbitrary extra vertical classes need not come from invariant ambient polynomials. Indeed K cannot itself be in the rational span of the tested products: it would then have zero square, contrary to (XIV.11.25). A matter restriction will exhibit directly what the inherited tests leave undetermined.

XIV.11.4 Splitting the matter spectrum

What line does the shared ten weight see, and which part of a matter count does it determine? First we must compute a divisor on the matter curve. Integrating it would give a number, but would discard the distinction between line classes of the same degree.

Then we will choose other lines explicitly to see how a change invisible to the degree can alter the cohomology.

Use r for the cubic coordinate class, and A, B, C, D for the total exceptional classes in the order of the blowups. The original x, y classes are $r+8H, r+12H$. The strict Cartans have classes $A-B, C-D, D, B-C$. The common ambient locus $W_0 = (e_2 = e_4 = 0)$ lies in the $W = 1$ chart, where $r = 0$. In the first exceptional plane the third center eventually selects the direction $[x_1 : y_1 : w_1] = [0 : 0 : 1]$. This is the line of class $2h$ in the first normal bundle, since it is the direction of the quadric equation w. The first exceptional normal is tautological, so $A|_{W_0} = 2h$.

At the second blowup the normal directions are cut by $y_1 = 0$ and $e_1 = 0$. They are transverse coordinate divisors. The classes of their normal lines on the selected section are $12h - 2h = 10h$ and $2h$. This is a split normal bundle: for a transverse complete intersection, the two defining equations give the direct sum description of its conormal, and dualizing gives the two lines. The remaining projective directions $[y_1 : e_1]$ therefore give

$$p : W_0 \simeq \mathbb{P}_{\text{lines}}\big(\mathcal{O}_S(10h) \oplus \mathcal{O}_S(2h)\big) \longrightarrow S, \qquad B|_{W_0} = c_1\big(\mathcal{O}_{W_0}(-1)\big). \quad \text{(XIV.11.33)}$$

Figure XIV.11.3 locates the two lines and the directions chosen in the last two blowups. In the third exceptional line the strict second divisor meets it at $[x_1 : e_4] = [1 : 0]$. This keeps every second exceptional direction. The fourth center meets this locus at the Cartier section where the current y vanishes. Blowing up a Cartier divisor on the relative line leaves it isomorphic to the original relative line. On its strict transform the direction of that last blowup is the y direction. Thus the final strict x, y never vanish there. Their classes on W_0 are respectively $6h - C$ and $10h - B - D$, which proves

$$r = 0, \qquad A = 2h, \qquad C = 6h, \qquad D = 10h - B \quad \text{on } W_0. \qquad \text{(XIV.11.34)}$$

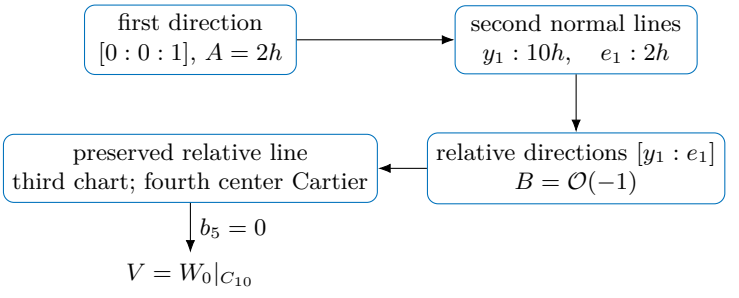


Figure XIV.11.3: The first selected direction sets the class of A. The two normal lines at the second center give the full projective line of directions. The third direction and fourth Cartier modification preserve that relative line. The last cut restricts its base to C_{10}.

The two projections of the tautological line to the summands in (XIV.11.33) cannot vanish simultaneously. Their divisor product vanishes, giving the projective-bundle

relation. The degree of B on the fiber is -1:

$$(B-10h)(B-2h)=0, \qquad p_*1=0, \qquad p_*B=-1. \tag{XIV.11.35}$$

On substituting (XIV.11.34) the four Cartans restrict as

$$(D_1,D_2,D_3,D_4)|_{W_0}=(2h-B,\ B-4h,\ 10h-B,\ B-6h). \tag{XIV.11.36}$$

Their fiber degrees give $(1,-1,1,-1)$, as expected for the common weight. The h terms in the same expressions are essential for the Chow calculation. They do not enter the fiber row.

The proper Tate polynomial on the common locus is b_5xy. To see the origin of this cut, use the total transform

$$(x_{\text{old}},y_{\text{old}},w_{\text{old}})=\big(xe_1e_4e_2^2e_3^2,\ ye_1e_4^2e_2^2e_3^3,\ e_0e_1e_2e_3e_4\big). \tag{XIV.11.37}$$

After the common exceptional factor is removed, all terms other than b_5xy still contain e_2 or e_4. Since x,y are units here, the cut is exactly the pullback of $b_5=0$. The curve is smooth and the cut has multiplicity one. This identifies V as the restriction of W_0 over C_{10}, with no additional vertical component in this common stratum.

We can now do the Chern calculation directly on W_0. For a blowup with exceptional class E and normal divisor classes z_j of its center, the multiplicative Chern factor is

$$(1+E)\prod_{j=1}^{k}\frac{1+z_j-E}{1+z_j}. \tag{XIV.11.38}$$

For the degree-two Newton sum this adds $E^2+\sum_j[(z_j-E)^2-z_j^2]=(k+1)E^2-2E\sum_j z_j$. The initial Chern roots restricted to W_0 are four h's and $0,8h,12h$, from the base and cubic bundle. The four ordered center lists on restriction and their contributions are

E	$(z_j)\|_{W_0}$	Δp_2
$2h$	$(8h,12h,2h)$	$-72h^2$
B	$(10h,2h)$	$3B^2-24Bh$
$6h$	$(6h,B)$	$-12Bh+36h^2$
$10h-B$	$(10h-B,6h)$	$B^2-8Bh-20h^2$.

(XIV.11.39)

The normal lists are taken in the spaces at the respective blowups, with their classes then pulled back. For example, the second list comes from $r+12H-A,A$; substituting the final strict y at that earlier stage would erase the $10h$.

Adjunction for the proper hypersurface subtracts its class $3r+24H-2A-B-C-D$, which restricts to $4h$. The resulting virtual first Newton sum is zero. Adding (XIV.11.39) to the initial $212h^2$ and subtracting $16h^2$ gives

$$p_2|_{W_0}=4B^2-44Bh+140h^2=4Bh+60h^2, \tag{XIV.11.40}$$

$$c_2|_{W_0}=-\tfrac{1}{2}p_2|_{W_0}=-2Bh-30h^2. \tag{XIV.11.41}$$

The last equality in the first line uses $B^2=12Bh-20h^2$. Here $c_2|_{W_0}$ denotes evaluation of the ambient polynomial for $c_2(\widetilde{Y})$; its restriction to V is the actual restricted Chern class.

For the witness α, the ambient expression uses the vector $(91, 24, -12, -18, -30, -14)$ on $H^2, ZH, HD_1, \dots, HD_4$, and a further term $-2D_2D_4$. The section term drops because $r = 0$. The linear Cartan terms give $10Bh - 168h^2$ before $91h^2$ is added. Inserting the last term gives

$$\begin{aligned}\alpha|_{W_0} &= 10Bh - 77h^2 - 2(B - 4h)(B - 6h)\\ &= -2B^2 + 30Bh - 125h^2 = 6Bh - 85h^2.\end{aligned} \tag{XIV.11.42}$$

Only terms proportional to B survive the relative push. The projective bundle restricts to C_{10} with the same relation and tautological line, so the push commutes with this restriction:

$$p_*c_2 = 2h, \qquad p_*\alpha = -6h, \qquad p_*(\alpha - c_2/2) = -7h. \tag{XIV.11.43}$$

To check the sensitivity to the normal lines, keep the same two degree conventions and test the counterfactual relation $(B - 10h)(B + 2h) = 0$ in the push computation. It changes B^2 to $8Bh+20h^2$, so the unreduced expressions in (XIV.11.41) and (XIV.11.42) give pushes $-6h$ and $-14h$ for c_2, α. The resulting $-11h$ disagrees with (XIV.11.43). This calculation changes the projective-bundle reduction; it does not supply another compact Tate resolution. The fiber row would be the same in this test because the degree of B is unchanged.

The divisor $-7h|_{C_{10}}$ has degree -56, recovering the earlier period. It also specifies the representative $\mathcal{O}_C(-7, -7)$ in rational Chow, with $C = C_{10}$. Now choose ruling representatives meeting C transversely away from the further enhancements. The restriction of $\Gamma_i(a)$ to V pushes to $a|_C$ times the i-th shared fiber degree, by intersecting each ruling with C before taking the fiber pairing. The K-correction is therefore

$$(2, 4, 6, 3) \cdot (1, -1, 1, -1) = 1, \qquad (p|_V)_*(K|_V) = f|_C. \tag{XIV.11.44}$$

The integral representative for the resulting rational Chow line class of $G_* + K$ is $\mathcal{O}_C(-6, -8)$. The spin line enters once: by adjunction $K_C = \mathcal{O}_C(2, 2)$, and we choose $\Theta = \mathcal{O}_C(1, 1)$. On the smooth curve of bidegree $(4, 4)$, the degree of $\mathcal{O}_C(a, b)$ is $4(a + b)$ and the genus is nine. Thus

$$M_{\mathrm{sh}} = \Theta \otimes \mathcal{O}_C(-6, -8) = \mathcal{O}_C(-5, -7), \tag{XIV.11.45}$$

$$\deg M_{\mathrm{sh}} = -48, \qquad (h^0, h^1)(C, M_{\mathrm{sh}}) = (0, 56). \tag{XIV.11.46}$$

There are no sections at negative degree and the index is $-48 + 1 - 9 = -56$. The smooth defect dictionary would assign the two cohomologies to a representation and its conjugate given a compatible refined background. This calculation supplies a Chow representative and its cohomology. It does not fix a differential lift or all the component lines. For example $\Theta \otimes \mathcal{O}_C(-7, -7) \otimes L|_C^q$ at the other ten weights is an explicit comparison ansatz, giving the same degree and cohomology, not an induced compact pushforward for those weights.

More generally, if a smooth matter support has class (d_u, d_v), the flux degrees from this ruling difference obey

$$\begin{aligned}\deg(L|_C) &= \int_S (u - v)(d_u u + d_v v) = d_v - d_u,\\ \chi(M \otimes L|_C^q) - \chi(M) &= q(d_v - d_u).\end{aligned} \tag{XIV.11.47}$$

The second equality is Riemann–Roch for a line M on that curve. A diagonal support cannot show the splitting in its degree even when a particular representative changes. A nondiagonal component, such as one of the graphs below, can respond in degree as well. On a union the total degree adds those contributions, but the sections must still agree at intersections. A zero degree change on the full support is therefore compatible both with nonzero changes on individual components and with rank changes at fixed degree.

To see how a degree-zero difference can affect matter pairs, choose a new baseline Θ, without the negative-degree factor just computed. Take the actual quartic $b_5 = X_0^4 + X_1^4 + X_2^4 + 2X_3^4 + \epsilon X_0^2 X_3^2$. With $x = u_1/u_0,\ y = v_1/v_0$ now base coordinates, its Segre restriction is

$$F_\epsilon = 1 + x^4 + y^4 + 2x^4y^4 + \epsilon x^2y^2, \qquad \epsilon = 0, 1. \tag{XIV.11.48}$$

Both curves are smooth. On a boundary of the torus the remaining coordinate satisfies a quartic with simple nonzero roots; at the four corners the constant coefficient in the corresponding chart is nonzero. In the torus set $a = x^2, b = y^2$. The two derivative equations, multiplied by a, b and subtracted, imply $a^2 = b^2$. If $b = sa$, $s = \pm 1$, a critical point has $a^2 = -(2 + \epsilon s)/4$ and hence

$$F_\epsilon = 1 - (2 + \epsilon s)^2/8 \neq 0. \tag{XIV.11.49}$$

Replacing the coefficient 2 of x^4y^4 by 1 at $\epsilon = 0$ instead gives $(1 + x^4)(1 + y^4)$, a reducible curve with crossings. It is outside the smooth calculation.

Write $M_q = \Theta \otimes L|_C^q = \mathcal{O}_C(1 + q, 1 - q)$. All these lines have degree eight, so Riemann–Roch only gives $h^0 = h^1$. To determine both dimensions, use the divisor exact sequence on S:

$$0 \longrightarrow \mathcal{O}_S(a - 4, b - 4) \xrightarrow{F_\epsilon} \mathcal{O}_S(a, b) \longrightarrow \mathcal{O}_C(a, b) \longrightarrow 0. \tag{XIV.11.50}$$

In the two affine charts of $\mathbb{P}^1$, a negative degree $m \leq -2$ contributes the Laurent classes with exponents $m + 1, \ldots, -1$ to H^1. Terms outside that range are coboundaries. A nonnegative degree n contributes the ordinary powers $0, \ldots, n$ to H^0. Taking products of these bases determines the two possible H^1 blocks on S. To form the map one multiplies by F_ϵ and keeps only the monomials in the target block.

For $q = -4$, the map is from $H^1(\mathcal{O}_S(-7, 1))$ to $H^1(\mathcal{O}_S(-3, 5))$. Both spaces have dimension twelve. Each target x exponent $j = -2, -1$ receives independent source terms from $j, j - 4, j - 2$ with coefficients $1 + y^4,\ 1 + 2y^4,\ \epsilon y^2$. Each source is a linear polynomial in y. The first two groups span $1, y, y^4, y^5$; the third adds y^2, y^3 when $\epsilon = 1$. The two target exponents use disjoint source exponents. Thus

$$\operatorname{rk}\bigl(H^1(-7, 1) \to H^1(-3, 5)\bigr) = \begin{cases} 8 & \epsilon = 0, \\ 12 & \epsilon = 1. \end{cases} \tag{XIV.11.51}$$

The neighboring H^0 spaces vanish, so the kernel gives four or zero sections.

For the $q = 6$ line we can compute the $q = -6$ case instead: the swap $x \leftrightarrow y$ is a symmetry of these quartics and exchanges the two bidegrees. Equivalently Serre duality interchanges $h^0(M_{-6})$ and $h^1(M_6)$, which here equal $h^0(M_6)$. For $q = -6$, the

H^1 map is from $(-9,3)$ to $(-5,7)$, of size 32 by 32. At $\epsilon = 0$ each target x exponent independently receives cubics in y multiplied by $1+y^4$ and $1+2y^4$. Their images span all degrees $0,\dots,7$, giving rank 32. At $\epsilon = 1$ split by the parity of x and y. There are four identical blocks. With $z = y^2$, write the four source polynomials A_0, B_0, C_0, D_0, each of degree at most one in z, in ascending x order. The two target x exponents give the kernel equations

$$(1+2z^2)A_0 + zB_0 + (1+z^2)C_0 = 0, \tag{XIV.11.52}$$

$$(1+2z^2)B_0 + zC_0 + (1+z^2)D_0 = 0. \tag{XIV.11.53}$$

The constant and cubic coefficients imply $C_{0,0} = -A_{0,0},\ C_{0,1} = -2A_{0,1}$ and $D_{0,0} = -B_{0,0},\ D_{0,1} = -2B_{0,1}$, where the second subscript denotes the power of z. The first quadratic and the second linear coefficients then give $B_{0,1} = -A_{0,0}$ and $B_{0,1} = C_{0,0}$. The first linear and second quadratic coefficients give $B_{0,0} = A_{0,1}$ and $B_{0,0} = 2A_{0,1}$; these force both to zero. The kernel in each block is therefore the span of $(1, -z, -1, 2z)$, and the rank is $4 \cdot 7 = 28$. This time the perturbed curve gains four sections. A matrix of the same size need not retain its rank when the map is changed.

For $q = 1$, the target line on S is $\mathcal{O}_S(2,0)$. Its three sections restrict isomorphically on H^0, since $\mathcal{O}_S(-2,-4)$ has no H^0 or H^1. The same argument with the exchanged rulings, or with $\mathcal{O}_S(1,1)$, gives $h^0(M_{-1}) = 3$ and $h^0(M_0) = 4$. In particular the complete comparison at the three cocharacter weights is

	$q=-4$	$q=1$	$q=6$
$\epsilon = 0$	$(4,4)$	$(3,3)$	$(0,0)$
$\epsilon = 1$	$(0,0)$	$(3,3)$	$(4,4)$

(XIV.11.54)

If we use root-sized relative differences and anchor the $q = 1$ line at Θ, the twists are $L|_C^{-1}, \mathcal{O}_C, L|_C$, with counts $(3,3),(4,4),(3,3)$. All entries in (XIV.11.54) have the same index. Neither these entries nor the root-sized comparison can be substituted for (XIV.11.46); the baseline line in that calculation has degree -48.

The three calculations on the ten curve may now be compared without identifying their inputs. For the shared weight, the common shift by $-7h$ comes from the compact intersection. The new rank calculation removes that common shift as a choice of starting line, and so lands at degree $g - 1 = 8$, where sections and their duals can coexist. For the root-sized comparison, the charge differences are divided by five only after choosing the line at $q = 1$. In formulas the respective assignments are

$$\text{shared weight only:} \quad \mathcal{O}_C(-5,-7), \tag{XIV.11.55}$$

$$\text{cocharacter comparison:} \quad \Theta \otimes L|_C^{q}, \tag{XIV.11.56}$$

$$\text{root-sized comparison:} \quad \Theta \otimes L|_C^{(q-1)/5}, \qquad q = -4, 1, 6. \tag{XIV.11.57}$$

In the last line the exponent is always integral, although $q/5$ is not. This is the curve version of the distinction between assigning relative twists and constructing a rank-five split bundle. The choices in the last two lines are useful calculations of possible line cohomology. Neither asserts the corresponding compact background.

We next change the support, not just a smooth-curve multiplication map. The actual homogeneous cubic

$$R = X_0^2 X_3 - 2X_1^3 - X_2^3 + 2X_0 X_3^2 \tag{XIV.11.58}$$

restricts to $(x - y^2)(y - 2x^2)$ in the finite Segre chart. Its two components D_A, D_B are graphs isomorphic to $\mathbb{P}^1$, of classes $(1,2), (2,1)$, respectively. Setting $b_3 = Rc_3,\ b_2 = Rc_2,\ b_0 = Rc_0$ with c_3, c_2, c_0 of degrees $5, 7, 11$ respects the Tate section classes. The five equation factors as

$$P = R\{R(b_4 c_3^2 - c_2 c_3 b_5) + c_0 b_5^2\}. \tag{XIV.11.59}$$

For general remaining coefficients the residual does not contain either graph: on each, its equation restricts to $c_0 b_5^2$, not identically zero. The residual class is $(19, 19)$, since P has degree 22 and R degree 3. The f-periods on the graphs are $1, -1$, and on the residual are zero. Their sum vanishes, even though the graph degrees respond with opposite signs. We will compute on the graph union $D_{\mathrm{gr}} = D_A \cup D_B$, without matching to the residual or assuming the entire tuned fourfold is regular.

In the finite chart the intersections satisfy $y - 2y^4 = 0,\ x = y^2$. The four roots are distinct, with derivative 1 at zero and -3 at the nonzero roots. At the point at infinity use $x' = 1/x,\ y' = 1/y$. The equations become $x' = y'^2,\ y' = x'^2/2$, with independent linear parts. The finite intersections and infinity exhaust the intersection product $(1,2) \cdot (2,1) = 5$. The normalization therefore has two rational branches with five transverse nodes, giving arithmetic genus $5 - 2 + 1 = 4$. Figure XIV.11.4 gives both the parameterization and the two types of matching conditions.

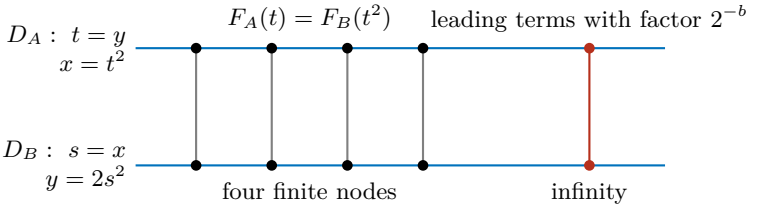


Figure XIV.11.4: The two normalized graph components, with four identifications in the finite chart and one at infinity. Each joining segment stands for one condition on the common fiber of the restricted ambient line, not for a new component of the curve.

An ambient line $\mathcal{O}_S(a, b)$ gives branch degrees $d_A = 2a + b,\ d_B = a + 2b$. Use the coordinates $t = y$ on D_A, $s = x$ on D_B, so $x = t^2$ and $y = 2s^2$ respectively. A section on the normalization is given by polynomials $F_A(t), F_B(s)$ bounded by the two degrees, with zero section on a branch of negative degree. The common finite frame is the one from $u_0^a v_0^b$. In the infinity frame $u_1^a v_1^b$, the polynomial is multiplied by $x^{-a} y^{-b}$. Its value at infinity is the degree-d_A coefficient on D_A, and 2^{-b} times the degree-d_B coefficient on D_B. Thus the five conditions are

$$F_A(t) = F_B(t^2) \quad (t - 2t^4 = 0), \qquad [t^{d_A}]F_A = 2^{-b}[s^{d_B}]F_B. \tag{XIV.11.60}$$

The infinity condition uses the actual transition factor. It is part of the gluing even when four finite conditions are already imposed.

Prescribe the already twisted $\overline{\mathbf{5}}$ triplet line $\mathcal{O}_{D_{\mathrm{gr}}}(2,-1)$. Its degrees are $(3,0)$; the finite conditions force F_A equal to the constant F_B, since a cubic vanishing at four distinct points is zero. The left side of the infinity condition is then zero, so the constant also vanishes. This proves the rank-five matching map for the triplet. The relative doublet charge is -5; at root size one the twist is $-f$, and the line has $(a,b)=(1,0)$. The finite conditions now force $F_A(t)=F_B(t^2)$ as polynomials of degree at most two. The infinity condition holds automatically because $b=0$, leaving both coefficients of F_B. The matching map has rank three.

At cocharacter size the doublet twist is $-5f$, giving $(a,b)=(-3,4)$ and branch degrees $(-2,5)$. Only F_B can be nonzero. The four distinct values of $s=t^2$ at the finite nodes obey $s(s^3-1/4)=0$. The infinity condition kills the degree-five term. Hence F_B is a multiple of $s(s^3-1/4)$, and the rank is again five. If the conjugate charge difference $+5$ is used with the same triplet baseline as a sign test, the line is instead $\mathcal{O}_{D_{\mathrm{gr}}}(7,-6)$, with degrees $(8,-5)$. Now only F_A survives. The four finite zeros and vanishing of its degree-eight coefficient leave four independent coefficients.

It is useful to check one of the glued counts directly on the surface. The graph union is a Cartier divisor of class $(3,3)$, so the restriction sequence now uses multiplication by

$$\begin{aligned} R|_S &= xy-2x^3-y^3+2x^2y^2,\\ 0\to\mathcal{O}_S(a-3,b-3)&\xrightarrow{R}\mathcal{O}_S(a,b)\to\mathcal{O}_{D_{\mathrm{gr}}}(a,b)\to 0. \end{aligned} \tag{XIV.11.61}$$

For the cocharacter doublet $(-3,4)$, the source $H^1(-6,1)$ and target $H^1(-3,4)$ both have dimension ten. Write a source representative as $\sum_{j=-5}^{-1}x^j(a_j+b_jy)$. On the target only x^{-2},x^{-1} remain. If $P_j=a_j+b_jy$, the coefficients of those two powers are

$$-2P_{-5}+2y^2P_{-4}+yP_{-3}-y^3P_{-2}=0, \tag{XIV.11.62}$$

$$-2P_{-4}+2y^2P_{-3}+yP_{-2}-y^3P_{-1}=0. \tag{XIV.11.63}$$

The displayed equalities impose the kernel conditions. Reading coefficients from y^0 to y^4 gives $a_{-5}=a_{-4}=b_{-2}=b_{-1}=0$, then $a_{-3}=b_{-5}=b_{-3}=a_{-1}=0$ and $a_{-2}=2b_{-4}$. Only b_{-4} is free. Thus the surface calculation also leaves one section. It reaches the glued answer without using a normalization, because the exact sequence restricts the line to the Cartier union as a scheme.

For a line M restricted from S, the normalization sequence subtracts one common fiber at each node. In particular

$$0\longrightarrow M\longrightarrow\nu_*(M_A\oplus M_B)\longrightarrow\bigoplus_{i=1}^{5}M|_{p_i}\longrightarrow 0, \tag{XIV.11.64}$$

$$\chi(M)=(d_A+1)+(d_B+1)-5. \tag{XIV.11.65}$$

All four comparisons have $a+b=1$, so $\chi=0$. The triplet, root-sized doublet, and cocharacter doublet give $(0,0),(2,2),(1,1)$; the changed sign gives $(4,4)$. Reading

sections on the normalization alone would give $5, 5, 6$ for the first three. These counts measure an induced line and its node matching on the connected union. They do not specify the Higgs or sheaf data of the full nodal matter locus or a physical triplet and doublet spectrum. In the next section we test which proposed flux sizes can even pass compact quantization.

XIV.11.5 Quantization and combined flux

Can the compact cocharacter cycle coexist with the chirality class? We now have its integral representative and its mixed pairings. Write $G_k = G_* + kK$, and keep the characteristic shift of Chapter 3. For $k \in \mathbb{Z}$,

$$G_k + \tfrac{1}{2}c_2(\widetilde{Y}) = \alpha + kK \quad \text{is integral.} \tag{XIV.11.66}$$

This argument uses an actual witness α and an integral algebraic cycle K. It does not require $c_2/2$ to be integral. On the stipulated smooth projective member the classes are of type $(2, 2)$ by algebraicity. The base and section transversality conditions, and the bulk Cartan gaugings tested against inherited base classes, are unchanged:

$$\int_{\widetilde{Y}} G_k H^2 = \int_{\widetilde{Y}} G_k Z H = 0, \tag{XIV.11.67}$$

$$\int_{\widetilde{Y}} G_k D_i H = 0 \qquad (i = 1, \dots, 4). \tag{XIV.11.68}$$

These are inherited periods, not the individual Cartan pushes to S. In particular (XIV.11.24) describes a nontrivial Cartan background despite (XIV.11.68).

The charge from G_k enters the leading compact D3 relation quadratically. In the ordinary normalization and with $\chi(\widetilde{Y}) = 6768$, $G_*^2 = 140$ from Chapter 3, (XIV.11.31) and (XIV.11.25) give

$$\tfrac{1}{2}G_k^2 = \tfrac{1}{2}G_*^2 + kG_* \cdot K + \tfrac{1}{2}k^2K^2 = 70 + 30k^2, \tag{XIV.11.69}$$

$$N_{\mathrm{D3}}^{\mathrm{formal}}(k) = \tfrac{\chi}{24} - \tfrac{1}{2}G_k^2 = 212 - 30k^2. \tag{XIV.11.70}$$

For $k = 1$ the formal budget is 182; for $k = 2$ it is 92; for $k = 3$ it is -58. The last value cannot be supplied by a nonnegative count of mobile D3-branes in the stated leading budget. The first two values pass that necessary sign test. Increasing k changes the self-pairing while leaving all the inherited mixed pairings unchanged. This is why a vanishing axion charge does not imply vanishing induced D3 charge.

The Kähler test asks a different question. At finite resolution, if $J \wedge G_k = 0$ in cohomology then pairing it with every divisor must give zero. In the span

$$J = aH + bZ + \sum_{i=1}^{4} j_i D_i \tag{XIV.11.71}$$

the H and Z contributions to the Cartan equations vanish. For ZD_i this also follows from disjointness of the section and the Cartans. The Cartan–Cartan matrix for G_k is

unchanged from G_* by the ambient projection proof. Explicitly the necessary equations are

$$56\begin{pmatrix}0&0&0&0\\0&1&0&-1\\0&0&-1&1\\0&-1&1&0\end{pmatrix}\begin{pmatrix}j_1\\j_2\\j_3\\j_4\end{pmatrix}=0,\qquad j_2=j_3=j_4. \tag{XIV.11.72}$$

Now evaluate the area of the effective fibral component with geometric row $(0,-1,0,1)$. Neither H nor Z pairs with it, so

$$J\cdot\gamma_{\mathrm{wall}}=-j_2+j_4=0. \tag{XIV.11.73}$$

An effective curve on a smooth projective member has positive area for an interior Kähler class. Thus the tested span contains no interior J satisfying the necessary primitivity pairings. This curve is not the shared component with row $(1,-1,1,-1)$. Testing that other component would not reproduce the wall. Setting all resolution parameters to zero can satisfy the inherited pairings on the base face; an equality there is not a supersymmetric F-theory limit, which would need separate control of the limiting background. In particular 182 is a charge budget, not a count of D3-branes in a constructed vacuum.

One can see which conditions are independent by solving the Cartan equations in a different order. The second and third rows say that the fourth coefficient equals the second and the third; the fourth row is then automatic. Thus the coefficient directions that survive the Cartan pairings are

$$(j_1,j_2,j_3,j_4)=j_1(1,0,0,0)+j_2(0,1,1,1). \tag{XIV.11.74}$$

The wall row annihilates each of these two directions separately. The shared row instead evaluates to j_1-j_2; it need not vanish throughout this kernel. Neither a nor b can reopen the wall since the two inherited divisors have zero degree on that component. In particular a test using only the shared surface and the charge budget would miss an effective curve with zero area. This failure persists on both sides of the budget sign change between $k=2$ and $k=3$, since k drops out of the matrix entirely.

What about the root size that removed the charged bulk fields? It uses $K/5$. Its square gives an obstruction before any choice of Kähler class:

$$(K/5)^2=60/25=12/5. \tag{XIV.11.75}$$

The square of an integral class on the free middle cohomology lattice is integral by the cup product evaluated on the fundamental class. A nonintegral square is sufficient to exclude integrality, though an integral square would not establish it. The difference of two classes obeying the same characteristic shift has to be integral. Therefore $G_*+K/5$ fails the shift since G_* obeys it.

Separate quantization of pieces of a total flux is not required. Can a rational increment along the existing chirality direction compensate for $K/5$? Consider $G_*+\rho G_*+K/5$, with $\rho\in\mathbb{Q}$. If it is shifted integral, then

$$I=\rho G_*+K/5\quad\text{is integral on the free lattice.} \tag{XIV.11.76}$$

Pair I with the integral surface V. Its K-pairing vanishes by (XIV.11.44), since $f|_C$ has degree zero. The earlier period gives

$$\int_V I = -56\rho \in \mathbb{Z} \quad \Longrightarrow \quad v_5(\rho) \geq 0. \tag{XIV.11.77}$$

Here v_5 is the exponent of five in a rational number, and $v_5(0) = +\infty$. The implication follows because 56 is prime to five. This is the use of the shared surface in the integral argument; testing inherited base periods would give no denominator bound.

By orthogonality the square of the difference would be

$$I^2 = 140\rho^2 + \frac{12}{5}. \tag{XIV.11.78}$$

The first term has $v_5 \geq 1$ and the second has $v_5 = -1$. With unequal valuations the valuation of a sum is the lesser one. Equivalently, for $\rho = m/n$ in lowest terms with $5 \nmid n$, the numerator of the square over $5n^2$ is $700m^2 + 12n^2$, nonzero modulo five. Thus the sum cannot be integral for any rational ρ. This calculation tests the whole single rational direction G_*, rather than a finite sample of coefficients or an assumption that both summands quantize separately.

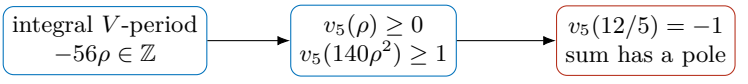


Figure XIV.11.5: The shared surface period constrains the denominator of the putative compensator. The two terms in the cup-square have different orders in five, so no cancellation can make the total square integral in this family.

There is a useful way to see how much information each of the two integral tests contributes. All rational increments $\rho = m/56$, $m \in \mathbb{Z}$, pass the shared-period test. In this family the term from ρG_* alone is $5m^2/112$. It can have other denominators but never a pole at five. Taking $\rho = 1/56$, for instance, gives

$$\int_V I = -1, \qquad I^2 = \frac{5}{112} + \frac{12}{5}. \tag{XIV.11.79}$$

At the other extreme, $\rho = 1/5$ has a denominator at five but already fails the period test. Passing a single period does not certify a class as integral; here it makes the square test decisive for all remaining rational choices.

The compact exclusion applies to this specified compensation space. It gives no exclusion for a class outside it. In the local spectral construction there is another, independent compensation space: line increments inherited from the projective bundle containing the spectral surface. Its obstruction is a condition on a norm map, which we can calculate without assuming a map into the compact fourfold.

XIV.11.6 Global extension and the resulting theory

How much of the shared compact line can a local spectral construction reproduce? Over $b_0 \neq 0$ the polynomial in the canonical bundle K_S can be made monic by

dividing by b_0. Its roots give the finite local Higgs eigenvalue data. Compactify K_S in $\mathcal{P} = \mathbb{P}_{\text{lines}}(\mathcal{O}_S \oplus K_S)$. Along $b_0 = 0$ the homogenized equation has a point at infinity. The compactified finite-flat cover alone does not give the spectral cover of an everywhere holomorphic Higgs field on S. This is a different ambient bundle from the gauge normal model of (XIV.11.20). It also has a different role from the compact elliptic fourfold. Write $c = c_1(S) = 2h$, and write σ, σ_∞ for the zero and infinity sections. They are disjoint, and the zero section has normal K_S. The two section classes and the relative canonical class satisfy

$$\sigma^2 = -\sigma c, \qquad \sigma_\infty = \sigma + c, \qquad K_{\mathcal{P}/S} = -\sigma - \sigma_\infty. \tag{XIV.11.80}$$

The relative canonical formula follows in the finite chart from the simple poles of the relative logarithmic differential at the two sections. Adding $K_S = -c$ gives $K_{\mathcal{P}} = -2\sigma - 2c$.

Use U, V_{sp} for homogeneous coordinates vanishing at σ, σ_∞, respectively. The actual equation for the cover is

$$0 = b_5 V_{\text{sp}}^5 + b_4 U V_{\text{sp}}^4 + b_3 U^2 V_{\text{sp}}^3 + b_2 U^3 V_{\text{sp}}^2 + b_0 U^5. \tag{XIV.11.81}$$

The trace term of fiber degree four in U is absent. To check that all displayed terms are global, recall that the i-th Tate coefficient is a section of $4iH$ before removing its prescribed power of the quadric equation. The respective residual degrees are

$$(4-0,\ 8-2,\ 12-4,\ 16-6,\ 24-10) = (4, 6, 8, 10, 14). \tag{XIV.11.82}$$

Their restrictions are full diagonal linear systems on S: any bidegree (d, d) monomial is a product of d Segre coordinates. In (XIV.11.81), $U^{5-j} V_{\text{sp}}^j$ contributes $5\sigma + jc$, and b_j contributes $(14 - 2j)h$. Thus every term has class $5\sigma + \eta$ for $\eta = 14h$. Intersecting with the zero section leaves $b_5 = 0$ and has class

$$[C_{\text{sp}}] = 5\sigma + \eta, \qquad \sigma \cap C_{\text{sp}} \simeq C_{10}, \qquad \delta = \eta - 5c = 4h. \tag{XIV.11.83}$$

Fix a smooth b_5 as in (XIV.11.48) and choose the remaining coefficients generally in the indicated systems. Along σ the derivative of the defining equation in a base direction transverse to $b_5 = 0$ is nonzero. Away from σ, the variable $b_0 U^5$ has a nonzero value available at each point, because $U \neq 0$ and the base linear system is base point free. Bertini for this family therefore gives smoothness there for general choices. To exclude a whole fiber, choose b_4 to meet b_5 at finitely many points and choose b_0 to avoid all of them. There is then no point at which every coefficient vanishes. The relative Cartier divisor has length five in each fiber, counting roots with multiplicity, and the projection $p_{\text{sp}} : C_{\text{sp}} \to S$ is proper and quasi-finite, hence finite. Flatness can be checked from the relative divisor sequence: the defining equation stays a nonzero divisor in each $\mathbb{P}^1$ fiber. Equivalently, after a local change of fiber coordinates putting infinity away from the five roots at a base point, the equation in the finite chart is monic of degree five over a base neighborhood. Its quotient is free of rank five. This proves finite flatness for the chosen family, without requiring five distinct sheets everywhere. It does not assert smoothness or flatness for the separate split-five or Yukawa tuning.

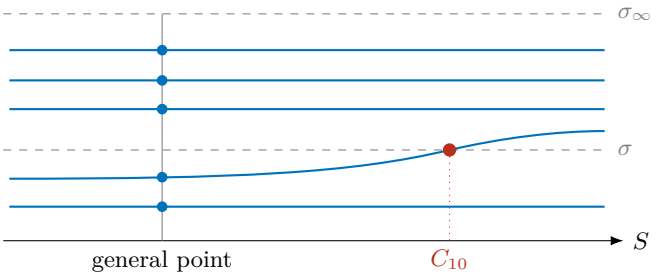


Figure XIV.11.6: The local spectral surface in the compactified canonical bundle. Over a general point there are five points counted by the finite map; the marked zero-section slice lies over C_{10}. The same slice restricts the tautological section class to $K_S|_{C_{10}}$.

We can now use the canonical divisor formula for the finite map. Adjunction gives $K_{C_{\mathrm{sp}}} = (3\sigma + \eta - 2c)|_{C_{\mathrm{sp}}}$. Subtract $p_{\mathrm{sp}}^* K_S$ to obtain the ramification class:

$$R_{\mathrm{sp}} = (3\sigma + \eta - c)|_{C_{\mathrm{sp}}}, \qquad (p_{\mathrm{sp}})_* \sigma = \delta, \qquad (p_{\mathrm{sp}})_* p_{\mathrm{sp}}^* a = 5a. \tag{XIV.11.84}$$

The second identity is the actual zero-section intersection (XIV.11.83); the third follows from degree five.

For a line N_{sp}, the degree-one part of Grothendieck–Riemann–Roch gives

$$c_1\big((p_{\mathrm{sp}})_* N_{\mathrm{sp}}\big) = (p_{\mathrm{sp}})_*\big(c_1(N_{\mathrm{sp}}) - R_{\mathrm{sp}}/2\big). \tag{XIV.11.85}$$

In fact the degree-one Todd correction on the source minus the pullback of the target correction is $(-K_{C_{\mathrm{sp}}} + p_{\mathrm{sp}}^* K_S)/2 = -R_{\mathrm{sp}}/2$. A traceless increment is therefore

$$\gamma = \tfrac{1}{2}(5\sigma - \delta), \qquad (p_{\mathrm{sp}})_* \gamma = \tfrac{1}{2}(5\delta - 5\delta) = 0. \tag{XIV.11.86}$$

This line computation is sensitive to the order of the two operations. For example the structure sheaf of the cover has determinant class

$$c_1\big((p_{\mathrm{sp}})_* \mathcal{O}_{C_{\mathrm{sp}}}\big) = -\tfrac{1}{2}(3\delta + 5(\eta - c)) = -36h. \tag{XIV.11.87}$$

A direct degree check comes from pushing the relative divisor sequence. Let $q : \mathcal{P} \to S$ and $Q = 5\sigma + \eta$. Then $q_* \mathcal{O}_{\mathcal{P}}(-Q) = 0$ by fiber degree and $R^1 q_* \mathcal{O}_{\mathcal{P}} = 0$. Relative duality gives

$$\big(R^1 q_* \mathcal{O}_{\mathcal{P}}(-Q)\big)^\vee = q_* \mathcal{O}_{\mathcal{P}}(3\sigma + \eta - c). \tag{XIV.11.88}$$

The four monomials of fiber degree three split the latter push into lines of classes $\eta - c - jc$ for $j = 0, 1, 2, 3$: $U^{3-j} V_{\mathrm{sp}}^j$ has class $3\sigma + jc$, so its coefficient accounts for the remainder. Their sum is $4(\eta - c) - 6c = 36h$. The divisor sequence adjoins one trivial summand in the determinant computation, so the dual has determinant class $-36h$, agreeing with (XIV.11.87). This nonzero determinant is why one cannot impose tracelessness by simply taking $c_1(N_{\mathrm{sp}}) = 0$.

The half-shift and γ need not each be integral; their sum in this example is integral:

$$\tfrac{1}{2} R_{\mathrm{sp}} + \gamma = 4\sigma + \tfrac{1}{2}(\eta - c - \delta) = 4\sigma + 4h, \qquad N_{\mathrm{sp}} = \mathcal{O}_{C_{\mathrm{sp}}}(4\sigma + 4h). \tag{XIV.11.89}$$

The cover line realizes a half-ramification condition on a surface. This operation is different from the fourfold characteristic shift in (XIV.11.66). Taking just $\gamma = 0$ in this construction would leave the half-integral coefficient $3/2$ on σ in the inherited expression and would miss the chosen trace-free contribution on the ten curve.

For the numerical square, integration over C_{sp} inserts $5\sigma + \eta$ into the projective bundle. Use $\sigma^2 = -c\sigma$ and push σ to one on S. This yields

$$\int_{C_{\mathrm{sp}}} \sigma^2 = -\int_S c\delta, \qquad \int_{C_{\mathrm{sp}}} \sigma\delta = \int_S \delta^2, \qquad \int_{C_{\mathrm{sp}}} \delta^2 = 5\int_S \delta^2, \tag{XIV.11.90}$$

$$\int_{C_{\mathrm{sp}}} \gamma^2 = \tfrac{1}{4}\int_S (-25c\delta - 5\delta^2) = -\tfrac{5}{4}\int_S \eta\delta = -140. \tag{XIV.11.91}$$

There is also a line comparison, stronger on this slice than comparing two numbers. On $\sigma \cap C_{\mathrm{sp}}$, the restriction of σ is $-c$. Thus N_{sp} restricts to $-8h + 4h = -4h$, $R_{\mathrm{sp}}/2$ to $(-6h + 12h)/2 = 3h$, and γ to $-7h$:

$$\big(N_{\mathrm{sp}}|_{C_{10}},\ \tfrac{1}{2}R_{\mathrm{sp}}|_{C_{10}},\ \gamma|_{C_{10}}\big) \ \leftrightarrow\ \big(\mathcal{O}_C(-4,-4),\ \mathcal{O}_C(3,3),\ \mathcal{O}_C(-7,-7)\big). \tag{XIV.11.92}$$

The last representative matches (XIV.11.43). Tensoring it with $L|_C$ for the shared weight matches the representative of $G_* + K$, and twisting once by Θ then gives (XIV.11.46). The coincidence of this slice and the opposite numerical squares of G_* and γ do not give a correspondence of cycles between the compact fourfold and the spectral cover. In particular there is no comparison yet of the restrictions at the other weights or of the gluing in the full Higgs system.

There is one more local extension test. In an $S(U(5) \times U(1))$ compensation construction a proposed determinant increment of $\pm f$ needs a line increment on the five sheets with trace $\pm f$, with the sign depending on the chosen compensating direction. For finite flat p_{sp}, the norm of a line is $\det(p_*\mathcal{L}) \otimes \det(p_*\mathcal{O})^{-1}$. Its first Chern class is the push of $c_1(\mathcal{L})$; the ramification terms cancel because the two bundles have rank one on the same cover. Restrict now to increments inherited from $\mathcal{P}$, with divisor $a\sigma + bu + dv$. The norm map in coordinates is

$$\begin{pmatrix} m \\ n \end{pmatrix} = \begin{pmatrix} 4 & 5 & 0 \\ 4 & 0 & 5 \end{pmatrix} \begin{pmatrix} a \\ b \\ d \end{pmatrix} = \begin{pmatrix} 4a + 5b \\ 4a + 5d \end{pmatrix}. \tag{XIV.11.93}$$

Every output satisfies $m \equiv n \pmod 5$. Conversely, if this congruence holds, take $a \equiv 4m \pmod 5$ and solve $b = (m - 4a)/5$, $d = (n - 4a)/5$ in integers. Since $\mathrm{Pic}(S) = \mathbb{Z}^2$, this is the exact image in the Picard group:

$$\operatorname{im} \mathrm{Nm}_{\mathrm{inh}} = \{(m, n) \in \mathbb{Z}^2 : m - n \equiv 0 \pmod 5\}. \tag{XIV.11.94}$$

Both $f = (1, -1)$ and $-f$ miss it; their differences are ± 2. But the pullback of L gives norm $5f$. The half-ramification of the fixed cover cannot change this congruence for an increment. The exclusion concerns inherited lines only, and does not determine all Picard classes on the cover or all possible refined data. It is a different calculation from the cup-square obstruction in (XIV.11.78).

The congruence measures one direction in the target lattice. The image contains $(1,1)$, for example as $4(4,4)-3(5,5)$, and contains $(5,0)$. These two classes generate all pairs with difference divisible by five. Hence the quotient is cyclic of order five, detected by the difference of the ruling degrees. For the subgroup generated by f itself,

$$kf \in \operatorname{im} \mathrm{Nm}_{\mathrm{inh}} \quad \Longleftrightarrow \quad 2k \equiv 0 \pmod 5 \quad \Longleftrightarrow \quad 5 \mid k. \tag{XIV.11.95}$$

This is an obstruction even if one allows all three inherited generators of the cover Picard sublattice and any integral combination of them. It would be weaker to test only pullbacks from S, whose norm has each coordinate divisible by five. For instance the inherited section class has norm $(4,4)$, allowed by the exact image but not by the pullback-only test. That distinction parallels the compact need to specify precisely which compensation space is being tested.

One can also see why a change in the local trace does not automatically give a compatible compact increment. In the inherited local group the diagonal direction can be adjusted with the section generator and the two base generators. To obtain f would require

$$4a + 5b = 1, \qquad 4a + 5d = -1, \qquad 5(b-d) = 2. \tag{XIV.11.96}$$

The last equation fails over integral line classes even though the first two admit rational solutions. Conversely the compact argument permits a *rational* compensating coefficient but tests the resulting fourfold class against the integral lattice. A rational solution of the local equations would still lack a line bundle; a local integral solution for a different determinant would still lack a compact cycle construction. The two obstructions concern different maps and cannot be combined to enlarge either exclusion.

The compact ruling cycles here realize the geometrical operation of fibering exceptional curves over a curve difference. Other realizations use different compact geometries: a weak-coupling quadric or a surface with an additional $U(1)$, or a stable-degeneration setting with a projected cylinder and compensating line. Those settings do not furnish a cylinder map for the $\mathbb{P}^3$ model. The common slice in (XIV.11.92) identifies exactly what the two descriptions agree on here.

We have an integral Cartan cycle, a shifted-integral cohomology sum, and vanishing inherited axion gaugings. At $k = 1$ its D3 budget is positive, but it fails the finite-resolution Kähler test in the indicated span and has charged pairs in the local zero-Higgs bulk calculation. The root-sized choice avoids those local pairs and fails in the two tested compensation spaces. A compact differential gauge background, a compatible Higgs and matter sheaf including their gluing, and a stable F-theory limit are still needed before a physical compact spectrum or physical couplings can be extracted. Neither a complete Standard Model supersymmetric spectrum nor an isolated four-dimensional theory follows.

Finally, the classical base cone has $J_B = tH$ with $t > 0$. In the leading volume dictionary at fixed microscopic couplings the gauge kinetic term measures $\mathrm{Vol}(S)$ and the gravitational term measures $\mathrm{Vol}(B)$. The two powers of the same parameter give

$$\mathrm{Vol}(S) = \tfrac{1}{2}(2H)(tH)^2 = t^2, \qquad \mathrm{Vol}(B) = \tfrac{1}{6}(tH)^3 = t^3/6 \tag{XIV.11.97}$$

with integration understood. Sending the bulk volume to infinity at fixed surface volume is impossible on this ray. A different compact embedding or a noncompact model would

need its own kinetic and boundary analysis. The absence of this particular volume limit does not exclude every other decoupling mechanism.

XIV.11.7 Exercises

1. **Change the polarization and the root size.** Take $J_S = 2u + 5v$. Give the color and weak slopes of the bundle in (XIV.11.9). Compute the charged bulk dimensions for the two signs of root size three. Explain why the cohomology calculation does not certify the split zero-Higgs solution at this polarization.

2. **Change the ruling class.** Use $a = 2u - v$ instead of f, with the same T. Find the two ruling periods in the order u, v, the hyperplane period, the four Cartan pushes as multiples of a, and the cycle square. Explain which of the inherited gauging and local root tests detect the change.

3. **Change the bundle relation.** For a formal test replace only the relation on W_0 by $(B-10h)(B-4h) = 0$. Keep the unreduced Newton and witness polynomials in (XIV.11.41) and (XIV.11.42) and $p_*B = -1$. Compute the three push coefficients of h and the fiber row. Explain why this test cannot establish the existence of another phase-I geometry.

4. **Change the ten curve.** In (XIV.11.48) set $\epsilon = 2$. Check smoothness by the same boundary and torus argument. For the Θ baseline, compute the H^1 map ranks and h^0, h^1 at $q = -4, 1, 6$. For the parity blocks of (XIV.11.53), multiply the two terms linear in z by the new ϵ before solving.

5. **Transport the graph matching.** Replace 2 by 3 in the graph $y - 2x^2$ and in the corresponding two coefficients of R. Keep the triplet baseline $(2, -1)$ and compare the two relative twists $+3f, -3f$. Give both branch degrees, the factor on the second branch in the infinity condition, the node-map rank, and the glued pair for each twist. Explain why knowing only the two branch degrees would not specify the evaluation map.

6. **Test both compensation spaces.** For $k = 4$, compute the formal D3 budget and the area of γ_{wall} after imposing the Cartan equations. For $\rho = 3/14$ and $1/5$ give the V-period of the proposed integral increment and say whether that period alone excludes it. For the local inherited norm, test $(7, 2)$ and $(3, -3)$, and give an integral preimage for the attainable target with $0 \le a < 5$. Explain why either restricted obstruction leaves possible flux or line classes outside the tested space.

Use `benchmark/tasks.json` to find the question IDs and `benchmark/PROTOCOL.md` for submission. Include the specified numerical results. The written smoothness, geometry, and physics explanations are human assessed.

Status and sources

§1. Geometry and inputs. The Segre and Tate class data are [MATH]; see Chapters 2–4 and Hayashi et al. (2013), arXiv:1304.1678v2, PDF pp. 15–17, §3, and pp. 36–37, Appendix A through (A.9). Their b_1 is our b_5. The calculation uses the Weierstrass convention $\Delta_{\text{book}} = 4f^3 + 27g^2$, the phase and electric sign of Chapter 2, the smooth projective crepant member and shifted class of Chapter 3, and the shared surface of Chapter 4. Whole-fourfold regularity at each coefficient choice is not claimed. The imported classical holomorphic Yukawa scope is [GEO-E], under the local twisted seven-brane premises of Chapter 5; it is not evaluated on the lines in this chapter.

§2. Hypercharge and bulk lines. The matrix weights, conditional group centralizer, slope and line integrality are [MATH]. The bulk multiplet assignment is [GEO-E] under the local twisted, zero-Higgs assumptions, with the cohomology calculated explicitly. See Beasley et al. (2008), arXiv:0802.3391v2, PDF pp. 33–34, (3.46)–(3.49), and Donagi and Wijnholt (2008), arXiv:0808.2223v2, PDF pp. 9–16, (2.7)–(2.22), (3.2), for the primitive root-size and compact quantization distinction.

§3. Pushforward and inherited moments. The ambient push, integral cycles, slice intersection and ambient orthogonality are [MATH]. The specified classical mass mechanism is [GEO-E] in the ordinary reduction with a positive dynamical axion metric. See Donagi and Wijnholt (2008), PDF pp. 9–10, (2.7)–(2.12), and Braun et al. (2014), arXiv:1402.4096v1, PDF pp. 9–13 and 16–18, (33)–(51), (65)–(76). The latter examples are a distinct weak-coupling quadric and a different $SU(5) \times U(1)$ construction; the geometric sign here uses the electric sign of Chapter 2 directly. The equivariance calculation concerns the named ambient products only.

§4. Line restriction and cohomology. The common stratum, relative Chow push, line and smooth and nodal curve calculations are [MATH]. See Hayashi et al. (2013), §3 and Appendix A, for the phase-I fiber data. The smooth physical interpretation is conditional [GEO-E]; see Bies et al. (2017), arXiv:1706.04616v1, PDF pp. 12–13, (2.19)–(2.25), and Beasley et al. (2008), PDF p. 71, (4.98)–(4.103). The computed shared line is an explicit rational Chow representative. No assertion of a unique flat or differential lift, a full nodal defect sheaf, or a compact multiplet count is needed for the cohomology calculations.

§5. Shift, budget and wall. The shifted lattice, charge arithmetic, finite Kähler obstruction and rational one-direction test are [MATH] with the integral witness and intersections of Chapter 3. The leading D3 relation is the conditional compact charge law of Chapter 3. The effective wall row and the shared row describe distinct components. The numerical test is not a finite-radius or limiting vacuum criterion.

§6. Local cover and comparison. The finite-flat family, ramification line, matching slice, inherited norm and volume-ray calculations are [MATH]. See Marsano et al. (2009), arXiv:0906.4672v2, PDF pp. 13, 18–21, (2.21)–(2.24), (2.37)–(2.48), (2.56)–(2.61); our C_{sp} is their spectral surface, while C_{10} denotes the base curve. For the sign choice of the compensating determinant in a separate compact geometry, see Donagi and Wijnholt (2008), PDF p. 65, (A.10)–(A.12). No compact spectral lift or refined background is

constructed here. The two compensation exclusions have different, explicitly restricted domains.

References

Beasley, C., J. J. Heckman, and C. Vafa (2008). "GUTs and Exceptional Branes in F-theory – I". In: arXiv: 0802.3391 [hep-th].

Bies, M., C. Mayrhofer, and T. Weigand (2017). "Gauge Backgrounds and Zero-Mode Counting in F-Theory". In: arXiv: 1706.04616 [hep-th].

Braun, A. P., A. Collinucci, and R. Valandro (2014). "Hypercharge Flux in F-Theory and the Stable Sen Limit". In: arXiv: 1402.4096 [hep-th].

Donagi, R. and M. Wijnholt (2008). "Breaking GUT Groups in F-Theory". In: arXiv: 0808.2223 [hep-th].

Hayashi, H., C. Lawrie, and S. Schäfer-Nameki (2013). "Phases, Flops and F-theory: $SU(5)$ Gauge Theories". In: arXiv: 1304.1678 [hep-th].

Marsano, J., N. Saulina, and S. Schäfer-Nameki (2009). "Monodromies, Fluxes, and Compact Three-Generation F-theory GUTs". In: arXiv: 0906.4672 [hep-th].

Chapter XIV.12

Strongly coupled sectors and conformal matter

XIV.12.1 When a matter curve stops being ordinary

What replaces ordinary matter when two seven-branes meet too singularly for the usual matter-curve calculation? In Chapter 2 a minimal enhancement at a curve supplied charged fiber curves, with their charges read from intersections. Here the first signal is different: the Weierstrass coefficients vanish strongly enough to permit a crepant blowup of the *base*. Over a point on the matter curve the blowup exposes a chain familiar from six-dimensional conformal matter. We will build the chain, compactify the corresponding sector with a supersymmetry twist, and calculate how it contributes when one of its flavor symmetries is weakly gauged. The two examples have the same local collision but different compact curves. The distinction will matter when we compute the four-dimensional anomaly.

Let $S = \mathbb{P}^2$, with H of degree one on a line. The base is $B = \mathrm{Tot}(N)$ with $N = \mathcal{O}_S(n)$, projection $\pi : B \to S$, and compact zero section also denoted S. Write z for the tautological section of π^*N. Its representative in a line frame is the normal coordinate; changing the frame changes that representative by the inverse frame factor. The relative tangent bundle of the line projection is π^*N. The tangent sequence and its determinant therefore give

$$0 \longrightarrow \pi^*N \longrightarrow TB \longrightarrow \pi^*TS \longrightarrow 0, \tag{XIV.12.1}$$

$$K_B = \pi^*(K_S \otimes N^{-1}), \qquad L = K_B^{-1} = \pi^*\mathcal{O}_S(3+n). \tag{XIV.12.2}$$

Use the ordinary relative plane with hyperplane class H_{rel}, in which the homogeneous coordinates Z, X, Y have classes $H_{\mathrm{rel}}, H_{\mathrm{rel}} + 2L, H_{\mathrm{rel}} + 3L$. We write addition of lines for tensor product in the class formulas. The equation $Y^2Z = X^3 + fXZ^2 + gZ^3$ then has class $3H_{\mathrm{rel}} + 6L$. The relative Euler sequence gives the relative canonical class $-3H_{\mathrm{rel}} - 5L$, since the three coordinate classes enter with a minus sign. Adjunction

gives the dualizing line of the Weierstrass hypersurface W:

$$K_W = \pi_W^*(K_B \otimes L) = \mathcal{O}_W. \tag{XIV.12.3}$$

The relative Euler sequence presents the relative tangent as the quotient of the three coordinate lines by the trivial Euler direction:

$$0 \longrightarrow \mathcal{O} \longrightarrow \mathcal{O}(H_{\mathrm{rel}}) \oplus \mathcal{O}(H_{\mathrm{rel}} + 2L) \oplus \mathcal{O}(H_{\mathrm{rel}} + 3L) \longrightarrow T_{\mathrm{rel}} \longrightarrow 0. \tag{XIV.12.4}$$

Taking its determinant before adding the base canonical line gives the $-5L$ in the relative class. The adjunction result is a statement about the hypersurface even where it is singular. The plane equation never becomes identically zero on a fiber and gives plane cubics of fixed Hilbert polynomial; over the generic point it is a smooth elliptic cubic with the section at infinity. Triviality of the dualizing line does not resolve the hypersurface.

To place a second seven-brane, choose the plane polynomial $F = X_0^d + X_1^d + X_2^d$, where X_i are base coordinates on S. We suppress the pullback symbol on F, H. Put $\Sigma = \{F = 0\} \subset S$, $T = \pi^{-1}(\Sigma)$ and take $f = 0,\ g = (zF)^4$. The two divisor classes enter the same section. Requiring g to have class $6L$ gives

$$4(n + d) = 6(3 + n), \qquad 4d = 18 + 2n. \tag{XIV.12.5}$$

In particular g has class $12H$ in the quartic example, yet its fourth normal coefficient $g/z^4|_S = F^4$ has class $16H$. Dividing out a normal factor changes the bundle: the fourth coefficient is in $(6L - 4N)|_S$. More generally the degree-j coefficient in a g-jet is in $(6L - jN)|_S$, whereas that for f is in $(4L - jN)|_S$. A negative normal line can thus make a jet coefficient more positive even though g itself has a smaller degree.

The derivatives dX_i^{d-1} have no common projective zero, so the two Fermat curves under consideration are smooth. A reducible positive-degree plane curve would have intersecting components by Bézout, and would be singular there. Adjunction on the plane and the two independent defining equations in B give

$$K_\Sigma = \mathcal{O}_\Sigma(d - 3), \qquad 2g_\Sigma - 2 = d(d - 3), \tag{XIV.12.6}$$

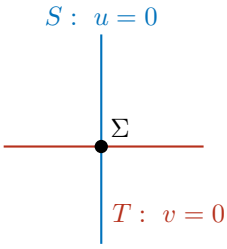
$$N_{\Sigma/B} = \mathcal{O}_\Sigma(n) \oplus \mathcal{O}_\Sigma(d), \qquad (\deg N_{\Sigma/S}, \deg N_{S/B}|_\Sigma) = (d^2, nd). \tag{XIV.12.7}$$

In the direct sum in (XIV.12.7) we put the normal of S first. The degree of $\mathcal{O}_\Sigma(1)$ is d, not one. These are actual classes of the two compact curves, not parameters of the local transverse germ:

	n	d	g_Σ	nd	d^2
CM4−Q	-1	4	3	-4	16
CM4−C	-3	3	1	-9	9

(XIV.12.8)

The cubic and quartic satisfy the same coefficient equation by changing N as well as F. Keeping $N = \mathcal{O}(-1)$ and replacing the quartic by a cubic without changing the ansatz would give $4(n + d) = 8$, not 12. We use the cubic as a different fourfold model, rather than as a smooth degree-changing deformation of the plane quartic.



	IV ends	IV* ends
g	$(uv)^2$	$(uv)^4$
$\mathrm{ord}_u(g)$	2	4
$\mathrm{ord}_{(u,v)}(g)$	4	8
curve blowup	pole	regular

Figure XIV.12.1: A transverse slice to the compact intersection curve Σ. The compact divisor S is $u = 0$; the line bundle T over Σ is $v = 0$. Away from the crossing the other variable is a unit. At the crossing both variables are in the ideal. The table compares the split IV and split IV* choices on this same transverse coordinate domain.

At any point of Σ choose $u = z,\ v = F$ in local frames and a third coordinate w along the curve. This is possible by the two independent normal directions. In these coordinates the Weierstrass section is $g = u^4v^4$, and our discriminant convention is $\Delta = 4f^3 + 27g^2$. Define $\mathrm{ord}(0) = \infty$. For a single divisor take the discrete valuation at its generic point; at Σ take the largest power of the ideal (u, v) containing the coefficient. As Figure XIV.12.1 shows, these operations give different triples:

$$\mathrm{ord}_u(f, g, \Delta) = \mathrm{ord}_v(f, g, \Delta) = (\infty, 4, 8), \qquad \mathrm{ord}_{(u,v)}(f, g, \Delta) = (\infty, 8, 16). \tag{XIV.12.9}$$

In the ordinary, relatively minimal transverse dictionary, the end fibers are IV*. To read their Lie algebras one must also test the monodromy cover. With m its variable, the covers are $m^2 - v^4$ and $m^2 - u^4$, both split in the relevant function fields. This gives $\mathfrak{e}_6$ on each end. Over a spectator function field one could instead take $g = \sigma(uv)^4$. The odd σ-valuation of σv^4 prevents it from being a square even though the u-valuation of g has not changed. This altered local equation has its own special loci; the comparison isolates the square test.

For comparison use the ordinary split IV jet $f = 0,\ g = (uv)^2$. In each divisor direction it has $(\infty, 2, 4)$, with cover $m^2 - v^2$ or $m^2 - u^2$. The ideal order is now $(\infty, 4, 8)$. On the quartic it has a lift away from the zeros of $G_3 = X_0X_1X_2$: $g = (zF)^2G_3^2$ has class $12H$, and the additional coefficient is a unit square there. Blow up the crossing by $u = a,\ v = ab$. The coefficient g in this split IV test pulls back to a^4b^2. A crepant base change at a smooth curve requires removal of the factor a^6 in g, giving

$$g'_{\mathrm{IV}} = a^{-6}a^4b^2 = a^{-2}b^2. \tag{XIV.12.10}$$

The pole is the concrete failure of this construction for that jet. It does not give a spectrum for the IV collision. By contrast, the IV* example has two extra powers of a after the same rescaling. We now follow them through the remaining charts.

XIV.12.2 What the three blowups separate

Which geometry appears over Σ when the base is allowed to change? A base blowup of a smooth codimension-two center has canonical discrepancy one, so $L' = \beta^* L - E$ on the blown-up base $\beta : B' \to B$. On a chart with exceptional coordinate e, the fiber variables satisfy $x = e^2 x',\ y = e^3 y'$. This explains the required divisibility of the pulled-back coefficients:

$$f' = \frac{\beta^* f}{e^4}, \qquad g' = \frac{\beta^* g}{e^6}, \qquad \Delta' = \frac{\beta^* \Delta}{e^{12}}. \tag{XIV.12.11}$$

The codimension of the center matters. Blowing up a point of this threefold base would have discrepancy two and require divisibility by powers $8, 12, 24$ rather than $4, 6, 12$.

For the first curve blowup we use two charts, keeping w fixed:

$$(u, v) = (a, ab), \qquad g' = a^2 b^4, \tag{XIV.12.12}$$

$$(u, v) = (cd, d), \qquad g' = c^4 d^2. \tag{XIV.12.13}$$

In the first chart $a = 0$ is the exceptional divisor and $b = 0$ is the proper transform of T. In the other chart $d = 0$ is the same exceptional divisor and $c = 0$ is the proper transform of S. On the overlap $c = b^{-1}, d = ab$. Thus the two corners are the zero and infinity directions in the exceptional $\mathbb{P}^1$ over each point of Σ. They are disjoint smooth sections over the curve. This statement glues: the proper transforms of the two distinguished divisors pick out the two lines of the normal bundle in (XIV.12.7). No global product structure over Σ has been used.

At either corner the first transformed g has total order $2+4 = 6$, and the discriminant has order twelve. The next blowup has exceptional g-order zero. In the chart with $g' = a^2 b^4$, write either $(a, b) = (s, st)$ or $(a, b) = (st, t)$. The rescaled coefficients are

$$(u, v) = (s, s^2 t), \qquad g'' = t^4, \tag{XIV.12.14}$$

$$(u, v) = (st, st^2), \qquad g'' = s^2. \tag{XIV.12.15}$$

The first of these contains the proper transform of T; the second contains the proper transform of the original exceptional divisor. On the other side $g' = c^4 d^2$; the two choices $(c, d) = (s, st), (st, t)$ give

$$(u, v) = (s^2 t, st), \qquad g'' = t^2, \tag{XIV.12.16}$$

$$(u, v) = (st^2, t), \qquad g'' = s^4. \tag{XIV.12.17}$$

These formulas show why both second-stage centers matter. Blowing up only the first corner would leave $c^4 d^2$ at the second. Conversely, the centers do not require further successive modifications of each other. Each lies in a different end of the first exceptional fiber.

A useful way to compare all four charts is to record the vanishing orders of (u, v) on their coordinate axes as rays. The first blowup inserts $(1, 1)$; the others insert the sums of that ray with each original ray. Figure XIV.12.2 orders the final rays from the

compact side to the noncompact side. Write $r_i = (r_{i,1}, r_{i,2})$ for each ray in this order, with $|r_i| = r_{i,1} + r_{i,2}$. On its cone with r_{i+1}, choose a, b such that

$$(u, v) = \left(a^{r_{i,1}} b^{r_{i+1,1}}, a^{r_{i,2}} b^{r_{i+1,2}}\right), \qquad J = \frac{\partial(u, v)}{\partial(a, b)} = a^{|r_i|-1} b^{|r_{i+1}|-1}. \tag{XIV.12.18}$$

Indeed the two terms in the Jacobian determinant have the same monomial and the difference of their integer coefficients is $\det(r_i, r_{i+1}) = 1$. The adjacent pairs form lattice bases, and so these are smooth affine transverse charts. In the indicated ordering the coordinates and transforms are

(r_i, r_{i+1})	(u, v)	J	g/J^6	$\mathrm{ord}_{(a,b)}(g/J^6)$
$((1,0),(2,1))$	(ab^2, b)	b^2	a^4	4
$((2,1),(1,1))$	(a^2b, ab)	a^2b	b^2	2
$((1,1),(1,2))$	(ab, ab^2)	ab^2	a^2	2
$((1,2),(0,1))$	(a, a^2b)	a^2	b^4	4

(XIV.12.19)

For instance in the second chart $u^4v^4 = a^{12}b^8$, and $J^6 = a^{12}b^6$. The b^2 remains on the middle divisor; along $a = 0$ with $b \neq 0$ the fiber is smooth. At the origin of this chart the remaining discriminant has order four, well below twelve. In the first chart the corresponding corner has discriminant order eight. None of the four corner orders permit another curve blowup of this kind. The middle two charts also make it possible to follow the rescaling on a common open. Write (a, b) for the second chart and (c, d) for the third. Where $a \neq 0$ the two monomial maps agree at

$$c = a^3 b, \qquad d = a^{-1}, \qquad J_2 = a^2 b, \qquad J_3 = cd^2 = ab. \tag{XIV.12.20}$$

Therefore $g/J_3^6 = a^6(g/J_2^6) = a^6 b^2 = c^2$. Both the exceptional coordinate and the Weierstrass line frame change. The leading g-coefficient on the middle divisor remains 1 relative to its local defining coordinate. If one changed only the coordinate b to c without changing the equation frame, one would keep a spurious coefficient a^{-6}. The same computation in local line frames at every point of Σ removes the nonminimal base collision. It does not give a smooth simultaneous fiber resolution.

One can also verify the crepant scaling by following the fourfold residue form on the chart with $y \neq 0$. Before the base change it is proportional to $du \wedge dv \wedge dw \wedge dx/(2y)$. With $x = J^2 x'$, $y = J^3 y'$, the numerator dx contributes $J^2 dx'$ plus base differentials that vanish after wedging. The factor J from $du \wedge dv$ completes the cancellation:

$$\beta^* \left(du \wedge dv \wedge dw \wedge \frac{dx}{2y} \right) = J \, \frac{J^2}{J^3} \, da \wedge db \wedge dw \wedge \frac{dx'}{2y'}. \tag{XIV.12.21}$$

This calculation identifies the pulled-back dualizing generator in this presentation. The blowup changes the base and the line of the equation together. Dividing a common factor in the original base would not supply the Jacobian in (XIV.12.21).

The middle divisor is $b = 0$ in the second chart and $a = 0$ in the third. Its two leading g-coefficients in those coordinates are both 1. The cover $m^2 - 1$ splits in both frames, so the middle transverse IV fiber gives $\mathfrak{su}(3)$. The end proper transforms still have split IV*, whereas the two new exceptional divisors have smooth generic elliptic

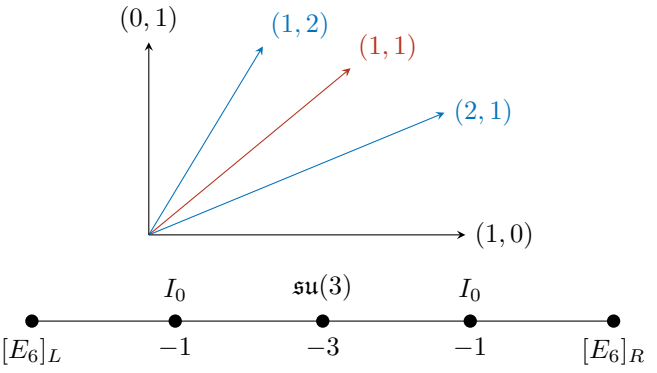


Figure XIV.12.2: The transverse fan and the ordered chain over a point of Σ. Each adjacent ray pair in the top panel gives a chart in (XIV.12.19). The end exceptional curves have smooth generic elliptic fibers, and the middle exceptional curve carries a split IV fiber. The self-intersections refer to curves in the transverse base surface.

fibers. To interpret the chain, take the transverse *surface* obtained by fixing w. The first exceptional curve starts with self-intersection -1. Blowing up a smooth point on a curve decreases its self-intersection by one, since the proper transform is the pullback minus the new exceptional curve. The two new curves are disjoint and each meets the proper transform of the first curve once. Thus, ordered from the compact to the noncompact side, the positive intersection pairing is

$$\Omega = -\big(C_i \cdot C_j\big) = \begin{pmatrix} 1 & -1 & 0 \\ -1 & 3 & -1 \\ 0 & -1 & 1 \end{pmatrix}. \tag{XIV.12.22}$$

The principal minors of order one are $1, 3, 1$; those of order two in index pairs $12, 13, 23$ are $2, 1, 2$. The determinant is 1. The leading principal minors $1, 2, 1$ prove positive definiteness. In the threefold base the curves are fibers of exceptional surfaces over Σ. The entries of Ω are not self-intersections of those surfaces, nor does the computation amount to three point blowups of the base.

A different calculation on the generic elliptic fiber illustrates a limit of the Lie algebra dictionary. Let $s_0 = (zF)^2$. Its class is $3L$, since $4(n+d) = 6(3+n)$. The marked point $P = (0, s_0)$ lies on $y^2 = x^3 + s_0^2$ and its tangent is $y = s_0$. Substituting that line leaves $-x^3 = 0$, so the tangent meets the curve three times at P. The chord-and-tangent law with the origin at infinity gives $3P = 0$, and $P \neq O$ makes its order exactly three. To test what this calculation depends on, keep g and add $f = z^4F^3$ on CM4-Q. This is a valid section of $4L$, since $4(-1) + 3(4) = 8$. The orders along S, T become $(4, 4, 8)$ and $(3, 4, 8)$; both covers still split. At the same marked point the slope is now $f/(2s_0)$. Substitution gives

$$\left(s_0 + \frac{fx}{2s_0}\right)^2 - x^3 - fx - s_0^2 = \frac{f^2}{4s_0^2}x^2 - x^3. \tag{XIV.12.23}$$

At the generic point $f \neq 0$, and the contact drops to two. The change preserves the end Lie algebras while losing the flex at that marked point. It does not exclude a different torsion section or determine a global gauge or flavor group. We next use the chain as a transverse description of the sector on Σ; the protected calculation needs the two end Lie algebras and the choice of a compactification on the curve.

XIV.12.3 Which six-dimensional theory is on the curve?

How does a transverse tensor branch become a four-dimensional matter sector? In the ordinary unfrozen F-theory dictionary, the collision of two split IV* ends in a base surface defines the minimal (E_6, E_6) conformal matter system. Its tensor branch, with positive curve labels, is

$$[E_6] \;-\; 1 \;-\; \overset{\mathfrak{su}(3)}{3} \;-\; 1 \;-\; [E_6]. \tag{XIV.12.24}$$

The three finite labels are the negatives of the three transverse self-intersections. In the six-dimensional description each compact curve supplies a tensor whose scalar controls its size; $\mathfrak{su}(3)$ is the gauge algebra over the middle curve. The square brackets denote flavor algebras before any four-dimensional gauging. The identification of the singular limit with a six-dimensional SCFT is a physical input. The blowup derivation tells us which input to use. Rank one means one copy of the minimal conformal-matter block, $Q = 1$; the branch still has three tensors. We will use the interacting anomaly, after removing a center-of-mass tensor and its associated flavor term.

A local patch along the common curve Σ is sufficient to compute the transverse jet. It is insufficient to decide which supercharges survive on the compact curve. The two normal lines in (XIV.12.7) have nonzero degrees of opposite signs, so no pair of coordinates u, v trivializes their normal directions over the whole quartic. The curve's canonical line can also be recovered by restricting base adjunction:

$$K_\Sigma = (K_B + S + T)|_\Sigma = \mathcal{O}_\Sigma\big(-(3+n) + n + d\big) = \mathcal{O}_\Sigma(d-3). \tag{XIV.12.25}$$

Neither normal line by itself is the spin line of the curve.

In the ordinary compactification of the six-dimensional system, the $SU(2)_{R_6}$ background reduces to its Cartan. Choose a theta characteristic Θ, a line satisfying $\Theta^{\otimes 2} \simeq K_\Sigma$. Write R_4 for the external $U(1)$ line for which the chosen four-dimensional supercharge has charge $+1$. In the twist, the positive weight of the $SU(2)_{R_6}$ doublet is tensored with Θ; the other weight is its dual. The internal spin line Θ^{-1} paired with the positive weight cancels its curve connection, $\Theta^{-1} \otimes \Theta \simeq \mathcal{O}_\Sigma$. To keep track of the other weight, consider the two internal spin lines Θ^{-1}, Θ. The R_6 doublet with internal weights Θ, Θ^{-1} gives the combinations

internal spin line	positive weight	negative weight
Θ^{-1}	$\mathcal{O}_\Sigma$	K_Σ^{-1}
Θ	K_Σ	$\mathcal{O}_\Sigma$

(XIV.12.26)

The trivial diagonal pair contains the chosen four-dimensional supercharge and its conjugate; the nontrivial canonical lines do not have a covariantly constant section on the curved example. Holomorphic sections of K_Σ do not supply extra unbroken supercharges. The pair gives the usual four real supercharges on the nonflat, unpunctured curve. Write $r = c_1(R_4)$, normalize $\eta \in H^2(\Sigma, \mathbb{Z})$ by $\int_\Sigma \eta = 1$ in the complex orientation, and set $h = g_\Sigma - 1$. The two Chern roots and their product are

$$\deg \Theta = h, \qquad \text{roots}(R_6) = \big(r + h\eta, -r - h\eta\big), \qquad C = c_2(R_6) = -(r + h\eta)^2. \tag{XIV.12.27}$$

The sign of the product matters for the mixed gravitational slot. Also $\eta^2 = 0$, so $C = -r^2 - 2hr\eta$, with the factor of two arising from the cross term. Using the full canonical line in this formula would double the four-dimensional anomaly.

On the quartic we can specify an actual Θ. Restrict the Fermat equation to the line $X_2 = -X_0 - X_1$:

$$X_0^4 + X_1^4 + (X_0 + X_1)^4 = 2(X_0^2 + X_0X_1 + X_1^2)^2. \tag{XIV.12.28}$$

At $X_1 = 0$ there is no projective zero, and in the chart $X_1 = 1$ the quadratic has discriminant -3. Its distinct roots give points P, Q, each occurring twice on the intersection divisor. Since $K_\Sigma = \mathcal{O}_\Sigma(1)$, the bitangent gives

$$K_\Sigma \simeq \mathcal{O}_\Sigma(2P + 2Q), \qquad \Theta = \mathcal{O}_\Sigma(P + Q), \qquad \deg K_\Sigma = 4, \quad \deg \Theta = 2. \tag{XIV.12.29}$$

The equation specifies one spin line, though only its degree enters the polynomial pushforward. Compare the coordinate line $X_0 = 0$. On $X_2 = 1$ the restriction is $X_1^4 + 1$, which has four distinct zeros, since its derivative can vanish only at $X_1 = 0$. There is no extra zero at $X_2 = 0$. The hyperplane has the same total intersection degree as the bitangent, but its divisor is not twice an effective divisor on the curve. Thus replacing the bitangent by this line would leave the canonical degree intact and lose the explicit construction of Θ. The twist uses a square root of a line bundle, not the numerical operation of halving an arbitrary chosen representative divisor. On CM4-C the cubic has trivial canonical line by adjunction. Choose the trivial theta line, with periodic supercharges on the flat torus and no Wilson lines. Degree zero alone would not specify those flat data.

Turning off flavor flux does not turn off the R-twist in Figure XIV.12.3. It means the E_6 flavor curvatures have only their external background parts for this calculation. We also choose no flat flavor holonomy, so there is no separate breaking of the end Lie algebras by transport around Σ. This compactification prescribes no punctures or additional defects. It does not construct a quantized compact G_4 or require that a hypothetical compact completion have zero G_4. On the chosen torus $h = 0$, so the ordinary polynomial integral will lose its curve leg. The torus block still exists in the sourced compactification dictionary; we will need a different rule for its protected observables.

XIV.12.4 Why only one flavor is gauged

What distinguishes a propagating gauge field from a background flavor current in this local model? In a leading reduction, start with a gauge kinetic term on a seven-brane

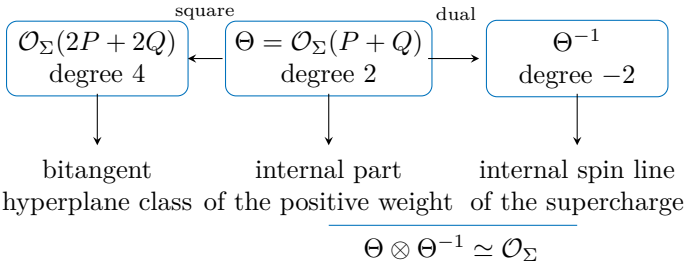


Figure XIV.12.3: The quartic hyperplane class restricted along the chosen bitangent gives the divisor $2P+2Q$. Its half defines a spin line. The positive R_6 weight and inverse internal spin line cancel on the chosen supercharge. The degrees $+2,-2$ concern the quartic and become zero for the chosen trivial spin line on the cubic.

and choose a gauge profile constant on its internal surface D. The coefficient contains $\int_D J^2/2$, with the external kinetic normalization and microscopic coupling held fixed. At fixed boundary values the constant mode can describe a dynamical four-dimensional vector only if its norm is finite. We compare the compact and noncompact surfaces using an explicit auxiliary Kähler metric on the quartic base.

For $N=\mathcal{O}_{\mathbb{P}^2}(-1)$, B is the incidence space $\{(x,[\ell]) : x\in\ell\}\subset\mathbb{C}^3\times\mathbb{P}^2$, the blowup of the origin in $\mathbb{C}^3$. Add the pullback of the flat Kähler form on the first factor to $t>0$ times the pullback of Fubini–Study on the second. Their sum is positive because a nonzero tangent to the incidence space cannot map to zero in both factors. On the punctured cone, use the radial action variable ρ, a circle connection ϑ with $\int_{S^1}\vartheta=1$, and the horizontal form ω_H with $\int_{\mathbb{P}^1}\omega_H=1$. Take $d\vartheta=\omega_H$ in this frame. Then

$$J=d(\rho\vartheta)+t\omega_H=d\rho\wedge\vartheta+(\rho+t)\omega_H. \tag{XIV.12.30}$$

The graph construction supplies the smooth extension to the zero section, where $J|_S=t\omega_H$. The curve area and compact surface volume are

$$A_\Sigma=4t, \qquad V_S=\int_S\frac{J^2}{2}=\frac{t^2}{2}. \tag{XIV.12.31}$$

For the noncompact quantities regulate at $\rho=U$. The radial two-form squares to zero, and on T the horizontal two-form squares to zero because its base is a curve. On B the only term of $J^3/3!$ with a radial leg is $d\rho\wedge\vartheta\,(\rho+t)^2\omega_H^2/2$. Thus

$$V_T(U)=4\int_0^U(\rho+t)\,d\rho=2\big[(U+t)^2-t^2\big], \tag{XIV.12.32}$$

$$V_B(U)=\frac{1}{2}\int_0^U(\rho+t)^2\,d\rho=\frac{(U+t)^3-t^3}{6}. \tag{XIV.12.33}$$

The 4 is $\int_\Sigma\omega_H$; in the second line $\int_S\omega_H^2=1$. The distinct powers of U reflect the dimensions of the horizontal spaces. Sending $U\to\infty$ at fixed t leaves the compact

norm fixed while the constant mode on T has divergent norm. Taking $t \to \infty$ would increase the compact norm and the curve area together. Those operations are not interchangeable ways of taking the four-dimensional coupling weak.

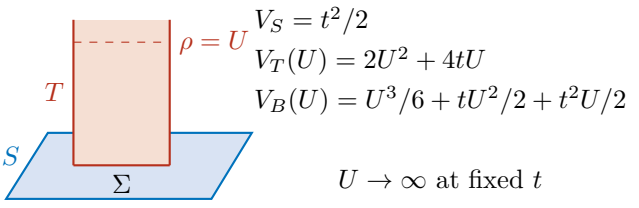


Figure XIV.12.4: The compact zero section and noncompact flavor surface meet on the quartic. The same radial cutoff on T and B gives the quadratic and cubic volume growth in (XIV.12.32)–(XIV.12.33). The compact volume is independent of U at fixed t.

In the local boundary prescription we treat the T constant mode as a flavor background and the S vector as dynamical. Figure XIV.12.4 explains this distinction in an unwarped auxiliary reduction. The metric is not a backreacted solution, and the comparison does not exclude localized or continuum modes on the noncompact side. It does not establish gravitational or Kaluza–Klein isolation in a compact limit or control the metric on the exceptional surfaces. We use the weakly gauged four-dimensional reference description below its compactification scales.

With trivial bulk gauge data and zero bulk Higgs profile, the ordinary twisted seven-brane dictionary of Chapter 2 gives a vector from $H^0(S, \mathcal{O}_S)$ and bulk adjoint chirals from $H^1(S, \mathcal{O}_S)$ and $H^0(S, K_S)$. For $S = \mathbb{P}^2$, the constants are the only degree-zero holomorphic polynomials, the intermediate line cohomology vanishes, and the negative-degree canonical line has no sections:

$$h^0(\mathcal{O}_S) = 1, \qquad h^1(\mathcal{O}_S) = 0, \qquad h^0(K_S) = 0. \tag{XIV.12.34}$$

Serre duality gives $h^2(K_S) = h^0(\mathcal{O}_S) = 1$, which is not an additional chiral in this dictionary. The twist is essential: this calculation does not assert that the plane is spin or that an untwisted spinor is a constant mode on it. The result motivates comparing a single $\mathcal{N} = 1$ E_6 vector with one compactified conformal-matter block. Any additional charged sector would change the weak-gauging test.

We need the *interacting* six-dimensional anomaly. Let $p = p_1(T_6)$, $p_2 = p_2(T_6)$, $C = c_2(R_6)$, and $Y_i = \mathrm{Tr} F_i^2/4$ for $i = L, R$, with $\mathrm{Tr} = \mathrm{tr}_{\mathrm{adj}}/h^\vee$. These are characteristic-class curvatures. In the rank-one E_6 source formula take

$$Q = 1, \quad |\Gamma| = 24, \quad \mathrm{rank}\, E_6 = 6, \quad d_G = 78, \quad h^\vee = 12, \quad u_G = 6, \quad t_G = 0, \tag{XIV.12.35}$$

$$A = |\Gamma|(\mathrm{rank}\, E_6 + 1) - 1 = 167. \tag{XIV.12.36}$$

Here u_G is the coefficient of $\frac{3}{4}(\mathrm{Tr} F^2)^2$ in the adjoint quartic trace when the independent quartic term t_G vanishes. The free six-dimensional vector polynomial in these

conventions is

$$V(Y) = -\frac{\frac{3}{4}u_G(4Y)^2 + 6Ch^\vee(4Y) + d_G C^2}{24} - \frac{(4h^\vee Y + d_G C)p}{48} - d_G\frac{7p^2 - 4p_2}{5760}. \tag{XIV.12.37}$$

The chirality sign gives the overall minus. The vector polynomial enters the inflow presentation with weight $-1/2$ at each end. Its Y^2 term is $-3Y^2$ and its CY term is $-12CY$. The source polynomial before removal is

$$I_8^{\mathrm{tot}} = \frac{|\Gamma|^2 C^2}{24} - \frac{A\,C(4C+p)}{48} - \frac{|\Gamma|}{2}C(Y_L + Y_R) + \frac{1}{8}\left(\frac{Cp}{6} - \frac{p_2}{6} + \frac{p^2}{24}\right) - \frac{1}{2}\big[V(Y_L) + V(Y_R)\big]. \tag{XIV.12.38}$$

The left and right contributions from V do not couple to one another, so there is no $Y_L Y_R$ term at this stage. The prescription for the interacting sector subtracts two terms:

$$I_8^{\mathrm{tensor}} = \frac{C^2}{24} + \frac{Cp}{48} + \frac{23p^2 - 116p_2}{5760}, \tag{XIV.12.39}$$

$$I_8^{\mathrm{cm,GS}} = \tfrac{1}{2}(Y_L - Y_R)^2, \qquad I_8 = I_8^{\mathrm{tot}} - I_8^{\mathrm{tensor}} - I_8^{\mathrm{cm,GS}}. \tag{XIV.12.40}$$

The first is the free tensor's anomaly. The second is the Green–Schwarz term of that center-of-mass tensor. The total coefficient of CY_L is $-24/2 + 12/2 = -6$; neither subtraction changes it. The total coefficient of Y_L^2 is $3/2$, and the second subtraction reduces it to 1. It simultaneously produces the $+Y_L Y_R$ term. For the C^2 slot the numerator before subtraction in units of $1/24$ is $576 - 2(167) + 78 = 320$; the free tensor changes it to 319. Thus omitting the two subtractions would have different effects.

For use in the pushforward, all eleven slots are

$$I_8 = \frac{319}{24}C^2 - \frac{89}{48}Cp + \frac{553}{5760}p^2 - \frac{79}{1440}p_2 + Y_L^2 + Y_R^2 + Y_L Y_R - 6C(Y_L + Y_R) + \tfrac{1}{2}p(Y_L + Y_R). \tag{XIV.12.41}$$

The total Cp numerator in units of $1/48$ is $-167 + 1 + 78 = -88$, giving -89 after removal. For p^2 the total numerator in units of $1/5760$ is $30 + 7(78) = 576$, giving 553 after removal. For p_2 it is $-120 - 4(78) = -432$, which becomes -316. The two source presentations agree on all eleven monomials once the normalization is translated. This checks the protected input algebraically. It is not an independent ultraviolet anomaly match. To compare the two subtractions without the long inflow formula, the grouped coefficients are as follows. A row with two monomials gives the coefficient of each.

Slot	$I_8^{\rm tot}$	tensor or GS removed	I_8
$24[C^2]$	320	1	319
$48[Cp]$	-88	1	-89
$5760[p^2]$	576	23	553
$5760[p_2]$	-432	-116	-316
$Y_L^2,\ Y_R^2$	3/2	1/2	1
$Y_L Y_R$	0	-1	1
$CY_L,\ CY_R$	-6	0	-6
$pY_L,\ pY_R$	1/2	0	1/2

The negative entry in the removed mixed-flavor slot is a consequence of the relative minus sign between the two backgrounds in the GS square, not a minus sign on the full square. The two removed terms will be distinguishable after reduction as well: one affects the R and gravitational slots, while the other matters when flavor curvature has a leg on the curve.

XIV.12.5 A protected weak-gauging test

Does the conformal matter contribute enough screening for one E_6 vector? The anomaly calculation gives a mixed-current coefficient. To use it for a physical beta function we will also need the superconformal current identity of the ungauged block. We first determine the coefficient without that assumption.

In (XIV.12.41) insert $C = -r^2 - 2hr\eta$, with $h = g_\Sigma - 1$ from (XIV.12.27). The external tangent Pontryagin classes can be written with the same symbols p, p_2 after integration: $p_1(T\Sigma) = c_1(T\Sigma)^2 = 0$, so the Whitney product contributes no curve two-form to either six-dimensional Pontryagin class. With flavor backgrounds pulled back from the external spacetime, only the C terms contribute. To see the sign in each slot, write

$$[C^2]_\eta = 4hr^3, \qquad [Cp]_\eta = -2hrp, \qquad [CY_i]_\eta = -2hrY_i. \tag{XIV.12.42}$$

Here brackets mean the coefficient of η, and integration over Σ takes this coefficient. It follows that

$$I_6 = \int_\Sigma I_8 = h\left(\frac{319}{6}r^3 + \frac{89}{24}rp + 12r(Y_L + Y_R)\right). \tag{XIV.12.43}$$

The $Y_L Y_R$ term does not enter this fluxless answer, since neither flavor field has an internal component. This is why that particular four-dimensional calculation cannot test whether the Green–Schwarz removal was made. For comparison, failing to remove $I_8^{\rm tensor}$ would add $h(r^3/6 - rp/24)$ to (XIV.12.43), shifting both R traces by h. At genus three the resulting shift in the trial a would be 3/8.

With the conventions of Volume I, the pure R and gravitational slots of I_6 are $\operatorname{Tr} R^3\, r^3/6 - \operatorname{Tr} R\, rp/24$, with traces over four-dimensional left Weyl fermions. Denote the coefficients of rY_L, rY_R by k_L, k_R in this polynomial frame. Then

$$(\operatorname{Tr} R^3, \operatorname{Tr} R, k_L, k_R) = (319h, -89h, 12h, 12h). \tag{XIV.12.44}$$

At genus three this is $(638, -178, 24, 24)$. If the block is a unitary $\mathcal{N} = 1$ SCFT with this exact superconformal R, the anomaly relations for its stress tensor give

$$a_{\text{block}} = \frac{3}{32}(3\,\mathrm{Tr}\,R^3 - \mathrm{Tr}\,R) = \frac{1569h}{16}, \tag{XIV.12.45}$$

$$c_{\text{block}} = \frac{1}{32}(9\,\mathrm{Tr}\,R^3 - 5\,\mathrm{Tr}\,R) = \frac{829h}{8}. \tag{XIV.12.46}$$

The quartic gives $a_{\text{block}} = 1569/8,\ c_{\text{block}} = 829/4$. The exact-$R$ qualification matters: the integrated polynomial would still describe the named background current if it were only a trial R, but then these numbers would not be its physical central charges.

To calibrate k_i, use the mixed term for a single left Weyl fermion of R-charge q in a representation ρ. In dimensionless characteristic-class curvatures the relevant term is $-qr\ \mathrm{tr}_\rho\, F^2/2$. Define the physics quadratic index $T(\rho)$ by $\mathrm{tr}_\rho(T^aT^b) = T(\rho)\delta^{ab}$ with $T(\mathrm{adj}) = h^\vee$. Since $Y = \mathrm{tr}_{\mathrm{adj}}\, F^2/(4h^\vee)$, we obtain

$$-\tfrac{1}{2}qr\ \mathrm{tr}_\rho\, F^2 = -2qT(\rho)\, rY, \qquad k_{\text{poly}} = -2\ \mathrm{Tr}(RT^aT^b)/\delta^{ab}. \tag{XIV.12.47}$$

As a sign check take a free $\mathcal{N} = 1$ fundamental chiral of $SU(N)$. Its scalar has $R = 2/3$, its Weyl fermion $q = -1/3$, and $T = 1/2$. Thus $k_{\text{poly}} = 1/3$. Its positive contribution to gauge screening is $1/2$, fixing the convention $b_{\text{matter}} = 3k_{\text{poly}}/2$ in this free example.

For an interacting block the free example establishes the normalization only. To compute physical weak screening, assume the ungauged block is a unitary $\mathcal{N} = 1$ SCFT with the exact R_{SCFT} specified in (XIV.12.44), and no other charged sectors in the weak-gauging problem. The protected current-multiplet relation then fixes the two-point coefficient of the flavor current by the mixed anomaly with R_{SCFT}. In our gauge beta convention this says

$$b_{\text{matter}} = -3\ \mathrm{Tr}(R_{\text{SCFT}}T^aT^b)/\delta^{ab} = \tfrac{3}{2}k_{\text{poly}}, \tag{XIV.12.48}$$

$$\mu\frac{dg_{\text{gauge}}}{d\mu} = -\frac{b_{\text{weak}}}{16\pi^2}g_{\text{gauge}}^3 + \cdots, \qquad b_{\text{weak}} = 3h^\vee - b_{\text{matter}}. \tag{XIV.12.49}$$

This is a relation at the decoupled reference point. If the R current used in the polynomial were a different trial current, its mixed trace would not give the physical two-point coefficient. The same premise is needed for the comparisons at other genera.

For the quartic, the matter contribution is 36 under these assumptions. The single adjoint gaugino has $q = 1$ and contributes $k_{\text{vec}} = -24$ in the polynomial, so the formal mixed $RE_{6,L}^2$ anomaly vanishes, and $b_{\text{weak}} = 36 - 36 = 0$ when the current identity applies. Explicitly

$$I_6^{\text{vec}} = 78\left(\tfrac{1}{6}r^3 - \tfrac{1}{24}rp\right) - 24rY_L, \tag{XIV.12.50}$$

$$[rY_L]\,(I_6 + I_6^{\text{vec}}) = 0, \qquad [rY_R]\,(I_6 + I_6^{\text{vec}}) = 24. \tag{XIV.12.51}$$

We added the vector on the compact side only. The right flavor anomaly persists. The vanishing of a pure cubic local E_6 gauge anomaly has a separate reason: the invariant degrees of $\mathfrak{e}_6$ are $2, 5, 6, 8, 9, 12$, with no invariant of degree three on the Lie algebra. For example the Coxeter polynomial of the E_6 root reflections is $\Phi_{12}(s)\Phi_3(s)$, giving

exponents $1, 4, 5, 7, 8, 11$ and these degrees by adding one. The cubic invariant on vectors of the 27 is a different tensor; it does not give a symmetric invariant on three adjoint Lie algebra arguments.

At zero gauge coupling one may also add the central charges of the free vector and of the block, since their stress tensors belong to a decoupled product. For the vector, using its 78 fermions of charge one gives

$$(a_{\text{vec}}, c_{\text{vec}}) = (117/8, 39/4), \qquad (a_{\text{product}}, c_{\text{product}}) = (843/4, 217). \tag{XIV.12.52}$$

These are not central charges of a calculated finite-coupling fixed point. Even with the assumed ungauged SCFT, a vanishing leading coefficient does not determine the next term in the running or prove exact marginality. The mixed trace identity also does not address global anomalies.

A change of genus illustrates the dependence of the weak test on the twist, even with the same six-dimensional input. In the abstract unfluxed, unpunctured compactifications with genus $2, 3, 4$, the predicted screening from (XIV.12.49) is $18, 36, 54$ if each has the stated exact SCFT current. Subtracting these from 36 gives $+18, 0, -18$. A positive b_{weak} makes the small gauge coupling decrease toward the ultraviolet in this convention. Negative b_{weak} reverses the leading tendency. These genus-two and genus-four tests are not additional members of the selected smooth plane family. They compare the polynomial reduction on other abstract curves.

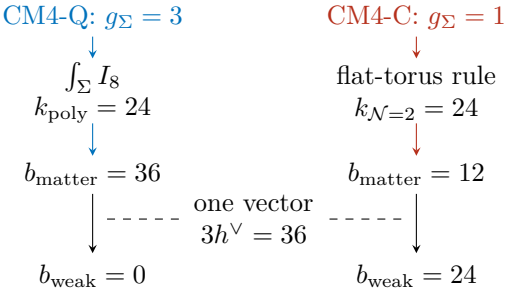


Figure XIV.12.5: Two inputs for the screening test. For genus greater than one, push the twist-dependent anomaly down the curve and use the exact R current of the assumed block. For the flat torus, use the very-Higgsable compactification rule. The final subtraction by the same vector contribution is common to the two calculations.

The actual CM4-C is a flat-torus control with periodic spin structure and trivial flavor backgrounds. Direct integration of (XIV.12.41) gives zero, because there is no curvature leg on the torus. That zero does not say that the torus block has no anomalies. The separate very-Higgsable compactification rule gives the protected data of the resulting $\mathcal{N} = 2$ block. To use it, let $\alpha, \beta, \gamma, \delta$ denote the coefficients of C^2, Cp, p^2, p_2 in I_8, and let κ be that of pY_L. In the normalization of the torus rule the coefficient of

$p\,\mathrm{Tr}F_L^2$ is $\kappa/4$, not κ. The rule gives

$$a_{T^2} = 24\gamma - 12\beta - 18\delta = \frac{613}{24}, \qquad c_{T^2} = 64\gamma - 12\beta - 8\delta = \frac{173}{6}, \quad \text{(XIV.12.53)}$$

$$k_{\mathcal{N}=2} = 192\,\frac{\kappa}{4} = 24, \qquad b_{\mathrm{matter},T^2} = \frac{k_{\mathcal{N}=2}}{2} = 12. \quad \text{(XIV.12.54)}$$

For example the a formula combines $553/240 + 89/4 + 79/80 = 613/24$; the C^2 slot does not enter this rule. Both the coefficient used and the operation on it differ from the twist integral. Here $k_{\mathcal{N}=2}$ is a flavor central charge in the $\mathcal{N}=2$ current convention, distinct from k_{poly} of (XIV.12.47). To use this screening, take the sourced torus block with its protected current and the inherited exact $\mathcal{N}=1$ subalgebra used for gauging, with no extra charged sectors. The gauging in this example uses the $\mathcal{N}=1$ vector, without its would-be adjoint chiral partner. Thus $b_{\mathrm{weak},T^2} = 36 - 12 = 24$, as opposed to zero for CM4-Q under its premises. The two values in Figure XIV.12.5 compare different reductions of the same transverse sector. The flat-torus value is not the $h=0$ substitution in (XIV.12.43), and neither value determines an infrared phase.

XIV.12.6 Changing flux or changing the geometry

Which inputs change the protected anomaly, and which can remove the collision itself? A right flavor line on the compactification curve changes the characteristic classes inserted into I_8. Changing the holomorphic equation instead can replace the two intersecting supports by a single support. We will perform these operations separately; the first does not deform the quartic Weierstrass polynomial, and the second does not specify a flux background.

Keep the left E_6 background and reduce the right flavor algebra to $\mathfrak{so}(10) \oplus \mathfrak{u}(1)$. Normalize the abelian generator by the adjoint decomposition

$$\mathbf{78} = \mathbf{45}_0 \oplus \mathbf{16}_3 \oplus \overline{\mathbf{16}}_{-3} \oplus \mathbf{1}_0, \qquad x = \frac{16(3)^2 + 16(-3)^2}{12} = 24. \quad \text{(XIV.12.55)}$$

The semisimple restriction has embedding index one. The trace in the Y convention includes a factor $1/4$. Hence with $j = c_1(U(1)_f)$, trial mixing parameter ϵ, and integral degree ℓ for the right flavor line of the chosen generator, the substitution is

$$Y_R = Y_D - \tfrac{x}{4}(j + \epsilon r + \ell\eta)^2 = U - 12\ell Q_0 \eta, \qquad Q_0 = j + \epsilon r, \quad U = Y_D - 6Q_0^2. \quad \text{(XIV.12.56)}$$

Here Y_D uses the normalized $\mathfrak{so}(10)$ trace. The sign in the abelian substitution is the Chern-class convention of (XIV.12.47). Choosing the displayed generator and an integral line does not establish the global flavor group or a set of all admissible fluxes.

Use the coefficients of (XIV.12.41): $\alpha = 319/24$, $\beta = -89/48$, $\xi = -6$ on $C(Y_L + Y_R)$, $\nu = 1$ on each Y_i^2, $\chi = 1$ on $Y_L Y_R$, and $\kappa = 1/2$ on $p(Y_L + Y_R)$. The η coefficient is the derivative with respect to C times $-2hr$, plus the derivative with respect to Y_R times $-12\ell Q_0$, evaluated at $(C, Y_R) = (-r^2, U)$. This gives

$$I_6 = 4\alpha h r^3 - 2\beta h r p - 2\xi h r (Y_L + U) - 12\ell Q_0 (2\nu U - \xi r^2 + \kappa p + \chi Y_L). \quad \text{(XIV.12.57)}$$

In particular the direct mixed slots at fixed r are $[jY_L]I_6 = -12\ell$ and $[jY_D]I_6 = -24\ell$. The first tests the $Y_L Y_R$ coefficient: if one forgot the center-of-mass Green–Schwarz removal and set $\chi = 0$, this term would vanish. It also tests the direction of flux, even when the protected central charges are unchanged under reversal.

Set $j = 0$ to extract the trial R traces. The first line of (XIV.12.57) contributes a term $-72h\epsilon^2 r^3$ from the shift in U, and the flux derivative contributes $(144\ell\epsilon^3 - 72\ell\epsilon)r^3 - 6\ell\epsilon rp$. Including the original terms gives

$$\operatorname{Tr} R^3_{\text{trial}} = 319h - 432h\epsilon^2 + 864\ell\epsilon^3 - 432\ell\epsilon, \tag{XIV.12.58}$$

$$\operatorname{Tr} R_{\text{trial}} = -89h + 144\ell\epsilon, \qquad k_L = 12h - 12\ell\epsilon, \qquad k_D = 12h - 24\ell\epsilon. \tag{XIV.12.59}$$

One can test the abelian substitution before making a choice of trial current. At $\epsilon = 0$ the terms containing j are

$$I_6\big|_{\epsilon=0} - I_6\big|_{\epsilon=j=0} = -72h\, rj^2 + 144\ell j^3 - 72\ell r^2 j - 6\ell pj - 12\ell j Y_L - 24\ell j Y_D. \tag{XIV.12.60}$$

For example the cubic term comes from $-12\ell j\,(2\nu)(-6j^2)$, so it is odd in ℓ, while the rj^2 term comes from the twist derivative and is independent of ℓ. Setting $j = 0$ at the start without recording its insertion would discard the very coefficient that detects flux orientation. Thus the function to extremize for the *ungauged* block is

$$a_{\text{trial}}(\epsilon) = \frac{1569h}{16} - 135\ell\epsilon - \frac{243}{2}h\epsilon^2 + 243\ell\epsilon^3. \tag{XIV.12.61}$$

This use of a-maximization assumes an admissible supersymmetric compactification with no additional mixable currents and a unitary infrared SCFT. The local maximum gives the candidate exact R under those premises. At $\ell = 0$ and $h > 0$ the function is quadratic with maximum at zero. At $\ell \neq 0$, solve

$$a' = 729\ell\epsilon^2 - 243h\epsilon - 135\ell = 0, \qquad a'' = 1458\ell\epsilon - 243h, \tag{XIV.12.62}$$

$$D = \sqrt{9h^2 + 60\ell^2}, \qquad \epsilon_\pm = \frac{3h \pm D}{18\ell}, \qquad a''(\epsilon_\pm) = \pm 81D. \tag{XIV.12.63}$$

The minus sign labels the maximum by curvature for either sign of ℓ; it need not label the smaller numerical root. The positive-curvature root would incorrectly reverse which trial current enters the weak test.

For $h = 2,\ \ell = 1$, the roots are $1/3 \pm 2\sqrt{6}/9$ and the Hessians are $\pm 324\sqrt{6}$. At the negative-curvature root, the conditional screening and weak coefficient are

$$b_{\text{matter}} = 18h - 18\ell\epsilon_- = 15h + D, \qquad (b_{\text{matter}}, b_{\text{weak}}) = (30 + 4\sqrt{6}, 6 - 4\sqrt{6}). \tag{XIV.12.64}$$

For a check independent of the weak coefficient, put $\epsilon = \epsilon_-$ in the two trace equations in (XIV.12.59). At $(h, \ell) = (2, 1)$ this gives

$$\operatorname{Tr} R_{\text{trial}} = -130 - 32\sqrt{6}, \qquad \operatorname{Tr} R^3_{\text{trial}} = 430 + \frac{928}{9}\sqrt{6}, \tag{XIV.12.65}$$

$$(a, c)_{\text{trial}} = \left(\frac{1065}{8} + 32\sqrt{6},\ \frac{565}{4} + 34\sqrt{6}\right), \qquad k_D = 16 + \frac{16}{3}\sqrt{6}. \tag{XIV.12.66}$$

The D_5 mixed coefficient differs from $k_L = 20 + 8\sqrt{6}/3$, because the Y_D term is affected by the right flavor square as well as the twist. This interprets the trial output physically only when the extremum gives the exact current of the ungauged SCFT with no other charged sectors. As a check, changing ℓ to -1 reverses the two stationary values with their curvature labels preserved, and leaves $\ell\epsilon_-$, a, c, k_L, k_D and b_{weak} fixed. In the full I_6 this is equivalent to also reversing the external generator j: terms odd in j flip. The sign of $[jY_L]I_6$ accordingly changes from -12 to $+12$ in the same external frame. For $h = 1$, $\ell = 2$ the two roots are $(3 \pm \sqrt{249})/36$, with Hessians $\pm 81\sqrt{249}$. The weak coefficient at the formal maximum becomes $21 - \sqrt{249} > 0$. Simultaneously changing genus and flux can therefore reverse the sign of the candidate weak coefficient.

The source warns that low flux, often degree one, can make this procedure inadequate for determining the physical four-dimensional anomalies. Alternative methods are then needed. The $\ell = \pm 1$ stationary values just computed are exact properties of the polynomial; they do not settle whether those backgrounds yield the assumed SCFT. No compact G_4 or compatible seven-brane gauge background on CM4-Q is constructed by this insertion. Moreover $[jY_L]I_6 \neq 0$ means the flavor $U(1)$ has a mixed anomaly with the left gauge algebra. It is not automatically a conserved flavor current after left gauging. One cannot rerun the ungauged extremization as if the same mixing space were available at finite gauge coupling.

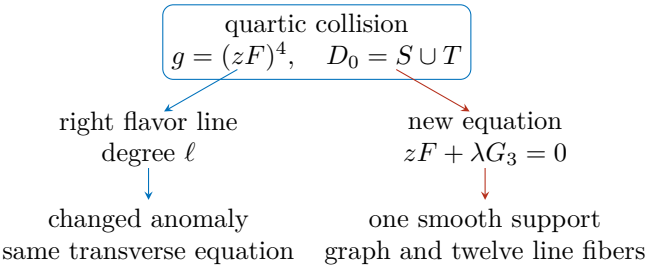


Figure XIV.12.6: Two different changes. Right flavor flux changes the curve leg of the anomaly while keeping the transverse equation. The deformation of the quartic equation changes the support itself; over the twelve common zeros of F, G_3, the deformed support includes whole line fibers. Neither operation establishes a compact background or a quantum vacuum.

We now change the equation instead. On CM4-Q, zF and $G_3 = X_0X_1X_2$ both have class $3H$. Thus the following path stays in the same space of g-sections:

$$D_\lambda = \{zF + \lambda G_3 = 0\}, \qquad g_\lambda = (zF + \lambda G_3)^4 \in H^0(B, 6L). \tag{XIV.12.67}$$

At $\lambda = 0$ the support is $S \cup T$. For $\lambda \neq 0$, away from $F = 0$ it is the graph of $z = -\lambda G_3/F$. At $F = 0$, membership requires $G_3 = 0$. Each coordinate line contains four simple quartic roots: for example, on $X_0 = 0$, $X_2 = 1$ they solve $X_1^4 + 1 = 0$, all nonzero with nonzero derivative. There are no roots at the coordinate vertices. Thus there are twelve common zeros, with F, G_3 independent local coordinates at each. In a

trivialization there,

$$d(zF + \lambda G_3)\big|_{F=G_3=0} = z\,dF + \lambda\,dG_3 \neq 0. \tag{XIV.12.68}$$

At $F \neq 0$ the derivative in the line direction is nonzero. More explicitly, at each common zero use $(s, t') = (F, G_3)$ as base coordinates. The equation for the support is $t' = -zs/\lambda$, so s, z are smooth coordinates on the deformed support even at $s = 0$. In this chart the projection to the plane forgets z and sends (s, z) to $(s, -zs/\lambda)$. For $s \neq 0$ there is one point above a base point, and for $s = 0$ the entire line maps to the common zero. Merely writing $z = -\lambda G_3/F$ would lose this part of the support. This proves smoothness on the whole support. The graph over $F \neq 0$ is irreducible, and every point of a line fiber over a common zero is in its closure, by approaching with $G_3 = -zF/\lambda$ at fixed z in the local chart. Hence the support is irreducible and noncompact. The generic split IV* locus remains, but there are no longer two divisors with the nonminimal collision of (XIV.12.9).

This classical support change is not a determination of a four-dimensional modulus. Its effect on the asymptotic support matters if the noncompact flavor boundary condition is held fixed. To promote λ to a field one would need the correct allowed variations and a finite kinetic norm; the constant-mode norm comparison on the original supports cannot answer that question. The source's quantum recombination proposal for a different confining example gives no instanton amplitude or generated superpotential in CM4-Q. The lesson for comparing construction mechanisms is that the same collision admits distinct questions about local geometry, protected responses and quantum dynamics. The first two supplied calculations here; the last requires new physical input.

XIV.12.7 Exercises

1. **Transport the coefficient classes.** Take a smooth Fermat curve of degree $d = 5$. Find the normal exponent n that makes $g = (zF)^4$ a section of $6L$. Submit the degrees of g and $g/z^4|_S$ on the plane, the genus, and the two normal degrees in the order S-normal, T-normal. Explain why this mathematical control does not establish a new physical compactification.

2. **Blow up a mixed crossing.** With $f = 0,\ g = u^4v^2$ in the transverse plane, submit the order triples along $u, v, (u, v)$, the two leading cover roots' orders in the respective spectator variables, and the exponents of the transformed g in the ordered charts $(u, v) = (a, ab)$ and $(u, v) = (cd, d)$. Give the next corner orders in both charts. Explain how the cover test and the crepant divisibility test use different data.

3. **Move to a different genus.** Use an abstract unfluxed genus-four curve. Submit the four reduced coefficients $\operatorname{Tr} R^3, \operatorname{Tr} R, k_L, k_R$, and add one left vector. Give the remaining left and right rY_i coefficients and the conditional weak coefficient. Explain the premise that makes the last quantity physical.

4. **Reverse the flux.** Take $g_\Sigma = 3, \ell = -1$. Submit the roots by curvature label, their Hessians, both jY_i coefficients and the conditional b_{weak} at the maximum.

Explain why the same trial flavor current need not survive left gauging and why the roots do not settle the unit-flux infrared theory.

5. **Regulate the mode norms.** Take $t = 2$, $U = 3$ for the quartic. Submit $A_\Sigma, V_S, V_T(U), V_B(U)$ and the two leading cutoff powers for T, B. Explain which volumes would change if one increased t while holding U fixed.

6. **Recombination and boundary data.** Prove that the line over a common zero of F, G_3 lies in the graph closure for nonzero λ. State what further kinetic and boundary conditions one would have to check before treating λ as a field. Why would that still leave the quantum superpotential undetermined?

Use `benchmark/tasks.json` for bounded answer fields and `benchmark/PROTOCOL.md` for submission. Written explanations require human assessment.

Status and sources

§1. The collision. Coefficient classes, the two Fermat realizations, normal degrees and ideal orders are [MATH]. The model is specialized from Apruzzi et al. (2018), arXiv:1803.00582v2, §5.1, eqs. (5.7)–(5.14), physical pp. 20–22. In eq. (5.11) the final g_j bundle uses $6 - j$ in the power of the normal line after expressing L by adjunction. Ordinary Kodaira and square-cover interpretation is [GEO-E]; see Katz et al. (2011), arXiv:1106.3854v1, §5 eq. (5.3), §7 eq. (7.1), physical pp. 17,21 and Table 2 p. 23, using the Weierstrass convention $\Delta_{\text{book}} = 4f^3 + 27g^2$. The same-order nonsquare jet is a separate local control.

§2. The blowups. The charts, residue factors, transverse intersection pairing and marked flex test are [MATH]; the ordinary fiber-algebra dictionary has the conditions above. See Apruzzi et al. (2018), v2 App. A eqs. (A.5)–(A.7), physical pp. 43–44, for the blowup transformation, and Del Zotto et al. (2015), arXiv:1407.6359v3, §2, eqs. (2.2),(2.5), physical pp. 8–9, for the chain interpretation. A marked three-torsion point is not a global form determination. The finite examples and selected variations test only the displayed cases, not every change of a transverse intersection or ordinary IV configuration. An ordinary IV flavor-flux label alone does not establish physical flux data. The singular Fermat example requires a derivative test in addition to the identity check. These calculations do not constitute a general model validator or assess a student derivation.

§3. The block and twist. The minimal conformal matter identification and supersymmetric compactification are [GEO-E]; see Del Zotto et al. (2015), v3 §2 and Apruzzi et al. (2018), v2 §2, eq. (2.2), physical pp. 6–7, and App. B.3, eqs. (B.19)–(B.21), physical pp. 48–49. The bitangent and the degrees are [MATH]. No flat flavor breaking, punctures or additional defects are inserted. The local chart does not trivialize the curve neighborhood.

§4. Gauging and six-dimensional input. The auxiliary metric integrals and plane cohomology are [MATH]; their ordinary kinetic and twisted field interpretations are [GEO-E]. See Apruzzi et al. (2018), v2 §5.1, and Chapter 2 for the ordinary twisted

dictionary. The complete interacting polynomial is sourced protected input, [GEO-E]. See Apruzzi et al. (2018), v2 App. B eqs. (B.1)–(B.2), Table 2, physical pp. 44–45, and Ohmori et al. (2014), published PTEP §3.2.2 eqs. (3.23)–(3.25), printed/physical p. 15 of 26, and App. A eqs. (A1),(A3)–(A8),(A10), pp. 20–22, with (A10) on p. 22. Section 3.3 starts below the cited equations.

§5. Pushforward and weak gauging. The formal reduction and polynomial identities are [MATH]. The physical screening interpretation uses the protected SCFT current-multiplet identity under the exact-R premise for every genus. For conventions and the Weyl calibration see Apruzzi et al. (2018), v2 §3 eqs. (3.3)–(3.7) and B.1 eqs. (B.3)–(B.16), physical pp. 46–47; the mixed trace is normalized by the Chern character, not by a literal reading of the sign in (B.5). The separate very-Higgsable torus prescription is [GEO-E]; see v2 eqs. (3.8),(B.17) and Ohmori et al. (2015), arXiv:1503.06217v1, §6.2 eqs. (6.3)–(6.4), physical p. 18, and §6.3 eqs. (6.42)–(6.46), p. 26. The genus-three candidate is discussed in AHMT v2 §5.4.1, physical p. 39. No finite-coupling fixed point or exact marginality is established.

§6. Flux and recombination. The formal flux reduction and extrema use Apruzzi et al. (2018), v2 App. B.3, eqs. (B.29)–(B.32), Table 3, and eqs. (B.39)–(B.45), Table 6. Section 2 explicitly warns that too little flavor flux, often degree one, can require a different method to obtain physical anomalies. In the fixed unit j and $Y = \mathrm{Tr}/4$, direct substitution in (B.1) using (B.31a) gives $-x\ell\chi/2$ and $-x\ell\nu$ for the mixed jY_L, jY_D slots. The standalone $U(1)$ entries of v2 (B.46) are twice these in the E_6 specialization. We use the directly consistent polynomial; the left trial-R coefficient and conditional screening agree with (B.44)–(B.45) and Table 6. Numbering here is for arXiv v2, not the journal version. Smooth irreducible recombination support is [MATH]. See Del Zotto et al. (2015), v3 §2.1 and AHMT v2 §5.4, eqs. (5.30)–(5.33), for related physical proposals. No normalizable modulus, compact completion, full spectrum or quantum confinement follows.

References

Apruzzi, F. et al. (2018). "4D Gauge Theories with Conformal Matter". In: *JHEP* 09, p. 088. DOI: 10.1007/JHEP09(2018)088. arXiv: 1803.00582 [hep-th].

Del Zotto, M. et al. (2015). "6d Conformal Matter". In: *JHEP* 02, p. 054. DOI: 10.1007/JHEP02(2015)054. arXiv: 1407.6359 [hep-th].

Katz, S. et al. (2011). "Tate's algorithm and F-theory". In: *JHEP* 08, p. 094. DOI: 10.1007/JHEP08(2011)094. arXiv: 1106.3854 [hep-th].

Ohmori, K. et al. (2014). "Anomaly polynomial of general 6D SCFTs". In: *PTEP* 2014, 103B07. DOI: 10.1093/ptep/ptu140. arXiv: 1408.5572 [hep-th].

Ohmori, K. et al. (2015). "6d $\mathcal{N} = (1, 0)$ theories on T^2 and class S theories: part I". In: *JHEP* 07, p. 014. DOI: 10.1007/JHEP07(2015)014. arXiv: 1503.06217 [hep-th].

Chapter XIV.13

Atlas of four-dimensional constructions

XIV.13.1 Choosing a construction from field-theory data

Suppose we want a four-dimensional gauge field with a primitive abelian charge direction over $\mathbb{P}^3$. Does specifying the base and the gauge datum determine the geometry? Chapters 2–12 supplied examples in the opposite direction: choose a geometry, compute a divisor, a charged curve, a flux moment or an anomaly, and then ask what the result means in four dimensions. We will now use those calculations to narrow a choice of geometry. To use the chapter, recall the intersection charge of a wrapped M2-brane, the role of the Shioda projection, and the distinction between a holomorphic zero-mode count and a normalized interaction.

A useful first question is what we actually want to compute. A split A_4 gauge sector calls for a relatively minimal split I_5 fiber along a surface. A primitive abelian direction calls for a section with an integrally normalized charge pairing. A neutral instanton calculation instead calls for a vertical divisor and an ordinary fermion zero-mode test. In particular, the existence of a specified section can answer a gauge question before any four-form flux is chosen. Its leading gauge kinetic term can still vary. In the two Morrison–Park (MP) section models below, write H for the hyperplane on $\mathbb{P}^3$, with $H^3 = 1$, and define the height b_σ using the fibration π:

$$b_\sigma = -\pi_*(\sigma^2) = hH, \qquad h = \int_{\mathbb{P}^3} H^2 b_\sigma. \tag{XIV.13.1}$$

The integral returns the coefficient in the specified primitive charge frame. Rescaling the generator by k rescales every charge by k and the height by k^2; it cannot be used to identify heights computed in the same primitive frame. The two twists give the

following bounded choices; we derive the entries in Section XIV.13.5.

$$\{\,\mathbb{P}^3,\ \text{one primitive abelian direction}\,\} \ \rightsquigarrow\ \{\mathrm{MP}(5),\mathrm{MP}(6)\}, \tag{XIV.13.2}$$

$$h=14 \ \rightsquigarrow\ \{\mathrm{MP}(5)\}, \qquad h=12 \ \rightsquigarrow\ \{\mathrm{MP}(6)\}. \tag{XIV.13.3}$$

Here and below a listed direction does not specify the full Mordell–Weil group. Even fixing the height leaves the admissible fluxes, Higgs expectation values and charged cohomology to be determined. If the target instead fixes $h=13$, both known heights disagree:

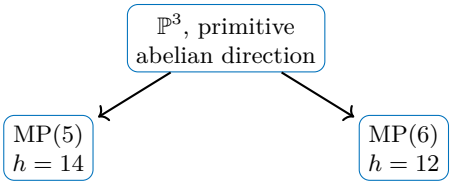
$$\{\,\mathbb{P}^3,\ \text{one primitive direction},\ h=13\,\} \ \rightsquigarrow\ \varnothing \quad \text{among these choices.} \tag{XIV.13.4}$$

This is an empty result within the comparison, with no consequence for existence in a different family.

A second question is how to combine the requirements. First ask whether the requirements make sense for the observable. A Shioda height constrains a gauge section, so it does not constrain the dressed M5 boundary calculation. An ordinary neutral index must be an integer, not a yes-or-no label. These requests are ill posed and stop before any model is tested. For a well-posed request, retain the constructions that address the observable, then compare each supplied condition with a fact about them. Write $p_i(M)$ for the truth of the i-th condition on a candidate M. There are three outcomes for the conjunction:

$$\bigwedge_i p_i(M) = \begin{cases} \text{confirmed}, & \text{all supplied conditions hold},\\ \text{excluded}, & \text{a supplied condition fails},\\ \text{unresolved}, & \text{none fails and at least one is unknown}. \end{cases} \tag{XIV.13.5}$$

This is physical reasoning with partial information. An unknown global gauge group cannot rescue a model whose base is the wrong threefold. Conversely, absence of a base determination is not evidence for the wrong base. Figure XIV.13.1 illustrates the distinction.



Split A_4, B_{bl}	SU5-Q: base disagrees
Dressed M5, B_{bl}	T_{11}: base undetermined here

Figure XIV.13.1: Three inverse questions. The height discriminates the two primitive section constructions on the same base. A known mismatch excludes the ordinary I_5 candidate on a different base; missing base data leave the charged instanton example unresolved.

For example let $B_{\mathrm{bl}} = \mathrm{Bl}_p\,\mathbb{P}^3$. The pullback hyperplane and the exceptional class are independent on B_{bl}, whereas $\mathbb{P}^3$ has Picard rank one. The ordinary split A_4 example SU5−Q has base $\mathbb{P}^3$; the T_{11} construction discussed below specifies a charged boundary calculation without a base determination for this comparison. Thus

$$\rho(\mathbb{P}^3) = 1, \qquad \rho(B_{\mathrm{bl}}) = 2, \tag{XIV.13.6}$$

$$p_{B_{\mathrm{bl}}}(\mathrm{SU5{-}Q}) = \text{false}, \qquad p_{B_{\mathrm{bl}}}(T_{11}) = p_{\mathbb{P}^3}(T_{11}) = \text{unknown}. \tag{XIV.13.7}$$

The second line concerns different starting observables: the first example is a candidate for a gauge algebra, and the second is a candidate for a charged instanton insertion. The two are not alternatives within a single request. For the neutral M5 test there is instead a known support with the desired ordinary index on the blowup base:

$$\{\, B_{\mathrm{bl}},\ \chi(\mathcal{O}_D) = 1,\ \text{ordinary neutral test} \,\} \ \rightsquigarrow\ \{\, \pi^{-1}(E) \,\}. \tag{XIV.13.8}$$

Section XIV.13.4 computes that index and the extra neutral counts for two comparison supports. These results neither rule out a split A_4 construction on B_{bl} nor identify the base of the charged instanton.

Table XIV.13.1 gives the scope of the choices used in this chapter. Keep separate calculations on the same geometry in separate rows. Otherwise, combining an available flux period with an available local pairing can silently assert a compatibility that neither calculation addresses. The observation to carry into the next section is that even the ordinary gauge geometry supplies its matter data in several steps.

Construction	Base	Output used here
SU5-Q geometry	$\mathbb{P}^3$	Ordinary split I_5, matter supports
SU5-Q flux	$\mathbb{P}^3$	Formal periods and D3 budget
SU5-Q local pairing	$\mathbb{P}^3$ (support)	Pairing on specified local modules
MP(5), MP(6) parents	$\mathbb{P}^3$	Primitive direction, heights $14H, 12H$
MP(5) child	$\mathbb{P}^3$	Period and index two on the smooth open
Witten $E, H, H-E$	$\mathrm{Bl}_p\,\mathbb{P}^3$	Three ordinary neutral tests
T_{11} dressed	Undetermined here	Charged M2 boundary condition
CM4-Q, CM4-C	$\mathrm{Tot}\,\mathcal{O}_{\mathbb{P}^2}(-1)$, (-3)	Same local link, different reductions

Table XIV.13.1: Geometric and protected data used in the comparison. Each grouped line lists distinct choices in the order of its outputs.

XIV.13.2 Ordinary seven-brane sectors

How much matter information follows from an ordinary split I_5 stack? In the ordinary, relatively minimal seven-brane dictionary, the split fiber supplies the algebra $\mathfrak{su}(5)$. The

model of Chapter 2 places the fiber over a smooth quadric $Q = (w = 0) \subset \mathbb{P}^3$. In the named split Tate presentation the coefficients are

$$(a_1, a_2, a_3, a_4, a_6) = (b_5, wb_4, w^2b_3, w^3b_2, w^5b_0). \tag{XIV.13.9}$$

Each a_i is a section of $\mathcal{O}(4iH)$ and w has degree two. Thus the five b's in descending order have degrees $4, 6, 8, 10, 14$. Over a generic point of Q, b_5 and the leading residual polynomial P are nonzero. The Tate discriminant has order five there. The leading double-root quadratic for the multiplicative fiber splits because its tangent slopes are determined by b_5 in the function field. Along Q the two ordinary matter loci are cut by

$$C_{10} : \ b_5 = 0, \qquad C_5 : \ P = b_4b_3^2 - b_5b_3b_2 + b_5^2b_0 = 0. \tag{XIV.13.10}$$

All terms of P have degree 22. Since the embedding of $Q = \mathbb{P}^1 \times \mathbb{P}^1$ is the Segre embedding, the hyperplane restricts to $h_1 + h_2$, the sum of the two ruling classes. Hence C_{10} and C_5 have bidegrees $(4, 4)$ and $(22, 22)$.

To find the genus, write $C = dh_1 + eh_2$ on Q. The ruling squares vanish, $h_1h_2 = 1$, and $K_Q = -2h_1 - 2h_2$, so adjunction gives

$$2p_a(C) - 2 = C \cdot (C + K_Q) = 2de - 2d - 2e, \tag{XIV.13.11}$$

$$p_a(C) = (d - 1)(e - 1), \qquad \big(g(C_{10}), p_a(C_5)\big) = (9, 441). \tag{XIV.13.12}$$

Take the open with C_{10} smooth and C_5 integral with precisely the 64 ordinary nodes. The node count uses the intersection of $b_5 = b_3 = 0$ on Q, of degrees $(4, 4), (8, 8)$. Locally P is quadratic in these two transverse coordinates, with a nondegenerate quadratic term on the stated open. Each node removes a one-dimensional quotient between the normalization and the original structure sheaf. Therefore

$$\#\text{nodes} = (4h_1 + 4h_2)(8h_1 + 8h_2) = 64, \qquad g(\widetilde{C}_5) = 441 - 64 = 377. \tag{XIV.13.13}$$

Computing cohomology on the normalization then requires deciding how values at the two branches are glued. The number 377 alone does not count any modes of the singular support.

The next step is to choose the oriented fibral curve whose charge will be measured. In the first resolved phase let $V = D_2D_4$ denote the shared effective surface over C_{10}, with generic fiber γ_{sh}. For the strict Cartans D_i, the ambient intersection reduction of Chapter 4 gives $\int_V HD_i = (8, -8, 8, -8)$. Since $\deg H|_{C_{10}} = 8$, dividing by eight gives the actual fiber intersections. The electric convention reverses their signs. For $\lambda_i = \mathbf{e}_i - \sum_j \mathbf{e}_j/5$, the weight $\lambda_2 + \lambda_4$ has simple-coroot pairings given by successive differences of $(0, 1, 0, 1, 0)$. We obtain

$$q_{\mathrm{geom}} = (1, -1, 1, -1), \qquad q_{\mathrm{el}} = (-1, 1, -1, 1). \tag{XIV.13.14}$$

The electric charge lists the coroot pairings of a weight of $\wedge^2\mathbf{5}$. The five strict fiber divisors sum to the pullback of Q, which has degree zero on the fiber. The four strict Cartan entries sum to zero, so the affine intersection also vanishes. Reversing the charge label is a convention change; reversing the orientation of V would instead negate every period of V.

The formal four-form G_* of Chapter 3 is expressed using the ordered ambient products $U = (H^2, ZH, HD_1, HD_2, HD_3, HD_4)$, with Z the zero section. The first two intersections of U with V vanish by dimension over the base curve and disjointness from Z. With $\int V^2 = -16$ and $\int_V c_2/2 = 8$ in the stated crepant phase, the period is

$$G_* = (91, 24, -12, -18, -30, -14) \cdot U - 2V - \tfrac{1}{2}c_2, \tag{XIV.13.15}$$

$$\int_V G_* = 8(-12 + 18 - 30 + 14) - 2(-16) - 8 = -56. \tag{XIV.13.16}$$

This calculation uses the complex orientation of V, even in the electric convention. Replacing V by the full second Cartan over C_{10} would give zero: $D_2(4H)$ lies among the ambient test products on which G_* has zero periods. The calculation identifies a formal flux period on one oriented weight surface. Physical chirality would additionally need a compatible background and the matter-sheaf identification.

Even when a chiral index has a sheaf interpretation, it does not give both dimensions. To see the difference explicitly, on the smooth genus-nine curve $C = C_{10}$ take the prescribed lines $M_q = \mathcal{O}_C(1 + q, 1 - q)$. These are a separate comparison, with spin factor $\mathcal{O}_C(1, 1)$ and ruling difference $\mathcal{O}_C(1, -1)$. For any of these lines, Riemann–Roch gives

$$\deg M_q = 4(1 + q) + 4(1 - q) = 8, \qquad h^0(M_q) - h^1(M_q) = 8 + 1 - 9 = 0. \tag{XIV.13.17}$$

To compute the dimensions choose the smooth quartic whose affine equation is $F = 1 + x^4 + y^4 + 2x^4y^4$. The restriction exact sequence is

$$0 \longrightarrow \mathcal{O}_Q(a - 4, b - 4) \xrightarrow{F} \mathcal{O}_Q(a, b) \longrightarrow \mathcal{O}_C(a, b) \longrightarrow 0. \tag{XIV.13.18}$$

For $q = 1$, the three sections of $\mathcal{O}_Q(2, 0)$ restrict isomorphically on H^0, since H^0 and H^1 of the source $\mathcal{O}_Q(-2, -4)$ vanish. For $q = -4$, sections are the kernel of $H^1(-7, 1) \to H^1(-3, 5)$. Each target Laurent exponent of x receives linear polynomials in y multiplied by $1+y^4$ and $1+2y^4$. These span $1, y, y^4, y^5$. The two target x exponents are independent, so the rank is eight and the dimension of the kernel is $12 - 8 = 4$. For $q = 6$, Serre duality and the zero index let us compute $q = -6$ instead. For that line the map $H^1(-9, 3) \to H^1(-5, 7)$ has four target Laurent exponents of x; in each, the same two multipliers now act on cubics in y. They span the eight powers $1, \ldots, y^7$. The rank is 32 in a 32-dimensional target and the kernel is zero. We conclude

$$(h^0, h^1)(M_{-4}, M_1, M_6) = \big((4, 4), (3, 3), (0, 0)\big). \tag{XIV.13.19}$$

Adding x^2y^2 to F adds the two missing powers y^2, y^3 for each target exponent in the $q = -4$ map. The rank becomes twelve without changing the degree or index. This change takes place in the map of Laurent classes. It cannot be detected by an integrated charge. These degree-eight lines are prescribed comparisons. The separate rational Chow restriction for the shared component of $G_* + K$ instead has representative $\mathcal{O}_C(-6, -8)$, giving spin-twisted degree -48 and $(0, 56)$ for that representative. It does not determine a globally compatible physical sheaf.

A local interaction needs still different data. In the transverse residue of Chapter 5, the two defining equations have Jacobian determinant -1 at the point in the chosen

order. Evaluating profiles $(1, x)$ on the specified local generator gives $Y = \mathrm{diag}(-1, 0)$. In the distinct double-point comparison, let t be the local coordinate in the quotient $\mathcal{A} = \mathbb{C}[t]/(t^2)$. If $h = h_0 + h_1 t$ represents the third profile in the quotient, the residue on two profiles a, b is $-[t](hab)$. On $(1, t)$ it gives

$$Y_h = -\begin{pmatrix} h_1 & h_0 \\ h_0 & 0 \end{pmatrix}, \qquad \mathrm{rk}(Y_1, Y_t, Y_{t^2}) = (2, 1, 0). \tag{XIV.13.20}$$

Here changing the external profile changes the rank while the support and local module stay fixed. These profiles are not three Higgs vacua. Figure XIV.13.2 compares the inputs for the index and residue calculations. Neither the representative line nor the residue provides a global generation basis or a metric normalization for this cubic.

Smooth C_{10}, $\chi = 0$

q	(h^0, h^1)
-4	$(4, 4)$
1	$(3, 3)$
6	$(0, 0)$

Fixed support, $t^2 = 0$

profile	rank
1	2
t	1
t^2	0

Figure XIV.13.2: Two different maps at fixed numerical or geometric input. Left: the Laurent multiplication rank gives different pairs at index zero. Right: multiplication in the length-two quotient followed by extraction of the t coefficient detects different profiles on the same support.

The leading Tate weak-coupling limit gives an independent geometric comparison. The D7 factor is $(B_4^2 - B_2 B_6)/4$, where $B_2 = a_1^2 + 4a_2$, $B_4 = a_1 a_3 + 2a_4$, $B_6 = a_3^2 + 4a_6$ are evaluated before scaling. Substituting (XIV.13.9), the two terms of order four cancel:

$$\frac{B_4^2 - B_2 B_6}{4} = w^5\big[-P + w(b_2^2 - 4b_4 b_0)\big]. \tag{XIV.13.21}$$

At $b_5 P \neq 0$, this reproduces multiplicity five on the distinct local cover sheets. If $b_5 = b_3 = b_2 = b_0 = 1$ and $b_4 = 0$, the leading D7 polynomial instead starts at w^6; that change does not compute a finite-coupling enhancement. Neither comparison supplies global ordered monodromy or identifies this model with the K3 orientation example of Chapter 1. The next section asks what a different fiber geometry can say about a gauge group even before these flux and spectrum choices.

XIV.13.3 Continuous and discrete gauge data

When can the circle of an abelian gauge symmetry be replaced by a sign? There are two pieces to the answer. A smooth genus-one fibration can carry a bisection in place of the two sections of its elliptic parent. Separately, a four-dimensional field of charge two can leave a group of order two when it acquires an allowed expectation value. We can test the geometry and the stabilizer in the same charge frame without assuming a compact vacuum interpolates between them.

Use the $\beta = 5$ Morrison–Park parent on $\mathbb{P}^3$. In the resolved toric fiber write the coordinates u, v, w, s; the ambient divisors $u = 0$ and $s = 0$ restrict to U and S. The section polynomial is

$$P_1 = sw^2 + (b_0 s^2 u^2 + b_1 suv + b_2 v^2)w \\ + c_0 s^3 u^4 + c_1 s^2 u^3 v + c_2 s u^2 v^2 + c_3 u v^3. \tag{XIV.13.22}$$

The toric blowdown uses $u' = su,\ v' = v,\ w' = sw$ of fiber weights $(1, 1, 2)$. Multiplying P_1 by s and substituting gives $w'^2 + B_2 w' + C_4^{(0)}$, where $B_2 = b_0 u'^2 + b_1 u' v' + b_2 v'^2$ and $C_4^{(0)}$ has no v'^4 term. At $u' = 0$ the equation factors as $w'(w' + b_2 v'^2) = 0$. The ordered images are

$$U \mapsto [0 : 1 : -b_2], \qquad S \mapsto [0 : 1 : 0]. \tag{XIV.13.23}$$

In particular these are distinct over $b_2 \neq 0$. The degree-six term $c_4 v'^4$ is allowed in this child. Putting $C_4 = C_4^{(0)} + c_4 v'^4$, we complete the square:

$$z = 2w' + B_2, \qquad z^2 = F = B_2^2 - 4C_4, \tag{XIV.13.24}$$

$$u' = 0 : \quad \delta_2 = b_2^2 - 4c_4. \tag{XIV.13.25}$$

The equation $u' = 0$ cuts a degree-two divisor over the base function field $K_B^{\mathrm{rat}} = \mathbb{C}(\mathbb{P}^3)$. A nonsquare δ_2 prevents this divisor from splitting over that field. This does not yet rule out a rational point somewhere else on the generic fiber.

To rule one out in the full smooth family, place F on $Y = \mathbb{P}_{\mathbb{P}^3}(\mathcal{O} \oplus \mathcal{O}(H))$, the projective bundle of one-dimensional quotients. If ζ is its quotient class, the two coordinates have classes $\zeta - H, \zeta$. Set $L = 2\zeta + 3H$, so F is a section of $2L$. The quotient class is induced by the generated bundle embedding into $\mathbb{P}^3 \times \mathbb{P}^4$; L is ample as the restriction of $\mathcal{O}(3, 2)$. At fixed b_i the coefficients of the binary quartic F can vary independently with base degrees $10, 9, 8, 7, 6$ by varying all the c_i. Thus this is a full linear system, rather than a claim about a fixed one-parameter c_4 slice. Its sections generate $2L$: the leading and trailing coefficients are basepoint free, and at least one of u', v' is nonzero. Over $\mathbb{C}$ a general branch divisor $\mathcal{B} = (F = 0)$ is smooth. We restrict to the smooth open and take the double cover $q : X \to Y$ defined by $z^2 = F$.

Let $\mathcal{R} = (z = 0)$ on X. The map $\mathcal{R} \to \mathcal{B}$ is an isomorphism, $\mathcal{B}$ is ample, and $\mathcal{R}$ is ample by finite pullback. The two ambient fourfolds are smooth. The integral Picard restriction theorem applies to both pairs: regular local rings supply the depth and parafactoriality hypotheses, and for $i = 1, 2$ the needed groups on each smooth threefold divisor A vanish:

$$H^i(A, \mathcal{O}_A(-nA))^\vee = H^{3-i}(A, K_A \otimes \mathcal{O}_A(nA)) = 0, \qquad n > 0. \tag{XIV.13.26}$$

The last step is Kodaira vanishing. The two restriction isomorphisms commute with q^*. Since the pullback on the divisors is an isomorphism, so is the pullback

$$q^* : \mathrm{Pic}(Y) \xrightarrow{\sim} \mathrm{Pic}(X). \tag{XIV.13.27}$$

The integral statement matters: equal Picard ranks alone do not exclude a degree-one line on X.

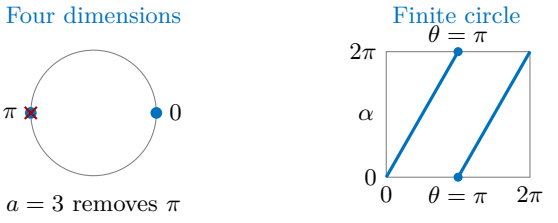


Figure XIV.13.3: Left: a charge-two VEV leaves two angles on the four-dimensional gauge circle; an additional periodic charge three removes the angle π. Right: the line $\alpha = 2\theta \bmod 2\pi$ wraps the angle torus with generator $(2, 1)$, so its separated segments in the square are parts of one connected circle.

The generic curve X_K (write $K = K_B^{\mathrm{rat}}$) is a smooth degree-two cover of $\mathbb{P}^1_K$ with four simple branch points, hence genus one. The closure of any closed point P of X_K is a Cartier divisor in the regular X. Its line descends by (XIV.13.27), so

$$[K(P) : K] = \deg(\mathcal{O}_{X_K}(P)) = 2\deg(\mathcal{M}|_{Y_K}) \quad \text{for some } \mathcal{M} \in \mathrm{Pic}(Y). \tag{XIV.13.28}$$

The displayed degree-two divisor supplies the upper bound on the index; evenness gives the lower bound. Moreover the curve is a nontrivial torsor for its Jacobian J_K since it has no K-point. The torsor $\mathrm{Pic}^d(X_K)$ has class $d[X_K]$: choosing a geometric point as origin for the line of degree one multiplies the corresponding Galois cocycle by d. The degree-two divisor gives a K-point on Pic^2. Thus

$$\mathrm{ind}(X_K) = 2, \qquad 0 \neq [X_K] \in H^1(K, J_K), \qquad 2[X_K] = 0. \tag{XIV.13.29}$$

The Weil–Châtelet period is two. No claim of local triviality over the base follows. To see why the hypotheses matter, take $F = v'(X_0^9 u'^3 + X_0^5(X_0 + X_1)v'^3)$. The branch polynomial is nonsquare at $u' = 0$ by its odd X_0 valuation, but $v' = z = 0$ gives a rational point elsewhere. The branch is singular at $[0 : 1 : 0 : 0]$, $v' = 0$, where its base derivatives and its v' derivative vanish. A nonsplit displayed divisor by itself could not have given (XIV.13.28).

The charge test is independent. On the resolved parent the two C_1 curves in exceptional, residual order have abelian charges $(-2, 2)$; the C_2 curves in the section order described in Section XIV.13.5 have $(1, -1)$. Suppose a charge-two field acquires a four-dimensional expectation value and there are no further charged backgrounds. In the primitive frame $\theta \sim \theta + 2\pi$, a state of charge Q transforms by $e^{iQ\theta}$. The VEV and an optional periodic axion of integer charge a constrain θ by

$$2\theta \in 2\pi\mathbb{Z}, \quad a\theta \in 2\pi\mathbb{Z}, \qquad |\,\mathrm{Stab}_{4d}\,| = \gcd(2, a). \tag{XIV.13.30}$$

This follows because the subgroup of $\mathbb{Z}$ generated by $2, a$ is $\gcd(2, a)\mathbb{Z}$. At $a = 0$ the C_2 states are odd and the C_1 charges are even. In the ordinary local square degeneration of the $\beta = 5$ child, the two C_2 branches are graphs $z = \pm Q(u', v')$ with distinct marked

points at $u' = 0$. Each graph is met once by the bisection, so its intersection agrees modulo two with the corresponding parent charge. At $a = 3$ there is no order-two group in the stated joint stabilizer. The child is therefore excluded for an order-two target with that extra gauging, although its geometric index is unchanged. The integer a is extra periodic gauging data, not a real coefficient extracted from a leading flux calculation.

At finite circle radius the comparison instead uses two angles, one for momentum and one for the gauge symmetry. In the frame where the condensing mode has charge $(1, -2)$, the kernel equation is

$$\alpha - 2\theta = 0 \pmod{2\pi}, \qquad \ker(1,-2) = \{(2\theta, \theta) : \theta \in \mathbb{R}/2\pi\mathbb{Z}\}. \tag{XIV.13.31}$$

Every solution has this form; the kernel is connected with integer generator $(2, 1)$. Figure XIV.13.3 contrasts this circle with the isolated four-dimensional angles. The different kernels refer to different gauge groups. Neither the geometric period nor the connected finite-circle kernel proves an allowed compact Higgs transition.

XIV.13.4 Instanton supports and strongly coupled sectors

What can geometry tell us before computing either an instanton amplitude or strong dynamics? For the instanton the first test concerns the internal fermions and the allowed boundary of an inserted membrane. For conformal matter it concerns the transformed base geometry and the anomaly of a protected current. The two operations use different cycles and characteristic classes. In both cases a numerical match can be decisive for one test without completing the dynamics.

Start with the compact Witten example of Chapter 10. Let H be the pullback hyperplane and E the exceptional plane of the blowup at a point of $\mathbb{P}^3$. Write D for the inverse image of a smooth base surface S_0 under the elliptic map. It is vertical, type (b) in Witten's terminology. For the ordinary neutral, unfluxed calculation, the direct images of the structure sheaf are $\mathcal{O}_{S_0}$ and $L^{-1}|_{S_0}$, in degrees zero and one, where $L = -K_{B_{\mathrm{bl}}}$. The three rational supports have $H^1(\mathcal{O}) = H^2(\mathcal{O}) = 0$, so there are no surviving differentials between the rows of Leray. Serre duality on S_0 gives

$$h^{0,p}(D) = h^p(S_0, \mathcal{O}_{S_0}) + h^{p-1}(S_0, L^{-1}|_{S_0}), \qquad h^{0,3}(D) = h^0(S_0, K_{S_0} + L|_{S_0}). \tag{XIV.13.32}$$

For these three supports the other L^{-1} contributions vanish. On a plane this is line-bundle cohomology. On the blowup of the plane, the dual line consists of lines through one point: the evaluation map of the three linear forms at the center surjects onto one value and H^1 of its kernel line vanishes. Its H^2 also vanishes by duality with the negative L^{-1}.

Indeed $L = 4H - 2E$. On the exceptional plane $H|_E = 0,\ E|_E = -h$, where h is its line class; on the plane away from the center E restricts trivially. On the plane through the center the restrictions of H, E are the pullback line h and exceptional curve e, with

$K_{S_0} = -3h + e$. Therefore

S_0	E	H	$H - E$
$K_{S_0} + L\|_{S_0}$	$-h$	h	$h - e$
$h^{0,p}(D)$	$(1,0,0,0)$	$(1,0,0,3)$	$(1,0,0,2)$
$\chi(\mathcal{O}_D)$	1	-2	-1

(XIV.13.33)

The exceptional support passes the ordinary neutral superpotential screen; its contribution remains conditional. Neither this index nor the full neutral vector evaluates the determinant or tests charged modes and their lifting.

The volumes depend on the Kähler polarization. For $J = aH - bE$, an exceptional line and the strict transform of a line through the center have respective areas b and $a - b$; the interior cone here is $a > b > 0$.

Here $H^3 = E^3 = 1$ and the mixed products vanish. The resulting volumes are

$$\tau(S_0) = \tfrac{1}{2} \int_{B_{\mathrm{b1}}} J^2 S_0, \tag{XIV.13.34}$$

$$(\tau_E, \tau_H, \tau_{H-E}) = \tfrac{1}{2}(b^2, a^2, a^2 - b^2), \tag{XIV.13.35}$$

$$(\tau_E, \tau_H, \tau_{H-E})\big|_{(a,b)=(7,3)} = (9/2, 49/2, 20). \tag{XIV.13.36}$$

The leading Einstein-frame real E3 action in this normalization is $2\pi\tau$. Moving the support to the plane through the point changes both the action and the neutral count; a smaller or larger volume alone does not tell us whether a term is allowed. In a different test, $(a, b) = (3, 7)$ makes the strict-transform line area negative. The positive exceptional volume formula at that input does not give a Kähler action.

The T_{11} example changes the fourfold, not just the instanton support. Here a flux restricted to D has a specified dual curve class. A cohomological boundary condition for the three-form on the M5 is

$$dT_3 = G_4|_D - \delta_4(C), \qquad [C] = \mathrm{PD}_D[G_4|_D] \tag{XIV.13.37}$$

in the tested cohomology. At one transverse matter point the flux restriction has signed curve $5c_{24} + 2r_1 - r_2 + r_3 - 2r_4$, where r_i are root curves split over the point. In the ordered components $c_{14}, c_{2B}, c_{24}, c_{3C}, c_{4D}$ of this phase it becomes $(0, -1, 2, 1, -2)$. The five membrane ends are

$$c_{24} + c_{3C}, \quad c_{14} + c_{24}, \quad -c_{4D}, \quad -c_{2B}, \quad -c_{14} - c_{4D}. \tag{XIV.13.38}$$

Adding the columns cancels c_{14} and gives exactly the flux restriction. For the Cartan pairing, the c_{24} weight is $(1, -1, 1, -1)$ in the convention of this T_{11} calculation and each root curve pairs by the negative Cartan column. The signed root coefficients $(2, -1, 1, -2)$ have $A_4(2, -1, 1, -2)^{\mathsf{T}} = 5(1, -1, 1, -1)^{\mathsf{T}}$; the two contributions cancel. The section S_{MW} meets only c_{3C} once and the zero section meets none of the five components. In the ordered pairing with $(D_1, D_2, D_3, D_4, S_{\mathrm{MW}}, Z)$ the net boundary has

$$(q_{\mathrm{Cartan}}, q_{S_{\mathrm{MW}}}, q_Z) = \big((0,0,0,0), 1, 0\big), \qquad q_X = 5. \tag{XIV.13.39}$$

The X generator has coefficient five on the section in this normalization, with the vertical pairing zero and the summed Cartan pairing zero. This is not the primitive MP unit. Without the curve insertion the section witness remains nonzero; omitting a curve from the specified sum also leaves a residual pairing. The match is a condition for a dressed term, separate from neutral zero modes, quantized worldvolume flux and a nonzero contraction.

For the strong sector, take $B = \operatorname{Tot}\mathcal{O}_{\mathbb{P}^2}(n)$, z its normal coordinate in a line frame, and F_d a smooth Fermat plane polynomial of degree d. The compact curve is $\Sigma = (z = F_d = 0)$. Since the vertical tangent is the pullback of $\mathcal{O}(n)$, $L = -K_B$ has class $3 + n$ in line units. The ansatz $f = 0,\ g = (zF_d)^4$ then gives

$$4(n + d) = 6(3 + n), \qquad 4d = 18 + 2n, \tag{XIV.13.40}$$

$$K_\Sigma = \mathcal{O}_\Sigma(d - 3), \qquad 2g_\Sigma - 2 = d(d - 3). \tag{XIV.13.41}$$

This yields $(n, d, g_\Sigma) = (-1, 4, 3)$ for CM4-Q and $(-3, 3, 1)$ for CM4-C. Changing degree alone would no longer match the bundle of g. The normal degrees from z and F_d are nd and d^2, so the two compact curves have different normal data even though the transverse equation is the same.

In transverse coordinates $u = z,\ v = F_d$, the generic end divisors have split IV* fibers: their leading g coefficients v^4, u^4 are squares in the divisor function fields. At the crossing the order of g in (u, v) is eight. Under the blowup of the smooth curve, $K_{B'} = \beta^* K_B + E_{\mathrm{exc}}$. Hence the chart $u = e,\ v = ex$ requires the new section coefficients $f' = \beta^* f/e^4,\ g' = \beta^* g/e^6$. The same divisions apply in the other chart. With $\Delta = 4f^3 + 27g^2$, three tests are

(f, g)	$\operatorname{ord}_{(u,v)}(f, g, \Delta)$	(f', g')
$(0, u^2v^2)$	$(\infty, 4, 8)$	$(0, e^{-2}x^2)$
$(0, u^4v^4)$	$(\infty, 8, 16)$	$(0, e^2x^4)$
(u^2v^2, u^3v^3)	$(4, 6, 12)$	(x^2, x^3)

(XIV.13.42)

In the last line the discriminant is $31u^6v^6$, so no leading cancellation changes the order. The lower-order collision has an actual pole, whereas both other germs pass this first local test. This is not an obstruction theorem for other constructions.

For the Fermat collision the other chart has $g' = x^4e^2$ with e now the exceptional coordinate along the other end. The two corners of the exceptional line have total order six. Blowing up each once therefore gives a new exceptional with generic g-order zero. The first exceptional goes from self-intersection -1 to -3 in the transverse surface after the two corner blowups. The chain is $(-1, -3, -1)$, with the middle fiber split IV from the square leading coefficient of the order-two g. This is the transverse base slice of the rank-one E_6 link. Figure XIV.13.4 shows both the exceptional division and where the three curves lie. The slice does not establish a smooth resolution of every total-space stratum.

The genus changes the protected calculation. Put $C = c_2(R_6)$, $p = p_1(T_6)$, $p_2 = p_2(T_6)$, and $Y_i = \mathrm{Tr}F_i^2/4$ with $\mathrm{Tr} = \mathrm{tr}_{\mathrm{adj}}/h^\vee$ on each end. The sourced interacting six-dimensional polynomial has had both the center-of-mass free tensor and its Green–

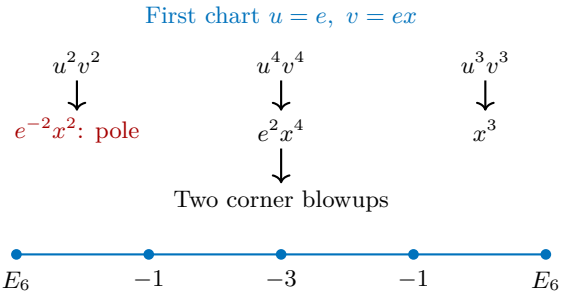


Figure XIV.13.4: The first exceptional power of g' is the total order of g minus six. For the Fermat E_6 germ, two more blowups at the end corners leave a central -3 curve between the new -1 curves. The distinct $(4, 6, 12)$ control is only compared at the first blowup.

Schwarz term removed. Its specialization is

$$I_8 = \frac{319}{24}C^2 - \frac{89}{48}Cp + \frac{553}{5760}p^2 - \frac{79}{1440}p_2 \\ - 6C(Y_L + Y_R) + \tfrac{1}{2}p(Y_L + Y_R) + Y_L^2 + Y_R^2 + Y_LY_R. \tag{XIV.13.43}$$

For the genus-three no-flux twist, write $r = c_1(R_4)$ and let η integrate to one on Σ. The twist replaces C by $-(r + (g_\Sigma - 1)\eta)^2$. With $\eta^2 = 0$ and no internal flavor curvature, p has no linear internal term either. Only C^2, Cp, CY_i contribute. In particular

$$[\eta](C^2, Cp, CY_i) = (g_\Sigma - 1)(4r^3, -2rp, -2rY_i). \tag{XIV.13.44}$$

At $g_\Sigma = 3$ the four surviving coefficients are

$$I_6 = \frac{319}{3}r^3 + \frac{89}{12}rp + 24rY_L + 24rY_R. \tag{XIV.13.45}$$

In left-Weyl trace conventions the pure terms give $\operatorname{Tr} R^3 = 638$, $\operatorname{Tr} R = -178$. The mixed term uses $k_{\text{poly}} = -2\operatorname{Tr}(RT^aT^b)/\delta^{ab} = 24$. An $\mathcal{N} = 1$ vector on the left contributes $-2h^\vee rY_L = -24rY_L$; hence the left slot cancels algebraically, while the right stays 24. If the inherited R is the exact ungauged superconformal R, the current multiplet identity gives the matter screening contribution for weak gauging without other charged sectors:

$$b_{\text{matter}} = -3\frac{\operatorname{Tr}(R_{\text{SC}}T^aT^b)}{\delta^{ab}} = \tfrac{3}{2}k_{\text{poly}} = 36, \qquad b_{\text{weak}} = 3(12) - 36 = 0. \tag{XIV.13.46}$$

The algebraic slot cancellation does not require this current interpretation. The weak coefficient, even under its assumptions, does not establish a fixed point at finite gauge coupling.

For the cubic, compare the separately sourced very-Higgsable compactification on a periodic flat torus without flux or holonomies. There is no twist curvature leg, so

the push of (XIV.13.43) with $g_\Sigma = 1$ is zero and does not compute the torus anomalies. The independent prescription uses the coefficient of $p\,\mathrm{Tr}F_L^2$, namely $1/8$, to give

$$\begin{aligned} k_{\mathcal{N}=2} &= 192(1/8) = 24, \\ b_{\mathrm{matter},T^2} = k_{\mathcal{N}=2}/2 = 12, &\qquad b_{\mathrm{weak},T^2} = 36 - 12 = 24. \end{aligned} \tag{XIV.13.47}$$

The last comparison uses only the $\mathcal{N} = 1$ vector in the specified weak gauging of the torus block. Despite the equal numbers 24, $k_{\mathcal{N}=2}$ and k_{poly} are different coefficients in different prescriptions. The two models share the local six-dimensional link, not the four-dimensional reduction. We now return to a case where a single line class changes and can follow exactly which earlier calculation survives.

XIV.13.5 Changing one input and checking the output

Which of the section and action results survive changing the twist? Keep $\mathbb{P}^3$, the toric fiber and its oriented sections fixed, and change the integer β from five to six. Write $\bar{K} = 4H$ and $\alpha = (\beta - 4)H$. The fiber coordinates have classes

$$[u] = U, \quad [v] = U + S + \alpha, \quad [w] = 2U + S + \beta H, \quad [s] = S. \tag{XIV.13.48}$$

The anticanonical class is their sum plus $\bar{K}$, namely $4U + 3S + 2\beta H$. Subtract the class of each monomial in (XIV.13.22). For instance v^2w leaves $2\bar{K} - \beta H$ and uv^3 leaves $3\bar{K} - \beta H$. For c_4 subtract the class of v'^4 from the class of sP_1. In units of H, the result is

	b_0	b_1	b_2	c_0	c_1	c_2	c_3	c_4
deg	β	4	$8-\beta$	2β	$4+\beta$	8	$12-\beta$	$16-2\beta$
$\beta = 5$	5	4	3	10	9	8	7	6
$\beta = 6$	6	4	2	12	10	8	6	4

(XIV.13.49)

In particular the old degree-six c_4 cannot be used as a degree-four section. No statement about the period or index of the retwisted child is needed for the parent comparison.

In the absence of an ordinary nonabelian divisor in this section construction, project $S - U$ by subtracting $d_\sigma H$ to make its pushforward against U vanish. The self-pushforwards of the two sections are $-\bar{K}$ by adjunction in the Calabi–Yau model. From (XIV.13.23) they meet over $b_2 = 0$ with a simple generic intersection, giving $\pi_*(SU) = (8 - \beta)H$. Also $\pi_*(UH) = \pi_*(SH) = H$ because each section has degree one, and $\pi_*(H^2) = 0$. Hence

$$\pi_*(U(S - U - d_\sigma H)) = (12 - \beta - d_\sigma)H, \tag{XIV.13.50}$$

$$\sigma = S - U - (12 - \beta)H, \tag{XIV.13.51}$$

$$-\pi_*(\sigma^2) = 2(12 - \beta)H. \tag{XIV.13.52}$$

For the height, the terms with a vertical factor vanish because $\pi_*(S - U) = 0$; the remaining square is $-2\bar{K} - 2\pi_*(SU)$ before the overall minus sign. This explains why

keeping the old subtraction $7H$ at $\beta = 6$ can leave the new height unchanged while giving a wrong gauge divisor: the mixed pushforward becomes $-H$. Both tests are needed.

The ordinary charge-two support C_1 has equations $b_2 = c_3 = 0$. On the smooth complete-intersection open let $d_1 = 8 - \beta,\ d_2 = 12 - \beta$. Its degree is $d_1 d_2$, and its canonical line is $\mathcal{O}_{C_1}(d_1 + d_2 - 4)$ by adjunction. Thus

$$(\deg C_1, g(C_1))_{\beta=5} = (21, 64), \qquad (\deg C_1, g(C_1))_{\beta=6} = (12, 25). \tag{XIV.13.53}$$

These genus statements concern the smooth open; the following sparse coefficient tuple tests two specified local fibers instead.

To realize those fibers for $\beta = 6$, take $p = [1 : 0 : 0 : 0]$ and $q = [0 : 1 : 0 : 0]$ in base coordinates X_i. For a coefficient of degree d, X_0^d, X_1^d prescribe its values at p, q, and $X_0^{d-1}X_i, X_1^{d-1}X_i$ for $i = 2, 3$ prescribe derivatives in two transverse directions. All degrees used are at least two, so the desired value and transverse derivative at one point do not constrain the other. Use the following sections:

$$\begin{aligned} &b_0 = 5X_1^6, && b_1 = 2X_1^4, && b_2 = 2X_0X_2 + X_1^2, \\ &c_0 = -X_0^{12} + 6X_1^{12} + 5X_1^{11}X_2, && c_1 = 5X_1^{10} + 7X_1^9X_3, && \\ &c_2 = -X_0^8 + 3X_1^8, && c_3 = 3X_0^5X_3 + X_1^6. && \end{aligned} \tag{XIV.13.54}$$

At p, $b_2 = c_3 = 0$; their Jacobian in (X_2, X_3) in the chart $X_0 = 1$ is $\operatorname{diag}(2, 3)$. In $u = 1$ the parent factors as $s(w^2 - v^2 - s^2)$. The conic is smooth (determinant 1); it meets $s = 0$ at the two simple points $w/v = \pm 1$. Thus the C_1 cut and the ordinary two-component fiber are both visible at p. In the $v = 1$ chart the residual toric weights of (u, w, s) are $(1, 1, -1)$. The exceptional component is the full $[u : w]$ line. On it $u = 0$ cuts one point and $s = 0$ has degree -1, since the divisor contains the component and its coordinate has weight -1. On the residual conic $u \neq 0$ and $s = 0$ cuts the two simple points. The differences of section degrees give $(-1 - 1, 2 - 0) = (-2, 2)$ in exceptional, residual order.

At q, $b_2 = 1$. To find the C_2 locus for $b_2 \neq 0$, try the factors $w + Asu^2 + Buv$ and $sw + Ds^2u^2 + Esuv + b_2v^2$. The coefficients of w and the terms with highest v powers give

$$B = c_3/b_2, \qquad E = b_1 - B, \qquad A = (c_2 - BE)/b_2, \qquad D = b_0 - A, \tag{XIV.13.55}$$

$$f_0 = c_0 - AD, \qquad f_1 = c_1 - AE - BD. \tag{XIV.13.56}$$

The last two equations $f_0 = f_1 = 0$ enforce the remaining constant terms. At q, $(A, B, D, E) = (2, 1, 3, 1)$ and the factorization is

$$F_q = 2su^2 + uv + w, \qquad G_q = 3s^2u^2 + suv + sw + v^2. \tag{XIV.13.57}$$

In the chart $s = u = 1$, put $w = -2 - v$ on $F_q = 0$. Then $G_q = 1 + v^2$ has two simple roots. The first derivatives of A, B, D, E in the two prescribed directions vanish, so the cut Jacobian is that of c_0, c_1:

$$J_{C_2} = \frac{\partial(f_0, f_1)}{\partial(X_2, X_3)} = \begin{pmatrix} 5 & 0 \\ 0 & 7 \end{pmatrix}. \tag{XIV.13.58}$$

Move the c_1 jet from X_3 to X_2, replacing its last term by $7X_1^9X_2$. The values at q and the two nodes stay fixed. Yet the rows of J_{C_2} become $(5,0),(7,0)$ and its rank drops to one. The transverse rank test fails even though the fiber polynomial and its component degrees are unchanged.

The sections meet the two branches once each. On $s=0, u=v=1$, $F_q=w+1$ and $G_q=1$, so S meets the first branch. On $u=0, v=w=1$, $F_q=1$, $G_q=s+1$, so U meets the second branch. The toric exclusions permit these charts at the corresponding intersections. The vertical subtraction has zero degree on each fiber curve, giving ordered charges $(1,-1)$. A unit pairing with an integral curve rules out divisibility of this normalized direction in the integral charge frame. Figure XIV.13.5 compares the two jet directions and shows which section pairs with which factor. Along $X_0=X_1=0$ the sparse tuple instead has all coefficients zero and $P_1=sw^2$; even the fibers of this one tuple need not be ordinary. The witness supplies one primitive direction from local fiber geometry, with no global smoothness, full Mordell–Weil rank or physical spectrum assertion.

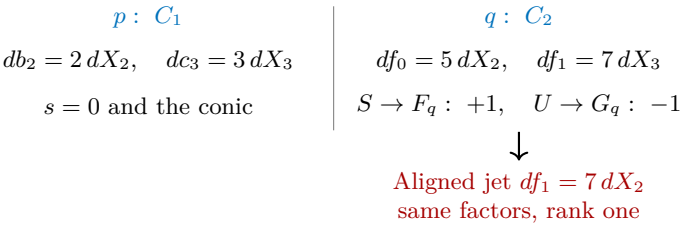


Figure XIV.13.5: Two transverse Jacobians for the $\beta=6$ construction. At q the sections meet opposite factors, giving $+1,-1$ in the displayed order. Moving the c_1 derivative into the X_2 direction keeps the factors but makes the two defining differentials dependent.

We can now transport the height to the leading action under a specified trial flux. Keep $J_B=tH$, $t>0$, and $G=mH\sigma$ with fixed integer coefficient m, without assuming admissibility of that flux. In the real gauge kinetic frame of Chapter 8 take $\tau=\operatorname{Re}T=t^2/2$, $K=-3\log\tau$ up to an additive constant, and h the numerical height coefficient. Denote the unhalved flux pairing by P.

The covariant derivative uses the half-pairing Θ. The leading kinetic coefficient and the two pairings are

$$P=\int G\,H\sigma=-hm, \qquad \Theta=P/2, \qquad \operatorname{Re}f=ht^2/2. \tag{XIV.13.59}$$

The raw pairing follows from $\pi_*(\sigma^2)=-hH$ and $H^3=1$. The factor $1/2$ in Θ is part of the leading reduction convention. It does not fix a primitive periodic axion charge. Since $\partial_T\tau=1/2$, we have

$$K_T=-\frac{3}{2\tau}, \qquad K_{T\bar T}=\frac{3}{4\tau^2}. \tag{XIV.13.60}$$

Inserting these derivatives in the leading one-vector action gives

$$D = K_T\Theta = \frac{3hm}{2t^2}, \tag{XIV.13.61}$$

$$V_D = \frac{D^2}{2\,\mathrm{Re}\,f} = \frac{9hm^2}{4t^6}, \tag{XIV.13.62}$$

$$m_A^2 = \frac{2K_{T\bar{T}}\Theta^2}{\mathrm{Re}\,f} = \frac{3hm^2}{t^6}. \tag{XIV.13.63}$$

The last expression uses a canonically normalized vector and is the leading mass diagnostic in this action, not a full mass eigenvalue in an arbitrary compactification. At $t = 8, m = 1$, changing β gives

β	$\mathrm{Re}\,f$	D	V_D	m_A^2
5	448	21/64	63/524288	21/131072
6	384	9/32	27/262144	9/65536

(XIV.13.64)

At either nonzero m, using P as Θ instead would double D and multiply both quadratic observables by four. At $m = 0$ those three observables vanish, while $\mathrm{Re}\,f$ still distinguishes the two heights. The old $\beta = 5$ trial flux contribution $\frac{1}{2}\int G^2 = -7m^2$ follows from its height and does not supply flux data for a different child. A controlled parent comparison thus transports the form of the leading action and recomputes its coefficients. It leaves the existence of compatible backgrounds to a separate test.

XIV.13.6 What remains unspecified

Can an apparently satisfactory compact charge budget certify a physical background? Return to the named smooth crepant phase of SU5-Q. Chapter 11 constructs an integral algebraic cycle K from differences of Cartan surfaces over the two rulings of Q. If $f = h_1 - h_2$, then $f \cdot H|_Q = 0$ and $f^2 = -2$. For the ordered Cartans let A_4 denote the Cartan matrix and $v = (2, 4, 6, 3)$ the integral coefficients up to common sign. Combining the negative Cartan intersection form with the negative ruling square gives

$$K^2 = 2v^{\mathsf{T}} A_4 v = 2(2, 4, 6, 3) \cdot (0, 0, 5, 0) = 60. \tag{XIV.13.65}$$

In this phase $G_*^2 = 140$ and $G_* \cdot K = 0$. To see the cross pairing, write $\Gamma_i(f)$ for the difference of the two ruling surfaces in the i-th Cartan. An inherited product P_2 of two divisors pairs with $\Gamma_i(f)$ by first pushing $P_2|_{D_i}$ to Q. At the level of the ambient construction, exchanging the rulings preserves the ambient blowup centers, divisor classes and hypersurface class. The pushed divisor is therefore symmetric in h_1, h_2, and its pairing with f vanishes. This argument does not require the chosen Tate coefficients to be symmetric. The Chern term of G_* is ambient as well, and the zero section has the rational Chow representative $r/3$ for the cubic coordinate class r. The same projection then gives $G_* \cdot K = 0$. Under the inclusion $i : Q \hookrightarrow \mathbb{P}^3$, each ruling is a line of degree one and both push to the same class:

$$i_* h_1 = i_* h_2 = H^2, \qquad i_* f = 0. \tag{XIV.13.66}$$

This last test can remove the specified leading hypercharge mass obstruction in the corresponding reduction; it does not solve the full gauging or vacuum problem.

For integer n, define $G_n = G_* + nK$. The characteristic and pairing numbers in the stated normalization give

$$\tfrac{1}{2}\int G_n^2 = \tfrac{1}{2}(140 + 2n\cdot 0 + 60n^2) = 70 + 30n^2, \tag{XIV.13.67}$$

$$N_{\mathrm{formal}}(n) = \frac{\chi(\widetilde{Y})}{24} - \tfrac{1}{2}\int G_n^2 = \frac{6768}{24} - 70 - 30n^2 = 212 - 30n^2. \tag{XIV.13.68}$$

The integral cycle is K, not the rational $K/5$ in the root normalization; the latter has square $12/5$ and fails the separate free quantization test for the named perturbation. Using its square here would answer a different question. Figure XIV.13.6 gives the integer comparison. At $n = 1$, the formal residual budget is 182. At $n = 3$ it is -58, so the ordinary compact D3 charge equation with nonnegative mobile D3 number rejects that flux choice under its stated assumptions. This sign condition retains only $|n| \le 2$ within the integer family; it does not promote the surviving entries to vacua.

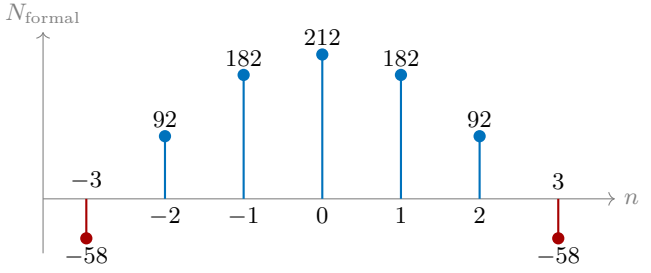


Figure XIV.13.6: The D3 budget for integer multiples of the integral ruling-difference cycle. The positive values at $|n| \le 2$ pass the necessary sign test. The $|n| = 3$ value would require a negative mobile D3 number under the stated convention.

What would a surviving entry require? In the stipulated smooth member G_* passes the stated shifted free-lattice test, and adding an integral cycle preserves it:

$$G_n + \tfrac{1}{2}c_2 = (G_* + \tfrac{1}{2}c_2) + nK. \tag{XIV.13.69}$$

This is a separate calculation: positivity of N_{formal} neither proves the shift condition nor checks refined flux data. For the usual resolved Calabi–Yau supersymmetry test one also asks that

$$G_n \in H^{2,2}(\widetilde{Y}), \qquad J \wedge G_n = 0. \tag{XIV.13.70}$$

The condition on J is sensitive to the choice of Kähler chamber. At finite resolved volume the named flux direction in Chapter 11 retains its explicit Kähler-wall obstruction. It cannot be discarded on the strength of the sign test; the physical F-theory limit needs its own analysis.

For matter, one needs the map from the refined background to compatible defect sheaves, not just their proposed degrees or a formal period. Then the spaces of

holomorphic modes and their pairings must be computed on those actual sheaves. For a normalized action one also needs a metric, the identification and normalization of the gauge and axion variables, and a limit in which the desired degrees of freedom can be isolated. A leading pairing does not give the periodic data that appeared in (XIV.13.30). These are different calculations. The value of a selective comparison is that it tells us which ones we can already perform and which inputs we would have to supply next.

XIV.13.7 Exercises

Use the signed charge frames and the volume conventions of the chapter. Exact rational arithmetic is sufficient for the bounded answers. Explanations, including the final comparison, are assessed by a reader.

1. **Select a section model.** For a primitive abelian direction over $\mathbb{P}^3$, list the candidates with no height constraint, at height $12H$, and at height $14H$. Use the row names `mp-parent-beta5` and `mp-parent-beta6`. Explain why an unresolved base for T_{11} is different from the known base mismatch for SU5-Q.

2. **Transport the action and test a jet.** At $\beta = 6, t = 4, m = -2$, calculate the subtraction d_σ, the degree and genus of smooth C_1, the signed raw pairing P, $\Theta, \operatorname{Re} f, D, V_D, m_A^2$. With the original c_0 derivative from (XIV.13.54), replace the c_1 transverse jet at q by $3X_2 + 4X_3$ in the chart $X_1 = 1$. Submit the new cut rank, and submit the ordered abelian charges at p (exceptional, residual) and q (F_q, G_q). Explain why an aligned c_1 jet would leave the factorization in place.

3. **Impose two periodic conditions.** For a charge-two Higgs VEV and axion charges $0, 3, 4$, give the three orders of the joint four-dimensional stabilizer. For the finite-circle vector $(1, -2)$ give the integer generator with positive second coordinate and the order of the component group.

4. **Test the budget.** Compute the formal budget at $n = 2$ in integral K units. State whether the sign rejects this class and whether the sign alone certifies a physical background.

5. **Move the instanton support.** At $(a, b) = (8, 5)$, give the real action factors $S_{\mathrm{E3}}/(2\pi)$ and the ordinary neutral vectors for $E, H - E$, in that order. At $(a, b) = (4, 5)$, give both curve areas and decide whether this is in the cone.

6. **Compare the protected quantities.** For the quartic give the left mixed slot, the conditional matter screening and the conditional weak coefficient. For the cubic give the separately sourced torus current central charge, screening and weak coefficient. Explain why substituting $g_\Sigma = 1$ in the twist formula does not reproduce the torus result.

7. **Specify what would have to be computed.** Give one flux-to-sheaf step and one metric or periodic-gauging step that the chapter leaves open. For each, name the extra input and calculation, then explain why a matched finite invariant would not perform it.

Status and sources

§1. Selection. The two primitive section choices and their height and base predicates are [MATH] at the scope of the examples in Chapters 6 and 8. The calculation uses the stated ordered geometric charges and the leading action of Chapter 8.

§2. Ordinary sectors. The ordinary split I_5 reading is [GEO-E]. The genus, oriented charge, period and curve cohomology are [MATH]; see Chapters 2–5 and 11, Hayashi et al. (2013), v2 §3, (3.12)–(3.14), and Bies et al. (2017), v1 (2.15), (2.17), (2.21). The local pairing uses Cecotti et al. (2009), v2 (3.45)–(3.46), in the stated Chapter 5 modules. The leading Sen comparison is contextual from Chapter 9. See Sen (1997), v2 (4)–(7) for the starting ansatz, (18) for the cover, and (21)–(23) (PDF pp. 5–6) for the χ deformation and leading discriminant. No finite-coupling monodromy is deduced here. The G_* and K calculations retain the phase and orientations of Chapters 2, 4 and 11.

§3. Discrete data. The full smooth double-cover Picard, index and period result and the two kernel calculations are [MATH]; the VEV is a physical premise. See Chapter 7, Mayrhofer et al. (2014), v4 (2.1)–(2.3), (2.12)–(2.17), and Grothendieck (1968), Exposé XII, §3, Corollaries 3.5–3.6. The index and period concern the stated curve over the base function field.

§4. Instantons and strong sectors. The ordinary neutral vectors, T_{11} boundary pairing, local blowups and plane-curve computations are [MATH] in their named settings. The conditional neutral interpretation is [GEO-E]; see Witten (1996), v2 (2.9), §3 type (b) and the exceptional example (PDF pp. 15,17), and Martucci and Weigand (2015), v2 (2.10)–(2.12), (5.12)–(5.13), with Chapter 10. The quartic anomaly and conditional screening comparison are [ANOM]; see Chapter 12, Apruzzi et al. (2018), v2 (5.10)–(5.14), Appendix B (B.1), (B.16), (B.19)–(B.21), and Ohmori et al. (2015), v1 (6.42)–(6.46). The latter uses a different compactification prescription.

§5. Retwist. The projection, height, homogeneous local witness and degree change are [MATH]; see Chapters 6–7 and Morrison and Park (2012), v2 (3.4)–(3.8), for the projection framework. The action comparison is [SUGRA] in the leading Chapter 8 frame; compare Grimm (2011), v2 (3.38), (5.16). The physical use of a non-torsional Shioda direction presumes the ordinary F-theory limit and a background that leaves the direction available.

§6. Compact budget. The quadratic intersection calculation is [MATH]; the compact D3 sign test is [SUGRA]. See Chapters 3 and 11 for the shifted lattice, the exact cycle and finite-resolution obstruction. No compact physical completion is established by the budget.